Investigating a Novel Pathway for Hypertension and Pharmacologic Response Involving the Dicarboxylic Acid, Hexadecanedioate

Nora Hassan J Alharbi

BSc, MSc

Submitted In fulfilment of requirements for the degree of Doctor of Philosophy (Ph.D.) in the Institute of Cardiovascular and Medical Sciences, College of Medical, Veterinary and Life Sciences, University of Glasgow

December 2018

BHF Glasgow Cardiovascular Research Centre
Institute of Cardiovascular and Medical Sciences
College of Medical, Veterinary, and Life Sciences
University of Glasgow

Author's Declaration

I declare that this thesis has been written by myself and is a record of research performed by myself with the exception of the metabolomics analysis in Chapter 4, which was carried out at Metabolon© laboratories, USA and the statistical analysis was performed under the guidance of Dr Desmond Campbell. Biochemistry analysis in Chapter 3 was performed by Mrs. Elaine Butler at Institute of Cardiovascular and Medical Sciences, University of Glasgow. Quantitative analysis of hexadecanedioate level in rat plasma samples was carried out by Dr Christian Reichel and Dr Anja Huber at Seibersdorf laboratories, Austria. This work has not been submitted previously for a higher degree. It was carried out under the supervision of Dr Delyth Graham and Professor Sandosh Padmanabhan in the Institute for Cardiovascular and Medical Sciences.

Nora H. J. Alharbi

December 2018

Acknowledgement

Firstly, I would like to thank my supervisors Dr Delyth Graham and Professor Sandosh Padmanabhan for their continual support, motivation, expertise, immense knowledge and guidance throughout the course of this project. I would gratefully thank them for opportunities, experiences and trust afforded to me. Their insightful advice always kept me on the right track, and helped me to shape my research towards something more meaningful. I am also grateful to Dr Martin McBride, for his time, support, advice and guidance throughout this project.

My gratitude also goes out to everyone in the Cardiovascular Research Centre who I have had the pleasure of working with over the last four years. A special mention to Elisabeth Beattie for her advice, patience in teaching me myography and valuable help organising all of the animal studies. I wish to thank Andrew Carswell for his technical expertise in histology. I also thank Elaine Butler and Josephine Cooney for their kindness and assisting with the biochemistry analysis. Thank you to Christine, Charlie, Emad and the BHF GCRC biological services team for all your assistance. I would like to extend my gratitude to Dr Desmond Campbell for his help and guidance in metabolomics analysis.

My gratitude also goes out to Dorothy Ronney for her kindness and her support.

I must further extend my gratitude to my colleagues in McBride/Graham group and all my friends for their support, enthusiasm, unforgettable time during my PhD study.

I would like to acknowledgment Professor Omar Al-theeb, King Saud University, KSA for his support and advice throughout the course of my study.

I would like to express my deepest appreciation to my family, particularly my beloved parents for their continuous encouragement and support. My thanks also goes to my mother-in-low for her support and good wishes. I offer my regards, love and blessings to my other half, Faisal Alfouzan for his support and encouragement throughout conducting and writing my thesis and in my life in general. My love goes to the apple of my eye, my beautiful and gorgeous daughter, Joud. I am sure one day you will understand why mummy had to be a doctor. Last

but not least, I would like to dedicate this work to my brother Muhammad who I lost before I start my PhD.

As this research was supported and funded by Saudi Arabian Government represented by Hail University, I am immensely grateful for giving me this opportunity, and for providing everything I needed for my studies. It would not have been possible to complete this research without the support and funding I received.

Lastly, I sincerely thank everyone who has made this project possible.

Table of Contents

List of Tables

List of Figures

Glossary of terms and abbreviations

ACC	Acetyl-CoA carboxylase
ACE	Angiotensin Converting Enzyme
ACEI	Angiotensin converting enzyme inhibitors
ACTH	Adrenocorticotropic hormone
ADH	Antidiuretic hormone
ADHs	Alcohol dehydrogenases
ADP	Adenosine 5`-diphosphate
AKT	Protein kinase B
ALDHs	Aldehyde dehydrogenases
ALT	Alanine Aminotransferase
AME	Apparent mineralocorticoid excess
AMP	Adenosine 3`-monophosphate
Ang I	Angiotensin I
Ang II	Angiotensin II
Ang III	Angiotensin III
ANOVA	Analysis of variance
APA	Aminopeptidase A
ARBs	Angiotensin II receptor blockers
AST	Aspartate Aminotransferase
AT1R	Angiotensin II Type 1 Receptor
AT2R	Angiotensin II Type 2 Receptor
ATP	Adenosine triphosphate
ATPase	Adenosine triphosphatase
AUC	Area under the curve
AV	Atrioventricular
AWT	Anterior Wall thickness
BH4	Tetrahydrobiopterin
BMI	Body mass index
BP	Blood Pressure
BSEP	Bile salt export pump
CACT	Carnitine AcylCarnitine Translocase
cAMP	Cyclic adenosine monophosphate
CCB	Calcium channel blockers
CEMS	Capillary Electrophoresis- Mass Spectrometry
CK	Creatine Kinase
Cl^-	Chloride

CLCNKB	Voltage-gated chloride channel Kb
CNS	Central Nervous System
CO_2	Carbon dioxide
COX	Cyclooxygenase
CPT-1	Carnitine Pamitoyl Transferase 1
CPT-2	Carnitine Pamitoyl Transferase 2
Ct	cycle threshold
CVD	Cardiovascular disease
CYP450	Cytochrome P450
DALYS	Disability adjusted life years
DBP	Diastolic Blood Pressure
DCT	Distal convoluted tubule
DETC	N-diethyldithiocarbamate
DETC-SO	DETC-sulfoxide
DFAs	Dicarboxylic fatty acids
DHP	Dihydropyridine
DHT	Dihydrotestosterone
DIO2	Type 2 iodothyronine deiodinase
DOCA	Deoxycorticosterone acetate
EC50	50% of the maximum response
EDD	End diastolic dimension
EDHF	Endothelium- Derived Hyperpolarizing Factor
EDV	End-diastolic volume
EF	Ejection fraction
EGFR	Epidermal Growth Factor Receptor
ELISA	Enzyme Linked Immunosorbent Assay
ENaC	Epithelial sodium channels
eNOS	Endothelial Nitric Oxide Synthase
ER	Endoplasmic Reticulum
ESC/ ESH	European Society of Cardiology and the European Society of Hypertension
ESD	End Systolic dimension
ESV	End-systolic volume
ET-1	Endothelin-1
$FADH_2$	Flavin adenine dinucleotide
FS	Fractional shortening
FXR	Farnesoid X Receptor
g/L	Gram/liter

G3P	glycerol-3-phosphate
G6Pase	Glucose-6-phosphatase
GAPDH	Glyceraldehyde-3-phosphate dehydrogenase
GC- MS	Gas Chromatography- Mass Spectrometry
GCS	Gamma-glutamylcysteine synthetase
GGT	Gamma-glutamyltransferase
GnRH	Gonadotropin-releasing hormone
GPCRs	G- Protein- Coupled Receptors
GS	Glutathione synthetase
GSH	Glutathione
GSK3β	Glycogen Synthase Kinase 3β
GSSH	Glutathione disulfide
GWAS	Genome wide association studies
H_2	Hydrogen
HEXA	Hexadecanedioic acid
HR	Heart Rate
HRP	Horseradish Peroxidase
HSD11β2	11β- hydroxysteroid dehydrogenase Type 2
IL-1	Interleukin-1
IL-6	Interleukin-6
iNOS	Inducible Nitric Oxide Synthase
IP	Prostacyclin receptors
IP_3	Inositol triphosphate
JNC VI	Sixth Report of the Joint National Committee on Prevention, Detection, Evaluation, and Treatment of High Blood Pressure
LC-MS/MS	Liquid chromatography–mass spectrometry
LDL	Low- Density Lipoprotein
LIMS	Laboratory Information Management System (LIMS)
L-NMMA	N^G-monomethyl-L-arginine
LV	Left ventricular
L-VDCC	L-type voltage dependent Ca_2^+ Channel
LVM	Left ventricular mass
MAP	Mean Arterial Pressure

Me-DDTC	N-diethyldithiocarbamate
Me-DDTC-SO	*S*-methyl-*N*, *N*-diethylthiocarbamate-sulfoxide
Me-DDTC-SO_2	Sulfone
mmHg	Millimetres of mercury
mmol/L	Millimole/lite
MRs	Mineralocorticode Receptors
MS	Mass Spectrometry
Na^+	Sodium
Na+/Cl− co-transporters	sodium-chloride cotransporters
NAD^+	Nicotinamide adenine dinucleotide
NADP	Nicotinamide adenine dinucleotide phosphate
NANC	Non-noradrenergic non-cholinergic transmitter
NCC	Sodium chloride cotransporter
NEDD4-2	Neural precursor cell-expressed developmentally down-regulated 4-2
NICE	National Institute for Health and Care Excellence
NKCC	Sodium-potassium chloride cotransporter
NMR	Nuclear Magnetic Resonance
nNOS	Neuronal Nitric Oxide Synthase
NO	Nitric Oxide
NOS	Nitric Oxide Synthase
NTCP	Na^+/taurocholate cotransporting polypeptide
NPY	Neuropeptide Y
O_2	Oxygen
$ONOO^-$	Peroxynitrite
PC	Phosphotidylcholine
PCA	Principle Component Analysis
PDK1	Phosphoinositide-dependent protein kinase 1
PECK	Phosphoenolpyruvate carboxykinase
PGE_2	Prostaglandin E_2
PGI_2	Prostacyclin
PHA	Pseudohypoaldosteronism
PHA II	Pseudohypoaldosteronism type II
PKCf	Protein kinase C zeta
PNS	Parasympathetic Nervous System
PP	Pulse pressure
PPARα/RXR	Peroxisome proliferator receptors alpha subunit/ the retinoid X receptor
PWT	Posterior wall thicknesses
PXR	Pregnane X Receptor

qRT-PCR	Quantitative real-time PCR
RAAS	Renin Angiotensin Aldosterone System
RI	Renin Inhibitor
RNA	ribonucleic acid
ROMK	Renal outer medullary potassium channel
ROS	Reactive Oxygen Species
RQ	Relative Quantification
RSP	Ribose-5-Phosphate
S1PR2	Sphingosine- 1-Phosphate Receptor 2
SAH	S- adenosylhomocysteine
SARCKATP	Sarcolemnal adenosine triphosphate-dependent potassium channels
SBP	Systolic Blood Pressure
SDS	Sequence Detection Software
SHP	Small heterodimeric partner
SHR	Spontaneously hypertensive rat
SHRSP	Stroke-prone spontaneously hypertensive rat
SILAC	Stable isotope labeling using amino acids in cell culture
SNS	Sympathetic Nervous System
SREBP	Sterol regulatory element-binding protein
SV	Stroke volume
TAL	Thick ascending limb
TGR	Transgenic rat
TGRS	Takeda G- protein- coupled Receptors
TNF-α	Tumour necrosis factor-α
TXA_2	Thromboxane
U/L	Units per litre
umol/L	Micromole/liter
VIP	Vasoactive intestinal peptide
VLCFAs	Very-long-chain fatty acids
WHO	World Health Organization
WKY	Wistar-Kyoto
α	Alpha
ß	Beta
ω	Omega

Oral presentations, publications, and awards

Abstracts for Poster Presentation

Alharbi, N., McBride, M., Graham, D. and Padmanabhan, S. 26th European Meeting on Hypertension and Cardiovascular Protection, Paris, France, 10-13 June 2016. METABOLOMIC STUDY OF PATHWAYS UNDERLYING HEXADECANEDIOATE INDUCED BLOOD PRESSURE ELEVATION.

Alharbi, N., McBride, M., Graham, D. and Padmanabhan, S. 15th Annual Meeting of the Complex Trait Community in collaboration with the 10th Annual Meeting of Rat Genomics and Models, Memphis, USA, 13-17 June 2017. INVESTIGATING A NOVEL PATHWAY UNDERLYING HEXADECANEDIOATE- INDUCED BLOOD PRESSURE ELEVATION.

Alharbi, N., McBride, M., Graham, D. and Padmanabhan, S. The American Heart Association, San Franciscio, USA, 14-17 Sep 2017. THE OMEGA OXIDATION PATHWAY UNDERLIES HEXADECANEDIOATE INDUCED BLOOD PRESSURE ELEVATION.

Abstracts for Oral Presentation

Alharbi, N., McBride, M., Graham, D. and Padmanabhan, S. Scottish Cardiovascular Forum, Glasgow, UK, 4 Feb 2017. INVESTIGATING A NOVEL PATHWAY UNDERLYING HEXADECANEDIOATE INDUCED BLOOD PRESSURE ELEVATION.

Published Work

Menni, C., Graham, D., Kastenmüller, G., **Alharbi, N**., Alsanosi, S., McBride, M., Mangino, M., Titcombe, P., Shin, S., Psatha, M., Geisendorfer, T., Huber, A., Peters, A., Wang-Sattler, R., Xu, T., Brosnan, M., Trimmer, J., Reichel, C., Mohney, R., Soranzo, N., Edwards, M., Cooper, C., Church, A., Suhre, K., Gieger, C., Dominiczak, A., Spector, T., Padmanabhan, S. and Valdes, A. (2015). Metabolomic Identification of a Novel Pathway of Blood Pressure Regulation Involving HexadecanedioateNovelty and Significance. Hypertension, 66(2), pp.422-429.

Summary

Human hypertension is the biggest contributor to the global burden of cardiovascular disease and it is the most prevalent modifiable risk factor for cardiovascular morbidity and mortality. The causation of hypertension is multifactorial and is related to perturbation in the pathways that regulate blood pressure. The known blood pressure regulating pathways include those that regulate intravascular volume, vascular tone and peripheral vascular resistance through renal, the renin-angiotensin-aldosterone and autonomic systems, which are targets of the commonly used antihypertensive drugs. In the largest investigation of blood pressure using a metabolomics approach, a novel pathway for blood pressure regulation was identified, involving a dicarboxylic acid, hexadecanedioate. Hexadecanedioate is a long chain dicarboxylic acid, which is generated during fatty acid omega-oxidation pathway (ω-oxidation). Higher circulating levels of hexadecanedioate were significantly associated with both high blood pressure and mortality.

This research project aimed to examine the functional role of hexadecanedioate and investigate its underpinning mechanisms in blood pressure regulation using *in*-vivo, *ex*-vivo and metabolomics studies in two animal models; the Wistar Kyoto (WKY) and the Spontaneously Hypertensive Stroke Prone rats (SHRSP).

In the first results chapter (chapter 3), we conducted three independent interventional studies to examine the effects of hexadecanedioate on blood pressure regulation. Circulating levels of hexadecanedioate were significantly increased in WKY rats after treatment with oral hexadecanedioic acid leading to blood pressure elevation and impairment of vascular function in WKY rats. However, hexadecanedioic acid treatment was unable to further increase circulating hexadecanedioate levels or blood pressure in SHRSP rats, indicating that hexadecanedioate levels may already be maximally elevated in the hypertensive model. The data also show an increase in adiposity index despite reduced body weight in SHRSP rats after treatment with hexadecanedioic acid. These results may indicate muscle wasting and altered cellular energy homeostasis such as an impairment of the beta-oxidation pathway (ß-oxidation).

In the second results chapter (chapter 4), a global metabolomics study was carried out in WKY rats to demonstrate the metabolic effect of hexadecanedioic acid treatment in cardiovascular tissues (i.e. heart, kidney, liver, aorta, adipose and brain) in order to identify the metabolic pathways leading to hexadecanedioate-induced blood pressure elevation. Several alterations in metabolic readouts, including changes in metabolites related to lipid and glucose metabolisms, bile acid metabolism, redox homeostasis, and uric acid cycle were observed after hexadecanedioic acid treatment. Hexadecanedioate increased in all tested tissues of hexadecanedioic acid-treated WKY rats except brain, where this metabolite was below the threshold of detection. Our data indicated significant increases in peroxisomal ω-oxidation metabolites (i.e. dicarboxylic fatty acids) along with marked changes in mitochondrial fatty acid β-oxidation metabolites such as phospholipids, lysolipid, sphingolipid, monoacylglycerol and acyl carnitine in all tested tissues. These changes in fatty acid availability indicate that hexadecanedioic acid treatment induced changes in mitochondrial β-oxidation and a shift toward increased use of peroxisomal ω-oxidation.

In the third results chapter (chapter 5), the ω- oxidation pathway was investigated by measuring the expression levels of the different enzymes involved in the pathway (i.e. CYP4A, alcohol dehydrogenase (ADH), and aldehyde dehydrogenase (ALDH)) in two different rat strains; the normotensive WKY and hypertensive SHRSP rat models. The gene expression results show significant reduction in expression of the ALDH isoform, ALDH1L2, in the liver tissues of SHRSP rats compared to WKY. In addition, the levels of ALDH enzyme were measured in the liver tissues using ELISA assay, which showed a trend towards an increase in SHRSP rats compared to WKY rats.

Blood pressure was assessed after modulation of endogenous hexadecanedioate levels by perturbing the ω-oxidation pathway in both WKY and SHRSP by either inhibition or stimulation of enzymes critical to ω-oxidation. Inhibition of the final ω-oxidation pathway enzyme, ALDH by disulfiram resulted in a significant lowering of blood pressure in the hypertensive SHRSP rat. A pilot study was also conducted to examine the effect of HET0016 (CYP4A antagonist) on blood pressure of SHRSP rats, which showed no significant changes. However, stimulation of the ω-oxidation pathway enzyme, CYP4A by fenofibrate caused a significant reduction

of blood pressure in WKY rats, along with significant increase in the CYP4A expression in kidney and liver tissues.

In the final results chapter (chapter 6), an alternative mechanism was examined that may lead to elevated circulating levels of hexadecanedioate via altered activity of the solute carrier organic anion transporter (SLCO), which encodes the protein organic anion transporting polypeptide (OATP). It has been found that the human SLCO1B1 gene is associated with elevated levels of circulating hexadecanedioate. SLCO1B1 may have a role in hexadecanedioate elimination from the body, and any alteration in this liver transporter may cause increases in circulating hexadecanedioate levels leading to blood pressure elevation. A preliminary investigation was performed to identify the sequence variants in the rat homolog, the Slco1b2 gene. Genotype analysis of the $SHRSP_{Gla}$ and WKY_{Gla} genome sequence identified an insertion of 9 nucleotides (GTCTATCTA) within an intronic region (intron 3/14) on chromosome 4 at position 240,062,637 bp, band 4q44 forward strand in the WKY_{Gla} strain rather than a G nucleotide in the $SHRSP_{Gla}$ strain. The deletion of 4 nucleotides (TATC) within the 3'untranslated region (UTR) was also detected on chromosome 4 at position 240,102,755 bp of the WKY_{Gla} genome sequence. Total Slco1b2 mRNA expression was measured in liver tissues of WKY and SHRSP, which showed significantly decreased levels in SHRSP compared to WKY. These genetic variants within the Slco1b2 gene may contribute to altered function of the Oatp1b2 transporter, which may in turn contribute to elevated levels of circulating hexadecanedioate in the SHRSP rat model of hypertension.

In summary, we have investigated the functional role of hexadecandioate in blood pressure regulation. The findings presented in this thesis demonstrate novel targets associated with hexadecandioate; including the ω-oxidation pathway and the solute carrier organic anion mechanism in regulation of blood pressure.

Chapter 1 Introduction

1.1 Cardiovascular disease

Cardiovascular disease (CVD) is a complex set of disorders, involving pathological changes in heart, blood vessels, kidneys and brain; including hypertension, angina, stroke, coronary heart disease, myocardial infractions, renal diseases and metabolic syndromes (Nichols *et al.*, 2014). According to the World Health Organization (WHO), cardiovascular disease is the number one cause of worldwide deaths, accounting for 30% (17.7 million people) of total global deaths in 2015 (World Health Organization, 2018). Cardiovascular disease is the main cause of mortality burden in European countries (51% of deaths among women and 42% among men), which is considered a greater risk for mortality than cancer (19% of deaths among women and 23% among men) (Nichols *et al.*, 2014). The main CVD disorders representing the common cause of death are coronary heart disease (7.4 million) and stroke (6.7 million) (World Health Organization, 2018). The most important risk factors identified for developing of CVD are divided into controllable risk factors, including smoking, poor diet, high alcohol consumption, high blood cholesterol, high blood pressure, lack of exercise, obesity, and diabetes (Saeidi *et al.*, 2015; Mozaffarian *et al.*, 2015). Additionally, there are major non controllable risk factors that include ethnicity (George *et al.*, 2017), age, sex, family history and genetics (Mozaffarian *et al.*, 2015). Two types of interventions are used to reduce the burden of CVD. The cost effective primary intervention, includes control of smoking and alcohol, reducing the intake of foods that are high in fat, sugar and salt and increased physical activity (Piepoli *et al.*, 2016, 2014). Secondary prevention of cardiovascular disease includes use of medications such as antiplatelet therapy (aspirin), blood pressure-lowering agents (i.e. beta-blockers and angiotensin-converting enzyme inhibitors), where a systolic BP ≥140 mm Hg and lipid-lowering agents (statins) where low-density lipoprotein (LDL) cholesterol ≥2.5 mmol/L (Bansilal *et al.*, 2015). In addition, there are more expensive surgical interventions that include coronary artery bypass (Kulik *et al.*, 2015), balloon angioplasty (Matsuzawa *et al.*, 2015) and valve repair and replacement (Acker *et al.*, 2014).

1.2 Blood pressure: definition

Blood circulates in the arteries and veins, and carries essential substances such as oxygen, nutrients and hormones to cells, tissues and organs, also transports the waste products such as carbon dioxide away from those cells, tissues and organs. The pressure of the blood against the inner walls of the blood vessels is called blood pressure. Blood pressure is measured in millimetres of mercury (mmHg) and recorded as a fraction with the maximum pressure (systolic) representing the peak pressure during heart contraction over the minimum pressure (diastolic) that represents the pressure during heart relaxation. Blood pressure is categorised into pulsatile (pulse arterial pressure) and steady components (mean arterial pressure), which are considered to be important predictor of cardiovascular disease.(Haider *et al.*, 2003; Sesso *et al.*, 2000). Pulse pressure is the difference between systolic and diastolic blood pressure, which is associated with vessel stiffness, left ventricular ejection fraction, development of large-vessel atherosclerosis and small-vessel disease (Haider *et al.*, 2003; Sesso *et al.*, 2000). Mean arterial pressure (MAP) is a function of left ventricular contractility, heart rate, and vascular resistance (Haider *et al.*, 2003; Sesso *et al.*, 2000). The main factors of diastolic blood pressure (DBP) are the mean circulatory filling pressure, total peripheral vascular resistance and the interval between heart beats (Ackermann, 2004). Mean arterial blood pressure is the average pressure, which is calculated from diastolic and pulse pressure values using the following formula (Ackermann, 2004):

Mean arterial blood pressure = diastolic pressure +1/3 pulse pressure

The normal value of mean arterial blood pressure is about 100 mmHg. Small variations from this value occur regularly during daily life, but compensatory mechanisms control the pressure within a normal range (Ackermann, 2004). Normal blood pressure readings are <120 mmHg systolic and <80 mmHg diastolic, although there is some variability between normal healthy people (O'Shea *et al.*, 2017).

1.3 Physiological blood pressure regulation

Blood pressure refers to the pressure imposed by circulating blood on the walls of blood vessels. It is a quantitative feature, which is variable between individuals, and it is mainly determined by cardiac output and total peripheral resistance. Cardiac output and total peripheral resistance are controlled by homeostatic regulatory mechanisms, which are a complex system of cooperating physiological pathways, including neural, hormonal, vascular and renal mechanisms to regulate blood pressure (Taylor and Abdel-Rahman, 2009). Three cardiovascular factors are involved in blood pressure regulation, including total peripheral vascular resistance, stroke volume and heart rate (Ackermann, 2004). The first of these, peripheral vascular resistance regulation, is specified by the luminal diameter of arterioles, which is determined by the degree of constriction of vascular smooth muscles cells around the arterioles (Ackermann, 2004; Martinez-Lemus, 2012). The vascular smooth muscles cells are regulated by vasodilation factors (e.g. nitric oxide) and by vasoconstrictor factors (e.g. sympathetic nervous system activity), as well as vasoconstrictor substances, for example angiotensin II, adrenaline and vasopressin (Brozovich *et al.*, 2016; Ackermann, 2004). Overall regulation of total peripheral vascular resistance is accomplished via sympathatic vasoconstriction, as well as stroke volume regulation, which is determined by cardiac performance via heart contractility, preload (initial stretching of the cardiac myocytes prior to contraction), afterload (the pressure against which the heart must work to eject blood) and heart rate (Ackermann, 2004; Poole and Erickson, 2014). Heart rate is regulated by generation of action potentials in dominant pacemaker cells in the heart, enhanced by cardiac sympathatic nervous activity (positive chronotropic) and is reduced by cardiac parasympathetic nervous activities (negative chronotropic) (Ackermann, 2004; Gordan *et al.*, 2015) (Figure 1-1).

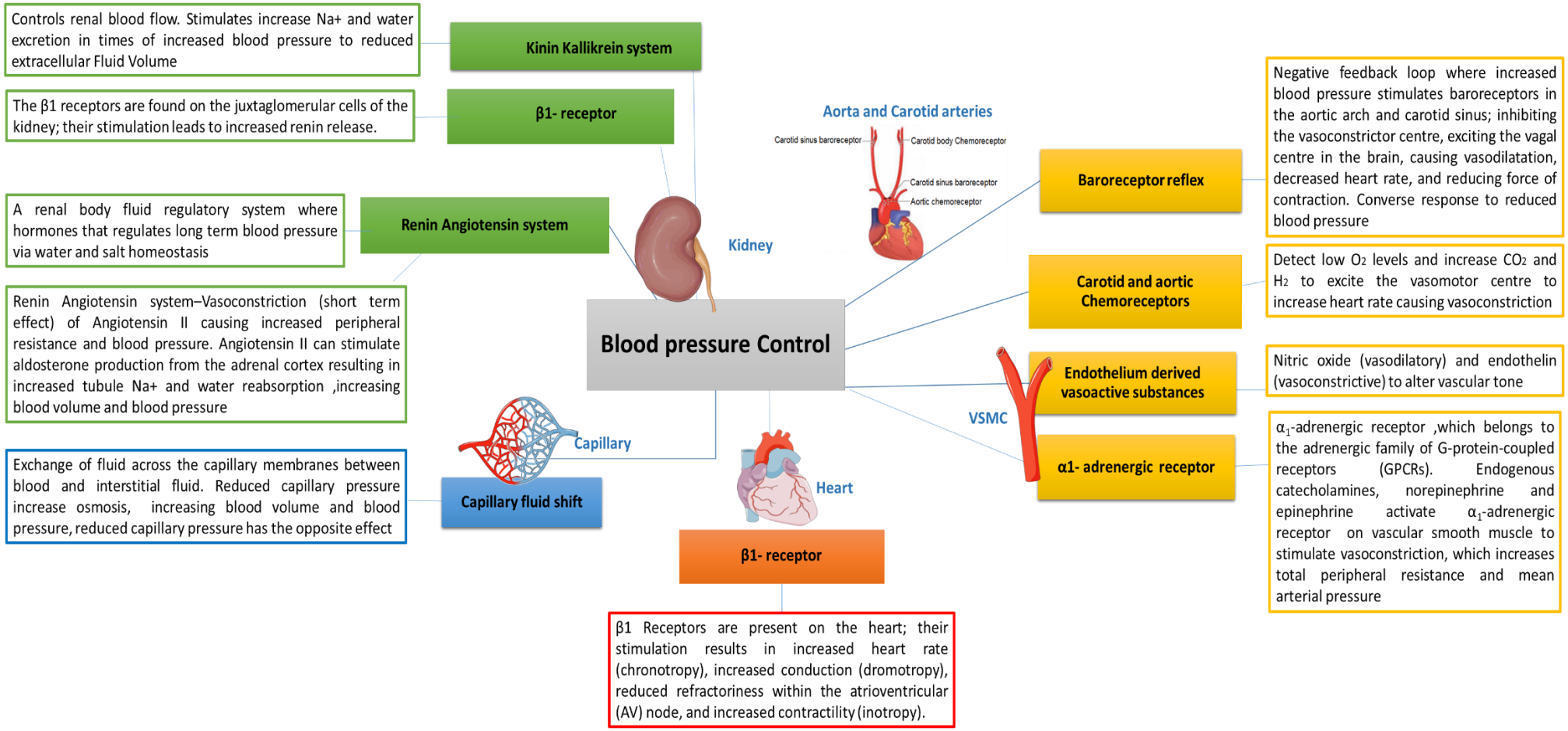

Figure 1-1: Schematic diagram showing physiological factors that regulate blood pressure.

Abbreviation: Na^+, Sodium; β1- receptor, Beta 1- receptor; α1- adrenargic receptor, Alpha 1-adrenargic receptor; O_2, Oxygen; CO_2, Carbon dioxide; H_2, Hydrogen; GPCRs, G-protein-coupled receptors.

1.3.1 Role of the central nervous system in blood pressure regulation

Two types of autonomic nervous system have an essential role in controlling cardiovascular functions; there are the sympathatic nervous system (SNS) and the parasympathatic nervous system (PNS). Both nervous systems mainly regulate heart rate, physical activity, the sleep/awake phase and the emotional state of the individual. In addition, PNS has a minor role in vascular resistance regulation (Taylor and Abdel-Rahman, 2009). The central nervous system (CNS) plays an important role in short-term and long-term regulation of blood pressure (Taylor and Abdel-Rahman, 2009). In the short-term (seconds to hours), the autonomic nervous system regulates the circulation compatible with behaviour (i.e. exercise), the environment (i.e. thermoregulation) and emotions (i.e. fright and shock) (Guyenet, 2006).

Baroreceptors are the only identified neural sensor that regulate blood pressure, and have a dominant role in short-term blood pressure regulation. However, their impact on the long-term regulation of blood pressure is less well understood (Guyenet, 2006). An elevation in arterial blood pressure occurs as a consequence of baroreceptor stimulation, which send nerve impulses to the medullary vasomotor centres and causes central inhibition of sympathetic tone and a rise in parasympathetic tone. In contrast, a reduction in arterial pressure causes baroreceptor reflex-mediated withdrawal of vagal tone and sympathetic activation, leading to cardiac acceleration, improved myocardial performance, and decreased arterial resistance (Marr and Reimer, 2009).

The autonomic nervous system also regulates both vascular resistance and cardiac output, which consequently regulates blood pressure. Cardiac output is dependent on end-diastolic volume, myocardial contractility and heart rate. End-diastolic volume is the volume of blood achieved by the ventricular chamber before contraction and the beginning of filling, which is related to venous smooth muscle tone and blood volume, both are under sympathetic control. Furthermore, myocardial contractility and heart rate are controlled by both the sympathetic and parasympathetic autonomic nervous system (Guyenet, 2006). The definitive consequences of increased activity of the sympathatic nervous system are an increase in heart rate and heart contractility due to activation of beta 1 receptor

(β1 receptor), and a rise in vascular resistance due to activation of alpha 1 receptor (α1 receptors) (Ackermann, 2004) (Figure 1-1).

The vascular system is mainly innervated by sympathetic adrenergic nerves that release noradrenaline as a neurotransmitter. However, some blood vessels are innervated by either parasympathetic cholinergic or sympathetic cholinergic nerves. Both of them release acetylcholine as their neurotransmitter. These neurotransmitters bind to the adrenergic and cholinergic receptors, which activate signal transduction pathways causing changes in vascular function (Taylor and Abdel-Rahman, 2009). Vascular smooth muscle are usually innervated by sympathetic vasodilating innervation, while there is no parasympathetic innervation to the vascular smooth muscle. Sympathetic vasodilating innervation to the skeletal muscle vasculature in certain vascular beds is mediated by the release of acetylcholine from these sympathetic nerve terminals. Circulating acetylcholine can contribute to vascular resistance by two mechanisms. Firstly, acetylcholine stimulation of presynaptic cholinergic nicotinic receptors on noradrenergic nerve terminals lead to increase noradrenaline release. Inversely, acetylcholine stimulation of presynaptic muscarinic receptors cause inhibition of noradrenaline release from noradrenergic nerve terminals. Secondly, stimulation of muscarinic cholinergic receptors on endothelial cells increases nitric oxide (NO) release. These different effects of cholinergic modulation of noradrenaline and NO release contribute differentially to vascular tone control (Taylor and Abdel-Rahman, 2009).

A non-noradrenergic, non-cholinergic transmitter (NANC) is also known as a neurotransmitter of the autonomic nervous system besides two main transmitters (i.e. noradrenaline and acetylcholine). The transmitters for NANC include purine bodies (ATP), neuropeptide (e.g. neuropeptide Y (NPY), vasoactive intestinal peptide (VIP), gonadotropin-releasing hormone (GnRH), substance P), and nitric oxide. These transmitters are co-released with noradrenaline and acetylcholine as the neurotransmitters to control the vascular tone and contraction or relaxation of smooth muscle cells (Uno and Hisa, 2016).

The sympathetic nervous system also has a role in stimulation of the chromaffin cells in the adrenal medulla to release epinephrine, as well as simulating renal juxtaglomerular cells to release renin, and peripheral synapses to release

noradrenaline, located in cardiac muscle cells and the vascular smooth muscles that surround the blood vessels.(Ackermann, 2004; Bakris and Mensah, 2003; Singh *et al.*, 2010).

1.3.2 Role of kidney in blood pressure regulation

The kidney has an important role in regulation of blood pressure through adjusting electrolyte balance, salt and water homeostasis and the total fluid volume as well as through its role in the renin angiotensin aldosterone system (RAAS) (Ko and Bakris, 2008). RAAS is considered to be a major hormonal system, which controls functions of the cardiovascular and renal systems, as well as the adrenal glands by regulating blood pressure, fluid volume, fluid homeostasis and electrolytes (i.e. sodium and potassium) balance, and also is known to be involved in hypertension pathophysiology (Pacurari *et al.*, 2014; Te Riet *et al.*, 2015). Renin is released from juxtaglomerular cells in the media layer of the afferent glomerular arterioles of the kidney into the circulation (Friis *et al.*, 2013). Renin expression and secretion are regulated at the juxtaglomerular cell by three different mechanisms: intrarenal baroreceptors of the afferent arteriole, the influence of sympathetic nerves on the arterioles of the juxtaglomerular apparatus and alterations in the delivery of sodium chloride to the macula densa cells (Sparks *et al.*, 2014; Friis *et al.*, 2013; Harrison-bernard, 2009).

The first mechanism, via renal baroreceptors, is an independent mechanism for renin regulation. Intrarenal baroreceptors act as high-pressure baroreceptors, which are able to detect any change in blood pressure. An elevation of renal arterial pressure inhibits renin release, whereas reductions in renal arterial pressure and calcium concentration lead to enhanced release of renin from the juxtaglomerular apparatus (Chapleau, 2012; Harrison-bernard, 2009; Sparks *et al.*, 2014; Friis *et al.*, 2013). Secondly, renin release is increased by activation of sympathetic nerves and ß-adrenergic receptors (Harrison-bernard, 2009).Thirdly, increased distal delivery of sodium chloride to the macula densa of the thick ascending limb of the loop of Henle leads to reduction in renin secretion and vice versa (Harrison-bernard, 2009). Increase in release of cyclooxygenase 2 in the macula densa cells leads to increased prostaglandin E_2 (PGE_2) production and PGE_2 receptor activation causing stimulation of adenylyl cyclase, and subsequently increases in the second messenger for renin secretion cyclic adenosine monophosphate (cAMP).

Increased renin secretion results in an increase in the level of the potent vasoconstrictor Angotensin II, which results in increased blood pressure (Harrison-

bernard, 2009). Angiotensin II (Ang II) is produced from angiotensin I (Ang I), by angiotensin converting enzyme (ACE) that is mainly expressed by the lungs. Angiotensin (AngIII) is then generated from Ang II (precursor) via aminopeptidase A (APA), which has been shown to be involved in central control of blood pressure (Taylor and Abdel-Rahman, 2009) (Figure 1-2). This mechanism is essential for systemic arterial pressure regulation as well as tissue perfusion through reduced vascular volume (Harrison-bernard, 2009).

Ang II has a range of actions on different vascular and organ systems. It increases peripheral resistance and blood pressure by vasoconstriction of renal and systemic arterioles. In addition, Ang II causes an increase of arginine and vasopressin release from the posterior pituitary gland leading to increases in fluid retention in the renal collecting duct of the kidneys in order to maintain blood volume (Harrison-bernard, 2009). Ang II is released in response to blood pressure changes through circulatory depression, blood volume depletion or sodium depletion. It enhances sodium reabsorption through activation of aldosterone secretions, this results in hemodynamic effects and epithelial transport. Constriction of efferent arterioles is mediated by angiotensin II, causing reduction of renal blood flow, hydrostatic pressure of peritubular capillary and elevating osmotic pressure of peritubular colloid. Ang II activates exchange of Na+/H+ and enhances Na+/ K+ adenosine triphosphatase (ATPase) activity in proximal renal tubules (Harrison-bernard, 2009). Ang II also activates angotensin II type 1 receptors (AT1R), leading to aldosterone release from the adrenal cortex and increase reabsorption of sodium chloride and fluid in the distal nephron to increase extracellular fluid volume (Harrison-bernard, 2009). Aldosterone is a sodium retaining hormone, which affects blood pressure regulation by increasing renal reabsorption of sodium in the collecting ducts, distal tubules and cortical collecting tubules. Aldosterone works by binding to intracellular mineralocorticoid receptors (MRs), leading to activation of Na+/K+ ATPase pump at the basolateral epithelial membrane and stimulation of amiloride-sensitive sodium channels at the luminal epithelial membrane (Hall *et al.*, 2013).

In the brain, sympathoexcitatory effects are produced by Ang II, while intracerebroventricular action of Ang II and Ang III cause identical increases in blood pressure and identical agonist activation of central AT1R receptors (Figure 1-2). Thus, the RAAS acts to produce a balancing effect on vascular resistance

resulting in blood pressure homeostasis. However, impaired AT1R signalling due to imbalanced effects causes hypertension known as high-renin hypertension (Taylor and Abdel-Rahman, 2009).

An alternative pathway for blood pressure regulation by Ang II is via angotensin II type 2 receptor (AT2R) (Mas receptors) and other angiotensin fragments (i.e. Ang1–7). The roles of Ang1–7 and AT2R receptors in blood pressure regulation and in the pathophysiology of hypertension have recently been identified. Activation of AT2R receptors by Ang II and Ang1-7 results in vasodilation and reduction of vascular resistance. Stimulation of Mas receptors via Ang1-7 results in increased of bradykinin–nitric oxide release, anti-proliferation, natriuresis and vasodilation. Ang1-7 reduces blood pressure by central and peripheral mechanisms that involve nitric oxide and bradykinin, generating antifibrotic and antihypertrophic effects (Taylor and Abdel-Rahman, 2009; Carey *et al.*, 2001; Singh and Karnik, 2016).

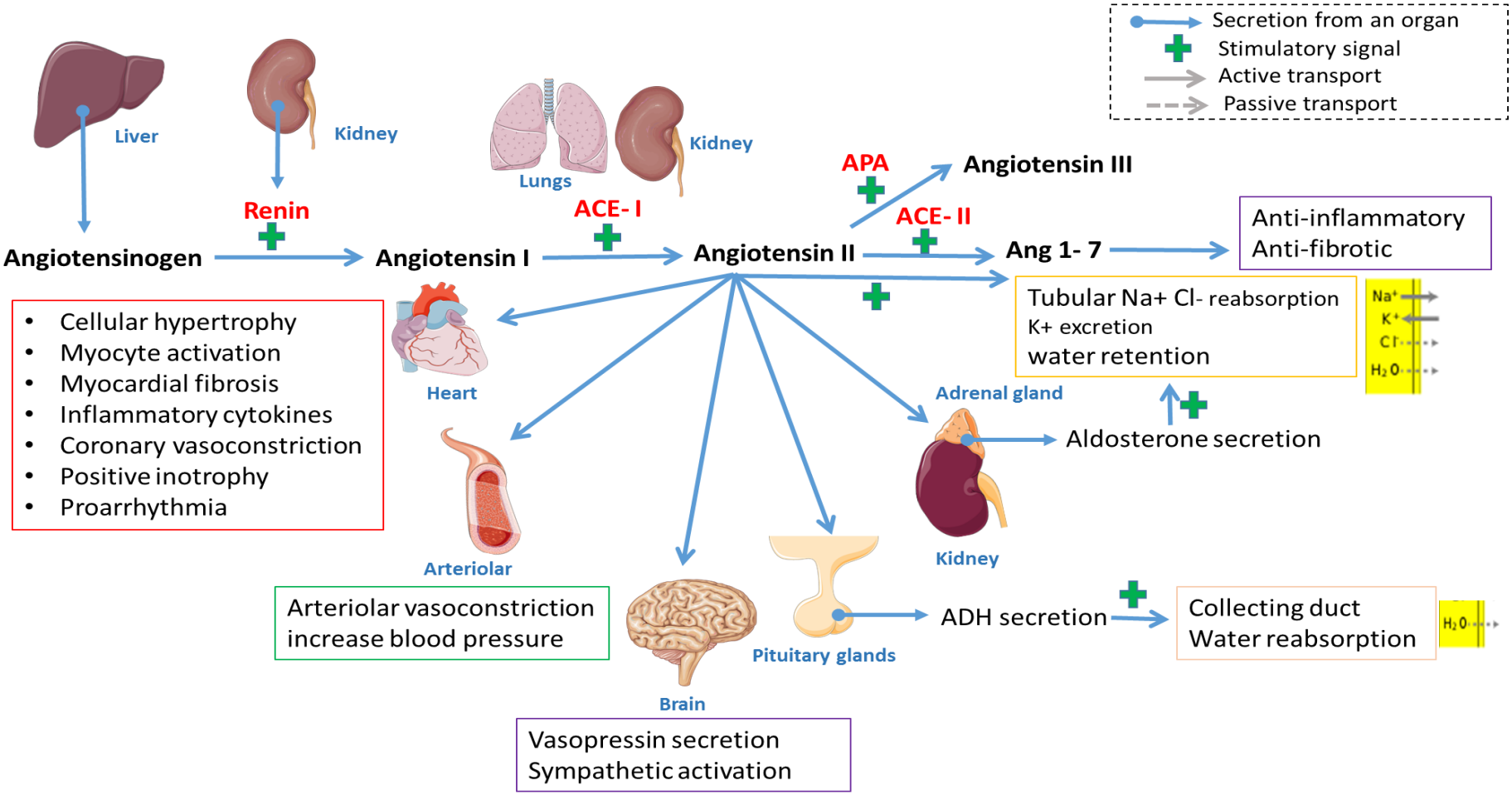

Figure 1-2: Renin-angotensin-aldestrone system.

Abbreviation: ACE, Angiotensin Converting Enzyme; APA, aminopeptidase A; Na^+, Sodium; Cl^-, Chloride; K^+, Potassium; H_2O, Water; ADH, antidiuretic hormone.

1.3.3 Role of Endothelium in blood pressure regulation

The endothelium plays an important role in the regulation of vascular tone via release of vasoactive factors, such as nitric oxide (NO), prostacyclin (PGI_2) and endothelium derived hyperpolarizing factor (EDHF) or vasoconstrictive factors such as thromboxane (TXA_2) and endothelin-1 (ET-1) (Taylor and Abdel-Rahman, 2009). NO is an endothelium-dependent vasodilator of the smooth muscle, which is produced from L- arginine by nitric oxide synthase (NOS) enzymes. Three isoforms of NOS, includes neuronal isoform (nNOS), which yields NO to act as a neuronal messenger that controls synaptic neurotransmitter release. Inducible isoform (iNOS), which is only expressed in cells that have been exposed to inflammatory mediators or damage activated macrophages, and endothelial NOS (eNOS), which produces nitric oxide in the vasculature (Hall *et al.*, 2013).

NO is released from renal tubular cells and vascular endothelial cells, which maintain blood pressure regulation through vasodilatation via an increase in the production of intracellular cyclic GMP in vascular smooth muscle cells (Taylor and Abdel-Rahman, 2009). Long-term blockade of nitric oxide synthase reduces renal pressure natriuresis and hypertension. Also, a decrease of nitric oxide synthesis leads to an increase in Na+ reabsorption and alteration of renal interstitial hydrostatic pressure (Hall *et al.*, 2013). eNOS couples with tetrahydrobiopterin (BH4) and caveolin to maintain the enzyme activities within the physiological limit, while uncoupling leads to formation of superoxide and reactive oxygen species that impair the function and structure of cardiac and vascular smooth muscles and elevation in peripheral resistance leading to hypertension (Köhler *et al.*, 2001; Taylor and Abdel-Rahman, 2009). Reactive oxygen species (ROS) may play a role in the development of cardiovascular diseases related to high blood pressure. ROS are formed from nicotinamide adenine dinucleotide phosphate (NADPH) oxidases, which generate superoxide and cause uncoupling of endothelial nitric oxide synthases. There are four types of NADPH oxidase (Nox enzymes), which are considered main sources of reactive oxygen species; these are Nox1, Nox2, Nox4, and Nox5. Elevation of renal oxidative stress causes renal vascular resistance, reduction of glomerular filtration rate, decreasing the excretion of sodium via an increase of renal tubular reabsorption leading to impaired renal pressure natriuresis (Hall *et al.*, 2013).

The synergistic actions of prostacyclin (PGI_2) and thromboxane (TXA_2) also regulate vascular function. Their production is catalyzed by cyclooxygenase (COX) enzymes, which are classified into two isoforms COX-1 and COX-2. COX-1 is expressed in endothelial cells, whereas COX-2 is only expressed when the endothelium is damaged and exposed to inflammatory cytokines (Hall *et al.*, 2013). COX-2 converts arachidonic acid to prostaglandin H_2, which is then synthesized into PGI_2 by prostacyclin synthase. PGI_2 binds to the prostacyclin receptors (IP), which are located on vascular smooth muscle cells, which activates adenylate cyclase that induces cyclic adenosine monophosphate (cAMP) synthesis. cAMP then activates protein kinase A, which allows relaxation of the smooth muscle (Sandoo *et al.*, 2010).

Endothelium-derived hyperpolarizing factor (EDHF) is a substance or electrical signal, which hyperpolarizes the smooth muscle to generate the membrane potential of the vascular smooth muscle cell, causing vasodilation. The identity of EDHF is still unknown. Indeed, NO and PGI_2 can also dilate the vessel by hyperpolarizing the smooth muscle cells but for a short period (Sandoo *et al.*, 2010; Hall *et al.*, 2013).

Endothelin (ET) is a vasoconstrictor, which is expressed in the body in three isoforms, ET-1, ET-2, and ET-3. ET-1 causes potent vasoconstriction, which stimulates ETA receptors, leading to hypertension, systemic and renal vasoconstriction and impaired renal pressure natriuresis (Hall *et al.*, 2013). ET-1 receptors have been identified on smooth muscle cells; are ET_A and ET_{-B2}, also ET_{-B1} on endothelial cells. Regulation of ET-1 production is stimulated by inflammatory cells; such as interleukins and TNF-α and decreased by NO and PGI_2 (Sandoo *et al.*, 2010). ET-1 binds to ET_A or ET_{-B2} receptors, which cause smooth muscle Ca^{2+} channels to open allowing extracellular Ca^{2+} into the cell. This causes vasoconstriction of smooth muscle cells. ET_{-B1} receptors on the endothelial cells are downregulated, though ET_{-B2} receptors on smooth muscle cells are upregulated, therefore enhancing vasoconstriction (Hall *et al.*, 2013; Sandoo *et al.*, 2010).

1.4 Human essential hypertension

Hypertension is considered a main risk factor for CVD and mortality and is characterised by chronically increased arterial blood pressure (Carretero and Oparil, 2000). The Sixth Report of the Joint National Committee on Prevention, Detection, Evaluation, and Treatment of High Blood Pressure (JNC VI) previously classified hypertension in adults (Chobanian *et al.*, 2003) and has been recently updated to be comprehensive and incorporates new information from studies regarding blood pressure related risk of CVD, and blood pressure thresholds to initiate antihypertensive drug treatment (Whelton and Carey, 2018), as shown in Figure 1-3. Human hypertension is diagnosed when a systolic blood pressure (SBP) is ≥140 mm Hg and a diastolic blood pressure (DBP) is ≥90 mm Hg (Muntner *et al.*, 2014).

Essential hypertension accounts for approximately 90-95% of all hypertension cases, however around 5-10% of hypertension cases are caused by identifiable secondary pathological conditions; such as renal vascular hypertension, primary hyperaldosteronism, cushing's syndrome, pheochromocytoma and gestational hypertension (Carretero and Oparil, 2000). Essential or primary hypertension is a multi-factorial disease involving major contribution from both genes and environmental factors (Carretero and Oparil, 2000). Several risk factors underlying essential hypertension have also been identified including age, sex, genetics and demographic factors (Ruppert and Maisch, 2003). Thirty to fifty percent of genetic elements found to contribute to hypertension. Genetic variations can affect hypertension genesis, which demonstrates risk factor for development of stroke, ischemic heart disease, peripheral vascular disease and renal damage (Larsson *et al.*, 2013). Genome wide association studies (GWAS) have identified more than 100 loci associated with blood pressure (Russo *et al.*, 2018). A number of candidate genes have been identified, including those coding for components of renin angiotensin system, sodium epithelial channels, catecholaminergic/adrenergic function, lipoprotein metabolism, hormone receptors and growth factors (Pintérová *et al.*, 2011).

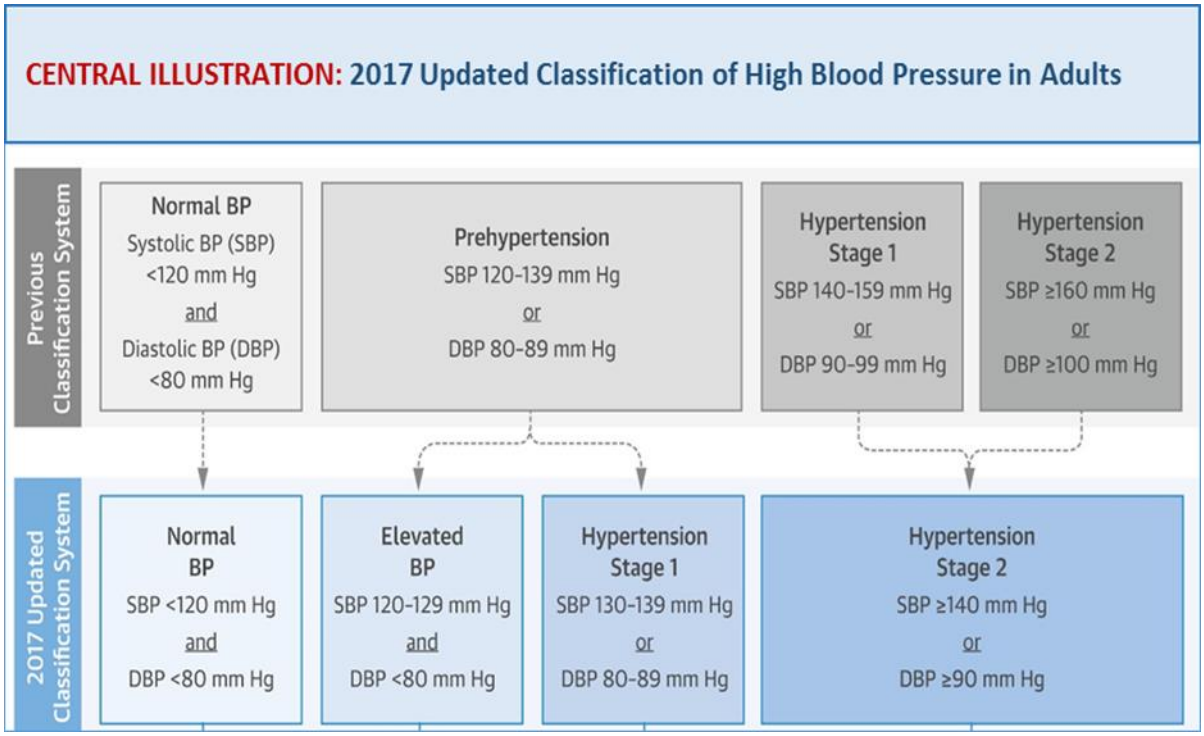

Figure 1-3: Hypertension classifications, adapted from (Whelton and Carey, 2018).

1.4.1 Hypertension prevalence

Hypertension is predominant within the population; affecting 40% of adults aged 25 years and older in 2008. The prevalence of uncontrolled hypertension increased in the population from 600 million in 1980 to nearly 1 billion in 2008. In addition, it caused 7.5 million deaths around the world and 57 million disability adjusted life years (DALYS) (World Health Organization, 2018).

The prevalence of Hypertension is highest in Africa with 46% for both sexes. However, the Americas had the lowest prevalence of hypertension with 35%, where men have higher prevalence than women (39% for men and 32% for women). These differences in blood pressure between sex were also statistically significant in Europe (World Health Organization, 2018).

The 2018 WHO statistical report revealed that low and middle income countries had highest prevalence of hypertension at around 40%. However, the prevalence in high-income countries was lower, at 35% (World Health Organization, 2018).

1.4.2 Hypertension risk factors

Hypertension risk factors are classified into modifiable risk factors such as weight, smoking, high alcohol intake, diabetes, insulin resistance, low physical activity, stress/depression, caffeine intake, low potassium intake, low calcium intake, vitamin D deficiency and high salt intake and unmodifiable risk factors such age, sex, ethnicity and family history (Cohen, 2009; Gong *et al.*, 2014).

1.4.2.1 Environmental risk factors

It is been identified that environmental risk factors account for approximately 80% of hypertension prevalence (Beilin, 2004). Epidemiologic studies show that 10–20 mmHg of the average systolic blood pressure levels among Western population in adolescence ages can be attributed to many life style factors; obesity, low physical activity, high alcohol intake, unbalanced diet containing high salt, saturated fat and sugar, and low in fruit and vegetables (Beilin, 2004). It has been found obesity is associated with increased prevalence of cardiovascular risks including hypertension worldwide (Rahmouni, 2014). A strong association has been observed between increased body mass index (BMI) and systolic/diastolic blood pressures (Timpson *et al.*, 2009). This might be due to the underlying mechanisms of increased tubular sodium reabsorption in obese patients with hypertension; including increased renal interstitial pressure of the kidneys by retroperitoneal visceral and renal sinus fat, thus reducing tubular and medullary blood flow and increasing sodium reabsorption in the loop of Henle. Also, stimulation of the RAAS system promotes sodium/fluid retention through increased renal tubular sodium reabsorption. Increased angiotensin II and aldosterone levels activate vascular production of reactive oxygen species by NADPH oxidase resulting in oxidative stress in obese individuals. In addition, increased activity of mineralocorticoid receptors (MRs) by leptin, which is a 167 amino acid hormone released by adipose tissue, plays an important role in energy expenditure and storage. Leptin contributes to the progression of hypertension in obese individuals through activation of sympathetic nervous system by modulation of the brain melanocortin system and increases peripheral vascular resistance by activation of arterial MRs (Samson *et al.*, 2017). Furthermore, obesity leads to insulin resistance, a condition where cells fail to response to normal insulin, which is also associated with elevated blood pressure through reduction of tyrosine kinase activity in

adipocytes. It is also associated with increased insulin secretion and the production of inflammatory biomarkers such as leptin, Interleukin-1 (IL-1), Interleukin-6 (IL-6), tumour necrosis factor-α (TNF-α), which lead to dysregulation of carbohydrate and lipid metabolism (D'Elia and Strazzullo, 2018) (Figure 1-4). Previous clinical and animal studies have determined that weight gain can increase arterial pressure, however weight loss has a beneficial effect on controlling of blood pressure (Weisbrod *et al.*, 2013; Haufe *et al.*, 2012; De Ciuceis *et al.*, 2011). Lifestyle modifications are mostly recommended as the first line of hypertension treatment (non-pharmacologic therapy) to help weight loss (Rahmouni, 2014) (Figure 1-3).

1.4.3 Salt sensitivity

Sodium is an important nutrient in the body, which is essential for nerves and muscles to function correctly and is involved in the regulation of the water homeostasis (Ha, 2014). However, high dietary salt intake is a challenge to the kidneys requiring eliminating of large amounts of salt administered, and excessive sodium intake predisposes to hypertension and cardiovascular diseases (Ha, 2014; Choi *et al.*, 2015; Stanhewicz and Kenney, 2015). A large international epidemiologic study of salt and blood pressure (INTERSALT) examined the association between urinary sodium excretion level and blood pressure. Results of the study showed a significant association between excessive salt intake and hypertension (Ha, 2014). The World Health Organization (WHO) strongly recommend restricting dietary salt intake to less than 5 g/day as one of the top priority actions to lower rate of hypertension and cardiovascular diseases prevalence and reduce approximately 2.5 million deaths per year (World Health Organization, 2018). Currently, salt intake remains high because of highly salted processed foods (Frisoli *et al.*, 2012).

However, blood pressure responses to dietary salt intake can differ either between hypertensive patients or between normotensive individuals. Some individuals can efficiently eliminate high dietary salt intake without an increase in blood pressure, who are considered salt insensitive. However, salt sensitive individuals are unable to excrete high salt intake leading to an increase in blood pressure (Choi *et al.*, 2015). The mechanisms underlying hypertension associated with salt-sensitivity have not been clearly identified (Stanhewicz and Kenney, 2015). The possible

mechanisms relating to salt induced hypertension involve an impairment in the ability of the kidneys to excrete sodium by inhibition of the sodium pump, which causes increased intracellular sodium, low potassium levels and drives calcium into cells leading to vascular smooth muscle contraction, increased blood volume and increased peripheral vascular resistance (Frisoli *et al.*, 2012). The effects of a high-salt diet are related to the function of the RAAS, whereby high-salt diet suppresses angiotensin II level through physiological blood pressure level control mechanisms (Drenjacnevic-Peric *et al.*, 2011). Also, there is an association between the level of angiotensin II and an increase in the production of reactive oxygen species, which leads to decreased nitric oxide bioavailability, and impairment of endothelium-dependent relaxation to acetylcoline in salt-sensitive hypertensive rats (Zhou *et al.*, 2006, 2003). Early studies by Bragulat *et al.* identified impairment of endothelium-derived nitric oxide system and acetylcholine-induced vasodilation in salt-resistant hypertensive individuals due to impairment of the L-arginine– nitric oxide pathway (Bragulat *et al.*, 2001).

1.4.4 Genetic risk factors

Twin studies and nuclear family studies have identified significant variances in systolic blood pressure (SBP) and diastolic blood pressure (DBP) due to genetic effects that contribute 30–50% of heritability of blood pressure (Tarnoki *et al.*, 2014). A previous study evaluated familial aggregation of blood pressure and found that the relative risks of hypertension are 4.1 times in men and 5 times in women aged 20–39 who had two first-degree relatives affected by hypertension (Hunt *et al.*, 1986). The early adoption study identified significant correlations in blood pressure between biological parent and siblings than parent and adopted siblings (Mongeau *et al.*, 1986). Furthermore, the Victorian family Heart study showed correlations are more likely between hypertension and identical twins (monozygotic) than non-identical twin (dizygous) twins and non-twin siblings (Harrap *et al.*, 2000). The identification of genetic mechanisms involved in hypertension is challenging due to many genes each with mild effects responding to different environmental stimuli contributing to blood pressure (Tarnoki *et al.*, 2014).

1.4.4.1 Mendelian forms of inheritance

A number of monogenic or Mendelian forms of hypertension have been identified by positional cloning using large family pedigrees, showing an inheritance pattern (Padmanabhan *et al.*, 2018). Rare mutations affect a range of genes involved in common pathways of hypertension including increased distal tubular re-absorption of sodium and chloride and volume expansion that suppresses plasma renin activity (Padmanabhan *et al.*, 2018; Luft, 2003).

1.4.4.2 Glucocorticoid- Remediable Aldosteronism or Familial Hyperaldosteronism Type 1

Glucocorticoid-remediable aldosteronism is an autosomal dominant disorder characterised by an early onset of hypertension with normal or elevated aldosterone levels despite lower or suppressed renin activity and hypokalemia (McMahon and Dluhy, 2004). This is caused by a chimeric gene fusing nucleotide sequence between two closely related aldosterone steroid biosynthesis genes; the 5′ regulatory sequences of 11ß-hydroxylase (CYP11B1) that is fused with the distal coding sequences of aldosterone synthase (CYP11B2). This leads to aldosterone synthase being expressed in the adrenal gland under the regulation of adrenocorticotropic hormone (ACTH) rather than angiotensin II as the main regulator of aldosterone secretions. Aldosterone secretions become linked to cortisol secretions leading to increased volume expansion, metabolic alkalosis with hypokalemia, low renin, high aldosterone, and hypertension (Toka, 2018; McMahon and Dluhy, 2004).

1.4.4.3 Apparent Mineralocorticoid excess

Apparent mineralocorticoid excess (AME) is an autosomal recessive disorder characterised by early onset hypertension with hypokalaemia, metabolic alkalosis, low plasma renin activity, aldosterone concentration and responsiveness to spironolactone. This is due to the impaired activity of the enzyme 11ß-hydroxysteroid dehydrogenase Type 2 (HSD11ß2). The normal function of HSD11ß2 is converting cortisol into its inactive metabolites to prevent cortisol from binding to the mineralocorticoid receptor. Activation of the mineralocorticoid receptor results in aldosterone like effect, sodium and water retention, volume expansion, low renin, low aldosterone, and hypertension (Toka, 2018; Funder, 2017).

1.4.4.4 Liddle Syndrome

Liddle syndrome is an autosomal dominant disorder with early onset of hypertension. This condition occurs due to mutations in the genes coding the ß or γ subunits of epithelial sodium channel (ENaC) by deletions of proline-rich regions, which are essential for binding of Nedd4-2 (neural precursor cell-expressed developmentally down-regulated 4-2) as a regulatory repressor that promotes ENaC degradation. Disruption of the ß and γ subunits ability to bind Nedd4 leads to increase epithelial sodium channels, increased ENaC activity at the renal distal tubule apical cell surface, resulting in increased sodium reabsorption, hypokalemia alkalosis, suppressed plasma renin activity, and low plasma aldosterone levels and hypertension (Toka, 2018).

1.4.4.5 Hypertension brachydactyly syndrome

Hypertension with brachydactyly is an autosomal dominant disorder, which is an inherited condition affecting individuals at the juvenile stage. This condition is characterised by shortened finger bones with severe development of hypertension. In this syndrome, blood pressure is not salt-sensitive, there is normal function of the renin-angiotensin-aldosterone and catecholamine axis and no evidence of left ventricular cardiac hypertrophy. However, baroreceptor reflex response is impaired due to a structural variation within chromosome 12, resulting in an excessive increase of blood pressure (Toka, 2018).

1.4.4.6 Gitelman Syndrome

Gitelman syndrome is an autosomal recessive condition diagnosed with hypotension and symptoms similar to individuals who are on thiazide diuretics; include hypokalemia, hypomagnesemia, metabolic alkalosis, and renal sodium wasting. This condition is associated with a loss function of the thiazide-sensitive sodium chloride cotransporter (NCC) gene (i.e. SLC12A3 (Solute Carrier Family 12 Member 3)) (Toka, 2018).

1.4.4.7 Bartter Syndrome

Bartter syndrome is an autosomal transmitted condition characterised by hypotension, renal salt wasting, hypokalemic, metabolic alkalosis, and hypercalciuria. This condition results from mutations in genes responsible for the

reabsorption of sodium chloride in the thick ascending limb (TAL). Neonatal bartter syndrome is the most common and life threatening, which is characterised by hypotension, polyuria, polydipsia and hypercalciuria. This is caused by mutations in three genes that are important in sodium reabsorption in the TAL (i.e. NKCC2, ROMK and CLCNKA). Bartter type 1 is caused by loss-of-function mutation in the sodium-potassium-2 chloride cotransporter (NKCC2) gene. Bartter type 2 is caused by mutation in the renal outer medullary potassium channel (ROMK) gene, whilst type 3 bartter is caused by loss-of-function in the voltage-gated chloride channel Kb (CLCNKB) gene and is usually identified at school age. Bartter type 4 is caused by mutations in barttin (BSND), a ß-subunit for CLCNKB in the TAL. Barttin is also expressed in stria vascularis cells of the inner ear. Mutation in barttin leads to renal salt wasting, hypercalciuria and sensorineural hearing loss (Toka, 2018).

1.4.4.8 Pseudohypoaldosteronism Type I

Pseudohypoaldosteronism (PHA) type features severe neonatal hypotension with salt wasting and elevation of aldosterone levels. There are two genetic subtypes, autosomal dominant and autosomal recessive. The dominant form arises from mutation in the mineralocorticoid receptor gene. In early stages, affected children exhibit hyponatremia, hyperkalemia, and urinary salt wasting, frequent vomiting, failure to thrive, and short stature. The dominant form can improve with age. The autosomal recessive type form arises from loss of function mutation in any of the ENaC subunits causing decreased channel activity, renal salt wasting and hypotension in neonates. Unlike the dominant form these individual do not improve with age (Toka, 2018).

1.4.4.9 Pseudohypoaldosteronism type II

Pseudohypoaldosteronism type II (PHA II), also known as Gordon's syndrome, is an autosomal dominant disorder characterised by hypertension, hyperkalaemia, hyperchloraemia, and metabolic acidosis. Hypercalciuria has also been reported in some cases of Gitelman syndrome. This is the result of mutation in serine-threonine kinase genes, WNK1 and/or WNK4, causing an increase in sodium re-absorption by stimulation of the sodium chloride cotransporter (NCC) in the distal convoluted tubule despite volume status. Decreases in renal tubular potassium

excretion in PHA II occur via inhibition of ROMK, the apical renal outer medullary potassium channel resulting in hypertension (Toka, 2018).

1.4.5 Treatment of hypertension

As first line therapy, several non-pharmacological strategies have been recommended to control blood pressure in order to improve life style choices such as good diet, exercise, weight loss, smoking cessation and reasonable consumption of alcohol, tobacco and caffeine. These strategies help to reduce blood pressure and consequently reduced the risk of cardiovascular diseases (Liu *et al.*, 2018). Nevertheless, pharmacologic therapy is the required treatment for the management of blood pressure in hypertensive patients.

Pharmacological treatments of hypertension are classified to five main classes according to the mechanism of actions. These include ß-blockers, diuretics, angiotensin converting enzyme inhibitors, angiotensin II receptor antagonists, and calcium channel blockers. Also, four additional pharmacological classes are renin inhibitors, alpha-adrenergic receptor blockers, centrally acting agents, and direct acting vasodilators (Laurent, 2017) (Figure 1-5).

1.4.5.1 Angiotensin converting enzyme inhibitors

Angiotensin converting enzyme inhibitors (ACEI) are considered to be a first-line therapy in treatment of stage 1 hypertension as recommended by NICE guidelines for antihypertensive treatment (Figure 1-5). ACEI blocks the formation of angiotensin II and consequently downstream effects through angiotensin II type 1 (AT1) receptor and angiotensin II type 2 (AT2) receptor, which leads to reduced vascular tone and extracellular fluid volume and thus reduce blood pressure. In addition, ACE inhibitors down regulate sympathetic adrenergic activity via blocking the effects of angiotensin II on sympathetic nerve release and reuptake of noradrenaline (Wang *et al.*, 2014). ACE inhibitors may also be used in hypertension caused by renal artery stenosis, which causes renin-dependent hypertension due to increased release of renin by the kidneys. ACE inhibitors inhibit the breakdown of kinins leading to increased concentration of bradykinin that is probably responsible for the unwanted side effects of cough and allergic reactions (Sear, 2013; Laurent, 2017) (Table 1-1).

1.4.5.2 Angiotensin II receptor blockers

Angiotensin II receptor blockers (ARBs) have effects that are similar to angiotensin converting enzyme (ACE) inhibitors. ARBs block the binding of angiotensin II to the AT1 receptor and facilitate stimulation of the AT2 receptor. Thus, ARBs may additionally cause vasodilation and natriuresis, which contribute to blood pressure reduction (Sear, 2013; Laurent, 2017) (Table 1-2).

ARBs and ACE inhibitors are less effective in lowering blood pressure in African Americans population. Therefore, the recommendations for first-line drug therapy differ between Caucasian and African American population (Lund, 2016). However, current recommendations are that ACE inhibitors and ARBs are appropriate for use in African Americans, but not as monotherapy. A diuretic or calcium-channel blocker should be used with an ACE inhibitor or ARB to achieve the target reduction in blood pressure, as recommended by NICE guidelines for antihypertensive treatment (Figure 1-5).

1.4.5.3 Diuretics

Diuretics are one of major therapeutic class of antihypertensive drugs, which help to reduce blood pressure by increasing sodium excretion and diuresis. Diuretics are classified into three different classes according to different mechanism of actions (Table 1-2). Thiazide diuretics inhibit sodium-chloride cotransporters (Na^+/Cl^- co-transporters) in the proximal diluting segment of the distal collecting tubule. Loop diuretics act on the medullary and cortical thick ascending limb segments of the nephron to prevent sodium, chloride and water reabsorption. Loop diuretics are not used as first-line therapy for treatment of hypertension due to a short duration of action. The third class is the potassium-sparing diuretics such as amiloride, triamterene and spironolactone. Both amiloride and triamterene have weak antihypertensive effects. However, spironolactone, which also acts as an aldosterone antagonist, is useful as an antihypertensive treatment in primary or secondary hyperaldosteronism (Sear, 2013; Laurent, 2017).

1.4.5.4 Calcium-channel blockers

Calcium channel blockers act as vasodilators of small resistance arteries by blocking Ca^{2+} influx through L type voltage-gated Ca^{2+} channels in the smooth

muscle cells of the resistance vessels. Also, CCBs reduce the increase in intracellular Ca^{2+} in response to membrane depolarization, thus reduce total peripheral resistance and mean blood pressure. Some calcium channel blockers also reduce heart rate and myocardial contractility, which leads to decreased cardiac output and mean blood pressure (Sear, 2013; Laurent, 2017) (Table 1-2). All calcium channel blockers (CCB) are effective in reducing blood pressure, although there is some argument over the side effect of short-acting drugs (Sear, 2013; Laurent, 2017).

1.4.5.5 Beta-blockers

ß adrenoceptor blocking drugs act on receptors by competitive antagonism, and reduce blood pressure elevation by reducing cardiac output (Laurent, 2017) and by inhibiting the release of renin from the kidneys (Marr and Reimer, 2009). B-blockers are used as effective treatment for angina, cardiac arrhythmia, hypertension, glaucoma and migraine (Ladage *et al.*, 2013). Reduced cardiac output by ß-blockade can be an effective treatment for hypertension in conjugation with other antihypertensive agents i.e. diuretics (Laurent, 2017). However, acute treatment with a ß-blocker is not very effective in decreasing arterial pressure due to a compensatory increase in systemic vascular resistance.

There are several ways of classifying the pharmacologic effects of the ß-blockers, depending on their receptor specificity, lipophilicity or hydrophilicity and the presence of either intrinsic sympathomimetic or vasodilator activity. The ß1 selective drugs such as atenolol, bisoprolol, and metoprolol are cardioselective. These drugs reduce the myocardial remodelling effects, while the ß adrenoceptor blocking drugs do not cause vasodilation effects. Nonselective (ß1 and ß2) drugs such as propranolol, oxprenolol, timolol, alprenolol and nadolol, which have similar effects to the selective agents on blood pressure (Sear, 2013; Laurent, 2017) (Table 1-2).

1.4.6 Rationale for combination anti-hypertensive therapy

A combination of antihypertensive drugs is used when hypertensive patients do not achieve the target level of control of their blood pressure. Antihypertensive effect of a combination of drugs is greater than that obtained by monotherapy as

a result of combined action on several different hypertensive mechanisms (Guerrero-García and Rubio-Guerra, 2018). Both the eighth report of the Joint National Committee for the Prevention, Detection, Evaluation and Treatment of Hypertension (JNC8) published in 2014 (James *et al*., 2014) and the guidelines of the European Society of Cardiology and the European Society of Hypertension (ESC/ ESH) for the management of hypertension published in 2018 (Brown, 2018) recommend the use of combinations of antihypertensive agents from the beginning for individual in which the probability of achieving the recommended treatment targets in hypertension with monotherapy is low, i.e. in patients with systolic pressure SBP>150 mmHg or DBP> 90 mmHg.

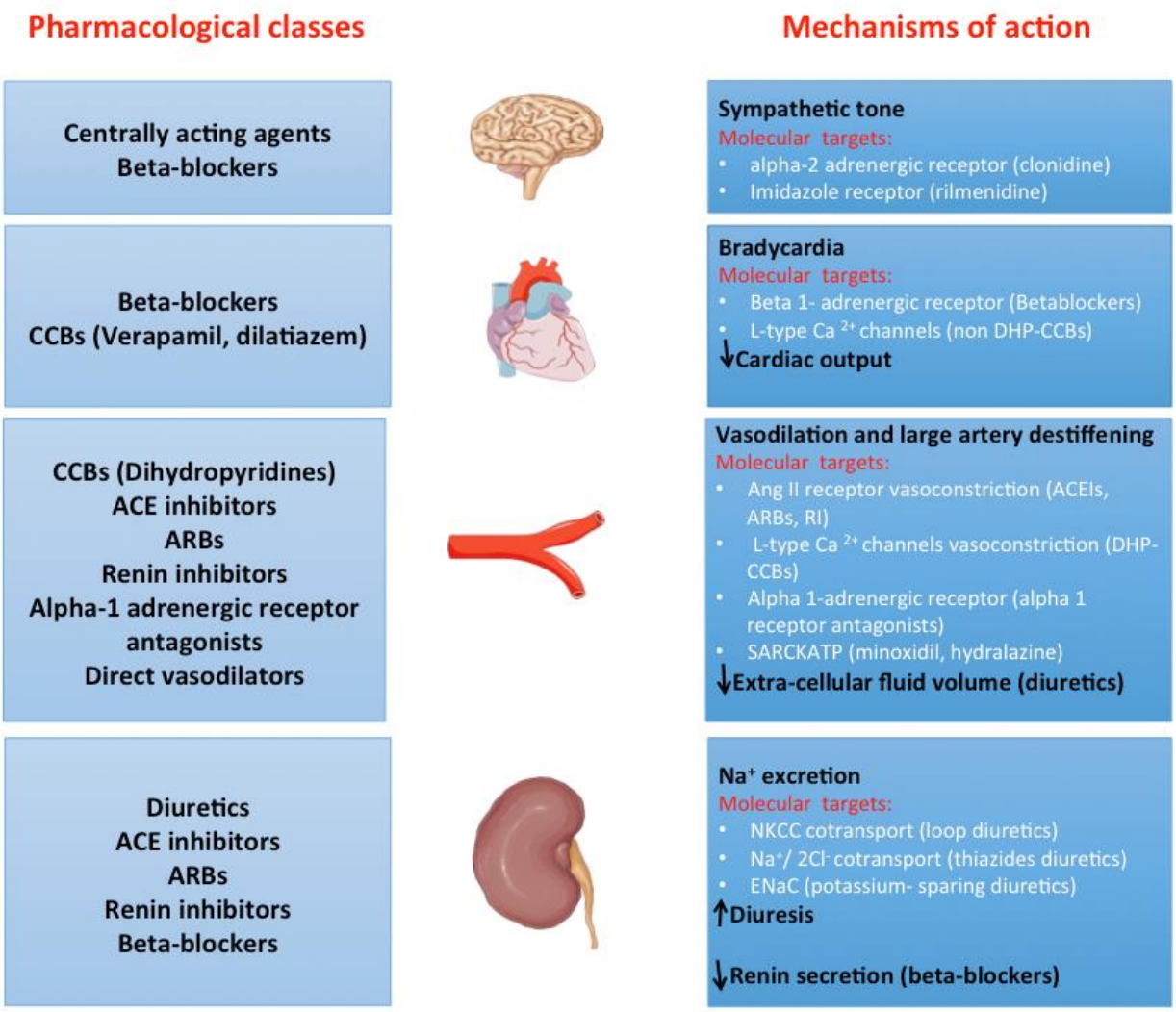

Figure 1-4: Pharmacological classes and related mechanisms of action of the antihypertensive effect (adapted from Laurent, 2017).

Bold names mean that this is the main mechanism of action. Molecular targets are given for each mechanism of action. Abbreviations: ACEIs, angiotensin converting enzyme inhibitors; ARBs, angiotensin receptor blockers; CCBs, calcium channel blockers; DHP, dihydropyridine; $SARCK_{ATP}$, sarcolemnal adenosine triphosphate-dependent potassium channels; NKCC, Na-K-Cl cotransporter; ENaC, the epithelial sodium channels; RI, renin inhibitor**.**

Table 1-1: Pharmacological classes and sub-classes of antihypertensive drugs (adapted from Laurent, 2017).

Pharmacological classes	Sub-classes	Molecules
Major classes **Beta-blockers**	Non-vasodilating with ß1 Non-vasodilating without ß 1-selectivity Vasodilating	Acebutolol, Atenolol, Betaxolol, Bisoprolol Carteolol, Esmolol, Metoprolol, Nadolol, Oxprenolol, Penbutolol, Propranolol, Timolol Celiprolol, Carvedilol, Labetalol, Nebivolol, Pindolol
Diuretics	Loop diuretics Thiazides diuretics Potassium sparing diuretics	Furosemide, Bumetanide, Torsemide Bendroflumethiazide, Chlorothiazide, Chlortalidone, Hydrochlorothiazide Amiloride, Eplerenone, Spironolactone, Triamterene
Angiotensin-converting enzyme inhibitors		Benazepril, Captopril, Cilazapril, Enalapril, Fosinopril, Imidapril, Lisinopril, Moexipril, Perindopril, Quinapril, Ramipril, Trandolapril, Zofenopril
Angiotensin II receptor blockers		Candesartan, Eprosartan, Irbesartan, Losartan, Olmesartan, Telmisartan, Valsartan
Calcium-channel blockers	Non-dihydropyridines Dihydropyridines	Diltiazem, Verapamil Amlodipine, Felodipine, Isradipine, Lacidipine, Lercanidipine, Manidipine, Nicardipine, Nifedipine, Nitrendipine
Other classes **Renin inhibitors** **Alpha-adrenergic receptor antagonists** **Centrally acting agents** **Direct acting vasodilators**		 Aliskiren Doxazosin, Prazosin, Terazosin Clonidine, Methyl-dopa, Rilmenidine Hydralazine, Minoxidine

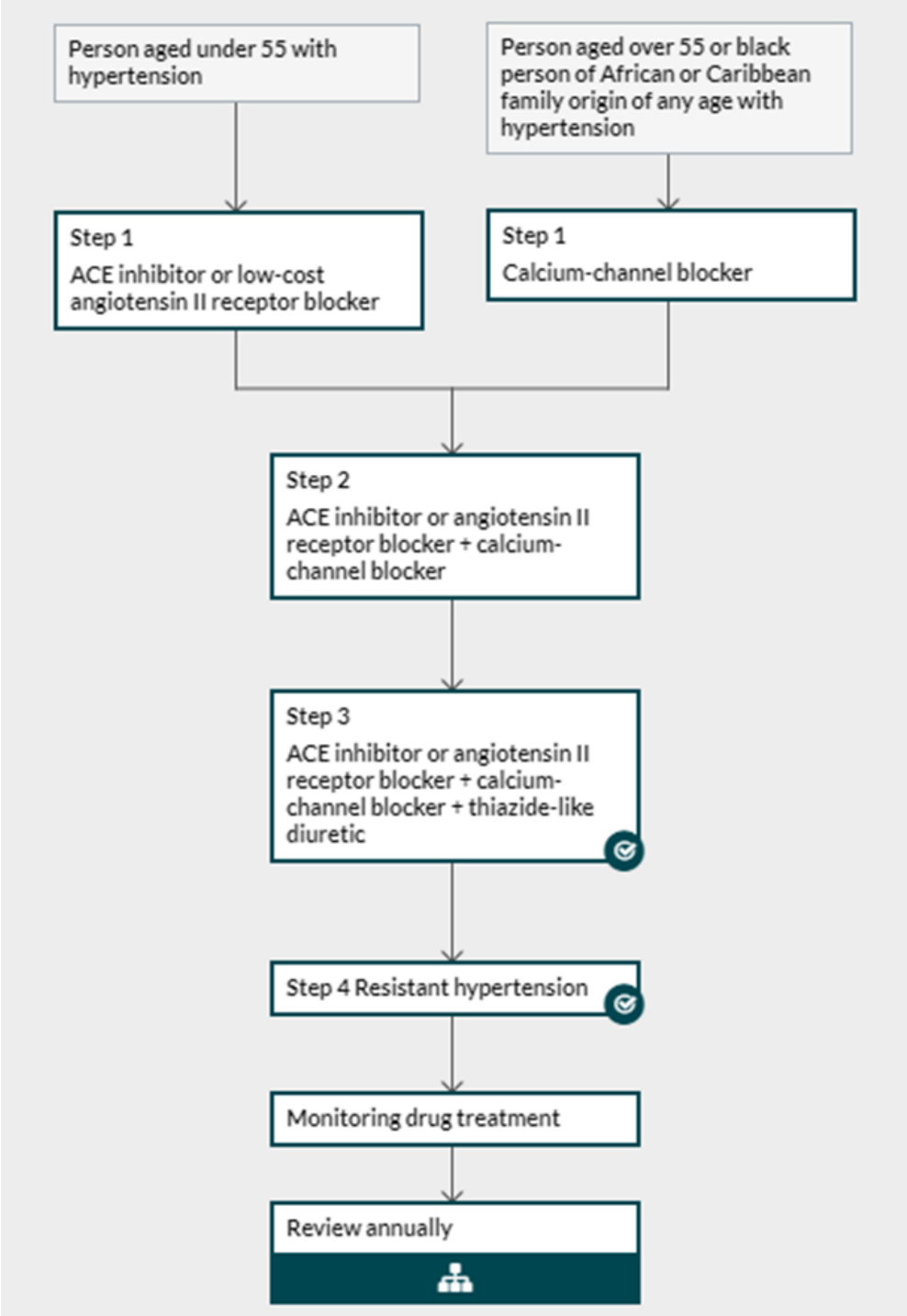

Figure 1-5: NICE guidelines for antihypertensive treatment (Adapted from the National Institute for Health and Care Excellence, 2018).

1.5 Resistant hypertension

Resistant hypertension is uncontrolled blood pressure (>140/90 mm Hg) after treatment with more than three antihypertensive medications (Sheppard *et al.*, 2017). Resistant hypertensive patients have four times higher risk of cardiovascular diseases than patients diagnosed with primary hypertension (Tobe and Lewanczuck, 2009). Prevalent resistant hypertension increased between 1996 to 2004, then plateaued and decreased in recent years. Nevertheless, resistant hypertension remains common in the UK hypertensive population (Sinnott *et al.*, 2017).

Several factors can contribute to resistant hypertension include pseudo-hypertension that is caused by poor clinic blood pressure measurement technique, patient non-adherence to antihypertensive therapy, white-coat effect (i.e. blood pressure is high in the clinic but is controlled at home) and life style factors (obesity, alcohol, smoking, high salt dietary) (Sarwar *et al.*, 2013; Sheppard *et al*, 2017). In addition, many drugs may encourage development of hypertension; such as non-steroidal anti-inflammatory drugs, oral contraceptives, adrenal steroids and antineoplastic drugs (Sarwar *et al.*, 2013). There are common secondary causes of resistant hypertension such as sleep apnea, renal artery stenosis, renal parenchymal disease, and primary aldosteronism. However, there are also some uncommon causes such as pheochromocytoma, cushing's disease, thyroid and parathyroid dysfunction (Sarwar *et al.*, 2013)

National Institute for Health and Care Excellence (NICE) guidelines suggest pharmacological and non-pharmacological therapy to control resistant hypertension. Three classes of hypertension with optimal doses should be used to control resistant hypertension; including an ACE inhibitor, a calcium channel blocker and a diuretic (NICE, 2018).

1.6 New treatments for hypertension

Despite combining multiple antihypertensive medications together with lifestyle modification, there is still not sufficient control of blood pressure in some hypertensive patients who suffer from multiple comorbidities. For that reason, the need for new treatment for the hypertension is still an area demanding further research. There are several studies which aimed to identify novel drugs or strategies to enhance antihypertensive effects (Makani *et al.*, 2013; Kunz *et al.*, 2008).

1.6.1 Vasopeptidase inhibitor

Angiotensin-converting enzyme, neutral endopeptidase (neprilysin) and endothelin converting enzyme are pharmacological targets for treatment of hypertension. Therefore, inhibition of all these enzymes in a single drug has been investigated in order to help improve the control of blood pressure as well as reduce organ damage. Vasopeptidase inhibitors, which provide dual inhibition of neprilysin and angiotensin-converting enzyme have been developed and reached the clinical stage. Both neprilysin and angiotensin-converting enzyme share similar structure and catalytic mechanisms, which allowed for the design of dual vasopeptidase inhibitors that have the same inhibitory activities against both enzymes (Laurent *et al.*, 2012).

Omapatrilat is a dual vasopeptidase inhibitor, which is highly specific, non-peptidergic, orally active and more effective for lowering blood pressure than angiotensin-converting enzyme inhibitors (ACEIs) alone. Conversely, angioedema incident was higher with omapatrilat than with ACEIs. This is due to increased bradykinin and reduced levels of substance P and neurokinin, resulting from the synergistic inhibition of their degradation by the dual vasopeptidase inhibition. Therefore, this drug failed in clinical trials as a potential treatment for congestive heart failure and was never marketed.(Laurent *et al.*, 2012).

LCZ696 (Entresto™) is a first class inhibitor of dual-acting angiotensin-2 type-1 receptor and neprilysin inhibitors, which was innovated by Novartis Pharmaceuticals Canada Inc. Entresto™ was developed by combining the diprotic ARB valsartan and the neprilysin inhibitor prodrug sacubitril in a 1:1 ratio. A

number of ongoing phase 2 randomised clinical trials are assessing the role of valsartan/sacubitril combination in the treatment of heart failure and hypertension (Hubers and Brown, 2016; Laurent *et al.*, 2012; Shaddy *et al.*, 2017).

1.6.2 Aldosterone synthase inhibitors

Novartis Pharmaceuticals developed LCI699, the first-in-class oral inhibitor of aldosterone synthase, which has been shown to reduce blood pressure in primary hypertensive patients. This drug was designed to overcome side effects that are associated with mineralocorticoid receptor-antagonist or aldosterone antagonist (i.e. spironolactone and eplerenone). These side effects include hyperkalaemia, and increased plasma level of aldosterone and gynaecomastia due to the poor selectivity of spironolactone. However, LCI699 also partially inhibited 11-ß-hydroxylase, which catalyses conversion of 11-deoxycortisol to cortisol. Therefore, LCI699 development was stopped in 2010, and research focused more on selective aldosterone synthase (Laurent *et al.*, 2012; Namsolleck and Unger, 2014).

1.6.3 Endothelin antagonists

TRACLEER® (bosentan) is an endothelin-A and endothelin-B receptor antagonist. Bosentan was developed by Actelion Pharmaceuticals US, Inc and is suitable for long-term treatment of pulmonary artery hypertension, however, its use has been investigated in patients with resistant hypertension. In resistant hypertension it reduced blood pressure, but it was associated with side-effects such as increased levels of liver transaminase, oedema, and water retention.

1.7 Animal Models

Animal models have been widely used for investigation of cardiovascular disorders for many years, in order to study a range of cardiovascular diseases mechanisms, including hypertension. This allows in depth understanding of the functional, biochemical, and genetic level effects on development of the disease. Animal models are also useful in pre-clinical studies in the development of strategies for the prophylaxis, diagnosis and treatment of diseases.(Bähr and Wolf, 2012; Hewitson *et al*., 2015).

The use of animals is not only based on the biology of most mammals, but also based on the fact that human diseases affect other animal species. It is mainly the case for most infectious diseases, but also for other common disorders; such as cancer, hypertension, diabetes and epilepsy. These diseases share the same mechanisms, also the veterinary drugs used to treat animals are similar to those used to treat humans. Many human surgical techniques have been designed and improved by using a range of animal species before being applied to humans. Therefore, many advances in basic science and medical research have been possible due to investigation of animal models (Barré-Sinoussi and Montagutelli, 2015). The most widely used experimental models are rodents models (Olson and Graham, 2014).

1.7.1 Mouse models

Mice have been the species of choice for geneticists for many years due to the ease of manipulating their genes. Use of the mouse has become an important part of many research fields such as embryology, pharmacological, cancer, and infectious disease, however, they have been less well studied in CVD. The development of genome research and genetic manipulation (i.e. transgenic and knockout mouse models) was made the mouse a favoured model for investigating the relationship of molecular makeup to disease conditions (Olson and Graham, 2014).

1.7.2 Rat model

Rats are the favoured species for hypertension research. There are a variety of genetically hypertensive strains and non-genetic models, which demonstrate excellent pathophysiological similarities to human diseases. A wide range of hypertensive rat strains have been produced over the last 30 years, which are good models for both essential and secondary hypertension. Genetic models range from inbred strains, such as the spontaneously hypertensive rat (SHR) and stroke-prone spontaneously hypertensive rat (SHRSP) to genetically modified rats generated by CRISPR/Cas9 protein genetic engineering (Graham *et al.*, 2005; Leong *et al.*, 2015; Remy *et al.*, 2017). In addition, non-genetic hypertensive rat models include surgically induced hypertension, such as ligation of renal artery (Segarra *et al.*, 2016), and diet-induced hypertension through increased salt intake, for example the Dahl salt-sensitive and Sabra rats (Leong *et al.*, 2015). More details regarding some of the animal models used for hypertension and their different aetiologies are given in Table 1-2.

1.7.2.1 The Stroke-Prone Spontaneously Hypertensive Rat

The Stroke-Prone Spontaneously Hypertensive Rat (SHRSP) is a sub-strain of SHR, which were obtained by selective inbreeding of normotensive Wistar-Kyoto (WKY) rats in the laboratory of Okamoto and colleagues at the Kyoto University Faculty of Medicine, Japan (Yamori *et al.*, 1974; Okamoto *et al.*, 1975). The SHR was developed by selective inbreeding of WKY with high systolic blood pressure. The blood pressure of SHR spontaneously increase from 4 weeks of age reaching an SBP in males of 180-200 mmHg relative to 130 mmHg in the WKY strain. Consequently, the SHR was divided into three sub-strains (A-C); where sub-strain A consistently exhibited higher SBP and an increased susceptibility for cerebrovascular disease. Inbreeding of offspring from sub-strain A produced the SHRSP (Okamoto *et al.*, 1975; Yamori *et al.*, 1974), as shown in Figure 1-6.

SHRSP rats are characterised by severe hypertension (220-240 mmHg) and high incidence of cerebral stroke (approximately 80%) when compared with the SHR. (Yamori *et al.*, 1974; Okamoto *et al.*, 1975). The SHRSP model exhibits end-organ damage phenotypes similar to human essential hypertension, such as left ventricular hypertrophy, stroke, and renal failure (Graham *et al.*, 2005). However,

spontaneous heart failure and atherosclerosis have not been observed in the SHRSP (Nabika *et al.*, 2012).

The Glasgow colony of SHRSP rats ($SHRSP_{Gla}$) was established in 1991 and originated from rats provided by Dr DF Bohr at the University of Michigan (more details are provided in Chapter 2, Section 2.2.1). Both male and female $SHRSP_{Gla}$ are hypertensive and display cardiac hypertrophy and endothelial dysfunction, however males are more severely affected than females and are more likely to display evidence of stroke, typically after 5 months of age (Graham *et al.*, 2004). $SHRSP_{Gla}$ are salt sensitive and display severe renal disease after 3 weeks of salt-loading with 1% NaCl in drinking water (Caline Koh-Tan *et al.*, 2017).

Table 1-2: Common rodent models for hypertension with different aetiology (adapted from Leong *et al*., 2015).

Experimental model	Description
Genetic hypertension (i) SHR (ii) Dahl salt-sensitive (iii) Transgenic	**(i) SHR** is developed by inbreeding Wistar rats (brother-to-sister) with the highest BP. The BP increases from week 6 and reach systolic BP of 180–200 mmHg. SHR may develop cardiac hypertrophy, cardiac failure, renal dysfunction, and impaired endothelium-dependent relaxation. **(ii) Dahl salt-sensitive rats** derived from Sprague-Dawley rats on the basis of administering high NaCl diet. Salt-sensitive rats become hypertensive when given normal salt diets; however these rats develop severe and fatal hypertension with high salt diet (8% NaCl).These rats may develop cardiac hypertrophy severe cardiac failure, hypertensive nephropathy, impaired endothelium-dependent relaxations. **(iii) Transgenic model** can be generated by overexpression of a specific gene, for example, the mouse Ren-2 gene, and TGR (mREN2)27. Manifestations include marked cardiac hypertrophy, moderate proteinuria, and impaired endothelium-dependent relaxations.
Endocrine hypertension	**(i)** Administration of DOCA in a combination with high salt diet and unilateral nephrectomy. **(ii)** DOCA-induced hypertension induces a low renin model of hypertension. **(iii)** Increased cardiac weight, proteinuria, glomerulosclerosis, and impaired endothelium-dependent relaxations.
Pharmacological hypertension	**(i)** Nitric oxide-deficient model by administering NOS inhibitors such as L-NAME. **(ii)** Increase in BP was reported during long-term oral treatment with NOS inhibitors. **(iii)** Development of endothelial dysfunction is gradually with increased of BP.
Renal hypertension	**(i)** This includes two-kidney one-clip hypertension (2K1C; constriction of one renal artery while the contralateral kidney is left intact), one-kidney one-clip hypertension (1K1C; one renal artery is constricted and the contralateral kidney is removed), and two-kidney two-clip hypertension (2K2C; constriction of aorta or both renal arteries). **(ii)** In the two-kidney model, circulating renin and aldosterone levels are increased, which are most notably in the early phase of hypertension.
Abbreviations: SHR, spontaneously hypertensive rat; BP, blood pressure; NaCl, sodium chloride; TGR, transgenic rat; RAAS, renin-angiotensin-aldosterone system; DOCA, deoxycorticosterone acetate; NOS, nitric oxide synthase; L-NAME, N^{ω}-nitro-L-arginine methyl ester.	

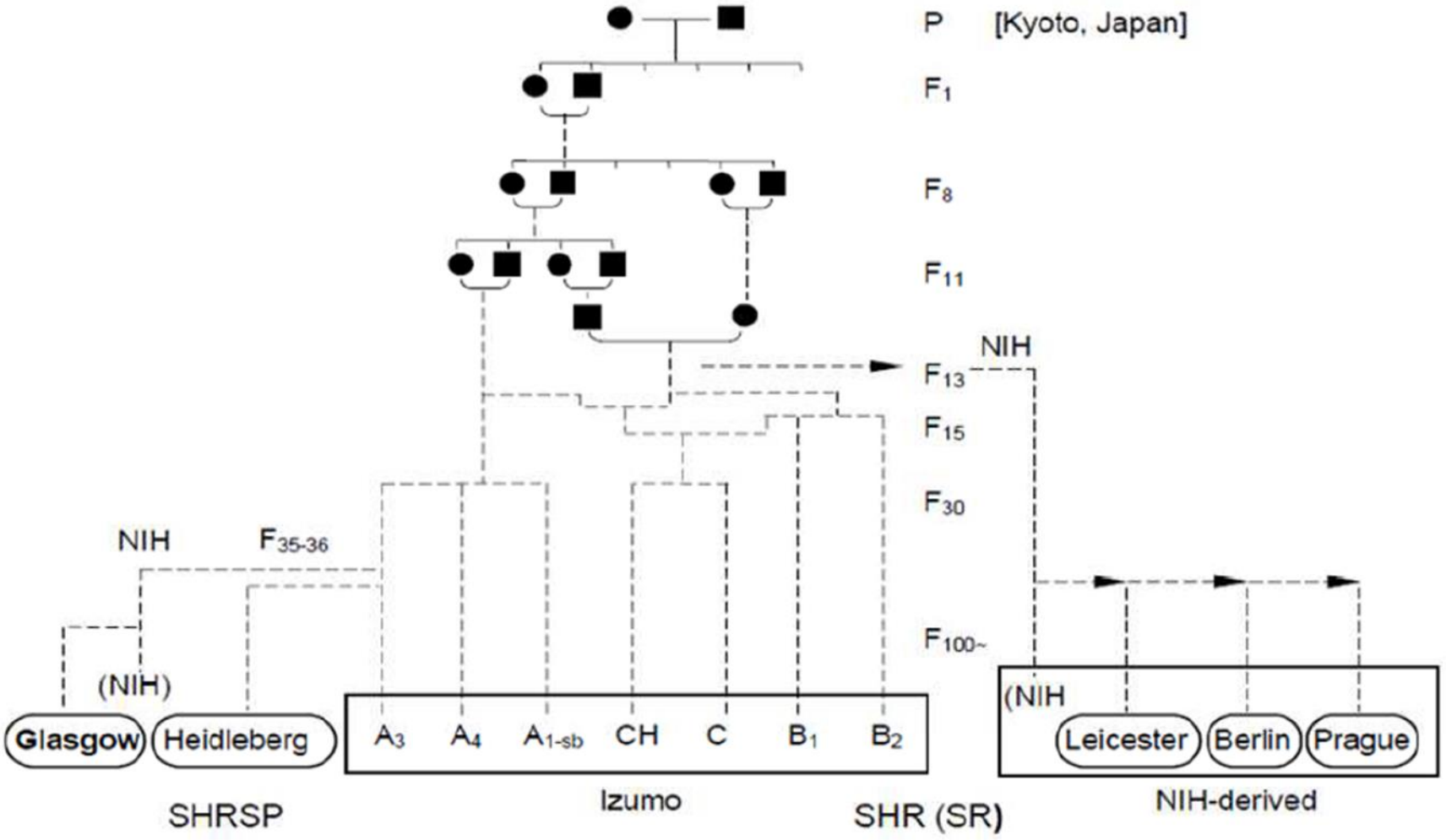

Figure 1-6: Genealogical background of the Stroke Prone Spontaneously Hypertensive Rat (SHRSP).

1.8 The role of fatty acids in cardiovascular disease

Fatty acids are long chains of lipid-carboxylic acid found in fats and cell membranes as a component of phospholipids and glycolipids. Carboxylic acid is an organic acid containing the functional group –COOH. Fatty acids are classified into saturated fatty acids, unsaturated fatty acids, monounsaturated fatty acids, the omega-6 and omega-3 polyunsaturated, and very long chains fatty acids (Lecerf, 2009). Fatty acids are metabolised by two different process; catabolic processes to produce energy, and anabolic processes to generate biologically important molecules such as triglycerides, phospholipids, hormones and ketone bodies. The main role of fatty acids metabolism is energy production. Fatty acids are oxidized to CO_2 and water by beta oxidation (ß- oxidation) and the citric acid cycle to produce ATP (Lopaschuk *et al.*, 2010). Alterations in fatty acid metabolism have been found to be associated with pulmonary arterial hypertension, resulting from elevations in the levels of circulating free fatty acids and long chain acylcarnitines (Brittain *et al.*, 2016). In pulmonary arterial hypertension patients, it has been found that increased fatty acid levels promote left ventricular dysfunction, which are characterized by decreased rate of fatty acids oxidation and increased accumulation of lipotoxic compounds (Talati and Hemnes, 2015). In addition to pulmonary arterial hypertension, alterations in fatty acid oxidation are common in many heart diseases such as heart failure, ischaemic heart disease and diabetic cardiomyopathies. These impairments include mitochondrial dysfunction and defects in energy production, which are characterised by elevations in the relative amount of fatty acids oxidised by the mitochondria in relation to oxidized carbohydrates, which contributes to decreased heart function (Fillmore *et al.*, 2014). Studies suggest that cardiac function can be improved by enhancing glucose oxidation through inhibition of fatty acid oxidation (Fruchart, 2009; Keech *et al.*, 2005; Yue *et al.*, 2003; Rubins *et al.*, 2002; Tsunoda *et al.*, 2016).

1.9 Fatty acid beta oxidation pathway

The major pathway for fatty acid degradation is mitochondrial fatty acid beta-oxidation. This pathway plays an essential role in energy homeostasis in heart, liver and skeletal muscles. In such conditions as fasting, glucose levels become low, thus these tissues switch to using fatty acids to generate energy (Houten and Wanders, 2010). ß-oxidation takes place within mitochondria to generate acetyl-

CoA units. Four different enzymes are involved in ß-oxidation pathway, which degrade acyl-CoAs into acetyl-CoA units. Firstly, an acyl-CoA-ester is dehydrogenated to produce a trans-2-enoyl-CoA, followed by hydration of the double bond to yield L-3-hydroxy-acyl-CoA. Subsequently, L-3-hydroxy-acyl-CoA is dehydrogenated to 3-keto-acyl-CoA, which is then cleaved to generate an acyl-CoA shortened by two carbon atoms; an acetyl-CoA, one nicotinamide adenine dinucleotide (NADH) and one flavin adenine dinucleotide ($FADH_2$). The resulting acyl-CoA can then enter another fatty acid oxidation cycle or enter the citric acid cycle (Houten and Wanders, 2010) (Figure 1-7).

1.9.1 Impairment of fatty acids β oxidation pathway

High energy demand tissues such as heart, liver and skeletal muscle depends on fatty-acid oxidation to produce energy. Therefore, in conditions of fatty acid oxidation stress such as impairment of hepatic ketogenesis, glycogen and glucose stores, free fatty acids cannot be metabolised and stored in the cytosol as triglycerides. This causes weakness and lipid storage myopathy along with fatty acid oxidation disorders such as fatty liver, hypertrophic and dilated cardiomyopathy (Tein, 2014). In addition, deficiency in gluconeogenesis, ß-oxidation, and the citric acid cycle are caused due to increased levels of short or medium-chain fatty acids as well as dicarboxylic fatty acids metabolites from the ω-oxidation pathway (Tein, 2014).

Mitochondrial fatty acid ß-oxidation disorders are heterogeneous defects in transportation of fatty acid and mitochondrial ß-oxidation. These disorders, which are inherited as autosomal recessive disorders include; defects in the uptake of long-chain fatty acids into mitochondria, and also, intramitochondrial ß-oxidation deficiencies of long-chain fatty acids and very long chain fatty acids affecting membrane bound enzymes (Sim *et al.*, 2002; Vishwanath, 2016). It has been found that elevations in levels of long-chain fatty acids may lead to acute muscle breakdown or myoglobinuria (Tein, 2014).

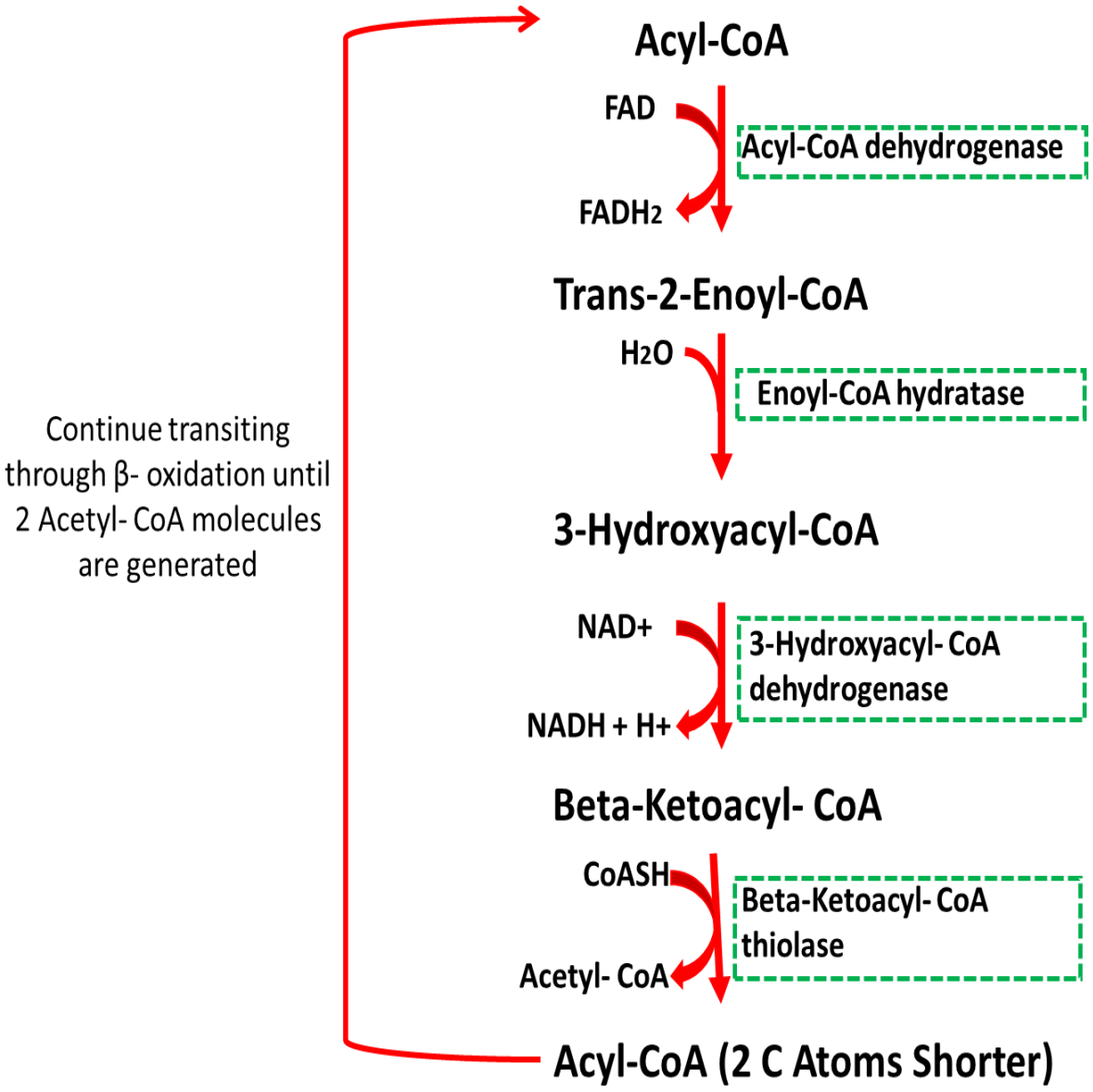

Figure 1-7: Steps of β-oxidation pathway of fatty acids.

Fatty acyl-CoA is dehydrogenased by an enzyme acyl-CoA dehydrogenase, which is FAD dependent to form trans-2-enoyl-CoA. Hydration occurs at the double bond resulting in the formation of β-hydroxyacyl-CoA, which then dehydrogenased to form β-ketoacyl-CoA by β-hydroxyacyl-CoA dehydrogenase. β-ketoacyl-CoA is celvaged by β-ketoacyl-CoA thiolase to form acetyl CoA, which can then enter another fatty acid oxidation cycle or enter the citric acid cycle.

1.10 Fatty acid omega oxidation pathway

Very-long-chain fatty acids (VLCFAs) are known to be degraded in peroxisomes via the ß-oxidation pathway. An alteration in this pathway leads to increases in VLCFAs levels which then undergo an alternative fatty acid omega-oxidation pathway for breakdown (Sanders *et al.*, 2006, 2008a). ω-oxidation of fatty acids consists of the conversion of the ω-methyl group of the fatty acid into an ω-hydroxyl group by cytochrome P450 enzymes. This step requires NADPH and oxygen. Consequently, the ω-hydroxy fatty acid is oxidised into a ω-carboxylic acid by an NAD+-dependent alcohol and aldehyde dehydrogenase system to produce dicarboxylic acids. Finally, dicarboxylic acids can be ß-oxidised in peroxisomes and/ or mitochondria to shorter-chain dicarboxylic acids, which are then excreted into the urine (Sanders *et al.*, 2006, 2008a) (Figure 1-8).

1.10.1 Enzymes involved in fatty acids ω- oxidation pathway

There are three enzymatic steps within the ω-oxidation pathway (Figure 1-8). First, the CYP4A family of enzymes, which introduced the hydroxyl group onto the omega carbon to generate fatty-ω-hydroxyl acid. Secondly, alcohol dehydrogenase, which oxidised the hydroxyl group to an aldehyde to generate fatty-ω-aldo acid. Finally, aldehyde dehydrogenase, which oxidised the aldehyde group to a carboxylic acid to produce a dicarboxylic fatty acid (Sanders *et al.*, 2006, 2008a).

1.10.1.1 CYP4A enzymes

Hepatic cytochome P450 enzymes contain a superfamily of heme-containing proteins that are involved in oxidative metabolism of a large range of endogenous and exogenous compounds; including drugs, steroids and fatty acids (Miura, 2013). It has been demonstrated that enzyme systems involving the microsomal or mitochondrial cytochrome P-450 catalyse the ω-oxidation of many fatty acids, and it has been recognised that cytochrome P-450 enzymes family have an essential role in the ω-oxidation of fatty acids (Dhar *et al.*, 2008; Fer *et al.*, 2008; Johnston *et al.*, 2011).

The mammalian CYP4 family of P450 enzymes catalyses the ω-hydroxylation of fatty acids and eicosanoids. This family include CYP4A1, CYP4A2, CYP4A3, and

CYP4A8, which have been well investigated in terms of their fatty acid ω-hydroxylase activities in mice, rabbits and other mammals. In humans the properties and functions of CYP4A11, CYP4B1, CYP4F2, CYP4F3, CYP4F8, CYP4F11, CYP4F12 are well defined, whereas the other five members of the family, CYP4A22, CYP4F22, CYP4V2, CYP4X1, and CYP4Z1 are less well examined (Johnston *et al.*, 2011).

1.10.1.2 Alcohol dehydrogenases (ADHs)

Human alcohol dehydrogenases (ADHs) are a family of enzymes that catalyse oxidative conversion of several alcohols to aldehydes. Five kinds of subunits (alpha, beta, gamma, pi and chi) governed by 5 non allelic genes have been identified; which are ADH1, ADH2, ADH3, ADH4, and ADH5 (Yasunami *et al.*, 1991). ADH isoenzymes encoded by these genes, are classified into three different classes (Yasunami *et al.*, 1991), which show different physiological functions due to their specificity and distribution in tissues. Class I and III are identified in liver and class IV in stomach, where all are involved in the oxidation of ω-hydroxyl fatty acids. In addition, class I and IV are responsible in retinol oxidation and retinal reduction, whereas class IV has an important role in retinoic acid generation (Boleda *et al.*, 1993).

1.10.1.3 Aldehyde dehydrogenases (ALDHs)

Aldehyde dehydrogenases (ALDHs) are a group of enzymes catalysing the conversion of aldehydes to the corresponding acids. ALDH activity was first detected in mammalian liver over 50 years ago and two ALDH genes were identified in 1985 (Yoshida *et al.*, 1998; Hsu *et al.*, 1985). Since then, 12 genes have been elucidated in the human ALDH family, of which the coding enzyme subunits consists of 500 amino acids residues (Yoshida *et al.*, 1998). In humans, there are many forms of ALDH divided into two groups. Firstly, cytoplasmic forms include ALDH 1, ALDH 3, ALDH 7, ALDH 8 and ALDH 9. Mitochondrial forms include ALDH 2, ALDH 4, ALDH 5, and ALDH 6. The ALDH classes are distributed widely in the human body, while ALDH 3 is only expressed in stomach, lungs, liver, skin and the cornea. These isoenzymes play a role in elimination of toxic aldehydes, which are produced during lipid peroxidation. They are also involved in metabolism of

bile acids, prostaglandin and steroids dehydrogenation (Orywal and Szmitkowski, 2017).

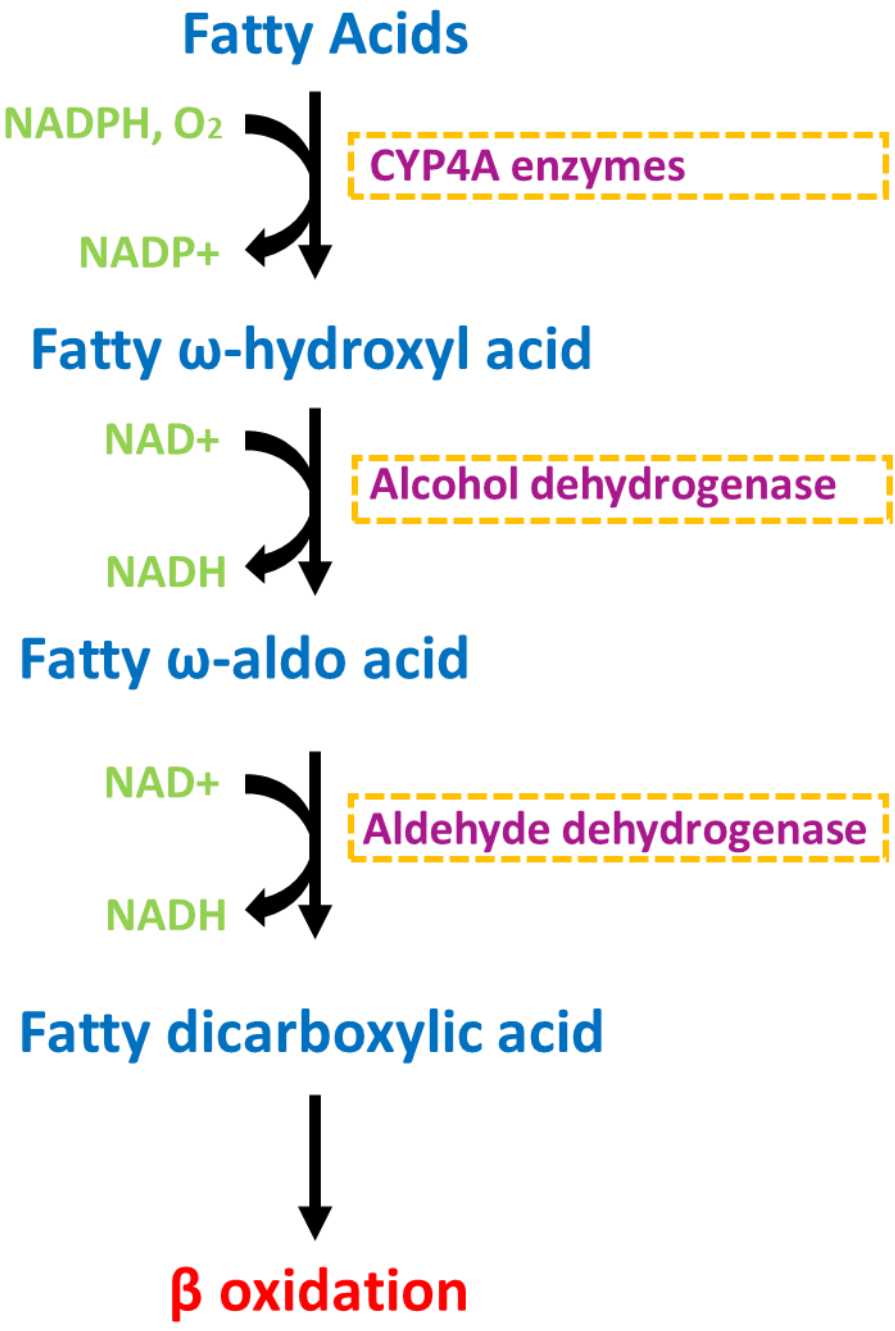

Figure 1-8: Conversion of fatty acids to fatty dicarboxylic acids via Omega-oxidation pathway.

Fatty acids is converted to fatty-ω-hydroxyl acid by a cytochrome P450 and oxidised the hydroxyl group to an aldehyde by alcohol dehydrogenase to generate fatty-ω-aldo acid. Aldehyde dehydrogenase then oxidised the aldehyde group to a carboxylic acid to produce a dicarboxylic fatty acid.

1.11 Dicarboxylic acid

Dicarboxylic acids are generated from omega-oxidation of monocarboxylic acids. The process involves fatty acid conversion into ω-hydroxymonocarboxylic acids by a microsomal cytochrome P450 and oxidised to ω-ketomonocarboxylic acids and then by the sequential action of cytosolic long-chain alcohol and aldehyde dehydrogenases to produce dicarboxylic acid (Ferdinandusse *et al.*, 2004). Dicarboxylic acids are numbered according to chain length, including adipic (C6), suberic (C8), sebacic (C10) and dodecanedioic (C12) acids. Medium chain fatty acids are derived from ß-oxidation of long chain dicarboxylic acids (Mingrone *et al.*, 2013). Short-chain dicarboxylic acids (i.e. 4-carbon) and medium-chain dicarboxylic acids (i.e. 8-carbon) are capable of crossing the outer and inner mitochondrial membranes as free fatty acids to enter the mitochondrial matrix, while long chain fatty acids (i.e.16-carbon) are not able to enter the mitochondria. Long-chain dicarboxylic acids are shortened in the peroxisome and the products are either excreted in the urine or move to the mitochondrion for the ß–oxidation (Ferdinandusse *et al.*, 2004).

Dicarboxylic fatty acids can be transported through the mitochondrial membrane by four different pathways, including electrophoretic transport by an inner membrane anion channel, by passive diffusion, via tributyltin-mediated transport or via transport by the dicarboxylate carrier (Mingrone *et al.*, 2013). The dicarboxylate carrier works for short-chain dicarboxylic acids since this transportation does not need the carnitine shuttle (i.e. carnitine palmitoyltransferase1, carnitine palmitoyltransferase 2 and carnitine acetyltransferase).

1.12 Hexadecanedioate

Hexadecanedioic acid (HEXA) is a long chain dicarboxylic acid ($HOOC(CH_2)_{14}COOH$) generated during fatty acid ω-oxidation, which is then metabolised by ß-oxidation in peroxisomes or mitochondria (Reddy and Rao, 2006). The transport of HEXA through the inner mitochondrial membrane is facilitated via the carnitine acyltransferase enzyme, which catalyses the reversible transfer of acyl groups from acyl-CoA to L-carnitine (Pettersen, 1973). However, HEXA can also be ß-oxidized at both peroxisomes and inner mitochondrial membrane components via a carnitine-independent pathway (Aarsland *et al.*, 1989; Grego and Mingrone, 1995). Activation of HEXA transportation is localised in liver, in particular the mitochondrial and microsomal fractions in presence of CoA, ATP, and Mg^{2+} (Pettersen, 1973; Pettersen and Aas, 1974).

HEXA has been reported to have hypotriglyceridemia and hypocholesterolemia functions by affecting lipid metabolism through modifying lipid and lipoprotein synthesis and degradation. These effects are caused by stimulation of peroxisomal ß-oxidation and peroxisome proliferation. (Aarsland *et al.*, 1989). The modulating capacity of long-chain fatty acids, as opposed to their role as substrates, has initiated the design of nonmetabolic long-chain fatty acyl analogues (i.e. MEDICA 16) (Tzur *et al.*, 1988). MEDICA 16 is a non-metabolic long-chain fatty acyl analogue of hexadecanedioic acid, which contains a chain length of C14 to C18 (i.e. HOOC-CH2- C(CH3)2- (CH2)n-C(CH3)2-CH2-COOH). MEDICA 16 is designed to work as a hypolipidemic, hypoglycemic-hypoinsulinemic and antiobesity agent (Tzur *et al.*, 1988). It inhibits liver lipogenesis and cholesterogenesis by inhibition of liver ATP-citrate lyase, thus decreasing the levels of plasma very-low-density lipoprotein (VLDL)-triacylglycerol, VLDL-cholesterol, chylomicrons, triacylglycerol and apolipoprotein C III (Tzur *et al.*, 1988; Bar-Tana *et al.*, 1988; Frenkel *et al.*, 1988, 1994). The decrease in plasma apolipoprotein C-III is due to activation of peroxisome proliferator receptors alpha subunit/ the retinoid X receptor (PPARα/RXR) (Mayorek *et al.*, 1997). Peroxisome proliferators are known to activate dicarboxylation of fatty acids. Interestingly, HEXA is the most potent activator of PPARs (Desvergne and Wahli, 1995).

Previous studies showed that treatment of obese-insulin-resistant rats by MEDICA 16 caused decreased content of neutral lipids of the epididymal, perirenal, and

omental fats leading to decrease in body weight (Tzur *et al.*, 1988; Atkinson *et al.*, 2002). Moreover, treatment with MEDICA 16 caused an insulin-induced decrease in production of hepatic glucose as well as increase in total-body glucose disposal. It activated intracellular reesterification of lipolysed free fatty acids in adipose tissue causing reduction in free fatty acid release and plasma free fatty acids (Tzur *et al.*, 1988; Mayorek *et al.*, 1997; Atkinson *et al.*, 2002). In addition, increased glucose disposal for free fatty acids reesterification was estimated by the role of glycerol-3-phosphate (Mayorek *et al.*, 1997). The glycerol-3-phosphate shuttle maintains intracellular redox balance and allows the synthesis of NADH in the cytosol by glycolysis to contribute to the oxidative phosphorylation pathway in the mitochondria to generate ATP (Larsson *et al.*, 1998). In addition, long term treatment of MEDICA 16 inhibits the secretion of arginine and potassium (K^+) that helps to stimulate insulin secretion, inhibition of glucose-induced proinsulin biosynthesis and depletion of insulin in the islets of Langerhans (Frenkel *et al.*, 1988).

Atkinson *et al* study exhibited that chronic treatment of MEDICA 16 reduced the activity of hepatic acetyl-CoA carboxylase (ACC), followed by reduction in plasma triacylglycerol in obese-insulin-resistant JCR:LA-cp rats (Atkinson *et al.*, 2002). ACC is the rate-limiting enzyme in fatty acids synthesis and it has an essential role in the energy metabolism by regulation of fatty acid biosynthesis and oxidation in liver and adipose tissue. ACC catalyses the synthesis of malonyl-CoA, the substrate for synthesis of fatty acid and the regulation of fatty acid oxidation. In addition, ACC enzyme is considered as a target to regulate cardiovascular diseases such as obesity and diabetes (Wakil and Abu-Elheiga, 2009).

1.13 Hexadecanedioate and hypertension

A putative novel pathway for blood pressure regulation involving the dicarboxylic acid, hexadecanedioate has been identified in a metabolomics study associating blood pressure and mortality outcomes with fasting blood metabolites (Menni *et al.*, 2015). A total of 3980 adult females not on blood pressure medications and free of renal diseases from the TwinsUK cohort study (Moayyeri *et al.*, 2013) were included in the metabolomics study (Menni *et al.*, 2015). The metabolomics analysis showed that three metabolites (i.e. hexadecanedioate, dihomo-linoleate and caffeine) significantly associated with all-cause mortality. However, hexadecanedioate was the only metabolite that showed a direct association with blood pressure and mortality, indicating consistent impact of higher levels of hexadecanedioate on blood pressure elevation (Menni *et al.*, 2015).

This result was verified in two additional clinical cohorts (i.e. KORA and Hertfordshire). Both studies included male and female participants on antihypertensive medications (Menni *et al.*, 2015). The KORA cohort included 1494 subjects (males=776 and females=718) (Holle *et al.*, 2005), while the Hertfordshire cohort included 1515 subjects (males=765 and females=750) (Syddall *et al.*, 2010). In these additional cohorts hexadecanediote was again found to be significantly associated with systolic blood pressure and diastolic blood pressure (Menni *et al.*, 2015).

In vivo animal experiments were subsequently conducted to provide functional evidence of a role for hexadecanedioate in blood pressure regulation. In these studies circulating levels of hexadecanedioate and systolic blood pressure (SBP) significantly increased in hexadecanedioic acid treated WKY rats compared to untreated controls. Baseline circulating hexadecanedioate levels were significantly higher in SHRSP rats compared to untreated aged-matched WKY rats Three weeks of 1% NaCl administration in drinking water significantly elevated SBP in SHRSP rats, though plasma hexadecanedioate levels were not modified by this salt-challenge (Menni *et al.*, 2015) (Figure 1-9).

These studies provide strong evidence for a link between hexadecanedioate levels and blood pressure control. Therefore, investigating of the functional role and the pathway underlying hexadecanedioate induced blood pressure elevation are necessary.

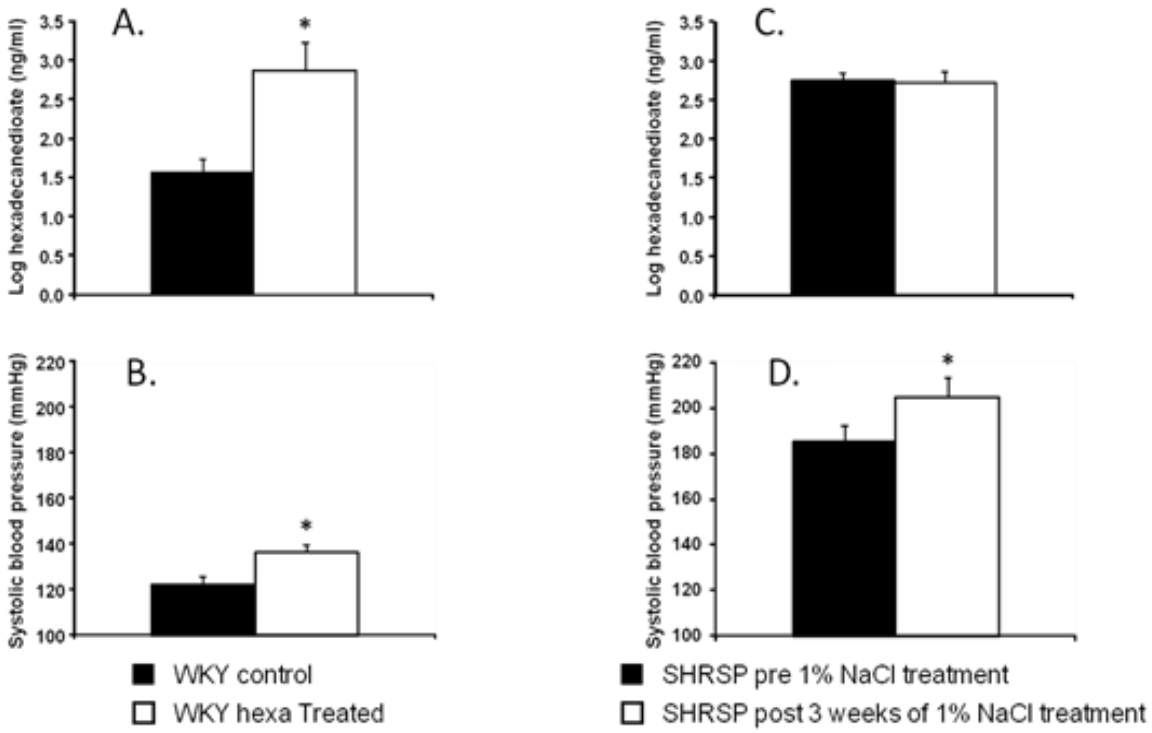

Figure 1-9: *In vivo* experiments using WKY and SHRSP rat model to examine the effect of hexadecanedioate on blood pressure regulation (Menni *et al*., 2015).

(A) Plasma hexadecanedioate levels (ng/ml) and (B) systolic blood pressure (mmHg) in WKY rats treated with 250 mg/kg/day hexadecanedioate or vehicle for 4 weeks (n=6). (C) Plasma hexadecanedioate levels (ng/ml) and (D) SBP (mmHg) in SHRSP rats (n=6) pre- and post-administration of 1% NaCl in drinking water for 3 weeks. *P<0.05 versus respective untreated group.

1.14 Proteomic and mRNA expression of ALDH and ADH in SHRSP and WKY

Previous unpublished studies by Dr Sofia Tsiropoulou, 2015 at the University of Glasgow have generated 'omics' datasets from cardiovascular tissues (e.g. kidneys and vascular tissue) derived from SHRSP and WKY rats. The results of these studies showed expression of key enzymes involved in the ω-oxidation pathway are perturbed in the hypertensive model in both vascular and renal tissues (Figure 1-9). For example, microarray expression profiling demonstrated significantly increased mRNA expression of the alcohol dehydrogenase family of enzymes, in particular ADH1C*, in whole kidney homogenates from SHRSP rats compared to WKY. In addition, significantly increased protein expression of aldehyde dehydrogenase isoenzymes was identified using SILAC proteomics in cultured vascular smooth muscle cells from mesenteric resistance arteries from SHRSP rats when compared to WKY. These results indicate that the SHRSP rat may be a useful model for examining the ω-oxidation pathway and its potential link with development of hypertension.

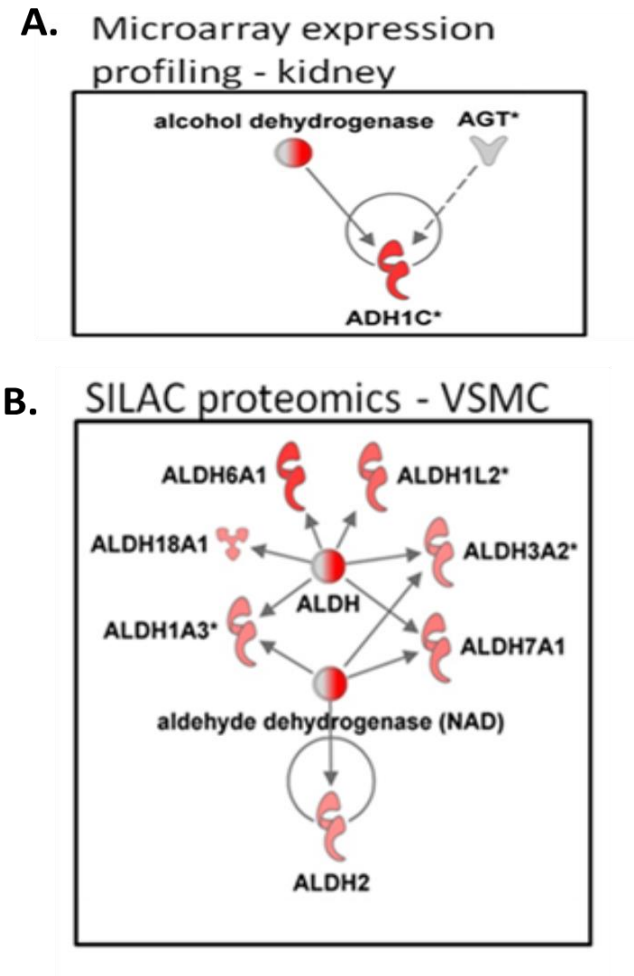

Figure 1-10: Ingenuity Pathway Analysis of 'omics' datasets identifies significant expression differences in omega oxidation pathway enzymes between SHRSP and WKY for (A) renal mRNA expression and (B) VSMC proteomic analysis in SHRSP and WKY rats. (Tsiropoulou, 2015).

1.15 Hypothesis

We hypothesised that the dicarboxylic acid, hexadecanedioate plays a causal role in blood pressure regulation. Elucidating the underpinning mechanism will expand our understanding of blood pressure regulation and inform new drug discovery.

1.16 Aims

The aims which would allow us to address this hypothesis were as follows:

1. To investigate the relationship between blood pressure and hexadecanediote by assessing the impact of exogenous hexadecanedioic acid on blood pressure and end organ damage in a normotensive WKY and hypertensive SHRSP rats models.

2. To examine the metabolic effects of hexadecanedioic acid administration in WKY rats.

3. To assess hemodynamic changes after modulation of endogenous hexadecanedioate levels by perturbing the ω-oxidation pathway in both a WKY and SHRSP rat models.

4. To investigate the role of anion transporter Slco1b2 as a regulator of circulating hexadecanedioate levels.

Chapter 2 Materials and Methods

This chapter contains details on general laboratory practice and methods routinely used during this PhD project. Methods specific to particular aspects of the project are described in the relevant chapters.

2.1 General laboratory practice

A laboratory coat and non-latex powder-free gloves were worn during all procedures. Hazardous reagents were kept in labelled cabinet and handled as described in the Control of Substances Hazardous to Health regulations. Booking systems were available for laboratory equipment were communally and routinely used. Laboratory glassware was cleaned in Decon 75 detergent (Decon Laboratories Ltd, East Sussex, UK), rinsed with distilled water and dried at 37°C. Sterile disposable plastic ware were also commonly used, including 0.5 ml, 1.5 ml and 2 ml microcentrifuge tubes (Greiner Bio-one, Stonehouse, UK), 15 ml and 50 ml centrifuge tubes (Corning, Birmingham, UK). Certified nuclease-free reagents and plastic ware, including RNase-free microcentrifuge tubes, RAININ nuclease-free filtered pipette tips and Ambion nuclease-free water were used in experiments involving ribonucleic acid (RNA). Pipettes and benches were wiped with Ambion RNaseZap reagent before all RNA experiments. Laboratory-ware and liquids requiring sterilisation were autoclaved in a Priorclave Tactrol 2. Reagents were weighed using an Ohaus Portable Advanced balance (sensitive to 0.01 g), or a Mettler HK160 balance (sensitive to 0.0001 g). PH of solutions were measured using a Mettler Toledo digital pH meter calibrated with pH 4.0, 7.0 and 10.0. Volumes from 0.1 µl to 1,000 µl were dispensed with Thermo fisher pipettes (Thermo fisher Scientific, Loughborough, UK). All producers carried out according to risk assessment and relevant COSHH forms were read and signed before commencement of procedures.

2.2 In vivo experimental procedures

2.2.1 Experimental animals

The animal strains used in this thesis were the Spontaneously Hypertensive Stroke Prone rats (SHRSP$_{Gla}$) and Wistar Kyoto rats (WKY$_{Gla}$) where Gla is used as short for Glasgow). The animals were housed individually in cages on a 12 hours light/dark cycle at room temperature (21± 3°C). A standard rat chow (rat and mouse No. 1

maintenance diet, Special Diet Services) and water *ad libidum* were provided daily to the rats. All work with experimental animals were approved by the Animals' Scientific Procedures Act 1986 under the project license of Dr Delyth Graham (70/9021). Offspring were weaned, sexed, ear-tagged (National Band and Tag. Co.) at 3 to 4 weeks of age and then caged, with a maximum of 3 animals per cage, according to sibling group and sex.

Colonies of WKY and SHRSP rats have been maintained at the University of Glasgow since 1991 by brother-sister mating. These colonies originated from 13 SHRSP and 13 WKY rats (6 males and 7 females of each strain), provided by Dr D.F. Bohr, at the Department of Physiology, University of Michigan (USA) who originally obtained this breeding stock from the National Institutes of Health, Bethesda, Maryland, USA. Rats were phenotyped for blood pressure level before breeding to ensure the normotensive and hypertensive phenotypes were maintained within the following ranges of blood pressure: 170-190 mmHg (males) and 140-170 mmHg (females) for SHRSP adult breeders, and 120-140 mmHg (males) and 100-130 mmHg (females) for WKY adult breeders. Routine microsatellite screening was also used to confirm the maintenance of homozygosity of all loci within strains.

2.2.2 Hemodynamic profile

2.2.2.1 Blood pressure measurements by tail cuff plethsymography

Systolic blood pressure (SBP) measurement was carried out using the well-established method of tail cuff plethysmography in conscious rats as described previously (Evans *et al.*, 1994). Rats were placed in an insulated box and a direct heat source (overhead lamp) was applied at 30°C for 15-20 minutes for vasodilation of the tail artery. Rats were then wrapped in a soft cloth to restrain them and an inflatable cuff placed on their tail along with a piezoceramic transducer (Hartmann & Braun type 2) for pulse detection. The pressure in the cuff was controlled in 1 mmHg steps over a 300-mmHg range. Numerous cuff inflation and deflation steps were carried out over tail cuff session and the resulting pulsation detected by the transducer. The detected pulsatile signal was then visualised as pressure function and displayed on a computer using Microsoft Windows compatible software. A minimum of six readings was taken for each rat per session and the average values were taken for systolic blood pressure.

2.2.2.2 Blood pressure measurements telemetry

The animals were anesthetized by isoflurane anesthetic in an induction chamber (2.5% isofluorane in 1.5 L/min O_2) and their abdomens were shaved and the area cleaned with betadine solution (Purdue Pharma L.P., Stamford). The surgical procedure was carried out under sterile conditions. The incision was prepared on the mid line of the abdomen and opened using retractors. The intestines were gently externalised, wrapped in sterile gauze swabs and kept moist with sterile PBS (Sigma Aldrich Co Ltd, Irvine, UK). The internal organs were protected by use of gauze pads and the descending aorta was exposed by blunt dissection using long handled sterile cotton buds. Blood flow along the abdominal aorta was transiently prevented by placing silk ties (sloops) on the abdominal aorta (below the renal arteries) and on each iliac artery, after which an incision was made immediately above the aortic bifurcation with 23 gauge needle. The gel-filled catheter of the telemetric probe (TA11PA/C40) was implanted into the distal descending abdominal aorta pointing towards the proximal end of the animal (i.e. towards the heart), against the flow of blood, and secured with VetBond™ biological glue (Data Sciences International, Sheffield, UK). After the silk ties were removed this probe was sutured to the wall of the peritoneum cavity with non-absorbable sutures to prevent the movement of the probe. After that, the animals were injected with carprofen (5 mg/kg) a non-steroidal anti-inflammatory analgesic for pain control and allowed to recover for one week for recovery before haemodynamic parameters were monitored (i.e. systolic blood pressure (SBP), diastolic blood pressure (DPB), mean arterial blood pressure (MAP), pulse pressure (PP), heart rate (HR) and locomotors activity). In this process, telemetric probes send signals to receiver panels situated under each cage, then measured signals were sent to the matrix linked with a computer. Dataquest A.R.T. (system version 4.2) acquisition software acquired and recorded the raw data. Briefly, heart rate, blood pressure, pulse pressure, and activity were recorded for 10 seconds every 5 min throughout the day and night. Cycles of scheduled sampling occurred every 5 minutes over a 24-hour period. Blood pressure were recorded and data points displayed as daytime/night time averages (averages of daytime (7:00 am - 7:00 pm) and night time (7:00 pm - 7:00 am)) (Anderson *et al.*, 1999). Data was analysed using Microsoft Excel spread sheet macro and the daytime and night time averages were used to calculate daily averages which were plotted in the graphs for clarity.

2.2.3 Echocardiography

Transthoracic echocardiography was carried out using an ACUSON Sequoia C512 ultrasound system with a 15-MHz linear array transducer to assess cardiac geometry, function and contractility. Echocardiography was performed at baseline and weekly during drug administration. Animals were sedated by isoflurane anesthetic in an induction chamber (2.5% isoflurane in 1.5 L/min O_2) and their chest was shaved. After shaving the chest of animals, aquasonic 100-ultrasound transmission gel (Parker Laboratories, INC., USA) was applied and rats were placed in supine position and a 15-MHz linear array transducer was placed directly on the shaved chest wall. 2-dimensional guided M-mode images at a 2-mm depth were recorded at the tip of papillary muscles. Averaged data from three consecutive cardiac cycles from each M-mode were used to measured anterior wall thickness (AWT), posterior wall thicknesses (PWT), end diastolic dimension (EDD) and end systolic dimension (ESD) of the left ventricular (LV) chamber during systolic and diastolic cycles. Subsequently, the following equations were used to calculate left ventricular mass (LVM) (ASE-cube formula with Devereux correction factor) (LVM =0.8 [1.04 [(EDD + PWT + AWT) 3 – EDD3]] +0.6). The value of LVM was then normalised for both body weight and tibia length. End-systolic volume (ESV) and LV end-diastolic volume (EDV) was calculated from two-dimensional images according to a modified Simpson's rule. Ejection fraction (EF), stroke volume (SV) and fractional shortening (FS) were then determined from EDV and ESV. Ejection fraction [(EDV-ESV)/ ESDx100]. Fractional shortening [(EDD-ESD)/ EDDx100] and stroke volume= [(EDV-ESV)] Cardiac output was derived as follows: cardiac output [(ESV-EDV) *HR], where HR is heart rate.

2.2.4 Metabolic cages

Metabolic cages were used for housing individual rats for 24 hours for the collection of urine and the monitoring of water in-take, at baseline and before sacrifice of the animals. The metabolic cages (Techniplast, model number 3700M022, Buguggiate, Italy) consist of an upper chamber with a support grid that allows the rat to stand while allowing urine and feces to pass through the grid and into a funnel, which separates and collects the feces and urine. A small feeder and marked water bottle on the outside of the cage allows access to standard rat chow and water. Urine output and fluid intake were saved and recorded at the end of the 24 hours. Urine was collected, allocated into 1 ml samples and stored at -80°C for biochemical analysis.

2.3 Ex vivo experimental procedure

2.3.1 Tissue preparation

At sacrifice animals were anesthetized by isoflurane (5% isoflurane in 1.5 L/min O_2) and the thoracic cavity was opened to expose the heart. Blood samples were collected by cardiac puncture with a 23-gauge needle. Tissues (heart, aorta, kidneys, lungs, liver, brain and fat) were harvested, either snap frozen in liquid nitrogen and stored at -80°C for RNA extraction and protein assays or fixed for histological assessment in a 10% formalin solution overnight at room temperature and subsequently transferred into 70% ethanol. The fixed samples were later embedded in paraffin blocks, which then were cut and baked onto silanised slides at 60°C for 3 hours followed by 40°C overnight. Both the paraffin blocks and sections were kept at room temperature and stored in appropriate boxes. Mesenteric resistance arteries were collected to assess vascular function and morphology by wire myography (more specific details in section 2.3.3). Also, blood samples collected in VACUETTE® heparin lined tubes (Greiner Bio-One, Stonehouse, UK) during sacrifice were kept on ice until centrifugation using VWR® Mega Star 3.0 / 3.0R centrifuge (VWR International, Leicestershire, UK) at 2400 RPM for 20 minutes at 4°C. Plasma was then extracted and stored at -80°C for further experiments.

2.3.2 Organ mass index

Organ weight for whole heart, left ventricle plus septum, kidneys, liver, epididymal fat and retroperitoneal fat were measured at the time of tissue harvest. This was correlated for both body weight and tibia length. After sacrifice, a scalpel blade (Swann-Morton, Sheffield, UK) was used to expose the knee and ankle joint on an extended hind limb, the tibia length was determined using a double-pointed drawing compass and was subsequently measured with a ruler. Both body weight and tibia length were used to measure organ mass index. The absolute values are different but the pattern of change is comparable.

2.3.3 Wire myography

Wire myography is used to examine the functional response and vascular reactivity of isolated small mesenteric resistance arteries. Third order mesenteric resistance arteries were dissected from fat and connective tissue under a dissecting microscope (Carl Zeiss Ltd, Cambridge, UK) and stored in Krebs buffer overnight at 4°C before use. An approximately 2-mm length of artery was mounted onto two stainless steel 40 micron wires on a four channel small vessel myograph (Danish Myotechnology, Denmark). Changes in force were measured by connecting the force transducer to a myo-interface and changes in tension were then recorded using a data acquisition package (ADI Instruments Powelab systems). The vessels were maintained in Krebs buffer (0.25 M NaCl; 0.001 M KCl; 2 mM $MgSO_4$; 50 mM $NaHCO_3$; 2 mM KH_2PO_4; 2 nM $CaCl_2$) warmed to 37°C and bubbled with 95% O_2 and 5% CO_2 (pH 7.4). Following a 30 minutes equilibrium period, vessels were set to a normalized internal diameter (L1) in order to achieve optimal contraction. Internal diameter was calculated using the following equation, $L1 = 0.9*L_{100}$; whereas L_{100} was determined using the LaPlace equation ($P=T/r$; where P is effective pressure, T is wall tension and r is the internal rediau. After 1 hour, contractile response of the vessel was tested by a pretreatment of KCl (10 µmol/L) (wake up technique) to determine the maximum active tension development, which allowed for standardization of initial experimental conditions. Vessels were then washed 4 times with Krebs buffer and were allowed to rest for 30 minutes. A cumulative concentration curve to noradrenalin, 10 nmol/L to 30 µmol/L, was performed followed by a carbachol dose response curve, 10 nmol/L to 10 µmol/L. The dose response to carbachol was performed to determine the percentage of

relaxation in response to the stimulated contraction. The dose response curves were followed by a Krebs buffer wash out to baseline. The concentration required to achieve 50% of the maximum response (EC50) and area under the curve (AUC) were calculated from the response curves.

2.4 General molecular biology

2.4.1 mRNA expression

2.4.1.1 Total RNA extraction from heart, aorta, liver and kidney tissues

Total RNA was extracted from animal tissue using Qiagen column based miRNeasy Mini kits (QIAGEN, Manchester, UK). Whole tissues (≤50 mg) were homogenised in 700 µl buffer RLT lysis solution, containing 0.01% (v/v) β-mercaptoethanol (Qiazol). Tissues were homogenised either with a Polytron 2100 rotor homogeniser at full speed, then centrifuged at 5000 g to collect lysates or by using 5 mm (mean diameter) stainless steel beads and homogenised on the TissueLyser (QIAGEN, Manchester, UK) for 2 minutes at 20 Hz. 140 µl of Chloroform is added to each tube and centrifuge for 15 minutes at 12,000 x g at 4°C. The upper aqueous layer was collected and transferred to a new collection tube containing 525 µl of 70% ethanol. 700 µl of the sample was then transferred into an RNeasy Mini spin column in a 2ml collection tube and centrifuge at 8,000 x g for 15 seconds at room temperature. The flow through was discarded and 700 µl of buffer RW1 was added to the spin columns, samples were spun as before and the flow though discarded. An optional on column DNA digest was carried out (refer to section 2.4.1.3). Spin columns were then transferred to new collection tubes and 500 µl of buffer RPE added, and centrifugations repeated as before. The flow through was discarded prior to another 500 µl of buffer RPE. The spin column was then centrifuged for 2 minutes, at 8000 x g, at room temperature. RNase-free water (50 µl) was then added to the column and centrifuge for 1 minute at 8,000 x g. The first eluate was pipetted back onto the membrane in the columns and spun for 1 minute. The resulting eluate was quantified as described in section 2.4.1.4.

2.4.1.2 Total RNA extraction from adipose tissue

Total RNA was isolated from adipose tissue using Qiagen RNeasy lipid tissue Mini kit (QIAGEN, Manchester, UK). Fatty tissues (≤100 mg) were homogenised in 1 ml

Qiazol lysis reagent using 5 mm stainless steel beads and a TissueLyser for 2 minutes at 20 Hz. The lysates were transferred into fresh microcentrifuge tubes and then 200 µl of chloroform is added to each tube and centrifuged for 15 minutes at 12,000 x g at 4°C. The upper aqueous layer was collected and transferred to a new collection tube containing 600 µl of 70% ethanol. 700 µl of the sample was then transferred into an RNeasy Mini spin column in a 2 ml collection tube and centrifuged at 8,000 x g for 15 seconds at room temperature. The flow through was discarded and 700 µl of buffer RW1 was added to the spin columns, samples were spun as before and the flow though discarded. An optional on column DNA digest was carried out (refer to section 2.4.1.3). Spin columns were then transferred to new collection tubes and 500 µl of buffer RPE added, and centrifugations repeated as before. The flow through was discarded prior to another 500 µl of buffer RPE. The Spin column was then centrifuged for 2 minutes, at 8000 x g, at room temperature. RNase-free water (50 µl) was then added to the column and centrifuged for 1 minute at 8,000 x g. The first eluate was pipetted back onto the membrane in the columns and spun for 1 minute. The resulting eluate was quantified as described in section 2.4.1.4.

2.4.1.3 DNase treatment of extracted total RNA

Extracted total RNA was treated with DNase using the reagents provided in the QIAGEN miRNeasy mini kit (QIAGEN, UK) following the manufacturer's recommendations. The on-column digestion of DNA during the RNA purification is as follows; 350 µl of buffer RWT was added to the spin column and centrifuged for 15 seconds at 8000 x g. 10 µl of DNase I stock was added to 70 µl of buffer RDD which then added to the spin column and left to incubate for 15 minutes at room temperature. Afterwards, 350 µl of buffer RWT was added to the column and centrifuged for 15 seconds. All flow through were discarded and spin columns were used for completion of RNA purification.

2.4.1.4 Measuring nucleic acid concentration

RNA concentrations were quantified using a Nanodrop® ND-1000 spectrophotometer (Thermo fisher Scientific, Loughborough, UK). Absorbance ratios (260 nm/280 nm) of approximately 2.0 for RNA indicated that the nucleic acid preparations were sufficiently free from protein contamination for

downstream experiments. Also, the ratio of absorption at 260 nm and 230 nm was utilised as an indicator of RNA purity; pure RNA has a ratio of (2.0-2.2). A common contaminant, phenol, absorbs at 230 nm. The equation of Beer-Lambert Law of absorption is used to calculate the concentration of the RNA (µg/ml). Concentration of RNA (µg/ml) = (A260 reading – A320 reading) x 40.

2.4.1.5 Reverse transcription (RT)-PCR

The preparation of cDNA from RNA templates by reverse transcription for quantitative real-time PCR (qRT-PCR) was performed using Applied Biosystems High Capacity cDNA Archive Kit (Applied Biosystems). All steps were performed according to manufacturer's instructions. 1 µg of RNA samples were reverse transcribed into cDNA in a 20 µl reaction containing a final concentration of 10X reaction buffer, 25 mM $MgCl_2$, 2.5 mM dNTP mixture, 20 u/µl RNase inhibitor, 50 µM of random hexamers, 50 U/µl of reverse transcriptase (Multiscribe) in a 96-well plate (Thermo Fischer Scientific, Loughborough, UK). The reaction was then placed on a thermocycler and underwent the following two-step reaction conditions: 25°C for 10 minutes, 48°C for 30 minutes, 95°C for 5 minutes, 4°C for 10 minutes then 12°C forever. The plate was then stored at -20°C until use.

Applied Biosystems TaqMan Reverse Transcription Reagents:

Reagent	Volume (µl)
10X Reaction Buffer	2 µl
25 mM $MgCl_2$	4.4 µl
2.5mM dNTPs	4 µl
50 µM Random hexamers	1 µl
20 U/µl RNase Inhibitor	0.4 µl
50 U/µl MultiScribe RT	0.5 µl
1 µg RNA	1 µl
RNAse free water	7.7µl
Total Volume	20 µl

2.4.1.6 Real-Time Polymerase Chain Reaction

Relative real-time RT-PCR quantitation of the samples was carried out using the QuantStudio™ 12K Flex Real-Time PCR System from Applied Biosystems in a multiplex reaction. Expression of the gene of interest was always measured relative to the housekeeping control gene. The gene of interest and ß-actin, B2M or glyceraldehyde-3-phosphate dehydrogenase (GAPDH) probe (housekeeper) were amplified in duplex PCR reactions, probes for the gene of interest were tagged to 'FAM' labelled fluorescent dyes, while housekeeper probes were labelled with 'VIC' dye, they fluoresce at different wavelengths, allowing them to be measured in the same reaction. All reactions were performed in 5 µl volumes in 384-well plates.

Reaction mix	**Volume (µl)**
2X Taqman Master Mix	2.5
Probe FAM labelled	0.25
Housekeeper VIC labelled	0.25
cDNA	2.0
Total Volume	5 µl

All samples were amplified in triplicate. Fluorescence of FAM and VIC dyes were measured for all reactions during temperature cycling. Data was analysed using a combination of Applied Biosystems SDS (Sequence Detection Software) and Microsoft Excel (2016) software.

Temperature cycling:

Heat Cycle	**Time**	
50 °C	2 min	**Stage 1**
95 °C	7.14 min	
95 °C	15 sec	**Stage 2**
60 °C	1 min	**X40**

2.4.1.7 Analysis of qRT-PCR

The exponential phase of the PCR reaction releases the fluorescence from the respective qRT-PCR probe (FAM and VIC), which is measured by QuantStudio™ 12K Flex Real-Time PCR System. Sequence Detection Software (SDS) plotted the amplification curves as cycle number versus fluorescence for both dyes in every well. A threshold of fluorescence is set during the exponential phase of amplification. The cycle number at which the fluorescence signal crosses this set threshold is termed the cycle threshold (C_t) (Figure 2-1). qRT-PCR results were analysed using the relative quantification (RQ) method of comparative C_t. The 'cycle threshold value' (C_t value) for each amplification. The housekeeper acts as a normalising control for RNA concentrations and its stability and consistency were tested in triplicate for each experimental condition. Housekeeping gene expression was used to calculate the ΔC_t for gene of interested and the equation to calculate ΔC_t is as follows:

$$\Delta C_t = C_{t\,(Sample)} - C_{t\,(Housekeeper)}$$

All experiments were compared to a reference control (calibrator) to calculate the $\Delta\Delta C_t$ as follows: $\Delta\Delta C_t = \Delta C_{t\,(Sample)} - \Delta C_{t\,(Reference)}$

Relative quantification (Fold of change) was calculated as follows:

$$\text{Relative Quantification (RQ)} = 2^{-\Delta\Delta Ct}$$

The calibrator is untreated or control group which all samples are compared to. The calibrator has a RQ value of 1.

Range of possible RQ values was calculated by the standard error of the ΔC_t using RQ min and RQ max as follows:

Pre RQ min= $2^{-\Delta\Delta Ct}$ + standard error

Pre RQ max= $2^{-\Delta\Delta Ct}$ - standard error

From these equations, RQ min and RQ max were calculated as follows:

RQ min= RQ - Pre RQ min

RQ max= RQ + Pre RQ max

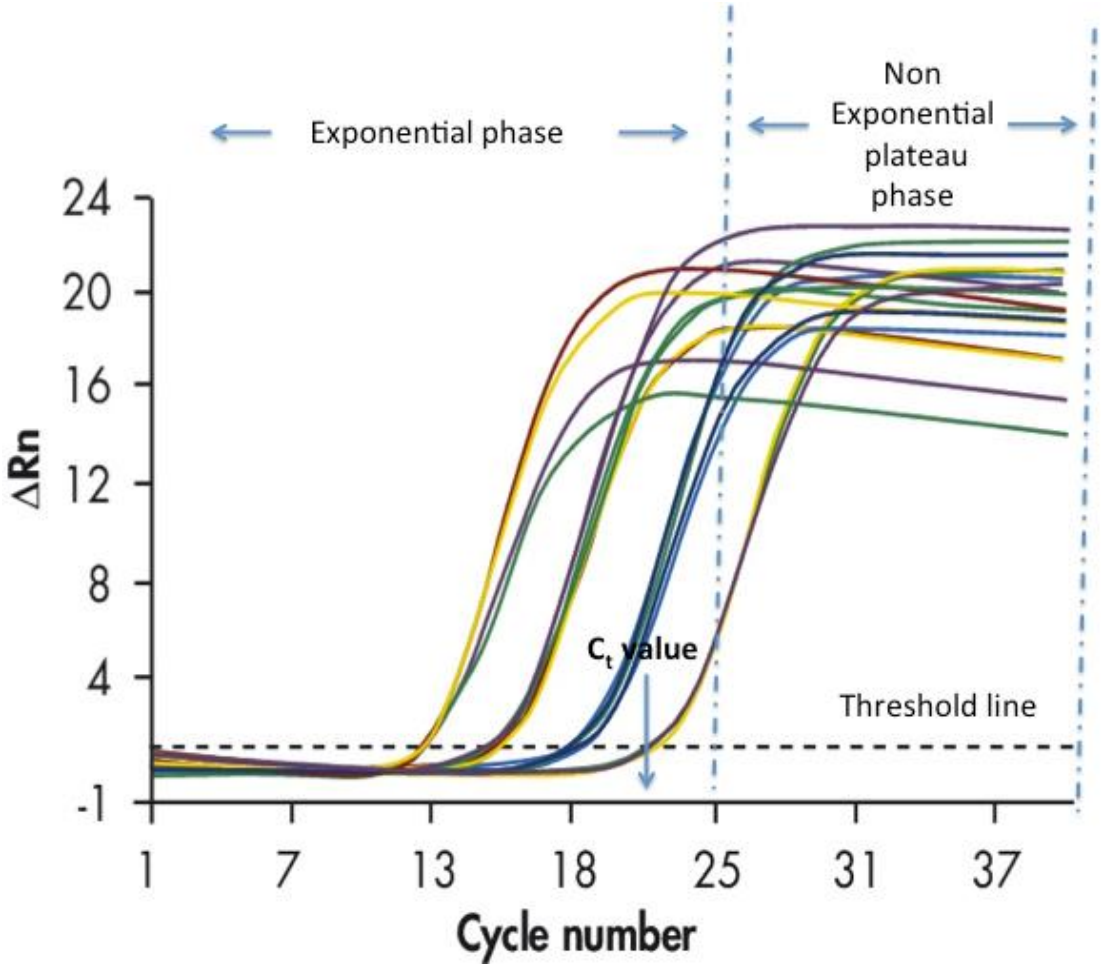

Figure 2-1: Example of qPCR amplification curve.

Amplification plots are created when the fluorescent signal from each sample is plotted against cycle number over the duration of the real-time PCR experiment. Threshold cycle (Ct) is the cycle number of which the fluorescent signal of the reaction crosses the threshold.

2.5 Quantification of hexadecanedioate level in plasma samples

Quantitative analysis of hexadecanedioate level in serum samples of WKY and SHRSP rats were carried out by Dr Christian Reichel and Dr Anja Huber (Seibersdorf laboratories, Austria) using Liquid chromatography–mass spectrometry (LC-MS/MS). The method was provided by Dr Christian Reichel.

2.5.1 Sample preparation

100 µl of rat serum were mixed with 50 ng of hexadecanedioate-d28 internal standard (CDN Isotopes, UK). For protein precipitation, 850 µl of methanol (Merck, USA) were added, the mixture was vortexed two times for 5 seconds and centrifuged for 3 minutes at 10°C and 14.000 rcf. The supernatant was transferred into a new V-vial (Phenomenex, USA) and dried under vacuum pressure for 45 minutes at 45°C. The dried material was redissolved in 100 µl of 20% methanol and hexadecanedioate was measured using LC-MS/MS.

2.5.2 Calibration

To generate a calibration curve for hexadecanedioate, six different concentrations (5, 10, 20, 30, 40 and 50 ng/ml; in the result table referred to as standards 1, 2, 3, 4, 5 and 6) of the substance were each mixed with 50 ng of hexadecanedioate-d28 internal standard in new V-vials. The mixture was dried under vacuum for 45 minutes at 45°C. The dried material was redissolved in 100 µl of 20% methanol and hexadecanedioate was measured using LC-MS/MS. Standard mixtures 1, 2, 3 and 4 were measured two times on two different days to guarantee reproducibility. When fragmented in MS/MS mode, hexadecanedioate dissociates into several product ions. The fragment ion showing the most intense mass signal was used for quantification (m/z 223) (Figure 2-2).

2.5.3 LC-MS/MS

For all analyses, an LC-MS/MS instrument of the TSQ Vantage series (Thermo Scientific), a reversed-phase C-18 column (Dionex Acclaim PolarAdvantage II, 4.6 x 50 mm, 3 µm) and following chromatographic conditions were used: 100% water/0.2% formic acid (1 min, isocratic), linear gradient to 100% methanol/0.1% formic acid (3 min), 100% methanol/0.1% formic acid (2.5 min, isocratic) and linear gradient back to 100% water/0.2% formic acid (1.5 min). Hexadecanedioate was analysed in negative ion mode (ESI-, transition 285→223), meaning that negatively charged iones were detected in the mass analyser.

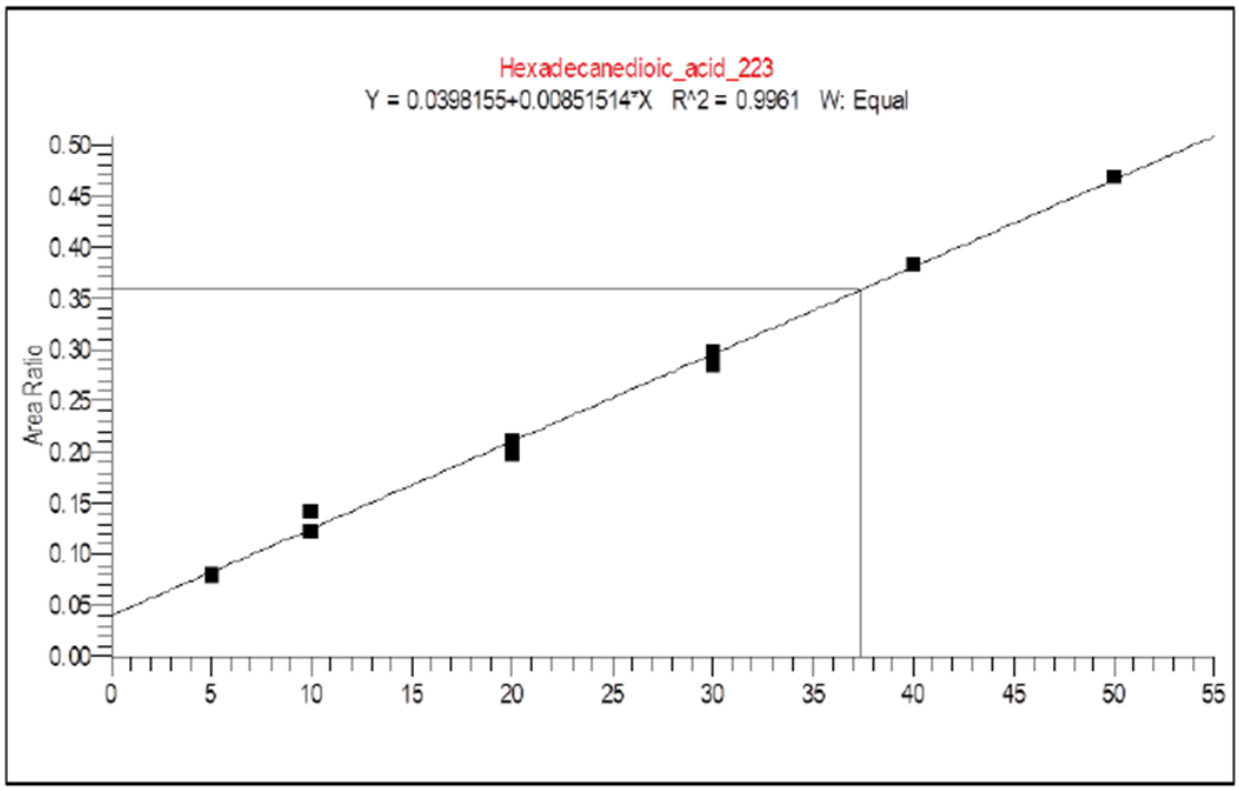

Figure 2-2: Calibration curve of hexadecanedioate.

The product ion showing the most intensive mass peak was used for quantification (*m/z* 223). On the x-axis hexadecanedioate concentration [ng/ml] and on the y-axis the area ratio (ratio between signal of standard and internal standard) are shown.

2.6 Statistical Analysis

Statistical analysis was performed using Minitab 17. Data are presented by mean ± standard error of mean using Graphpad Prism 5 (San Diego, California, USA). Statistical significance was assumed at P-value less than 0.05. For comparisons of a continuous variable between two experimental groups, paired and two Student's t-tests were applied as appropriate. For statistical comparisons in data sets with more than two groups, analysis of variance (ANOVA) was applied, followed by post-hoc Tukey's test. Repeated measures ANOVA (a general linear model ANOVA) was used to compare radiotelemetry and echocardiography data between groups. Detailed statistical analyses for certain experiments are specified in the relevant results chapters.

2.6.1 Power calculations:

Sample size estimates were based on power calculations from previous radiotelemetry blood pressure studies in rats. It was estimated that 9-10 rats per group would allow 90% power at α=0.05 to detect differences of 10 mmHg. The pressor response to noradrenaline measured by wire myography was also determined in a previous pilot study, which revealed physiological effects in the order of 2 SDs or greater with 90% power at α=0.05 with 9 rats per group.

Chapter 3 Effect of exogenous hexadecanedioate on blood pressure regulation

3.1 Introduction

Hexadecanedioate is a long chain dicarboxylic fatty acid, which has been found to be associated with blood pressure elevation and mortality (Menni *et al.*, 2015). The mechanisms through which hexadecanedioate regulates blood pressure are currently unknown, and require elucidation. This chapter aimed to verify the causal role of hexadecanedioate in blood pressure regulation, by carrying out intervention studies using normotensive Wistar Kyoto (WKY) rats and Stroke Prone Spontaneously Hypertensive Rats (SHRSP).

Previous studies in humans and rat models have already demonstrated links between fatty acids (FAs) and hypertension. For example levels of several fatty acids were found to be highly correlated with development of high blood pressure in the spontaneously hypertensive rat (SHR) when compared with Wistar Kyoto (WKY) rats (Lu *et al.*, 2008). Also, a cross sectional study performed by Wang *et al* in 232 randomly selected subjects aged between 35 and 60 years, showed that essential hypertensive patients had marked alteration in FA metabolism compared to normotensive subjects (Wang *et al.*, 2008). Moreover, a study by Guo *et al.* showed that increased free FA level is an independent risk factor for prevalence of hypertension (Guo *et al.*, 2015). Therefore, it is suggested that abnormal FA metabolism may play an essential role in the pathogenesis of hypertension.

Although there is evidence that long-chain fatty acids can impact blood pressure regulation and influence vasodilatation via large-conductance Ca^{2+}- and voltage-activated K^+ channels (Hoshi *et al.*, 2013), currently there is no evidence regarding the mechanism of how hexadecanedioate affects blood pressure elevation. Therefore, this study was designed to investigate the relationship between the dicarboxylic acid and blood pressure regulation and to identify any underlying pathological changes.

3.2 Hypothesis

Increased circulating hexadecanedioate levels mediate blood pressure elevation, which leads to target organ damage.

3.3 Aims

1. To determine the effect of elevated hexadecanedioate on blood pressure, vascular function and end organ damage in normotensive WKY rats using exogenous hexadecanedioic acid administration.

2. To examine the dose response of hexadecanedioic acid on blood pressure in adult male WKY rats by oral administration of a range of doses (e.g. 250, 300, 350, 400, 450 and 500 mg/kg/day) over six-week treatment period.

3. To examine the impact of longer-term hexadecanedioic acid treatment on blood pressure, vascular function and end organ damage in normotensive WKY rats and in a hypertensive rat model (SHRSP).

3.4 Methods

3.4.1 Animals

Three intervention studies were carried out to examine the effects of hexadecanedioate on blood pressure regulation and end-organ damage.
In the first intervention study, male Wistar Kyoto (WKY) rats were purchased from Harlan (Hillcrest, UK). In the second and third intervention studies male Wistar Kyoto (WKY_{Gla}) rats and male Stroke Prone Spontaneously Hypertensive rats ($SHRSP_{Gla}$) were obtained from breeding colonies maintained at the University of Glasgow. The $_{Gla}$ suffix identifies that strains originate from the Glasgow colonies. The rats were housed individually in cages on a 12 hours light/dark cycle at room temperature (21± 3°C). Rats were given *ad libidum* access to food and water. The study protocols were approved by the Animals' Scientific Procedures Act 1986 under the project license of Dr Delyth Graham (70/9021).

3.4.2 Experimental protocol for examination the impact of hexadecanedioic acid treatment on blood pressure regulation

The first intervention study was carried out in adult male WKY rats aged 10 weeks. The oral hexadecanedioic acid treatment (250 mg/kg/day) (Sigma Aldrich Co Ltd, Irvine, UK) doses were prepared in baby food (egg custard with rice, Heinz Co. Ltd., Hayes, Middx.) on a weekly basis (n=10) and frozen until required, and the control group (n=9) was given the same amount of the baby food without the drug. The treatment was administered for four weeks with monitoring of the haemodynamic parameters carried out using the Dataquest V telemetry system (Data Sciences International) and cardiac functions measured by echocardiography. Kidney function was assessed using 24 hours urine collections by metabolic cages. At sacrifice, blood samples were collected by cardiac puncture (Chapter 2, Section 2.3.1), main organs (i.e. heart, liver, kidney and vascular tissue) samples were harvested, and mesenteric arteries were dissected to assess vascular function and morphology by wire myography (Figure 3-1).

3.4.3 Experimental protocol for dose response curve of hexadecanedioic acid on blood pressure

To determine the concentration range at which hexadecanedioic acid levels have an impact on blood pressure regulation, WKY_{Gla} rats (n=3) implanted with radiotelemetry probes, were administered increasing dosages of oral hexadecanedioic acid at aged 12 weeks. The dose increased weekly by 50 mg (i.e. 250 mg/kg, 300 mg/kg, 350 mg/kg, 400 mg/kg, 450 mg/kg and 500 mg/kg). The starting dose of hexadecanedioic acid (250 mg/kg/day) was selected based on previous studies (Russell *et al.*, 1991; Frenkel *et al.*, 1994). The drug was discontinued at dose 500 mg/kg/day to ensure the dose remained palatable for the rats and to avoid potential toxicity. Blood pressure parameters were monitored via the telemetry system for 7 weeks including at baseline and during treatment (Figure 3-2).

3.4.4 Experimental protocol for longer-term hexadecanedioic acid treatment

Six-week-old male WKY_{Gla} and $SHRSP_{Gla}$ were treated orally with hexadecanedioic acid (250 mg/kg per day; n=3) or vehicle (n=3) for 9 weeks. Blood pressure was measured weekly by tail cuff plethysmography and cardiac function was assessed at two week intervals by echocardiography. At sacrifice the main organs (i.e. heart, liver, kidney and vascular tissue) were harvested, snap frozen and formalin fixed for histological analysis (Figure 3-3).

3.4.5 *In vivo* analysis

3.4.5.1 Radiotelemetry surgery

Systolic (SBP) and diastolic blood pressure (DBP), heart rate and activity were directly monitored using the Dataquest V telemetry system (Data Sciences International). The animals were anesthetised by isoflurane in an anesthetic induction chamber (anaesthesia was induced at 5% Isoflurane in 1.5 L/min O_2, and subsequently maintained at 2.5% Isoflurane in 1.5 L/min O_2) and the operation was conducted under sterile conditions. The incision was prepared on the mid line of the abdomen and opened by retractors. The intestines were externalised and kept moist using sterile gauze soaked in sterile PBS. The internal organs were protected with sterile cotton gauze pads to expose the descending aorta. The telemetric

probe (TA11PA/C40) was introduced into the peritoneal cavity, and the catheter inserted into the distal descending aorta and then secured with biological glue. The probe was sutured to the peritoneum muscle wall with non-absorbable sutures (Ethilon) (Ethicon, USA), and the outer skin layer secured with absorbable sutures (Vicryl) (Ethicon, USA). After that, the animals were left for one week for recovery. A more detailed description of the procedure is provided in Chapter 2, Section 2.2.2.2.

3.4.5.2 Tail Cuff Plethsymography

Measurement of systolic blood pressure was carried out as described in the main methods section (Chapter 2, Section 2.2.2.1) and was used for blood pressure measurement in the longer-term intervention study. Male WKY_{Gla} and $SHRSP_{Gla}$ rats, starting from the age of 6 weeks old, were measured every week in order to measure SBP. Multiple cuff inflation/deflation values were obtained through the duration of each tail-cuff session and an average was taken for each animal.

3.4.5.3 Echocardiography

Echocardiography was performed on anesthetised rats (1.25%-1.5 % isoflurane in 1.5l/min O_2). Left ventricular motion mode (M-mode) measurements at the level of the papillary muscles were used to delineate wall thickness and internal diameter at systole (s) and diastole (d). Images were captured using an Acuson Sequoia C512 ultrasound system and then used to assess cardiac function and contractility. The cardiac index was estimated as cardiac output adjusted for tibia length or body weight, as previously described in Chapter 2, Section 2.2.3.

3.4.5.4 Metabolic cages

WKY rats were housed in metabolic cages for 24 hours for the collection of urine and the monitoring of water in-take at baseline and prior to sacrifice. Urine was kept on ice and stored at -80°C, until required for biochemical analysis. More information on this process is available in Chapter 2, Section 2.2.4.

3.4.6 *Ex vivo* analysis

3.4.6.1 Tissue collection

At sacrifice, animals were anesthetised by isoflurane (5% Isoflurane in 1.5 L/min O_2) and the thoracic cavity was opened to expose the heart. Blood samples were collected by cardiac puncture with a 23-gauge needle. Tissues were excised and any excess blood removed by blotting before weighing the kidneys, whole heart, left ventricle plus septum, liver and fat after dissection. Tissue/organ weights were corrected to tibia length and body weight. Further details are provided in Chapter 2, Sections 2.3.1 and 2.3.2.

3.4.6.2 Wire myography

Mesenteric resistance arteries were carefully dissected and cleaned from fat and connective tissue under a microscope. The arteries were then mounted onto 40 micron wires in the myograph (Multimyograph Model 610, DMT Denmark) and the lengths of arteries were measured by calibrated eyepiece in a microscope. All baths of the multimyograph (model 610M) were set at a temperature of 37°C and then gassed with 95% O_2 and 5% CO_2 to place the vessels in standard conditions. The evaluation of the physiological responses of the vessels was recorded using computer software (Lab chart 7). A normalization technique was used to determine the internal circumference the vessel would have under a transmural pressure of 100 mmHg (13.3 KPa) by carrying out a number of stepwise stretches of the vessel, measuring micrometer (x) and force (y) readings, until a force of 13.3 KPa is reached. This gives the micrometer reading required to set the vessels at the required tension. Forty minutes after normalisation, a wake-up procedure was performed. The aims of this technique were to reactivate the signalling mechanism of the vessels and validate the function and response of the vessels that have not been damaged through the dissection process. This technique was implemented following warming, equilibration and stretching with specific passive tension (X1). Vessels were then subject to a wake up technique as previously described in Chapter 2, Section 2.3.3. To establish the vessel's contractile response curve, noradrenaline was added at the following cumulative concentrations: $1x10^{-9}$, $3x10^{-9}$, $1x10^{-8}$, $3x10^{-8}$, $1x10^{-7}$, $3x10^{-7}$, $1x10^{-6}$, $3x10^{-6}$, $1x10^{-5}$ and $3x10^{-5}$ M. To determine the vessel's endothelium-dependent relaxation response, carbachol was added at the following increasing concentrations: $1x10^{-}$

^{8}, $3x10^{-8}$, $1x10^{-7}$, $3x10^{-7,}$ $1x10^{-6}$, $3x10^{-6,}$ $1x10^{-5}$ M. The maximum response (EC50) and area under the curve (AUC) were then calculated from the response curves. More details are available in Chapter 2, Section 2.3.3.

3.4.7 Histology

3.4.7.1 Tissues preparation for histology

Tissues (heart, liver and kidney) were fixed for 24 hours in 10% formalin at room temperature. After 24 hours, the formalin was replaced with 70% ethanol and kept overnight. The next day, tissues were then placed in histology cassettes (Thermo Fisher, Paisley, UK) and placed in a Citadel 1000 processor (Fisher Scientific, Loughborough, UK) at the following settings: 70 % ethanol 30 minutes, 95 % ethanol 30 minutes, 100% ethanol 30 minutes, 100% ethanol 30 minutes, 100% ethanol 45 minutes, 100% ethanol 45 minutes, 100% ethanol 60 minutes, 100% ethanol/xylene 30 minutes, xylene 30 minutes, xylene 30 minutes, wax 30 minutes, wax 30 minutes, wax 45 minutes, wax 45 minutes. The total running time was 8 hours and 30 minutes. Tissues were embedded using Shandon Histocentre 3 embedding centre (Thermo Fisher Scientific, Loughborough, UK) and Histoplast paraffin (Thermo Fisher Scientific, Loughborough, UK). Paraffin sections of 5 µm were cut using a Leica Finese 325 Microtome (Thermo Fisher Scientific, Loughborough, UK) and placed in an oven at 60°C overnight. Eight to ten slides were taken per sample per animal and then stored at room temperature until used. Paraffin blocks were stored at 4°C.

3.4.7.2 Haematoxylin and Eosin staining

Immediately prior to staining, slides were deparaffinised twice in histoclear for 7 minutes then rehydrated through an ethanol gradient (100%, 95% and 75%; 7 minutes each) into distilled H_2O for 7 minutes. Slides were stained with Harris haematoxylin (CellPath Ltd, Newtown, UK) for 2 minutes and then washed under a running tap water for 5 minutes. The sections were transferred to 70% ethanol for 30 seconds and then to eosin (CellPath Ltd, Newtown, UK) for 3 minute. Sections were then dehydrated through a reverse ethanol gradient of 95% twice for 30 seconds at each stage. The sections were then transferred to 100% ethanol for 1 minute followed by 100% ethanol for 5 minutes. Subsequently, sections were washed twice with Histoclear for 7 minutes and mounted using DPX (Phthalate

free) mounting medium (CellPath Ltd, Newtown, UK). Examination was performed under a microscope Olympus BX41 (Olympus America Inc, Center Valley), where the nuclei appeared purple and the cytoplasm pink. Eight to ten images were taken using a QImaging Go3 camera (QImaging, Canada) attached to the microscope and analysed by QCapture pro6 software (Qimaging, Canada). Double-blind histological analysis was performed using Image J 1.52a (National Institutes of health, USA). Percentage of renal artery wall thickness (%WT) was calculated by measuring the external diameter and the inner lumen.

3.4.8 Biochemistry analysis

3.4.8.1 Biochemistry analysis on plasma and urine samples

Biochemistry analysis on plasma and urine samples obtained from hexadecanedioic acid treated and control WKY rats were carried out by Mrs. Elaine Butler at the clinical biochemistry lab (British Heart Foundation Glasgow Cardiovascular Research Centre, Glasgow, UK). The quantitative determination of alanine aminotransferase (ALT) (U/L), aspartate aminotransferase (AST) (U/L), urea (mmol), creatinine (mmol), bilirubin (mmol), albumin (g/L), sodium (Na) (mmol), potassium (K) (mmol) and chloride (Cl) (mmol) levels were measured using Roche/Hitachi cobas c 311 systems.

3.4.8.2 Quantification of hexadecanedioate level in plasma samples

Quantitative analysis of hexadecanedioate levels in plasma samples of WKY rats was carried out by Dr Christian Reichel and Dr Anja Huber (Seibersdorf laboratories, Austria) using liquid chromatography–mass spectrometry (LC-MS/MS). More details are provided in Chapter 2, Section 2.5.

3.4.9 Statistics and Data analysis

Data are presented by mean ± standard error of mean by Graphpad Prism 5 (San Diego, California, USA). Statistical analyses for haemodynamic parameters and echocardiography were carried out by repeated measures ANOVA (general linear model). For metabolic cage results, paired t-tests were used. One way ANOVA was applied to analyse the results of more than two groups, followed by a post-hoc Tukey's test. Two sample t-tests were used in analysis of other data using Minitab

16 statistical software. Statistical significance was assumed at P-value less than 0.05.

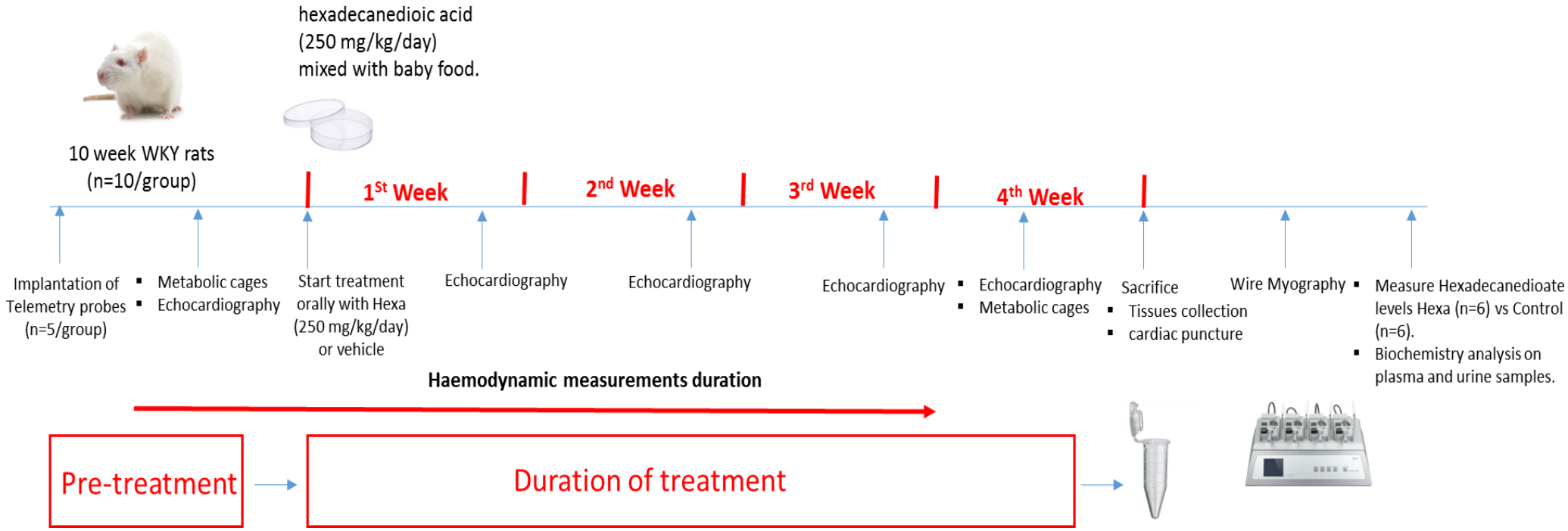

Figure 3-1: Timeline of the first intervention study to examine the impact of hexadecanedioic acid treatment (250 mg/kg/day) on blood pressure regulation.

Harlan WKY rats (n=10) treated orally with hexadecanedioic acid for four weeks with monitoring of the haemodynamic parameters carried out using the Dataquest V telemetry system and cardiac functions measured by echocardiography. Kidney function was assessed using 24 hours urine collections by metabolic cages. At sacrifice, blood samples were collected by cardiac puncture and organs samples were harvested, and mesenteric arteries were dissected to assess vascular function by wire myography.

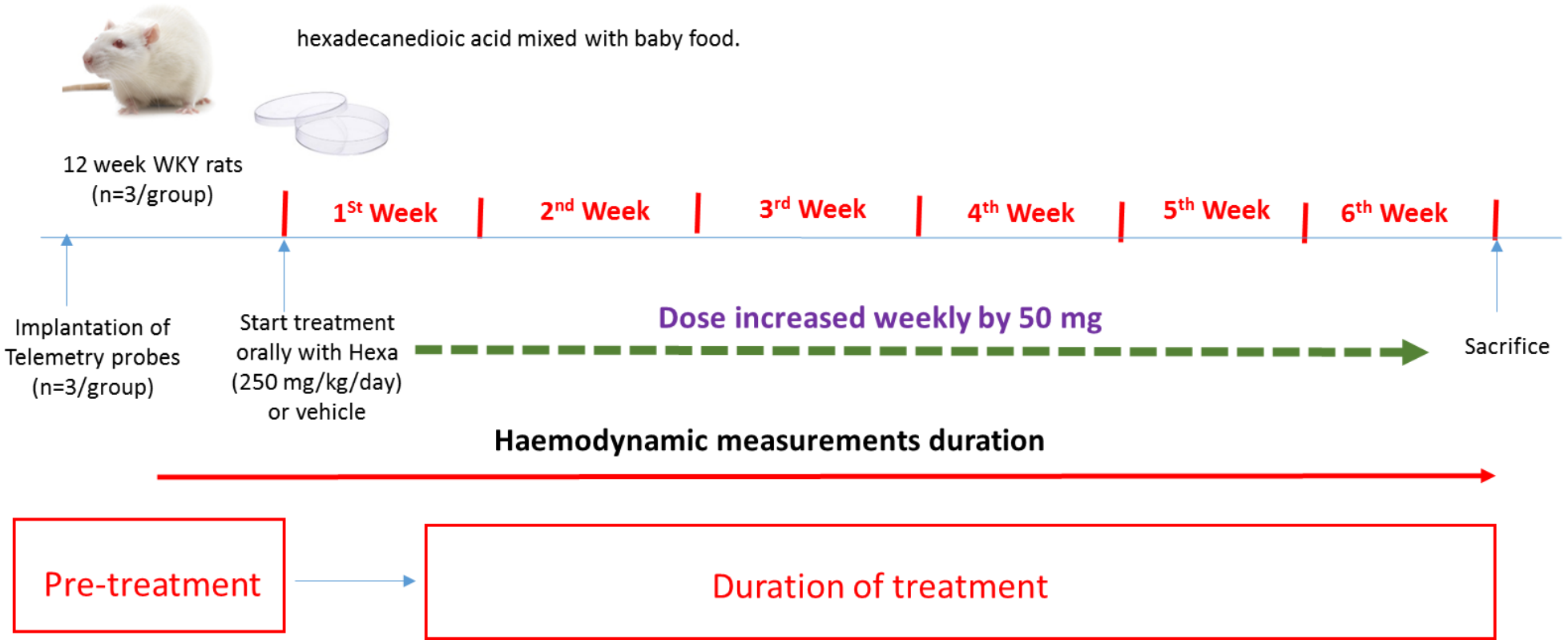

Figure 3-2: Timeline of dose response curve of hexadecanedioic acid on blood pressure.

Twelve-week-old male WKY_{Gla} (n=3/group) treated with hexadecanedioic acid or vehicle. The dose increased weekly by 50 mg (i.e. 250 mg/kg, 300 mg/kg, 350 mg/kg, 400 mg/kg, 450 mg/kg and 500 mg/kg). Blood pressure parameters were monitored via the telemetry system for 7 weeks including at baseline and during treatment.

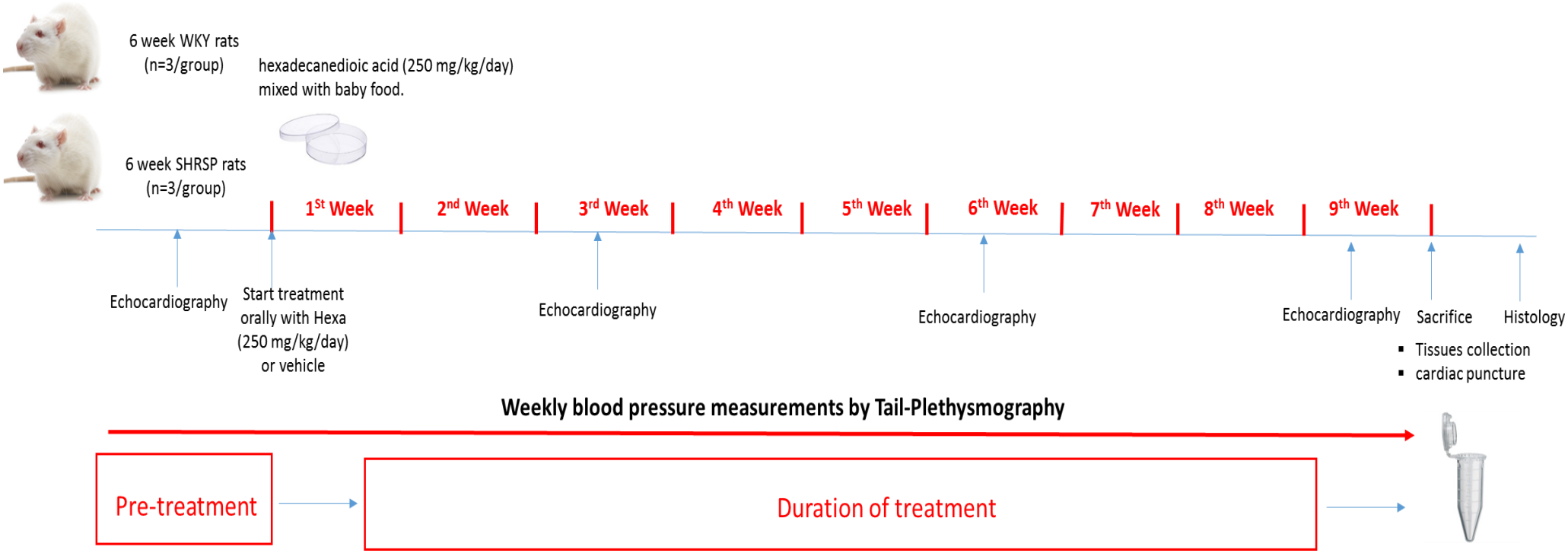

Figure 3-3: Timeline of longer-term hexadecanedioic acid treatment.

Six-week-old male WKY_{Gla} and $SHRSP_{Gla}$ were treated orally with hexadecanedioic acid (250 mg/kg per day; n=3) or vehicle (n=3) for 9 weeks. Blood pressure was measured weekly by tail cuff plethysmography and cardiac function was assessed at two week intervals by echocardiography. At sacrifice, the main organs were collected, snap frozen and formalin fixed for histological analysis.

3.5 Results

3.5.1 The impact of hexadecanedioic acid (250 mg/kg/day) on blood pressure and end organ damage

3.5.1.1 The effect of hexadecanedioic acid on haemodynamic parameters

After the recovery period from the radiotelemetry surgery, a delayed separation of systolic blood pressure (SBP) and mean arterial pressure (MAP) were observed between hexadecanedioic acid-treated WKY rats and vehicle-treated WKY rats occurring one week after the start of hexadecanedioate treatment. However, this hexadecanedioic acid-induced rise in blood pressure did not reach statistical significance (SBP, P=0.084), (MAP, P=0.057); respectively (Figure 3-4 A, B). There was no change in diastolic blood pressure (DBP) between the hexadecanedioic acid-treated rats and control rats (P=0.773) (Figure 3-4 C). Also no change was observed in heart rate over the course of the study between the hexadecanedioic acid-treated rats compared to the control rats (P=0.813) (Figure 3-4 D) (Menni, *et al.*, 2015). The activities of hexadecanedioate-treated rats showed no significant difference compared to control WKY rats (P=0.10) (Figure 3-5).

3.5.1.2 Echocardiography

M-mode echocardiographic findings are summarised in Table 3-1. The levels of left ventricular mass normalised either to body weight or tibia length showed no significant difference during the study period between hexadecanedioic acid-treated rats compared with vehicle-treated rats (LVM/ Body weight, P=0.13), (LVM/tibia length, P=0.39); respectively. However, final echocardiography measurement showed a significant reduction in left ventricular mass normalised to body weight in hexadecanedioic acid-treated rats compared to their respective controls (P=0.017). Also, no significant changes in left ventricular mass normalised to tibia length in hexadecanedioic acid-treated rats compared to their respective controls (P=0.092).

Relative wall thickness (RWT), fractional shortening (FS) and ejection fraction (EF) showed no significant changes between hexadecanedioic acid-treated rats compared with vehicle-treated rats (Table 3-1). Stroke volume and cardiac output

for hexadecanedioic acid-treated rats also showed no difference compared with the vehicle-treated rats (SV, P=0.95), (CO, P=0.200); respectively (Table 3-1).

3.5.1.3 Vascular responses to exogenous noradrenaline and carbachol

Vascular reactivity to noradrenaline was significantly increased in the mesenteric resistance arteries of hexadecanedioic acid-treated rats compared with controls. The mesenteric resistance arteries of rats treated with hexadecanedoic acid started contraction at lower noradrenaline concentration compared with the mesenteric resistance arteries of control rats, indicating a significantly increased sensitivity to noradrenaline. This is illustrated as a shift to the left of the concentration response curve in the mesenteric resistance arteries of hexadecanedoic acid-treated rats (hexadecanedioate area under the curve 100.8±9.3 versus control area under the curve 81.7±8.8 AUC; P=0.013; EC50, P=0.044) (Figure 3-6 A). Relaxation in response to carbachol did not differ between the mesenteric resistance arteries from control or hexadecanedioic acid-treated WKY rats (Figure 3-6 B).(Menni, *et al.*, 2015).

3.5.1.4 Plasma hexadecanedioate levels

Plasma levels of hexadecanedioate were significantly increased in WKY rats after treatment with oral hexadecanedioic acid for four weeks compared with controls WKY (2.86 ± 0.36 ng/ml vs 1.56 ± 0.18 ng/ml, P=0.014), as shown in figure 3-7 (Menni *et al.*, 2015).

3.5.1.5 Renal functions

No changes were observed in water intake between hexadecanedioic acid-treated rats compared to control rats (hexadecanedioic acid-treated water intake 38.7 ± 4.8 ml versus control water intake 35.9 ± 3.5 ml, P=0.352), as shown in Figure 3-8 A. Also, no significant difference in water intake levels were observed in hexadecanedioic acid-treated rats after treatment with hexadecanedioic acid (Δ water intake=3.4 ml, P=0.57). Moreover, no significant difference was observed in urine output of hexadecanedioic acid-treated rats compared to control rats (hexadecanedioic acid-treated urine output 17.9 ± 2.2 ml versus control urine output 12.96 ± 1.22 ml, P=0.09). In addition, no change was observed in urine

output level after hexadecanedioic acid administration when compared with pre-hexadecanedioic acid treatment urine output (16 ± 2.5 ml, P=0.26) (Figure 3-8 B).

3.5.1.6 Biochemical findings

The levels of AST, ALT, bilirubin and albumin were measured in plasma samples as liver function biomarkers. The hexadecanedioic acid treatment did not affect the liver specific enzymes. No changes were observed in the ALT, AST, bilirubin or albumin levels of hexadecanedioic acid-treated rats compared to control rats (Table 3-2). In addition, the levels of serum kidney biomarkers (i.e. urea, creatinine) showed no changes in hexadecanedioic acid-treated rats compared to control rats. Also, no changes were observed in the levels of sodium, potassium and chloride between hexadecanedioic acid-treated rats or control rats, as presented in Table 3-2. However, creatine kinase enzyme levels were significantly decreased in hexadecanedioic acid-treated rats compared to control rats (P=0.015).

The levels of bilirubin and creatinine were also measured in urine samples. The creatinine levels showed no significant difference between hexadecanedioic acid-treated rats and control rats (P=0.804). However, bilirubin levels were significantly increased in hexadecanedioic acid-treated rats compared to control rats (P=0.041), as shown in Table 3-3.

3.5.1.7 Organ mass index

Organ mass indexes for whole heart, left ventricle plus septum, liver, kidneys, and adipose tissues were measured at time of tissue collection. No significant differences were observed in the heart weight when normalised to body weight of hexadecanedioic acid-treated rats compared to control rats (P=0.513). To compare the accuracy of the left ventricular mass estimated by echocardiography, the left ventricular plus septal wall weight of the sacrificed rats was also measured. The left ventricular plus septal wall weight normalised to body weight showed no significant difference in hexadecanedioic acid-treated rats compared to control rats (P=0.18) (Table 3-4). Similarly, there was no significant difference in the weight of either right or left kidneys, when normalised to body weight in hexadecanedioic acid-treated rats compared to control rats (left kidney, P=0.93; right kidney P=0.59) (Table 3-4). Additionally, statistical analysis showed no

significant differences in liver weight normalised to body weight of hexadecanedioic acid-treated rats compared to controls (P=0.88) (Table 3-4). Furthermore, the weight of epididymal fat and retroperitoneal fat pads normalised to body weight did not show any differences between hexadecanedioic acid-treated rats compared to control rats (epididymal fat, P=0.64; retroperitoneal fat, P=0.89). The same pattern was shown when normalised to tibia length, as shown in (Table 3-4).

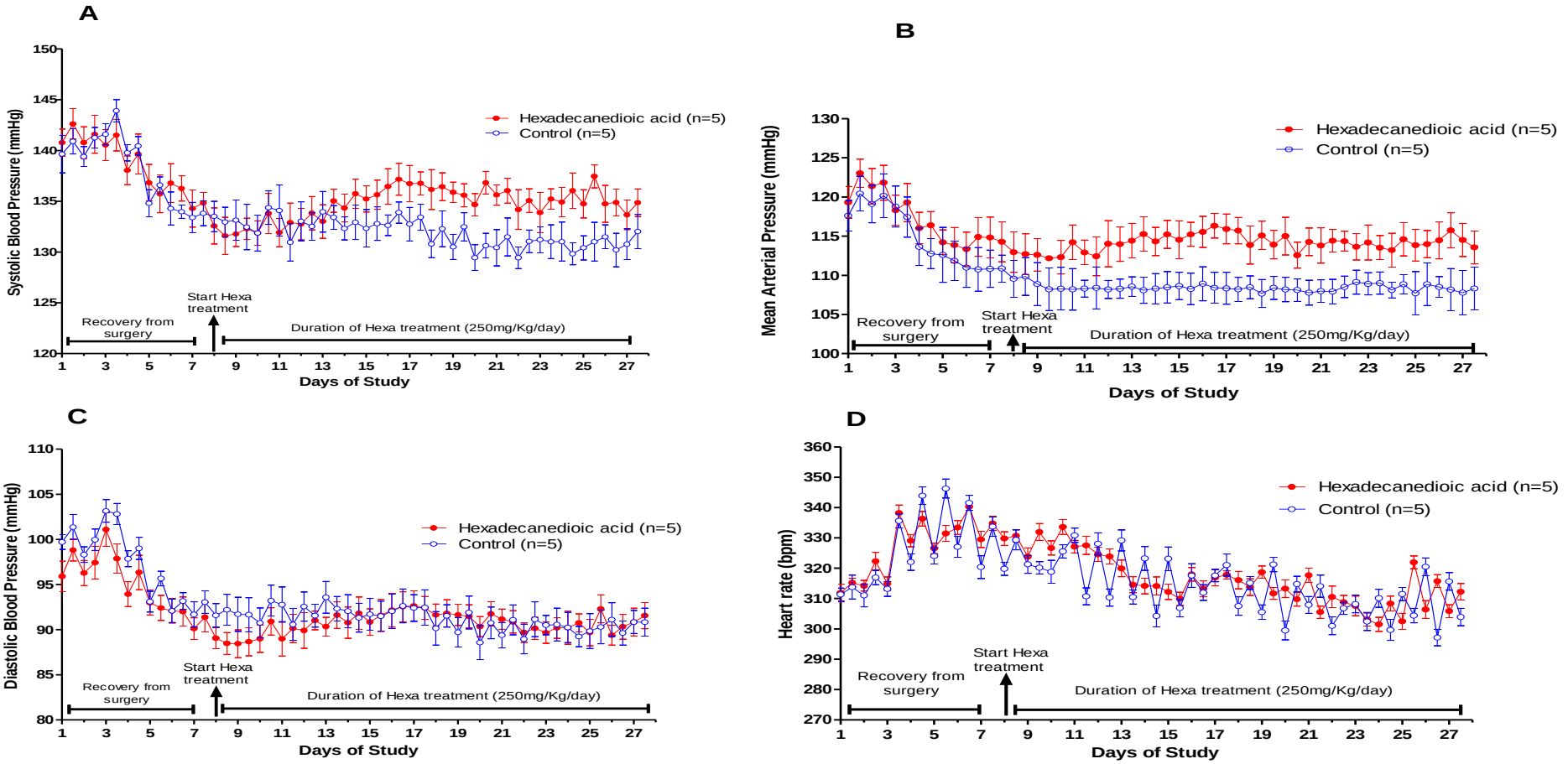

Figure 3-4: Radiotelemetry measurement (24-h averages) of haemodynamic parameters for hexadecanedioic acid-treated WKY rats and control WKY rats.

The levels of (A) systolic blood pressure and (B) mean arterial pressure increased in hexadecanedioic acid (250 mg/kg per day, n=5)-treated WKY compared to vehicle-treated WKY (n=5). There was no significant difference in (C) diastolic blood pressure, and (H) heart rate observed in WKY rats treated with hexadecanedioic acid or vehicle. Each point represented as mean ± standard error of mean**.**

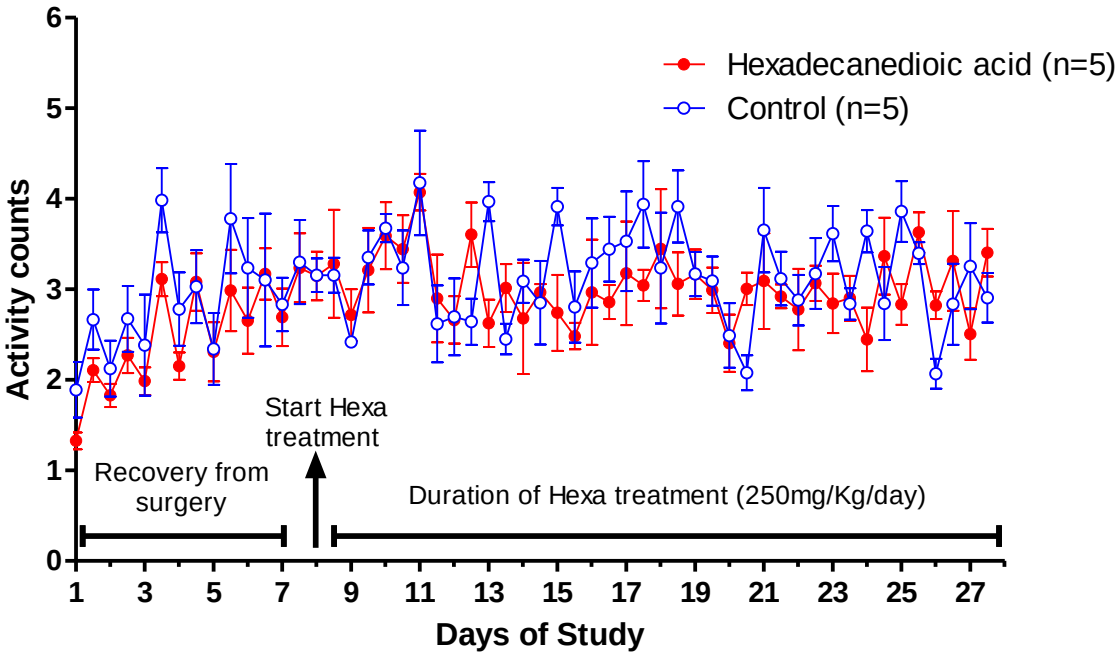

Figure 3-5: Radiotelemetry measurement (24-h averages) of activity in hexadecanedioic acid-treated WKY rats and control WKY rats.

There was no significant difference in activity of WKY rats treated with hexadecanedioic acid (n=5) compared to vehicle-treated WKY rats (n=5). Each point represented as mean ± standard error of mean.

Table 3-1: Echocardiographic measurements for WKY treated with hexadecanedioic acid (250 mg/kg per day) or vehicle for 4 weeks.

Parameters	Pre-treatment		1st week of treatment		2nd week of treatment		3rd week of treatment		4th week of treatment		ANOVA (general linear model)
	control	Hexa	Control	Hexa	control	Hexa	control	Hexa	control	Hexa	P value
LVM (mg)	0.69 ± 0.05	0.65 ± 0.02	0.65 ± 0.04	0.70 ± 0.04	0.69 ± 0.05	0.72 ± 0.09	0.64 ± 0.07	0.64 ± 0.02	0.80 ± 0.08	0.69 ± 0.02	0.640
LVM/BWt (mg/g)	2.94 ± 0.13	2.60 ± 0.09	2.44 ± 0.13	2.55 ± 0.19	2.52 ± 0.19	2.49 ± 0.29	2.19 ± 0.12	2.13 ± 0.05	2.67 ± 0.14	2.24 ± 0.08 *	0.130
LVM/tib (mg/mm)	18.30 ± 0.09	17.30 ± 0.06	16.60 ± 0.10	17.70 ± 0.09	17.30 ± 0.13	17.40 ± 0.19	15.50 ± 0.14	15.30 ± 0.03	19.40 ± 0.18	16.60 ± 0.04	0.390
FS %	45.57 ± 1.33	43.11 ± 1.83	48.27 ± 1.76	49.16 ± 2.37	42.39 ± 3.93	46.99 ± 1.98	44.14 ± 1.08	44.73 ± 1.82	40.71 ± 0.39	43.47 ± 2.46	0.490
RWT (mm)	0.49 ± 0.03	0.47 ± 0.02	0.48 ± 0.02	0.55 ± 0.04	0.46 ± 0.05	0.44 ± 0.03	0.43 ± 0.03	0.42 ± 0.02	0.48 ± 0.04	0.46 ± 0.02	0.940
SV (mls)	0.32 ± 0.02	0.31 ± 0.02	0.32 ± 0.04	0.28 ± 0.02	0.34 ± 0.02	0.38 ± 0.02	0.36 ± 0.06	0.36 ± 0.01	0.35± 0.01	0.34 ± 0.01	0.950
CO (mls/min)	112.59 ± 11.83	114.01 ± 6.74	110.41 ± 15.67	105.96 ± 6.15	114.09 ± 7.74	140.82 ± 4.61	125.44 ± 20.64	128.26 ± 5.916	112.85 ± 5.06	122.42 ± 5.67	0.200
EF %	85.80 ± 2.16	81.29 ± 1.86	86.01 ± 1.51	86.42 ± 1.93	80.09 ± 3.87	84.79 ± 1.69	82.51 ± 1.05	82.84 ± 1.62	77.76 ± 1.43	81.40 ± 2.62	0.460
Bwt g	236.25 ± 15.95	250 ± 2.96	265 ± 15.44	276 ± 4.59	275.25 ± 15.69	288.5 ± 4.61	288 ± 17.18	299.33 ± 5.29	298.75 ± 18.56	310.33 ± 4.51	0.0001

Abbreviations: LVM, Left Ventricular Mass; LVM/BWt, Left Ventricular Mass normalised to body weight; LVM/tib, Left Ventricular Mass normalised to tibia length; FS, Fractional Shortening; RWT, Relative Wall Thickness; SV, Strock Volume; CO, Cardiac Output; EF%, % Ejection Fraction; BWt g, Body Weight in gram. Unites: mg, milligram; mg/g, milligram per gram; mm, millimetre; mg/mm, milligram per millimetre; mls, millilitres; mls/min, milliliters/ minute. All data are mean ± SEM. (P*<0.05; Student Ttest used to compare hexa-treated WKY rats to their respective controls).

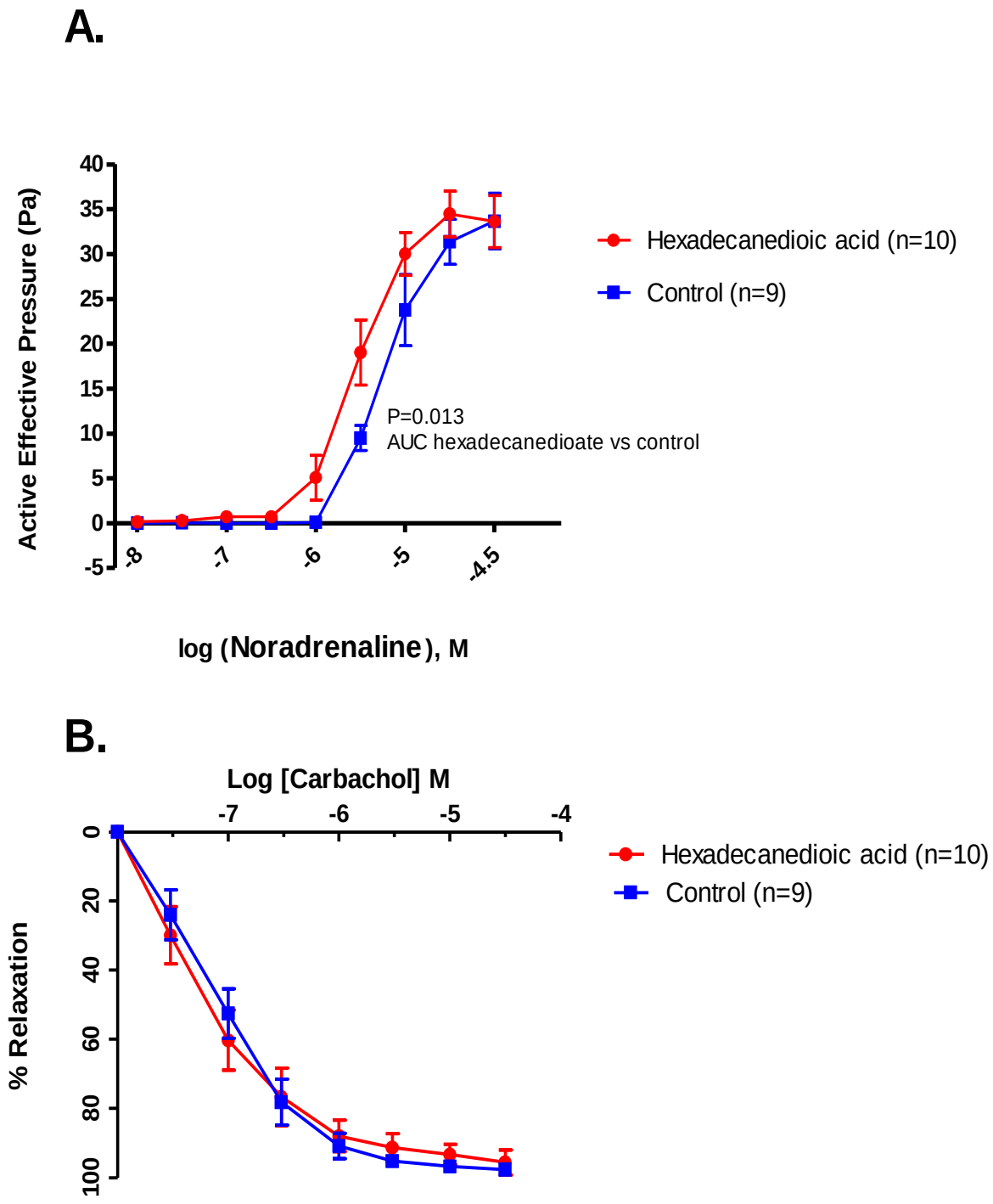

Figure 3-6: Mesenteric resistance artery function in response to noradrenaline and carbachol.

(A) Contractile responses to noradrenaline in the mesenteric resistance arteries showed significant increase in the mesenteric resistance arteries of 4 weeks hexadecanedioate-treated rats (250 mg/kg/day, n=10) compared with controls (n=9) (B) relaxation responses to carbachol, which showed no significant difference between hexadecanedioate-treated rats and controls (each point represents Mean ± Standard error of mean).

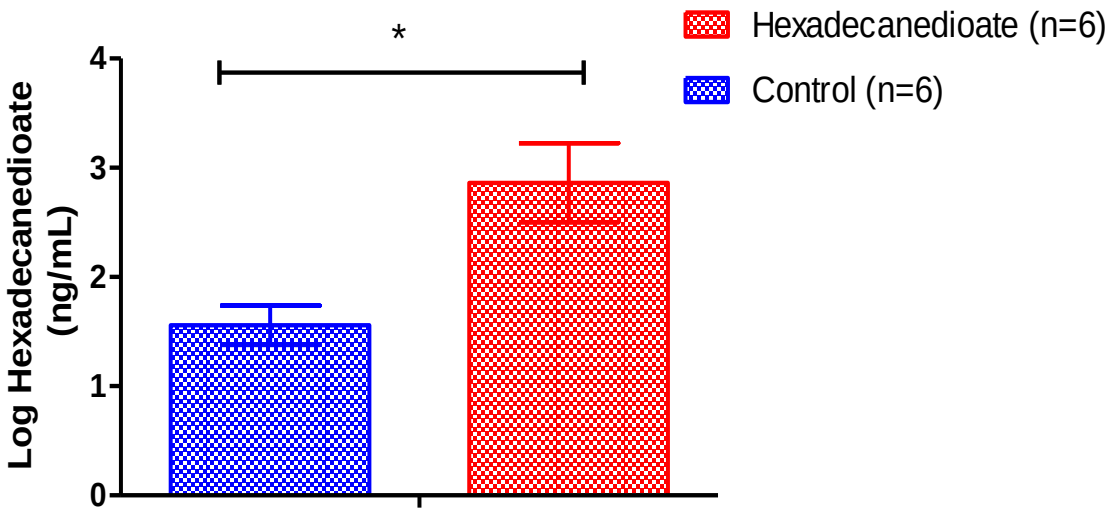

Figure 3-7: Plasma hexadecanedioate levels (ng/ml) in WKY rats treated with (250 mg/kg/day, n=6/group) hexadecanedioic acid or vehicle for 4 weeks.

Hexadecanedioate levels significantly increased in hexadecanedioic acid-treated WKY rats compared to control WKY rats (Each point represents Mean ± Standard error of mean) (P*< 0.05).

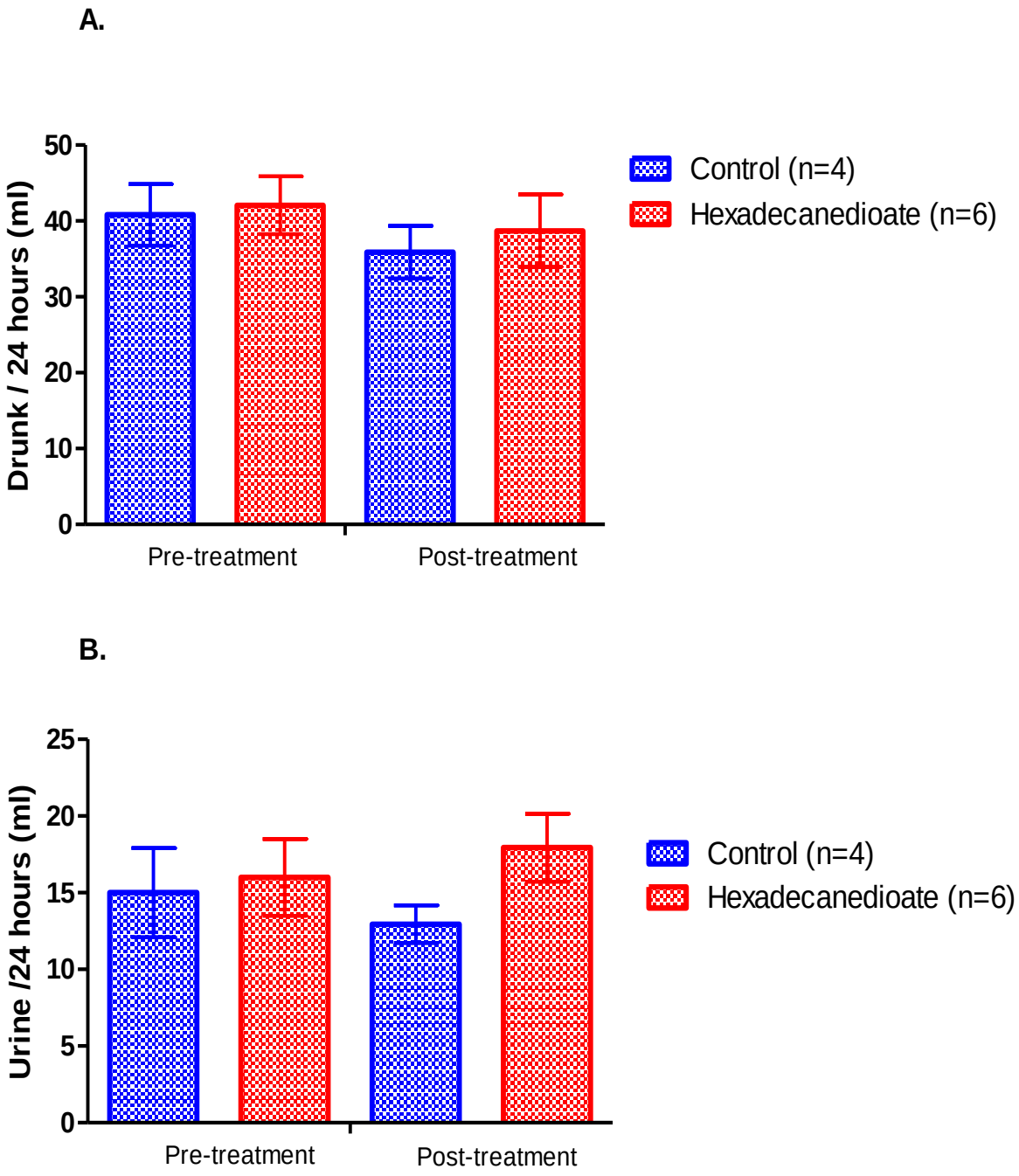

Figure 3-8: Renal function was assessed by metabolic cages over 24 hours for hexadecanedioic acid (n=6) or vehicle-treated WKY rats (n=4).

(A) Water intake and (B) urine output were measured pre and post treatment with hexadecanedioic acid or vehicle. The results showed no significant difference between hexadecanedioic acid-treated WKY rats and vehicle-treated WKY rats. Values are presented as Mean ± SEM.

Table 3-2: Biochemical analysis for plasma sample obtained from hexadecanedioic acid-treated rats and control rats.

Parameters	Control	Hexadecanedioate	P value
CK (U/L)	269.15 ± 13.78	218.39 ± 13.55	0.015*
ALT (U/L)	33.62 ± 3.82	37.97 ± 3.78	0.430
AST (U/L)	76.97 ± 2.91	69.66 ± 2.35	0.063
Urea (umol/L)	3.54 ± 0.14	3.83 ± 0.21	0.260
Creatinine (umol/L)	1.30 ± 0.02	1.30 ± 0.01	0.863
Bilirubin (g/L)	1.20 ± 0.09	1.23 ± 0.07	0.790
Albumin (mmol/L)	19.42 ± 0.39	19.20 ± 0.38	0.690
Na (mmol/L)	124.69 ± 2.59	122.08 ± 1.73	0.410
K (mmol/L)	3.79 ± 0.19	3.89 ± 0.17	0.720
Cl (mmol/L)	86.42 ± 1.83	83.86 ± 1.33	0.270

Abbreviations: CK, Creatine Kinase; ALT, Alanine Aminotransferase; AST, Aspartate Aminotransferase; Na, sodium; K, potassium; Cl, chloride. Units: mmol/L, millimole/liter; umol/L, micromole/liter; g/L, gram/liter; U/L, units per litre. All data are mean± SEM. (P*<0.05; Student Ttest used to compare hexadecanedioic acid-treated WKY rats to their respective controls).

Table 3-3: Biochemical analysis for urine sample obtained from hexadecanedioic acid-treated rats and control rats.

Parameters	Control	Hexadecanedioate	P value
Creatinine (umol/L)	3.47 ± 0.16	3.43 ± 0.07	0.548
Bilirubin (g/L)	0.46 ± 0.68	0.77 ± 0.46	0.041*
Abbreviations: umol/L, micromole/liter; g/L, gram/liter. All data are mean± SEM. (P*<0.05; Student Ttest used to compare hexadecanedioic acid-treated WKY rats to their respective controls).			

Table 3-4: Organ weights normalised to body weight and tibia length of WKY rats treated with hexadecanedioic acid (250 mg/kg per day) or vehicle for 4 weeks at sacrifice.

Parameters	Control	Hexa	Ttest Control vs Hexa
H/Bwt (mg/g)	3.42 ± 0.03	3.47 ± 0.01	0.513
H/tib (mg/mm)	24.77 ± 0.22	24.45 ± 0.34	0.731
LV+S/Bwt (mg/g)	2.31 ± 0.02	2.41 ± 0.02	0.181
LV+S/tib (mg/mm)	16.72 ± 0.25	16.99 ± 0.28	0.750
RK/Bwt (mg/g)	2.92 ± 0.02	2.93 ± 0.05	0.931
RK/tib (mg/mm)	21.09 ± 0.22	20.64 ± 0.53	0.730
LK/Bwt (mg/g)	2.81 ± 0.03	2.89 ± 0.06	0.595
LK/tib (mg/mm)	20.36 ± 0.33	20.39 ± 0.53	0.984
Epi/Bwt (mg/g)	13.92 ± 0.40	13.27 ± 0.45	0.640
Epi/tib (mg/mm)	100.50 ± 2.44	93.49 ± 3.62	0.493
Retro/Bwt (mg/g)	14.41 ± 0.84	13.99 ± 0.96	0.886
Retro/tib (mg/mm)	103.99 ± 5.89	99.09 ± 7.30	0.821
Liver/Bwt (mg/g)	32.44 ± 0.57	32.76 ± 0.73	0.883
Liver/tib (mg/mm)	234.29 ± 2.57	229.26 ± 2.35	0.537
Bwt (g)	289.56 ± 2.83	283.10 ± 4.59	0.606
Tib (mm)	40.20 ± 0.26	40.20 ± 0.26	0.792

Abbreviations: H/Bwt, Heart normalised to body weight; H/tib, Heart normalised to tibia length; LV+S/Bwt, Left Ventricular plus Septal wall normalised to body weight; LV+S/tib, Left Ventricular plus Septal wall normalised to tibia length; RK/Bwt, Right Kidney normalised to body weight; RK/tib, Right Kidney normalised to tibia length; LK/Bwt, Left Kidney normalised to body weight; LK/tib, Left Kidney normalised to tibia length; Epi/Bwt, Epididymal fat normalised to body weight; Epi/tib, Epididymal fat normalised to tibia length; Retro/Bwt, Retroperitoneal fat normalised to body weight; Retro/tib, Retroperitoneal fat normalised to tibia length; Liver/Bwt, Liver normalised to body weight; Liver/tib, Liver normalised to tibia length. Units: mg/g, milligram per gram; mg/mm, milligram/ millimetre; g, gram; mm, millimetre. All data are mean± SEM.

3.5.2 Dose response of hexadecanedioic acid on blood pressure regulation

The dose response curve was applied to examine the concentration range at which hexadecanedioic acid levels have an impact on blood pressure in adult male WKY_{Gla} rats by oral administration of a range of doses (e.g. 250, 300, 350, 400, 450 and 500 mg/kg/day) over a six-week treatment period. The step-wise increment in hexadecanedioic acid levels induced a gradual increase in the blood pressure of WKY_{Gla} rats with increasing doses. SBP levels shows a separation between hexadecanedioic acid-treated WKY_{Gla} rats and vehicle-treated WKY_{Gla} rats at 250 mg/kg/day (P=0.085) and at 300 mg/kg/day (P=0.16), while it did not reach statistical significance. SBP significantly increased after treatment with hexadecanedioate at 350 mg/kg/day ($P=2.3 \times 10^{-6}$), 400 mg/kg/day ($P=2.8 \times 10^{-10}$), 450 mg/kg/day ($P=3.1 \times 10^{-10}$) and 500 mg/kg/day ($P=4.04 \times 10^{-12}$) (Figure 3-9).

Gradual elevations in mean arterial pressure (MAP) and diastolic blood pressure (DBP) were shown in hexadecanedioic acid-treated rats compared to control rats. There were no significant differences in MAP after treatment with hexadecanedioate at 250 mg/kg/day (P=0.079) and after a dose of 300 mg/kg/day (P=0.31). However, after increasing the dose by 50 mg, the MAP significantly increased i.e. 350 mg/kg/day ($P=1.8 \times 10^{-6}$), 400 mg/kg/day ($P=9.14 \times 10^{-9}$), 450 mg/kg/day ($P=2.34 \times 10^{-8}$) and 500 mg/kg/day ($P=2.34 \times 10^{-8}$). Similarly, significant differences in DBP were observed between hexadecanedioate-treated rats and control rats after dose increment. The levels of DBP showed no significant difference after treatment with hexadecanedioic acid at 250 mg/kg/day (P=0.383) and 300 mg/kg/day (P=0.50). However, DBP was significantly elevated after treatment with hexadecanedioic acid at 350 mg/kg/day ($P=4.34 \times 10^{-7}$), 400 mg/kg/day ($P=2.65 \times 10^{-7}$), 450 mg/kg/day ($P=1.13 \times 10^{-8}$) and 500 mg/kg/day ($P=1.92 \times 10^{-11}$) as shown in Figure 3-9. It should be noted that an unexpected fall in blood pressure was observed at day 11 of hexadecanedioic acid treatment, occurring at a dose of 300 mg/kg/day.

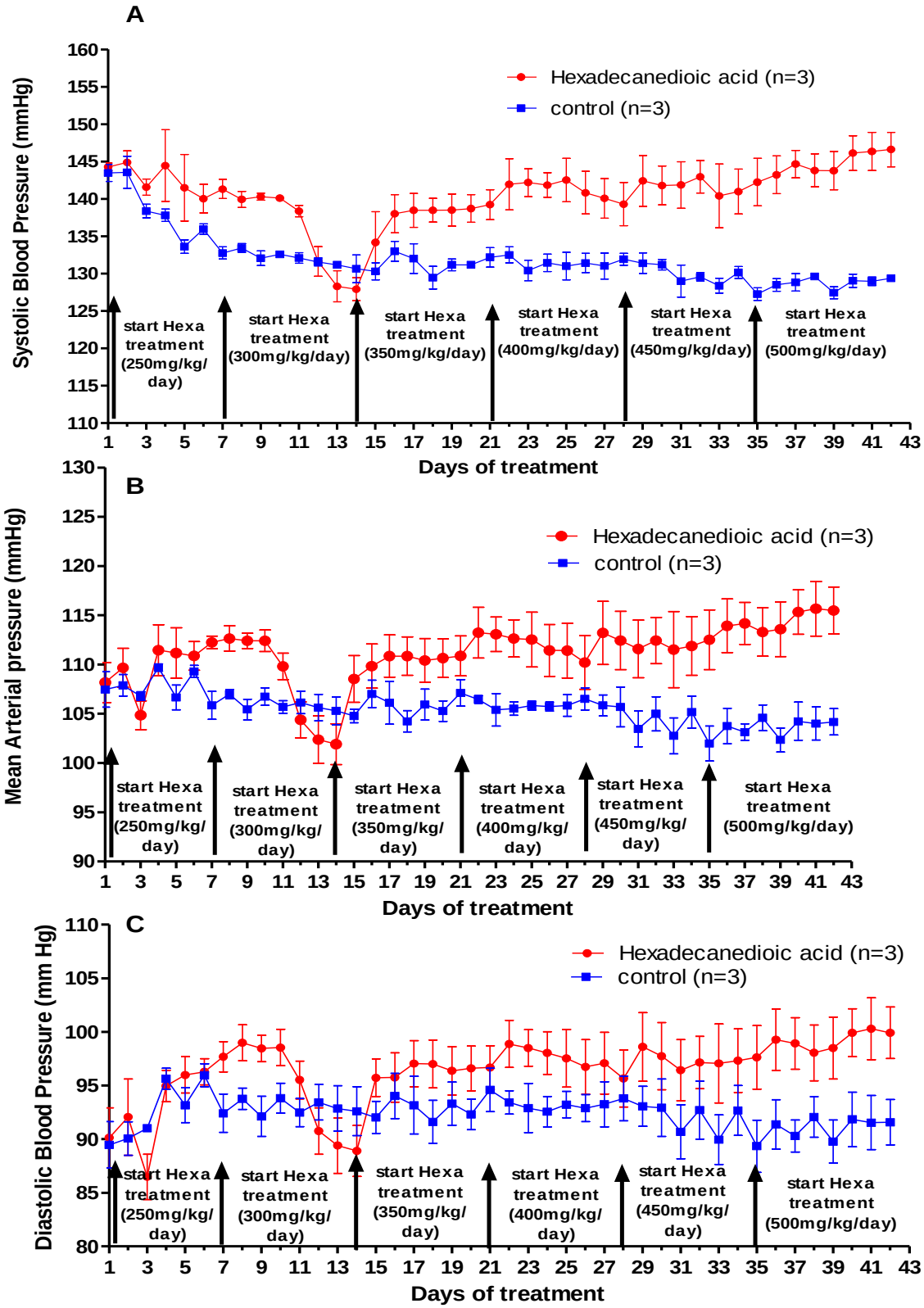

Figure 3-9: Dose response curves measured by radiotelemetry of (24-h averages) of WKY_{Gla} rats-treated with hexadecanedioic acid or vehicle for 6 weeks.

(A) Systolic blood pressure (mmHg), (B) mean arterial pressure (mmHg) and (C) diastolic blood pressure (mmHg) of WKY_{Gla} rats treated with hexadecanedioic acid (250 mg/kg per day, 300 mg/kg per day, 350 mg/kg per day, 400 mg/kg per day, 450 mg/kg per day and 500 mg/kg per day, n=3) or control (n=3) for a total treatment period of 6 weeks. The step-wise increase in hexadecanedioic acid dose induced a gradual increase in the blood pressure of WKY_{Gla} rats. Each point represents (mean ± standard error of mean).

3.5.3 Longer term hexadecanedioic acid treatment

3.5.3.1 Effect of longer term hexadecanedioic acid treatment on blood pressure of WKY_{Gla} and $SHRSP_{Gla}$

Blood pressure for both strains (i.e. WKY_{Gla} and $SHRSP_{Gla}$) increased with time, over the ten weeks study period. The blood pressure measurements began in young animals (i.e. 6 weeks of age) and followed to adulthood. Longer-term treatment with hexadecanedioic acid caused a significant elevation in the systolic blood pressure of hexadecanedioic acid-treated WKY_{Gla} rats compared to controls (P=0.0154). The difference in blood pressure between hexadecanedioic acid-treated WKY_{Gla} rats and control WKY_{Gla} rats was observed at 13 weeks of age (i.e. at week 8 of treatment) and the elevation was sustained until the last measurement. However, there was no changes in the systolic blood pressure of hexadecanedioic acid-treated $SHRSP_{Gla}$ rats compared with the control untreated $SHRSP_{Gla}$ rats (P=0.96), as shown in Figure 3-10.

3.5.3.2 Effect of longer term hexadecanedioic acid treatment on cardiac function of WKY_{Gla} and $SHRSP_{Gla}$

Cardiac function of WKY_{Gla}

The main echocardiographic parameters were measured at baseline and after treatment at two-week intervals (Table 3.5 and Table 3.6). Significant reduction in the levels of left ventricular mass was observed in hexadecanedioic acid-treated WKY_{Gla} rats compared to vehicle-treated WKY_{Gla} rats (Table 3-5). However, no significant difference was observed when the levels of LVM were normalised either to body weight (P=0.234) or tibia length (P=0.097) (Table 3-5).

A significant reduction was observed in relative wall thickness (RWT) in hexadecanedioic acid-treated rats compared to control WKY_{Gla} rats during the study period (P=0.049). This significant reduction was observed during the second echocardiography measurement, when compared to the respective controls (0.38 mm± 0.01 vs 0.49 mm± 0.01, P=0.001), and it remained lower at the final echocardiography measurement, but did not reach significance (0.46 mm± 0.03 vs 0.55 mm± 0.04, P=0.131).

Other parameters, such as fractional shortening, stroke volume, ejection fraction and cardiac output levels showed no difference between WKY_{Gla} rats treated with either hexadecanedioic acid or vehicle, as shown in Table 3-5.

The body weights of hexadecanedioic acid-treated WKY_{Gla} rats decreased significantly during the study timeline when compared to controls (P=0.0002), as shown in Table 3-5.

Cardiac function of $SHRSP_{Gla}$

Echocardiography measurement showed no difference in LVM either normalised to body weight or tibia length of $SHRSP_{Gla}$ treated either with hexadecanedioic acid or vehicle. In addition, no difference was observed in RWT of $SHRSP_{Gla}$ treated with hexadecanedioic acid compared to control (P=0.183) (Table 3-6).

Fractional shortening, stroke volume, ejection fraction and cardiac output levels also showed no difference between $SHRSP_{Gla}$ rats either treated with hexadecanedioic acid or vehicle, as shown in Table 3-6.

The body weights of hexadecanedioic acid-treated $SHRSP_{Gla}$ rats was also significantly decreased compared to control rats (P=0.002). This significant reduction was observed in the final echocardiography measurement (P=0.035) (Table 3-6).

3.5.3.3 Organ mass index

Organ weights were measured during collection of the tissues at sacrifice and then normalised to animal weight or tibia length to identify morphological changes after treatment with hexadecanedioic acid. Analysis of the data showed no significant change in heart weight normalised to rats' body weights between hexadecanedioic acid-treated WKY_{Gla} rats compared to controls (P=0.067). In addition, no significant difference was observed in the heart weight normalised to body weight of hexadecanedioic acid-treated $SHRSP_{Gla}$ rats compared to controls (P=0.937).

The left ventricular plus septal wall weight of the sacrificed rats was also measured to verify the accuracy of the left ventricular mass measurements

estimated by echocardiography. Left ventricular plus septal wall weight normalised to body weight did not show any significant difference in either WKY_{Gla} or $SHRSP_{Gla}$, treated with hexadecanedioic acid or vehicle, as shown in Table 3-7.

Renal indexes were also measured which showed no significant differences in the weight of left or right kidneys normalised to body weight between either hexadecanedioic acid or vehicle-treated $SHRSP_{Gla}$ and WKY_{Gla} (Table 3-7). In addition, no changes were observed in liver weight normalised to body weight of hexadecanedioic acid-treated $SHRSP_{Gla}$ or WKY_{Gla} rats compared to controls, as shown in Table 3-7.

Adiposity indexes were measured for both epididymal and retroperitoneal fat pads. Analysis demonstrated no significant differences in epididymal fat pad weight normalised to body weight of hexadecanedioic acid-treated WKY_{Gla} or $SHRSP_{Gla}$ rats compared to controls, as shown in Table 3-7. Furthermore, no significant difference in retroperitoneal fat weight normalised to body weight was observed in hexadecanedioic acid-treated WKY_{Gla} rats compared to control rats (P=0.070). However, there was a significant elevation in retroperitoneal fat weight normalised to body weight of hexadecanedioic acid-treated $SHRSP_{Gla}$ rats compared to controls (P=0.048). The same pattern was shown when normalised to tibia length (Table 3-7).

Significant reduction was observed in body weight of hexadecanedioic acid-treated WKY_{Gla} (P=0.004) and $SHRSP_{Gla}$ (P=0.03) rats compared to control rats (Table 3-7)

3.5.3.4 Histology

Histological evaluation using haematoxylin staining was carried out to identify evidence of cardiac, hepatic and renal morphology changes during chronic treatment with hexadecanedioic acid. No changes were shown in the heart tissues of hexadecanedioic acid-treated WKY_{Gla} or $SHRSP_{Gla}$ rats compared to their respective control rats (Figure 3-11). Moreover, no histopathologic alterations were observed in liver tissues of hexadecanedioic acid-treated WKY_{Gla} or $SHRSP_{Gla}$ rats compared to their respective controls (Figure 3-12).

No gross histopathological changes were observed in kidney sections of WKY_{Gla} and $SHRSP_{Gla}$ rats treated with hexadecanedioic acid when compared with vehicle (Figure 3-13). Renal artery wall thickness was measured which showed no significant differences in WKY_{Gla} rats treated with hexadecanedioic acid compared to control WKY_{Gla} rats (P=0.36), or in $SHRSP_{Gla}$ rats compared to control $SHRSP_{Gla}$ rats (P=0.48) (Figure 3-14).

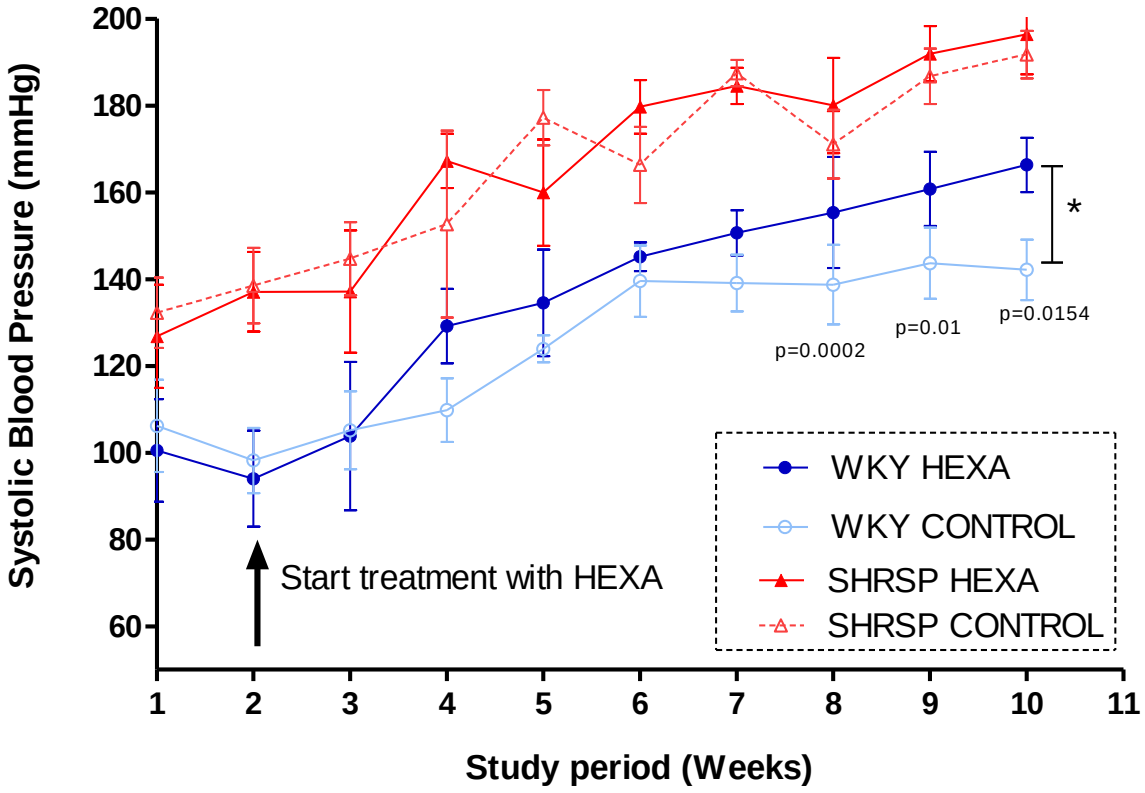

Figure 3-10: Systolic blood pressure of WKY_{Gla} and $SHRSP_{Gla}$ rats treated with hexadecanedioic acid (250 mg/kg per day, n=3) or vehicle (n=3) for 9 weeks.

A significant elevation in the SBP of WKY_{Gla} rats was observed after longer-term treatment with hexadecanedioic acid compared to control WKY_{Gla} rats (blue lines). However, there was no significant difference in SBP of $SHRSP_{Gla}$ after longer-term treatment with hexadecanedioic acid compared to control $SHRSP_{Gla}$ rats (red lines). Each point represents (mean ± standard error of mean) (P*< 0.05).

Table 3-5: Echocardiographic measurements for WKY_{Gla} treated with hexadecanedioic acid (250 mg/kg per day, n=3) or vehicle (n=3) for 9 weeks.

Parameters	Baseline		1st measurement		2nd measurement		3rd measurement		ANOVA (general linear model)
	WKY_{Gla}		WKY_{Gla}		WKY_{Gla}		WKY_{Gla}		P value
	Control	Hexa	Control	Hexa	Control	Hexa	Control	Hexa	
LVM (mg)	0.33 ± 0.02	0.32 ± 0.001	0.57 ± 0.02	0.48 ± 0.04	0.79 ± 0.03	0.69 ± 0.03	0.99 ± 0.019	0.88 ± 0.043	0.001
LVM:weight (mg/g)	2.65 ± 0.12	2.91 ± 0.11	2.59 ± 0.09	2.55 ± 0.20	2.56 ± 0.01	2.61 ± 0.07	2.82 ± 0.07	2.95 ± 0.12	0.234
LVM:tl (mg/mm)	11.20 ± 0.06	12.60 ± 0.01	17.50 ± 0.07	15.10 ± 0.12	21.0 ± 0.03	19.60 ± 0.11	24.90 ± 0.04	22.90 ± 0.09	0.097
FS %	34.23 ± 3.57	36.95 ± 4.50	46.44 ± 1.56	44.55 ± 0.92	44.34 ± 1.48	39.09 ± 3.84	37.03 ± 3.77	43.74 ± 4.95	0.626
RWT (mm)	0.51 ± 0.013	0.53 ± 0.02	0.47 ± 0.01	0.47 ± 0.035	0.49 ± 0.01	0.38 ± 0.01*	0.55 ± 0.04	0.46 ± 0.03	0.049
SV (mls)	0.12 ± 0.017	0.12 ± 0.01	0.28 ± 0.002	0.23 ± 0.01	0.35 ± 0.002	0.40 ± 0.03	0.34 ± 0.03	0.43 ± 0.03	0.275
CO (mls/min)	48.52 ± 6.15	46.43 ± 2.55	112.78 ± 3.17	89.03 ± 7.09	134.48 ± 3.73	129.41 ± 16.23	113.49 ± 16.61	147.25 ± 15.63	0.935
EF %	71.05 ± 4.76	76.49 ± 5.23	84.56 ± 1.31	82.92 ± 0.85	82.68 ± 1.32	76.88 ± 4.11	74.49 ± 4.74	81.35 ± 4.97	0.629
weight g	119 ± 2.91	117 ± 4.37	222 ± 4.26	188 ± 2.33**	310 ± 11.02	264 ± 6.36*	352 ± 6.94	298 ± 5.17**	0.0002

Abbreviations: LVM, Left Ventricular Mass; LVM/BWt, Left Ventricular Mass normalised to body weight; LVM/tib, Left Ventricular Mass normalised to tibia length; FS, Fractional Shortening; RWT, Relative Wall Thickness; SV, Strock Volume; CO, Cardiac Output; EF%, % Ejection Fraction; BWt g, Body Weight in gram. Unites: mg, milligram; mg/g, milligram per gram; mm, millimetre; mg/mm, milligram per millimetre; mls, millilitres; mls/min, milliliters/ minute. All data are mean± SEM. ($P^{*}<0.05$, $P^{**}<0.01$; Student Ttest used to compare hexa-treated WKY_{Gla} rats to their respective controls).

Table 3-6: Echocardiographic measurements for $SHRSP_{Gla}$ treated with hexadecanedioic acid (250 mg/kg per day, n=3) or vehicle (n=3) for 9 weeks.

Parameters	Baseline		1st measurement		2nd measurement		3rd measurement		ANOVA (general linear model)
	$SHRSP_{Gla}$		$SHRSP_{Gla}$		$SHRSP_{Gla}$		$SHRSP_{Gla}$		P value
	Control	Hexa	Control	Hexa	Control	Hexa	Control	Hexa	
LVM (mg)	0.35 ± 0.01	0.31 ± 0.02	0.54 ± 0.017	0.61 ±0.04	0.78 ± 0.07	0.87 ± 0.02	1.10 ± 0.06	0.95 ± 0.06	0.953
LVM:weight (mg/g)	3.41 ± 0.10	3.51 ± 0.33	2.78 ± 0.04	3.10 ± 0.30	3.01 ± 0.23	3.46 ± 0.12	3.79 ± 0.19	3.54 ± 0.27	0.653
LVM:tl (mg/mm)	13.30 ± 0.02	12.00 ± 0.08	17.50± 0.06	19.40 ± 0.12	20.80 ± 0.16	24.60 ± 0.08	28.90 ± 0.16	25.40 ± 0.13	0.741
FS %	55.97 ± 7.11	54.36 ± 6.02	54.78 ± 2.69	52.79 ± 1.11	61.40 ± 3.16	56.05 ± 3.48	36.97 ± 3.34	48.36 ± 5.57	0.818
RWT (mm)	0.56 ± 0.01	0.57 ± 0.06	0.53 ± 0.02	0.54 ± 0.06	0.61 ± 0.02	0.74 ± 0.09	0.66 ± 0.02	0.68 ± 0.05	0.183
SV (mls)	0.15 ± 0.01	0.12 ± 0.011	0.24 ± 0.02	0.26 ± 0.03	0.29 ± 0.01	0.25 ± 0.04	0.29 ± 0.01	0.28 ± 0.03	0.38
CO (mls/min)	65.12 ± 4.39	60.95 ± 2.16	100.24 ± 7.16	105.27± 12.64	112.75 ± 4.00	101.07 ± 16.03	93.89 ± 4.49	86.48 ± 4.37	0.287
EF %	90.17 ± 3.86	89.48 ± 4.13	90.56 ± 1.64	89.44 ± 0.73	94.02 ± 1.37	91.18 ± 2.16	74.55 ± 3.80	85.75 ± 4.47	0.773
weight g	104 ± 2.52	90 ± 4.48	196 ± 4.91	199 ± 6.65	259 ± 2.89	251 ± 4.33	290 ± 3.61	270 ± 3.00*	0.002

Abbreviations: LVM, Left Ventricular Mass; LVM/BWt, Left Ventricular Mass normalised to body weight; LVM/tib, Left Ventricular Mass normalised to tibia length; FS, Fractional Shortening; RWT, Relative Wall Thickness; SV, Strock Volume; CO, Cardiac Output; EF%, % Ejection Fraction; BWt g, Body Weight in gram. Unites: mg, milligram; mg/g, milligram per gram; mm, millimetre; mg/mm, milligram per millimetre; mls, millilitres; mls/min, milliliters/ minute. All data are mean± SEM. ($P^{*}<0.05$; Student Ttest used to compare hexa-treated $SHRSP_{Gla}$ rats to their respective controls).

Table 3-7: Organ weights normalised to body weight and tibia length of WKY_{Gla} and $SHRSP_{Gla}$ rats treated with hexadecanedioic acid (250 mg/kg per day, n=3) or vehicle (n=3) for 9 weeks at sacrifice.

Parameters	WKY_{Gla}		Ttest	$SHRSP_{Gla}$		Ttest	One Way ANOVA
	Control	Hexa	Control vs Hexa	Control	Hexa	Control vs Hexa	WKY_{Gla} vs $SHRSP_{Gla}$
H/Bwt (mg/g)	3.38 ± 0.10	3.31 ± 0.088	0.067	4.43 ± 0.03	4.41 ± 0.23	0.937	0.000
H/tib (mg/mm)	29.94 ± 0.83	28.88 ± 0.37	0.303	33.62 ± 0.34	31.72 ± 0.91	0.100	0.003
LV+S/Bwt (mg/g)	2.48 ± 0.04	2.70 ± 0.11	0.107	3.13 ± 0.16	3.17 ± 0.02	0.768	0.004
LV+S/tib (mg/mm)	22.03 ± 0.28	21.05 ± 0.95	0.381	24.55 ± 1.02	22.81 ± 0.44	0.290	0.071
RK/Bwt (mg/g)	2.73 ± 0.16	2.75 ± 0.06	0.894	3.86 ± 0.12	3.69 ± 0.06	0.349	0.000
RK/tib (mg/mm)	24.16 ± 1.45	21.39 ± 0.64	0.155	29.34 ± 0.85	26.54 ± 0.22	0.086	0.004
LK/Bwt (mg/g)	2.70 ± 0.05	2.84 ± 0.04	0.112	3.67 ± 0.06	3.72 ± 0.09	0.641	0.000
LK/tib (mg/mm)	23.96 ± 0.59	22.09 ± 0.53	0.079	27.86 ± 0.52	26.79 ± 0.04	0.215	0.000
Epi/Bwt (mg/g)	8.94 ± 0.36	9.21 ± 0.21	0.539	12.87 ± 0.97	14.80 ± 0.78	0.255	0.001
Epi/tib (mg/mm)	79.17 ± 2.72	71.74 ± 2.67	0.123	97.84 ± 7.81	106.49 ± 2.98	0.464	0.007
Retro/Bwt (mg/g)	10.46 ± 0.40	11.93 ± 0.44	0.070	13.58 ± 0.44	18.80 ± 2.02	0.048*	0.001
Retro/tib (mg/mm)	92.66 ± 2.77	92.91 ± 4.49	0.964	103.13 ± 3.18	135.05 ± 11.27	0.042*	0.001
Liver/Bwt (mg/g)	33.98 ± 0.25	36.65 ± 1.36	0.125	37.59 ± 1.09	38.65 ± 0.34	0.515	0.003
Liver/tib (mg/mm)	301.19 ± 0.69	285.30 ± 12.34	0.268	285.69 ± 9.57	278.33 ± 4.38	0.605	0.006
Bwt (g)	351.67 ± 6.94	298.33 ± 5.17	0.004*	290 ± 3.61	270 ± 3.00	0.030*	0.000
Tib (mm)	37.50 ± 0.50	38.33 ± 0.33	0.148	38.17 ± 0.17	37.50 ± 0.50	0.219	0.000

Abbreviations: H/Bwt, Heart normalised to body weight; H/tib, Heart normalised to tibia length; LV+S/Bwt, Left Ventricular plus Septal wall normalised to body weight; LV+S/tib, Left Ventricular plus Septal wall normalised to tibia length; RK/Bwt, Right Kidney normalised to body weight; RK/tib, Right Kidney normalised to tibia length; LK/Bwt, Left Kidney normalised to body weight; LK/tib, Left Kidney normalised to tibia length; Epi/Bwt, Epididymal fat normalised to body weight; Epi/tib, Epididymal fat normalised to tibia length; Retro/Bwt, Retroperitoneal fat normalised to body weight; Retro/tib, Retroperitoneal fat normalised to tibia length; Liver/Bwt, Liver normalised to body weight; Liver/tib, Liver normalised to tibia length. Units: mg/g, milligram per gram; mg/mm, milligram/ millimetre; g, gram; mm, millimetre. All data are mean± SEM. (P*<0.05; Student Ttest used to compare hexa-treated rats to their respective controls).

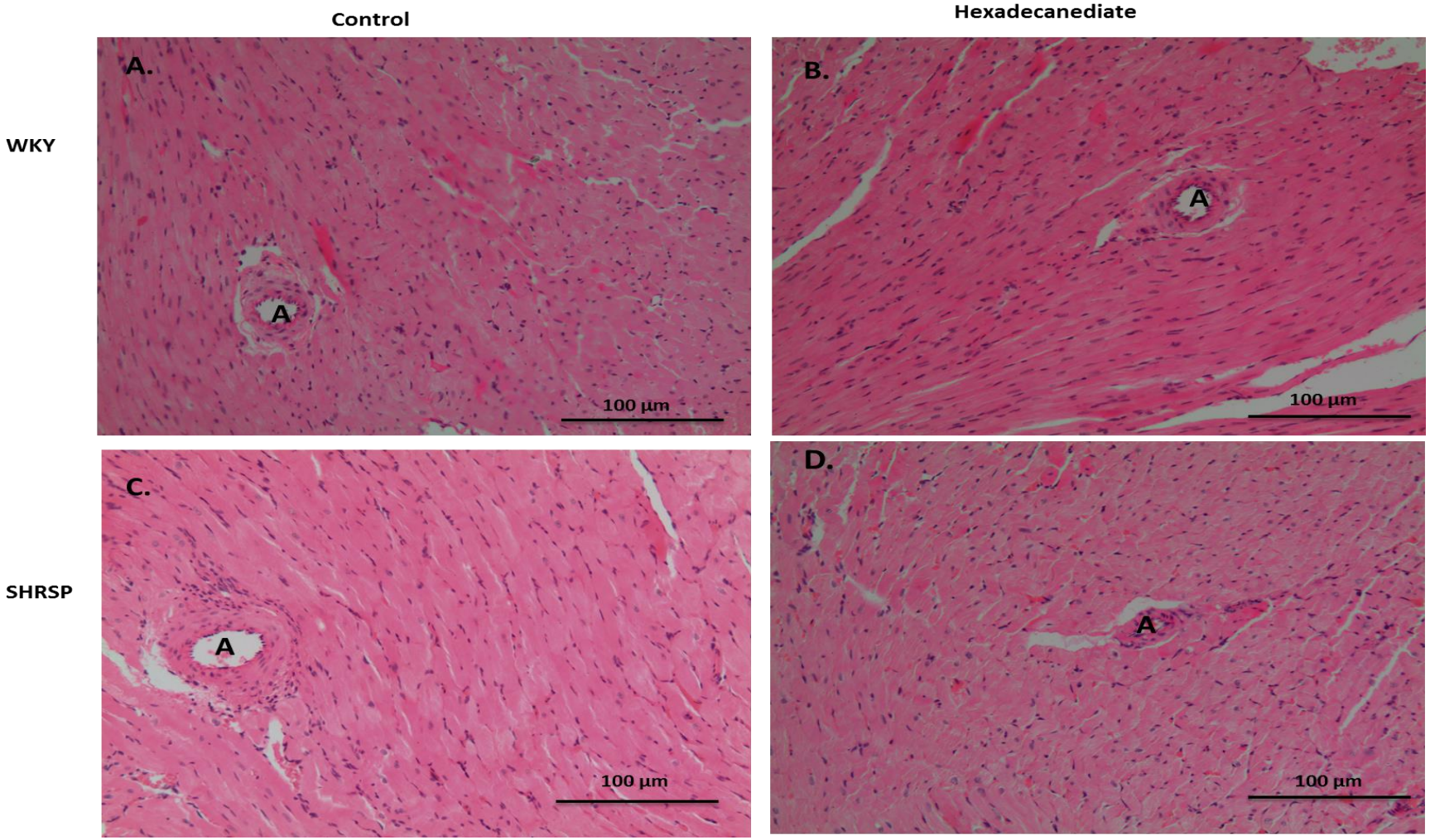

Figure 3-11: Haematoxylin and Eosin staining in heart sections from WKY_{Gla} and $SHRSP_{Gla}$ rats treated with hexadecanedioic acid or vehicle for 9 weeks.

There was no changes were shown in the heart tissues of hexadecanedioic acid-treated WKY_{Gla}/ $SHRSP_{Gla}$ rats (B, D) compared to control WKY_{Gla}/ $SHRSP_{Gla}$ rats (A, C). Abbreviation: Artery, A. Magnification=X100; scale bar=100 µm, n= 8-10 slides per animal.

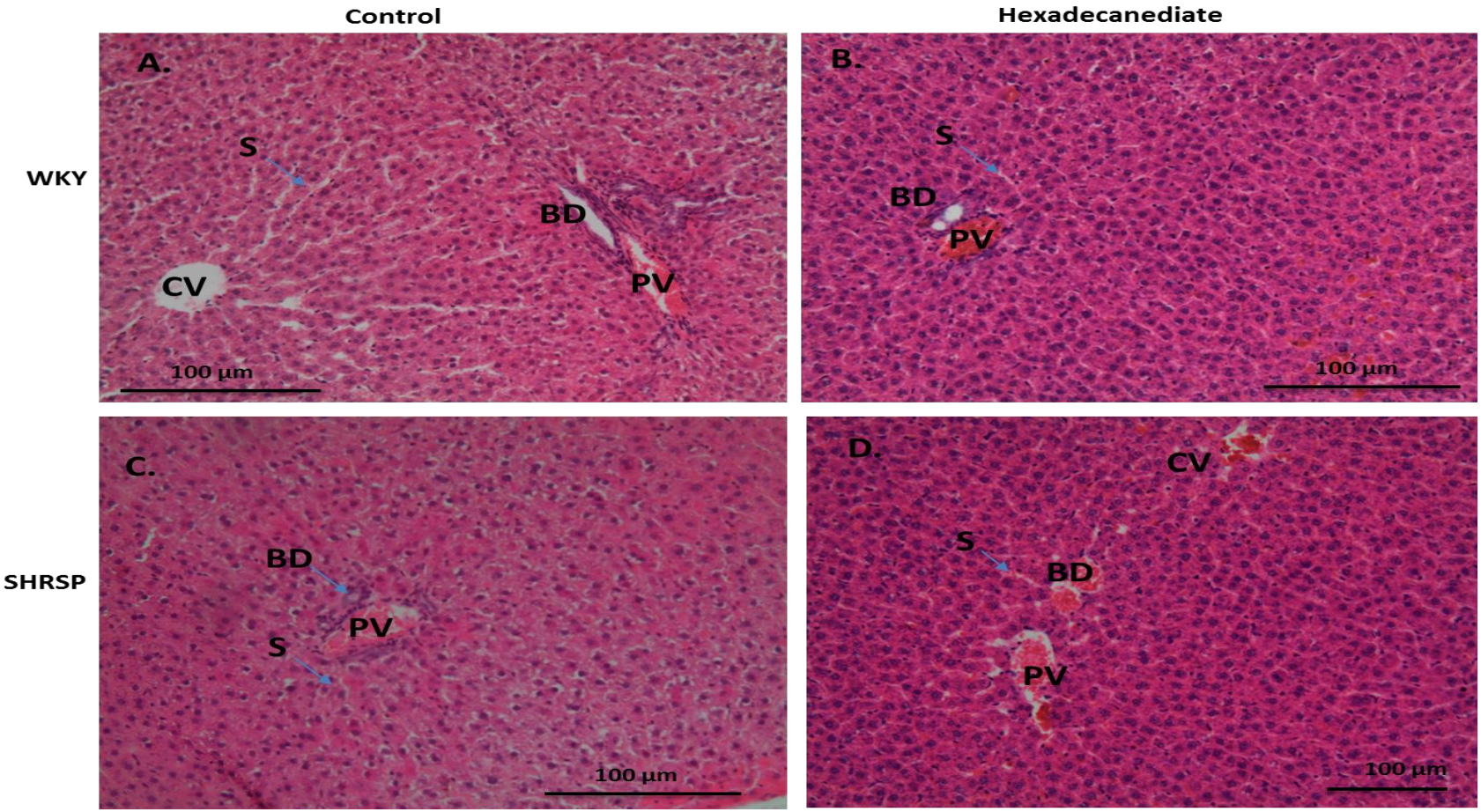

Figure 3-12: Haematoxylin and Eosin staining in liver sections from WKY_{Gla} and $SHRSP_{Gla}$ rats treated with hexadecanedioic acid or vehicle for 9 weeks.

No changes were detected in liver tissues obtained from WKY_{Gla} and $SHRSP_{Gla}$ rats after treatment with hexadecanedioic acid (B, D) compared to control (A, C). Abbreviation: Central Vein, CV; Portal Vein, PV; Bile Duct, BD; Sinusoid, S. Magnification=X100; scale bar=100 µm, n= 8-10 slides per animal.

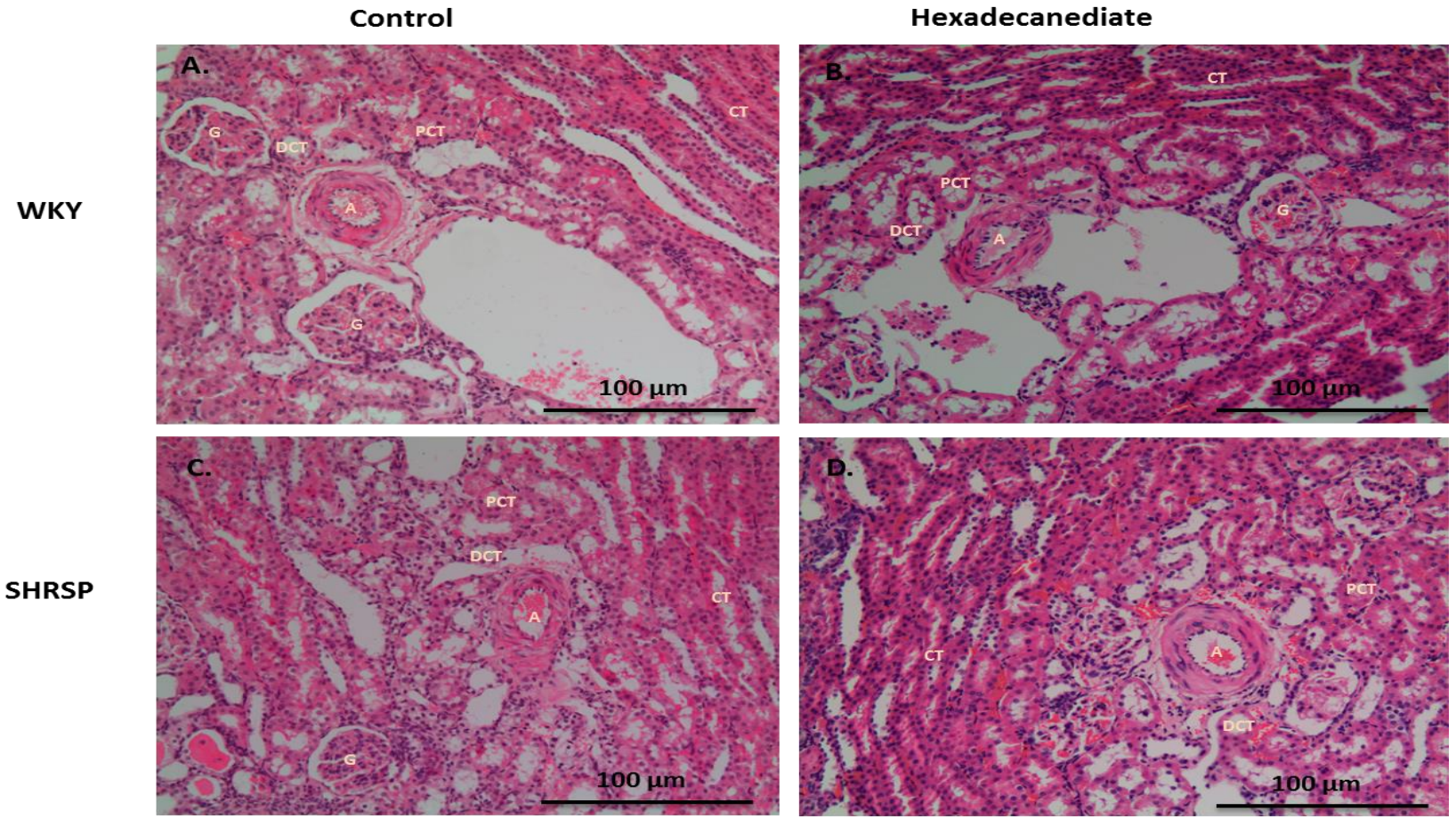

Figure 3-13: Haematoxylin and Eosin staining in kidney sections from WKY_{Gla} and $SHRSP_{Gla}$ rats treated with hexadecanedioic acid or vehicle for 9 weeks.

No changes were detected in kidney tissues obtained from WKY_{Gla} and $SHRSP_{Gla}$ rats after treatment with hexadecanedioic acid (B, D) compared to control (A, C). Abbreviation: Glomeruli (G), proximal convoluted tubules (PCT), distal convoluted tubules (DCT), collecting tubules (CT), and arteries (A). Magnification=X100; scale bar=100 µm, n= 8-10 slides per animal.

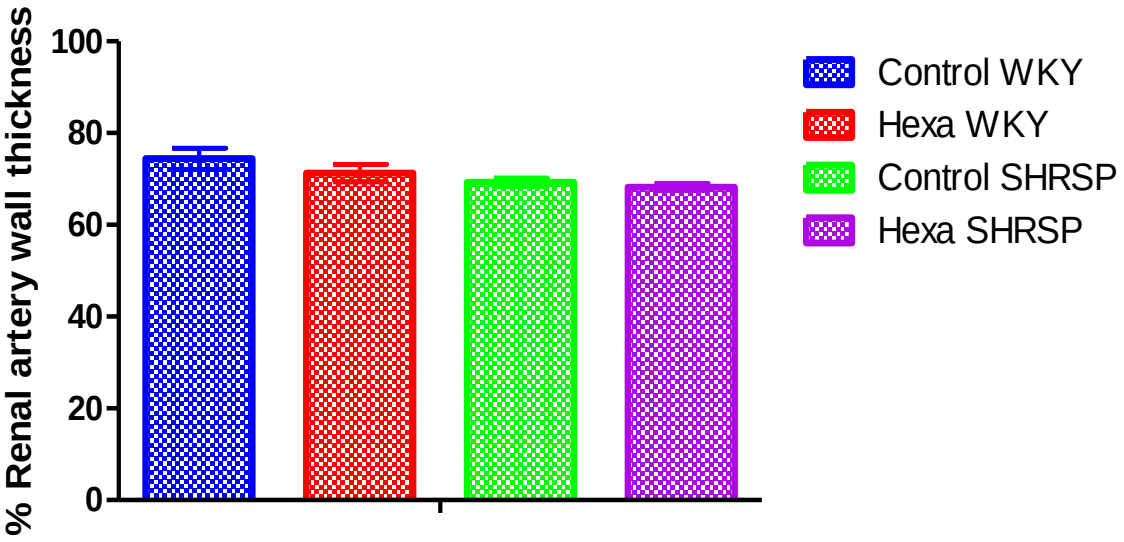

Figure 3-14: Percentage of renal vascular thickness of WKY_{Gla} and $SHRSP_{Gla}$ rats treated with hexadecanedioic acid or vehicle for 9 weeks.

No changes were observed in the renal artery wall thickness of WKY_{Gla} or $SHRSP_{Gla}$ rats treated with hexadecanedioic acid (n=3) compared to control rats (n=3) (mean ± standard error of mean).

3.6 Discussion

The data presented in this chapter validate the findings from the metabolomics studies conducted in the TwinsUK, KORA and Hertfordshire Cohorts (Menni *et al.*, 2015) demonstrating that hexadecanedioate levels are associated with blood pressure regulation (more details in Chapter 1, Section 1.13). Blood pressure was increased in adult WKY rats after treatment with hexadecanedioic acid (250 mg/kg/day) for 4 weeks in parallel with significant elevations in plasma hexadecanedioate levels. Furthermore, significant elevation in blood pressure of WKY_{Gla} rats was observed after chronic treatment with hexadecanedioic acid (250 mg/kg/day) over a 9 week study period. This elevation in blood pressure was observed once the rats reached maturity (i.e. at 13 weeks of age). However, chronic treatment with hexadecanedioic acid was unable to further increase blood pressure levels in $SHRSP_{Gla}$ rats. In a previous publication, we showed that systolic blood pressure in $SHRSP_{Gla}$ was significantly increased after 1% NaCl administration in drinking water for three weeks in order to enhance the level of hypertension and end organ damage. Plasma hexadecanedioate levels were already elevated in untreated $SHRSP_{Gla}$ compared to WKY_{Gla} and showed no further elevation after salt challenge (Menni *et al.*, 2015) (Figure 1-9). This suggests that elevating blood pressure *per se* does not stimulate hexadecanedioate production.

The original dose of hexadecanedioic acid (i.e. 250 mg/kg/day) was chosen based on previous studies to investigate it's in vivo effects on circulating lipid levels (Russell *et al.*, 1991; Frenkel *et al.*, 1994). The blood pressure response to higher doses was examined using a careful step-wise protocol in rats implanted with radiotelemetry probes. This dose-response study showed significantly increased blood pressure levels in WKY_{Gla} rats with progressively higher doses of hexadecanedioic acid. Potential toxicity effects prevented higher doses of hexadecanedioic acid being administered over longer study periods, since body weight was significantly reduced during longer-term treatment in $SHRSP_{Gla}$ and WKY_{Gla} rats even at the 250mg/kg/day dose (Table 3-5), (Table 3-6) and (Table 3-7).

The increased vascular reactivity to noradrenaline shown in the mesenteric arteries of hexadecanedioic acid-treated rats indicates a vascular mechanism underlying the association between hexadecanedioate and blood pressure (Figure

3-6 A). It is well established that hypertension is associated with changes in vascular structure, mechanics, and function, which reduce the lumen size of arteries and hence increase vascular resistance in hypertension (Intengan and Schiffrin, 2000). Previous experimental studies in hypertension have demonstrated amplified sensitivity to noradrenaline, increased myogenic tone, impaired endothelium-dependent relaxation and decreased acetylcholine-induced and flow-mediated vasodilatation responses in a range of hypertensive animal models investigated (de Wit *et al.*, 1998; Kang, 2014; Lüscher and Vanhoutte, 1986; Intengan and Schiffrin, 2000; Izzard and Heagerty, 1999). The stimulation of vascular smooth muscle cells with noradrenaline causes Ca^{2+} influx from intracellular Ca^{2+} stores via the inositol trisphosphate pathway (IP_3). IP_3 acts to release Ca^{2+} from the endoplasmic reticulum by binding to receptors that are ligand-gated Ca^{2+} channels to regulate vascular smooth muscle cell contraction (Liskova *et al.*, 2014). K^+ channels also play an important role in modulating contraction of vascular smooth muscle, which is mediated by Ca^{2+} release through L-type voltage dependent Ca^{2+} channels (L-VDCC) (Liskova *et al.*, 2014). Increased sensitivity of mesenteric arteries to noradrenaline during hexadecanedioic acid treatment may therefore suggest a role for hexadecanedioate on intracellular Ca^{2+} signalling. In systematic metabolomics study performed by Hiltunen *et al*, which verified the role of hexadecanedioate on intracellular Ca^{2+} signalling. This is further indicated by a recent metabolomics study conducted by Hiltunen *et al*, which aimed to identify the metabolic biomarkers related to four classes of anti-hypertensive drugs. They found that amlodipine (i.e. calcium channel blocker) was the only class of drug associated with decreased circulating levels of hexadecanedioate in hypertensive patients (Hiltunen *et al.*, 2017). These findings suggest that further investigation is needed to examine the role of hexadecanedioate on intracellular Ca^{2+} signalling.

In this study, no significant alterations were found in the relaxation response to carbachol in rats treated with hexadecanedioic acid compared with control rats (Figure 3-6 B). Carbachol is a synthetic analogue of acetylcholine and like other vasodilatation agents such as substance P, bradykinin, histamine, thrombin, and serotonin, it produces endothelium-dependent relaxation of blood vessels via nitric oxide (NO) signalling (Sumbria and Fisher, 2017). During hypertension, the formation of reactive oxygen species (ROS) increases, leading to increased

vascular smooth muscle proliferation and hypertrophy (Loperena and Harrison, 2017). Particularly, the superoxide radical (O_2^-) interacts with endothelium-derived nitric oxide (NO), to form the strong oxidant peroxynitrite ($ONOO^-$), which causes a reduction in NO bioavailability, leading to reduced dilation of the arteries and enhancement of systemic vascular resistance (Harrison *et al.*, 2007; Loperena and Harrison, 2017). The lack of impact of hexadecanedioic acid on carbachol-induced vasodilation therefore suggests that hexadecanedioate is unlikely to exert it's effect via endothelial–derived relaxation response and NO signalling. It would have been beneficial to measure the effect of hexadecanedioate on basal tone and NO bioavailability by incorporating an additional dose-response curve into the myography protocol to examine the relaxation-reponse to carbachol in the presence of L-NAME. However, due to the already extensive tissue harvest and analysis protocol on the day of sacrifice it was not posible to carry out this more in-depth investigation.

In hypertension, the function of resistance-artery reactivity may be altered due to hypertrophic remodelling which decreases lumen diameter leading to increased peripheral resistance (Intengan and Schiffrin, 2001). Hypertrophic vascular remodelling characterised by decreased outer and inner wall diameters, unaltered cross-sectional area and increased media/lumen ratio without stiffening has been shown in spontaneously hypertensive rats and essential hypertensive patients (Renna *et al.*, 2013). Unfortunately, time constraints in our study prevented assessment of vessel morphology using pressure myography alongside the wire myography for functional analysis in mesenteric arteries. This would have allowed investigation of any hexadecanedioic acid-induced changes in vessel size, wall thickness and elastic properties. However, as a surrogate we examined the % wall thickness of the renal arteries by histological analysis. In this analysis, no differences in renal wall thickness were observed in hexadecanedioic acid-treated WKY_{Gla} or $SHRSP_{Gla}$ rats compared to control rats. Previous histological studies have shown that vascular changes including hyperplasia and smooth muscle cell vaccuolation were observed in kidneys from salt-loaded $SHRSP_{Gla}$ rats indicating accelerated hypertension (Koh-Tan *et al.*, 2013). Renal damage during hypertension has been related to growth or migration of vascular smooth muscle cells through alterations in inflammatory responses, dysfunction of endothelial cells, and degradation or synthesis of extracellular matrix components (Renna *et*

al, 2013). The lack of obvious changes in renal histology suggests that hexadecanedioic acid treatment does not impact on these mechanisms, or that the effects are too mild to elicit renal damage.

In accordance with the lack of renal pathology, there were also no changes observed in renal mass index or renal function in terms of urine output or levels of biomarkers (i.e. urea, creatinine) in urine or plasma in WKY rats after 4-weeks of hexadecanedioic acid treatment. However, bilirubin levels in urine samples were significantly increased in hexadecanedioic acid-treated rats compared to control rats (Table 3-3). Increasing evidence suggests that mildly elevated serum bilirubin levels inhibit inflammation and the proliferation of vascular smooth muscle cells, which suggests a relationship between serum bilirubin levels and cardiovascular disease (Chen *et al.*, 2017; Demir *et al.*, 2014; Yang *et al.*, 2009). Studies by Chin *et al.*, 2009 identified that serum bilirubin was inversely associated with systolic blood pressure and with the prevalence of hypertension. In addition, bilirubin is considered to be a potent anti-oxidant and plays a role in oxidative stress by inhibiting the synthesis of reactive oxygen species in vascular smooth muscle cells (Wang and Bautista, 2015). However, in this study hexadecanedioic acid treatment induced an increase in bilirubin levels only in the urine but not in plasma. Increased bilirubin levels in urine may indicate an impairment of liver function or obstruction of biliary drainage leading to leakage of bilirubin out of liver cells, which is eliminated in the urine.

In our study, no changes were observed in liver mass index in hexadecanedioic acid-treated rats compared to control rats. In addition, biochemical analysis of plasma samples from hexadecanedioate–treated rats exhibited no significant differences in the liver enzymes alanine aminotransferase (ALT) and aspartate aminotransferase (AST). Histological examination of liver sections from WKY_{Gla} and $SHRSP_{Gla}$ rats also showed no major pathological changes after chronic treatment with hexadecanedioic acid for 9 weeks (Figure 3-12). Therefore, liver function and morphology appear to remain normal in hexadecanedioic acid-treated rats despite elevated urine bilirubin levels. However, the lack of pathological changes in these studies may be due to the treatment period not being long enough for end-organ damage to become apparent.

In the longer-term treatment study, significant increases were observed in retroperitoneal fat pad weight of $SHRSP_{Gla}$ rats treated with hexadecanedioic acid compared to control rats. This is in contrast to findings from a previous study carried out by Tzur *et al*. (1988), which demonstrated that treatment with ß, ß'-tetramethyl-substituted hexadecanedioic acid (MEDICA 16) caused an acute reduction in adiposity. However, the Sands rats used in the Tzur *et al* study are a model of obesity rather than spontaneous hypertension, which may in part explain the contrasting results. Flachs *et al*. (2005) identified that reduced lipid accumulation in abdominal fat results in stimulation of fatty acid beta-oxidation (ß oxidation); where hexadecanedioate is principally metabolised. Elevations in fatty acid ß-oxidation are found to be negatively correlated with body mass index. Therefore, increased fatty acid ß-oxidation leads to increased weight loss (Rupasinghe *et al*., 2016). In our study, $SHRSP_{Gla}$ and WKY_{Gla} rats treated with hexadecanedioic acid significantly lost weight during the study period as shown in Table 3-5, Table 3-6 and Table 3-7. These results may indicate that treatment with hexadecanedioic acid causes an alteration in fatty acid ß-oxidation, potentially leading to increase in an alternative fatty acid oxidation pathway (i.e. the omega oxidation pathway).

In the current study, cardiac function was also assessed during treatment with hexadecanedioic acid for 4 weeks and during chronic treatment for 9 weeks by echocardiography. Relative wall thickness was significantly reduced in the hexadecanedioic acid-treated WKY_{Gla} rats compared to control rats during the 9 week-treatment period (Table 3-5). However, there were no significant differences in heart function parameters such as fractional shortening, stroke volume and cardiac output after hexadecanedoic acid treatment in $SHRSP_{Gla}$ or WKY_{Gla}. Cardiac morphology was also evaluated by applying haematoxylin staining to heart histology sections, which showed no changes in either WKY_{Gla} or $SHRSP_{Gla}$ rats after chronic treatment with hexadecanedioic acid (Figure 3-11).

The significant reductions in body weight despite significantly increased epididymal fat pad weight and no change in volume drank/urine output in $SHRSP_{Gla}$ rats may indicate that muscle wasting is induced in treated rats. Accordingly, we observed a significant reduction in plasma levels of creatine kinase (CK) in WKY rats after 4 weeks of hexadecanedioic acid treatment (Table 3-2). CK is a sensitive marker of muscle injury and low levels in plasma may indicate reduced muscle

mass. Creatine has an essential role in cellular energy homeostasis in tissues such as brain, gut, heart and skeletal muscles which have high dynamic energy demands (Kitzenberg *et al.*, 2016). Creatine and its enzyme, CK, enable the transfer of high-energy phosphates in the form of phosphocreatine between sites of ATP generation such as mitochondrial oxidative phosphorylation and glycolysis (Kitzenberg *et al.*, 2016). Reductions in CK levels may occur due to substantial changes in cardiac metabolism and myocardial energetics, and plasma CK is used as a biomarker to indicate damage to the myocardium and cardiovascular functional ability (Stambuk and Konjevoda, 2002). Previous studies have demonstrated that CK activity is reduced in humans with left ventricular hypertrophy and impaired myocardial contractile function (Intengan and Schiffrin, 2001; Ingwall *et al.*, 1985). In addition to these observations, decreased expression of CK was observed in heart tissues obtained from rats with pulmonary artery hypertension and right ventricular failure (Fowler *et al.*, 2015). Furthermore, impaired contractile function and independent contributors to heart failure development have been found to be associated with reduced CK ATP delivery in animal models (Ye *et al.*, 2001b, 2001a; Fowler *et al.*, 2015). Hypertension may cause alterations in cardiac metabolism through increased myocardial energy demand to compensate for changes in glycolytic intermediates and high energy-phosphates (Dodd *et al.*, 2012). Unfortunately, CK levels were not examined in plasma from the longer term treatment rats. These measurements would need to be completed in order to determine whether CK levels were similarly reduced in hexadecanedioic acid-treated $SHRSP_{Gla}$ rats. However, the absence of cardiac dysfunction together with significant loss of body weight would suggest that skeletal muscles rather than cardiac muscles are being impacted by hexadecanedioic acid treatment in the longer term intervention studies.

Study limitations

There were a number of limitations to these studies, including the small number of animals used in both longer-term and dose-response hexadecanedioic acid studies. These studies were designed to comply with animal welfare regulations under the guidance of our vet (NVS)/Home Office Inspector, since we did not know how higher doses of hexadecanedioic acid would be tolerated, or potential toxicity issues over a longer treatment period. Therefore, the studies were conducted on

small batches of animals only. In addition, not all of the studies were carried out using WKY rats obtained from the Glasgow colony due to issues with animal supply at times, requiring the use of WKY rats from Harlan (Hillcrest, UK). This may create variability in the results since WKY rats from different colonies can have varying phenotypes (Zhang-James *et al.*, 2013).

Although blinding was conducted for ex vivo analysis, it was difficult to remain blinded during in vivo procedures since the hexadecanedioic acid-treated WKYs displayed behavioural issues during handling and restraint for the tail cuff method of blood pressure measurement. WKY rats' activity, measured by radiotelemetry in the 4 weeks study, showed no significant difference between control and treated groups (i.e. when the rats were unrestrained in their home cage) (Figure 3-5). However, the treated group resented being handled during tail cuff measurements during the longer-term intervention study.

In conclusion, our data suggests that increased circulating levels of hexadecanedioate leads to blood pressure elevation and impairment of vascular function in WKY rats. The data also indicate increased adiposity index despite reduced body weight in SHRSP rats. These results may indicate muscle wasting and altered cellular energy homeostasis such as an impairment of the ß-oxidation pathway. Further studies to validate and clarify the mechanisms by which hexadecanedioate affects blood pressure, are described in the following chapters.

Chapter 4 Global metabolomics profiles of pathways underling hexadecanediate-induced blood pressure elevation

4.1 Introduction

The metabolomics field is currently one of the most influential bioanalytical approaches that creates quantitative or semi-quantitative information about biochemical metabolites (final products) of the metabolism. It is used to obtain a clear picture of the metabolites in biological mechanisms and determining specific metabolites related to phenotype, diseases or drug treatments (Sussulini, 2017; Van der Hooft *et al.*, 2016). Metabolomics analysis has been widely used in recent studies to discover metabolites, drug-metabolites or biomarkers that are related to specific disease. (Maltesen *et al.*, 2016; de Oliveira *et al.*, 2016; Cowan *et al.*, 2016; Van der Hooft *et al.*, 2016).

Metabolome can be a very sensitive measure of organisms' phenotypes due to metabolites being the final products of several genome-wide or proteome-wide interactions. In fact, metabolites are related to the phenotype and any changes in metabolites such as amino acids, lipids, and carbohydrates can reflect consequences of disease or disease-related conditions (Monteiro *et al.*, 2013; Peng *et al.*, 2015). Cardiovascular, neurological, cancer and metabolic diseases have been studied by using metabolomics methods (i.e. mass spectrometry and nuclear magnetic resonance). This has provided a significant improvement in the discovery of biomarkers that are related to these diseases (Gowda and Raftery, 2013). For instance, increases in branched-chain amino acids (BCAA) such as leucine, isoleucine, and valine contribute to development of obesity-associated insulin resistance (Newgard *et al.*, 2013). Moreover, increases in methylated arginine species are related to the inhibition of nitric oxide production, leading to increased risk of coronary artery disease, myocardial infarction, and stroke (Wang *et al.*, 2009).

The method selected for metabolomics study varies depending on the research type, such as targeted analysis of metabolites (i.e. measurement of selected compounds, which belong to metabolic pathway). Metabolic fingerprinting (untargeted analysis), which is used to detect all metabolites present in a biological sample (urine, plasma or tissues) to identify specific metabolites related to a particular condition. The fingerprinting approach is also beneficial in the discovery of novel pathways and biomarkers to assess new therapeutic targets (Monteiro *et al.*, 2013; Sussulini, 2017; Spratlin *et al.*, 2009). In a standard

metabolomics analysis, several chemical detection platforms have been used; including mass spectrometry (MS) and nuclear magnetic resonance (NMR) However, a single analytical technique is not ideal to use for covering a whole metabolome due to chemical diversity of the metabolites. Therefore, a combination of platforms has been utilised over recent years (Sussulini, 2017). Detection of metabolites by using mass spectrometry is a powerful tool for investigations of metabolism because of its flexibility for the detection of multiple chemical molecular classes and its sensitivity to low-abundant molecules. A combination of a separation technique and MS is called a metabolomics platform and the most commonly used metabolomics platforms are: capillary electrophoresis–mass spectrometry (CEMS), gas chromatography-mass spectrometry (GC-MS) and liquid chromatography–mass spectrometry (LC-MS) (Wang *et al.*, 2009).

Ultra-high-resolution and high mass accuracy MS application differentiates the molecular classes accurately and identifies the molecular formula. Also, it provides a high lateral resolution imaging and highly dense data. However, data complexity exists, including challenges in analysing the results by using advanced computational analysis programmes and development of technical methodology to examine specific classes of metabolites that differentiate between groups (Van der Hooft *et al.*, 2016; Madsen *et al.*, 2010). Advanced spectral analysis includes multivariate analyses such as principal component analysis (PCA), which are often used for sample overview and classification. Also, univariate analysis based on the Student's t-test and Mann-Whitney U test are used for verification (Griffiths *et al.*, 2010; Madsen *et al* , 2010; Zhao *et al.*, 2014).

Biological interpretation is a crucial step in any metabolomics study. When putative metabolites are identified, metabolic pathways are the next step to be investigated. The metabolomics process for biological interpretation is divided into three main types based on their strategies in metabolite identification. Firstly, the chemometrics approach, which mainly emphasises classifying and understanding the subset of spectral features as the only significant features (Madsen *et al* , 2010; Sussulini, 2017). The second method is the metabolic profiling approach which generally focuses on classification of all detectable metabolites from the spectral data before subsequent functional analysis (Sussulini, 2017). Consequently, the third approach, the chemo-enrichment

analysis approach is mainly focused on an estimation of biological activities directly from the spectral features by mapping all detected metabolites, then linking them with pathways. (Booth *et al*., 2013; Barupal and Fiehn, 2017).

The general aims of metabolomics studies are to measure the up-regulation and down-regulation of metabolites in abundance. They are also used for determining the impact of metabolites variations on metabolic pathways and identifying biomarkers to understand physiological variations in response to environmental changes (Peng *et al* , 2015). Our study is design to understand the metabolic impact of hexadecanedioate on the Wistar Kyoto (WKY) rats in order to identify metabolic pathways underlying hexadecanedioate-induced hypertension.

4.2 Hypothesis

Distinct metabolite signatures are associated with elevated circulating hexadecanedioate levels, which will allow identification of dysregulated pathways underlying hypertension.

4.3 Aims

The aim of this chapter is to investigate the metabolic effect of hexadecanedioic acid administration on cardiovascular tissues (i.e. heart, kidney, liver, aorta and brain) obtained from Wistar Kyoto (WKY) rats which were treated with hexadecanedioic acid (hexa) or vehicle. This will allow identification of the metabolic pathways leading to hexadecanedioate-induced hypertension.

4.4 Methods

4.4.1 Experimental animals

Eleven-week-old male WKY rats (Harlan, UK) were treated orally with hexadecanedioic acid mixed with baby food (250 mg/kg per day; n=5) or vehicle (n=5) for 4 weeks. The rats were housed individually in cages on a 12 hours light/dark circle at room temperature (21± 3˚C). Food and water were provided daily to the rats. The study protocols were approved by the Animals' Scientific Procedures Act 1986 under the project license of Dr Delyth Graham (70/9021).

4.4.2 Sample preparation

At sacrifice, liver, kidney, heart, aorta, brain and retroperitoneal fat tissues were collected from hexadecanedioic acid-treated and control WKY rats. The tissues were harvested, frozen in liquid nitrogen and maintained at -80 ºC. Tissues were then sent to Metabolon©, Inc. (Research Triangle Park, Durham, NC) for metabolomics analysis. Once the samples arrived at Metabolon©, the samples were inventoried and immediately stored at -80 ºC. Each sample received was recorded into the Metabolon LIMS system (Laboratory Information Management System) and assigned with a unique identifier code. Samples were prepared using the automated MicroLab STAR® system from Hamilton Company. Several recovery standards were added prior to the first step in the extraction process for quality control (QC) purposes. Following data acquisition and processing, proteins were precipitated with methanol under vigorous shaking for two minutes (Glen Mills GenoGrinder 2000) followed by centrifugation to remove protein, dissociate small molecules bound to protein or trapped in the precipitated protein matrix, and to recover chemically diverse metabolites. The resulting extract was divided into five fractions (platforms): (i) early and (ii) late eluting compounds for analysis by ultra-high performance LC-MS/MS (UPLC-MS/MS) using positive ionization, (iii) for analysis by UPLC-MS/MS using negative ionization, (iv) for analysis using a UPLC-MS/MS polar platform with negative ionization, and (v) a sample reserved for backup if needed. Samples were placed on a TurboVap® (Zymark) to remove the organic solvent. The sample extracts were stored overnight under nitrogen before preparation for analysis.

4.4.3 Metabolomic analyses using Ultra-High Performance Liquid Chromatography-Tandem Mass Spectroscopy (UPLC-MS/MS)

All methods utilised a Waters ACQUITY ultra-performance liquid chromatography (UPLC) and a Thermo Scientific Q-Exactive high resolution/accurate mass spectrometer interfaced with a heated electrospray ionization (HESI-II) source and Orbitrap mass analyser operated at 35,000 mass resolution. The sample extract was dried, then reconstituted in solvents compatible to each of the four methods. Each reconstitution solvent contained a series of standards at fixed concentrations to ensure injection and chromatographic consistency. One aliquot was analysed using acidic positive ion conditions and chromatographically optimised for more hydrophilic compounds. In this method, the extract was gradient eluted from a C18 column (Waters UPLC BEH C18-2.1x100 mm, 1.7 µm) using water and methanol, containing 0.05% perfluoropentanoic acid (PFPA) and 0.1% formic acid (FA). The second aliquot was also analysed using acidic positive ion conditions. In this method, the extract was gradient eluted from C18 column using methanol, acetonitrile, water, 0.05% PFPA and 0.01% FA and was operated at a higher organic content. The third aliquot was analysed using basic negative ion optimized conditions using a separate dedicated C18 column. The basic extracts were gradient eluted from the column using methanol, water and with 6.5 mM Ammonium Bicarbonate at pH 8. The fourth aliquot was analysed via negative ionization following elution from a HILIC column (Waters UPLC BEH Amide 2.1x150 mm, 1.7 µm) using a gradient consisting of water and acetonitrile with 10 mM Ammonium Formate, pH 10.8.

4.4.4 Metabolomics bioinformatics analysis

For bioinformatic analysis, Metabolon© used informatics systems consisting of the Laboratory Information Management System (LIMS), the data extraction and peak-identification software, data processing tools for quality control and compound identification, and a collection of information interpretation and visualization tools to analyse the data. The hardware and software foundations for these informatics components were the LAN backbone, and a database server running Oracle 10.2.0.1 Enterprise Edition.

4.4.5 Statistical analysis

4.4.5.1 Methods for identifying treatment-associated metabolites

R statistical software (a free software environment for statistical computing and graphics) was used under the guidance of Dr Desmond Campbell to analyse the raw data, which was provided by Metabolon©. Following the log transformation and imputation of missing values, comparisons between the groups' metabolomic profiles were performed using Welch's two-sample t-test, Student's T Test, Shrinkage T Test, and Random Forest to identify biochemical metabolites that significantly differed between hexadecanedioic acid-treated rats and controls. The level of significance was set at $p<0.05$. Also, the false discovery rate was assessed using the q-value to correct for multiple testing. The q-value ($q<0.10$) is an indication of high confidence in the results. A q-value of 0.1 means that we should expect 10% of tests with q-values of less than 0.1 to be false positives.

4.4.5.2 Wilcoxon Rank Sum (Man Whitney test)

The samples were ranked according to metabolite level. The Wilcoxon Rank Sum test is applied to see whether the ranks of one treatment group are significantly higher or lower than control group. The Wilcoxon Rank Sum test's power is low because it is rank (not value) based and the sample size is small (i.e. 5 rats/group). Under the null hypothesis, each arrangement of treatments and controls is equally likely. Number of all possible cases when five observations were selected from the set with 10 observations:

$$\frac{10!}{5!\,5!} = 252$$

The most extreme Wilcoxon Rank Sum statistics are given by arrangements completely separating the groups, i.e. AAAAABBBBB and BBBBBAAAAA. In fact, the most significant (one sided test) p-value that the test could generate for a dataset is (p value for one-sided test = 5/252 = 0.0198. p value for two-sided test = 2 * (5/252) = 0.0396).

4.4.5.3 Student's T Test

A Student's T-test is most commonly applied when the test statistic would follow a normal distribution. This test is based on the ratio of between groups or within group distribution. Assumption of student t-test is that the variable under test is assumed to be normally (Gaussian) distributed and with equal variances. In the dataset, the majority of metabolite distributions looked Gaussian, but a minority were skewed and/or had outliers. Such departures from normality might cause very significant t-test p-values. We found the T test to be conservative when the data contained outliers or distributions that were skewed, as shown in Figure (4-1), Figure (4-2) and Figure (4-3). The distribution in figure (4-1) is heavier tailed, meaning that outliners are more common. We simulated datasets of 10 samples in which 5000 variables had been observed. Samples were divided into two groups of five. Data followed the null hypothesis (i.e. no significant difference between the means of the two groups).

4.4.5.4 Welch's T test (unequal variances t-test)

Welch's T test is used in cases where the Student's T test is not applicable. Distribution within group is not the same across groups. Welch's T test allows for distribution to differ across groups. Welch's t-test is used for unequal variances, but the assumption of normality is maintained.

4.4.5.5 Shrinkage T Test

When sample sizes are small, the Student's T test lacks power because the ratio between and within group variance is poorly estimated. The shrinkage t-statistic is used to overcome this by incorporating a James Stein estimator, which estimates the metabolite's variance. When applied to a set of (three or more) metabolites, the vector of shrinkage t-statistics generated is guaranteed to be closer (on average) to the true t-statistic vector than the corresponding vector composed of Student t-statistics. In brief, metabolite ranking based on shrinkage t-statistics should be more accurate than ranking based on Student t alone.

Skewed and heavy Tailed

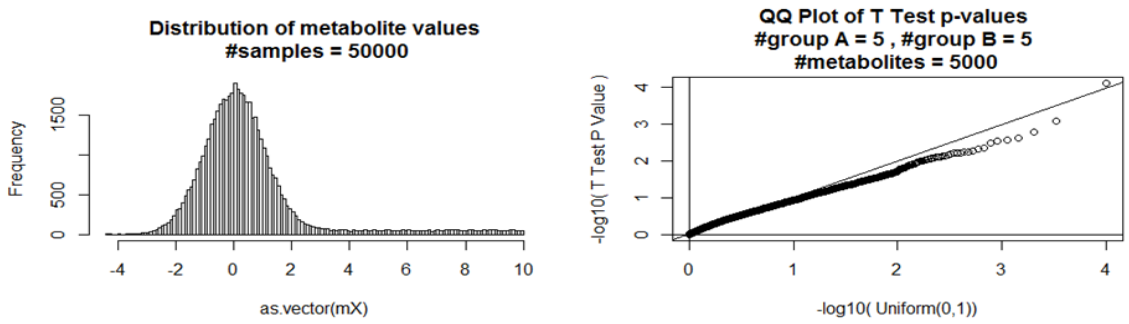

Figure 4-1: Skewed distribution is heavy tailed. Based on 5000 variables of 10 samples.
(Values taken from a mixture distribution of 0.9× Normal (0,1) +0.1×Uniform (0,10)).

Heavy Tailed

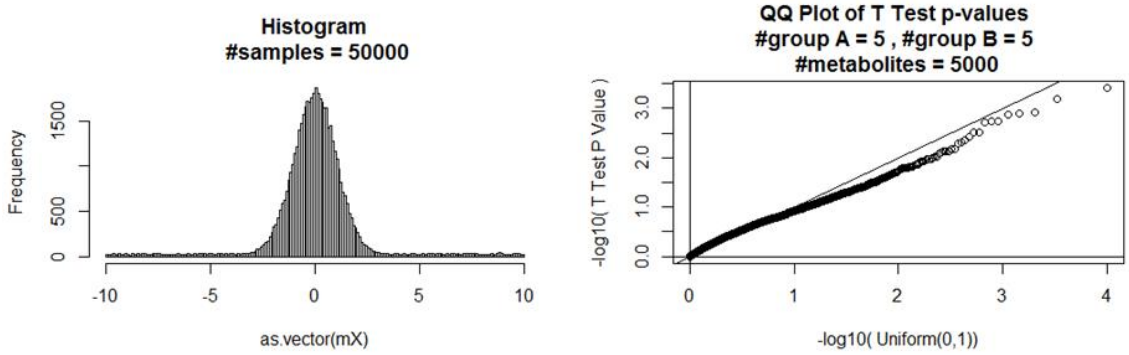

Figure 4-2: Heavy tailed distribution based on 5000 variables of 10 samples.
(Values taken from a mixture distribution of 0.9×Normal (0,1 +0.1×Uniform (10,10)).

Light tailed

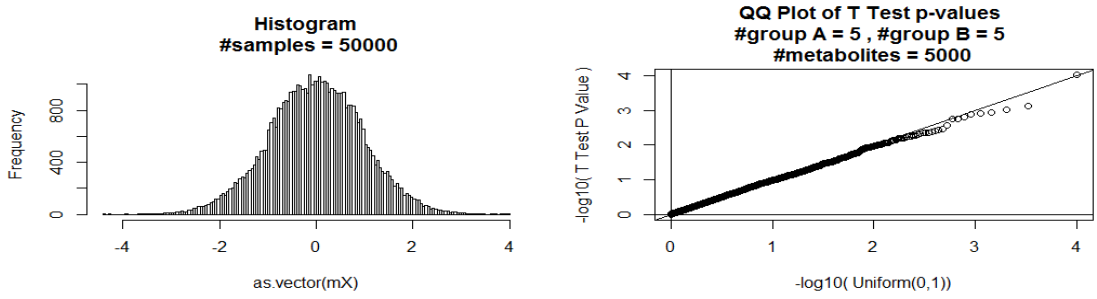

Figure 4-3: Light tailed distribution based on 5000 variables of 10 samples.
(Values from taken a mixture distribution of 0.9×Normal (0,1) +0.1×Uniform (1,1)).

4.4.5.6 Empirical Cumulative Distribution Functions

An empirical cumulative distribution function is a non-parametric estimator of the underlying cumulative distribution function of a random variable. Empirical cumulative distribution function is usually represented by;

$$\hat{F}_n(x) = \hat{P}_n(X \leq x) = n^{-1} \sum_{i=1}^{n} I(x_i \leq x)$$

Where, $\hat{F}_n(x) = \hat{P}_n(X \leq x)$ is empirical cumulative distribution function and $I(x_i \leq x)$ is the indicator function which has two possible values; ($x_i = 1, 2, 3, 4, \ldots\ldots, n$) is an independent, random variable.

$$I(x_i \leq x) = \begin{cases} 1 \; x_i \leq x \\ 0 \; x_i > x \end{cases}$$

4.4.5.7 Random Forest (RF)

Random forest analysis (RFA) is a statistical tool utilizing a supervised classification technique based on an ensemble of decision trees and can aid in the identification of biomarkers differentiating classification groups. For a given decision tree, a random subset of the data with identifying true class information is selected to build the tree and then the remaining data are passed down the tree to obtain a class prediction for each sample. This process is repeated thousands of times to produce the forest. The final classification of each sample is determined by computing the class prediction frequency (votes). For example, suppose the random forest consists of 50,000 trees and that 25,000 trees had a prediction for sample 1. Of these 25,000, suppose 15,000 trees classified the sample as belonging to Group A and the remaining were 10,000 classifieds belonging to Group B. Then the votes are 0.6 for Group A and 0.4 for Group B, and hence the final classification is Group A. This method is unbiased, since the prediction for each sample is based on trees built from a subset of samples that do not include that sample. When the full forest is grown, the class predictions are compared to the true classes, generating a measure of prediction accuracy.

4.4.5.8 Correlation

Inter specimen correlation in metabolite deviations is applied by a heatmap representation of the specimen metabolite deviations correlation matrix (10 by 10). Correlations were calculated as Kendal's Tau which is a non-parametric measure of correlation between two ranked variables. Correlations are in range (-0.2, 1). 1 is highly correlated and < 0 is intended low correlated.

4.4.5.9 Pathway enrichment

Two tests were used to measure pathway enrichment. Firstly, the hypergeometric test, which is used to measure the statistical significance of having samples containing of a defined number of successes from a population. Also, the fisher method test is used to combine the results from several independent tests with the same overall hypothesis. Enrichment values are based on the significant compounds relative to all detected compounds in the pathway. Enrichment = (number of significant metabolites in pathway/ total number of detected metabolites in pathway)/ (total number of significant metabolites/ total number of detected metabolites).

4.4.5.10 Principle component analysis (PCA)

Principal components analysis is an unsupervised, uncorrelated analysis that reduces the dimension of the data (i.e. reduces a large correlated number of variables to a small uncorrelated number of variables that still contains most of the information in the large set). Each principal component is a linear combination of every metabolite and the number of principal components is equal to the number of observations. The first principal component accounts by determining the coefficients of the metabolites that maximise the variance of the linear combination. The first principal component has the largest possible variance, that is it accounts for as much of the variability in the data as possible. The second component finds the coefficients that maximise the variance with the condition that the second component is orthogonal to the first. The second principal component captures the highest variance from what is left after the first principal component. The third component is orthogonal to the first two components and so on. The total variance is defined as the sum of the variances of the predicted values of each component (the variance is the square of the standard deviation),

and for each component, the proportion of the total variance is accounted. For example, if the standard deviation of the predicted values of the first principal component is 0.4 and the total variance = 1, then 100*0.4*0.4/1 = 16% of the total variance is explained by the first component.

4.5 Results

4.5.1 Quality control

4.5.1.1 Kidney

The missingness distribution helps to develop the quality control strategy and to improve analysis of the datasets. Approximately 10% of metabolites (missing) were dropped from the kidney dataset during quality control process and 469 of metabolites remained.

The dataset consisted of 10 samples (5 controls, 5 treated) containing 469 metabolites. The distribution of values within each metabolite cannot easily be characterised, as the sample size is 10. However, investigating the relationship between summary statistics across metabolites and across the samples can be performed. Scatterplots (Figure 4-4) show the relation between the mean and standard deviation per metabolite (A and B) and per sample (C and D). There is a linear relationship between mean and standard deviation per metabolite on the log scale, as shown in B. Also, there is an outlier (sample number K1_A_6469), as shown in C and D.

The empirical cumulative mass of metabolite deviation was also performed per sample stratified by platform to evaluate the distribution of our data. All samples performed well except for sample (K1_A_6469) (marked in blue colour) since this sample has unusual values for metabolites as measured by the LC/MS (Figure 4-5).

4.5.1.2 Heart

Twenty percent of metabolites (missing) were dropped from the heart dataset during the quality control process and 435 of metabolites remained. Scatterplots (Figure 4-6) show the relation between the mean and standard deviation per metabolite (A and B) and per sample (C and D). There is a linear relationship between mean and standard deviation per metabolite on the log scale, as shown in (Figure 4-6 B). Also, the empirical cumulative mass of metabolite deviations per subject stratified by platform illustrated that all samples were well distributed for metabolites measured by LC/MS, as shown in Figure 4-7.

4.5.1.3 Liver

Following initial quality control, the remaining dataset consisted of 10 samples (5 controls, 5 treated) containing 558 metabolites. No outliers were observed in liver samples. Scatterplots (Figure 4-8) show the relationship between the mean and standard deviation per metabolite (A and B) and per sample (C and D). There is a linear relationship between mean and standard deviation per metabolite on the log scale, as shown in (Figure 4-8 B). Also, the empirical cumulative mass of metabolite deviations per subject stratified by platform illustrate that all samples were well distributed for metabolites measured by LC/MS, as shown in Figure 4-9.

4.5.1.4 Aorta

380 metabolites were detected in aorta samples. There were no obvious outliers. Scatterplots (Figure 4-10) show the relationship between the mean and standard deviation per metabolite (A and B) and per sample (C and D). There is a linear relationship between mean and standard deviation per metabolite on the log scale, as shown in (Figure 4-10 B). The empirical cumulative mass of metabolite deviations per subject stratified by platform illustrate that all samples were well distributed for metabolites measured by LC/MS, as shown in Figure 4-11.

4.5.1.5 Brain

The remaining dataset consisted of 10 samples (5 controls, 5 treated) containing 454 metabolites. There were no obvious outliers. Scatterplots (Figure 4-12) show the relationship between the mean and standard deviation per metabolite (A and B) and per sample (C and D). There is a linear relationship between mean and standard deviation per metabolite on the log scale, as shown in (Figure 4-12 B). Also, the empirical cumulative mass of metabolite deviations per subject stratified by platform illustrate that all samples were well distributed for metabolites measured by LC/MS, as shown in Figure 4-13.

4.5.1.6 Adipose tissue

The remaining dataset consisted of 10 samples (5 controls, 5 treated) containing 380 metabolites. There were no obvious outliers. Scatterplots (Figure 4-14) show the relationship between the mean and standard deviation per metabolite (A and

B) and per sample (C and D). There is a linear relationship between mean and standard deviation per metabolite on the log scale, as shown in (Figure 4-14 B). Also, the empirical cumulative mass of metabolite deviations per subject stratified by platform illustrate that all samples were well distributed for metabolites measured by LC/MS, as shown in Figure 4-15.

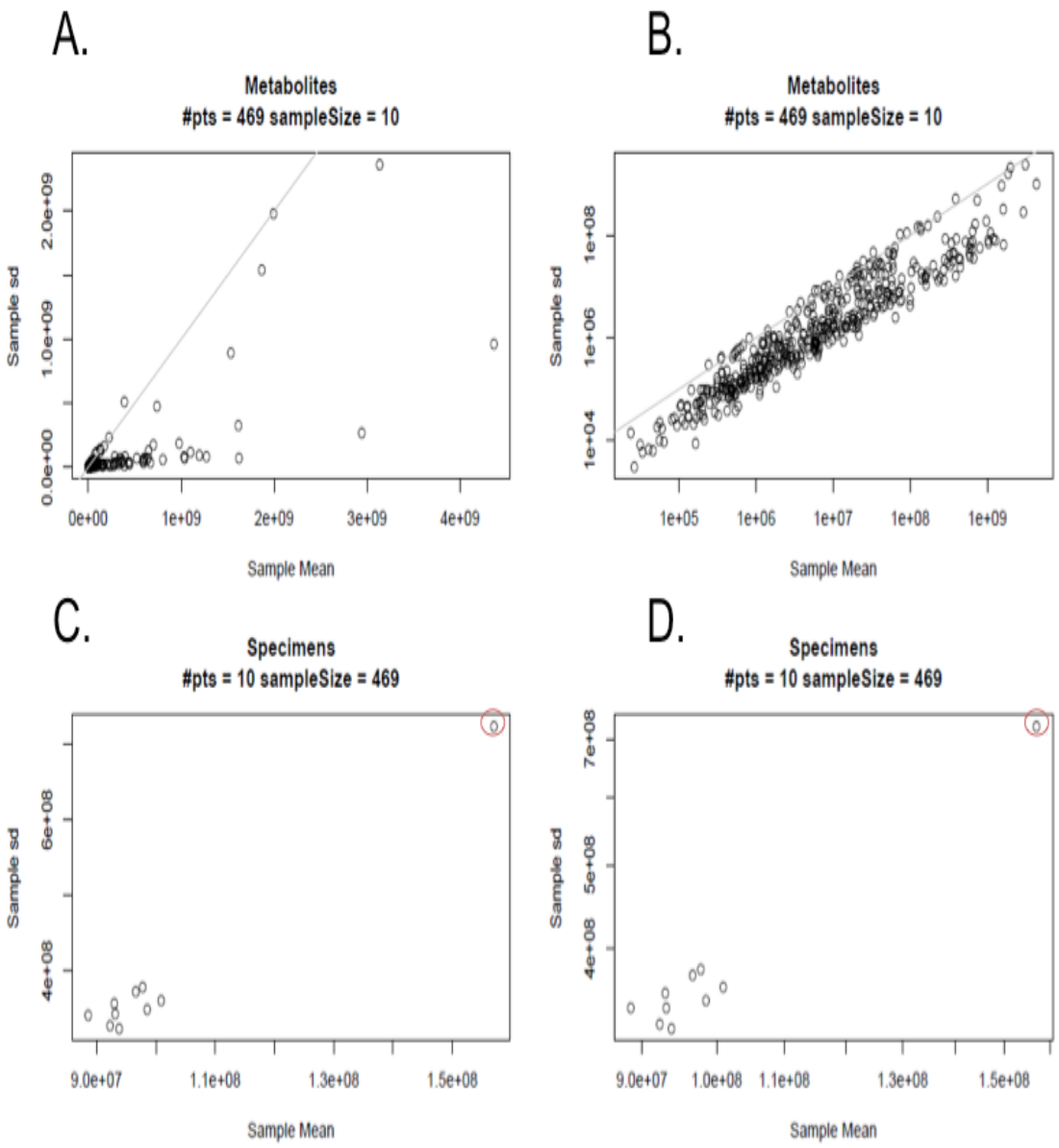

Figure 4-4: Scatterplots show the relationship between the mean and standard deviation per metabolite and per kidney sample.

The relationship between the mean and standard deviation per metabolite (A, B) and per kidney sample (C, D). Figures (A, C) represent the original scale and figures (B, D) represent the log scale. There is a linear relationship between mean and standard deviation per metabolite on the log scale (B). The red circle indicates the outlier (sample number K1_A_6469).

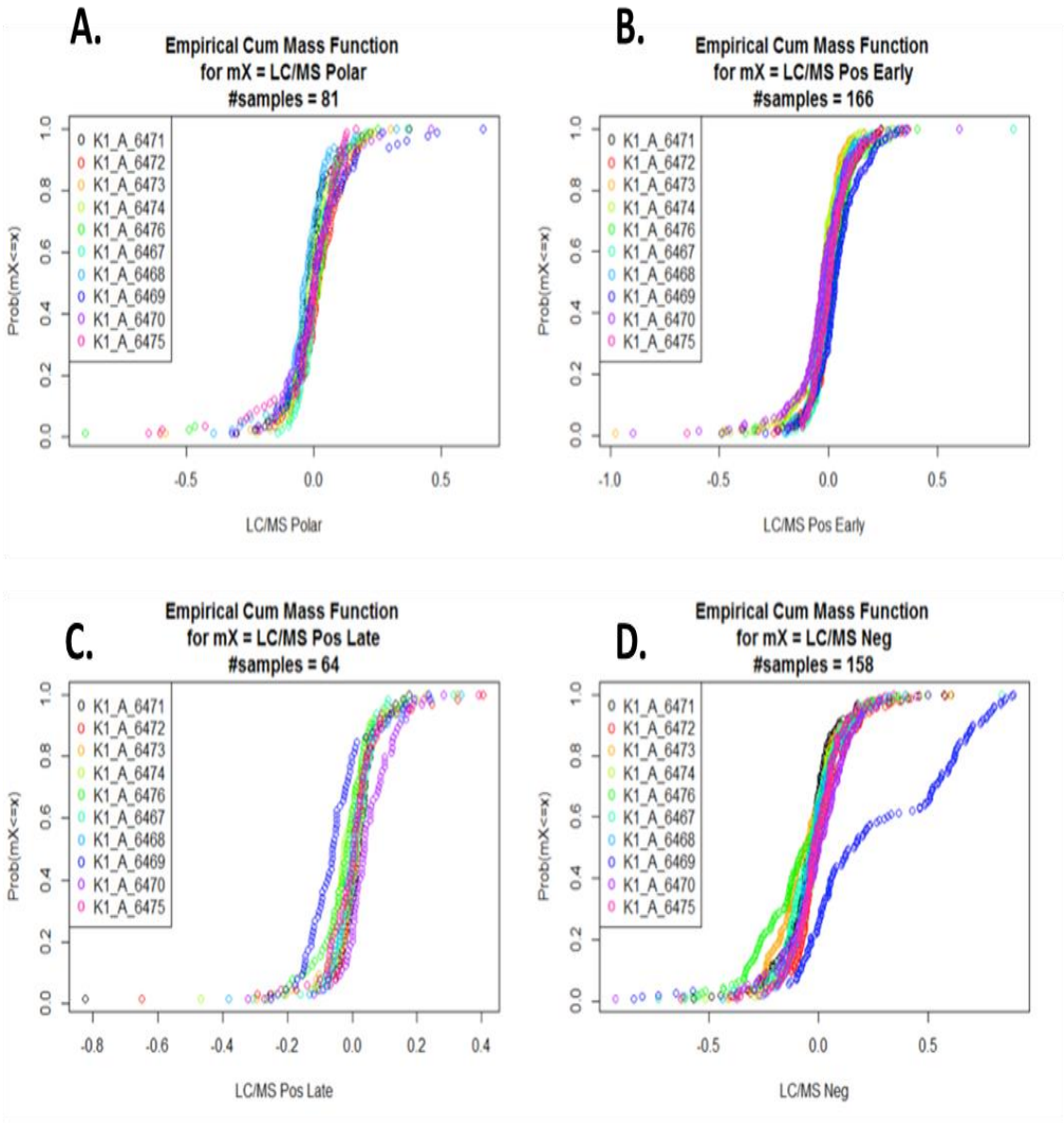

Figure 4-5: The empirical cumulative mass of metabolite deviation per kidney sample.

The empirical cumulative mass of metabolite deviation per kidney sample showed (A) 81 metabolites detected in LC/MS polar platform, (B) 166 metabolites detected in LC/MS positive early platform, (C) 64 metabolites detected in LC/MS positive late platform and (D) 158 metabolites detected in LC/MS negative platform. Y axis presents empirical cumulative mass function and X axis presents sample stratified by platform. Each colour represents an individual animal (sample). All samples performed well in all platforms except one sample (K1_A_6469) in the LC/MS negative platform, which appeared not well distributed (marked in blue colour).

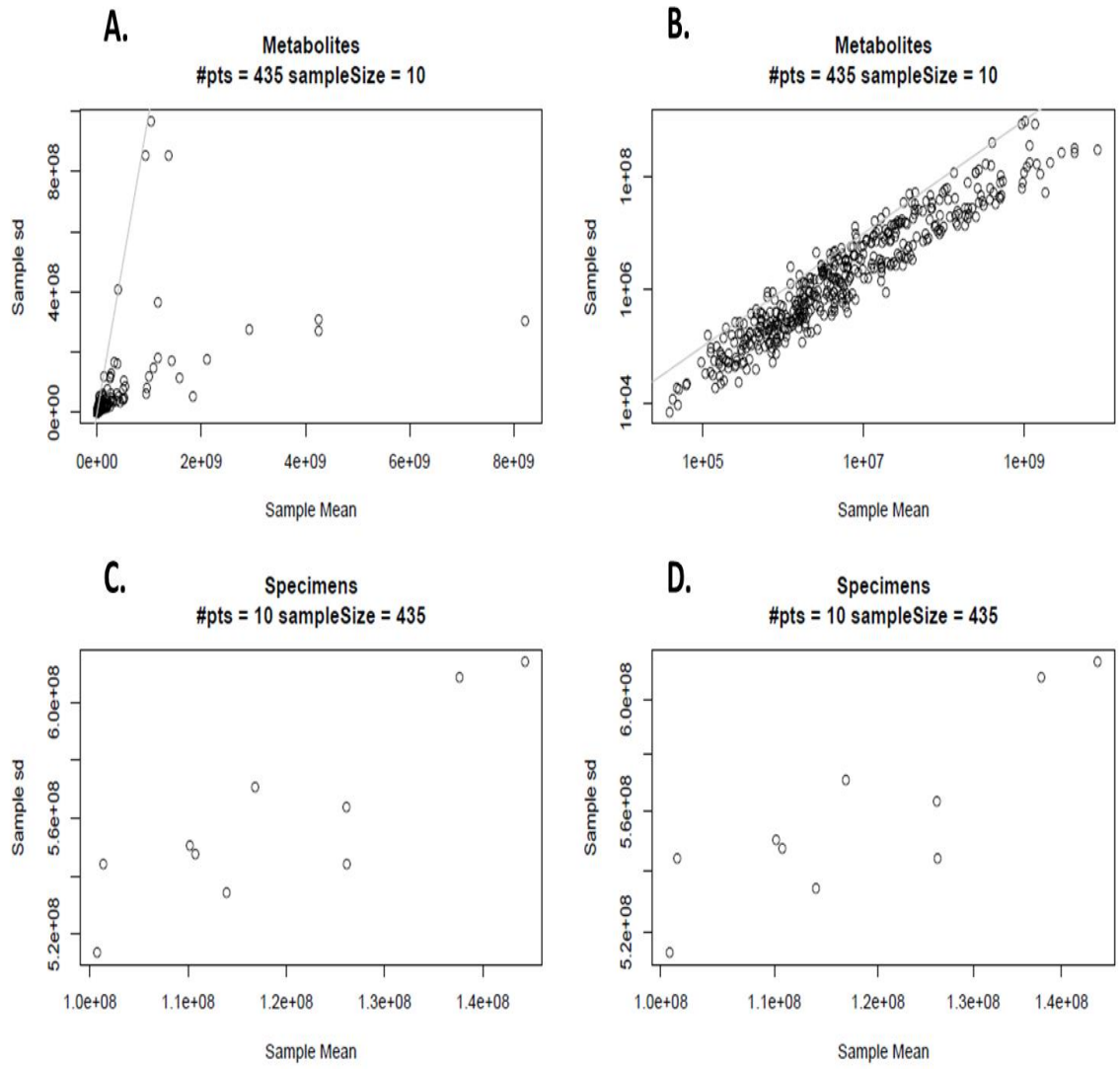

Figure 4-6: Scatterplots show the relationship between the mean and standard deviation per metabolite and per heart sample.

Linear relationship was observed between mean and standard deviation per metabolite on the log scale (B). Scatterplots show that no outliers were observed in the relationship between the mean and standard deviation per metabolite (A, B) and per heart sample (C, D). Figures (A, C) represent the original scale and Figures (B, D) represent the log scale.

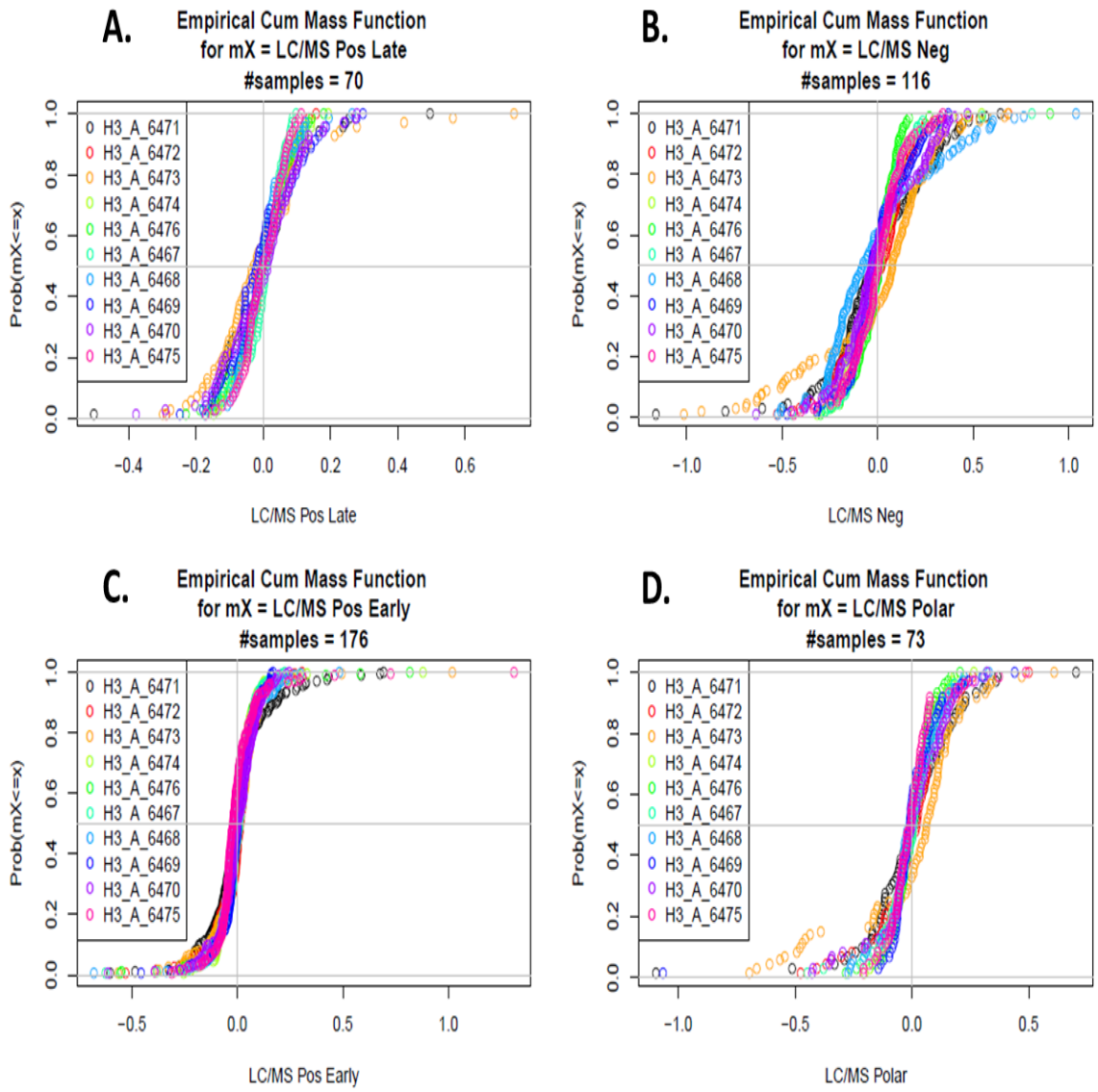

Figure 4-7: The empirical cumulative mass of metabolite deviation per heart sample.

The empirical cumulative mass of metabolite deviation per heart sample. (A) 70 metabolites detected in LC/MS positive late platform, (B) 116 metabolites detected in LC/MS negative platform, (C) 176 metabolites detected in LC/MS positive early platform and (D) 73 metabolites detected in LC/MS polar platform. Y axis presents empirical cumulative mass function and X axis presents samples stratified by platform. Each colour represents an individual animal (sample). All samples performed well in all platforms.

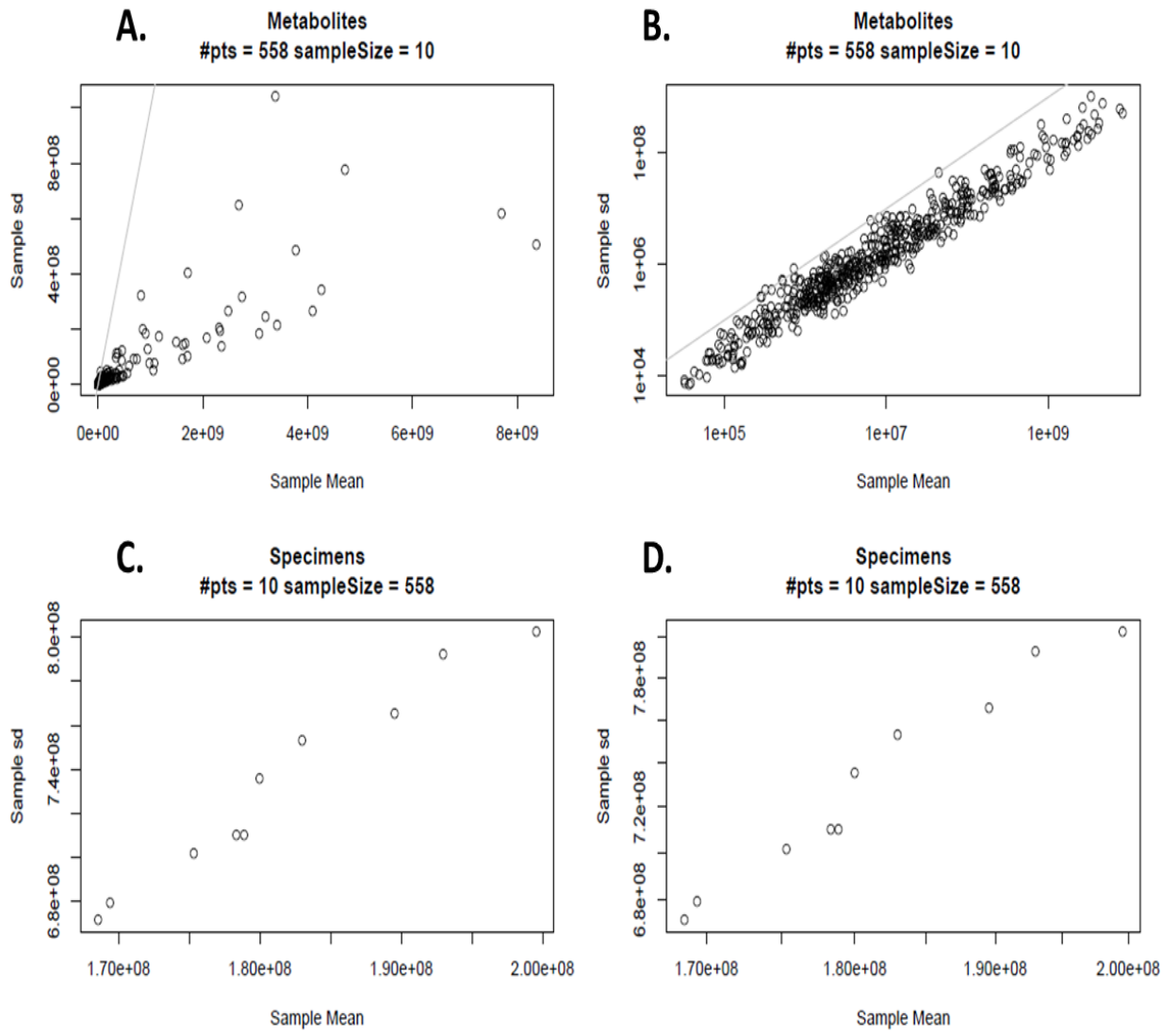

Figure 4-8: Scatterplots show the relationship between the mean and standard deviation per metabolite and per liver sample.

There is a linear relationship between mean and standard deviation per metabolite on the log scale (B).Scatterplots show that no outliers were observed in the relationship between the mean and standard deviation per metabolite (A, B) and per liver sample (C, D). Figures (A, C) represent the original scale and Figures (B, D) represent the log scale.

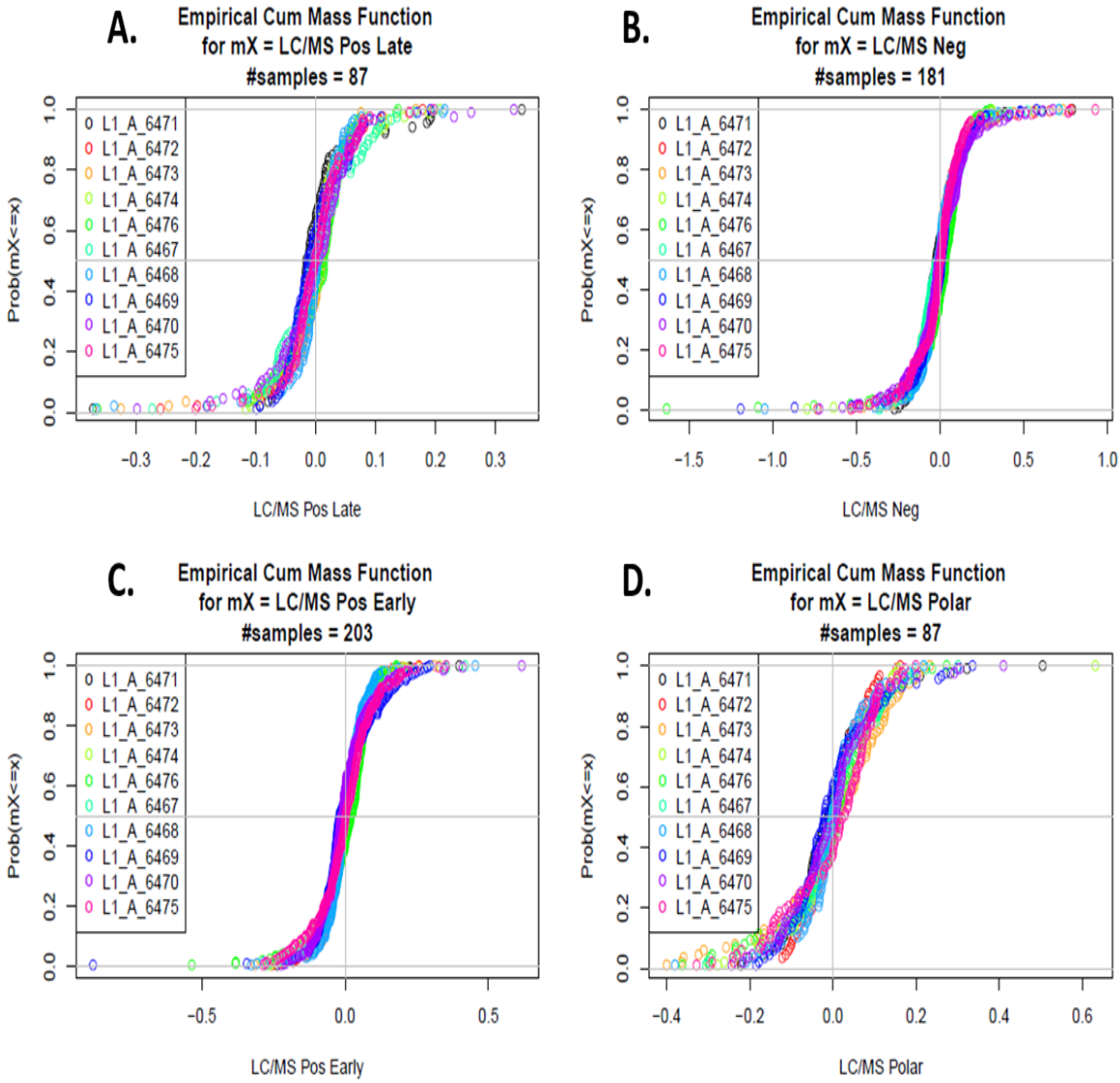

Figure 4-9: The empirical cumulative mass of metabolite deviation per liver sample.

The empirical cumulative mass of metabolite deviation per liver sample. (A) 78 metabolites detected in LC/MS positive late platform, (B) 181 metabolites detected in LC/MS negative early platform, (C) 203 metabolites detected in LC/MS positive early platform and (D) 87 metabolites detected in LC/MS polar platform. Y axis presents empirical cumulative mass function and X axis presents samples stratified by platform. Each colour represents an individual animal (sample). All samples performed well in all platforms.

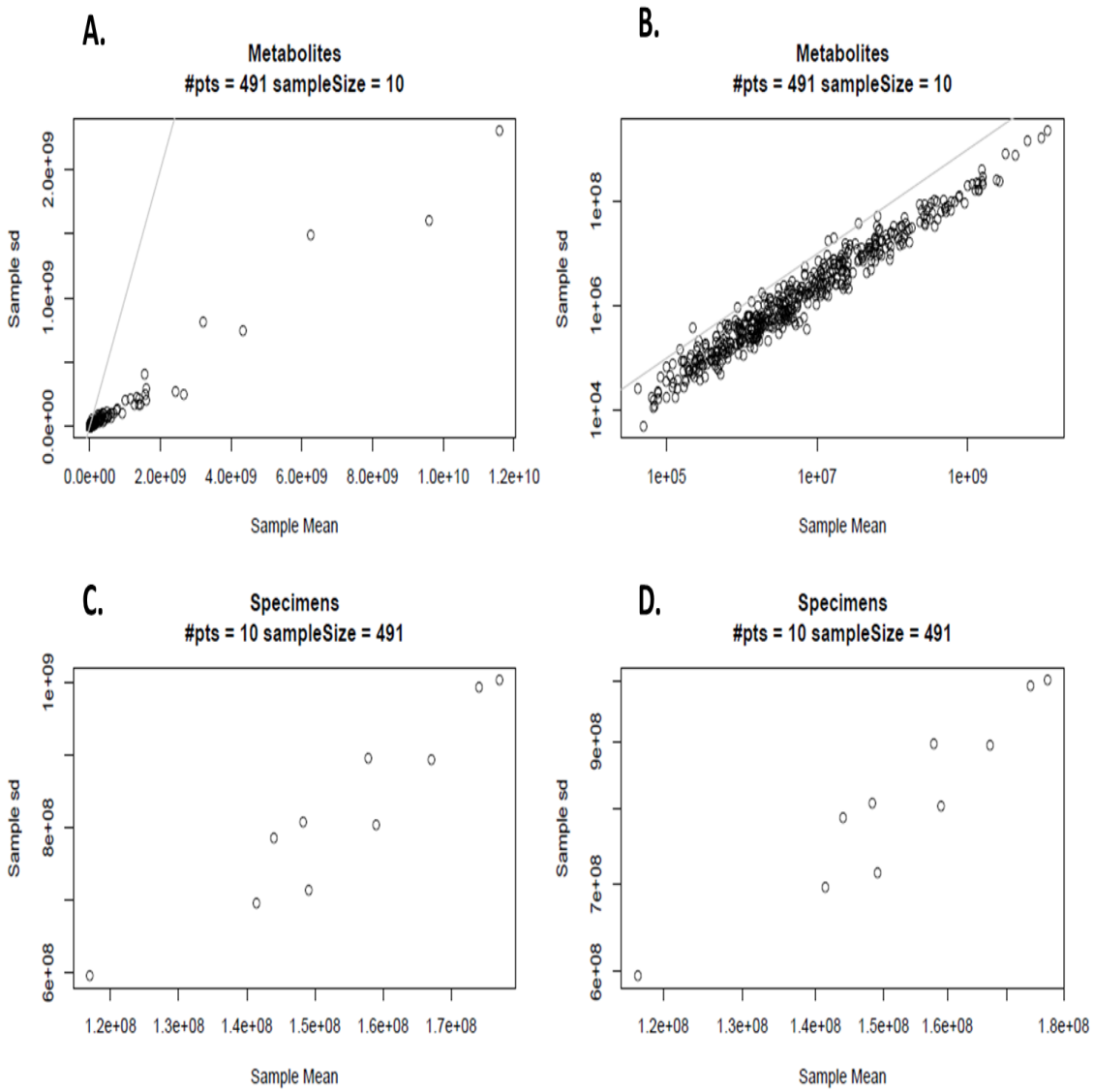

Figure 4-10: Scatterplots show the relationship between the mean and standard deviation per metabolite and per aorta sample.

Linear relationship between mean and standard deviation per metabolite on the log scale (B). Scatterplots show that no outliers were observed in the relationship between the mean and standard deviation per metabolite (A, B) and per aorta sample (C, D). Figures (A, C) represent the original scale and Figures (B, D) represent the log scale.

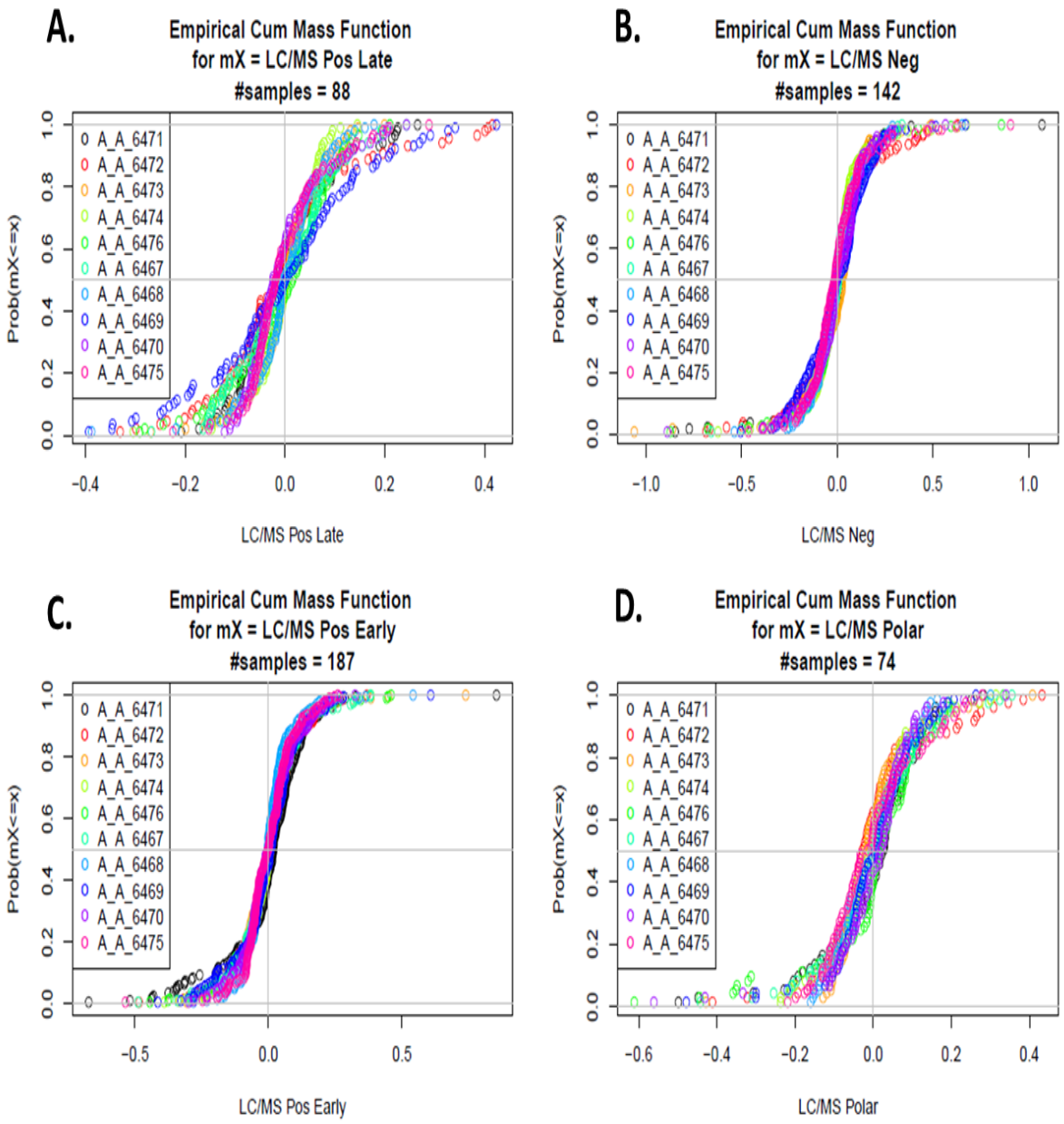

Figure 4-11: The empirical cumulative mass of metabolite deviation per aorta sample.

The empirical cumulative mass of metabolite deviation per aorta sample. (A) 88 metabolites detected in LC/MS positive late platform, (B) 142 metabolites detected in LC/MS negative platform, (C) 187 metabolites detected in LC/MS positive early platform and (D) 74 metabolites detected in LC/MS polar platform. Y axis presents empirical cumulative mass function and X axis presents samples stratified by platform. Each colour represents an individual animal number (sample). All samples performed well in all platforms.

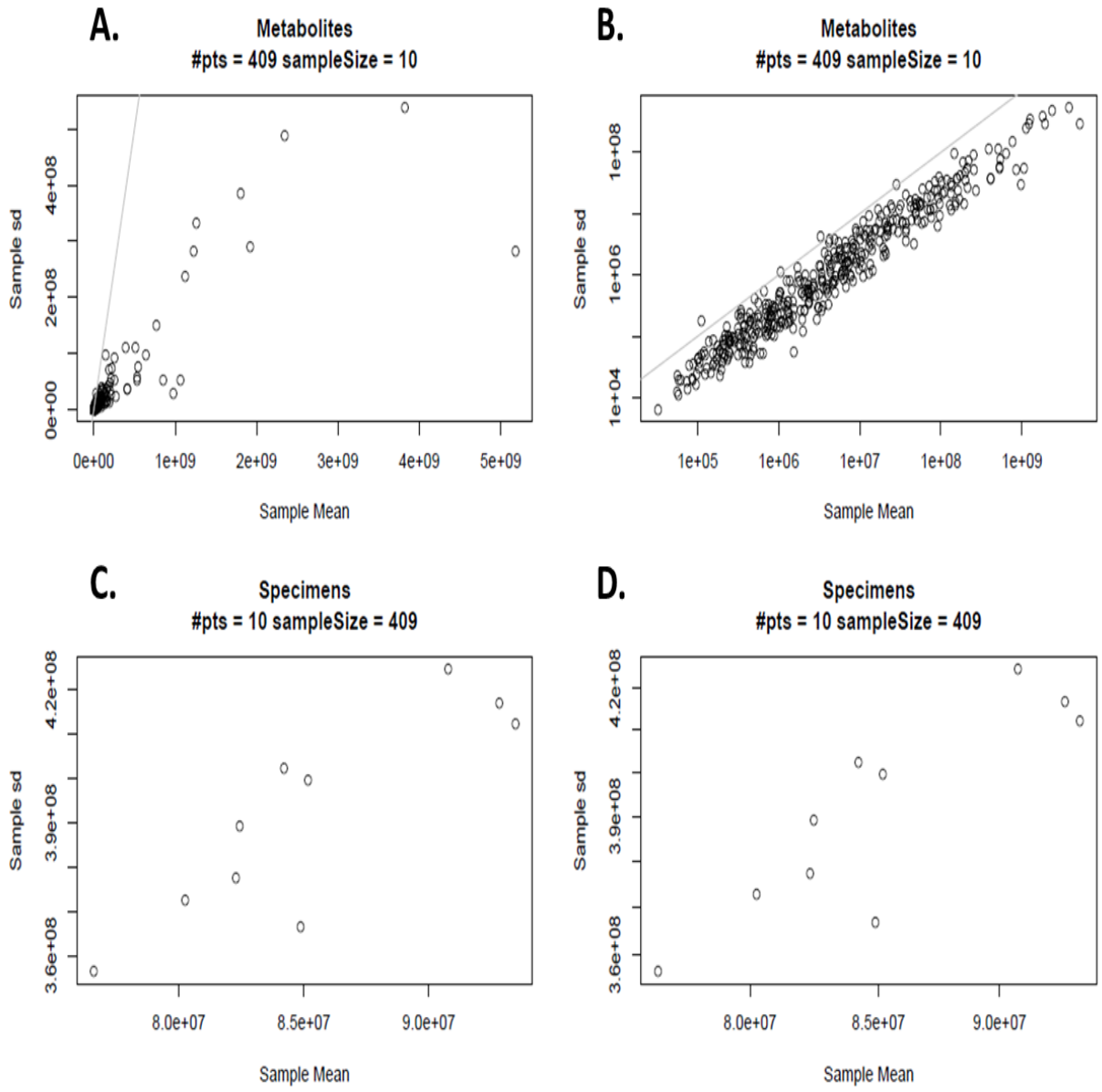

Figure 4-12: Scatterplots show the relationship between the mean and standard deviation per metabolite and per brain sample.

There is a linear relationship between mean and standard deviation per metabolite on the log scale (B). Scatterplots show that no outliers were observed in the relationship between the mean and standard deviation per metabolite (A, B) and per brain sample (C, D). Figures (A, C) represent the original scale and Figures (B, D) represent the log scale.

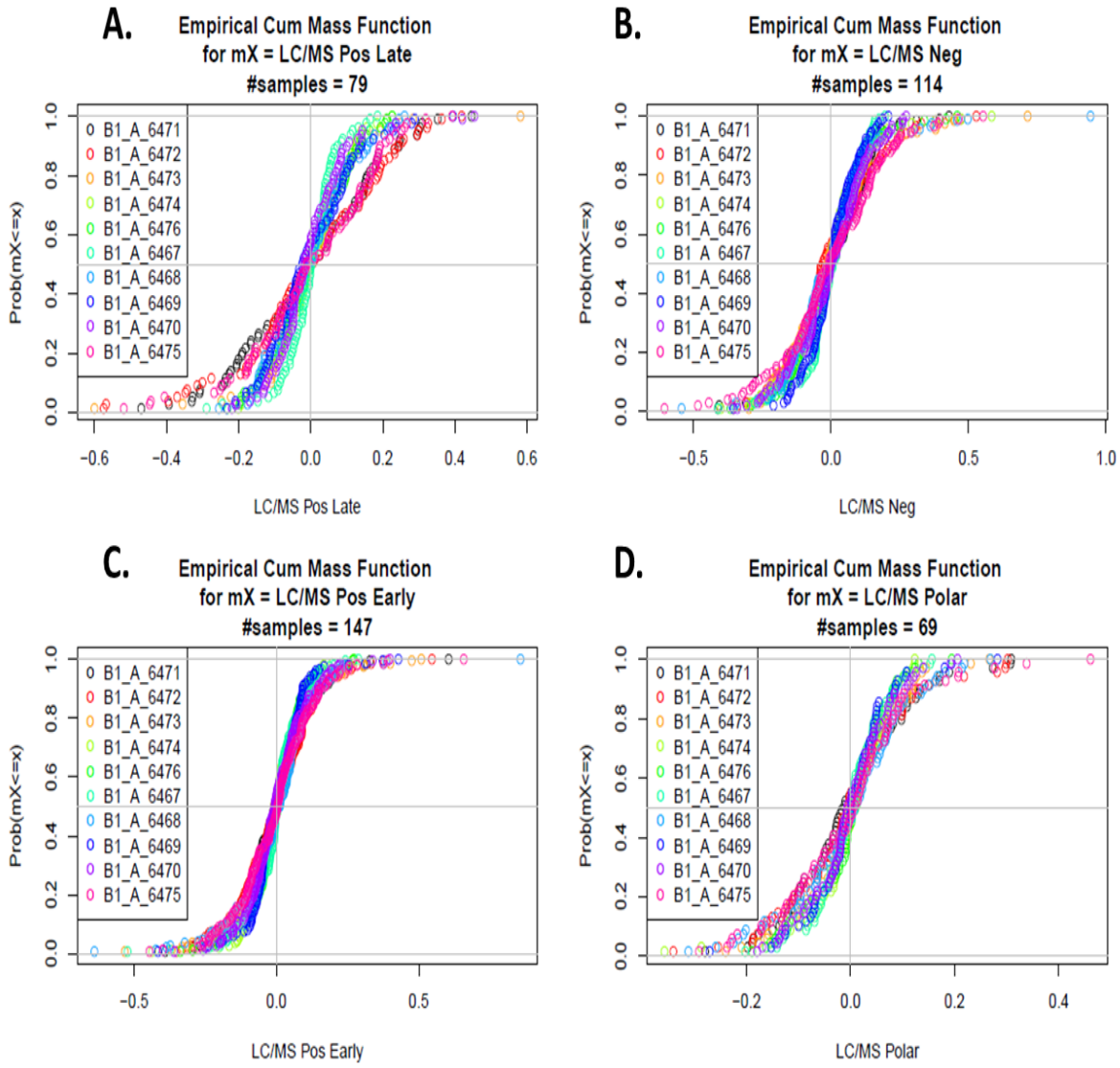

Figure 4-13: The empirical cumulative mass of metabolite deviation per brain sample.

The empirical cumulative mass of metabolite deviation per brain sample. (A) 79 metabolites detected in LC/MS positive late platform, (B) 114 metabolites detected in LC/MS negative platform, (C) 147 metabolites detected in LC/MS positive early platform and (D) 69 metabolites detected in LC/MS polar platform. Y axis presents empirical cumulative mass function and X axis presents samples stratified by platform. Each colour represents an individual animal number (sample). All samples performed well in all platforms.

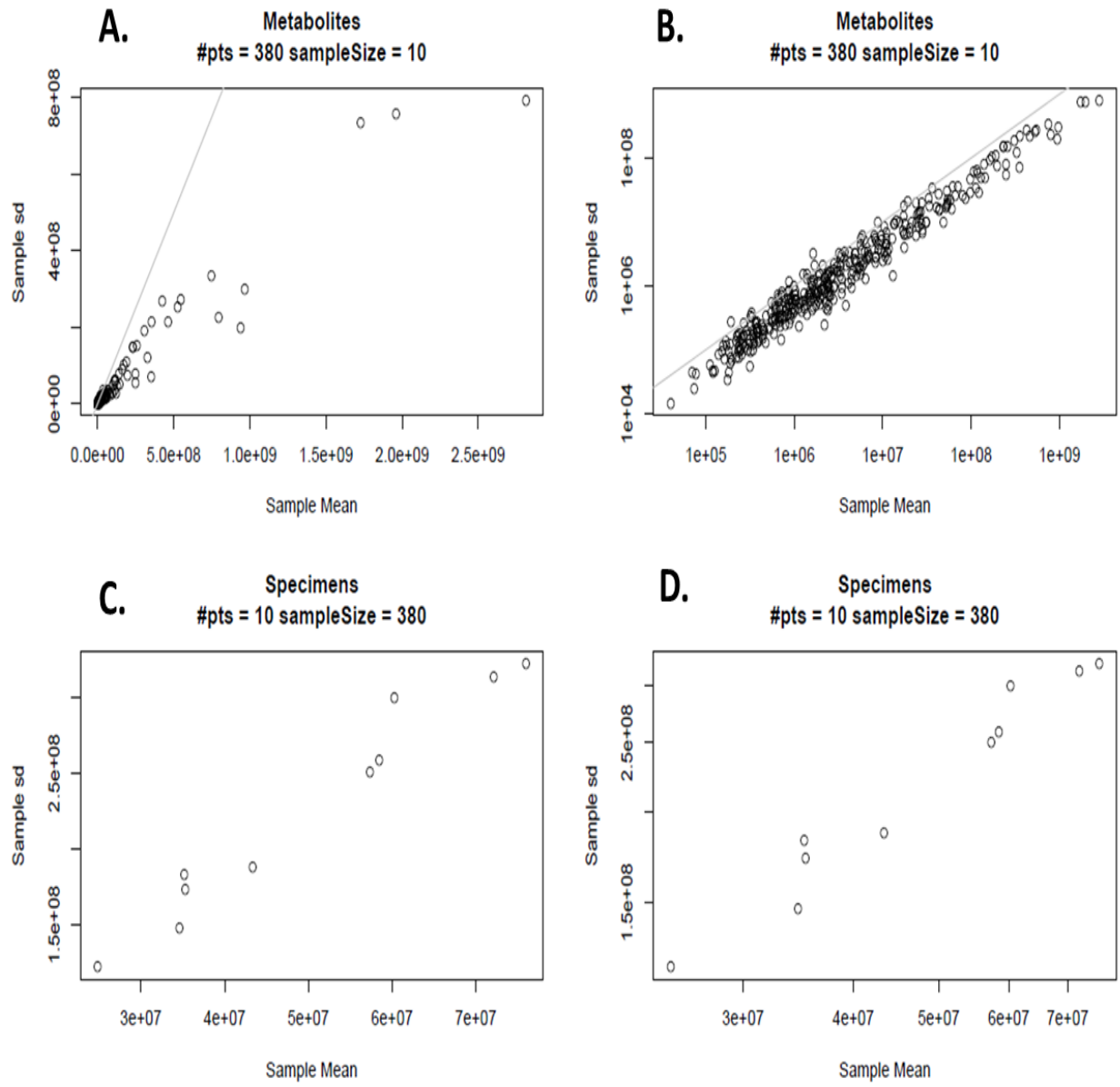

Figure 4-14: Scatterplots show the relationship between the mean and standard deviation per metabolite and per adipose sample.

There is a linear relationship between mean and standard deviation per metabolite on the log scale (B). Scatterplots show that no outliers were observed in the relationship between the mean and standard deviation per metabolite (A, B) and per adipose sample (C, D). Figures (A, C) represent the original scale and Figures (B, D) represent the log scale.

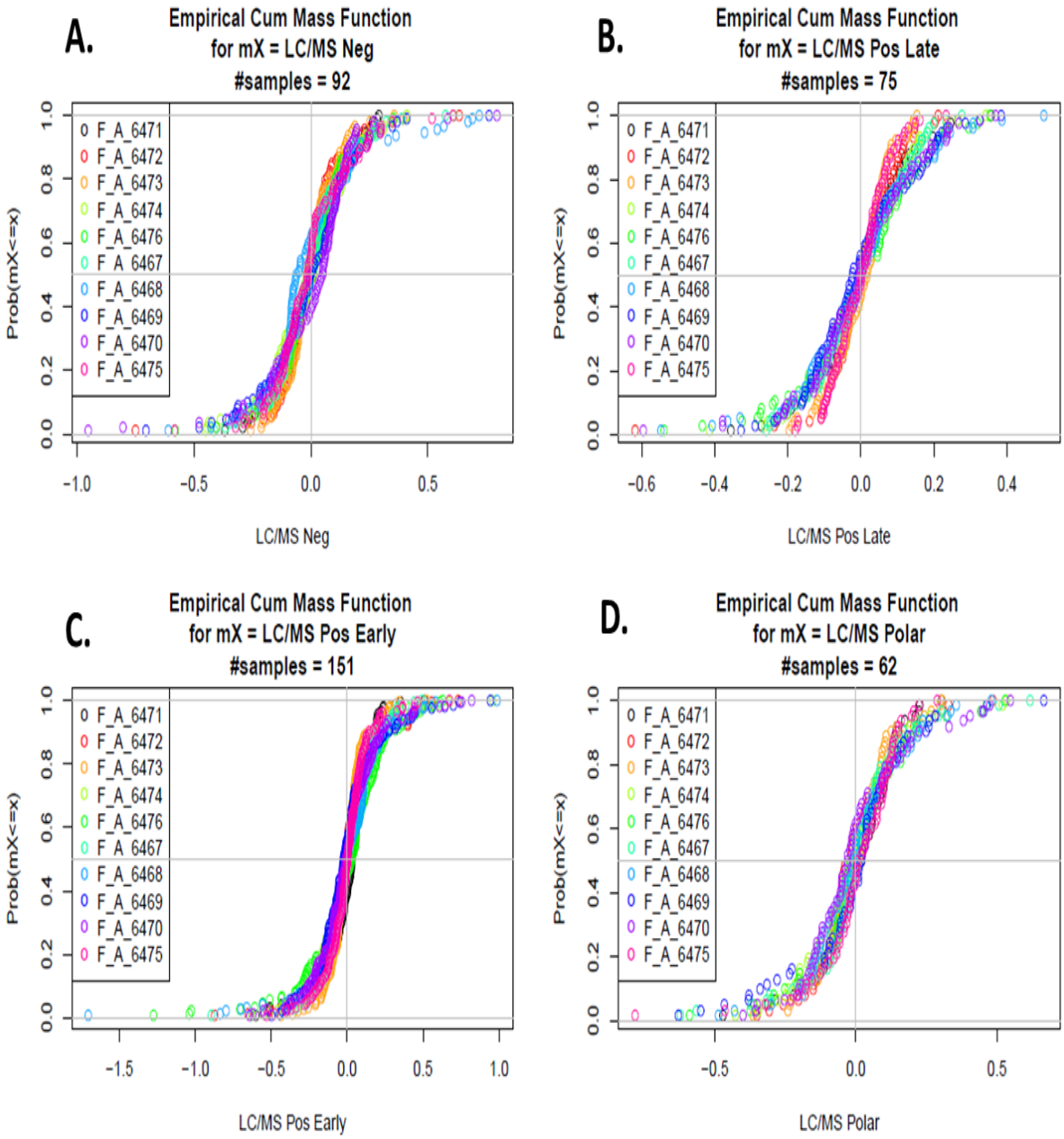

Figure 4-15: The empirical cumulative mass of metabolite deviation per adipose sample.

The empirical cumulative mass of metabolite deviation per adipose sample. (A) 92 metabolites detected in LC/MS negative platform, (B) 75 metabolites detected in LC/MS positive late platform, (C) 151 metabolites detected in LC/MS positive early platform and (D) 62 metabolites detected in LC/MS polar platform. Y axis presents empirical cumulative mass function and X axis presents samples stratified by platform. Each colour represents an individual animal number (sample). All samples performed well in all platforms.

4.5.2 Heat map

Inter specimen correlation in metabolite deviations is applied by a heatmap representation of the specimen metabolite deviations correlation matrix (10 by 10). Correlations were calculated as Kendal's Tau. The hypothesis is that there would be no correlation between the hexadecanedioic acid-treated group and the control group. The pattern in the kidney is not very strong; low correlation was observed between the hexadecanedioic acid-treated group and control group (Figure 4-16 A). A low correlation also occurred between the hexadecanedioic acid-treated group and the control group in heart and liver patterns (Figure 4-16 B) (Figure 4-16 C). The Aorta heatmap shows also low correlations between the hexadecanedioic acid-treated group and control group, as shown in Figure 4-16 D. In the brain and adipose, low correlation also shown between the hexadecanedioic acid-treated group and the control group (Figure 4-17 A) (Figure 4-17 B).

4.5.3 Principle components analysis (PCA)

Principle component analysis (PCA) was used to identify any separation between the hexadecanedioic acid-treated group and the control group. PCA for aorta, adipose, brain and liver matrices demonstrated overlapping populations when analysed by group. However, heart and kidney PCA showed a tendency to segregate by groups, which could suggest greater effects of hexadecanedioate on these matrices as shown in Figure 4-18.

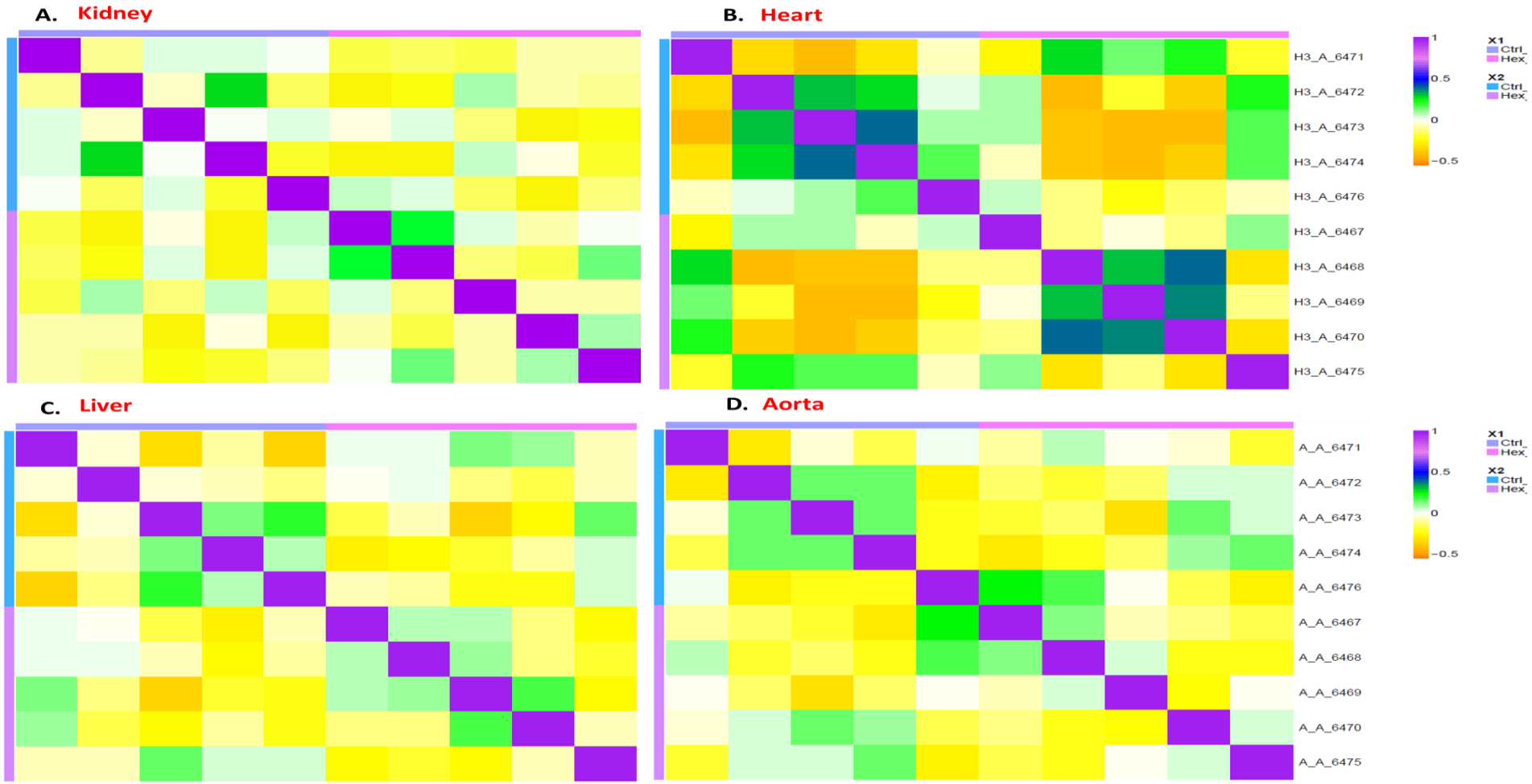

Figure 4-16: Heatmap representation of the samples' metabolite deviations correlation in (A) kidney, (B) heart, (C) liver and (D) aorta matrix.

Correlations are in range (-0.2, 1). 1 (purple colour) is highly correlated and < 0 (yellow colour) is low correlated.

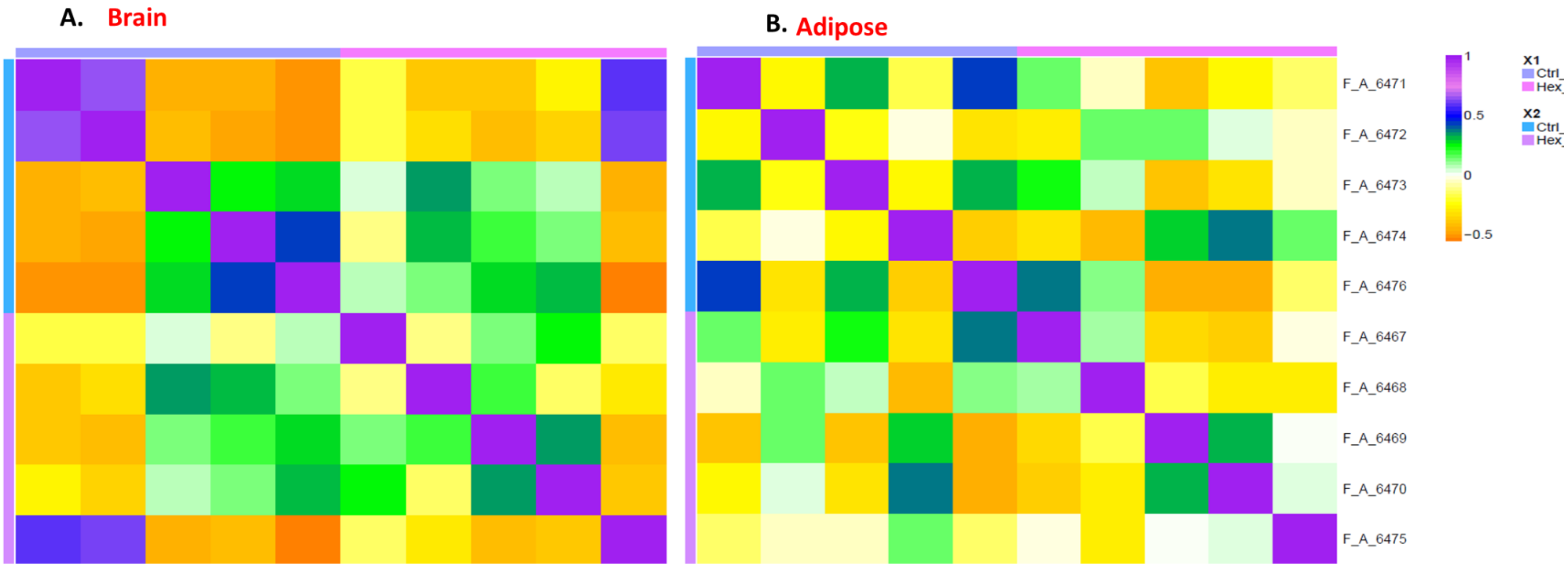

Figure 4-17: Heatmap representation of the samples' metabolite deviations correlation in (A) brain and (B) adipose matrix.

Correlation are in range (-0.2, 1). 1 (purple colour) is highly correlated and < 0 (yellow colour) is low correlated**.**

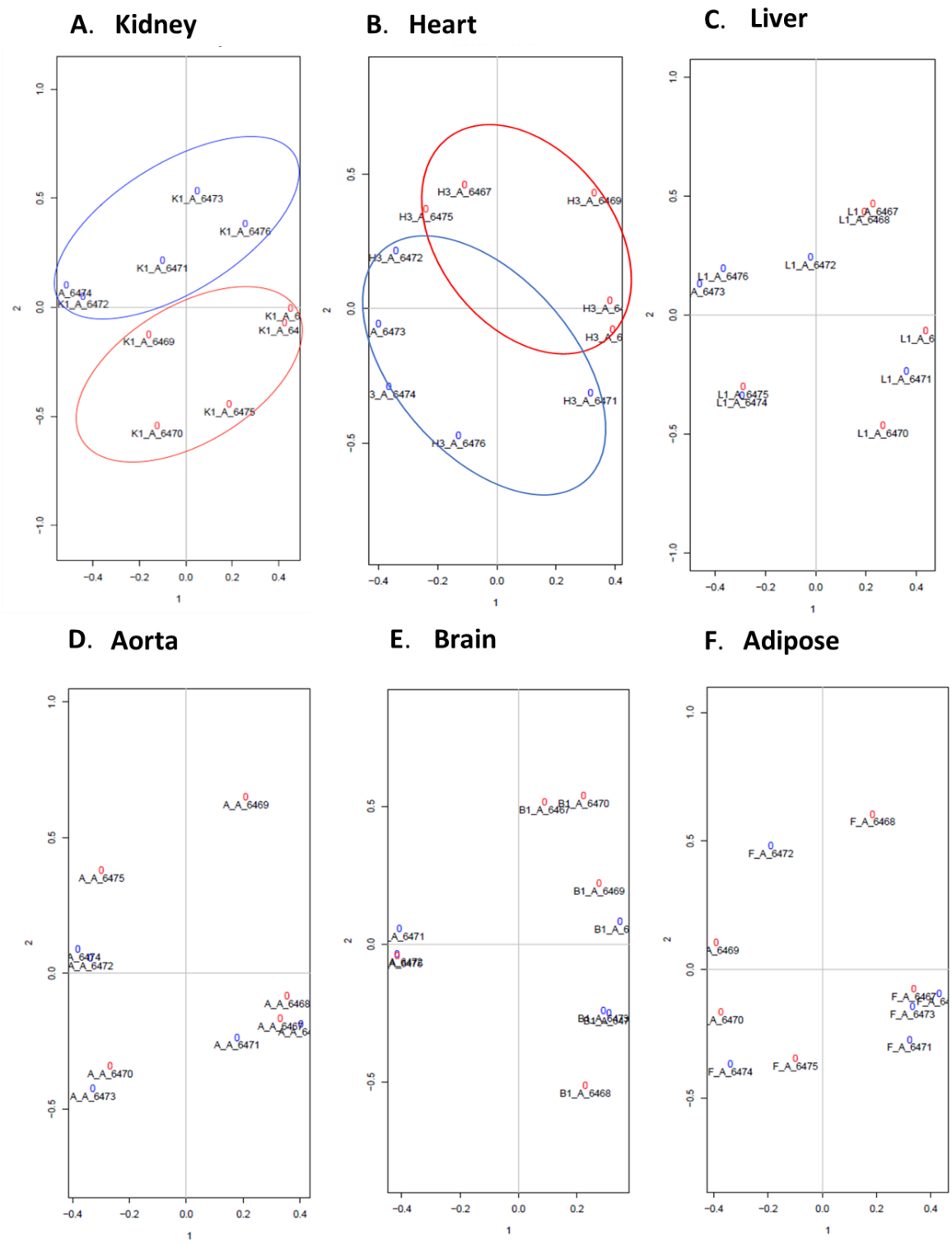

Figure 4-18: Principal Component Analysais (PCA).

PCA for (A) kidney and (B) heart showed a tendency to segregate by groups. However, (C) liver, (D) aorta, (E) brain and (F) adipose matrices demonstrated overlapping populations when analysed by group. Red symbols indicate samples from hexadecanedioic acid-treated animals. Blue symbols indicate samples from control animals.

4.5.4 Random forest analysis (RFA)

In the heart and kidney, the RFA was effective at separating samples into the appropriate group, with a predictive accuracy of 80% and 100% respectively (random chance would be expected to generate a predictive accuracy of 50%). RFAs for adipose, liver, aorta, and brain were not effective at classifying samples (with predictive accuracy approaching random chance). RFAs highlighted the top 30 metabolites important for segregating samples in the heart and kidney in related pathways, including carbohydrate metabolism (e.g. myo-inositol, maltose, maltotriose, and maltotetraose), lipid metabolism (e.g. acylcarnitines, malonylcarnitine, and hexadecanedioate) and in the kidneys, amino acid metabolism (e.g. alpha-hydroxyisovalerate). Several of these observations are discussed in more detail in Section 4.5.6.

4.5.5 Hexadecanedioate levels in tissues

The level of hexadecanedioate was significantly increased in heart (P=0.009), kidney (P= 0.003), liver (P= 0.042), adipose (P= 0.01) and with an increase in aorta (P=0.895) samples from hexadecanedioic acid-treated rats compared with control rats (Figure 4-19). However, hexadecanedioate levels were below the threshold of detection in the brain, which may reflect poor diffusion through the blood-brain barrier.

Ranking tests were used to identify association between hexadecanedioate and metabolites. The null hypothesis assumes that there is no association of metabolites with hexadecanedioate. Scatter plots (Upper diagonal) compare metabolite ranking for pairs of methods, where high rank (i.e. 400) indicates a strong association between metabolite levels and hexadecanedioate. Analyses are illustrated in the following order; Wilcoxon Rank Sum Test, Shrinkage T test (with and without equal within group variance assumption), Student T test (with and without equal within group variance assumption) and Random Forest.

The number of hexadecanedioate-associating metabolites is high in kidney, liver and adipose tissues, but low in heart tissue (Figure 4-20). In the aorta, T Test results were incompatible with Wilcoxon Rank Sum and Random Forest tests over hexadecanedioate drug ranking. This was probably caused by an outlier (Figure 4-

21 A). Nevertheless, there is little expectation of finding treatment-associating metabolites in the brain due to hexadecanedioate not being measurable in this tissue and because the principle component analysis did not show any separation between groups (Figure 4-21 B).

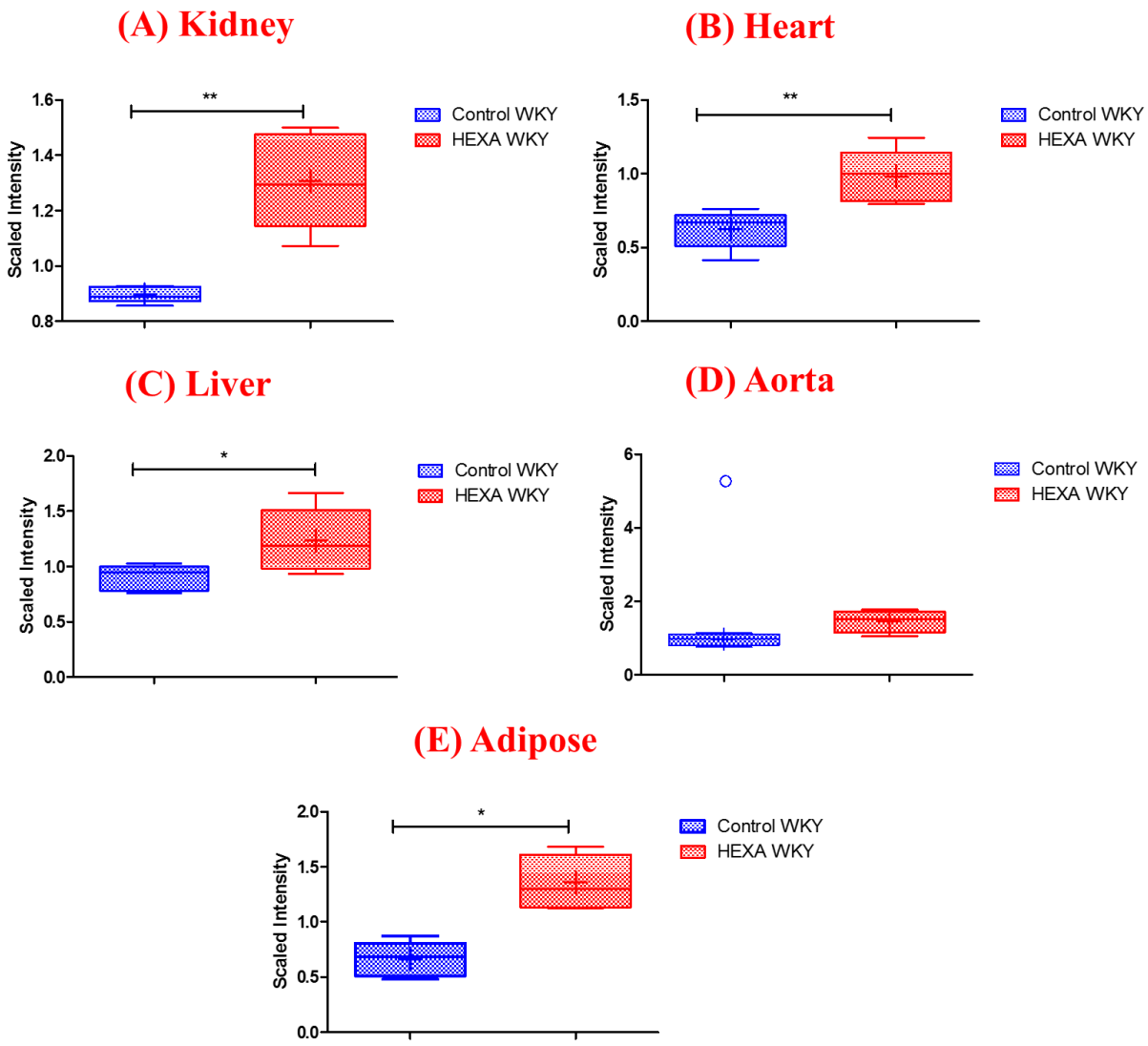

Figure 4-19: Hexadecanedioate metabolites levels.

Hexadecanedioate-treated rats (compared to control) showed significant increases in hexadecanedioate levels in the heart (P=0.009), kidney (P=0.003), liver (P=0.042), adipose tissue (P=0.01) and an increase in aorta (p=0.895), with no change in hexadecanedioate levels in the brain. (P*<0.05), (P**< 0.01).

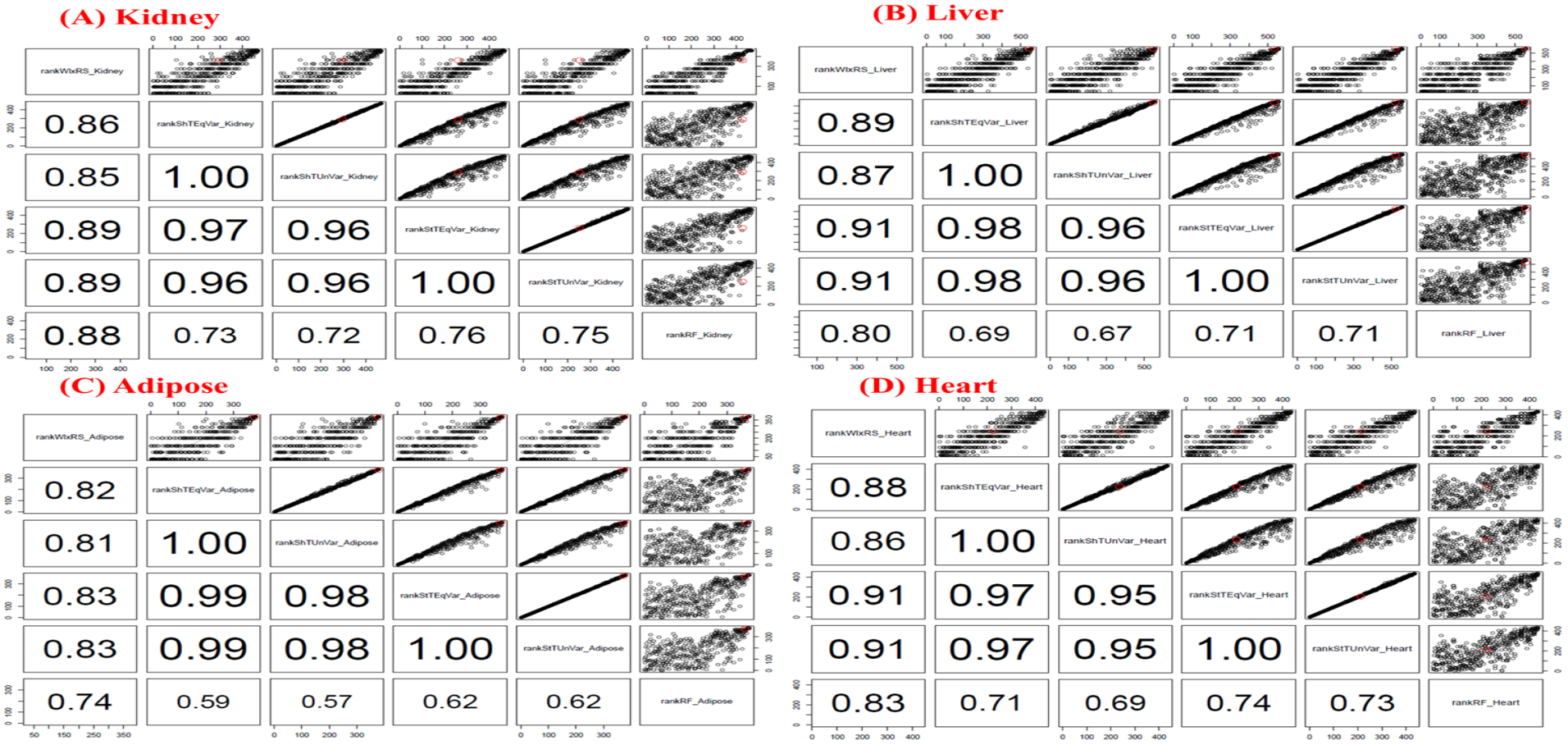

Figure 4-20: The rankings of association between hexadecanedioate and metabolites in (A) kidney, (B) liver, (C) kidney and (D) heart.

Upper diagonal - scatter plots compare metabolite ranking for pairs of methods, where >400 indicates strong association. Diagonal analyses are in order; Wilcoxon Rank Sum Test, Shrinkage T test (with and without equal within group variance assumption), Student T test (with and without equal within group variance assumption) and Random Forest. Lower diagonal – correlation. Red circle shows the hexadecanedioate drug.

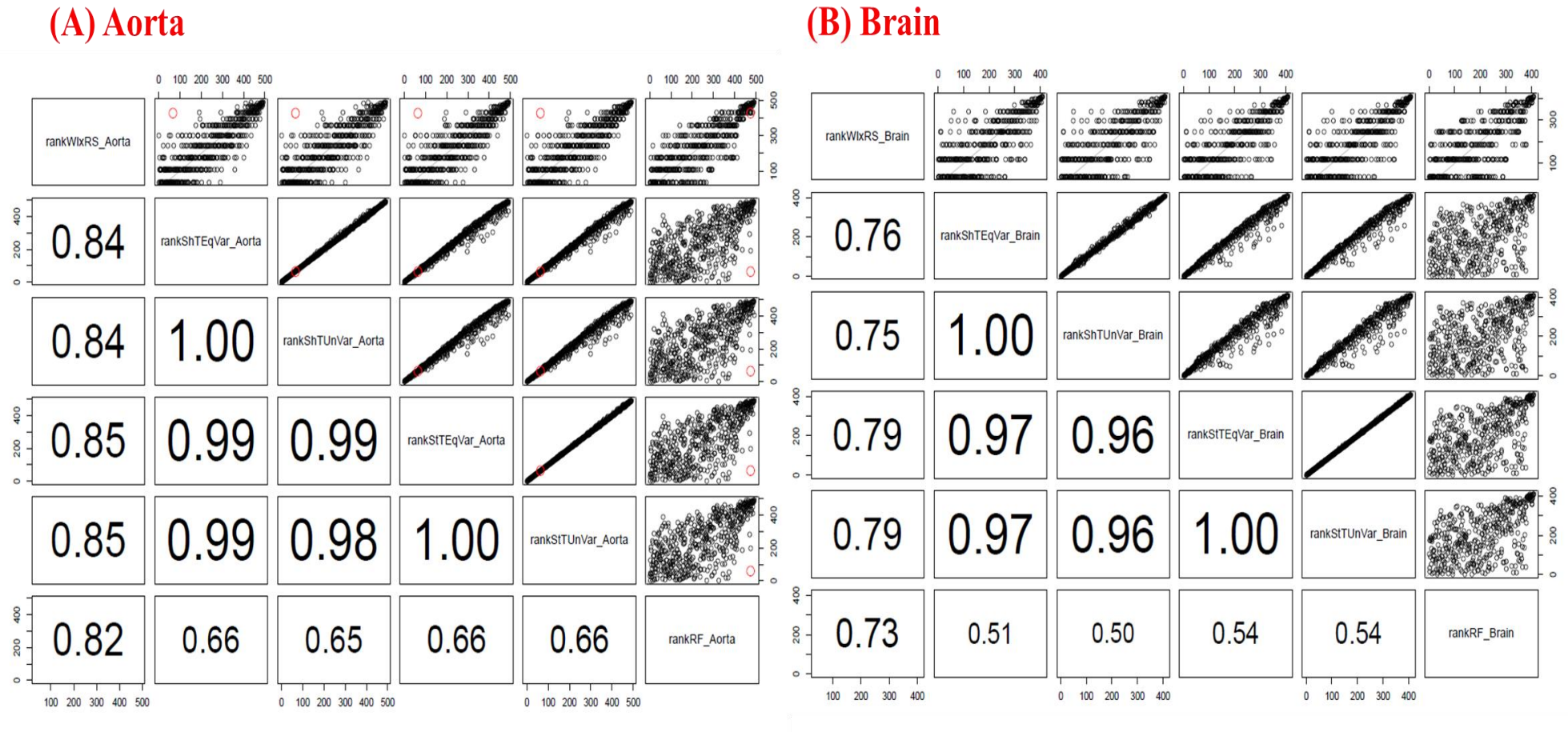

Figure 4-21: The rankings of association between hexadecanedioate and metabolites in (A) aorta, (B) brain.

Upper diagonal - scatter plots compare metabolite ranking for pairs of methods, where >400 indicates strong association. Diagonal analyses are in order; Wilcoxon Rank Sum Test, Shrinkage T test (with and without equal within group variance assumption), Student T test (with and without equal within group variance assumption) and Random Forest lower diagonal – correlation. Red circle shows the hexadecanedioate drug.

4.5.6 Enrichment of Metabolomic Pathways

A pathway enrichment overview of altered metabolites highlights lipids, carbohydrates and amino acid metabolism as being significantly enriched in the quantitative metabolomics of the heart, liver, kidney, aorta, adipose and brain tissues of hexadecanedioic acid-treated rats compared with control rats. Figure 4-22 illustrates enriched pathways, including only those that contain more than one detected metabolite. The size of the line indicates the number of metabolites enriched in the defined pathway. The greatest impact after three weeks of hexadecanedioic acid treatment include the dicarboxylate fatty acid pathway and bile acid metabolism (Figure 4-22).

4.5.6.1 Adipose

In adipose tissue, 10 metabolites achieved statistical significance ($p \leq 0.05$) and 11 approaching significance ($0.05 < p < 0.10$), as shown in the volcano plot (Figure 4-23 A). These altered metabolites are correlated to two super pathways, including lipid and carbohydrate metabolism. A pathway enrichment overview of altered metabolites highlights dicarboxylate fatty acids, primary and secondary bile acid, and pentose phosphate metabolisms as being significantly enriched in the quantitative metabolomics of adipose tissue from hexadecanedioic acid-treated rats compared with control rats (Figure 4-23 B).

Lipid metabolism

Our metabolomics results showed significantly increased levels of hexadecanedioate ($P=8x10^{-4}$), as well as the dicarboxylate fatty acids (DFAs) tetradecanedioate and octadecanedioate in the adipose tissues of hexadecanedioic acid-treated rats compared with control rats ($P=0.045$), ($P=0.042$); respectively, as listed in the appendix Table A1, (Figure 4-24). DFAs are the end products of ω-oxidation pathway generated by oxidation of the aldehyde group to a carboxylic acid.

The free fatty acids phospholipids (1,2-dipalmitoleoyl-GPC(16:1/16:1)*) were significantly increased in hexadecanedioic acid-treated rats compared with control rats ($P=0.039$), as shown in Figure 4-25 A. Lysolipid (1-oleoyl-GPI (18:1) *) (Figure 4-25 D), as well as acyl carnitine (myristoylcarnitine and oleoylcarnitine)

levels (Figure 4-25 E), decreased in hexadecanedioic acid-treated rats compared with control rats. Hexadecanedioic acid-treated WKY rats also demonstrated an increase in the levels of monohydroxy (i.e. 16-hydroxypalmitate) (Appendix, Table A1), sphingolipid (i.e. sphingomyelin (d18:1/20:1,d18:2/20:0)*) and monoacylglycerol (i.e. 1-palmitoleoylglycerol (16:1) *) compared with untreated control WKY rats (Figure 4-25 C, B).

Bile acid metabolism

Several taurine-conjugated primary bile acids (i.e. tauro-chenodeoxycholate, taurocholate) were significantly elevated in the adipose tissues of hexadecanedioic acid-treated rats compared with control rats (P=0.0151), ($P=3.5x10^{-3}$); respectively. Also, a marked increase in muricholic acids bile acids, tauro-alpha-muricholate (P=0.071) and tauro-beta-muricholate were observed ($P=1.3x10^{-3}$) (Figure 4-26 A). In addition, secondary (i.e taurodeoxycholate) bile acid was significantly elevated in the adipose tissues of hexadecanedioic acid-treated rats compared with control rats ($P=6.1\ x10^{-3}$) (Figure 4-26 B) (Appendix, Table A1).

Carbohydrate metabolism

Sedoheptulose-7-phosphate is an intermediate compound in the pentose phosphate pathway, which was significantly reduced in the adipose tissues of hexadecanedioic acid-treated rats compared with control rats (P=0.04) (Appendix, Table A1).

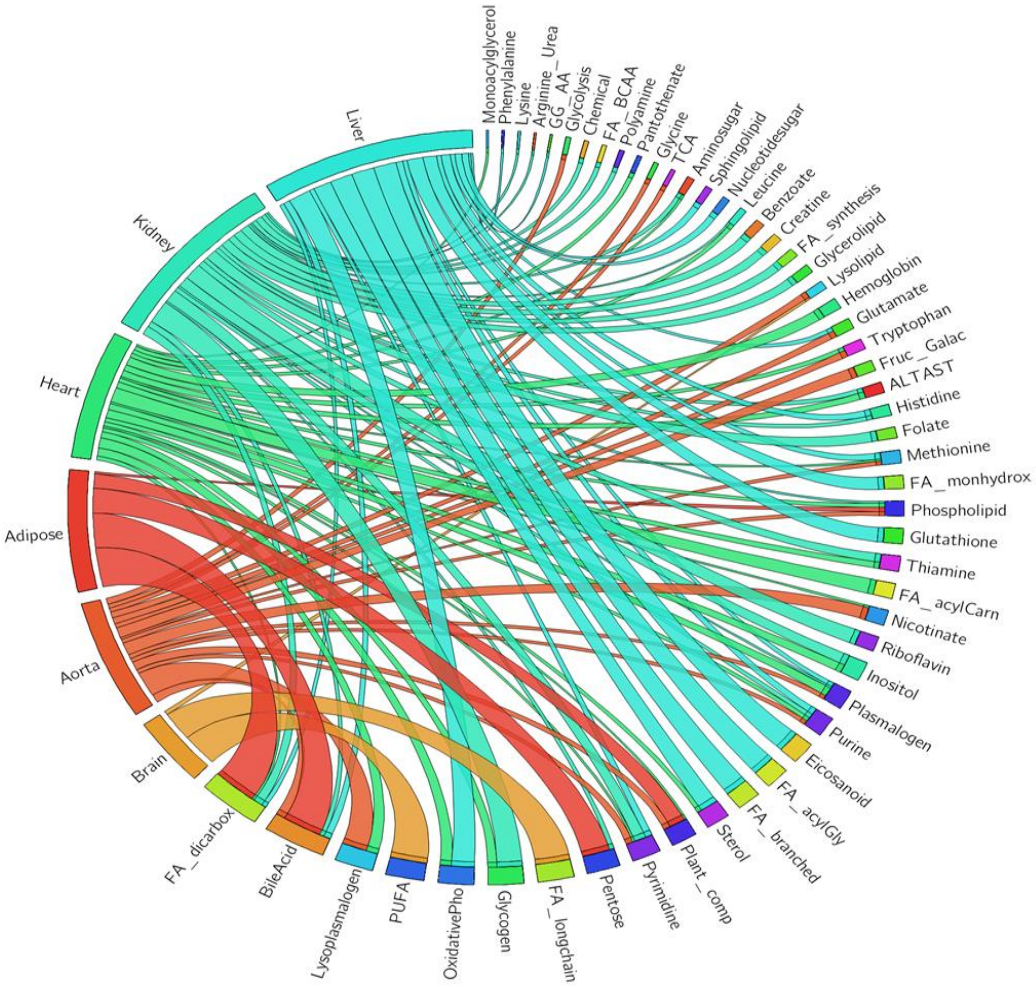

Figure 4-22: Circular visualisation of the metabolomics dataset.

Circular visualisation of the metabolomics dataset illustrating enrichment of metabolomic pathways and metabolites for the heart, liver, kidney, aorta, adipose and brain tissues analysed. The pathways demonstrating greatest impact after three weeks of hexadecanedioic acid treatment include the dicarboxylate fatty acid pathway and bile acid metabolism.

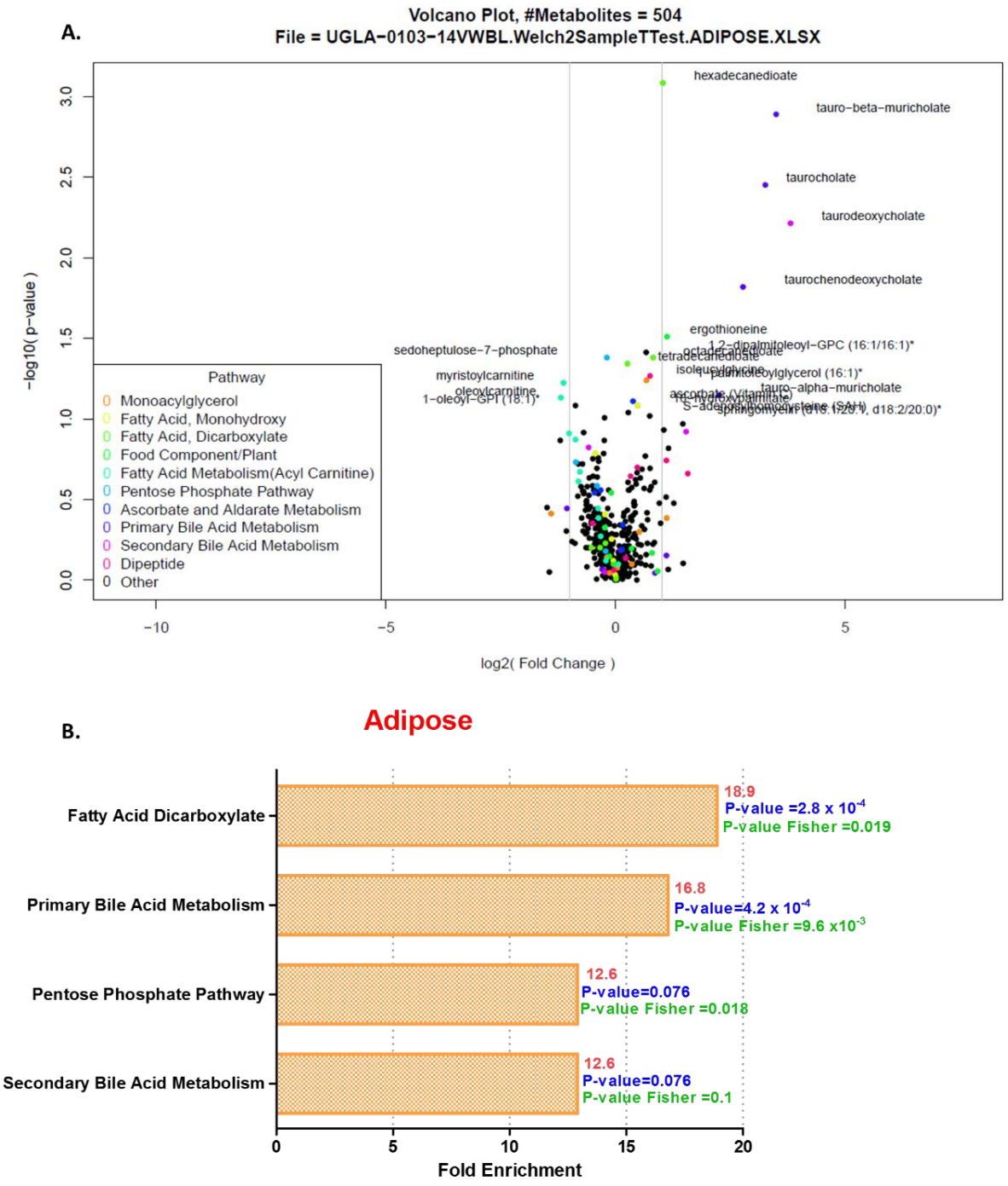

Figure 4-23: Enrichment pathway of significantly associated metabolites in adipose tissues.

(A) Volcano plot shows up to 21 metabolites are identified in adipose tissues, which are the top 10 by p-value with fold change. Colours indicate metabolite membership in the most significant pathways according to hypergeometric enrichment test p-value. (B) Fold enrichment pathway of significantly associated metabolites in adipose tissues. Enrichment values are based on the significant compounds relative to all detected compounds in the pathway. Enrichment = (number of significant metabolites in pathway/ total number of detected metabolites in pathway)/ (total number of significant metabolites/ total number of detected metabolites). Fold change is red labelled. Welch T- test p-value marked as blue and Fisher p-value is marked as green.

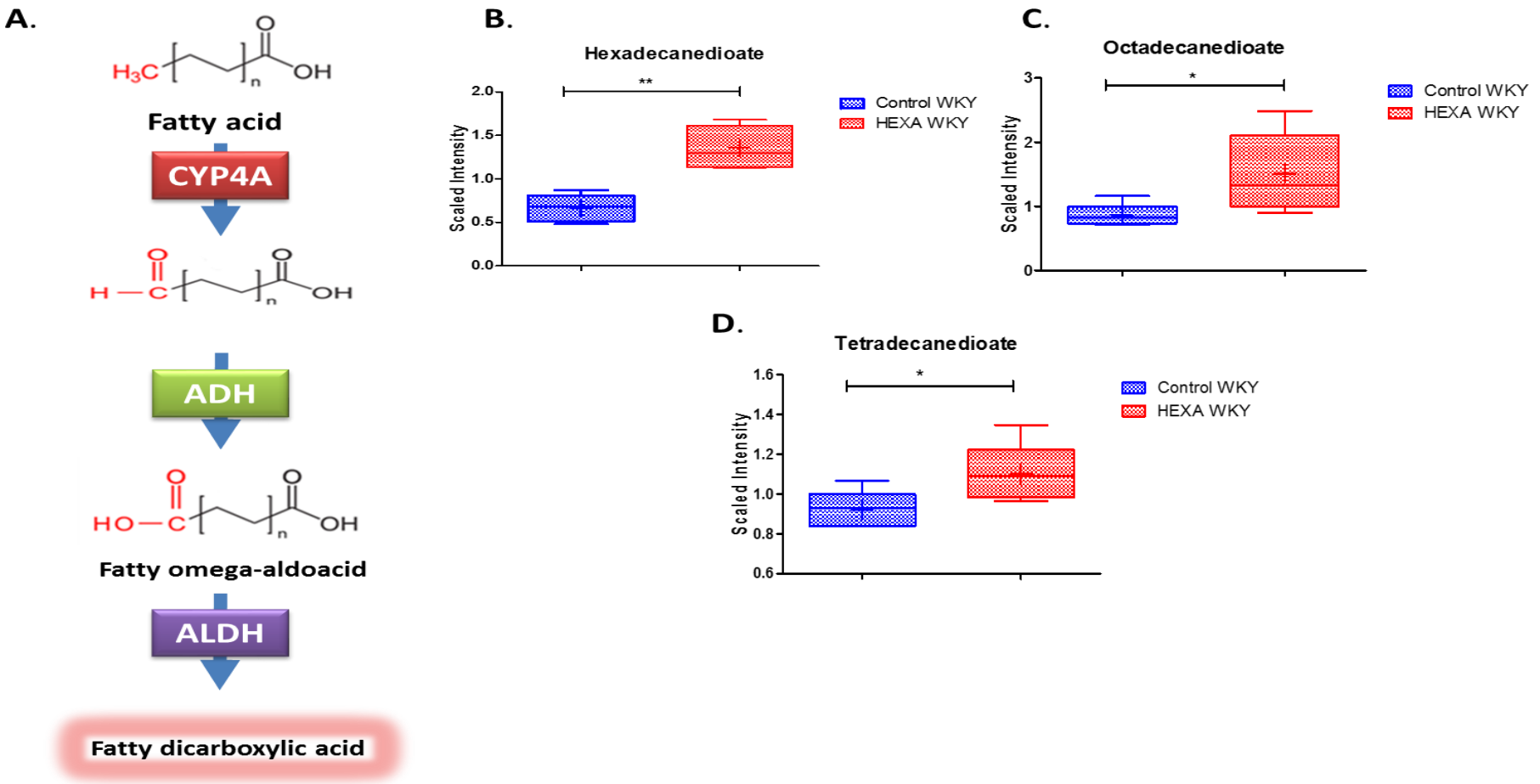

Figure 4-24: The levels of dicarboxylic fatty acids in adipose tissue of hexadecanedioic acid-treated rats compared with control rats.

(A) Fatty acid ω-oxidation pathway. (B) the level of hexadecanedioate ($P=8x10^{-4}$), tetradecanedioate ($P=0.045$) and octadecanedioate ($P=0.042$) significantly increased in adipose tissue of hexadecanedioic acid-treated rats compared with control rats. ($P^{*}<0.05$) ($P^{***}<0.001$).

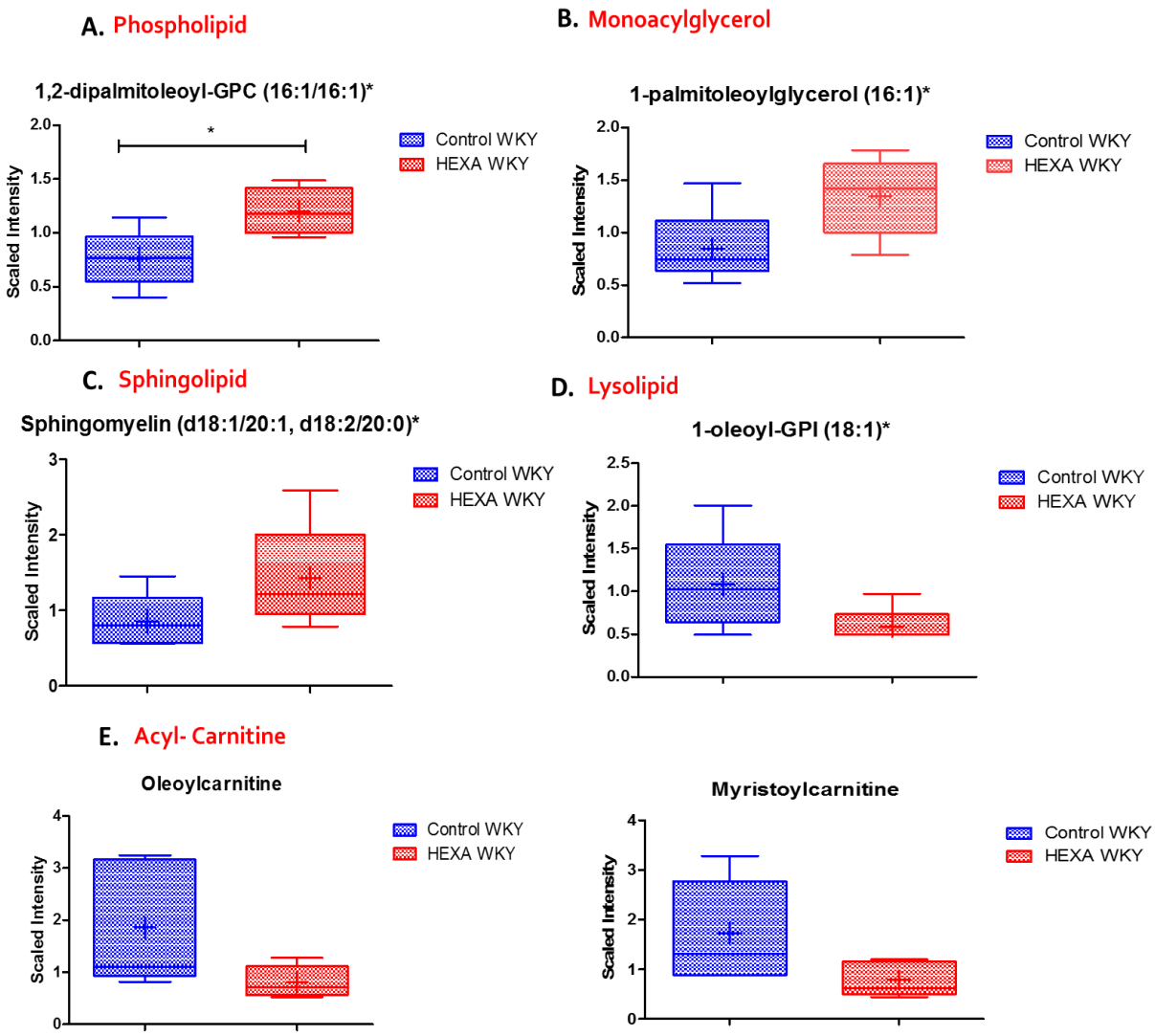

Figure 4-25: Fatty acid oxidation and carnitine metabolites in adipose tissues of hexadecanedioic acid- treated rats compared with control rats.

Fatty acid oxidation and carnitine metabolism pathways were significantly altered by hexadecanedioate. In adipose tissue, the level of (A) phospholipid, (B) monoacyl glycerol and (C) sphingolipid increased in hexadecanedioic acid-treated rats compared with control rats. Whereas, the level of (D) lysolipid and (E) acyl carnitine decreased in adipose tissue of in hexadecanedioic acid-treated rats compared with control rats.

.

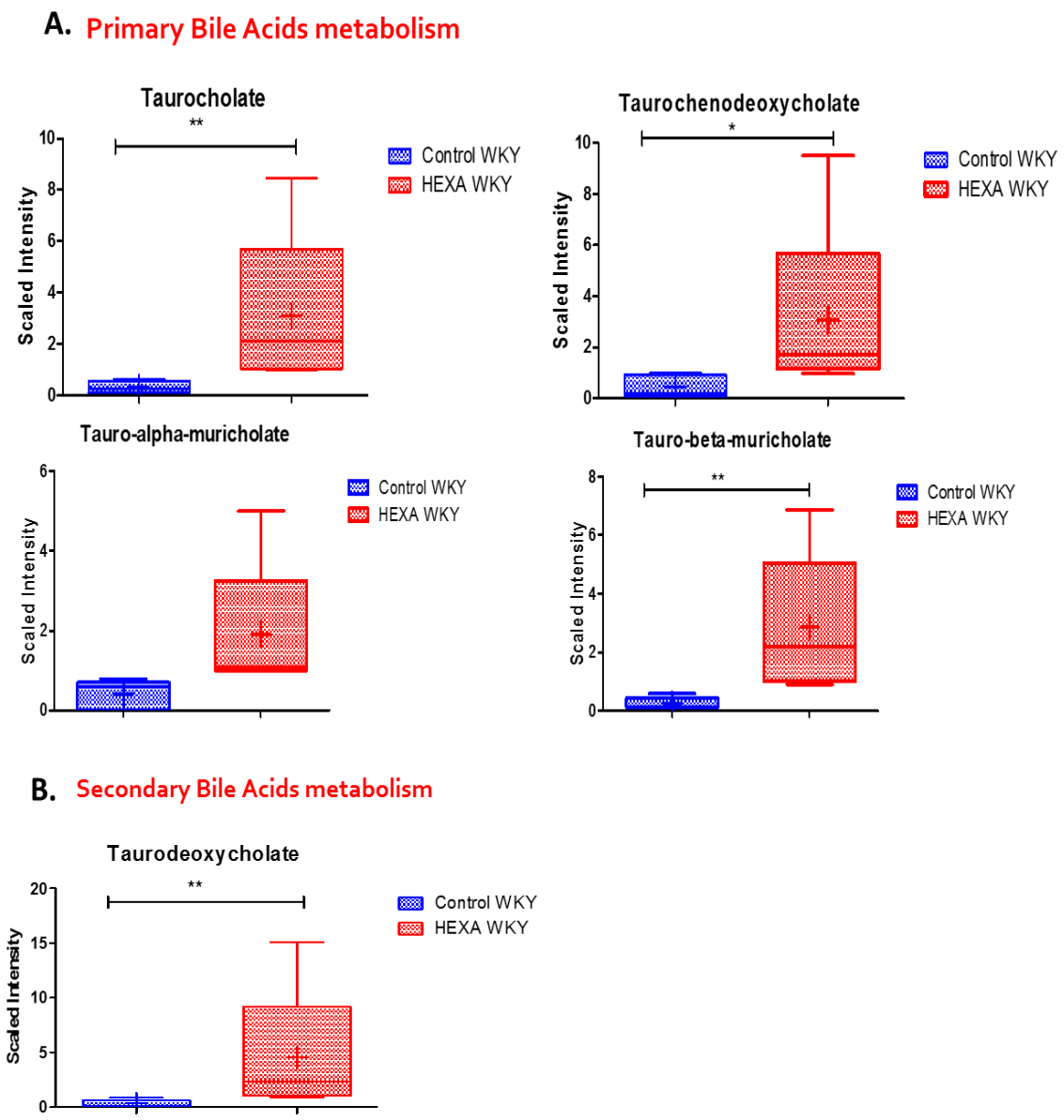

Figure 4-26: Bile acids metabolism in adipose tissues of hexadecanedioic acid-treated rats compared with control rats.

In adipose tissue, the level of (A) primary bile acids, tauro-chenodeoxycholate, taurocholate and tauro-beta-muricholate significantly increased in hexadecanedioic acid-treated rats compared with control rats. (B) The level of secondary bile acid, taurodeoxycholate also significantly increased in hexadecanedioic acid-treated rats compared with control rats.

4.5.6.2 Kidney

In kidney tissues, 49 metabolites achieved statistical significance ($p \leq 0.05$) and 39 approaching significance ($0.05 < p < 0.10$), as shown in the volcano plot (Figure 4-27 A). These perturbed metabolites are correlated to super pathways, including lipid, carbohydrate, and amino acid metabolisms (Appendix, Table A2). A pathway enrichment outline of altered metabolites that related to increase energy demands such as glycolysis, gluconeogenesis, glycogen, fatty acids (i.e. long chain fatty acid, dicarboxylate and phospholipid), ketone bodies, bile acid and co factors (i.e. FAD and FMN) were found in the kidney tissues of hexadecanedioic acid-treated rats compared with control rats (Figure 4-27 B).

Lipid metabolism

An increase in long-chain fatty acids (i.e. myristate, myristoleate, palmitoleate, 10-heptadecenoate and 10-nonadecenoate) as well as increase in branched fatty acid and acylcarnitine was observed in the kidney tissues of hexadecanedioic acid-treated rats compared with control rats (Figure 4-28 A, B). Also, the levels of dicarboxylic fatty acid; decanedioate (P=0.02) and inositol; myo-inositol (P=0.01) significantly decreased, with a significant increase in ketone bodies (BHBA) (P=0.015) in the kidney tissues of hexadecanedioic acid-treated rats compared with control rats (Figure 4-28 C, E and F).

There were significant increases in lysolipid, glycerolipid, monoacylglycerol and phospholipid observed in hexadecanedioic acid-treated rats compared with control rats. Nevertheless, reductions in sphingolipid, sterol and phospholipid (i.e. 1-stearoyl-2-arachidonoyl-GPI (18:0/20:4) and 1-oleoyl-2-linoleoyl-GPE (18:1/18:2)*), were observed in the kidney tissues of hexadecanedioic acid-treated rats compared with control rats (Figure 4-29), (Appendix Table A2).

A significant reduction in malonylcarnitine level (P=0.04) and plasmalogen (i.e. 1-(1-enyl-palmitoyl)-2-arachidonoyl-GPC (P-16:0/20:4)*) (P=0.007) was also observed in hexadecanedioic acid-treated rats compared with controls, as shown in (Figure 4-29), (Appendix Table A2).

Carbohydrate metabolism

Significant increases in the levels of glycogen breakdown products (i.e. maltotetraose (P=0.024), maltotriose (P=0.026) and maltose (P=0.039)) with significant reduction in glucose 6-phosphate level (P=0.028) were observed in kidney tissues of hexadecanedioic acid-treated rats compared with controls. In addition, a significant reduction in arabitol/xylitol level (P=0.018) in pentose phosphate, a parallel pathway to glycolysis, was observed in hexadecanedioic acid-treated rats compared with controls. Correspondingly, galactose 1-phosphate (fructose, mannose and galactose metabolism) and glucuronate (aminosugar metabolism) levels significantly decreased in the kidney samples from hexadecanedioic acid-treated rats compared with control rats (P=0.05), (P=0.017); respectively. (Figure 4-30) (Appendix, Table A2).

Bile acid metabolism

The levels of glycine-conjugated primary bile acids (i.e. glycocholate and glycochenodeoxycholate) and unconjugated bile acid (i.e. chenodeoxycholate) markedly decreased in the kidneys of hexadecanedioic acid-treated rats compared with control rats. Also, a significant increase in muricholic bile acid (tauro-alpha-muricholate (P=0.028) and tauro-beta-muricholate (P=0.024) was observed in hexadecanedioic acid-treated rats compared with control rats. In addition, reduction in the levels of secondary bile acids (i.e. glycodeoxycholate (P=0.007), glycolithocholate (P=0.08) and glycohyodeoxycholate (P=0.04)) was observed in hexadecanedioic acid-treated rats compared with control rats. While, tauroursodeoxycholate (secondary bile acid) levels significantly increased in hexadecanedioic acid-treated rats compared with control rats (P=0.015) (Figure 4-31) (Appendix, Table A2).

Amino acid metabolism

All amino acids are derived from intermediates in glycolysis, pentose phosphate pathway or the citric acid cycle. The metabolomics data shows changes in amino acid metabolism such as glycine, serine, threonine, histidine, lysine, tryptophan, leucine, isoleucine, valine, methionine, cysteine, and taurine metabolism. In the kidney samples, the levels of 3-phosphoserine (P=0.022), N2-acetyllysine (P=0.03) and N-acetylvaline (P=0.006) significantly downregulated in hexadecanedioic acid-treated rats compared with controls (Figure 4-32).

The levels of N-acetylglutamine, 1-methylhistidine, and N-acetyl-3-methylhistidine reduced in hexadecanedioic acid-treated rats compared with controls. Furthermore, the levels of imidazole lactate (P=0.043), 1-methylimidazoleacetate (P=0.001), alpha-hydroxyisovalerate (P=0.006), hypotaurine (P=0.002) and putrescine (P=0.017) significantly upregulated in hexadecanedioic acid-treated rats compared with controls (Figure 4-32).

The levels of kynurenine, taurine, N-acetylputrescine and guanidinosuccinate increased in hexadecanedioic acid-treated rats compared with controls (Appendix Table A2).

Differences between the groups (hexa vs control) were observed in some metabolites of urea and the citric acid cycle, for example arginine, N-delta-acetylornithine, and creatine, which showed a trend towards increase in hexadecanedioic acid-treated rats compared with controls. Also, proline (P=0.02), N-methylproline (P=0.037) and guanidinoacetate (P=0.01) showed a significant increase in the kidney tissues of hexadecanedioic acid-treated rats compared with controls (Figure 4-33) (Appendix Table A2).

Co-factors

A reduction in some of the co-factors related to many pathways such as 1-methylnicotinamide, flavin adenine dinucleotide (FAD), flavin mononucleotide (FMN), pterin, thiamin monophosphate, thiamin diphosphate and pyridoxamine phosphate were observed in the kidney tissues of hexadecanedioic acid-treated rats compared with control rats (Appendix, Table A2).

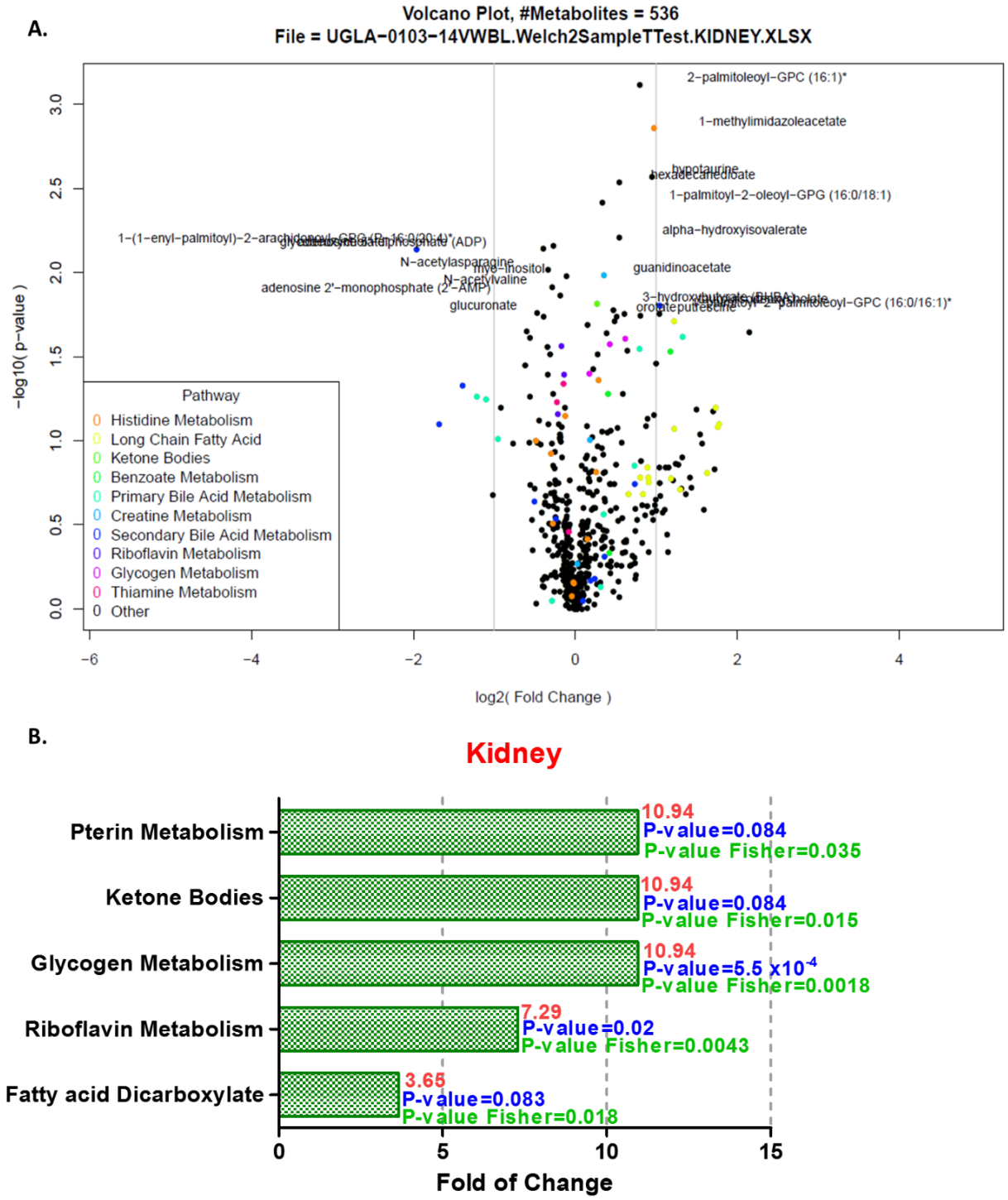

Figure 4-27: Fold enrichment pathway of significantly associated metabolites in kidney tissues.

(A) Volcano plot shows up to 88 metabolites identified in kidney tissues, which are the top 10 by p-value with fold change. Colours indicate metabolite membership in the most significant pathways according to hypergeometric enrichment test p-value. (B) Fold enrichment pathway of significantly associated metabolites in kidney tissues. Enrichment values are based on the significant compounds relative to all detected compounds in the pathway. Enrichment = (number of significant metabolites in pathway/ total number of detected metabolites in pathway)/ (total number of significant metabolites/ total number of detected metabolites). Fold change is red labelled. Welch T- test p-value marked as blue and Fisher p-value is marked as green.

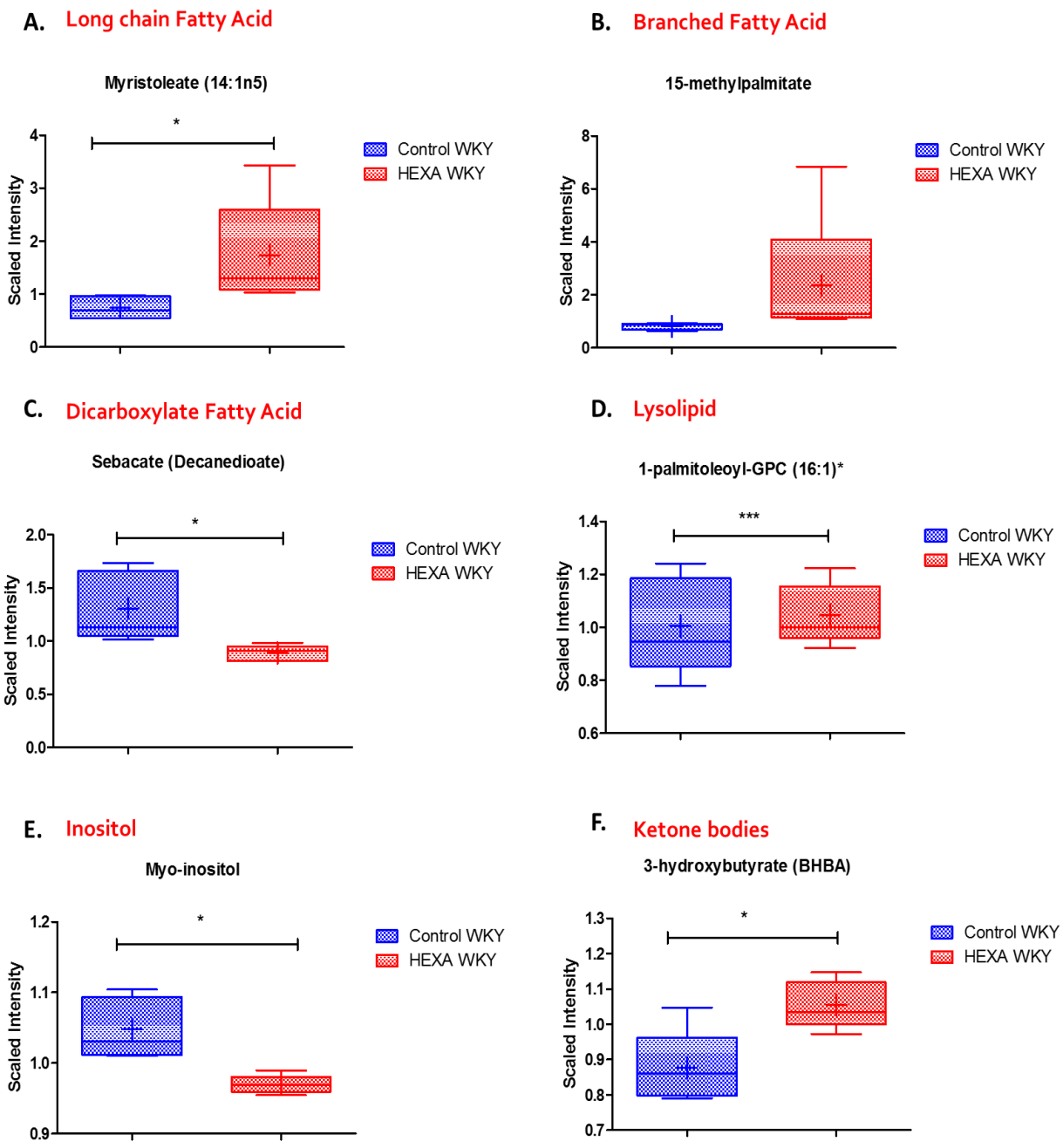

Figure 4-28: Alteration in fatty acid metabolic pathways detected in kidney tissues of hexadecanedioic acid- treated WKY rats compared to control WKY rats.

In kidney tissues, fatty acid metabolic pathways are affected by hexadecanedioate treatment. Hexadecanedioate induced increases in (A) Long chain fatty acid (B) branched fatty acid (15-methylpalmitate), and (D) lysolipid (1-palmitoleoyl-GPC (16:1)*). However, significant reduction in (C) dicarboxylate (i.e. sebacate) and (E) inositol (i.e. myo-inositol) was observed in hexadecanedioic acid-treated rats compared to control rats. Also, Ketone bodies levels significantly increased in the hexadecanedioic acid group compared to control rats (F). (P*<0.05), (P**<0.01), (P***<0.001).

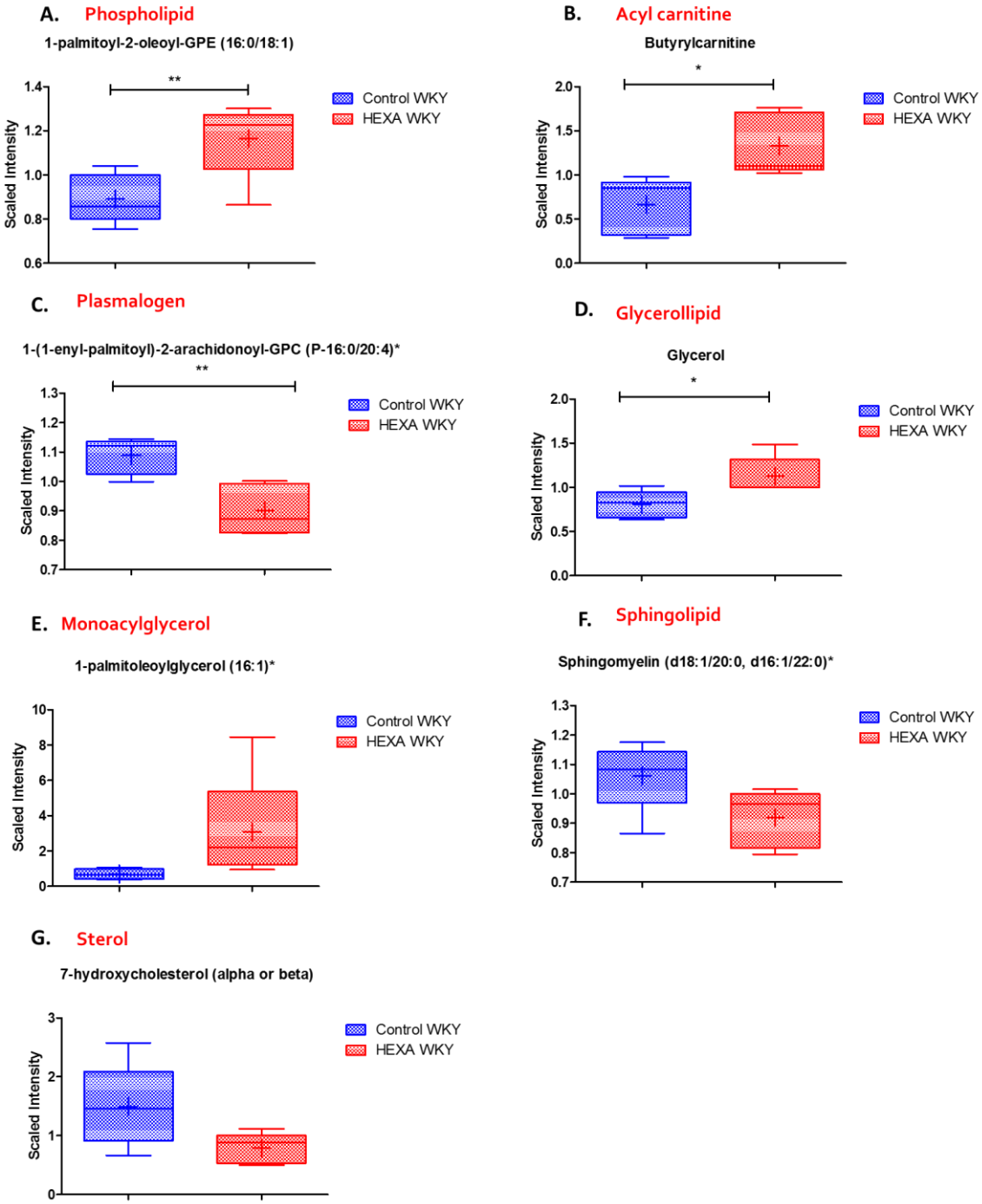

Figure 4-29: The levels of fatty acids in kidney tissues of hexadecanedioic acid-treated WKY rats compared to control WKY rats.

The levels of fatty acids (A) phospholipid, (B) acyl carnitine significantly increased, while (C) plasmalogen significantly decreased in hexadecanedioic acid-treated rats compared with control rats. (D) Glycerollipid level significantly increased in kidney tissue of hexadecanedioic acid-treated rats compared with control rats. Also, the level of (E) monoacylglycerol increased, though (F) sphingolipid and (G) sterol levels decreased in kidney tissues from the hexadecanedioic acid group compared to control rats. (P*<0.05), (P**<0.01), (P***<0.001).

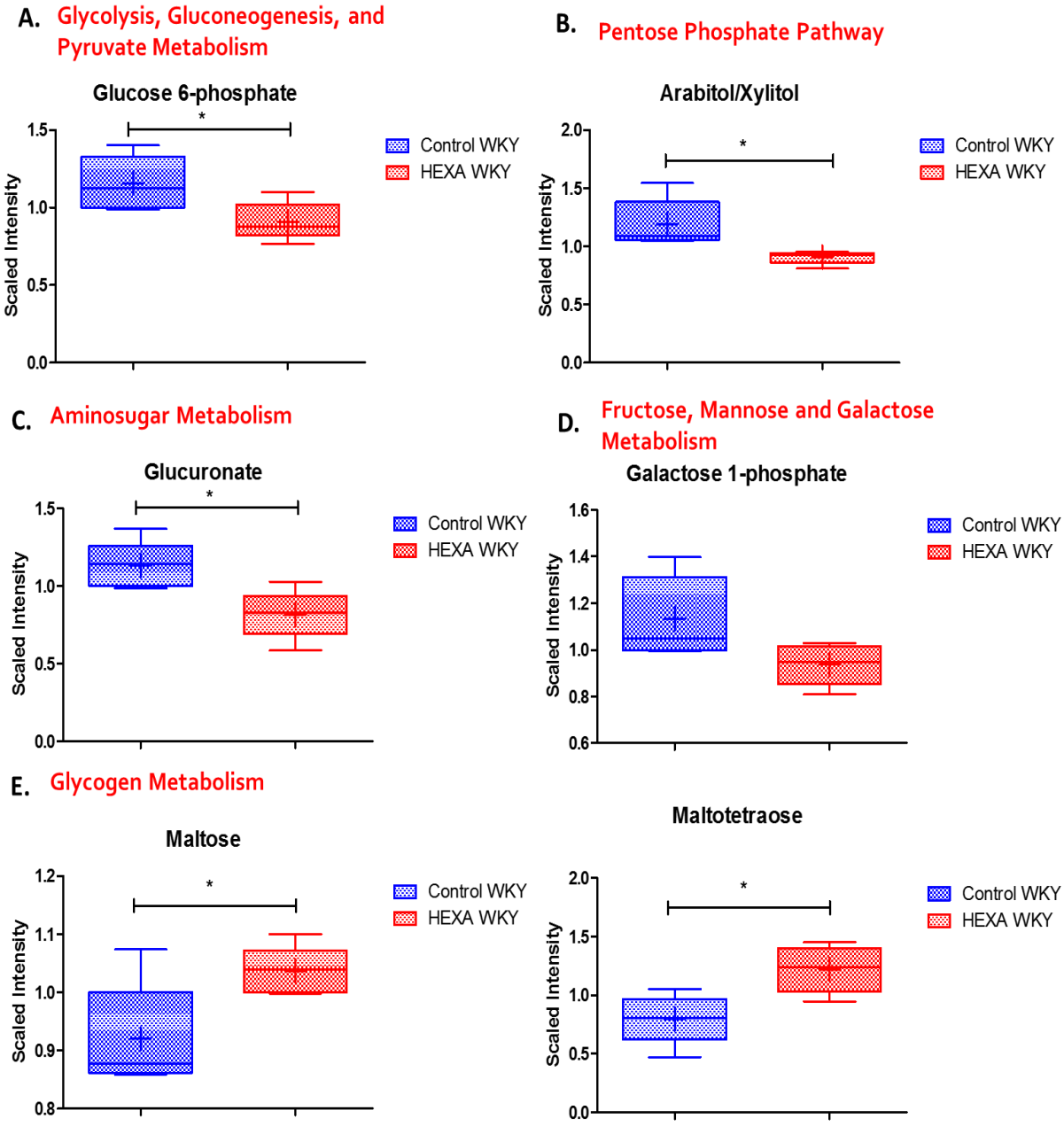

Figure 4-30: Alteration in carbohydrate metabolism in kidney tissues of hexadecanedioic acid-treated WKY rats compared with control WKY rats.

Hexadecanedioate induced significant changes in carbohydrate metabolism in kidney tissues. The levels of (A) glucose 6-phosphate, (B) arabotol/ xylitol and (C) glucuronate significantly decreased in kidney tissue of hexadecanedioic acid-treated rats compared with control rats. Also, the level of (D) galactose 1-phosphate decreased in the hexadecanedioic acid group compared to control rats. (E) Metabolites in glycogen metabolism (i.e. maltose and maltotetraose) showed a significant increase in hexadecanedioic acid-treated rats compared with control rats ($P^*<0.05$).

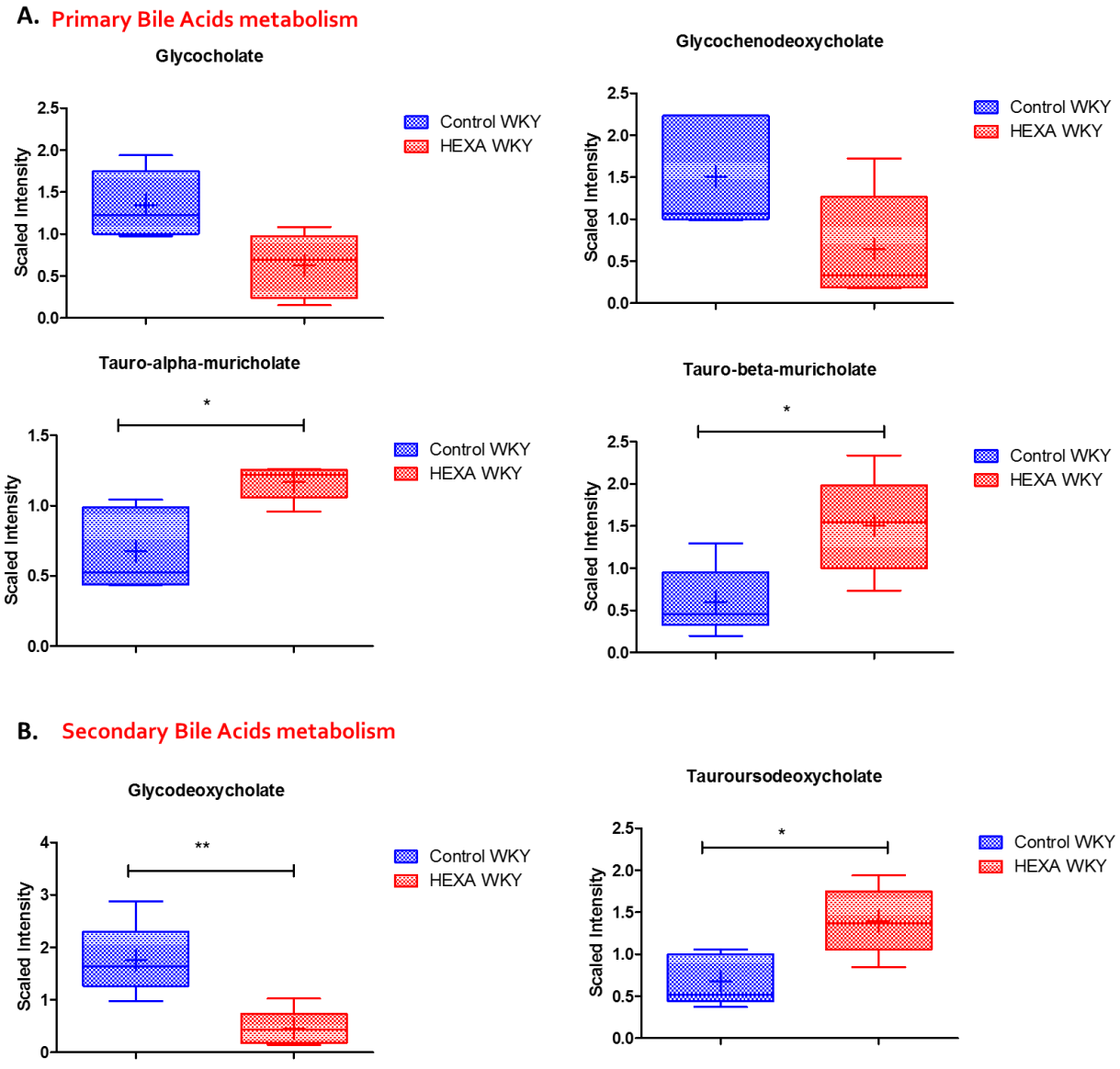

Figure 4-31: Bile acid metabolism in kidney tissues of hexadecanedioic acid-treated WKY rats compared with control WKY rats.

Hexadecanedioate induced significant changes in bile acid metabolism in kidney tissues. The levels of (A) primary bile acids (i.e. glycocholate and glycochenodeoxycholate) decreased, while tauro-alpha-muricholate and tauro-beta-muricholate showed a significant increase in kidney tissues from hexadecanedioic acid-treated rats compared with control rats. Also, the level of (B) secondary bile acids (i.e. glycodeoxycholate) showed a significant decrease, while tauroursodeoxycholate level significantly increased in the hexadecanedioic acid group compared to control rats. (P*<0.05) (P**<0.01).

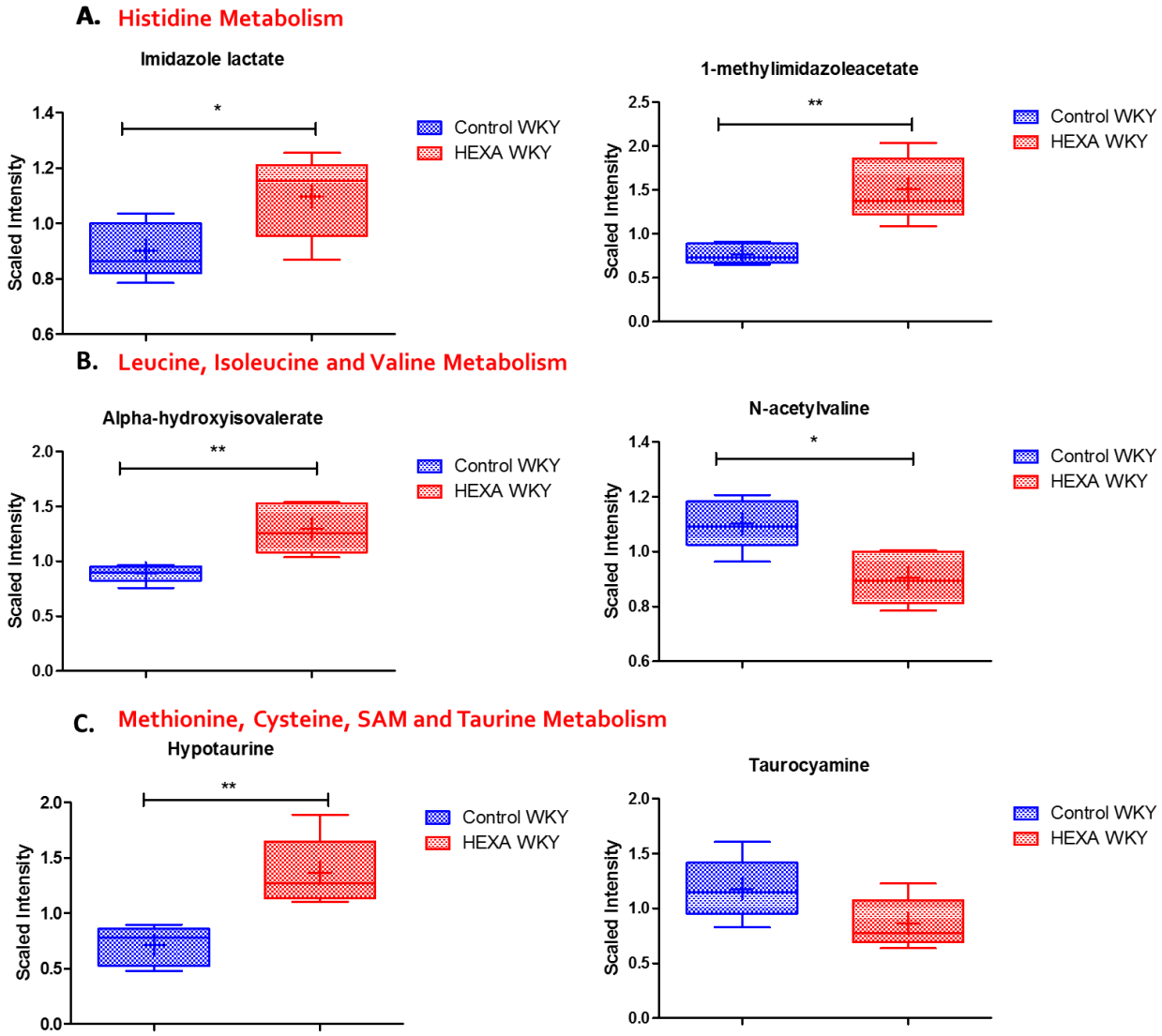

Figure 4-32: Amino acid metabolism in kidney tissues of hexadecanedioic acid-treated WKY rats compared with control WKY rats.

Hexadecanedioate induced significant changes in amino acid metabolism in kidney tissues. The levels of (A) histidine (i.e. imidazole lactate and 1-methylimidazoleacetate) significantly increased in kidney tissue of hexadecanedioic acid-treated rats compared with control rats. Also, the level of (B) leucine, isoleucine and valine Metabolism (i.e. alpha-hydroxyisovalerate and N-acetylvaline) significantly changes in hexadecanedioic acid-treated rats compared with control rats. (C) Methionine, Cysteine, SAM and Taurine Metabolism level (i.e. hypotaurine) significantly increased, though taurocyamine decreased in hexadecanedioic acid-treated rats compared with control rats. (P*<0.05), (P**<0.01).

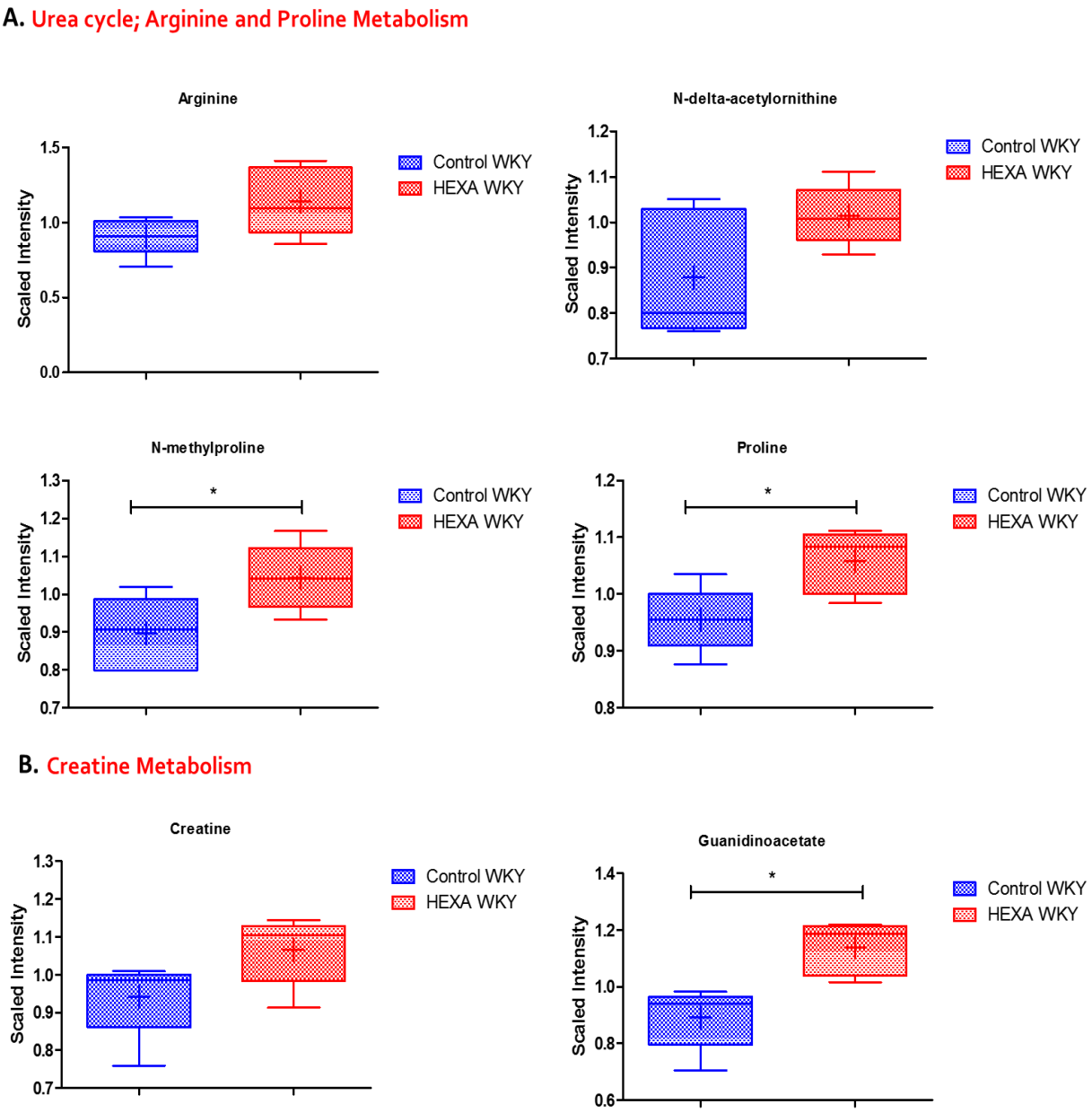

Figure 4-33: The citric acid cycle metabolism in kidney tissues of hexadecanedioic acid-treated WKY rats compared with control WKY rats.

Hexadecanedioate also induced significant changes in the urea cycle (A) related to the citric acid cycle metabolism in kidney tissues. The levels of arginine and N-delta-acetylornithine increased and the levels of N-methylproline and proline significantly increased in hexadecanedioic acid-treated rats compared with control rats. Also, the level of (B) creatine metabolism showed a significant increase in guanidinoacetate and a trend towards increase in creatine levels (P*<0.05).

4.5.6.3 Brain

In the brain tissues, 12 metabolites achieved statistical significance ($p \leq 0.05$) and 19 approached significance ($0.05 < p < 0.10$), as shown in the volcano plot (Figure 4-34 A). These perturbed metabolites are correlated to super pathways, including lipid and amino acid metabolism (Appendix, Table A3). Pathway enrichment (Figure 4-34 B) demonstrated the highly altered metabolites in brain of hexadecanedioic acid-treated rats compared with control rats; including long chain fatty acids, polyunsaturated fatty acids, and dihydrobiopterin cofactors in tetrahydrobiopterin metabolism.

Lipid metabolism

In the brain, long chain fatty acids such as myristate (P=0.018), palmitate (P=0.014), oleate (P= 0.006), stearate (P=0.024) and palmitoleate (P=0.045) significantly increased, while nonadecanoate (P=0.08) and arachidate (P=0.074) showed a trend towards increase in hexadecanedioic acid-treated rats compared with control rats. Moreover, polysaturated fatty acids showed a significant increase, such as docosahexaenoate (DHA; 22:6n3) (P=0.0036), adrenate (22:4n6) (P=0.0043), dihomo-linolenate (20:3n3 or n6) (P=0.0103), arachidonate (20:4n6) (P=0.018), and docosapentaenoate (n6 DPA; 22:5n6) (P=0.004) in hexadecanedioic acid-treated rats compared with control rats. Also, linoleate (18:2n6), eicosapentaenoate (EPA; 20:5n3) and dihomo-linoleate (20:2n6) levels increased in hexadecanedioic acid-treated rats compared with control rats. The levels of lysolipid (P=0.04), phospholipid, sphingolipid and corticosterone increased in hexadecanedioic acid-treated rats compared with control rats, as shown in Figure (4-35) (Appendix Table A3).

Amino acid metabolism

Small changes were observed in the levels of amino acids in brain tissues of hexadecanedioic acid-treated rats compared with control rats. An elevation in alpha and beta hydroxyisovalerate levels. An increase in urea level within the urea cycle with a decrease in levels of N-acetyl-3-methylhistidine and anserine, a dipeptide metabolite of histidine with anti-oxidant function could suggest increasing anti-oxidant use (Figure 4-36) (Appendix, Table A3).

Co-factors

An elevation in a number of co-factors such as flavin adenine dinucleotide (FAD), dihydrobiopterin (P=0.04) and pyridoxamine phosphate were observed in hexadecanedioic acid-treated rats compared with control rats (Appendix, Table A3).

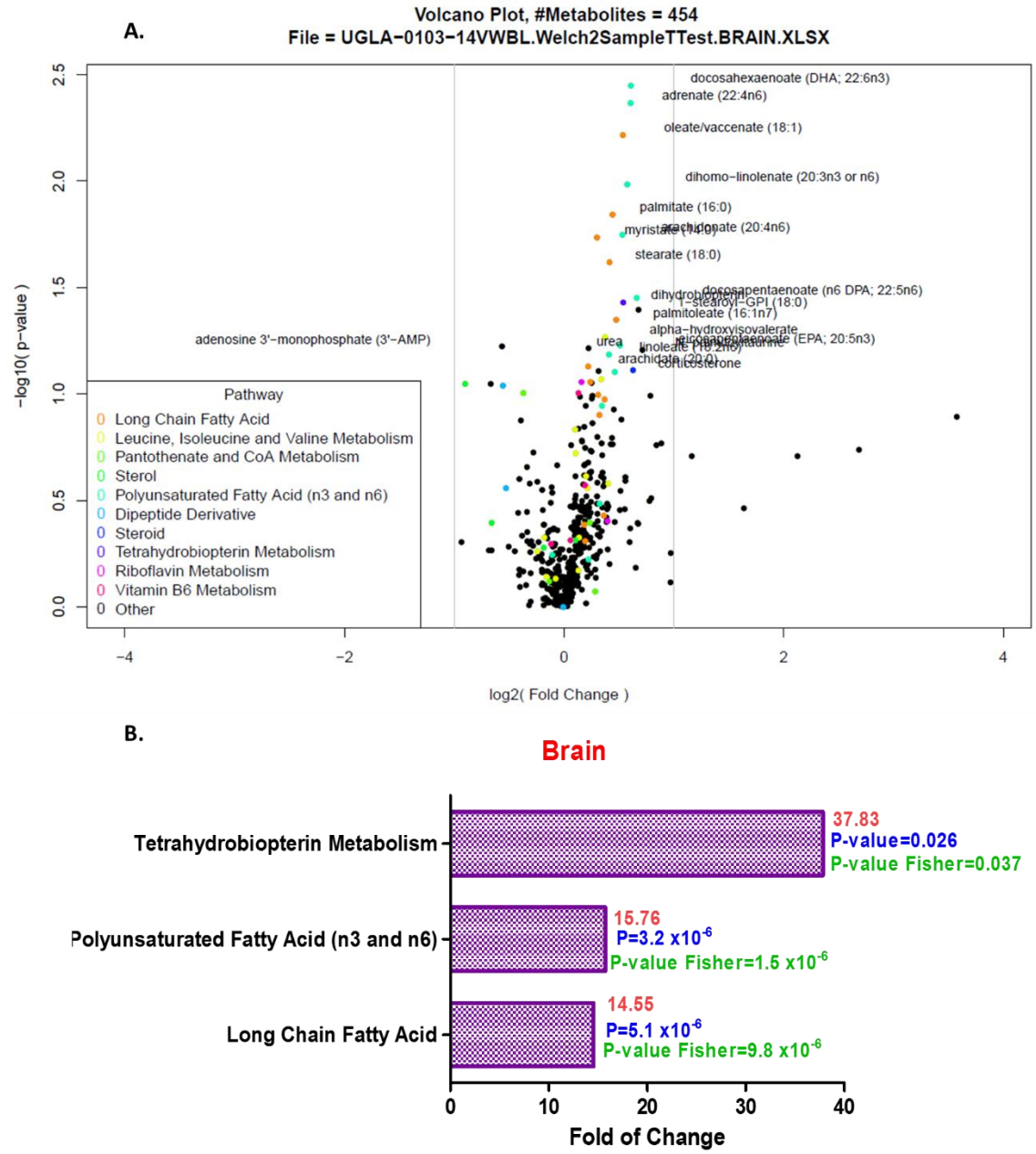

Figure 4-34: Fold enrichment pathway of significantly associated metabolites in brain tissues.

(A) Volcano plot shows up to 31 metabolites are achieved in brain tissues, which are the top 10 by p-value with fold change. Colours indicate metabolite membership in the most significant pathways according to hypergeometric enrichment test p-value. (B) Fold enrichment pathway of significantly associated metabolites in brain tissues. Enrichment values are based on the significant compounds relative to all detected compounds in the pathway. Enrichment = (number of significant metabolites in pathway/ total number of detected metabolites in pathway)/ (total number of significant metabolites/ total number of detected metabolites). Fold change is red labelled. Welch T- test p-value marked as blue and Fisher p-value is marked as green.

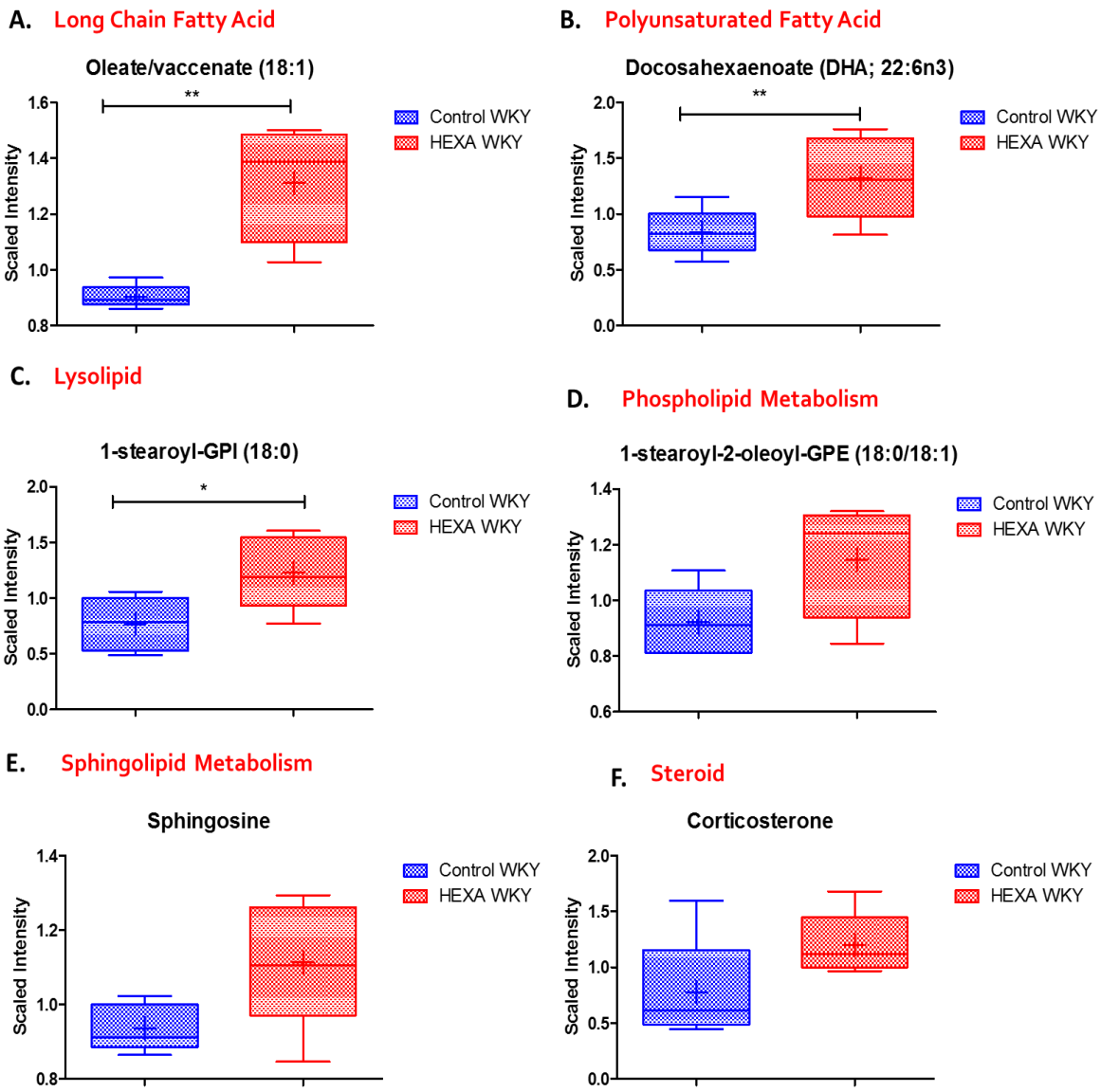

Figure 4-35: Fatty acids metabolism in brain tissues of hexadecanedioic acid-treated WKY rats compared with control WKY rats.

Hexadecanedioate also induced significant increases in (A) long chain fatty acid metabolism (i.e. oleate/ vaccinate), (B) polyunsaturated fatty acid (i.e. docosahexaenoate (DHA; 22: 6n3)), and (C) lysolipid (i.e. 1-stearoyl-GPI (18:0)). The levels of (D) phospholipid (1-stearoyl-2-oleoyl-GPE (18:0/ 18:1), (E) sphingolipid (i.e. sphingosine) and (F) steroid (I.e. corticosterone) increased in brain tissues of hexadecanedioic acid-treated rats compared with control rats (P*<0.05) (P**<0.01).

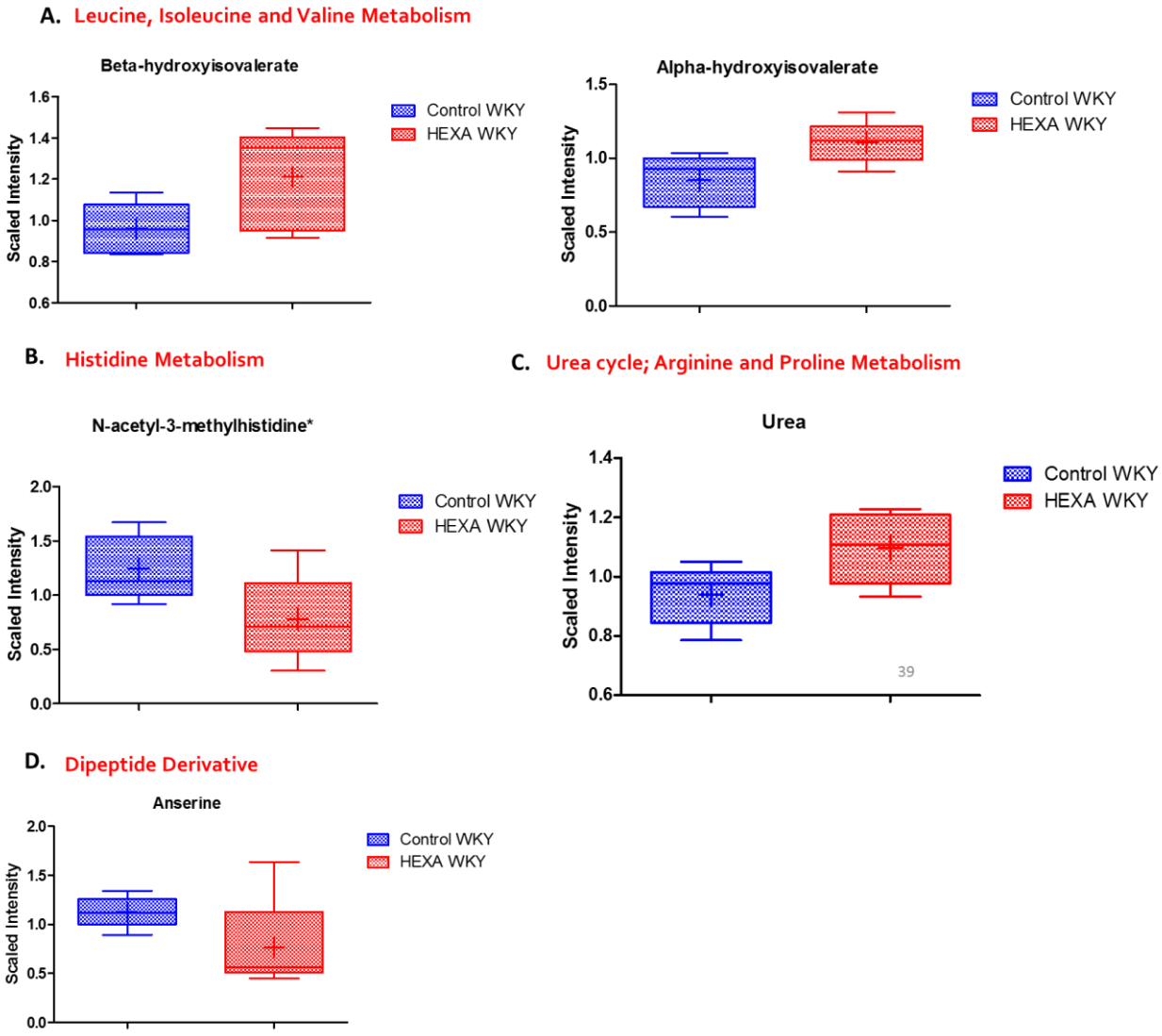

Figure 4-36: Amino acid metabolism in brain tissues of hexadecanedioic acid-treated WKY rats compared with control WKY rats.

Hexadecanedioate induced changes in amino acid metabolism in brain tissues of WKY rats. The level of (A) beta-hydroxyisovalerate and alpha-hydroxyisovalerate increased, while (B) N-acetyl-3-methylhistidine level decreased in hexadecanedioic acid-treated rats compared with control rats. (C) Urea metabolite in the urea cycle increased in brain tissues of in hexadecanedioic acid-treated rats compared with control rats. Also, (D) dipeptide derivative (anserine) decreased in hexadecanedioic acid-treated rats compared with control rats.

4.5.6.4 Liver

In the liver tissues, 30 metabolites achieved statistical significance ($p \leq 0.05$) and 54 approached significance ($0.05 < p < 0.10$), as shown in the volcano plot (Figure 4-37 A). These perturbed metabolites are correlated to super pathways, including lipid, carbohydrate, and amino acid metabolisms (Appendix, Table A4). A pathway enrichment overview of altered metabolites highlights branched fatty acid, acyl glycine fatty acid, sterol, eicosanoid, glutathione and oxidative phosphorylation metabolisms as being significantly enriched in the quantitative metabolomics of liver tissues of hexadecanedioic acid- treated rats compared with control rats (Figure 4-37 B).

Lipid metabolism

There were alterations in the lipid profiles in liver tissues. Long chain fatty acid products (i.e. margarate (17:0), 10-heptadecenoate (17:1n7) and 10-nonadecenoate (19:1n9)), branched fatty acids (i.e. 15-methylpalmitate and 17-methylstearate) and polyunsaturated fatty acid (i.e. dihomo-linoleate (20:2n6)) increased, with decreases in stearidonate (18:4n3) in hexadecanedioic acid-treated rats compared with control rats. Furthermore, an increase in phospholipid metabolism was observed in the liver tissue of hexadecanedioic acid-treated rats compared with control rats (Figure 4-38).

There was a significant elevation in sphingolipid metabolism as well as cholesterol ($P=0.0106$) and campesterol ($P=0.024$) levels of sterol metabolism in hexadecanedioic acid-treated rats compared with control rats. 1-(1-enyl-stearoyl)-2-linoleoyl-GPE (P-18:0/18:2)* level significantly increased with an elevation of other plasmalogen metabolites in hexadecanedioic acid-treated rats compared with control rats, as shown in Table A4 (Appendix)). Also, an increase in monoacylglycerol (i.e. 1-myristoylglycerol (14:0)) was shown in hexadecanedioic acid-treated rats compared with control rats (Figure 4-38).

Metabolomics data also shows that hexadecanedioate administration induced significantly decreased levels of monohydroxy fatty acid products (i.e.2-hydroxypalmitate), while 4-hydroxybutyrate significantly increased in hexadecanedioic acid-treated rats compared with control rats. Additionally,

lysolipid (i.e. 1-lignoceroyl-GPC (24:0)) and acyl carnitine (i.e. linoleoylcarnitine*) levels significantly increased in hexadecanedioic acid-treated rats compared with control rats. However, acyl glycine fatty acid (i.e. hexanoylglycine) and prostaglandin F2 alpha levels significantly decreased in liver tissues of hexadecanedioic acid-treated rats compared with control rats (Figure 4-38) (Appendix Table A4).

Bile acid metabolism

A marked increase in muricholic bile acid (i.e tauro-alpha-muricholate (P=0.054) and tauro-beta-muricholate (P=0.047) (Figure 4-39 A) in addition to significant reduction in secondary (i.e glycodeoxycholate) bile acid was observed in the liver samples from hexadecanedioic acid-treated rats compared with control rats (P=0.018), as shown in (Figure 4-39 B) (Appendix, Table A4).

Carbohydrate metabolism

Changes were found in carbohydrate metabolism in the liver tissues of hexadecanedioic acid-treated rats compared with control rats. Arabonate levels in pentose phosphate metabolism and glucuronate level in aminosuger metabolism reduced in hexadecanedioic acid-treated rats compared with control rats. The levels of N-acetyl-glucosamine 1-phosphate and nucleotide sugar (i.e. UDP-N-acetylgalactosamine and UDP-glucuronate) increased in hexadecanedioic acid-treated rats compared with control rats, as shown in (Appendix Table A4).

Amino acid metabolism

Our metabolomics data exhibited reductions in amino acids such as gamma glutamyl amino acids metabolites, as well as N-acetyltyrosine and o-tyrosine of phenylalanine and tyrosine metabolism in hexadecanedioic acid-treated rats compared with control rats (Appendix, Table A4) (Figure 4-40 C). Furthermore, N-acetylleucine, 4-methyl-2-oxopentanoate, N-acetylisoleucine, valine, and N-acetyltryptophan decreased in hexadecanedioic acid-treated rats compared with control rats (Appendix, Table A4). Glycine, betaine, betaine aldehyde and 4-hydroxyglutamate levels decreased, while N-acetylglutamate (P=0.026), S-methylcysteine (P=0.012) and taurocyamine (P=0.005) significantly reduced in

hexadecanedioic acid-treated rats compared with controls (Figure 4-40 A) (Appendix, Table A4).

Histidine levels decreased, with slightly increased 4-imidazoleacetate level in the histidine metabolism in hexadecanedioic acid-treated rats compared with controls (Appendix, Table A4). However, imidazole lactate (P=0.04) and 1-methylimidazoleacetate (P=0.0052) significantly increased in hexadecanedioic acid-treated rats compared with control rats (Figure 4-40 D). In liver, increases in cysteine-glutathione disulphide levels with significant decreases in 5-oxoproline level (P=0.0078) in hexadecanedioic acid-treated rats compared with controls (Figure 4-40 B). This could suggest an increase in oxidizing environment.

There was a reduction in ornithine metabolite in the urea cycle, with an increase in N-delta-acetylornithine level (P=0.068) in hexadecanedioic acid-treated rats compared with control rats (Appendix, Table A4).

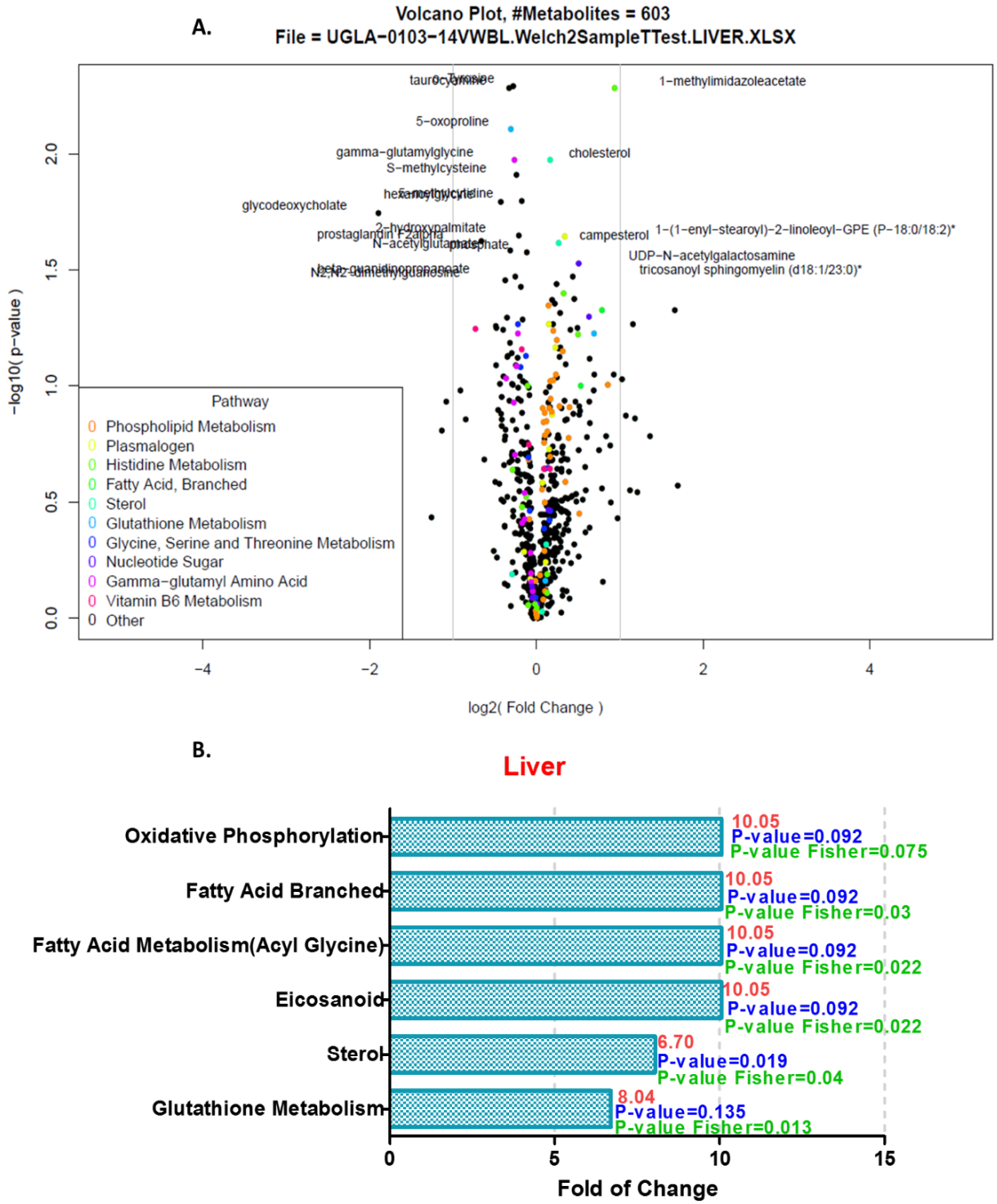

Figure 4-37: Fold enrichment pathway of significantly associated metabolites in liver tissues.

(A) Volcano plot shows up to 84 metabolites identified in liver tissues, which are the top 10 by p-value with fold change. Colours indicate metabolite membership in the most significant pathways according to hypergeometric enrichment test p-value. (B) Fold enrichment pathway of significantly associated metabolites in liver tissues. Enrichment values are based on the significant compounds relative to all detected compounds in the pathway. Enrichment = (number of significant metabolites in pathway/ total number of detected metabolites in pathway)/ (total number of significant metabolites/ total number of detected metabolites). Fold change is red labelled. Welch T- test p-value marked as blue and Fisher p-value is marked as green.

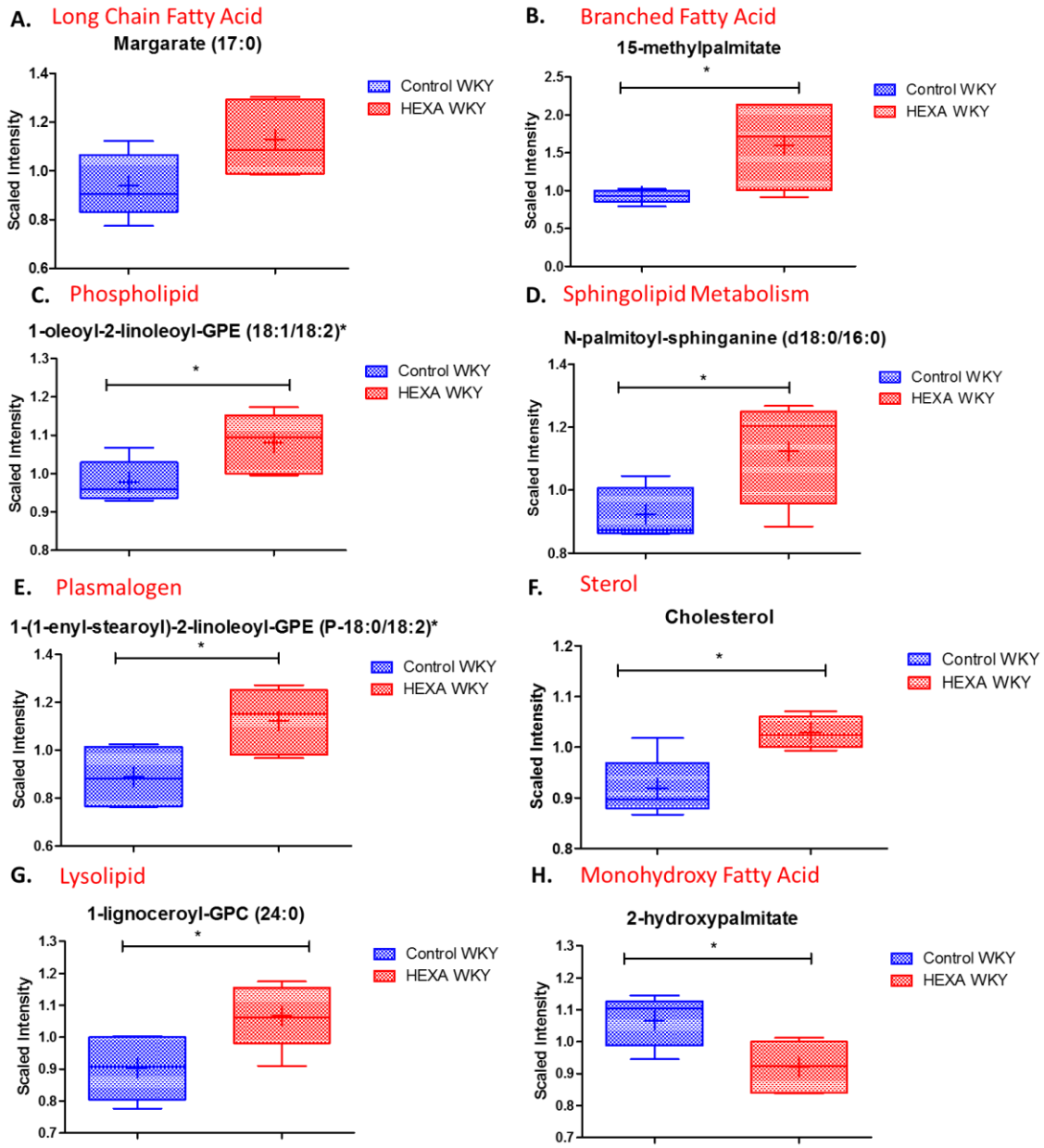

Figure 4-38: Fatty acids metabolism in liver tissues of hexadecanedioic acid-treated WKY rats compared to control WKY rats.

Hexadecanedioate induced marked elevation in (A) long chain fatty acids (i.e. margarate (17:0), (B) branched fatty acid (i.e. 15-methylpalmitate), (C) phospholipid (i.e. 1-oleoyl-2-linoleoyl-GPE (18:1/18:2)*, (D) sphingolipid (i.e. N-palmitoyl-sphinganine (d18:0/ 16:0), (E) plasmalogen (1-(1-enyl-stearoyl)-2-linoleoyl-GPE (P-18:0/18:2)*), (F) cholesterol, (G) lysolipid (1-lignoceroyl-GPC (24:0) in liver tissues of hexadecanedioic acid-treated rats compared with control rats. However, significant reductions were found in monohydroxy fatty acid (i.e. 2-hydroxypalmitate) in liver tissues of hexadecanedioic acid-treated rats compared to control rats (P*<0.05).

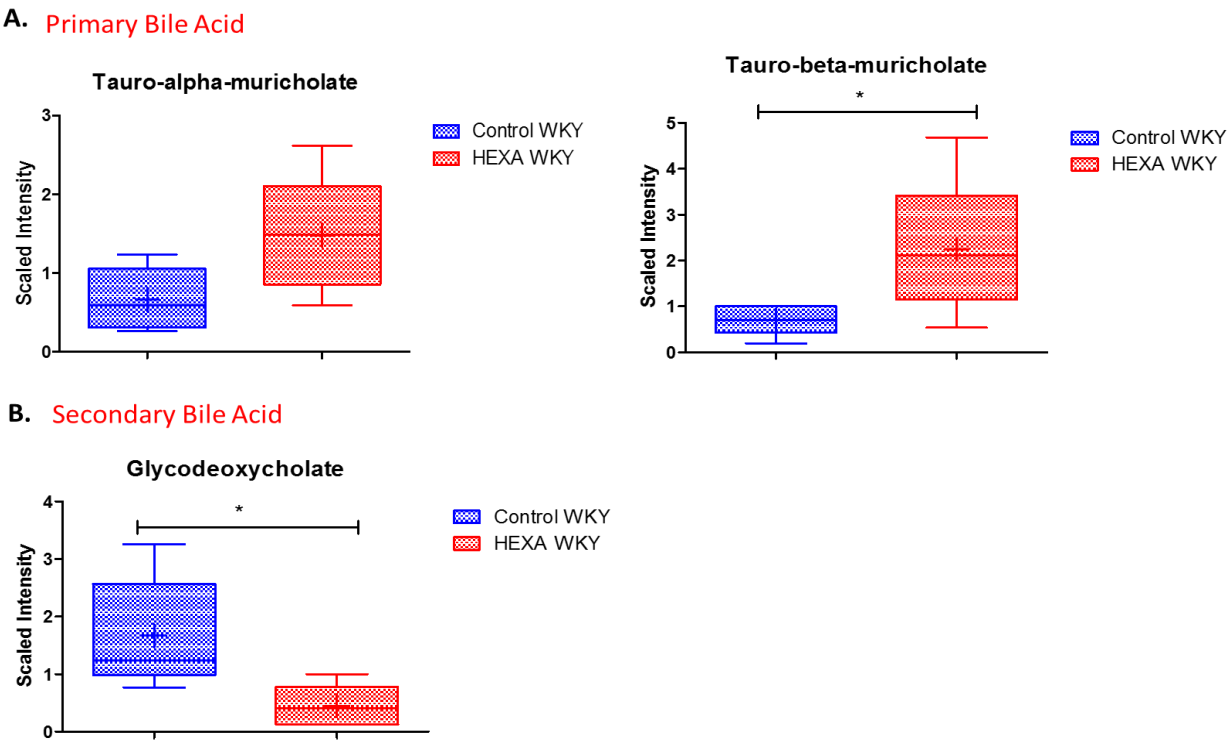

Figure 4-39: Bile acid metabolism in liver tissues of hexadecanedioic acid-treated WKY rats compared to control WKY rats.

Hexadecanedioate induced a marked increase in (A) primary bile acid and a significant decrease in (B) secondary bile acid metabolism in liver tissues of hexadecanedioic acid-treated rats compared to control rats (P*<0.05).

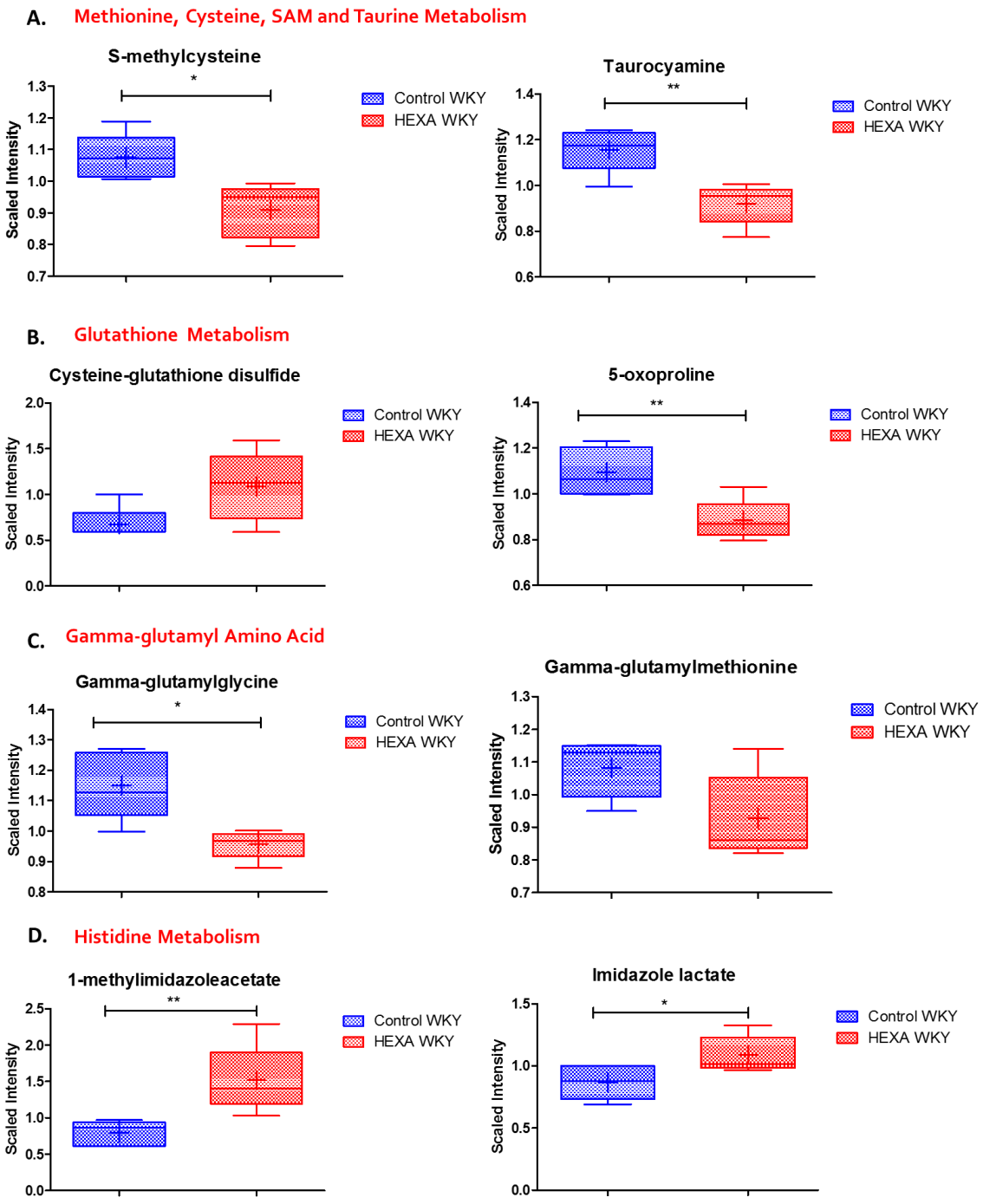

Figure 4-40: Alteration in metabolites within methionine, cysteine, and taurine metabolism, glutathione metabolism, and histidine metabolism detected in hexadecanedioic acid-treated WKY rats compared with control WKY rats.

Hexadecanedioate induced a significant reduction in (A) methionine, cysteine, SAM and taurine metabolism (i.e.s-methylcysteine and taurocyamine) and (B) 5-oxoproline metabolite in glutathione metabolism, while the levels of cysteine-glutathione disulphide increased. (C) Gamma-glutamyl amino acid (gamma-glutamylglycine) level significantly reduced and a trend towards decrease was shown in gamma-glutamylmethionine. Also, (D) a significant increase was observed in histidine metabolism metabolites in liver tissues in hexadecanedioic acid-treated rats compared with control rats. (P*<0.05) (P**<0.01).

4.5.6.5 Heart

In the heart tissues, 59 metabolites achieved statistical significance ($p \leq 0.05$) and 62 approached significance ($0.05 < p < 0.10$), as shown in the volcano plot (Figure 4-41 A). Heart samples from hexadecanedioic acid–treated rats displayed broad changes in lipids, carbohydrates, amino acid and nucleotide metabolisms (Appendix, Table A6). A pathway enrichment overview of altered metabolites highlights mevalonate, acyl carnitine fatty acid, oxidative phosphorylation, lysoplasmalogen, glycogen, leucine, lsoleucine and valine; and phospholipid metabolism as being significantly enriched in the quantitative metabolomics of heart tissues of hexadecanedioic acid-treated rats compared with control rats (Figure 4-41 B).

Amino acids metabolism

Heart samples from hexadecanedioic acid-treated rats exhibited a distinct amino acid metabolite signature in comparison to the control heart tissues. Significant elevations in most amino acid metabolites were shown such as threonine (P=0.0053), 1-methylimidazoleacetate (P=0.031), asparagine (P=0.038), isoleucine (P=0.026), beta-hydroxyisovaleroylcarnitine (P=0.04), tiglylcarnitine (P=0.01), phenyllactate (P=0.048), tryptophan (P=0.043), c-glycosyltryptophan (P=0.01), S-adenosylmethionine (SAM) (P=0.03) and methionine (0.026) (Appendix, Table A6).

The levels of leucine, alphahydroxyisovaleroylcarnitine*, N6,N6,N6-trimethyllysine, tyrosine, S-adenosylhomocysteine (SAH) and 3-(4-hydroxyphenyl) lactate increased in hexadecanedioic acid-treated rats compared to controls. Significantly lower levels of N-acetylaspartate (NAA) (P=0.002) and methysuccinate (P=0.014) were observed in hexadecanedioic acid-treated rats compared to control rats. However, a reduction in level of N-acetylglutamine was observed in hexadecanedioic acid-treated rats compared to control rats. Moreover, the urea cycle; arginine and proline metabolism metabolites were upregulated, such as argininosuccinate (P=0.04), dimethylarginine (SDMA+ ADMA) and N-delta-acetylornithine in hexadecanedioic acid-treated rats compared to control rats (Appendix, Table A6).

Carbohydrate metabolism

In the heart tissues, elevations in the levels of glucose and glucose 6-phosphat, with a decrease in the 3-carbon glycolytic intermediate 3-phosphoglycerate in hexadecanedioic acid-treated rats compared to control rats, are suggestive of changing glycolytic use (Figure 4-42 A). An increase in glycogen breakdown products (e.g. maltotetraose, maltotriose (P=0.043), and maltose (P=0.013)) could suggest increased glucose demand (Figure 4-42 B).

Increases in fructose could be consistent with increased glucose availability (Figure 4-43 B). However, the glycolytic end-products pyruvate and lactate were not changed between groups. Furthermore, pentose metabolite (i.e. ribulose/xylulose) and aminosugar (i.e. N-acetylneuraminate (P=0.042) and glucosamine-6-phosphate) increased in hexadecanedioic acid-treated rats compared to control rats (Figure 4-43 A, C). Also, a significant increase in the level of fumarate (P=0.014) along with a significant decrease in oxidative phosphorylation (i.e. phosphate) (P=0.04) in hexadecanedioic acid-treated rats compared to control rats, could suggest increasing demand for use in the TCA cycle though citrate levels did not change (Figure 4-43 D, E) (Appendix, Table A6).

Lipid metabolism

In the heart, fatty acids (i.e. malonyl carnitine and butyryl carnitine) levels increased, with significant increases in acylcarnitines (i.e. oleoylcarnitine (P=0.008), linoleoylcarnitine (P=0.002), 3-hydroxybutyrylcarnitine(1) (P=0.04), 3-hydroxybutyrylcarnitine(2) (P=0.02), palmitoylcarnitine (P=0.04) and stearoylcarnitine (P=0.02)) in hexadecanedioic acid-treated rats compared to control rats (Appendix, Table A6).

Significant increases were observed in the levels of phospholipids (i.e. trimethylamine N-oxide (P=0.026), 1,2-dioleoyl-GPC (18:1/18:1)* (P=0.043), 1-palmitoyl-2-oleoyl-GPE (16:0/18:1) (P=0.043), 1-stearoyl-2-oleoyl-GPE (18:0/18:1) (P=0.035), 1-palmitoyl-2-linoleoyl-GPE (16:0/18:2) (P=0.045), 1-stearoyl-2-linoleoyl-GPE (18:0/18:2)* (P=0.04), 1,2-dioleoyl-GPE (18:1/18:1) (P=0.03), 1,2-dilinoleoyl-GPC (18:2/18:2) (P=0.044) and 1-oleoyl-2-linoleoyl-GPE

(18:1/18:2)* (P=0.038) in hexadecanedioic acid-treated rats compared with controls (Appendix, Table A6).

There were also significant increases in the levels of lysolipids (i.e. 1-oleoyl-GPE (18:1) (P=0.045) and plasmalogen (i.e. 1-(1-enyl-palmitoyl)-2-oleoyl-GPE(P-16:0/18:1)* (P=0.039), 1-(1-enyl-palmitoyl)-2-oleoyl-GPC(P-16:0/18:1)* (P=0.048), 1-(1-enyl-stearoyl)-2-oleoyl-GPE(P-18:0/18:1) (p=0.014) as well as lysoplasmalogen (i.e. 1-(1-enyl-palmitoyl)-GPE(P-16:0)* (P=0.046) and 1-(1-enyl-oleoyl)-GPE (P-18:1)* (P=0.044) were observed as in hexadecanedioic acid-treated rats compared with controls (Appendix, Table A6).

An elevation in the levels of polyunsaturated fatty acid (i.e. linoleate), monoacylglycerol (i.e. 1-oleoylglycerol (18:1) (P=0.04) and 2-oleoylglycerol (18:1)), diacylglycerol (i.e. 1-palmitoyl-3-linoleoyl-glycerol (16:0/18:2)*) were observed in hexadecanedioic acid-treated rats compared with controls (Appendix, Table A6).

The levels of sphingolipids and sterol (i.e. cholesterol and beta-sitosterol (P=0.032)) increased in hexadecanedioic acid-treated rats compared with controls. However, myo-inositol (P=0.008) and melvalonate (i.e. 3-hydroxy-3-methylglutarate) (P=0.0024) levels significantly reduced in hexadecanedioic acid-treated rats compared with controls (Figure 4-44) (Appendix, Table A6).

Nucleotides metabolism

Elevations in several nucleotides were observed in the heart tissues of hexadecanedioic acid-treated rats compared with controls. For example purine metabolism, adenine containing metabolites (i.e. xanthinosine (P=0.04), adenosine 5'-diphosphate (ADP). Also, elevation in the levels of adenosine 3'-monophosphate (3'-AMP) (P=0.022), adenosine 2'-monophosphate (2'-AMP), adenosine, N1-methyladenosine (P=0.015), N6-succinyladenosine (0.034), pyrimidine metabolism, uracil, guanine and cytidine containing metabolites, and pyrimidine metabolism was observed in hexadecanedioic acid-treated rats compared with controls (Appendix Table A6).

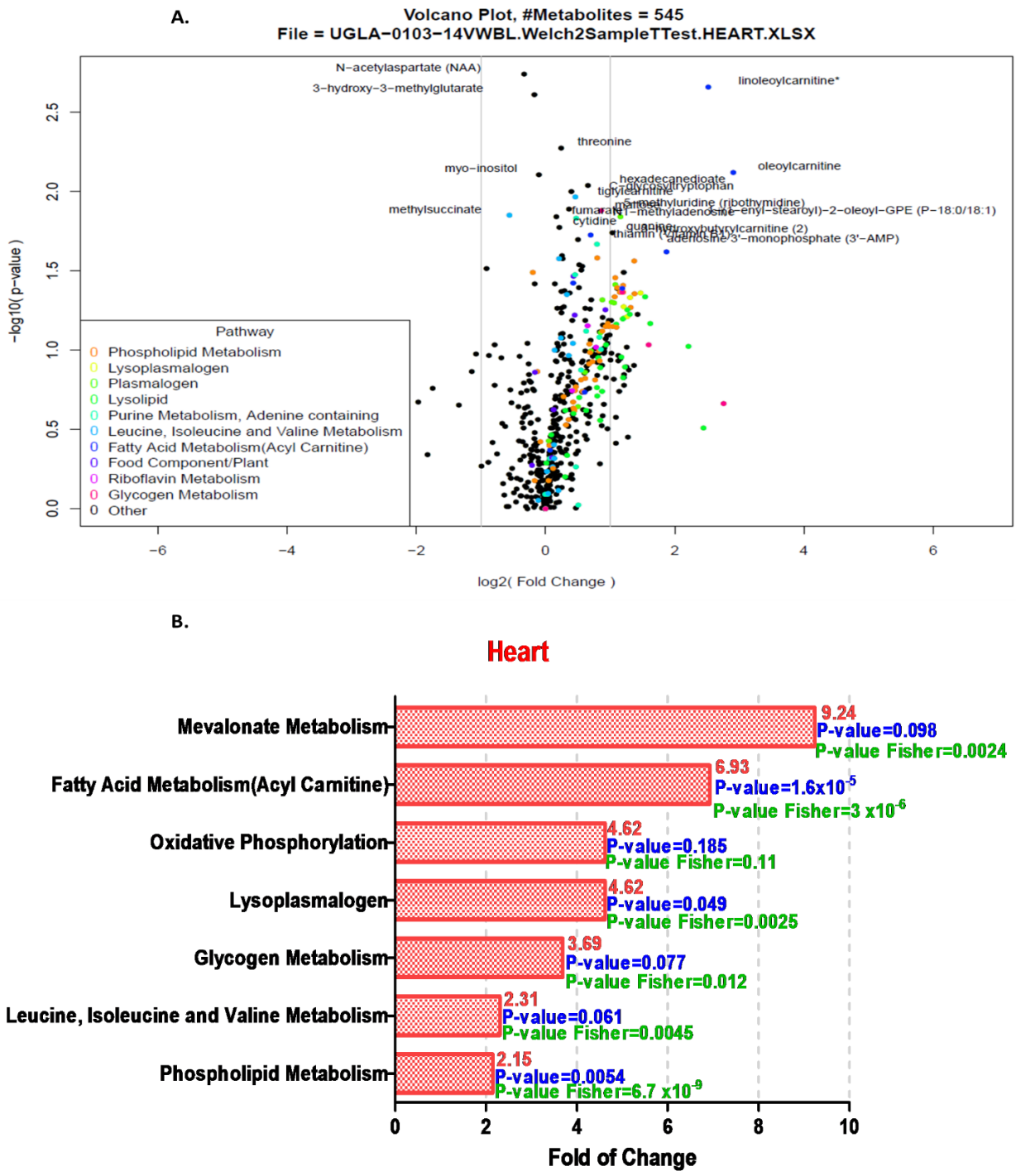

Figure 4-41: Fold enrichment pathway of significantly associated metabolites in heart tissues.

(A) Volcano plot shows up to 121 metabolites identified in heart tissues, which are the top 10 by p-value with fold change. Colours indicate metabolite membership in the most significant pathways according to hypergeometric enrichment test p-value. (B) Fold enrichment pathway of significantly associated metabolites in heart tissues. Enrichment values are based on the significant compounds relative to all detected compounds in the pathway. Enrichment = (number of significant metabolites in pathway/ total number of detected metabolites in pathway)/ (total number of significant metabolites/ total number of detected metabolites). Fold change is red labelled. Welch T- test p-value marked as blue and Fisher p-value is marked as green.

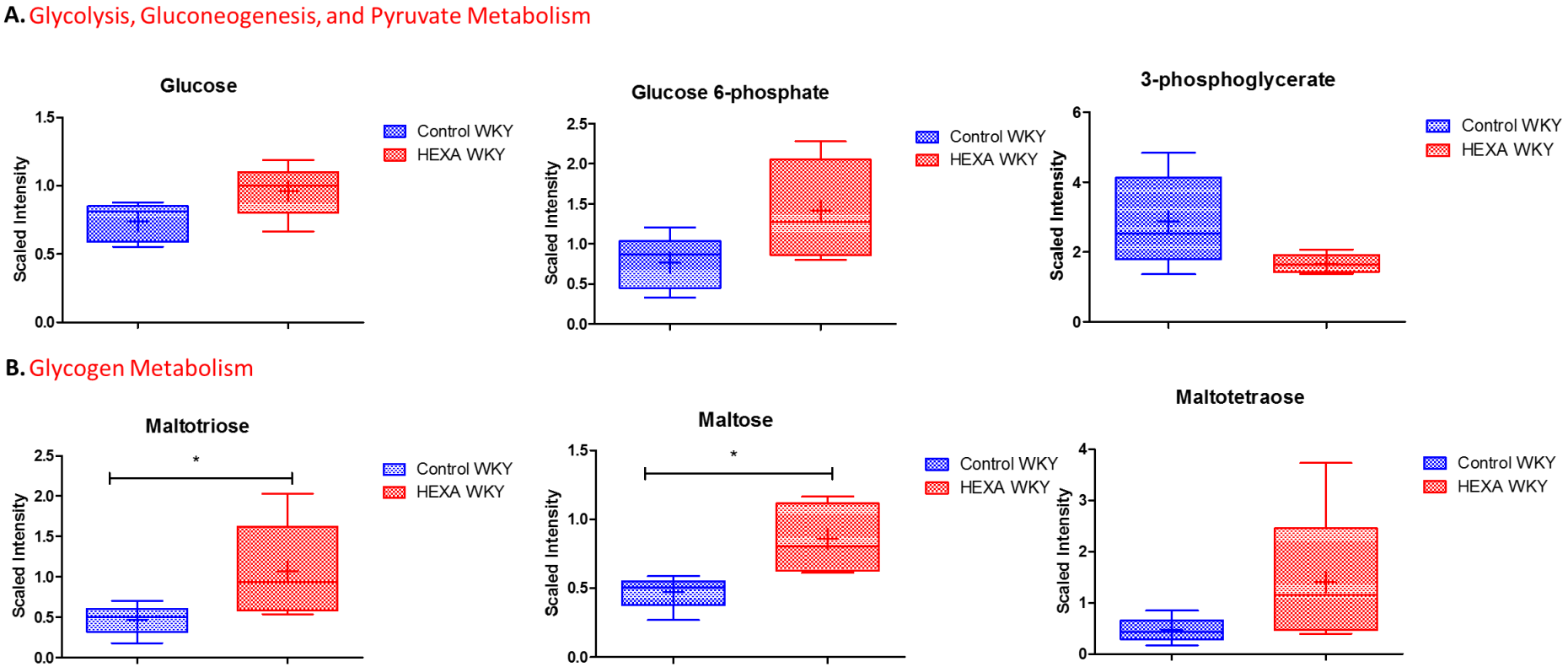

Figure 4-42: Glycolysis and glycogen metabolism in heart tissues of hexadecanedioic acid-treated WKY rats compared to control WKY rats.

In the heart, elevations in glucose and glucose 6-phosphate levels, with a decrease in the 3-carbon glycolytic intermediate 3-phosphoglycerate. Also, a marked increase in glycogen breakdown products (e.g. maltotetraose, maltotriose, and maltose) in hexadecanedioic acid-treated rats compared with control rats (P*0.05).

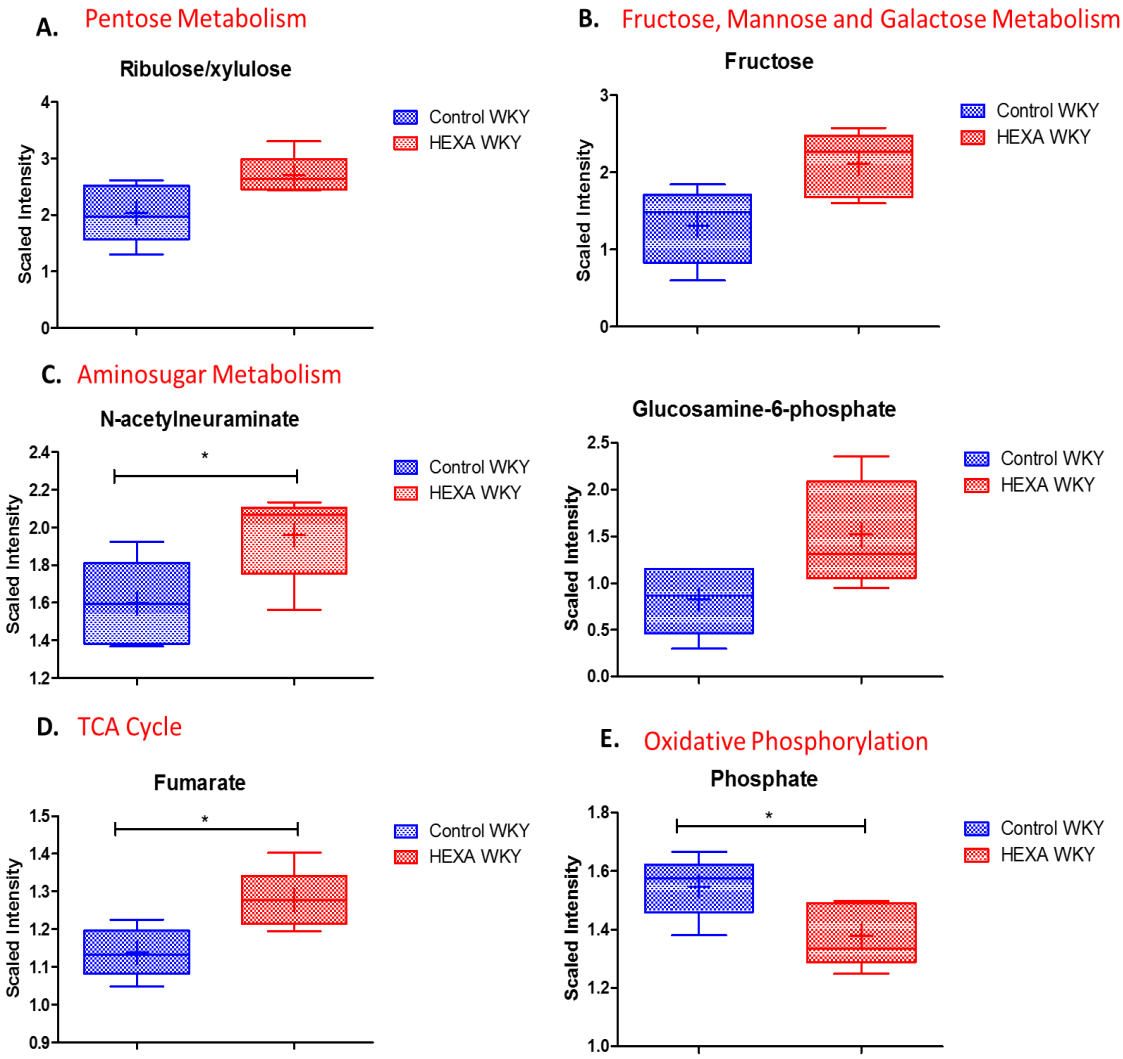

Figure 4-43: Carbohydrate metabolism in heart tissues of hexadecanedioic acid-treated WKY rats compared to control WKY rats.

The levels of (A) ribulose/xylulose and (B) fructose increased in heart tissues of hexadecanedioic acid-treated rats compared with control rats. Also, there was a marked increase in aminosugar metabolism products (i.e. N-acetylneuraminate and glucosamine-6-phosphate). The fumarate level in the TCA cycle significantly increased, as well as reduction in phosphate level within oxidative phosphorylation metabolism in hexadecanedioic acid-treated rats compared with control rats (P*0.05).

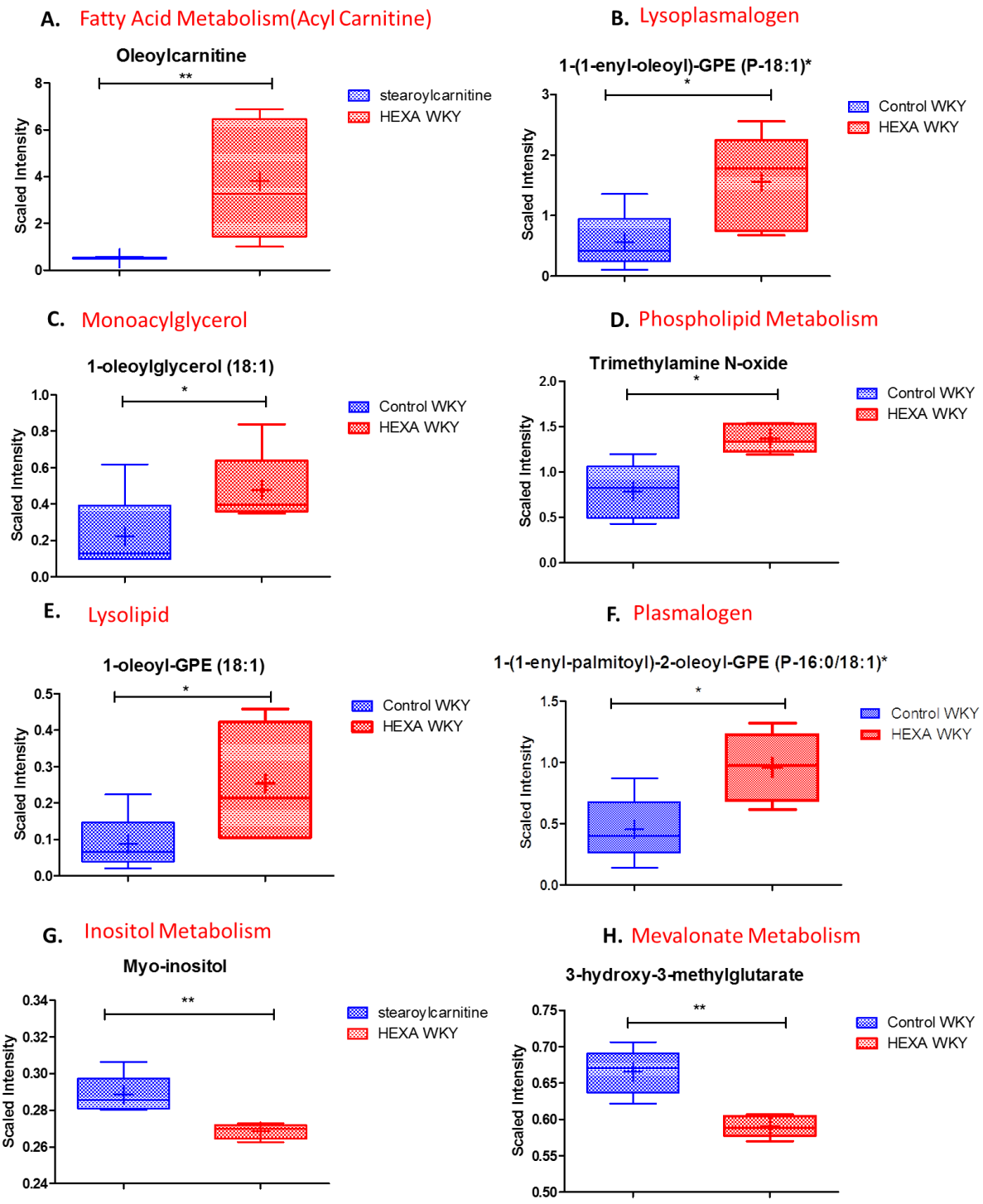

Figure 4-44: Fatty acids metabolism in heart tissues of hexadecanedioic acid-treated WKY rats compared to control WKY rats.

Hexadecanedioate causes notable changes in lipid profiles in heart tissues. The level of (A) oleoylcarnitine, (B) lysoplasmalogen (i.e. 1-(1-enyl-oleoyl)-GPE (P-18:1)*), (C) monoacylglycerol (i.e. 1-oleoylglycerol (18:1)), (D) phospholipid metabolites (i.e. trimethylamine N-oxide, (E) lysolipid (i.e. 1-oleoyl GPE (18:1)) and (F) plasmalogen fatty acids, significantly increased along with significant decreased in the level of (G) myo-inositol and mevalonate metabolite (i.e. 3-hydroxy-3-methylglutarate) (P*0.05) (P**<0.01).

4.5.6.6 Aorta

In aorta tissues, 23 metabolites achieved statistical significance ($p \leq 0.05$) and 23 approached significance ($0.05 < p < 0.10$), as shown in the volcano plot (Figure 4-45 A). These altered metabolites are correlated to super pathways, including lipid, carbohydrate, and amino acid metabolism (Appendix, Table A5). A pathway enrichment overview of altered metabolites highlights lysoplasmalogen, lysolipid and nicotinate and nicotinamide metabolisms as being significantly enriched in the quantitative metabolomics of aorta tissues from hexadecanedioic acid-treated rats compared with control rats (Figure 4-45 B).

Amino acids metabolism

Significant reductions were observed in some amino acid metabolites such as glycine (P=0.012), glutamate (i.e. pyroglutamine (P=0.047)) and taurocyamine (P=0.014) in hexadecanedioic acid-treated rats compared to control rats. Also, the levels of serine, asparagine, histidine, creatinine, 3-methoxytyrosine, valine and gamma-glutamylglycine decreased in hexadecanedioic acid-treated rats compared to control rats. Nevertheless, imidazole lactate, phenyllactate (PLA), indolelactate (P=0.049) and gamma-glutamylvaline levels increased in hexadecanedioic acid-treated rats compared to control rats, as shown in (Appendix, Table A5).

Carbohydrate metabolism

A significant reduction in the glycolysis metabolite (i.e. 1,5-anhydroglucitol) (P=0.045), with a significant increase in mannitol/sorbitol levels (P=0.037) in fructose metabolism was observed in hexadecanedioic acid-treated WKY rats compared to control rats. In addition, succinylcarnitine in the TCA cycle significantly increased (P=0.047), with an increase in citrate level in hexadecanedioic acid-treated rats compared to control rats that could suggest increased glucose and TCA demands (Appendix, Table A5).

Lipid metabolism

Downregulation was observed in the levels of lipid metabolites. There was a reduction in levels of polyunsaturated fatty acids (i.e. arachidonate (20:4n6)), 12-

HETE, sphingolipid (i.e. N-palmitoyl-sphingosine (d18:1/16:0)), phospholipids (i.e. 1-oleoyl-2-linoleoyl-GPC (18:1/18:2)*) and plasmalogen (i.e.1-(1-enyl-stearoyl)-2-arachidonoyl-GPE (P-18:0/20:4)*) in hexadecanedioic acid-treated WKY rats compared to controls rats. Also, significant reductions were observed in levels of phospholipids, lysolipid, plasmalogen and lysoplasmalogen in hexadecanedioic acid-treated WKY rats compared to controls rats. However, phospholipid (i.e. 1-stearoyl-2-oleoyl-GPG (18:0/18:1) increased in hexadecanedioic acid-treated aorta tissues compared to control rats (Figure 4-46) (Appendix Table A5).

Bile acids metabolism

Alteration in the bile acid profile was observed in hexadecanedioic acid-treated rats compared to control rats. Primary bile acids (i.e. tauro-beta-muricholate) level showed a significant increase in hexadecanedioic acid-treated rats compared to control rats (P=0.003). Also, secondary bile acid (i.e. glycodeoxycholate) (P=0.034) significantly decreased, with an increase in the level of deoxycholate in hexadecanedioic acid-treated rats compared to controls, as shown in (Appendix, Table A5).

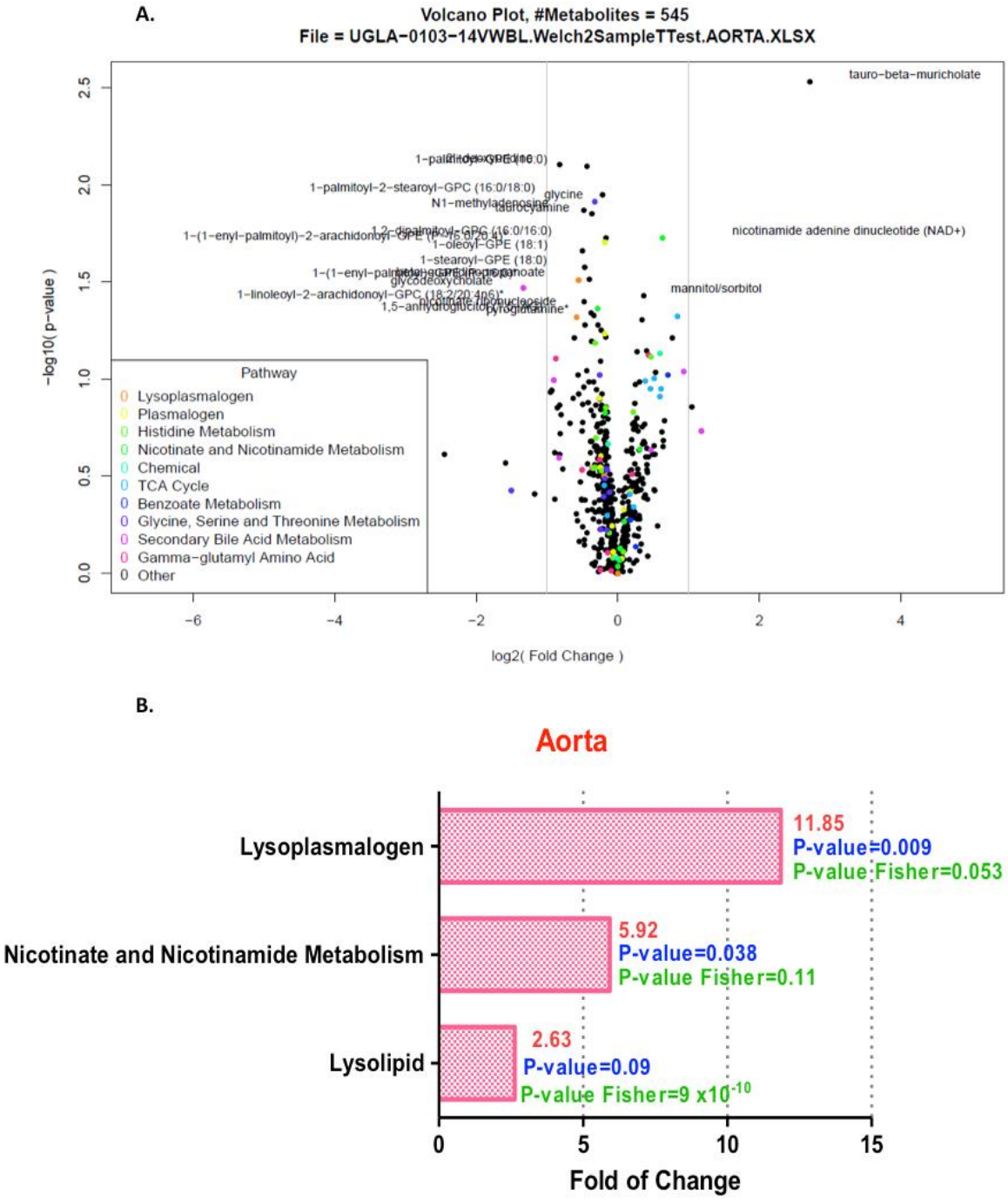

Figure 4-45: Fold enrichment pathway of significantly associated metabolites in aorta tissues.

(A) Volcano plot shows up to 46 metabolites identified in aorta tissues, which are the top 10 by p-value with fold change. Colours indicate metabolite membership in the most significant pathways according to hypergeometric enrichment test p-value. (B) Fold enrichment pathway of significantly associated metabolites in aorta tissues. Enrichment values are based on the significant compounds relative to all detected compounds in the pathway. Enrichment = (number of significant metabolites in pathway/ total number of detected metabolites in pathway)/ (total number of significant metabolites/ total number of detected metabolites). Fold change is red labelled. Welch T- test p-value marked as blue and Fisher p-value is marked as green.

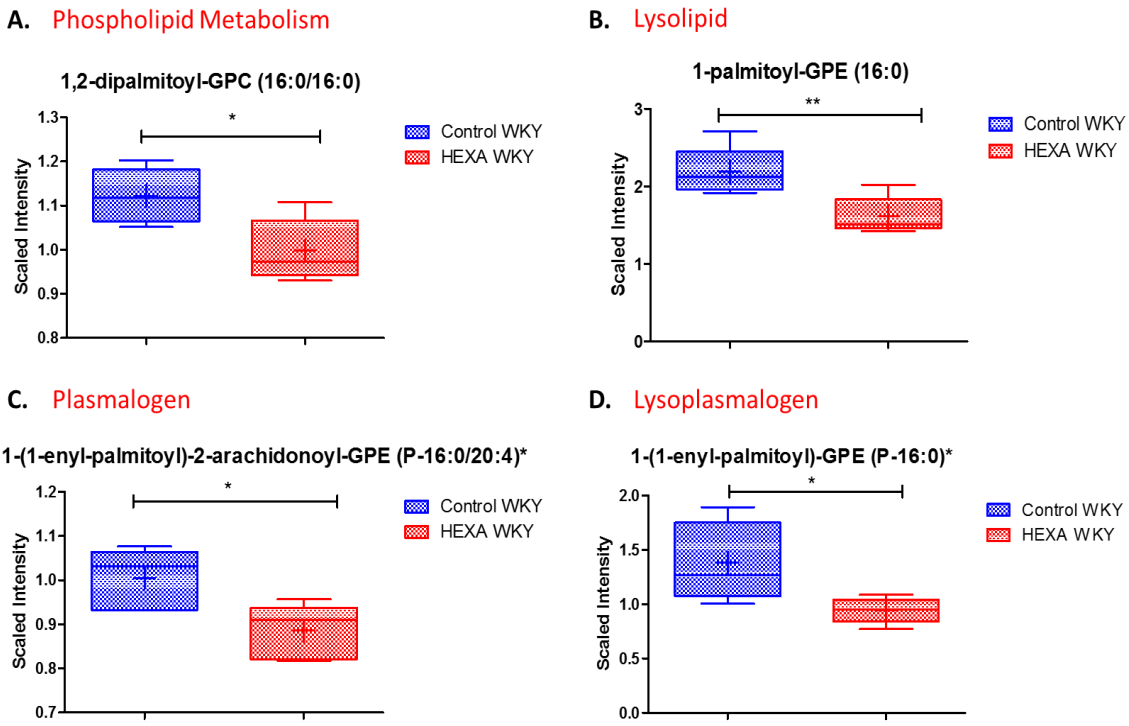

Figure 4-46: Fatty acids metabolism in aorta tissue of hexadecanedioic acid-treated WKY rats compared to control WKY rats.

Significant reductions were observed in the lipid metabolites of aorta tissues of hexadecanedioic acid-treated rats compared with control rats. (A) Phospholipids, (B) lysolipid, (C) plasmalogen and (D) lysoplasmalogen (P*<0.05).

4.6 Discussion

To understand the previously identified association between hexadecanedioate levels and elevation of blood pressure (Menni *et al.*, 2015), it is important to examine the metabolic pathways to identify hexadecanedioate-induced changes in production or consumption of important biochemicals such as fatty acids, amino acids and glucose. This chapter determined the impact of hexadecanedioate treatment in WKY rats by conducting a metabolomics profiling study. Most notably, there were disruptions in fatty acid metabolism through the ω-oxidation pathway, which is located within the smooth endoplasmic reticulum (ER), as well as ß oxidation in the mitochondria, and changes in glycolysis and glycogen metabolism, bile acid metabolism, the uric acid cycle, in addition to alteration in redox homeostasis.

4.6.1 Alterations in fatty acid metabolism

Analysis of the metabolomics dataset showed a significant increase in the DFA, hexadecanedioate, in all tested tissues except for the brain, where this metabolite was below the threshold of detection, as shown in Figure 4-19. This lack of detection in the brain may reflect poor diffusion through the blood-brain barrier. Also, the altered levels of DFAs, tetradecanedioate and octadecanedioate, in adipose tissues and decanedioate in the kidneys of hexadecanedioic acid-treated rats could suggest hexadecanedioate-induced changes in ß-oxidation and a shift towards the ω-oxidation pathway. The ω-oxidation pathway is a minor pathway for fatty acid oxidation, which is used when ß-oxidation is deficient. ω-oxidation is increased in conditions that are characterized by increased levels of mono-carboxylic free fatty acid (i.e. obesity, starvation, diabetes, or chronic alcohol consumption) as well as disturbances in ß-oxidation (Wanders *et al.*, 2011). ω-oxidation is considered to be a rescue pathway for many diseases, where an impairment occurs in mitochondrial fatty acid oxidation leading to an accumulation of fatty acids. ω-oxidation serves to break down accumulated fatty acids (Wanders *et al.*, 2011). In addition to significant increases in peroxisomal ω-oxidation metabolites, marked changes in mitochondrial fatty acid ß-oxidation metabolites were detected in tested tissues such as; phospholipids, lysolipid, sphingolipid, monoacylglycerol and acyl carnitine. Free fatty acids come from numerous biological molecules such as

triglycerides and phospholipids and are important sources of energy for mitochondrial oxidation and cellular ATP generation (Santos and Schulze, 2012). The ß-oxidation of long chain fatty acids is considered to be a main source of energy for organs, particularly heart and skeletal muscles. Conversely, other tissues, mainly liver, kidney, and adipose tissue use the products of ß-oxidation for the formation of ketone bodies in order to produce energy that can be utilized by other organs (Bartlett and Eaton, 2004). In our study, the levels of long-chain fatty acids significantly increased in kidney and liver tissues of hexadecanedioic acid-treated rats compared to control rats. A previous metabolomics study, which examine the effects of antihypertensive drugs on plasma metabolomic profiles of patients with essential hypertension, identified a reduction in plasma levels of long-chain fatty acids in bisoprolol-treated patients (Hiltunen *et al.*, 2017).

ß-oxidation pathways involve dehydrogenation catalysed by acyl-CoA dehydrogenase, followed by hydration catalysed by enoyl-CoA hydratase via addition of water to the double bond. Dehydrogenation takes place after that via ß-hydroxyacyl-CoA dehydrogenase to generate NADH. Acyl-CoA is formed and re-enters the ß-oxidation after being catalysed by ß-ketoacyl-CoA via thiolytic cleavage (Poirier *et al.*, 2006), as shown in Figure 4-47.

Elevation in acylcarnitine levels were also detected in heart and kidney tissues of hexadecanedioic acid-treated rats compared to control rats, which could suggest a subtle shift toward fatty acid biosynthesis and impairment of mitochondrial ß-oxidative function. It has been found that increased levels of acylcarnitine is associated with high risk of cardiovascular dieases (Rizza *et al.*, 2014). Adams *et al.*, (2009) showed that increase of fatty acylcarnitines is related to defects in the fatty acid ß-oxidation pathway. Fatty acids can enter the mitochondria by conjugating to carnitine, which forms a high-energy ester bond with long chain carboxylic acid through carnitine palmitoyl transferase 1 (CPT-1). Acylcarnitine is then produced and translocated transversely to the inner mitochondrial membrane via carnitine acylcarnitine translocase (CACT) and is cleaved by carnitine palmitoyl transferase 2 (CPT-2). Carnitine is then released in the mitochondrial matrix, whereas the fatty acid is conjugated back to coenzyme A and transferred to the ß-oxidation pathway with production of acetyl-CoA for oxidative phosphorylation (Longo *et al.*, 2006) (Figure 4-48). Alterations in acylcarnitine levels represents a defect in fatty acid oxidation, consequently

causing impairment in the utilization and production of glucose (Longo *et al.*, 2006; Longo, 2016). Hiltunen *et al.*(2017) provided evidence of an association between fatty acid metabolism and hypertension. The study identified a reduction in the plasma levels of acyl carnitine from hypertensive patients on antihypertensive medication (i.e. amlodipine, bisoprolol and losartan). In the same study amlodipine treatment also showed a significant reduction in the levels of circulating hexadecanedioate (Hiltunen *et al.*, 2017).

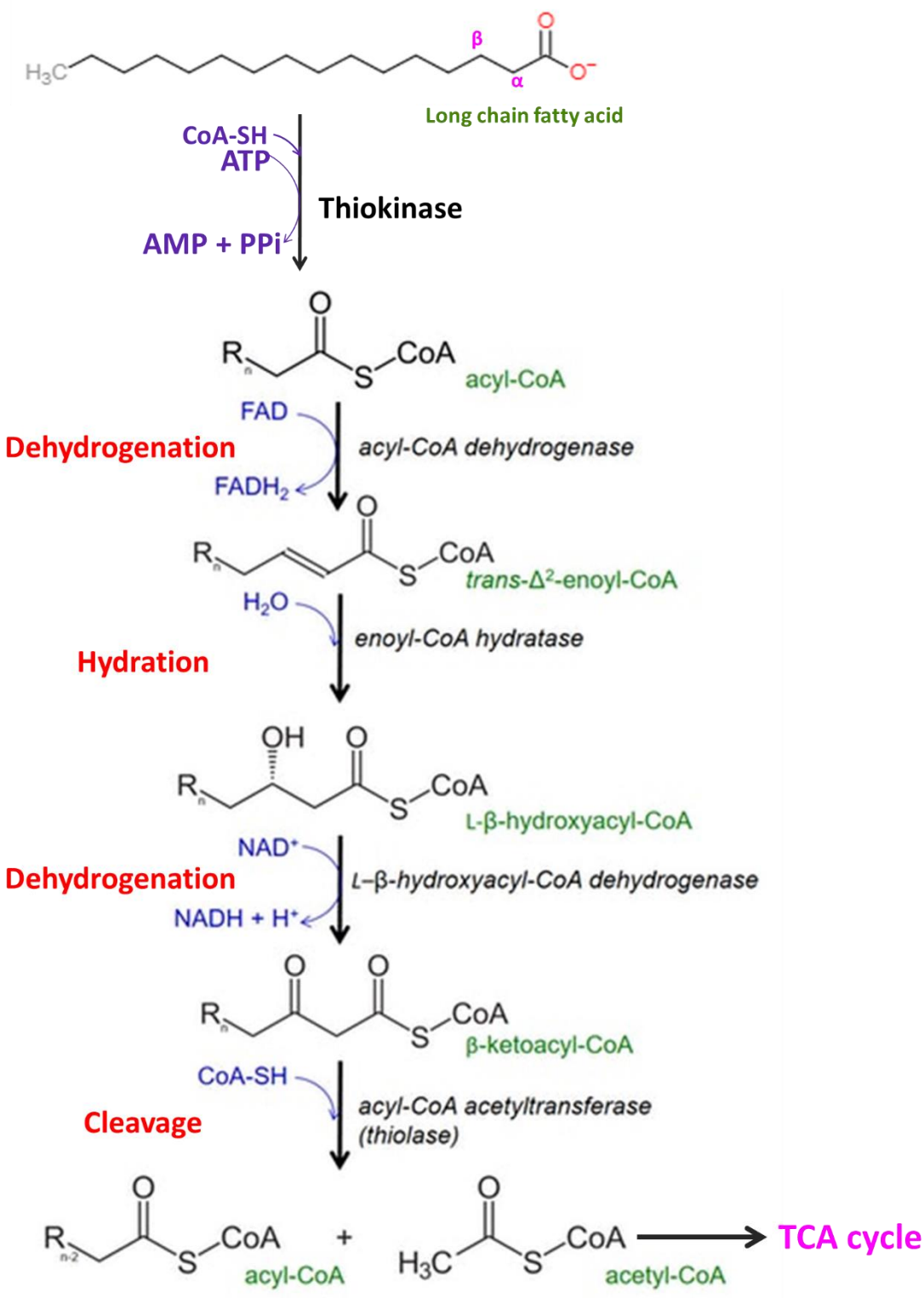

Figure 4-47: β-oxidation pathway.

β-oxidation pathways involve dehydrogenation and hydration to generate Acyl-CoA, which can then enter another β-fatty acid oxidation cycle or enter the citric acid cycle. Markedly changes in mitochondrial fatty acid β-oxidation metabolites were identified in tested tissues (e.g. heart, kidney, liver, adipose, aorta and brain) of hexadecanedioic acid-treated rats compared to control rats, which could suggest hexadecanedioate-induced changes in β-oxidation and a shift towards the ω-oxidation pathway.

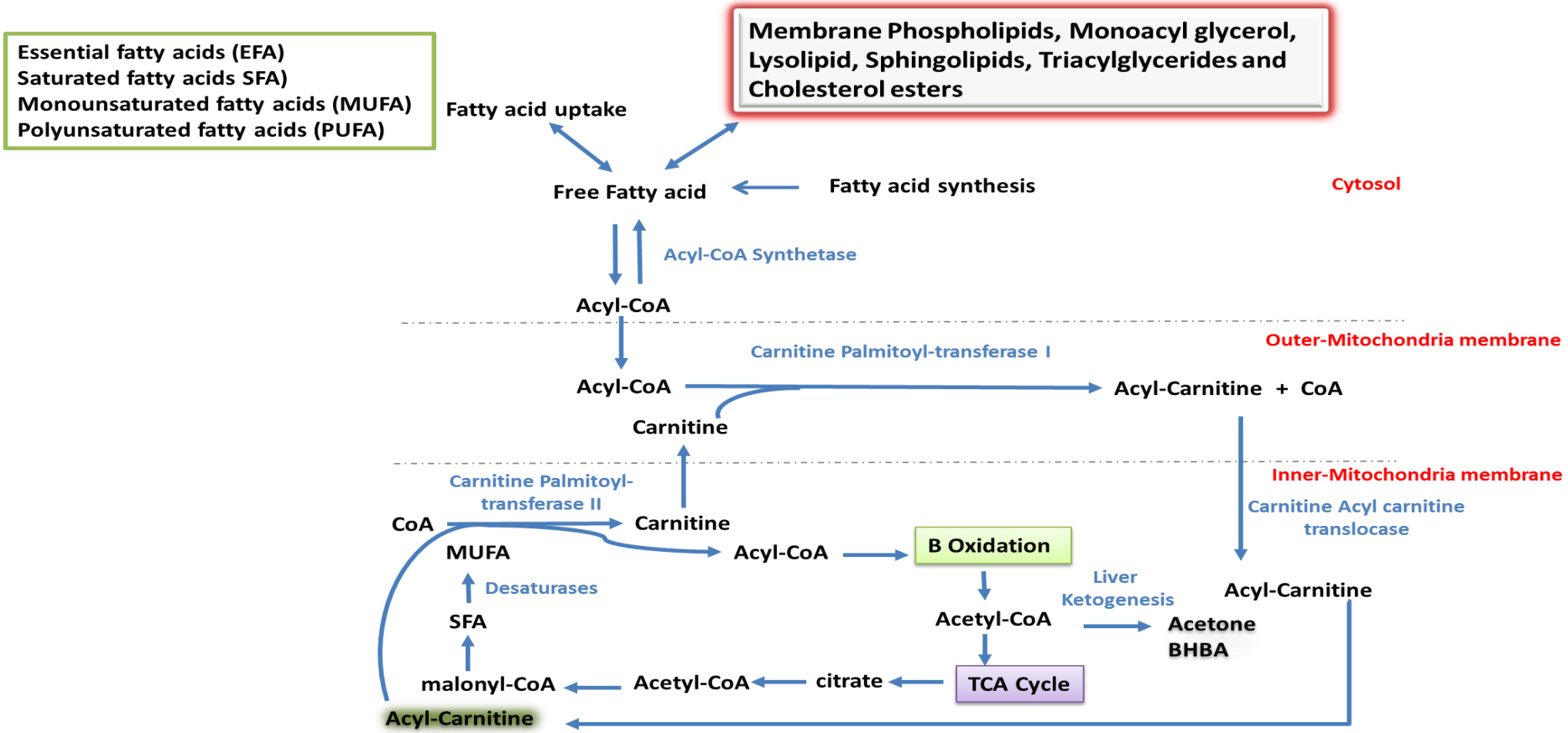

Figure 4-48: Lipid synthesis and metabolism.

Long-chain acyl-CoA esters are transported into mitochondria by a carnitine-dependent mechanism; these esters are then metabolised by β-oxidation within the mitochondria. Elevation in acylcarnitine levels was detected in heart and kidney tissues of hexadecanedioic acid-treated rats compared to control rats, which could suggest impairment of mitochondrial β-oxidative function.

4.6.2 Alterations in glucose utilization

Our metabolomics results have shown that there is an increase in glycolysis and glycogen metabolism, in particular increases in the levels of glucose and fructose, in the heart tissues of hexadecanedioate-treated rats compared to controls. In addition, an elevation was observed in levels of glucose-6-phosphate in the heart tissues of hexadecanedioate-treated rats compared to control, while it was decreased in kidney tissues. Glucose-6-phosphate is a key step in glycogenolysis and gluconeogenesis pathways for glucose production, anaerobic glycolysis, and storing glucose (Figure 4-49). Several studies have identified a direct association between an alteration in glycolysis, and glucose oxidation along with changes in fatty acid oxidation and pulmonary hypertension (Assad and Hemnes, 2015; Fessel *et al.*, 2012; Zhao *et al.*, 2014). Impairment in fatty acid oxidation has been found to be associated with high glucose utilization in the spontaneously hypertensive rat (SHR) to provide energy from fatty acid oxidation (Hajri *et al.*, 2001). Alterations in the glycolytic pathway are also reported to be associated with cardiac diseases, such as acute myocardial infarction (Carvajal and Moreno-Sánchez, 2003; Bolk *et al.*, 2001; Marsin *et al.*, 2000).

Glycolysis includes converting glucose into pyruvate, which is transformed into either acetyl CoA in the mitochondria, which enters the Krebs cycle (TCA cycle) or to lactate by fermentation (Feron, 2009; Jiang and Zhang, 2003; Zhao *et al.*, 2014). However, the glycolytic end-products pyruvate and lactate were not significantly changed in our samples, which could suggest increasing demand for use in the TCA cycle. Moreover, glucose-6 phosphate also convert to pentose phosphate by an oxidative, non-reversible pathway for generating ribose- 5-phsophate (R5P) for nucleotide synthesis (Wamelink *et al.*, 2008) (Figure 4-49). Our metabolomics results showed that a number of nucleotides were significantly increased in the heart tissues of hexadecanedioate-treated rats compared to controls, such as xanthine, adenosine 5'-diphosphate (ADP) and adenosine 3'-monophosphate (3'-AMP). Also, the significant reduction in the pentose-phosphate metabolism in adipose and kidney tissues of hexadecanedioate-treated rats compared to controls could suggest defects in the regulation of glucose and changes in glycolytic use. This outcome signposts that there is a strong shift in metabolism, as the adipose tissues of hexadecanedioate-treated rats are less dependent on glycolysis and more dependent on fatty acid oxidation. Increasing

ω-oxidation is characterised by increased end products due to insufficient glucose metabolism. Fatty acid oxidation and glucose oxidation both produce mitochondrial acetyl-CoA. Thus, the rate of glucose oxidation has a direct effect on the rate of fatty acid oxidation. More energy can be produced by stimulating fatty acid oxidation instead of glucose oxidation (Zhao *et al.*, 2014). In fact, fatty acid oxidation is considered to be more efficient mechanism for production of ATP and energy than glycolysis (Campbell *et al.*, 2002; Zhao *et al.*, 2014; Hajri *et al.*, 2001). Our metabolomics results identified increases in the levels of fatty acid metabolism in conjugation with altered glycolysis, which indicate alterations in the fatty acid oxidation pathway, which may be compensatory mechanisms to regulate elevations of blood pressure.

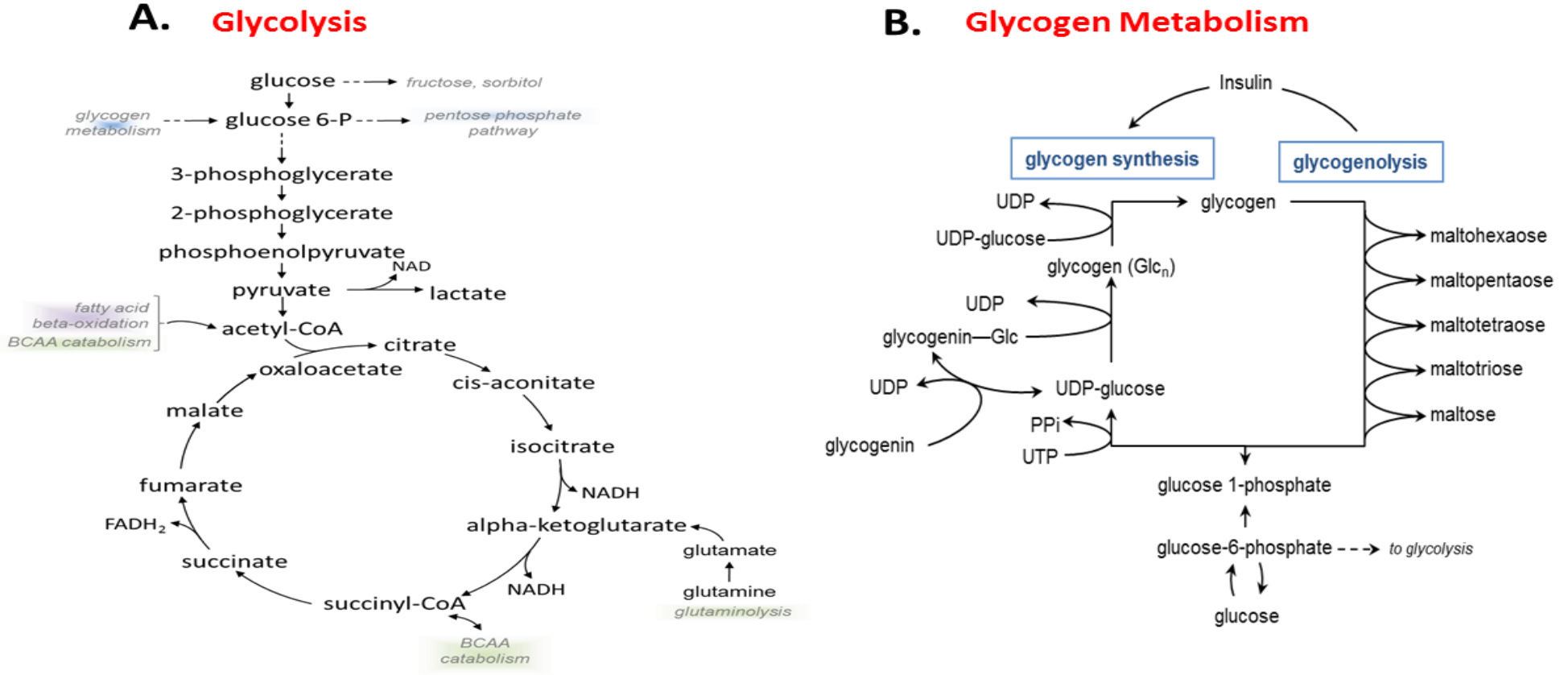

Figure 4-49: (A) Glycolysis metabolism and (B) glycogen metabolism.

In heart (Hexa vs control), elevations in glucose and glucose 6-phosphate levels, with a decrease in 3-phosphoglycerate are suggestive of changing glycolytic use. An increase in glycogen breakdown products (e.g. maltotetraose, maltotriose, and maltose) could suggest increased glucose demand. Increases in fructose could be consistent with increased glucose availability.

4.6.3 Alteration in bile acids

Our metabolomics results identified a significant elevation in taurine-conjugated primary bile acids in the adipose tissues of hexadecanedioic acid-treated rats compared with control rats. On the other hand, glycine-conjugated primary and unconjugated bile acids decreased in the kidney of hexadecanedioic acid-treated rats compared with control rats. In addition, several taurine-conjugated muricholic bile acids, as well as secondary bile acids, elevated in the kidney and adipose and liver tissues of hexadecanedioic acid-treated rats compared with control rats. Muricholic acid primary bile acids are formed only in the livers of rodents, and not formed in humans (Lefebvre *et al.*, 2009; Takahashi *et al.*, 2016) (Figure 4-52). The main primary bile acids produced in human livers are cholic acid and chenodeoxycholic acid, which are conjugated with taurine or glycine for secretion into bile (Chiang, 2013). In addition, both taurine and glycine conjugation are produced in rats, while taurine conjugated bile acids are mainly produced in mice (De Aguiar Vallim *et al.*, 2013). Primary bile acids are converted to secondary bile acids (i.e. deoxycholic (3 ,12 -dihydroxy-5-cholanoic acid)) and lithocholic (3 -hydroxy-5-cholanoic acid) acids in humans and ω-muricholic acid in rodents in the distal ileum by intestinal microbial flora (Ajouz *et al.*, 2014; Takahashi *et al.*, 2016; De Aguiar Vallim *et al.*, 2013) (Figure 4-50).

Bile acids have many essential functions, such as eliminating molecules resulting from cholesterol in the liver, facilitating solubilisation of cholesterol in the gallbladder, and the intestinal absorption of cholesterol, lipids, and lipophilic vitamins. Furthermore, bile acids have also a regulatory function in molecule signalling that regulate some metabolic pathways, including glucose, lipid and energy metabolism by activate several nuclear receptors (i.e. farnesoid x receptor (FXR), pregnane X receptor (PXR) and Vitamin D), and G protein-coupled receptors (GPCRs) (i.e. Takeda G-protein-coupled receptor 5 (TGR5), sphingosine-1-phosphate receptor 2 (S1PR2), and Muscarinic receptor) (Chiang, 2009, 2013; Hylemon *et al.*, 2009; Shapiro *et al.*, 2018; Zhou and Hylemon, 2014). Bile acids stimulate membrane G protein-coupled receptors (Gpbar-1, aka TGR5), which play a role in stimulating energy metabolism. TGR5 signalling activates cAMP, leading to stimulation of type 2 iodothyronine deiodinase (DIO2), which then converts thyroxine T4 to the biologically activate hormone T3. This results in increased levels of thyroid hormone and stimulation of mitochondrial oxygen consumption

and energy metabolism (Chiang, 2013, 2009; De Aguiar Vallim *et al.*, 2013) (Figure 4-51). Bile acids are also involved in the regulation of energy within certain tissues such as adipose tissues that are considered to be thermogenically competent (Fiorucci *et al.*, 2009).

Bile acids participate in the regulation of glucose, lipoprotein and lipid metabolism by activation of the $G\alpha_i$ GPCR, sphingosine-1-phosphate receptor 2 (S1PR2). Bile acids only activate S1P2 in hepatocytes. S1PR2 activates the insulin receptor/AKT pathway through activation of a tyrosine kinase, Src, and epidermal growth factor receptor (EGFR). The S1P2/AKT pathway regulates hepatic glucose and lipid metabolism via the inhibition of glycogen synthase kinase 3β (GSK3β), leading to stimulation of glycogen synthase, glycogenesis and decreasing serum glucose (Chiang, 2013; De Aguiar Vallim *et al.*, 2013) (Figure 4-52).

It is currently unclear what the physiological role of bile acids may be on blood pressure regulation. Feasibly, an important future direction of bile acid signalling research would be important to determine the association between bile acid signalling and blood pressure elevation.

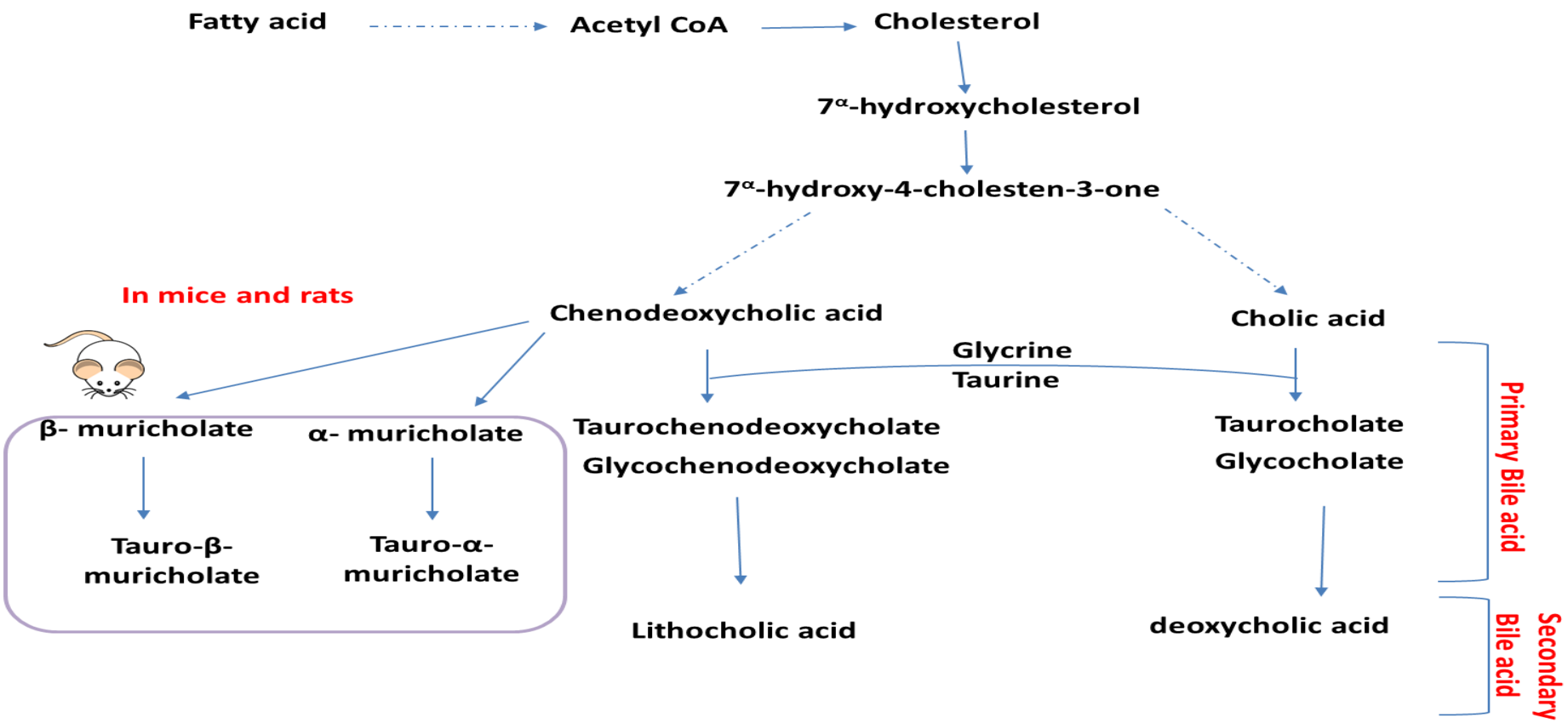

Figure 4-50: Primary and secondary bile acid metabolism pathways.

Bile acids are hydroxylated steroids, which produced in the liver from cholesterol. Primary bile acids are conjugated to the amino acids glycrine or taurine, which converted to secondary bile acids, deoxycholate and lithocholate by bacterial 7α-dehydroxylation. In rodents, chenodeoxycholic acid is converted to α- and β-muricholic acids. Several taurine-conjugated muricholic bile acids and secondary bile acids elevated in the kidney and adipose and liver tissues of hexadecanedioic acid-treated rats compared with control rats.

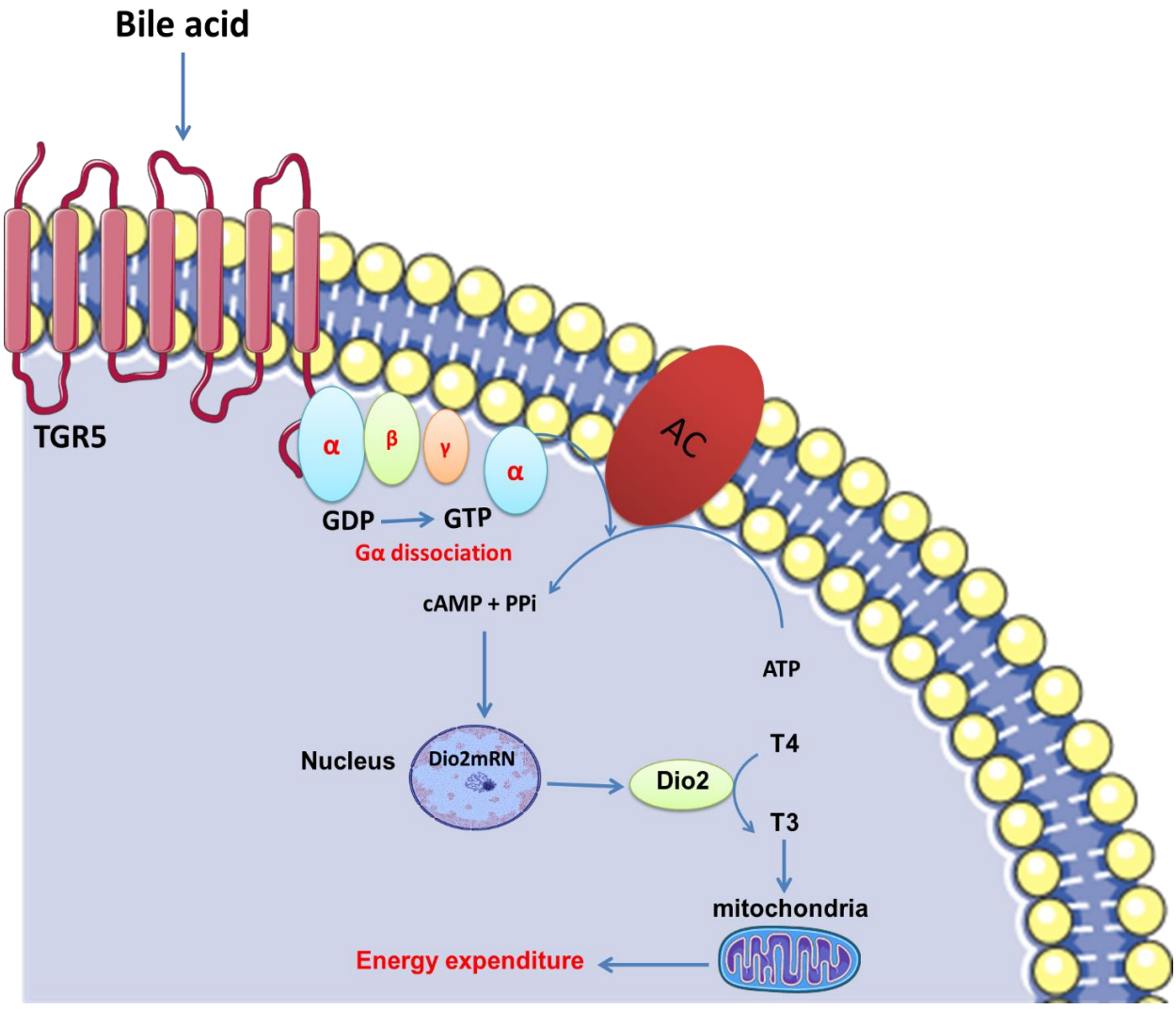

Figure 4-51: TGR5-signaling pathway leading to downstream signalling via cAMP stimulation.

Bile acids activate membrane G protein-coupled receptors (Gpbar-1, aka TGR5). TGR5 signalling activates cAMP, which leading to stimulation of type 2 iodothyronine deiodinase (DIO2), which then converts thyroxine T4 to the biologically activate hormone T3. This results in increased levels of thyroid hormone and stimulation of energy metabolism.

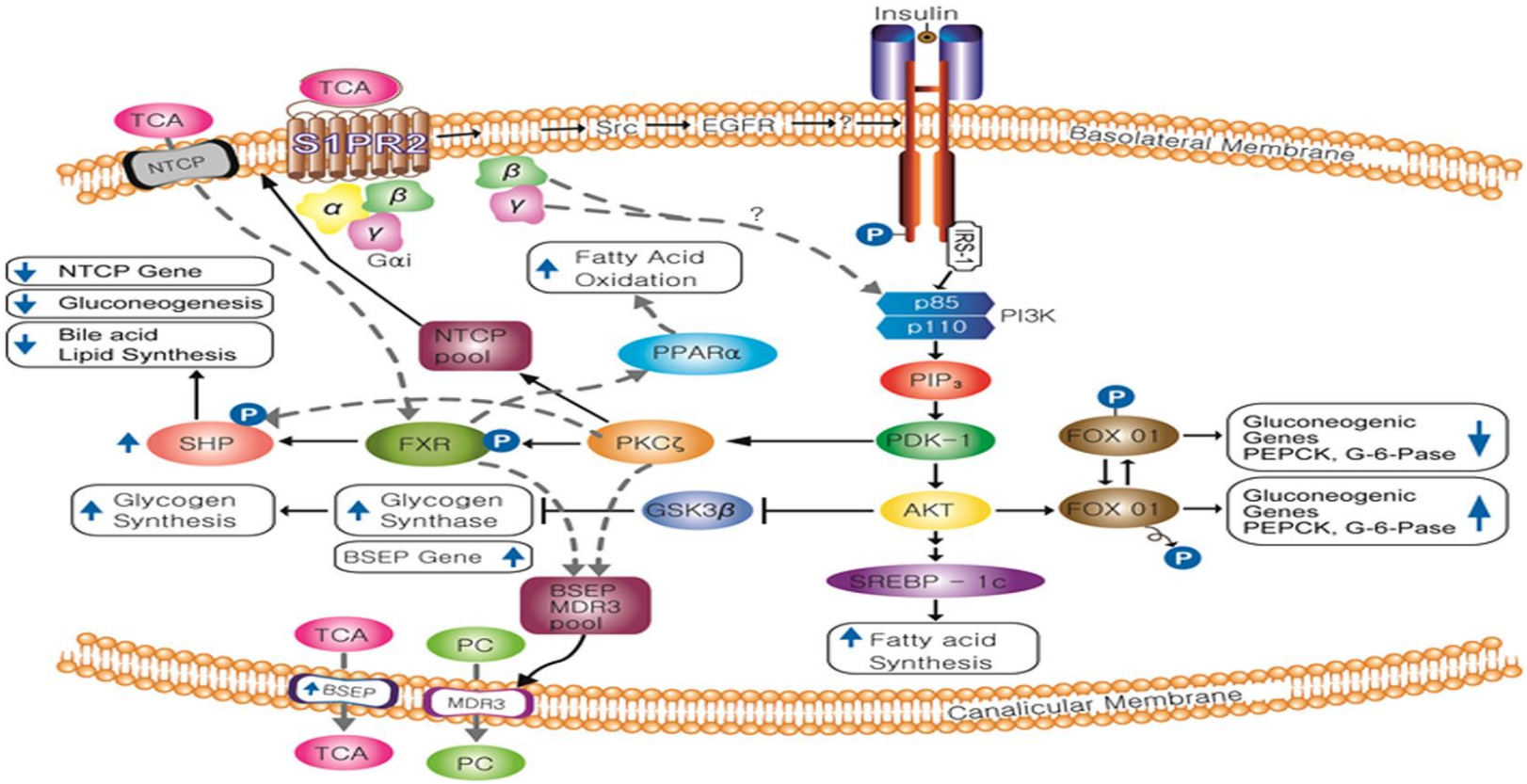

Figure 4-52: The role of bile acid in regulate hepatic downstream metabolism by activation of sphingosine 1-phosphate receptor 2 and the insulin signalling pathway (Zhou and Hylemon, 2014).

Bile acids are signaling molecules and metabolic regulators that activate nuclear receptors (FXR), sphingosine-1-phosphate receptor 2 and G protein-coupled receptor signaling to regulate hepatic lipid, glucose, and energy homeostasis and maintain metabolic homeostasis. Abbreviations: S1PR2, sphingosine 1-phosphate receptor 2; Src, Src Kinase; EGFR, epidermal growth factor receptor; PPARα, peroxisome proliferator-activated receptor alpha; NTCP, Na+/taurocholate cotransporting polypeptide; BSEP, bile salt export pump; PC, phosphotidylcholine; PECK, phosphoenolpyruvate carboxykinase; G6Pase, glucose-6-phosphatase; PDK1, phosphoinositide-dependent protein kinase 1; AKT, protein kinase B; SREBP, sterol regulatory element-binding protein; PKCf, protein kinase C zeta; FXR, farnesoid X receptor; SHP, small heterodimeric partner; GSK3b, glycogen synthase kinase 3 beta.

4.6.4 Alteration in Redox homeostasis

In this metabolomics study, increases in cysteine-glutathione disulphide with decreases in S-adenosylhomocysteine (SAH) and S-methylcysteine (i.e. a product of cysteine oxidation) were observed in the liver tissues of hexadecanedioic acid–treated rats. These metabolomic changes indicate alterations in cysteine availability, potentially reflecting use for the synthesis of glutathione, which was below the threshold of detection and could suggest an increasingly oxidizing environment.

Glutathione (GSH) is the main intracellular antioxidant, which helps to eliminate peroxides and other oxidants. Lower levels of glutathione and/or higher levels of its oxidized form (i.e. glutathione disulfide (GSSH)) are indicators of elevated intracellular oxidative stress (Ashfaq *et al.*, 2008). In addition, cysteine creates the main extracellular antioxidants that help to eliminate oxidants. Cysteine is more potent and reactive, so it is converted to its oxidized disulfide form. Released glutathione reacts with cysteine disulphide to generate glutathione-cycteine disulfide, the levels of which can be used to assess overall body oxidative stress (Ashfaq *et al.*, 2008). It has been found that cysteine has an antihypertensive function directly, or via its storage form (i.e. glutathione) through reduction of oxidative stress, increasing glucose metabolism and insulin resistance and controlling nitric oxide levels (Vasdev *et al.*, 2009).

Adequate levels of cysteine, glutamate and glycine are important to keep glutathione at appropriate levels. Therefore, many amino acids; such as glutamate, cysteine, and glycine are transported by gamma-glutamyl cycle into the cells (Vasdev *et al.*, 2009; Kageyama *et al.*, 2015). In our results, the reduction in gamma-glutamyl amino acids with decreased 5-oxoproline in the liver tissues of hexadecanedioic acid–treated rats compared to controls were detected, which may reflect decreased glutathione availability. Gamma-glutamyl peptide is catalysed to produce 5-oxoproline by gamma-glutamylcyclotransferase, which is one of the main enzymes in glutathione metabolism (Vasdev *et al.*, 2009; Kageyama *et al.*, 2015) (Figure 4-53). The association between the glutathione-related redox system, redox biology, and hypertension is not fully understood and further studies are required to identify the glutathione-related parameters that are altered in hypertension (Vasdev *et al.*, 2009).

In the brain tissues (hexadecanedioate vs control), decreases in anserine, a dipeptide metabolite of histidine with antioxidant function, could suggest increasing antioxidant use. Anserine has antioxidant functions, scavenging free radicals and metal chelation (Geissler *et al*., 2010). Also, anserine plays a major role in the regulation of matrix metalloproteinase protein which is responsible for cell proliferation, migration, differentiation, angiogenesis and apoptosis, in addition to its role in regulating glutathione levels (Geissler *et al*., 2010). These results indicate increased antioxidant activity in brain even though hexadecanedioate levels were not detected in brain tissues; may due to secondary mechanisms to prevent in disease progression.

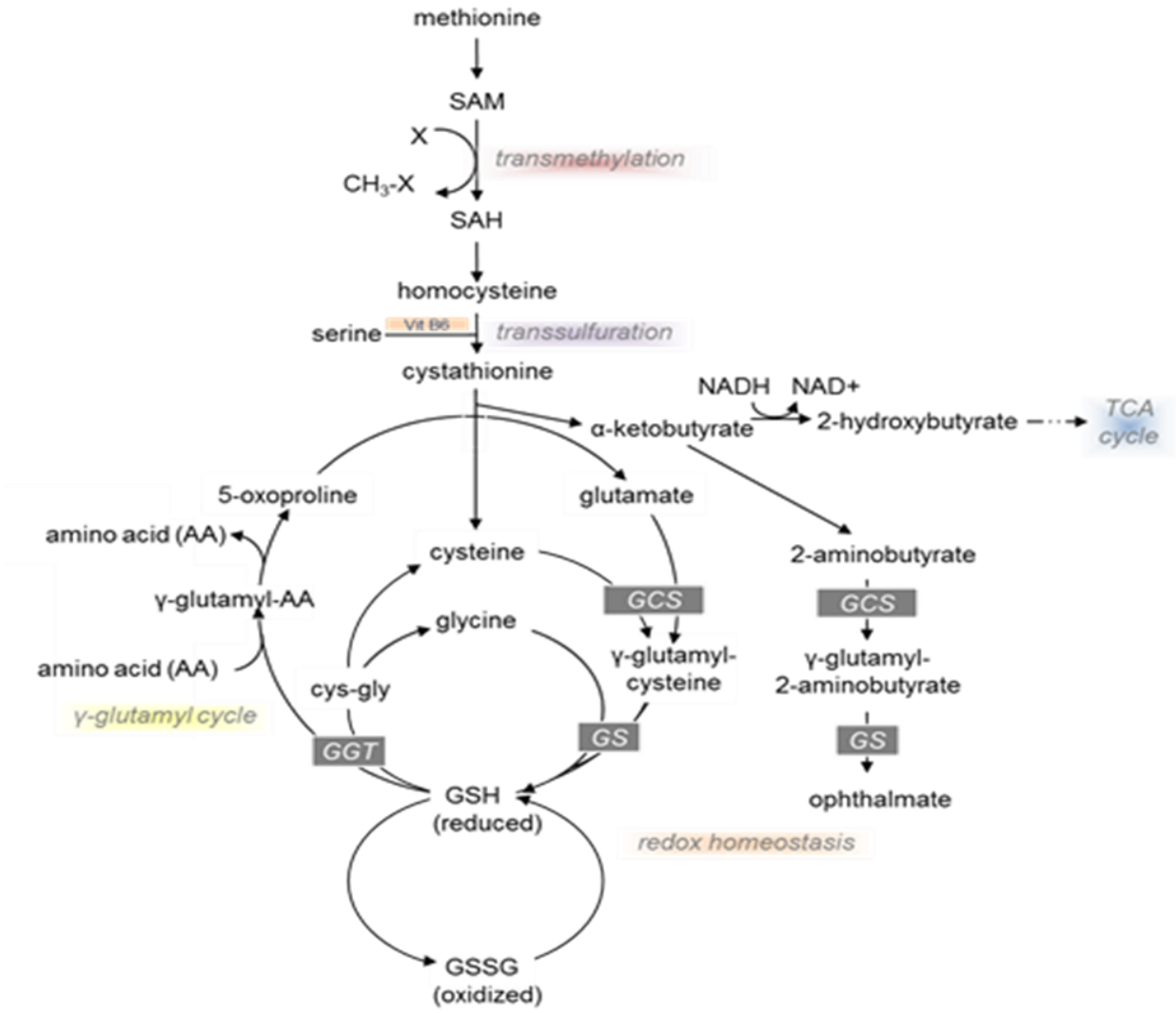

Figure 4-53: Glutathione synthesis pathway.

Glutathione is synthesised from glycine, glutamate and methionine-derived cysteine. Released glutathione reacts with cysteine disulphide to generate glutathione-cycteine disulphide. In liver tissues (Hexa vs control), an increase in cysteine-glutathione disulfide level, with a decrease in S-adenosylhomocysteine and S-methylcysteine levels could suggest an increasingly oxidizing environment. Also, a reduction in gamma-glutamyl amino acids and 5-oxoproline levels could reflect decreased glutathione availability. Abbreviations: (GGT), Gamma-glutamyltransferase; (GCS), gamma-glutamylcysteine synthetase; (GS), glutathione synthetase; (GSH), Glutathione; (GSSG), Glutathione disulphide.

4.6.5 Alteration in uric acid cycle

The metabolomics analysis also identified increases in arginine, N-delta-acetylornithine, creatine, proline, N-methylproline and guanidinoacetate in the kidney tissues of hexadecanedioic acid-treated rats. Arginine is converted by arginase to ornithine, an essential precursor of urea and polyamines in the urea cycle (Tapiero *et al.*, 2002). Arginine is also considered to be a precursor for creatine, which is important for energy metabolism. In addition, it has a role in the synthesis of nitric oxide and free radical molecules (Tapiero *et al.*, 2002). Arginine and its metabolites may be considered markers for the progression of cardiovascular diseases such as hypertension and atherosclerosis (Popolo *et al.*, 2014). The kidney is a main site for generation of endogenous arginine (Popolo *et al.*, 2014). In renal failure, the levels of arginine and nitric oxide are reduced. Any defect in arginine levels leads to a decrease in nitric oxide availability and a reduction in vascular relaxation, which results in hypertension and cardiovascular diseases (Gokce, 2004).

In conclusion, we have shown that exogenous administration of hexadecanedioic acid, in addition to increasing blood pressure, impacts a number of metabolic readouts; including changes related to lipid and glucose metabolism and redox homeostasis. Therefore, downstream effects of hexadecanedioate administration are multifactorial, however from the data it is not possible to determine whether the metabolic changes are due to a direct effect of hexadecanedioate on the various tissues/ organs or are a secondary effect of the elevated blood pressure.

Chapter 5 Haemodynamic changes after modulating circulating hexadecanedioate levels by perturbing the endogenous ω-oxidation pathway

5.1 Introduction

One of the major metabolic pathways impacted by hexadecanedioate administration is the ω-oxidation pathway (as identified in the previous chapter). Assessing the haemodynamic components of blood pressure regulation can give an insight into mechanisms that cause elevation in blood pressure (Ventura *et al.*, 2005). In this chapter, haemodynamic parameters are assessed to understand the mechanism by which hexadecanedioate-induced blood pressure elevation perturbs the endogenous ω-oxidation pathway. The ω-oxidation pathway consists of three steps involving three major enzymes. In the first step, the hydroxyl group is introduced onto the omega carbon by the CYP4A enzyme, followed by the oxidation of the hydroxyl group to an aldehyde by alcohol dehydrogenase to generate an oxo-fatty acid. In the last step, the oxidation of the aldehyde group to a carboxylic acid by aldehyde dehydrogenase produces a dicarboxylic fatty acid (Figure 4-24) (Sanders *et al.*, 2008b; Menni *et al.*, 2017; Kroetz *et al.*, 1998). Hexadecanedioic acid is a long chain dicarboxylic acid which is generated during fatty acid ω-oxidation which is then metabolised by ß-oxidation in peroxisomes (Reddy and Rao, 2006). As previously mentioned, ω-oxidation is a minor metabolic pathway that occurs in the smooth endoplasmic reticulum and also contributes to 5-10% of total fatty acid metabolism in the liver (Wanders *et al.*, 2011). In a previous association study, hexadecanedioate levels were found to be significantly correlated with gene expression of CYP4 and alcohol dehydrogenase in adipose tissues tested in 740 females from the TwinsUK cohort.(Menni *et al.*, 2017; Moayyeri *et al.*, 2013). This suggested that genetic variation may alter expression or activity of enzymes within the ω-oxidation pathway leading to altered levels of hexadecanedioate in hypertensive individuals

In this chapter the activity of several different enzymes of the ω-oxidation pathway were individually modified by utilisation of specific agonist or antagonist together with characterization of hemodynamic parameters in the hypertensive SHRSP model and WKY rat strains.

5.2 Hypothesis

Perturbing the endogenous ω-oxidation pathway via administration of specific enzyme inhibitors/activators will alter hexadecanedioate levels and lead to altered blood pressure.

5.3 Aims

The aims of this chapter were:

1. To investigate the expression of the genes encoding the main enzymes of the ω-oxidation pathway in heart, aorta, kidney, adipose and liver tissues obtained from normotensive WKY_{Gla} and hypertensive $SHRSP_{Gla}$ rats.

2. To assess haemodynamic changes after modulation of endogenous hexadecanedioate levels by perturbing the first step of the ω-oxidation pathway (i.e. CYP4A) by utilising the specific agonist (Fenofibrate) in a normotensive rat (WKY_{Gla}) and the specific antagonist (HET0016) in a hypertensive rat model ($SHRSP_{Gla}$).

3. To assess haemodynamic changes after modulation of endogenous hexadecanedioate levels by perturbing the last step of the ω-oxidation pathway (i.e. aldehyde dehydrogenase enzyme (ALDH)) by utilising a specific antagonist (disulfiram) in a hypertensive rat model ($SHRSP_{Gla}$).

4. To investigate levels of protein expression of ALDH in liver tissue obtained from five-week-old, 16-week-old and 20-week-old male WKY_{Gla} and $SHRSP_{Gla}$ rats.

5.4 Methods

This study was conducted to determine differences in expression of ω-oxidation genes between two different rat strains, WKY_{Gla} and $SHRSP_{Gla}$. In addition to identifying whether antagonism or stimulation of enzymes within the ω-oxidation pathway lead to effective inhibition/stimulation of circulating hexadecandioate levels and blood pressure lowering in $SHRSP_{Gla}$ or enhancing blood pressure in WKY_{Gla}. An overview of the study design is illustrated in Figure 5-1.

5.4.1 Animals

Adult male Wistar Kyoto (WKY_{Gla}) and the spontaneously hypertensive stroke prone rats ($SHRSP_{Gla}$) were obtained from breeding colonies maintained at the University Glasgow. The rats were housed in cages on a 12 hours light/dark circle at room temperature (21± 3°C). Food and water *ad libidum* were provided to the rats. The study protocols were approved by the home office and conducted in with complied the Animals' Scientific Procedures Act1986 under the project license of Dr Delyth Graham (70/9021).

5.4.2 Expression of main genes in ω oxidation pathways

5.4.2.1 Experimental animals

Gene expression study was carried out in tissues from adult male WKY_{Gla} (n=9) and $SHRSP_{Gla}$ rats (n=4) aged 16-week old, which had been used as untreated controls in previous intervention studies.

5.4.2.2 Samples

Liver, heart, kidney, aorta and adipose tissues were harvested and snap-frozen in liquid nitrogen and stored at -80°C for RNA extraction and gene expression, as described in section 2.4.1. Gene expression was carried out using the following probes from Thermo Fisher, Paisley, UK: CYP4A (Rn00598510_m1), ADH1C (Rn01522111_g1), ALDH1L2 (Rn01503718_m1) and ALDH6A1 (Rn00579182_m1).

5.4.3 Experimental protocol for first step of ω-oxidation pathway (CYP4A)

Twelve-week-old male WKY_{Gla} rats were treated orally with fenofibrate (Sigma Aldrich Co Ltd, Irvine, UK) mixed with baby food (egg custard with rice, Heinz Co.Ltd., Hayes, Middx.) (100 mg/kg per day; n=6) or vehicle (n=6) for 14 days (Figure 5-2). Male $SHRSP_{Gla}$ rats were treated with daily subcutaneous injection with HET0016 (Cambridge Bioscience, Cambridge, UK) dissolved in sulfobutyl ether ß-cycloodextrin (Sigma Aldrich Co Ltd, Irvine, UK) (4 mg/kg/day; n=3) or vehicle (n=2) for 14 days (Figure 5-3). Haemodynamic parameters were measured by radiotelemetry and kidney functions were assessed by 24 hrs metabolic cage collections. At sacrifice, blood samples were collected by cardiac puncture (Chapter 2, section 2.3.1). Main organs (i.e. heart, liver, kidney and vascular tissue) were snap frozen for molecular assessment and mesenteric arteries were taken to assess vascular function and morphology by wire myography.

5.4.3.1 Radiotelemetry

Telemetry probes (TA11PAC40, Dataquest IV Data Sciences International) were implanted at 10 weeks of age with 1 week of recovery before administration of the drugs and haemodynamic parameters (i.e. blood pressure, heart rate and locomotor activity) were monitored. More details are outlined in Section 2.2.2.2.

5.4.4 Experimental protocol for last step of ω-oxidation pathway (ALDH)

Twelve-week-old male $SHRSP_{Gla}$ rats were treated daily with disulfiram (Sigma Aldrich Co Ltd, Irvine, UK) diluted in 100 µl of 100% w/v dimethyl sulfoxide (DMSO, Sigma Aldrich Co Ltd, Irvine, UK) or vehicle (n=10) via intraperitoneal injection (25 mg/kg/day, n=10) for 14 days. Blood pressure was measured by tail cuff plethysmography and cardiac functions were assessed by echocardiography. The main organs (i.e. heart, liver, kidney and vascular tissue) samples were snap frozen for mRNA expression analysis and mesenteric arteries were d to assess vascular function by wire myography. (Figure 5-4).

5.4.4.1 Tail Cuff Plethysmography

Blood pressure was measured by tail cuff weekly for $SHRSP_{Gla}$ rats starting from the age of 10 weeks. More details are outlined in Section 2.2.2.1.

5.4.4.2 Echocardiography

Echocardiography was performed at baseline and weekly over two weeks of disulfiram administration for $SHRSP_{Gla}$ rats. Further details are mentioned in general methods Chapter 2, Section 2.2.3.

5.4.5 Renal Function

Renal function was assessed in WKY_{Gla} and $SHRSP_{Gla}$ rats at the baseline and at the end of the two-week study by means of metabolic cage measurements. The rats were placed in metabolic cages for 24-hour measurement of fluid intake and urine output, and for urine collection. Urine was kept on ice and stored at -80°C until required for further biochemical analysis. See Section 2.2.4 for more details.

5.4.6 Ex-vivo analysis

At the end of the two weeks study, all rats were sacrificed and organ/tissue samples were removed and cleaned of any connective tissue (for more details see Section 2.3.1). Body and tissue weight and tibia length were recorded. Organ weights were normalised to tibia length and body weight (see Section 2.3.2 for further information). Ex-vivo investigations included wire myography (Section 2.3.3) and mRNA expression (Section 2.4).

5.4.7 Measurement of hexadecandioate levels in plasma samples

Measurement of hexadecanedioate level in plasma samples of WKY_{Gla} and $SHRSP_{Gla}$ rats were carried out by Dr Christian Reichel and Dr Anja Huber (Seibersdorf laboratories, Austria) using liquid chromatography–mass spectrometry (LC-MS/MS). More details are given in Chapter 2, Section 2.5.

5.4.8 Measurement of Aldehyde dehydrogenase (ALDH) levels in liver samples

5.4.8.1 Experimental animals

Measurement of ALDH enzyme levels was carried out in liver tissues from untreated control male WKY_{Gla} (n=4/group) and $SHRSP_{Gla}$ (n=4/group) rats aged 5-week-old, 16-week-old and 20-week-old. These rats had been used as untreated controls in previous intervention studies.

5.4.8.2 Samples

Liver tissues were harvested into liquid nitrogen and stored at -80°C for ELISA assay to determine the level of aldehyde dehydrogenase.

5.4.8.3 Enzyme-linked immunosorbent assay (ELISA)

Aldehyde dehydrogenase (ALDH) levels were measured by using enzyme linked immunosorbent assay (ELISA), using a commercially available rat aldehyde dehydrogenase ELISA kit (MyBioSource, San Diego, USA), following the manufacturer's instructions. The ALDH kit is based on ALDH antibody-ALDH antigen interactions (immunosorbency) and a Horseradish peroxidase (HRP) colorimetric detection system to detect ALDH antigen targets in samples. The liver tissues were weighed before homogenisation. Tissues were minced into small pieces and homogenised in a specified amount of PBS (usually 10 mg of tissue in 100 µl of PBS). Homogenates were then centrifuged for 15 minutes at 1500 xg. The supernatants were then collected and stored at -80 ºC. On the day of the experiment, all the reagents and samples were left at room temperature for 30 minutes before starting. Standards (50 µl) and samples (50 µl) were added in duplicate to 96-well flat bottom plates. HRP (100 µl) were then added to each well. The plate was covered and incubated for 60 minutes at 37ºC. The microtiter plate was then washed four times using Wellwash™ Microplate Washer (Thermo Scientific, Loughborough, UK). Chromogen solution A (50 µl) and chromogen solution B (50 µl) were added respectively to each well and the plates were covered from the light and incubated for 15 minutes at 37 ºC. After that, a stop solution (50 µl) was added to each well and the colour in the wells changed from blue to yellow. Absorbance readings were measured at 450 nm using SpectraMax 190 Microplate Reader (Molecular Devices, USA).

5.4.9 Statistical analysis

Telemetry data and echocardiography were analysed using a repeated measures ANOVA (general linear model). The mRNA analysis is described in more detail in Section 2.4.1.6 and 2.4.1.7. For the metabolic cage results, paired t-tests were used. Two sample t-tests were used in analysis the data, as appropriate. Statistical significance was assumed at P-value less than 0.05. All data are displayed as a mean with standard error of the mean.

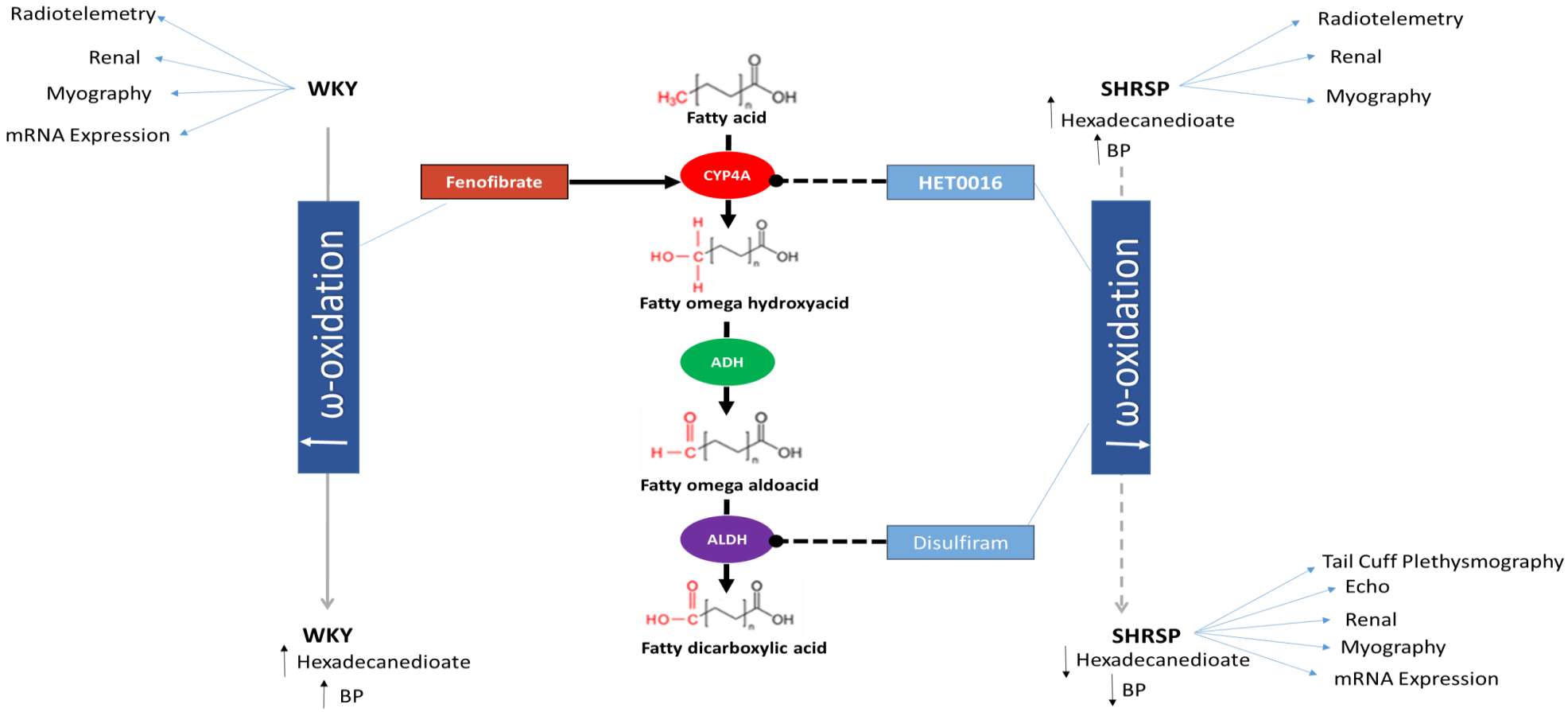

Figure 5-1: Experimental strategy to perturb the endogenous ω-oxidation pathway utilising specific inhibitors and agonists of ω-oxidation pathway enzymes.

Experimental strategy to assessing whether Inhibition/stimulation of a single or multiple enzymes in the ω-oxidation leads to effective inhibition/stimulation of circulating hexadecanedioate and blood pressure lowering in $SHRSP_{Gla}$ or enhancing blood pressure in WKY_{Gla}.

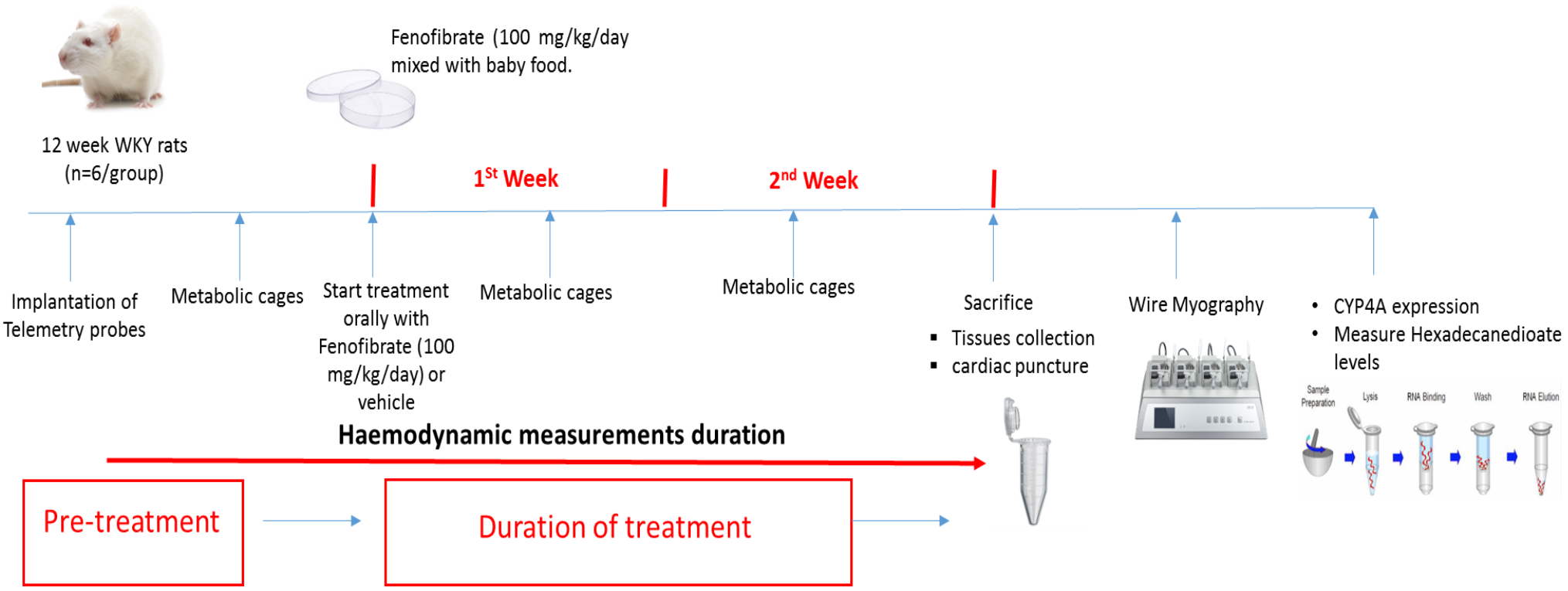

Figure 5-2: Timeline of fenofibrate (CYP4A agonist) study.

Twelve-week-old male WKY_{Gla} rats were treated orally with fenofibrate (100 mg/kg per day; n=6) or vehicle (n=6) for 14 days. Haemodynamic parameters were measured by radiotelemetry and kidney functions were assessed by 24 hrs metabolic cage collections. At sacrifice, blood samples were collected by cardiac puncture and main organs were harvested for molecular assessment. Mesenteric arteries were dissected to assess vascular function by wire myography.

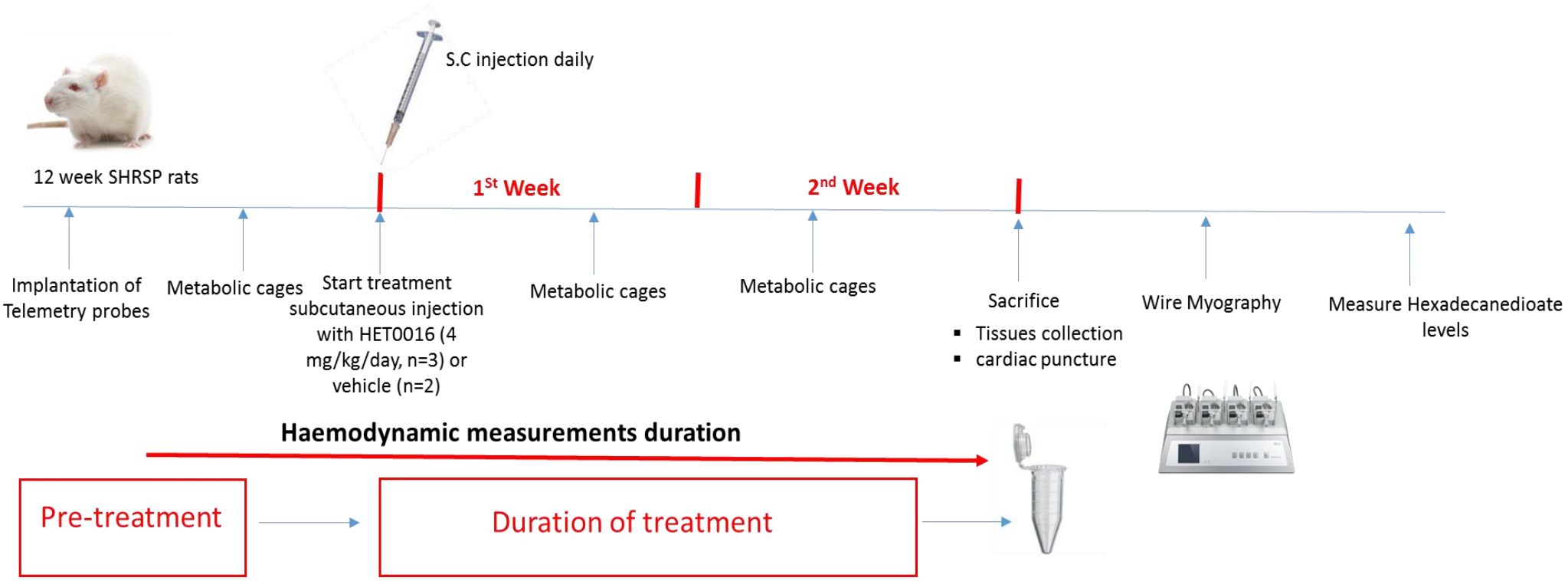

Figure 5-3: Timeline of HET0016 (CYP4A antagonist) study.

Twelve-week-old male $SHRSP_{Gla}$ rats were treated with daily subcutaneous injection with HET0016 (4 mg/kg/day, n=3) or vehicle (n=2) for 14 days. Haemodynamic parameters were measured by radiotelemetry and kidney functions were assessed by 24 hrs metabolic cage collections. At sacrifice, blood samples were collected by cardiac puncture and mesenteric arteries were dissected to assess vascular function by wire myography.

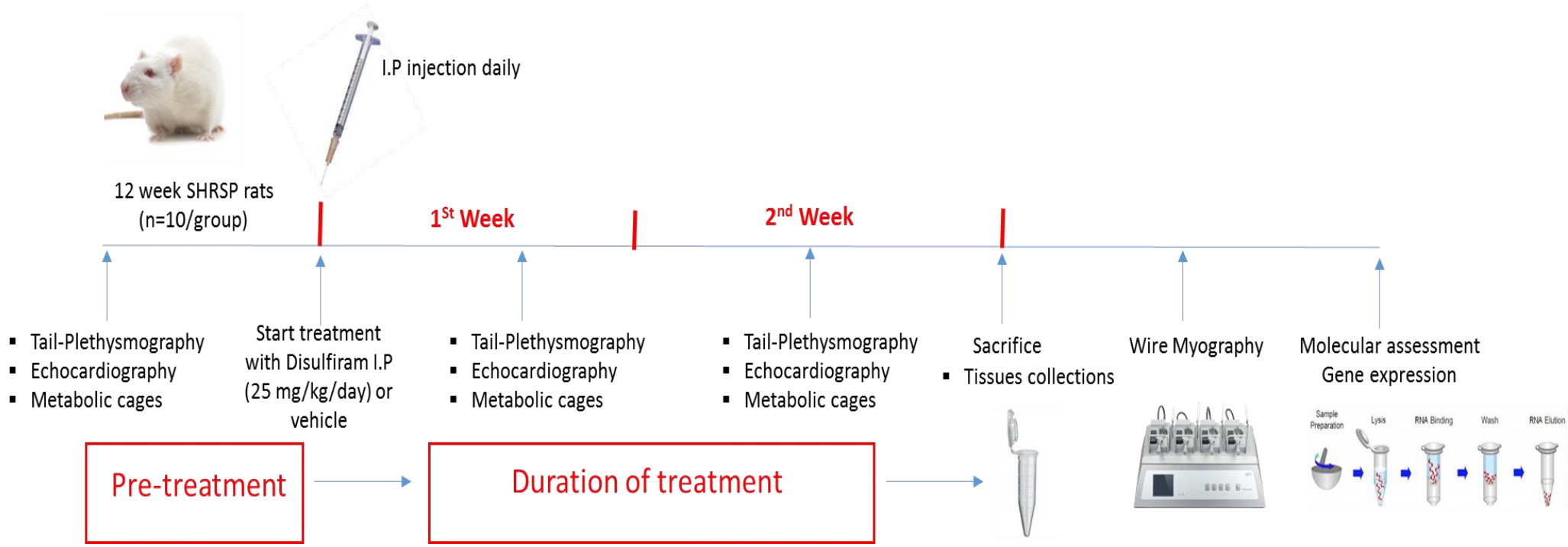

Figure 5-4: Timeline of disulfiram (aldehydehydrogenase antagonist) study.

Twelve-week-old male SHRSP$_{Gla}$ rats were treated with daily intraperitoneal injection with disulfiram (25 mg/kg/day, n=10) or or vehicle (n=10) for 14 days. Blood pressure was measured by tail cuff plethysmography and cardiac functions were assessed by echocardiography. The main organs were snap frozen for mRNA expression analysis and mesenteric arteries were dissected to assess vascular function by wire myography.

5.5 Results

5.5.1 Expression of major genes in ω oxidation pathways

In the heart, the expression of ALDH1L2 in $SHRSP_{Gla}$ increased compared to WKY_{Gla}, although this did not reach significance (P=0.12), however the level of ALDH1L2 expression for both strains was low (Table 5-1). There was no difference in ALDH6A1 expression in heart tissue between $SHRSP_{Gla}$ and WKY_{Gla} (P=0.25). In the heart, the levels of CYP4A and ADH1C were below the threshold of detection (Figure 5-5).

In the kidney, no significant differences were found in the expression of CYP4A (P=0.25) and ADH1C (P=0.53) in $SHRSP_{Gla}$ compared to WKY_{Gla} rats. In addition, there were no differences in expression of ALDH1L2 (P=0.10) and ALDH6A1 (P=0.24) between $SHRSP_{Gla}$ and WKY_{Gla} rats (Figure 5-6).

In liver, an increase in expression of CYP4A1 in $SHRSP_{Gla}$ rats compated to WKY_{Gla} rats, although this did not reach significance (P=0.146). The expression of ADH1C in $SHRSP_{Gla}$ decreased compared to WKY_{Gla}, although this did not reach significance (P=0.47). Interestingly, there was a significant reduction in expression of ALDH1L2 ($P=2X\ 10^{-3}$) in the liver tissues of $SHRSP_{Gla}$ rats compared to WKY_{Gla}, although no differences were observed in ALDH6A1 expression in the liver tissues from the strains (Figure 5-7).

In adipose tissue, CYP4A expression was below the threshold of detection. Also, no differences in expression of ADH1C (P=0.73) or in expression of ADH6A1 (P=0.77) were found between $SHRSP_{Gla}$ and WKY_{Gla}. In addition, there was no significant difference in expression of ALDH1L2 in adipose tissues of $SHRSP_{Gla}$ and WKY_{Gla} rats (P=0.33) (Figure 5-8) (Table 5-1). The expression of the ω-oxidation genes was below the threshold of detection in aorta tissues. Cycle threshold values are listed in Table 5-1.

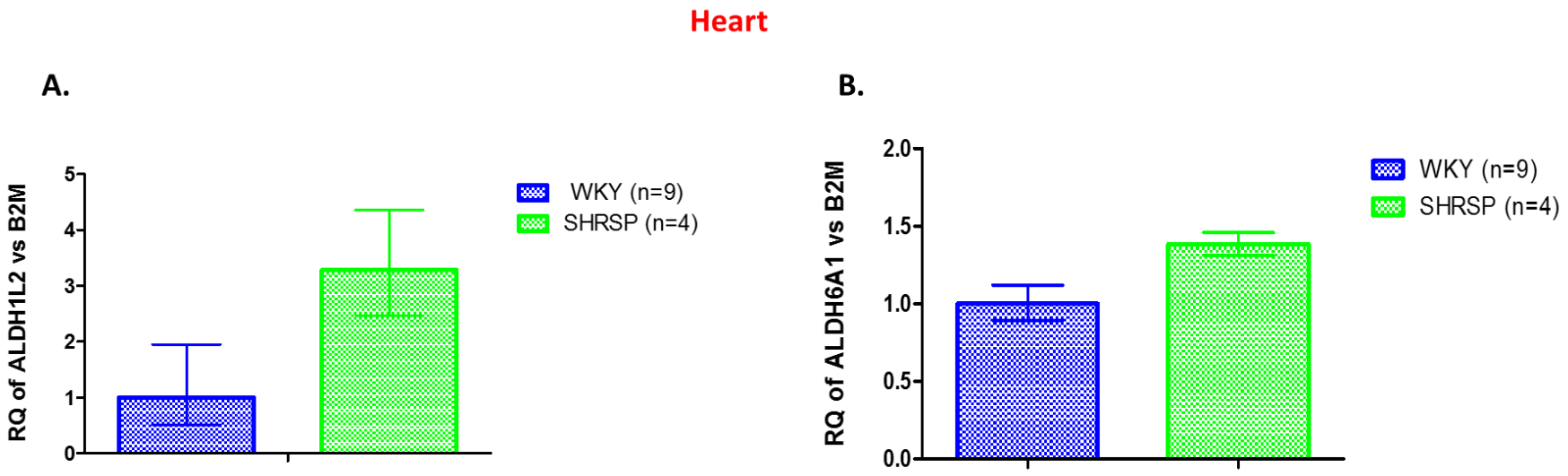

Figure 5-5: Expression of ALDH1L2 and ALDH6A1 in heart tissues of WKY_{Gla} and $SHRSP_{Gla}$ rats.

(A) An increase in expression of ALDH1L2 in heart tissue normalized to B2M of $SHRSP_{Gla}$ (n=4) compared to WKY_{Gla} (n=9) (B) No difference in the expression of ALDH6A1 normalized to B2M between WKY_{Gla} and $SHRSP_{Gla}$ rats. (Each point represents Mean ± Standard error of mean).

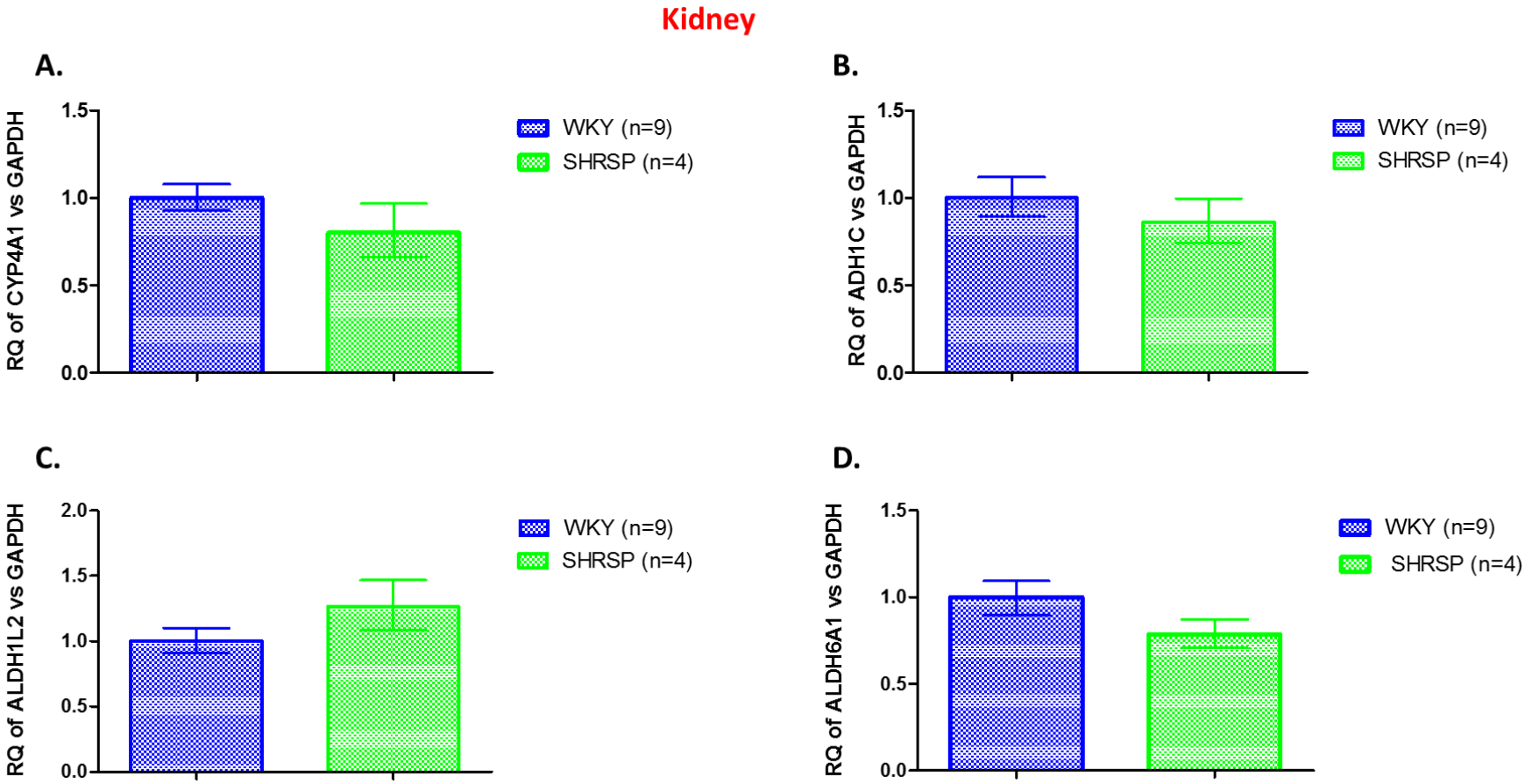

Figure 5-6: The expression of CYP4A1, ADH1C, ALDH1L2 and ALDH6A1 in kidney tissues of WKY_{Gla} and $SHRSP_{Gla}$ rats.

In Kidney, no difference in the expression of (A) CYP4A1, (B) ADH1C, (C) ALDH1L2 and (D) ALDH6A1 normalized to GAPDH between WKY_{Gla} (n=9) and $SHRSP_{Gla}$ (n=4) rats. (Each point represents Mean ± Standard error of mean).

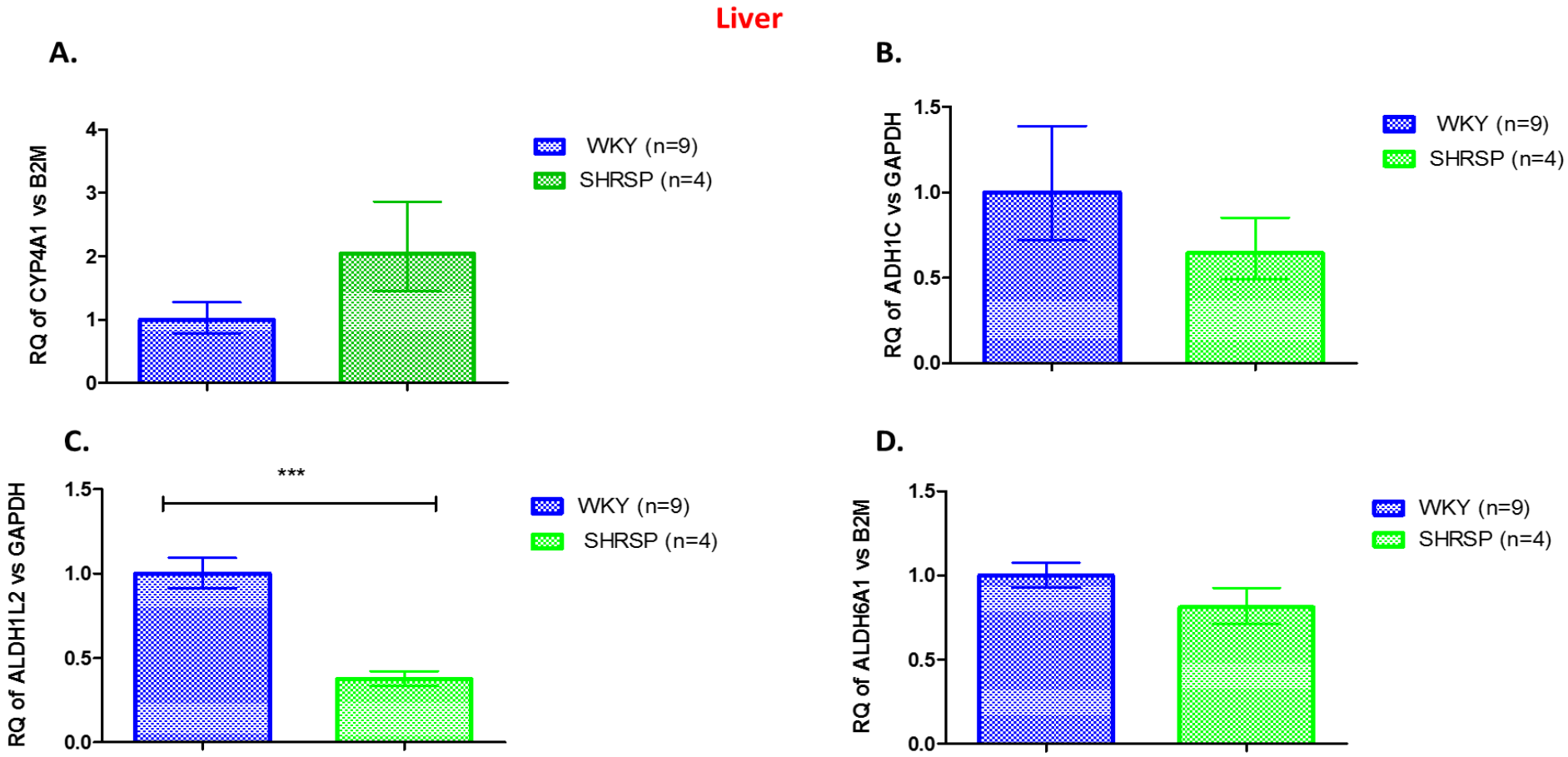

Figure 5-7: The expression of CYP4A1, ADH1C, ALDH1L2 and ALDH6A1 in liver tissues of WKY_{Gla} and $SHRSP_{Gla}$ rats.

An increase in expression of (A) CYP4A1 normalised to B2M in $SHRSP_{Gla}$ rats (n=4) compated to WKY_{Gla} (n=9) rats. (B) A decrease in expression of ADH1C normalised to GAPDH in $SHRSP_{Gla}$ rats compated to WKY_{Gla} rats. (C) The expression of ALDH1L2 normalised to GAPDH showed a significant reduction in $SHRSP_{Gla}$ rats compated to WKY_{Gla} rats. However, no change were observed in the expression of (D) ALDH6A1 normalized to B2M between WKY_{Gla} and $SHRSP_{Gla}$ rats. (Each point represents Mean ± Standard error of mean) (P***< 0.001).

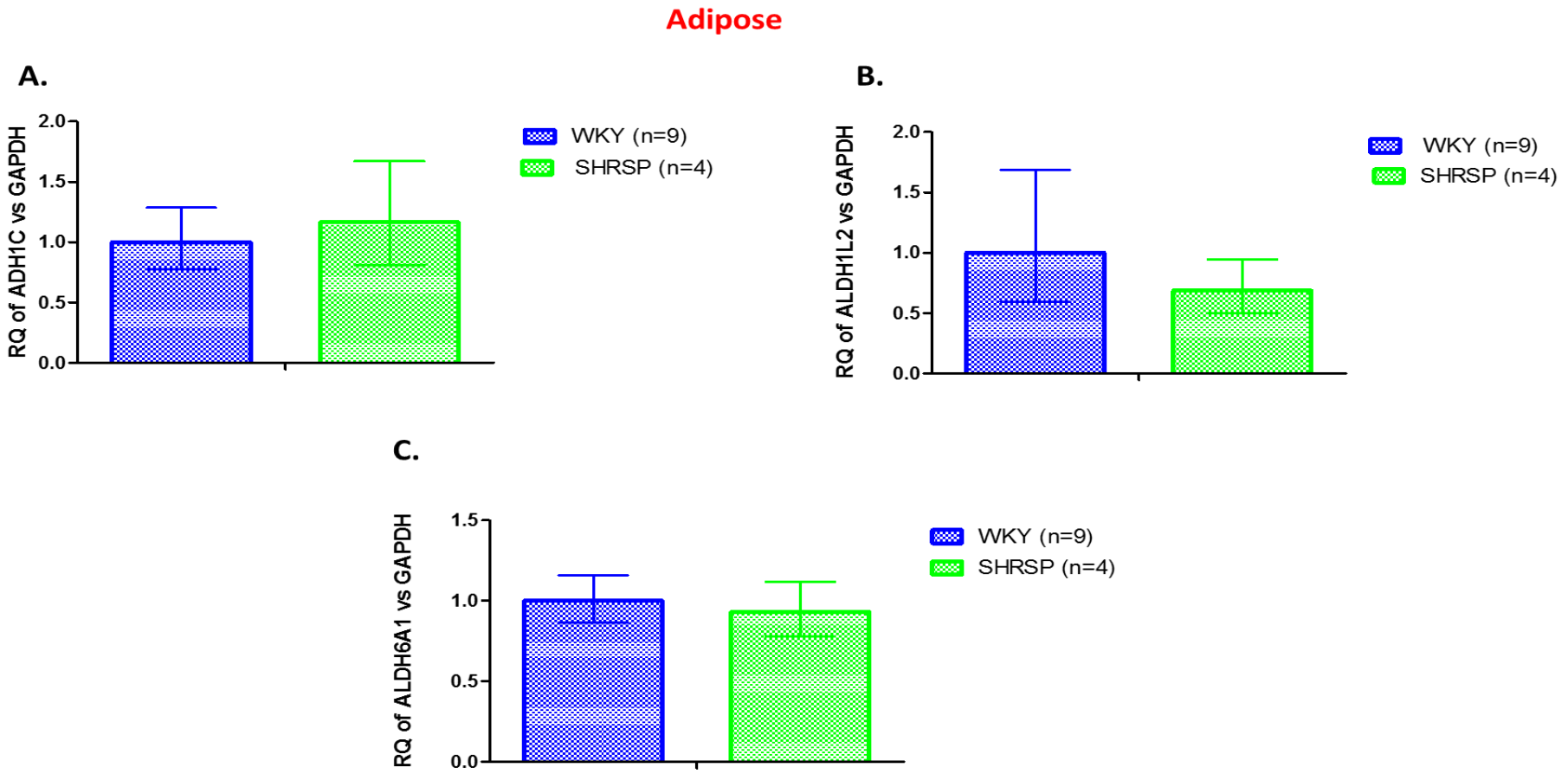

Figure 5-8: The expression of ADH1C, ALDH1L2 and ALDH6A1 in adipose tissues of control WKY_{Gla} and $SHRSP_{Gla}$ rats.

No differences in the expression of (A) ADH1C, (B) ALDH1L2 and (C) ALDH6A1 normalized to GAPDH in adipose tissues of WKY_{Gla} (n=9) and $SHRSP_{Gla}$ (n=4) rats. (Each point represents Mean ± Standard error of mean).

Table 5-1: Average Ct value of main genes in ω oxidation pathways and reference genes in heart, kidney, adipose and liver tissues.

Tissue	Group	Gene of interest	Mean Ct value	Reference gene	Mean Ct value
Heart	WKY_{Gla}	ALDH1L2	39	B2M	19
Heart	$SHRSP_{Gla}$	ALDH1L2	37	B2M	19
Heart	WKY_{Gla}	ALDH6A1	20.4	B2M	19
Heart	$SHRSP_{Gla}$	ALDH6A1	20.3	B2M	19
Kidney	WKY_{Gla}	CYP4A	27.9	GAPDH	20.4
Kidney	$SHRSP_{Gla}$	CYP4A	28.2	GAPDH	20.4
Kidney	WKY_{Gla}	ADH1C	24	GAPDH	20
Kidney	$SHRSP_{Gla}$	ADH1C	24.4	GAPDH	20.2
Kidney	WKY_{Gla}	ALDH2L1	34.9	GAPDH	20
Kidney	$SHRSP_{Gla}$	ALDH2L1	34.8	GAPDH	20
Kidney	WKY_{Gla}	ALDH6A1	22.4	GAPDH	21.5
Kidney	$SHRSP_{Gla}$	ALDH6A1	22.7	GAPDH	21.5
Liver	WKY_{Gla}	CYP4A	27.4	B2M	18.5
Liver	$SHRSP_{Gla}$	CYP4A	26.7	B2M	18.8
Liver	WKY_{Gla}	ADH1C	19.7	GAPDH	22.3
Liver	$SHRSP_{Gla}$	ADH1C	20.7	GAPDH	22.5
Liver	WKY_{Gla}	ALDH2L1	25.1	GAPDH	23
Liver	$SHRSP_{Gla}$	ALDH2L1	27.4	GAPDH	23.4
Liver	WKY_{Gla}	ALDH6A1	22	B2M	19.2
Liver	$SHRSP_{Gla}$	ALDH6A1	22.4	B2M	19.5
Adipose	WKY_{Gla}	ADH1C	31.4	GAPDH	26
Adipose	$SHRSP_{Gla}$	ADH1C	31.3	GAPDH	26
Adipose	WKY_{Gla}	ALDH2L1	33.5	GAPDH	26.2
Adipose	$SHRSP_{Gla}$	ALDH2L1	34.7	GAPDH	26.2
Adipose	WKY_{Gla}	ALDH6A1	28.1	GAPDH	26
Adipose	$SHRSP_{Gla}$	ALDH6A1	28.3	GAPDH	26

Ct= cycle threshold

5.5.2 Pharmacological Intervention: Fenofibrate (CYP4A agonist)

5.5.2.1 The effect of fenofibrate on haemodynamic parameters

Analysis of the data identified that fenofibrate significantly decreased blood pressure in WKY_{Gla} rats, as demonstrated by the significant separation of systolic blood pressure (SBP) between control and fenofibrate-treated animals (P=0.01); as shown in Figure 5-9A. There were no significant differences in diastolic blood pressure (DBP) between the fenofibrate-treated rats and control rats (P=0.087) (Figure 5-9B). In addition, no significant changes in the heart rate and activity were observed over the course of the study between control and fenofibrate groups (P=0.0513; P=0.098 respectively) (Figure 5-9C, D).

5.5.2.2 Vascular responses to exogenous noradrenaline and carbachol

The mesenteric resistance arteries of rats treated with fenofibrate showed a trend towards lower maximal response to noradrenaline compared with arteries obtained from control rats, but this did not achieve significance (fenofibrate area under the curve 56.98 ± 8.9 versus control area under the curve 68.9 ± 11.3; P=0.431, EC50 P=0.594), as shown in Figure 5-10 A. In addition, the mesenteric resistance arteries of fenofibrate-treated rats showed a significant reduction in relaxation response to carbachol (fenofibrate AUC 95.8 ± 15.4 verses control AUC 119.4 ± 12.17 P= 0.55, EC50 P=0.043), as shown in Figure 5-10 B.

5.5.2.3 CYP4A expression in cardiovascular tissues

The expression of CYP4A was assessed by quantitative real time PCR (qRT-PCR) in male WKY_{Gla} rats treated with fenofibrate or vehicle for two weeks. CYP4A was significantly higher in fenofibrate-treated rats compared to control in kidney (P=0.0001) and liver tissues ($P=3X10^{-4}$) (Figure 5-11). However, the expression of CYP4A was below the threshold of detection in heart and aorta tissues.

5.5.2.4 Renal function

There was a small reduction in water intake after treatment with fenofibrate, which did not reach significant levels (Δ water intake=5.3 ml, P=0.212). Furthermore, no change was observed in water intake between fenofibrate-treated rats compared to control rats (fenofibrate water intake 36 ± 3 ml versus

control water intake 34 ± 3 ml, P=0.61), as shown in Figure (5-12 A). In addition, there was no change in urine output between fenofibrate-treated rats and control rats (fenofibrate urine output 14.12 ± 1.4 ml versus control urine output 14.15 ± 2.4 ml, P=0.99). Moreover, no significant changes in urine output were found after fenofibrate administration (P=0.402) (Figure 5-12 B).

5.5.2.5 Organ mass index

Cardiac (whole heart) mass index and left ventricular (left ventricle+septum) mass index were measured to determine cardiac and left ventricular hypertrophy at sacrifice. There was no significant difference in left ventricular index of fenofibrate-treated rats (2.64 ± 0.26 mg/g; P=0.45) compared to the control rats (2.49 ± 0.09 mg/g). In addition, no significant difference was observed in whole heart normalised to body weight of fenofibrate-treated rats compared to the whole heart weight of control rats, normalised to body weight (Table 5-2).

There was also no significant difference between the left kidneys normalised to body weight between fenofibrate-treated rats (3.24 ± 0.09 mg/g) and control rats (3.03 ± 0.13 mg/g) (P=0.19). Furthermore, no change was observed in the right kidney of fenofibrate-treated rats (3.16 ± 0.12 mg/g, P=0.18) compared to control (2.94 ± 0.11 mg/g). There was also no changes in adiposity index of fenofibrate-treated rats compared to control rats (Table 5-2). Interestingly, there was a significant increase in hepatic index of fenofibrate-treated rats (58.18 ± 1.66 mg/g, P=4.07x 10^{-8}) compared to the control rats (36.46 ± 0.56 mg/g). Organs mass index adjusted to tibia length showed the same pattern for all, as shown in Table 5-2.

5.5.2.6 Hexadecandioate levels in plasma samples

Hexadecanedioate levels in plasma samples obtained from fenofibrate-treated WKY_{Gla} rats did not change after two weeks of treatment with fenofibrate compared to untreated control WKY_{Gla} rats (fenofibrate 1.20 ± 0.06 ng/ml versus control 1.24 ± 0.09; ng/ml, P=0.79), as shown in Figure 5-13.

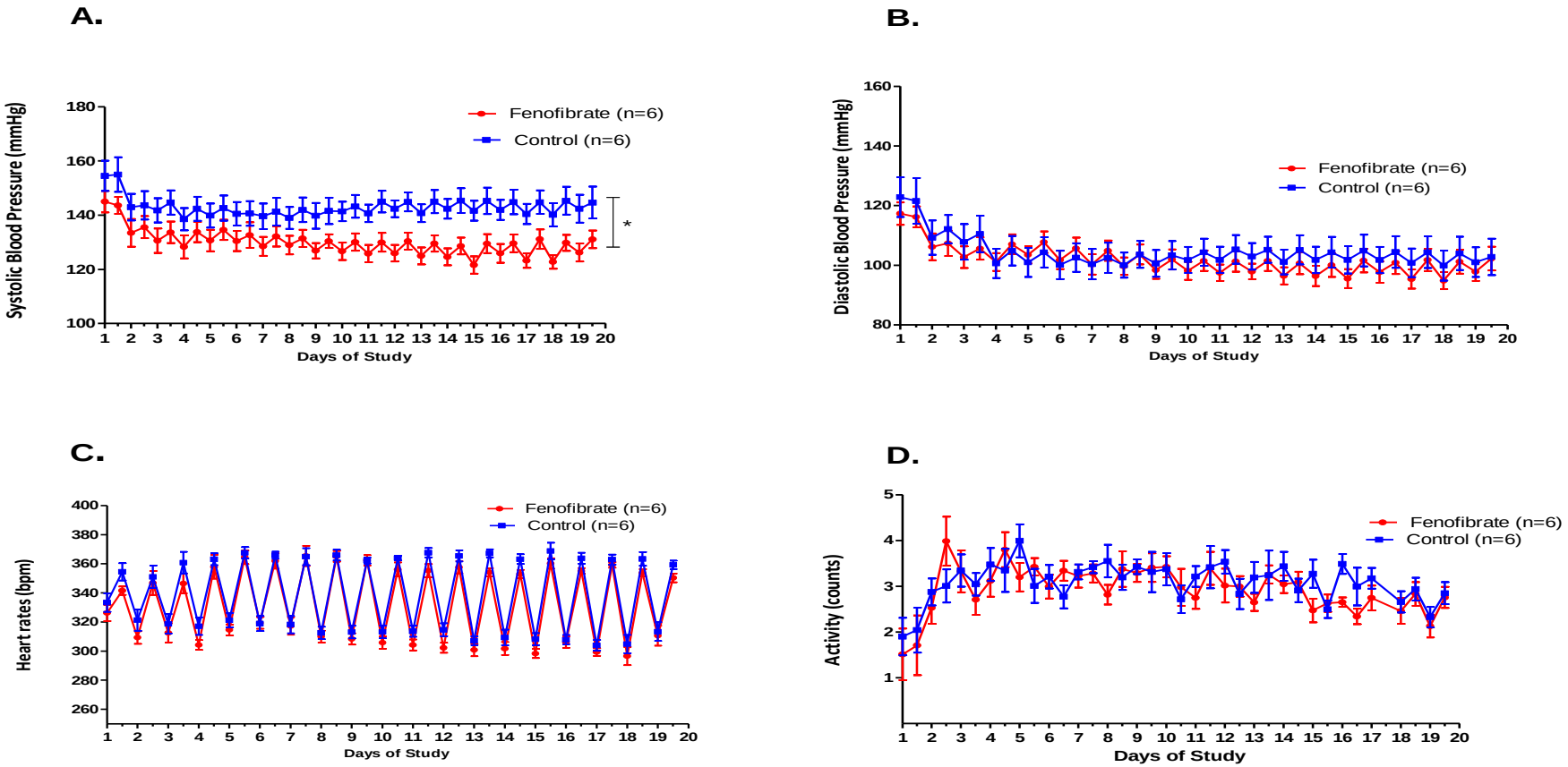

Figure 5-9: Radiotelemetry measurement (24-h averages) of haemodynamic parameters of fenofibrate-treated WKY_{Gla} rats (100 mg/kg per day, n=6) compared to control WKY_{Gla} rats (n=6) for 14 days.

(A) Systolic blood pressure (mmHg) significantly decreased in fenofibrate-treated rats compared to control rats. However, no changes were observed in (B) diastolic blood pressure (mmHg), (C) Heart rate (bpm) or (D) activity (counts) of WKY_{Gla} rats treated with fenofibrate compared to control rats. Each point represents (mean ± standard error of mean). (P*<0.05).

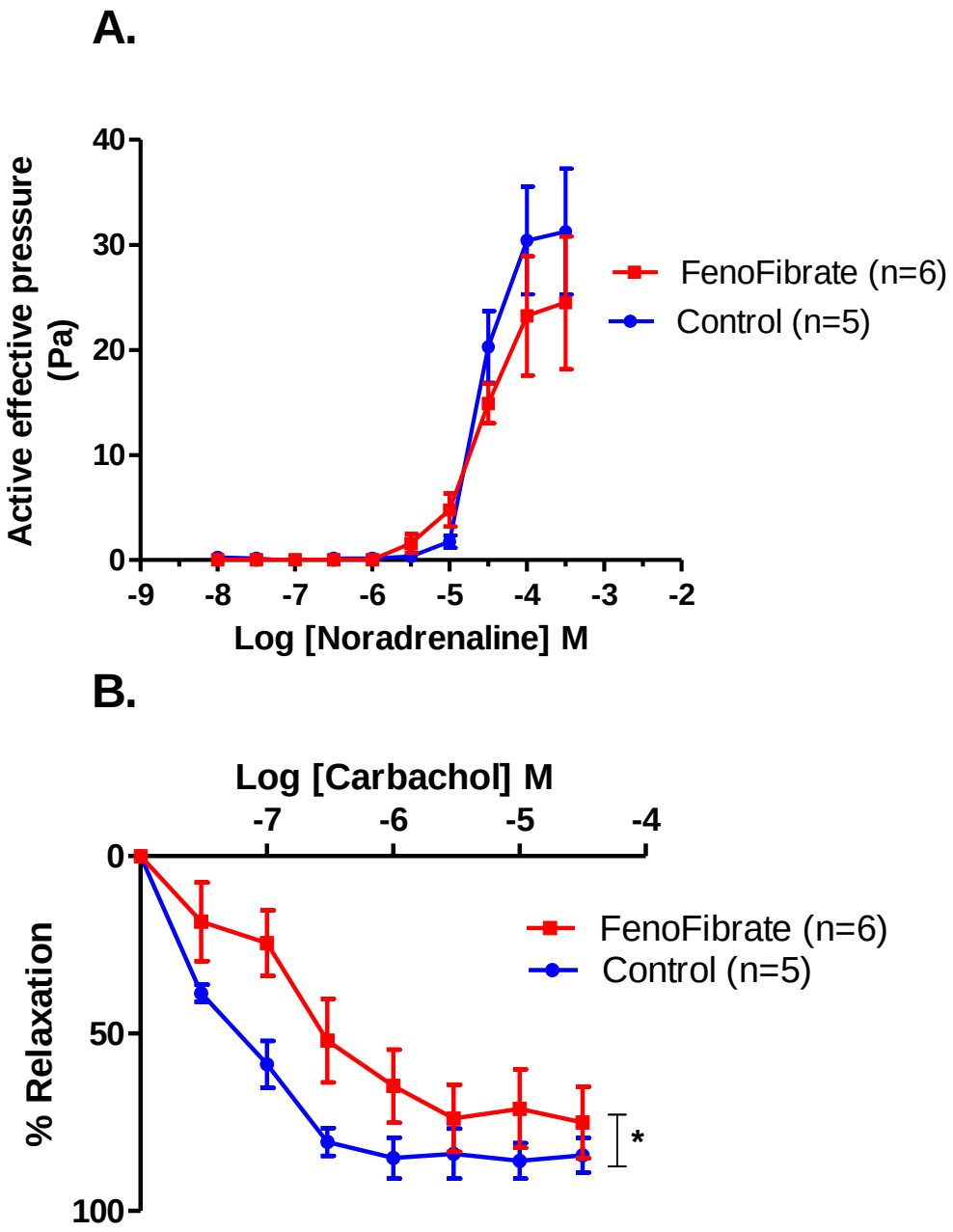

Figure 5-10: Mesenteric resistance artery contractile response to noradrenaline and carbachol in WKY_{Gla} rats treated with fenofibrate or vehicle.

Mesenteric resistance artery contractile response to noradrenaline (A) and relaxation to carbachol (B) in control (n=5) and fenofibrate treated (n=6) WKY_{Gla} rats. The mesenteric resistance arteries of rats treated with fenofibrate showed decrease in response to noradrenaline, and significant decrease in relaxation response to carbachol compared with arteries of control rats. Each point represents Mean ± Standard error of mean.

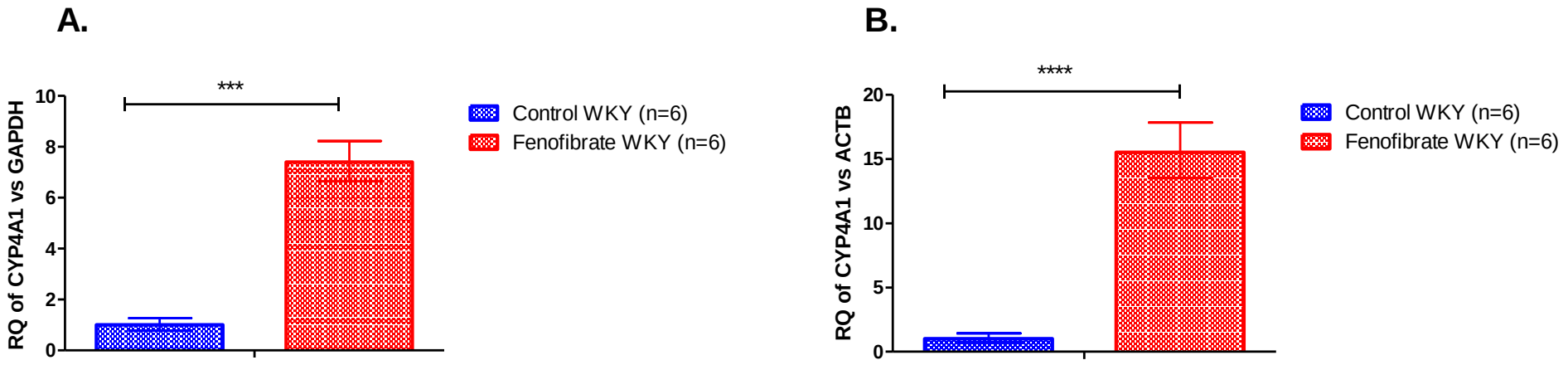

Figure 5-11: Expression of CYP4A in kidney and liver of fenofibrate-treated WKY_{Gla} rats compared to control WKY_{Gla} rats.

Expression of CYP4A was significantly increased in (A) whole kidney and (B) liver of fenofibrate-treated rats (n=6) compared to control rats (n=6). Values are represented as mean ± SEM (P***<0.001), (P****<0.0001).

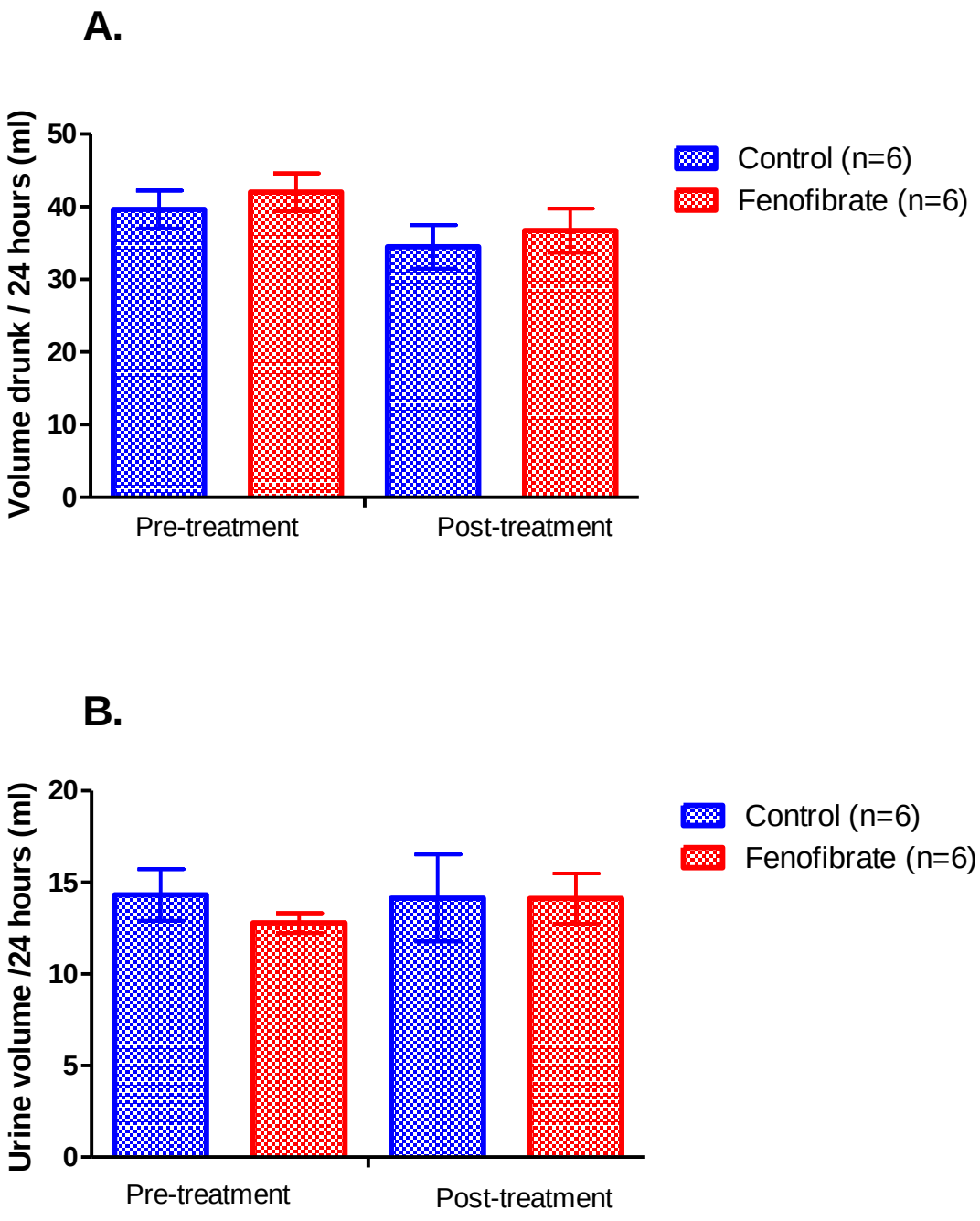

Figure 5-12: Renal function was assessed by 24 hours metabolic cage collections in fenofibrate or vehicle-treated WKY_{Gla} rats.

(A) Water intake and (B) urine output were measured pre and post treatment, which showed no significant difference between fenofibrate-treated WKY_{Gla} rats (n=6) and vehicle-treated WKY_{Gla} rats (n=6). Values are presented as mean ± SEM.

Table 5-2: Organ weight normalised to body weight and tibia length of fenofibrate-treated WKY_{Gla} rats (n=6) or vehicle (n=6) at sacrifice.

Parameters	Control	Fenofibrate	Ttest
H/Bwt (mg/g)	3.58 ± 1.45	3.92 ± 0.42	0.422
H/tib (mg/mm)	29.69 ± 1.45	30.68 ± 2.74	0.719
LV+S/Bwt (mg/g)	2.46 ± 0.09	2.64 ± 0.26	0.449
LV+S/tib (mg/mm)	20.47 ± 0.67	20.72 ± 1.63	0.870
RK/Bwt (mg/g)	2.94 ± 0.11	3.16 ± 0.12	0.178
RK/tib (mg/mm)	24.58 ± 1.29	24.64 ± 1.53	0.973
LK/Bwt (mg/g)	3.03 ± 0.13	3.24 ± 0.09	0.196
LK/tib (mg/mm)	25.28 ± 1.32	25.60 ± 1.20	0.848
liver/Bwt (mg/g)	36.46 ± 0.56	58.18 ± 1.66	0.000*
Liver/tib (mg/mm)	303.79 ± 8.33	458.50 ± 15.52	0.000*
EPI/Bwt (mg/g)	7.35 ± 0.35	7.27 ± 0.58	0.888
Epi/tib (mg/mm)	61.46 ± 4.06	57.34 ± 4.97	0.489
Retro/bwt (mg/g)	6.87 ± 0.73	6.19 ± 1.09	0.572
Retro/tib (mg/mm)	57.53 ± 6.75	49.25 ± 9.42	0.437
Bwt (g)	323.13 ± 4.83	302.33 ± 8.09	0.052
Tibia length (mm)	38.83 ± 0.60	38.33 ± 0.56	0.556

Abbreviations: H/Bwt, Heart normalised to body weight; H/tib, Heart normalised to tibia length; LV+S/Bwt, Left Ventricular plus Septal wall normalised to body weight; LV+S/tib, Left Ventricular plus Septal wall normalised to tibia length; RK/Bwt, Right Kidney normalised to body weight; RK/tib, Right Kidney normalised to tibia length; LK/Bwt, Left Kidney normalised to body weight; LK/tib, Left Kidney normalised to tibia length; Epi/Bwt, Epididymal fat normalised to body weight; Epi/tib, Epididymal fat normalised to tibia length; Retro/Bwt, Retroperitoneal fat normalised to body weight; Retro/tib, Retroperitoneal fat normalised to tibia length; Liver/Bwt, Liver normalised to body weigth; Liver/tib, Liver normalised to tibia length. Units: mg/g, milligram per gram; mg/mm, milligram/millimetre; g, gram; mm, millimetre. All data are mean± SEM. (P*<0.05; Student Ttest used to compare fenofibrate-treated WKY rats to their respective controls).

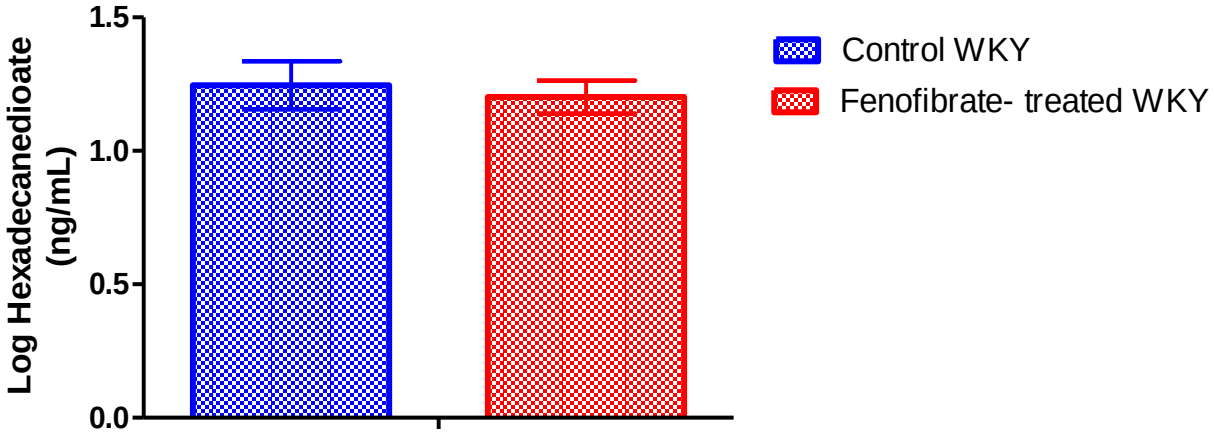

Figure 5-13: Plasma levels of hexadecanedioate in WKY_{Gla} rats after treatment with oral fenofibrate or vehicle for two weeks.

Circulating levels of hexadecanedioate did not show any differences in WKY_{Gla} rats after treatment with oral fenofibrate for two weeks (n=3) compared with controls (n=5). Values are presented as mean ± SEM.

5.5.3 Pharmacological Intervention: HET0016 (CYP4A antagonist)

Due to prohibitive cost of the HET0016 compound, a pilot study was conducted initially with n=3 HET0016-treated rats and n=2 control to determine any induction of drug induced changes in blood pressure before pursuing a full study with this compound.

5.5.3.1 The effect of HET0016 on haemodynamic parameters

The radiotelemetry data showed that the haemodynamic parameters (i.e. systolic blood pressure, diastolic blood pressure, heart rate and activity remained unchanged over the course of the study between control and HET0016 treated groups, as shown in Figure 5-14.

5.5.3.2 Vascular responses to exogenous noradrenaline and carbachol

The mesenteric resistance arteries of rats treated with HET0016 showed no change in contractile response to noradrenaline compared with mesenteric resistance arteries of control rats (HET0016 area under the curve 33.04 ± 15.2 versus control area under the curve 24 ± 8.8), as shown in Figure 5-15 A. In addition, there assumed to be no difference in vascular relaxation in response to carbachol (HET0016 area under the curve 65.9 ± 18.9 verses control AUC 48.2.4 ± 7.6), as shown in Figure 5-15 B, although n=2 values are currently too small to carry out statistical analysis. The quality of the curves are compromised by the low n values, however the major outcome parameter was blood pressure, which showed identical levels between HET0016-treated and control rats.

5.5.3.3 Renal function

No change was observed in water intake between HET0016-treated rats compared to control rats (HET0016 water intake 40 ± 9.9 ml versus control water intake 41.2 ± 1.7 ml), as shown in Figure (5-16 A). In addition, there was no change in urine output between HET0016-treated rats and control rats (HET0016 urine output 13 ± 2.9 ml versus control urine output 16.9 ± 3.2 ml (Figure 5-16 B). However, the small sample size is skewing the data. Urine output baseline for control SHRSP animals is normally around 8-10 ml.

5.5.3.4 Organ mass index

There was no change in cardiac index of HET0016-treated rats (4.23 ± 0.12 mg/g) compared to the control rats (4.06 ± 0.04 mg/g). In addition, no change in left ventricular index was observed between HET0016-treated rats (3.28 ± 0.12 mg/g) and the control rats (3.08 ± 0.04 mg/g) (Table 5-3).

There was no difference between left kidneys in the HET0016-treated rats normalised to body weight (3.79 ± 0.12 mg/g) and the control rats (3.63 ± 0.06 mg/g). Furthermore, no change was observed in the right kidneys of HET0016-treated rats (3.62 ± 0.09 mg/g) compared to control (3.83 ± 0.26 mg/g). There was also no difference in the hepatic and adiposity indexes of HET0016-treated rats compared to control rats, after they were normalised to body weight. Tibia length corrections showed identical level, as shown in Table 5-3.

5.5.3.5 Hexadecandioate levels in plasma samples

Hexadecanedioate levels in plasma samples obtained from HET0016-treated $SHRSP_{Gla}$ rats did not change after two weeks of treatment with HET0016 compared to untreated control $SHRSP_{Gla}$ rats (HET0016 1.083 ± 0.054 ng/ml versus control 1.26 ± 0.05 ng/ml), as shown in Figure 5-17.

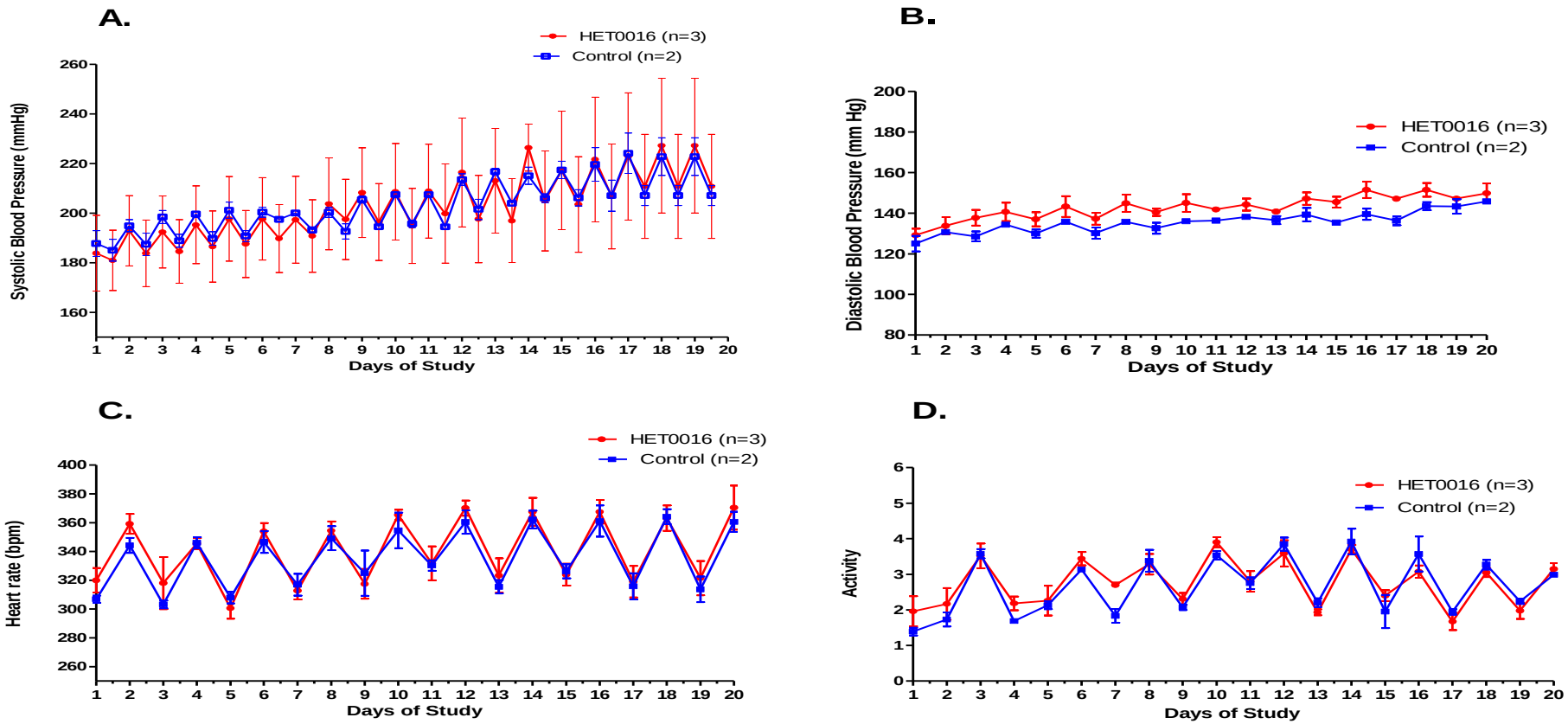

Figure 5-14: Radiotelemetry measurement (24-h averages) of haemodynamic parameters in SHRSP$_{Gla}$ rats treated with HET0016 (4 mg/kg per day, n=3) or control (n=2) for 14 days.

There was no changes in (A) systolic blood pressure (mmHg), (B) diastolic blood pressure (mmHg), (C) heart rats (bpm) and activity (counts) of SHRSP$_{Gla}$ rats treated with HET0016 over the course of the study. Each point represents (mean ± standard error of mean). Statistical analysis was not performed due to small n values.

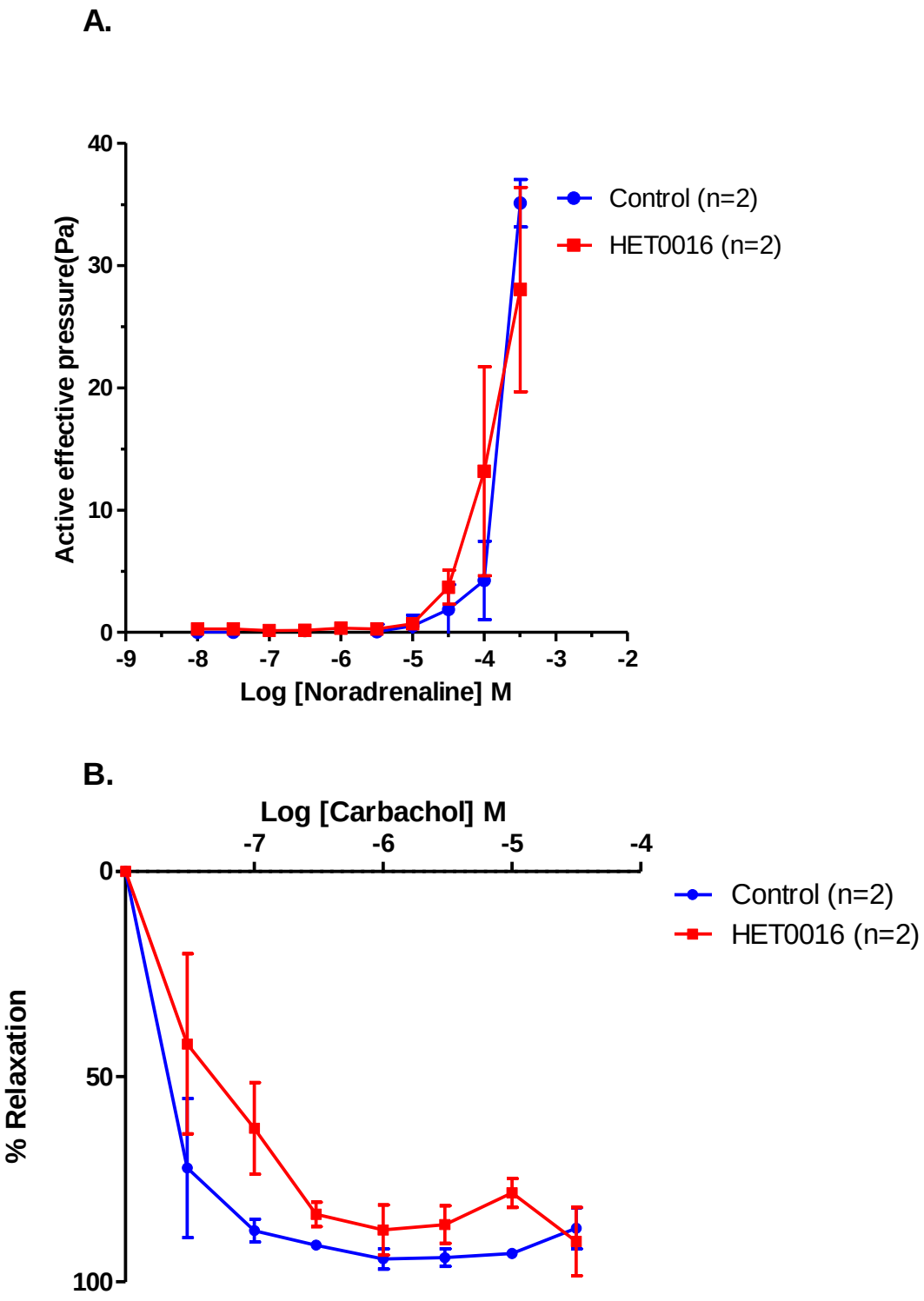

Figure 5-15: Mesenteric resistance artery contractile response to noradrenaline and carbachol in SHRSP$_{Gla}$ rats treated with HET0016 or vehicle.

Mesenteric resistance artery contractile response to noradrenaline (A) and relaxation to carbachol (B) showed no changes between control (n=2) and HET0016-treated SHRSP$_{Gla}$ rats (n=2). Each point represents Mean ± Standard error of mean. Statistical analysis was not performed due to small n values.

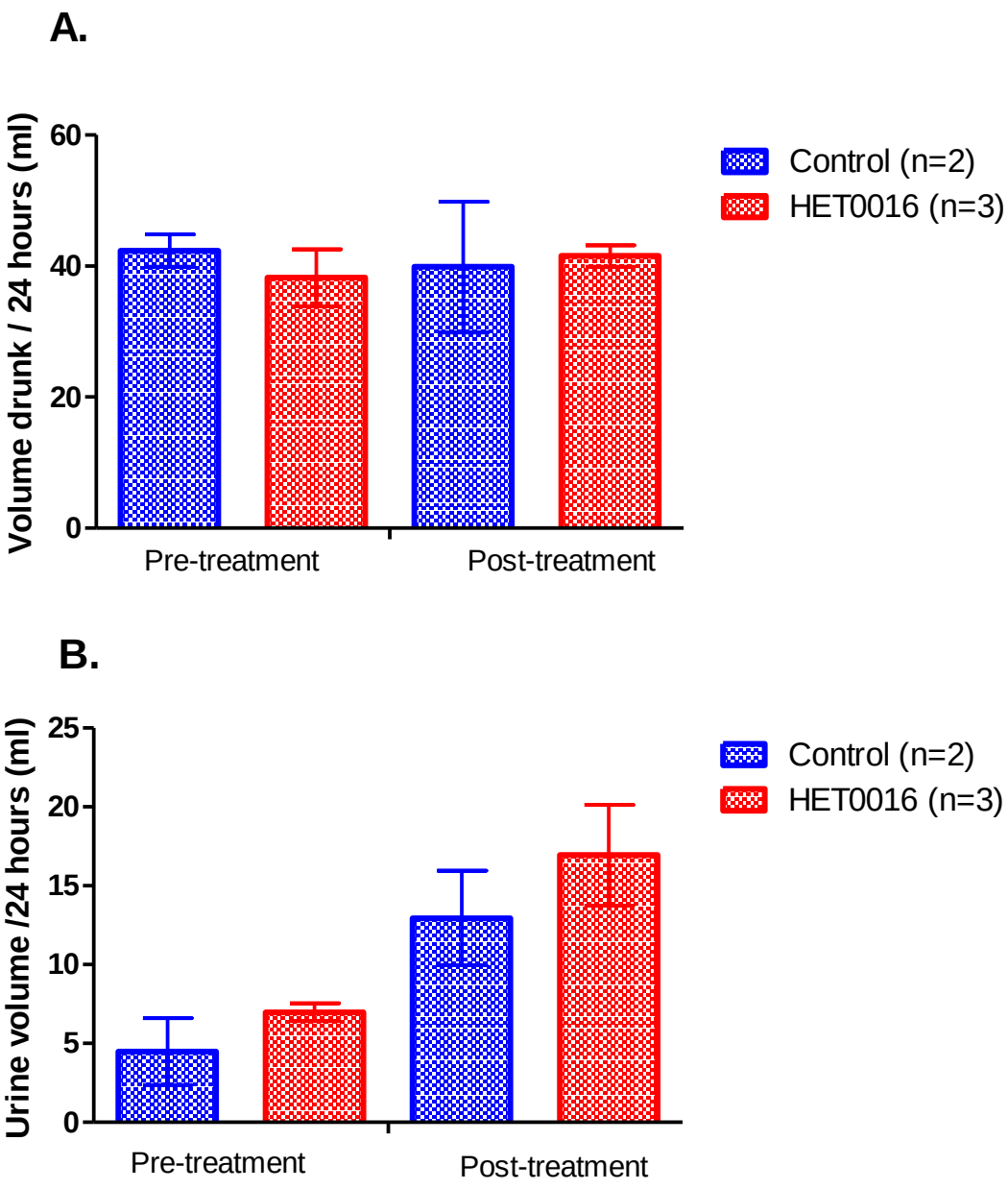

Figure 5-16: Renal function was assessed by metabolic cage collections during 24 hours in SHRSP$_{Gla}$ treated with HET0016 (n=3) or vehicle (n=2).

There were no apparent changes in (A) water intake and (B) urine output of SHRSP$_{Gla}$ rats pre or post treatment (n=3) when comparing vehicle or HET0016 treated rats. Values are presented as mean ± SEM. Statistical analysis was not performed due to small n values.

Table 5-3: Organ weight normalised to body weight and tibia length of HET0016-treated SHRSP$_{Gla}$ rats or vehicle at sacrifice.

Parameters	Control	HET0016
H/Bwt (mg/g)	4.23 ± 0.12	4.06 ± 0.04
H/tib (mg/mm)	29.48 ± 1.28	28.48 ± 0.19
LV+S/Bwt (mg/g)	3.28 ± 0.12	3.08 ± 0.04
LV+S/tib (mg/mm)	22.89 ± 1.19	21.66 ± 0.34
RK/Bwt (mg/g)	3.62 ± 0.09	3.83 ± 0.26
RK/tib (mg/mm)	25.21 ± 0.89	26.93 ± 1.93
LK/Bwt (mg/g)	3.79 ± 0.12	3.63 ± 0.06
LK/tib (mg/mm)	26.43 ± 0.37	25.50 ± 0.50
liver/Bwt (mg/g)	39.79 ± 0.69	40.95 ± 1.14
Liver/tib (mg/mm)	277.27 ± 8.38	287.51 ± 7.23
EPI/Bwt (mg/g)	11.68 ± 0.22	11.11 ± 0.24
Epi/tib (mg/mm)	81.38 ± 1.63	78.02 ± 1.45
Retro/bwt (mg/g)	8.33 ± 0.62	8.99 ± 0.9 1
Retro/tib (mg/mm)	57.92 ± 3.28	63.15 ± 6.57
Bwt (g)	256.25 ± 9.85	243.37 ± 9.66
Tibia length (mm)	36.50 ± 1.50	36.00 ± 2.00

Abbreviations: H/Bwt, Heart normalised to body weight; H/tib, Heart normalised to tibia length; LV+S/Bwt, Left Ventricular plus Septal wall normalised to body weight; LV+S/tib, Left Ventricular plus Septal wall normalised to tibia length; RK/Bwt, Right Kidney normalised to body weight; RK/tib, Right Kidney normalised to tibia length; LK/Bwt, Left Kidney normalised to body weight; LK/tib, Left Kidney normalised to tibia length; Epi/Bwt, Epididymal fat normalised to body weight; Epi/tib, Epididymal fat normalised to tibia length; Retro/Bwt, Retroperitoneal fat normalised to body weight; Retro/tib, Retroperitoneal fat normalised to tibia length; Liver/Bwt, Liver normalised to body weigth; Liver/tib, Liver normalised to tibia length. Units: mg/g, milligram per gram; mg/mm, milligram/millimetre; g, gram; mm, millimetre. All data are mean± SEM. Statistical analysis was not performed due to low n values.

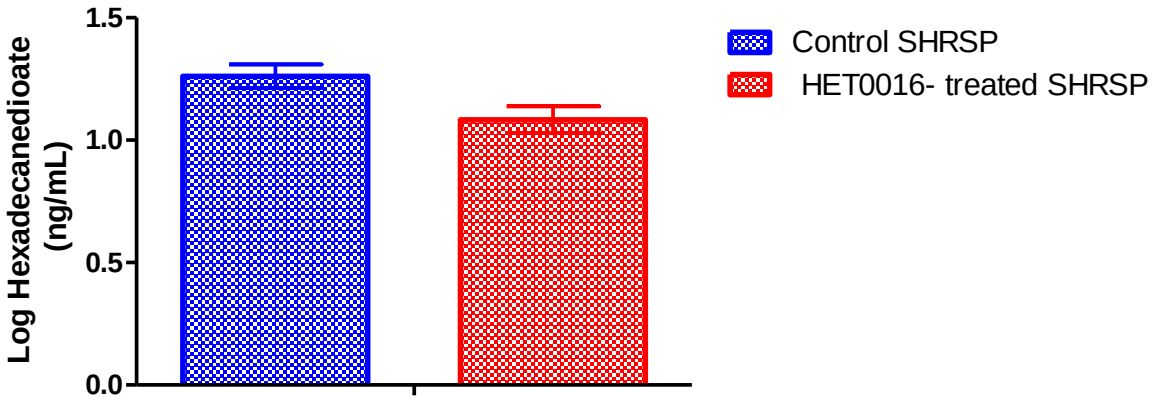

Figure 5-17: Plasma levels of hexadecanedioate in $SHRSP_{Gla}$ rats after treatment with HET0016 or vehicle for two weeks.

Circulating levels of hexadecanedioate did not show any differences in $SHRSP_{Gla}$ rats after treatment with HET0016 for two weeks (n=3) compared with untreated controls (n=2). Values are presented as mean ± SEM. Small n values prevented statistical analysis.

5.5.4 Pharmacological Intervention: Disulfiram (aldehyde dehydrogenase inhibitor)

5.5.4.1 The effect of disulfiram on blood pressure

A significant reduction in systolic blood pressure was observed in $SHRSP_{Gla}$ rats after treatment with the aldehyde dehydrogenase antagonist, disulfiram, for two weeks. The reduction was observed in the first week of treatment (ΔSBP 25.8 ± 6.9 mmHg; P=0.001) and was maintained in the second week of treatment (ΔSBP 24.9 ± 5.2 mmHg; $P=4.3x10^{-6}$), as shown in Figure 5-18.

5.5.4.2 Vascular responses to exogenous noradrenaline and carbachol

Significant lowering of maximal response to high doses of noradrenaline of the mesenteric resistance arteries obtained from disulfiram-treated $SHRSP_{Gla}$ rats, suggesting reduced vascular reactivity compared to control vessels (disulfiram area under the curve 68.05 ± 4.06 versus control area under the curve 86.08 ± 4.86; P=0.0127, EC50 P=0.15), as shown in Figure 5-19 A. Relaxation to carbachol was not significantly different in mesenteric resistance arteries of disulfiram-treated rats and control rats (disulfiram area under the curve 178.20± 22.53 versus control area under the curve 168.19± 23.35; P=0.76, EC50 P=0.65) as shown in Figure 5-19 B.

5.5.4.3 Echocardiography

Cardiac function and cardiac mass were assessed by echocardiography for $SHRSP_{Gla}$ rats at baseline and weekly after treatment with disulfiram. There was no significant difference in the left ventricular mass between the disulfiram-treated rats and the control group (P=0.07). No difference was observed after normalisation of left ventricular mass with body weight (P=0.701) or with tibia length (P=0.165). In addition, relative wall thickness (RWT) showed no significant change between disulfiram-treated rats compared with control rats (P=0.52), as shown in Table 5-4. Both fractional shortening (FS) and ejection fraction (EF), showed that there was no significant change in $SHRSP_{Gla}$ rats after treatment with disulfiram (P=0.152), (P=0.414). Stroke volume for disulfiram-treated rats showed no difference compared with the control rats (P=0.142) as well as cardiac output (P=0.128) (Table 5-4).

5.5.4.4 Renal function

There was no change in water intake between disulfiram-treated rats compared to control rats (disulfiram water intake 27.78 ± 1.22 ml versus control water intake 29.75 ± 2.25 ml, P=0.52), as shown in Figure 5-20 A. In addition, no change was shown in urine output between disulfiram-treated rats and control rats (disulfiram urine output 8.36 ± 0.95 ml versus control urine output 9.94 ± 1.12 ml, P=0.31). Furthermore, no differences in water intake (P=0.69) and urine output (P=0.82) were observed after treatment with disulfiram. (Figure 5-20 B).

5.5.4.5 Organ mass index

Disulfiram-treated rats demonstrated no cardiac (3.83 ± 0.11 mg/g; P=0.84) or left ventricular (2.69 ± 0.09 mg/g; P=0.74) hypertrophy when compared to the control rats (3.78 ± 0.18 mg/g), (2.74 ± 0.09 mg/g); respectively. There was no significant difference between the right kidneys of disulfiram-treated rats normalised to body weight (3.63 ± 0.10 mg/g) when compared to control rats (3.57 ± 0.09 mg/g) (P=0.70). Also, no change was observed in the left kidneys of disulfiram-treated rats (3.52 ± 0.09 mg/g, P=0.90) compared to the control rats (3.54 ± 0.12 mg/g). The disulfiram-treated rats also did not show any differences in liver weight compared to control rats after being normalised to body weight (disulfiram 39.65 ± 1.37 mg/g versus control 37.45 ± 1.22 mg/g; P=0.25). In addition, the result demonstrated that no changes were observed in either epididymal fat or retroperitoneal fat as a result of disulfiram treatment. Epididymal fat normalised to body weight was 8.89 ± 0.77 mg/g for disulfiram versus 9.99 ± 0.91 mg/g for control; P=0.37). Retroperitoneal fat normalised to body weight was 10.09 ± 0.74 mg/g for disulfiram versus 10.03 ± 0.79 mg/g for control; P=0.39). Organ mass index adjusted to tibia length showed the same pattern for all parameters and was not significantly different between treatment groups (Table 5-5).

5.5.4.6 mRNA expression

mRNA was extracted and prepared from kidney, heart, aorta and liver samples of control and disulfiram-treated rats to investigate the association between aldehyde dehydrogenase genes ALDH6A1 and ALDH1L2 and reduction of blood pressure in $SHRSP_{Gla}$-treated rats compared with control. There were no

differences detected in the expression of ALDH1L2 in heart (P=0.64), whole kidney (P=0.92) and liver (P=0.88), as shown in Figure 5-21 A, C, and E respectively. Moreover, no significant differences in the expression of ALDH6A1 between control and disulfiram-treated rats were observed in any of the tested tissues; heart (P=0.96), whole kidney (P= 0.91) and liver (P=0.87) between control and disulfiram-treated rats (Figure 5-21 B, D, F) (Table 5-6). However, both genes ALDH1L2 and ALDH6A1 were below the threshold of detection in aorta tissues.

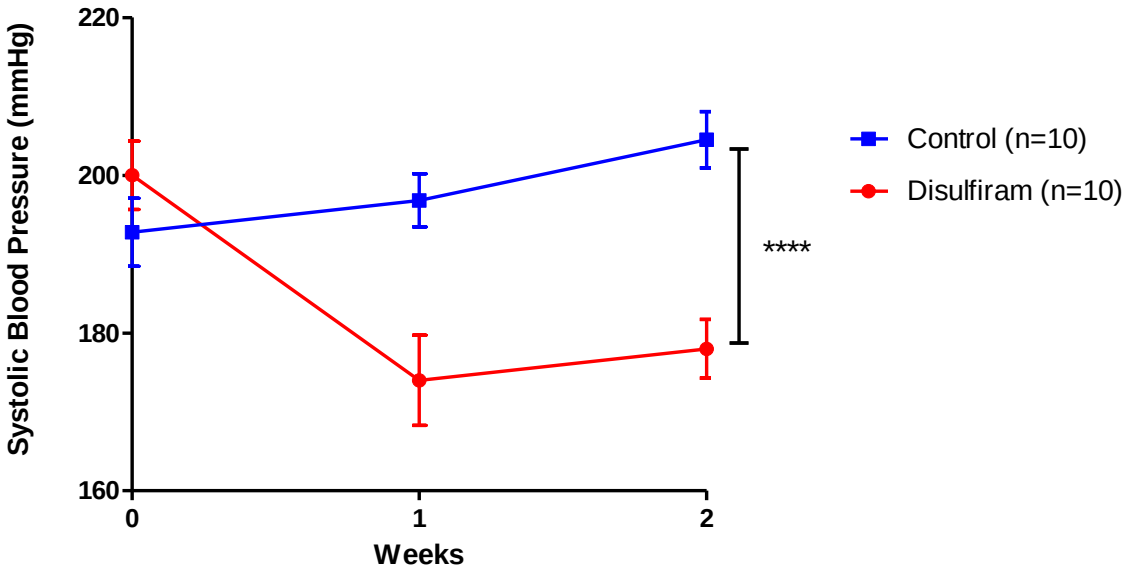

Figure 5-18: Systolic blood pressure (mmHg) of $SHRSP_{Gla}$ rats treated with disulfiram (25 mg/kg per day, n=10) or control (n=10) for 14 days by tail-cuff plethysmography.

Significant reduction was observed in SBP of disulfiram-treated $SHRSP_{Gla}$ rats (n=10) compared to control SHRSP rats (n=10), P****< 0.0001. Each point represents (mean ± standard error of mean).

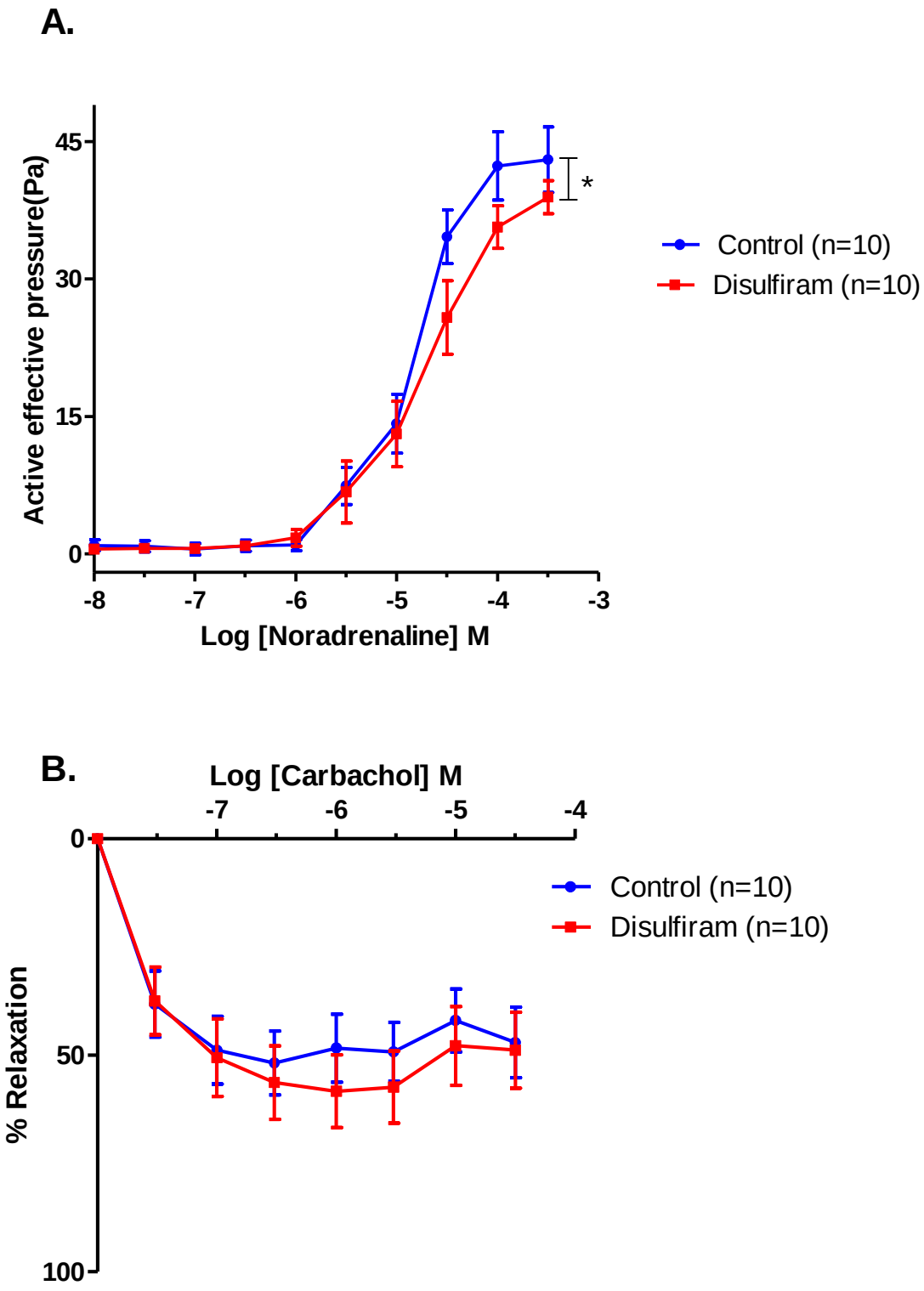

Figure 5-19: Mesenteric resistance artery contractile response to noradrenaline and carbachol in SHRSPGla rats treated with disulfiram or vehicle.

Mesenteric resistance artery contractile response to noradrenaline (A) and relaxation to carbachol (B) in control (n=10) and disulfiram-treated (n=10) SHRSPGla rats. (Each point represents Mean ± Standard error of mean). The mesenteric resistance arteries of rats treated with disulfiram showed significant reduction in response to noradrenaline, and no difference in relaxation response to carbachol compared to arteries of control rats. Each point represents Mean ± Standard error of mean.

Table 5-4: Echocardiographic measurements for $SHRSP_{Gla}$ rats treated with disulfiram (25 mg/kg per day, n=10) or vehicle (n=10) for 14 days.

Parameters	Pre-treatment		1st week of treatment		2nd week of treatment		ANOVA (general linear model)
	control	Disulfiram	control	Disulfiram	control	Disulfiram	P value
LVM (mg)	0.64 ± 0.02	0.59 ± 0.02	0.66 ± 0.02	0.67 ± 0.02	0.70 ± 0.03	0.65 ± 0.02	0.070
LVM/BWt (mg/g)	2.74 ± 0.09	2.67 ± 0.103	2.77 ± 0.09	2.97 ± 0.07	2.88 ± 0.10	2.82 ± 0.06	0.701
LVM/tib (mg/mm)	17.10 ± 0.05	16.04 ± 0.07	17.30 ± 0.05	17.50 ± 0.05	18.10 ± 0.08	17.80 ± 0.05	0.165
FS %	52.03 ± 3.01	55.64 ± 1.99	53.55 ± 2.02	47.87 ± 2.99	52.76 ± 1.74	50.59 ± 2.02	0.152
RWT (mm)	0.59 ± 0.03	0.54 ± 0.02	0.59 ± 0.024	0.55 ± 0.02	0.56 ± 0.02	0.55 ± 0.01	0.520
SV (mls)	0.24 ± 0.01	0.25 ± 0.01	0.25 ± 0.01	0.26 ± 0.01	0.28 ± 0.02	0.29 ± 0.01	0.142
CO (mls/min)	95.09 ± 6.33	104.80 ± 4.84	95.02 ± 6.81	96.13 ± 5.64	112.12 ± 7.23	109.99 ± 5.49	0.200
EF %	87.77 ± 2.18	90.79 ± 1.27	89.47 ± 1.33	84.60 ± 2.38	89.07 ± 1.26	84.19 ± 1.68	0.128
Bwt kg	234.4 ± 5.83	220.5 ± 5.31	242.3 ± 6.20	226.9 ± 6.98	243.4 ± 7.64	230.7 ± 6.71	0.000

Abbreviations: LVM, Left Ventricular Mass; LVM/BWt, Left Ventricular Mass normalised to body weight; LVM/tib, Left Ventricular Mass normalised to tibia length; FS, Fractional Shortening; RWT, Relative Wall Thickness; SV, Strock Volume; CO, Cardiac Output; EF%, % Ejection Fraction; BWt kg, Body Weight in Kilogram. Unites: mg, milligram; mg/g, milligram per gram; mm, millimetre; mg/mm, milligram per millimetre; mls, millilitres; mls/min, milliliters/ minute. All data are mean± SEM.

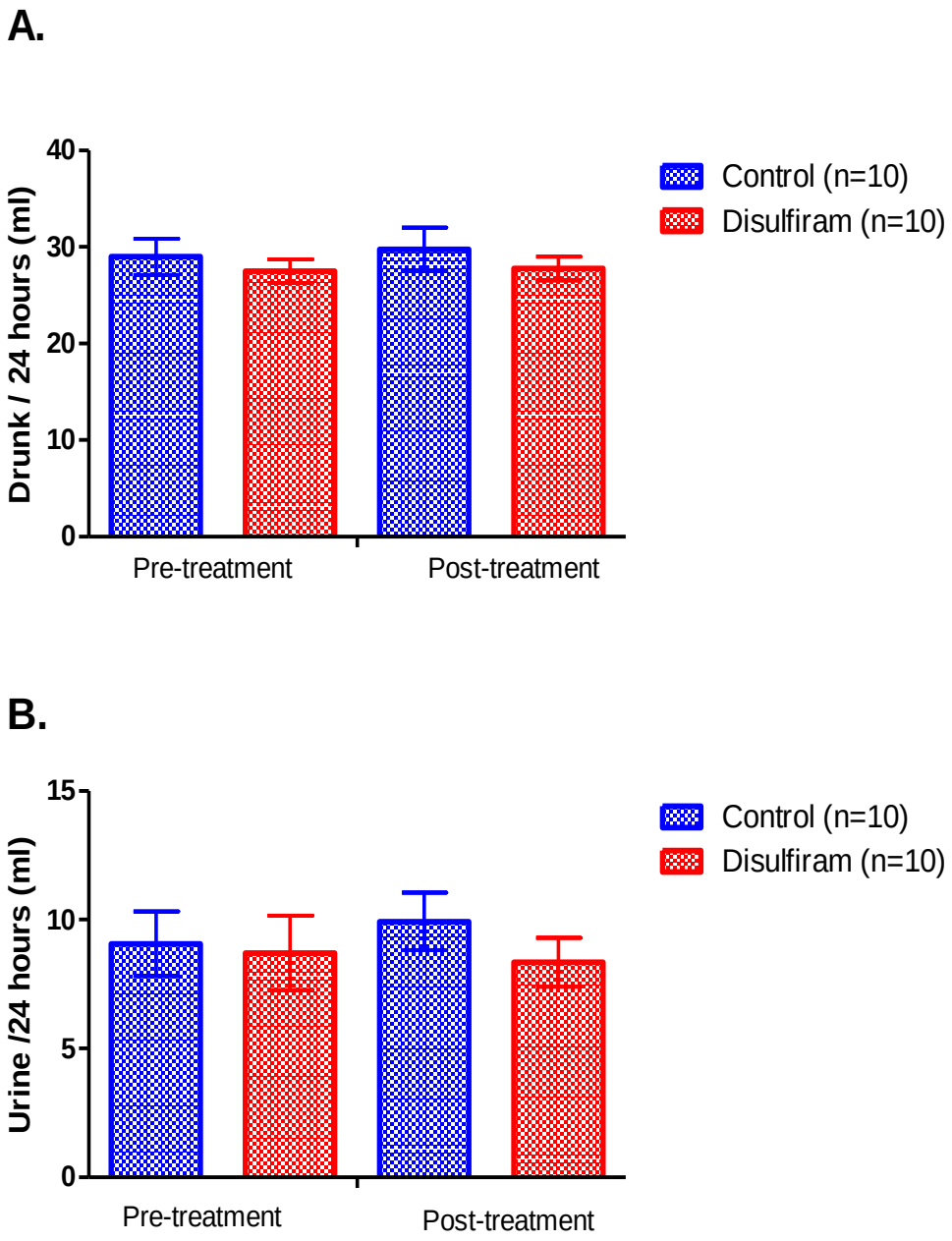

Figure 5-20: Renal function was assessed by 24 hours metabolic cage collections in SHRSP$_{Gla}$ rats treated with disulfiram or vehicle.

No change was observed in (A) water intake and (B) urine output, which were measured pre and post treatment with disulfiram (n=10) or vehicle (n=10). Values are presented as mean ± SEM

Table 5-5: Organ weight normalised to body weight and tibia length of disulfiram-treated $SHRSP_{Gla}$ rats (n=10) or vehicle (n= 10) at sacrifice.

Parameters	Control	Disulfiram	Ttest
H/Bwt (mg/g)	3.78 ± 0.18	3.83 ± 0.11	0.840
H/tib (mg/mm)	24.02 ± 1.11	22.86 ± 1.05	0.457
LV+S/Bwt (mg/g)	2.74 ± 0.09	2.69 ± 0.09	0.744
LV+S/tib (mg/mm)	17.29 ± 0.29	16.03 ± 0.68	0.102
RK/Bwt (mg/g)	3.57 ± 0.09	3.63 ± 0.10	0.700
RK/tib (mg/mm)	22.66 ± 0.51	21.48 ± 0.32	0.064
LK/Bwt (mg/g)	3.54 ± 0.12	3.52 ± 0.09	0.900
LK/tib (mg/mm)	22.52 ± 0.85	20.94 ± 0.69	0.168
liver/Bwt (mg/g)	37.45 ± 1.22	39.65 ± 1.37	0.246
Liver/tib (mg/mm)	236.92 ± 5.38	234.66 ± 5.69	0.776
EPI/Bwt (mg/g)	9.99 ± 0.91	8.89 ± 0.77	0.371
Epi/tib (mg/mm)	62.82 ± 5.03	53.29 ± 5.04	0.197
Retro/bwt (mg/g)	10.03 ± 0.79	10.09 ± 0.74	0.399
Retro/tib (mg/mm)	69.63 ± 4.60	59.93 ± 4.55	0.151
Bwt (g)	255.19 ± 9.99	236.14 ± 6.95	0.135
Tibia length (mm)	39.95 ± 0.30	39.65 ± 0.33	0.514

Abbreviations: H/Bwt, Heart normalised to body weight; H/tib, Heart normalised to tibia length; LV+S/Bwt, Left Ventricular plus Septal wall normalised to body weight; LV+S/tib, Left Ventricular plus Septal wall normalised to tibia length; RK/Bwt, Right Kidney normalised to body weight; RK/tib, Right Kidney normalised to tibia length; LK/Bwt, Left Kidney normalised to body weight; LK/tib, Left Kidney normalised to tibia length; Epi/Bwt, Epididymal fat normalised to body weight; Epi/tib, Epididymal fat normalised to tibia length; Retro/Bwt, Retroperitoneal fat normalised to body weight; Retro/tib, Retroperitoneal fat normalised to tibia length; Liver/Bwt, Liver normalised to body weigth; Liver/tib, Liver normalised to tibia length. Units: mg/g, milligram per gram; mg/mm, milligram/millimetre; g, gram; mm, millimetre. All data are mean± SEM.

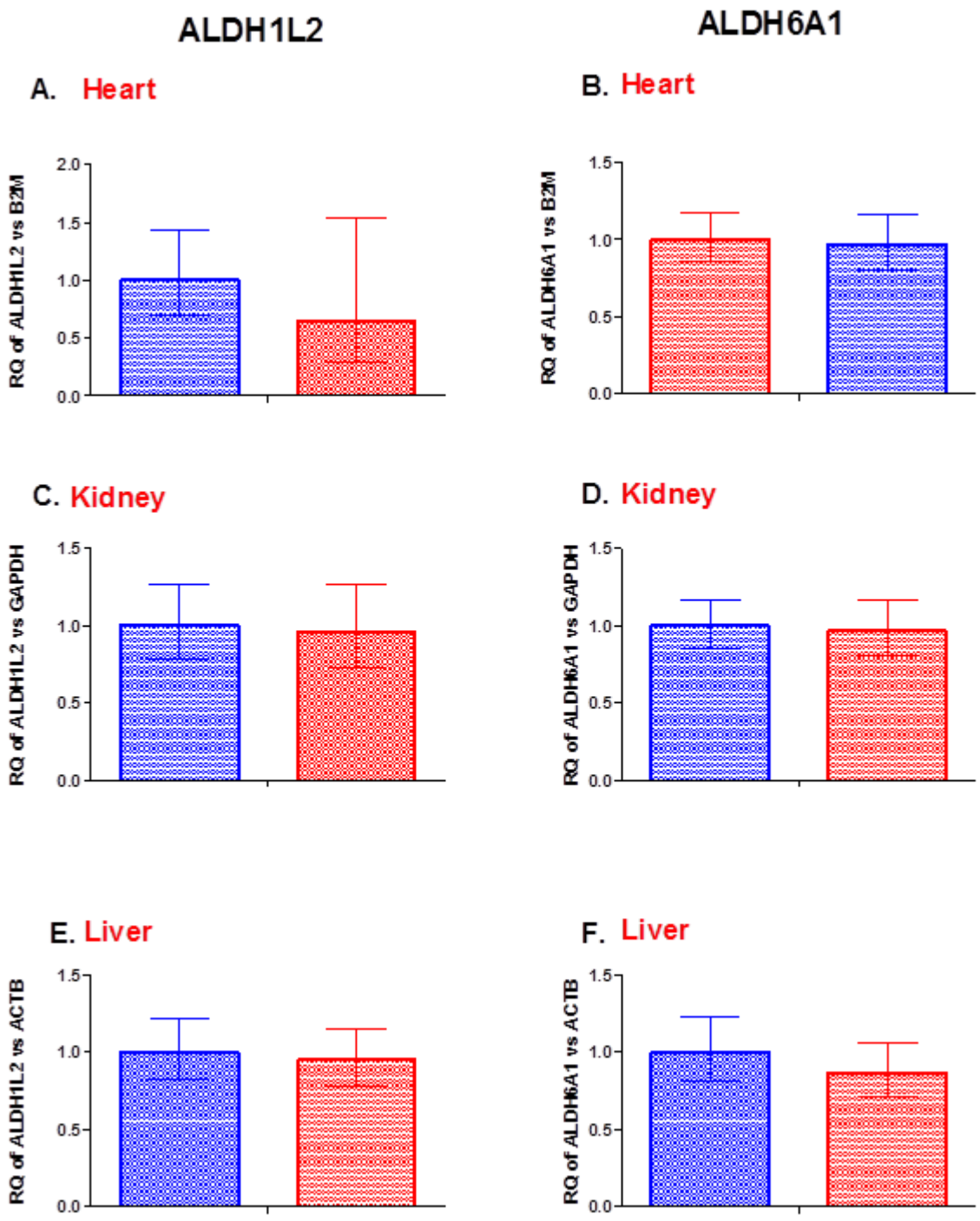

Figure 5-21: Expression of ALDH1L2 and ALDH6A1 in heart, kidney and liver of disulfiram-treated SHRSP$_{Gla}$ rats compared to control SHRSP$_{Gla}$ rats.

There was no change in expression of ALDH1L2 and ALDH6A1 in (A, B) heart (normalized to B2M), (C, D) kidney (normalized to GAPDH), and (E, F) liver (normalized to ACTB) between control (n=5) and disulfiram-treated rats (n=5). Each point represents Mean ± Standard error of mean.

Table 5-6: Average Ct value of ALDH1L2 and ALDH6A1 and deference genes in heart, kidney and liver tissues.

Tissue	Group	Gene of interest	Mean Ct value	Reference gene	Mean Ct value
Heart	Disulfiram	ALDH1L2	34.1	B2M	18.2
Heart	Control	ALDH1L2	34.4	B2M	18.2
Heart	Disulfiram	ALDH6A1	20.7	B2M	18
Heart	Control	ALDH6A1	20.7	B2M	18
Kidney	Disulfiram	ALDH1L2	34	GAPDH	22
Kidney	Control	ALDH1L2	34	GAPDH	22
Kidney	Disulfiram	ALDH6A1	23.1	GAPDH	22.5
Kidney	Control	ALDH6A1	23.2	GAPDH	22.7
Liver	Disulfiram	ALDH1L2	30.5	ACTB	25.5
Liver	Control	ALDH1L2	30	ACTB	25
Liver	Disulfiram	ALDH6A1	27.5	ACTB	25.5
Liver	Control	ALDH6A1	27	ACTB	25

Ct= cycle threshold

5.5.5 Aldehyde dehydrogenase levels in liver samples.

The levels of aldehyde dehydrogenase enzyme were measured in liver tissues from male $SHRSP_{Gla}$ and WKY_{Gla} rats at different ages (i.e. five-week-old, 16-week-old and 20-week-old) (n=4/group). Levels of aldehyde dehydrogenase showed an increase in five-week-old rats ($SHRSP_{Gla}$ 4.07 ± 0.20 ng/ml versus WKY_{Gla} 3.82 ± 0.22 ng/ml; P=0.453) (Figure 5-22 A) and in sixteen-week-old rats ($SHRSP_{Gla}$ 5.22 ± 0.25 ng/ml versus WKY_{Gla} 4.85 ± 0.103 ng/ml; P=0.242) (Figure 5-22 B) in $SHRSP_{Gla}$ rats compared to WKY_{Gla} rats. Interestingly, the increase in ALDH levels at 20-week-old in $SHRSP_{Gla}$ liver just failed to reach significance when compared to WKY_{Gla} rats ($SHRSP_{Gla}$ 4.73 ± 0.22 ng/ml versus WKY_{Gla} 4.07 ± 0.06 ng/ml; P =0.062) (Figure 5-22 C).

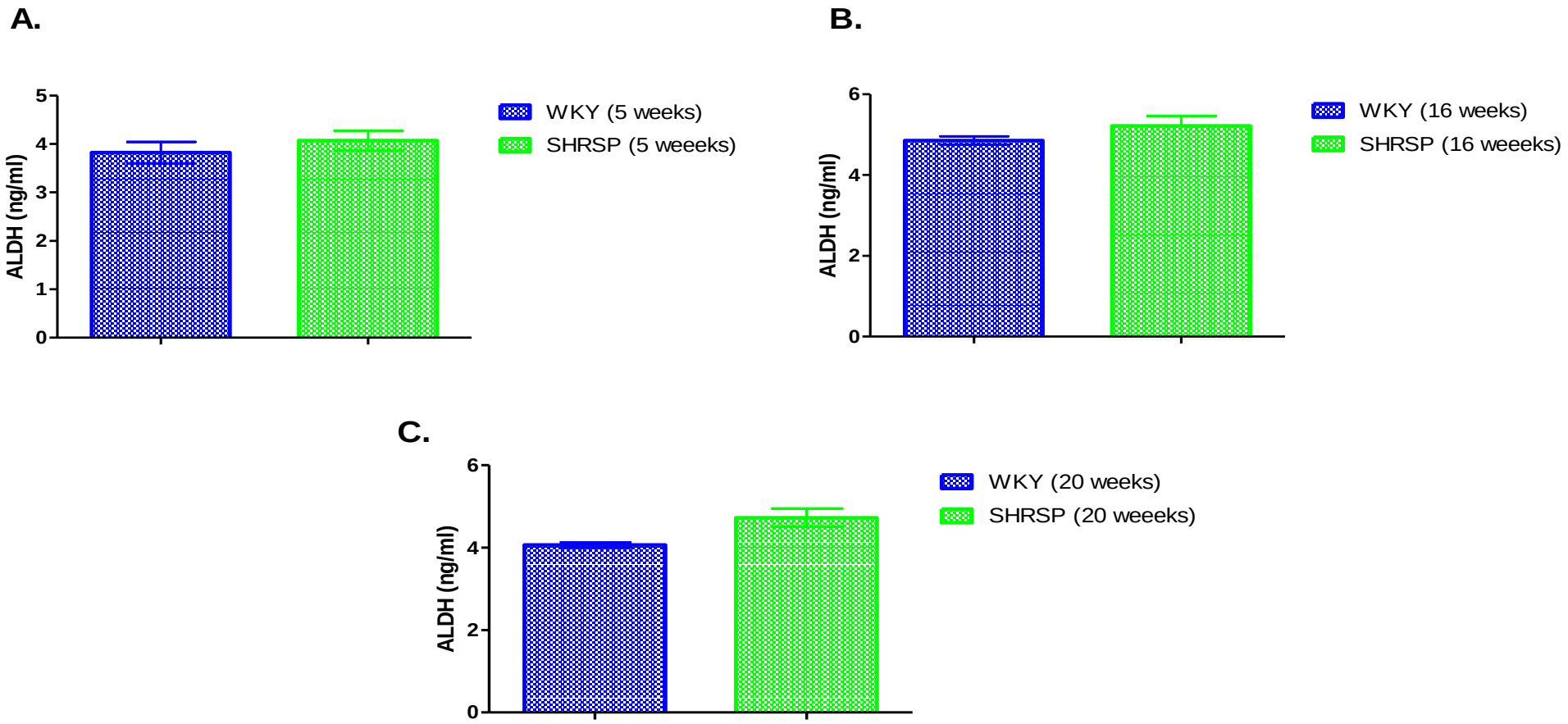

Figure 5-22: Aldehyde dehydrogenase enzyme level in liver tissues of (A) five-week-old, (B) 16-week-old and (C) 20-week-old male WKY_{Gla} and $SHRSP_{Gla}$ rats (n= 4/group).

There was a trend in elevation of ALDH levels at 20-week-old in $SHRSP_{Gla}$ liver compared to WKY_{Gla} rats. However, no difference was observed in ALDH levels at 5-week and 16 week in liver tissues of $SHRSP_{Gla}$ and WKY_{Gla} rats. Each point represents Mean ± Standard error of mean.

5.6 Discussion

There are multiple potential mechanisms by which hexadecanedioate may act to elevate blood pressure. In this chapter, the role of ω-oxidation pathway was addressed in the link between hexadecanedioate levels and development of hypertension. By individually manipulating enzyme activity of CYP4A and ALDH I was able to demonstrate alterations in blood pressure levels and vascular reactivity.

5.6.1 CYP4A

The hypothesis was stimulation of the ω-oxidation pathway, CYP4A with specific agonists (fenofibrate) raises the circulating levels of hexadecanedioate causing blood pressure elevation in adult male WKY_{Gla} rats. In this study, we found that fenofibrate treatment caused a significant reduction in systolic blood pressure in WKY_{Gla} rats. In addition, a reduction in vascular function of mesenteric resistance arteries in response to noradrenaline and relaxation in response to carbachol compared to control rats. It has been found that treatment with fenofibrate increased systolic blood pressure by 3 mmHg in healthy people (Subramanian *et al.*, 2006). Gilbert *et al.* (2013) found that fenofibrate decreased blood pressure in salt-sensitive hypertensive subjects but not in salt-resistant hypertensives; also it reduced heart rate and renal vasoconstriction. The study by Lee *et al.* demonstrated that fenofibrate causes a reduction in blood pressure in a model of DOCA-salt hypertension, thus decreasing renal cyclooxygenase-2 (COX-2) and increasing CYP4A expression (Lee *et al.*, 2011). Similarly, this study showed that the expression of CYP4A was significantly increased in fenofibrate-treated WKY_{Gla} rats compared to control rats.

Fenofibrate is used in the treatment of dyslipidaemia mainly associated with type 2 diabetes mellitus (Rakhshandehroo *et al.*, 2010). Fibrates and steroids are CYP4A inducers, which stimulate peroxisomal-proliferative responses through improving endothelial function and increasing the renal expression of cytochrome P450 enzymes responsible for the formation of epoxyeicosatrienoic acids (EETs) and 20-hydroxyeicosatetraenoicacid (20-HETE) (Gilbert *et al.*, 2013). Cytochrome P450 4A (Cyp4A) enzymes are members of the cytochrome P450 monoxygenase superfamily and catalyse microsomal-hydroxylation of fatty acids

(Rakhshandehroo *et al.*, 2010). Members of CYP4A enzyme family that catalyse ω-oxidation are dependent on PPARα (Hardwick *et al.*, 2009). Activation of PPAR-α has also been found to increase the generation of nitric oxide, promoting renal excretion of Na+ via reduced Na+-K+ ATPase in the proximal tubule (Lee *et al.*, 2011). PPAR-α increases renal tubular CYP4A expression, thus elevating 20-HETE production which reduces sodium retention and blood pressure (Lee *et al.*, 2011). It has been shown that 20-HETE, the major metabolite of CYP4A, has a different action on blood pressure regulation. It has a potent vasoconstriction action leading to increasing blood pressure (Williams *et al.*, 2011b, 2011a). 20-HETE depolarises vascular smooth muscles by blocking the open-state probability of Ca^{2+}-activated K^+-channels (Williams *et al.*, 2011b, 2011a). EETs also play a role in regulation of vascular tone by stimulation of smooth muscle large-conductance Ca^{2+}-activated K^+ channels, producing hyperpolarization and vasorelaxation (Williams *et al.*, 2011b, 2011a). Many studies have reported that sequence variants in the CYP4A gene that produce 20-HETE are linked with the development of hypertension in human population studies (Singh *et al.*, 2007; Gainer *et al.*, 2008; Williams *et al.*, 2011a). Previous experiments in mice suggested that PPAR-α might affect blood pressure. PPAR-α deficient mice are protected from hypertension induced by feeding a high-fat diet or by chronic treatment with glucocorticoids (Tordjman *et al.*, 2001; Bernal-Mizrachi *et al.*, 2003). The PPARa agonist fenofibrate has been reported to both decrease and increase blood pressure. These varying findings need further investigation.

In the second study of this chapter, the hypothesis was inhibition of CYP4A with the potent, selective antagonist HET0016 (N-hydroxy-N′-(4-butyl-2-methylphenyl)-formamidine) would result in a reduction in circulating hexadecandioate levels and blood pressure lowering in the hypertensive $SHRSP_{Gla}$ rat model. Our results showed that no significant changes were observed in blood pressure or vascular function of $SHRSP_{Gla}$ rats treated with CYP4A antagonist (HET0016) compared to vehicle treated rats. Due to prohibitive costs, the study was conducted as a pilot study with a small number of rats to determine if there any effect of HET0016 in blood pressure before pursuing a full study. Previous research performed by Toth *et al* showed that systolic blood pressure of spontaneously hypertensive rats (SHR) decreased after treatment with HET0016 (10 mg/kg·per day, in 10% lecithin solution; intraperitoneally for 5 days) (Toth *et al.*, 2013). In addition, Singh *et al*

showed that dihydrotestosterone (DHT)-induced hypertension was reduced in male Sprague–Dawley rats after treatment with HET0016 (Singh *et al.*, 2007). However, HET0016 had no effect on blood pressure in rats fed a low salt diet, while blood pressure increased by 18 mm/Hg after the rats were fed a high salt diet (Hoagland *et al.*, 2003). Further studies have shown that HET0016 prevents the development of hypertension induced by adrenocorticotrophic hormone in male Sprague-Dawley rats (Zhang *et al.*, 2009).

HET0016 has anti-oxidative and anti-inflammatory effects in the cerebral arteries of spontaneously hypertensive rats (SHR), and disturbing the 20-HETE-mediated autocrine/paracrine signalling pathways in the vascular wall causes a decrease in blood pressure (Toth *et al.*, 2013). Previous studies have indicated that the formation of 20-hydroxyeicosatetraenoic acid (20-HETE) is greater in hypertensive rat models than in normotensive rat, which may contribute to oxidative stress and endothelial dysfunction of hypertensive rats (Dunn *et al.*, 2008). These results suggest that the chronic blockade of 20-HETE formation prevents the development of hypertension, since HET0016 is a selective cytochrome P450 4A inhibitor, which has a potent inhibitory effect on epoxyeicosatrienoic acid (EETs) and 20-HETE (Miyata *et al.*, 2001).

The current study has limitations regarding the dose, route of administration, the solubility of the drug, and the study was not sufficiently powered (i.e. small sample size). The function of the cytochrome P450 metabolites of arachidonic acid in the regulation and maintenance of hypertension is complex and remains to be fully determined, considering that the pathway has both pro-hypertensive and antihypertensive actions (Tordjman *et al.*, 2001). Therefore, additional studies are required.

5.6.2 ALDH

The hypothesis was inhibition of aldehyde dehydrogenase (ALDH) with specific antagonists (disulfiram) leads to decrease the circulating levels of hexadecanedioate causing lowering of blood pressure in hypertensive $SHRSP_{Gla}$ rats. Our results agreed with the hypothesis demonstrating that inhibition of the ω-oxidation pathway enzyme, aldehyde dehydrogenase, results in a significant lowering of blood pressure in hypertensive $SHRSP_{Gla}$ rats after treatment with

disulfiram (aldehyde dehydrogenase inhibitor) for two weeks. A previous animal study found a reduction of blood pressure in spontaneously hypertensive rats treated with disulfiram by intraperitoneal injection 200 mg/kg for 4 consecutive days (Nikodijević *et al.*, 1971). In addition to decreasing systemic blood pressure, disulfiram reduced intraocular pressure in rabbit models (Nagai *et al.*, 2015). Conversely, one of the earlier systematic review studies identified no changes in blood pressure within six weeks of treatment with disulfiram (Peachey *et al.*, 1981).

Disulfiram (tetraethylthioperoxydicarbonic diamide) is an irreversible aldehyde dehydrogenase antagonist which is used for the treatment of alcoholism (Soyka and Müller, 2017). It has also been found that disulfiram is associated with stage-I and stage II hypertension, as an adverse reaction in patients with alcohol dependence (Kulkarni and Bairy, 2013; Grossman and Messerli, 2008; Kulkarni *et al.*, 2014). However, many studies have suggested that severe hypotension occurs after the disulfiram-ethanol reaction (Moreels *et al.*, 2012; Ho *et al.*, 2007; Prancheva *et al.*, 2010; Tummers-de Lind van Wijngaarden *et al.*, 2013). Reduction in peripheral vascular resistance was also observed in albino rabbits treated with disulfiram, which could be a main underlying cause of the hypotension during the disulfiram-alcohol reaction (Bygdeman *et al.*, 1962). In this study, the mesenteric resistance arteries of disulfiram-treated $SHRSP_{Gla}$ rats showed a significant reduction in response to noradrenaline compared to control vessels (Figure 5-19 A). In addition to the antialcoholism effects of disulfiram, it also has shown recent promise as a pharmacotherapy for treating cocaine dependence by inhibition of dopamine beta-hydroxylase, the enzyme that catalyses the conversion of dopamine to noradrenaline (Gaval-Cruz and Weinshenker, 2009). In our study, disulfiram was selected based on its selective inhibition of ALDH. However, disulfiram may have further underlying pleiotropic mechanisms of action, which target several regulatory proteins/signaling pathways.

The levels of ALDH enzyme were measured in our study in the liver tissues, which showed a trend to increase in 20-week-old $SHRSP_{Gla}$ rats compared to WKY_{Gla} rats (Figure 5-22 C). This increase occurred despite a significant reduction in mRNA expression of ALDH1L2 (Figure 5-7 C) indicating that ALDH1L2 mRNA and ALDH proteins are differentially expressed. From these observations, the ALDH ELISA

assay measures total ALDH protein levels, whereas ALDH1L2 is only one of a large superfamily. It is possible that we have just not assessed the particular gene(s) responsible for the elevated ALDH level. Also, mRNA expression is regulated by many factors, such as miRNA, which may inhibit or stimulate the translation of target mRNAs (Fabian *et al.*, 2010).

The aldehyde dehydrogenase (ALDH) gene superfamily encodes important enzymes for the detoxification of endogenous and exogenous aldehyde substrates and maintaining redox balance (Vasiliou and Nebert, 2005). Analysis of the ALDH gene superfamily in the Human Gene Nomenclature Committee (HGNC) database suggested that the human genome includes 19 functional genes and three pseudogenes (Vasiliou and Nebert, 2005; Jackson *et al.*, 2011). ALDH gene mutations cause defects in aldehyde metabolism, which are the basis of several diseases. For example, mutation in ALDH2 E504K raises the risk of Alzheimer's disease amongst the East Asian population (Jackson *et al.*, 2011). Systolic and diastolic blood pressure were lower in a Japanese population who harboured the ALDH2 genetic polymorphism (i.e. heterozygous (*1/*2) and homozygous (*2/*2)) when compared to the *1/*1 group (Ota *et al.*, 2016). The ALDH2*1/*1 genotype correlated with alcohol intake, and was found to be positively associated with hypertension (Yokoyama *et al.*, 2013). GWAS on Asian populations has identified a genetic locus within the ALDH2 gene with a functional variant (rs671), which is highly associated with systolic blood pressure and diastolic blood pressure (Kalra *et al.*, 2014). Also, the ALDH2 Glu504Lys polymorphism was associated with vascular endothelium-dependent dilation disorder in a Han Chinese population with hypertension (Ma *et al.*, 2016). The ALDH2 rs671 L-genotypes have been found to have a protective effect on hypertension in the Han Chinese population, independent of alcohol consumption (Yokoyama *et al.*, 2013). ALDH2 plays a protective role against oxidative stress through acetaldehyde oxidation. A deficiency in ALDH2 leads to increases in oxidative stress, which is a contributing factor for hypertension (Ohsawa *et al.*, 2003). Mutations of the ALDH2 gene occur differentially amongst races; it is common in the Asian population, but it occurs rarely in Caucasian, European or American populations (Ma *et al.*, 2016; Ota *et al.*, 2016). Accordingly, ALDH2 genetic polymorphism is mostly associated with alcohol intake which may affect systolic blood pressure and cardiovascular diseases (Ma *et al.*, 2016; Ota *et al.*, 2016).

It would be beneficial to measure hexadecanedioate levels in our disulfiram treated rats compared to controls to understand the actual role of ALDH in hypertension. However, time constraints and cost prevented a full investigation.

5.6.3 ADH

Alcohol dehydrogenase (ADH) is the second enzyme in the omega oxidation pathway. It has been found that expression of alcohol dehydrogenase 1B (class I), beta polypeptide (ADH1B) and alcohol dehydrogenase 1A (class I), Alpha polypeptide (ADH1A) are strongly associated with hexadecanedioate levels (Menni *et al.*, 2017). A mutation in alcohol dehydrogenase-1B was previously found to be associated with an increased risk of alcoholism (Yokoyama *et al.*, 2013; Borràs *et al.*, 2000). Since moderate-to-heavy alcohol intake is known to increase blood pressure (Mori *et al.*, 2015), the relationship between alcohol, hypertension and hexadecanedioate should be further investigated. Again, unfortunately time constraints meant that I was unable to carry out investigations to examine the effect of modulating ADH enzyme activity on blood pressure, but this would be beneficial for future studies.

Future pharmacological intervention studies could employ the ADH anatagonist, formepizole, or the ADH activator GW4064 (an agonist of the farnesoid x receptor (FXR)). Fomepizole interacts with ADH zinc element and coenzyme nicotinamide-adenine dinucleotide, which prevents its binding to the toxic alcohol and the formation of acidic ethylene glycol metabolites (Mégarbane, 2010). Fomepizole inhibits the formation of toxic metabolites by prolonging the elimination half-life of ethylene glycol and methanol, improving metabolic imbalance, and prevention of end-organ damage such as renal failure (Chu *et al.*, 2002). FXR activation via administration of GW4064 leads to an increase in endothelial nitric oxide synthase (eNOS) as well as a decrease an endothelin–1 (ET–1) expression in cultured human vascular endothelial cells. The regulatory effects of FXR on eNOS and ET–1 in endothelial cells suggests that FXR may have a potential role in blood pressure regulation (Li *et al.*, 2015). This is further supported by studies demonstrating GW4064 was able to reduced systolic blood pressure in SHR rats (Li *et al.*, 2015).

In conclusion, inhibition of the ω-oxidation pathway enzyme, aldehyde dehydrogenase, results in a significant lowering of blood pressure in hypertensive $SHRSP_{Gla}$ rats. We were unable to determine whether levels of hexadecanedioate were also modified by disulfiram treament, and this will be a necessary next step for subsequent investigations. Taken together, our findings suggest that the ω-oxidation pathway is a putative target for further research to elucidate the

mechanism by which hexadecanedioate affects blood pressure. However, increased endogenous levels of circulating hexadecanedioate may occur not only because of increased production through the ω-oxidation pathway but also because of decreased removal from the blood stream. In the next chapter I examine a potential mechanism that is linked to hexadecanedioate excretion from the body.

Chapter 6 Investigating the link between Slco1b2 anion transporter genetic variants and hexadecanedioate levels

6.1 Introduction

Results from previous chapters in this thesis have identified that elevation of circulating levels of hexadecanedioate is associated with increased blood pressure. To examine this relationship, we initially investigated the pathway responsible for hexadecandioate generation, the ω-oxidation pathway, which our results suggest is linked to increased production of the dicarboxylic acid during hypertension (chapter 5). An alternative mechanism that may lead to elevated circulating levels of hexadecanedioate is via altered activity of the solute carrier organic anion transporter (SLCO), which expresses the protein OATP (organic anion transporting polypeptide). This protein plays an important role in the clearance of a range of endogenous compounds from the blood stream, one of which has recently been identified as hexadecanedioate (Lai, 2013; Menni *et al.*, 2017). The current chapter focuses on preliminary investigation of $SHRSP_{Gla}$ and WKY_{Gla} genome sequence to identify variants in the rat Slco1b2 gene. The analysis identified variants within the 3'UTR of Slco1b2, which are located within predicted miRNAs binding sites and may therefore impact on post-transcriptional regulation of Slco1b2 gene expression.

Eleven functional human OATP isoforms encoded by SLCO genes have been discovered and are designated by numbering and letters according to the amino acid sequence identities (Lai, 2013). The proteins within the subfamily are: OATP2A1, OATP3A1, OATP4A1, OATP5A1, OATP6A1, OATP1B1, OATP1B3, OATP2B1, OATP1C1 and OATP4C1 (Roth *et al.*, 2012). OATPs are expressed in several organs; including the liver, muscle, intestine and the blood-brain barrier (BBB), where they control the absorption, distribution and excretion of a range of substrates (Lai, 2013).

In a recent human GWAS study conducted by Menni *et al.* on 6447 participants from the TwinsUK and KORA cohorts, an association was identified between SNP (rs11045656), encoding an Val174Ala amino acid change within the human SLCO1B1 gene, which encodes the OATP1B1 protein, and hexadecanedioate levels in adipose tissue. However, this SNP did not demonstrate an association with hypertension (Menni *et al.*, 2017). A genome-wide study discovered a functional variant of OATP1B1, OATP1B1-Val174Ala (rs4149056), which was significantly associated with 20 endogenous blood sample metabolites, including bile acids,

steroids and dicarboxylic fatty acids (Yee *et al.*, 2016). The dicarboxylic fatty acids, tetradecanedioate and hexadecanedioate were identified as novel substrates of OATP1B1 (Yee *et al.*, 2016). OATP1B1 is a protein that is selectively expressed and localized on the basolateral (sinusoidal) membrane of human hepatocytes (Lai, 2013; Roth *et al.*, 2012). It is encoded by the SLCO1B1 gene and it plays an important role as a specific carrier for removal of endogenous compounds such as organic anions, bile acids, bilirubin, leukotriene C4, estradiol, thyroxine and prostaglandins (Roth *et al.*, 2012; Lai, 2013). OATP1B1 also transports therapeutic drugs from the blood into the liver, for elimination from the body, such as statins, saquinavir, rifampicin, and valsartan (Lai, 2013; Roth *et al.*, 2012) (Figure 6-1). OATP1B1 is also referred to as liver specific transporter 1 (LST–1), OATP2 or OATP-C, and is involved in Na+- and ATP-independent transport of amphiphilic organic compounds (Hagenbuch, 2007).

Homologous protein of human OATPs are found in various species, for instance, humans have two OATP1B transporters (OATP1B1 and OATP1B3), while rodent have a single homolog of this human protein, Oatp1b2 (also known as Oatp4 and Lst-1) (Zaher *et al.*, 2008; Thakkar *et al.*, 2015; Clarke *et al.*, 2014).

In order to examine the potential impact of the anion transporter Slco1b2 in the circulating levels of hexadecanedioate and blood pressure regulation, the genome sequence was compared between normotensive WKY_{Gla} and hypertensive $SHRSP_{Gla}$ rats to identify putative genetics variants (SNPs) in the Slco1b2 gene. Atanur *et al.*(2013) previously carried out whole genome sequencing in 27 rat strains including the University of Glasgow maintained SHRSP and WKY rat strains. This dataset was used in this thesis to identify sequence differences in and near to the Slco1b2 gene.

In this chapter, preliminary investigation of the Slco1b2 gene variants and their putative role in regulating hexadecanedioate levels were examined in the Glasgow SHRSP and WKY rat models.

.

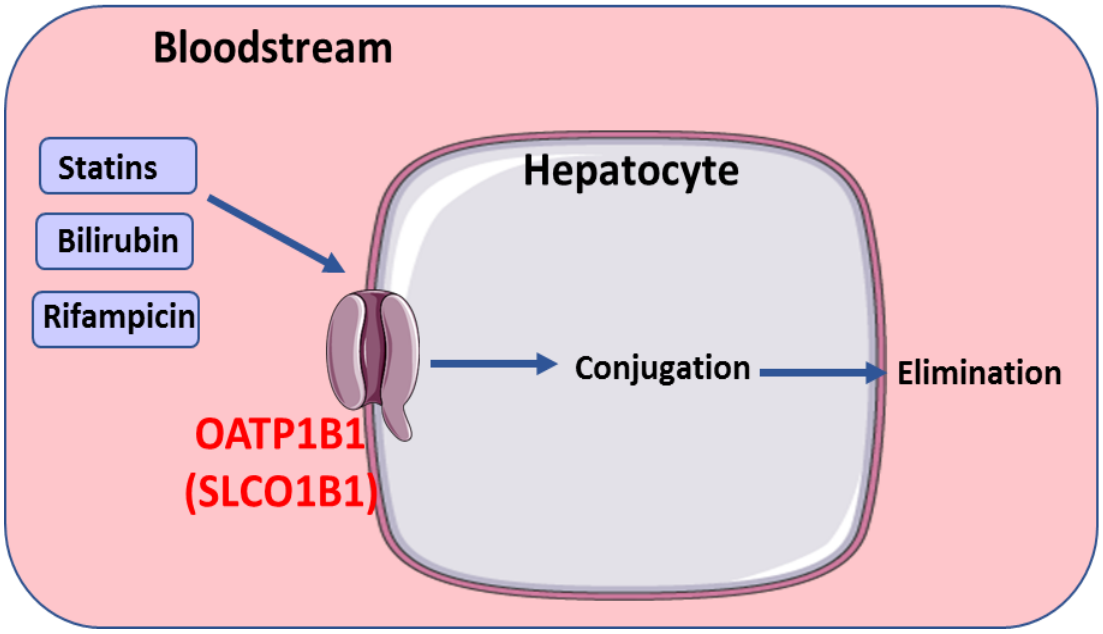

Figure 6-1: The role of OATP1B1 (SLCO1B1) in uptake and elimination of bilirubin, statins and other drugs by the liver.

The solute carrier organic anion transporter (SLCO), which encodes the protein organic anion transporting polypeptide (OATP). SLCO1B1 may have a role in hexadecanedioate elimination from the body. Any alteration in this liver transporter may cause increases in circulating hexadecanedioate levels leading to blood pressure elevation.

6.2 Hypothesis

Genetic variants in the Slco1b2 anion transporter contribute to elevated circulating levels of hexadecanedioate in SHRSP rats.

6.3 Aims

The aims of this chapter are:

1. To investigate the role of anion transporter Slco1b2 as a potential regulator of circulating hexadecanedioate levels by identifying genetic variants (SNPs) between the $SHRSP_{Gla}$ and WKY_{Gla} rat strains

2. To identify putative miRNA binding sites in the 3'UTR sequence of Slco1b2 in $SHRSP_{Gla}$ and WKY_{Gla} rats.

3. To investigate differences in mRNA expression of Slco1b2 in liver tissues of $SHRSP_{Gla}$ and WKY_{Gla} rats.

4. To investigate differences in protein expression of Oatp1b2 in liver tissues of $SHRSP_{Gla}$ and WKY_{Gla} rats.

6.4 Methods

6.4.1 The genome sequence of $SHRSP_{Gla}$ and WKY_{Gla}

The genome sequences for $SHRSP_{Gla}$ and WKY_{Gla} rats have been previously generated and published along with another 25 laboratory rat strains by Atanur *et al*. (2013). The annotated sequence variants in Slco1b2 between $SHRSP_{Gla}$ and WKY_{Gla} were identified using variant visualiser and Ensembl genome browser (Rat Rnor_5.0).

6.4.1.1 Variant visualiser on Rat Genome Database (RGD)

Variants (SNPs) and indels between $SHRSP_{Gla}$ and WKY_{Gla} rat strains were identified using variant visualiser on Rat Genome Database (RGD) using the the Rat Rnor_5.0 Genome assembly version 79. The Rat Genome Database (RGD); http://rgd.mcw.edu/offers tools for gene prediction, identification of variants (SNPs) and hosts a 'traits and phenotypes' database for several rat strains.

6.4.1.2 Rat Rnor_5.0 Genome assembly

Examination of the rat genome RNA was performed using assembly 79 to identify the annotated sequence variants in Slco1b2. Ensembl; http://www.Ensembl.org/ is a joint project between the European Bioinformatics Institute (EMBL – EBI) and the Wellcome Trust Sanger Institute which aims to maintain and update annotation of a wide range of species genomes. Genomic variants are annotated to highlight sequence variants based on their predicted effect and to identify genes affected by large structural variants that are unique to each rat strain.

6.4.1.3 Sequencing analysis

Sequencing was analysed using CLC genomics workbench 7.5. Experimental sequences were aligned with known sequences derived from the bioinformatics database Ensembl genome browser.

6.4.2 Computationally predicted target databases

All this information was cross referenced with known miRNA precursor sequences that are mapped and stored in the target prediction database. Information for

miRNA sequences, annotation and biological function interpretations for genes of interest are housed in number of databases such as miRTarBase and miRBase databases.

6.4.2.1 miRTarBase database

miRTarBase 7.0 database; http://miRTarBase.mbc.nctu.edu.tw/ is a comprehensively annotated, experimentally validated miRNA-target interactions database. miRNA-target interactions have been validated experimentally by western blot, microarray and next-generation sequencing experiments and by reporter assay that are available in the literature.

6.4.2.2 miRBase database

miRBase database; http://www.mirbase.org/ is a searchable database of published miRNA sequences and annotation. The miRBase Sequence database lists predicted mature miRNA sequence (termed miR) and stem loop miRNA (hairpin) (termed mir in the database). Also, this database provides information about the location and sequence of both stem loop and mature sequences.

6.4.3 Animals

Wistar Kyoto (WKY) and spontaneously hypertensive stroke prone rats (SHRSP) were obtained from breeding colonies in Glasgow University. The rats were housed in cages on a 12 hours light/dark circle at room temperature (21± 3°C). Food and water *ad libidum* were provided to the rats. The study protocols were approved by the home office and conducted in accordance with the Animals' Scientific Procedures Act1986 under the project license of Dr Delyth Graham (70/9021).

6.4.4 Samples

Liver tissues from male untreated WKY_{Gla} and $SHRSP_{Gla}$ rats were obtained at five, sixteen and twenty-weeks of age. At sacrifice, liver tissues were harvested and snap-frozen in liquid nitrogen and stored at -80°C for western blot assay to determine the level of Oatp1b2 protein expression and Taqman assay for mRNA expression.

6.4.5 mRNA expression

6.4.5.1 qRT-PCR

RNA was extracted, quantified, DNAse treated and reverse transcribed as described in section 2.4.1 in liver tissues of 16-week-old male WKY_{Gla} and $SHRSP_{Gla}$ rats. Total mRNA expression of Slco1b2 (Rn01492635_m1) was assessed by Taqman® assay systems. All samples were amplified in triplicate. Fluorescence of FAM and VIC dyes was measured for all reactions during temperature cycling as detailed in section 2.4.1.6. GAPDH was used as the housekeeping gene. Data was analysed as detailed in section 2.4.1.7.

6.4.6 Western Blot

6.4.6.1 Protein Extraction

Protein from liver tissues was extracted using a 1X RIPA buffer (20 mM Tris HCl, pH 8, 150 mM NaCl, 0.5% nonidet P-40 (NP-40), 0.5% sodium deoxycholate, 0.1% sodium dodecyl sulphate (SDS), and 5 Mm ethylenediaminetetraacetic acid (EDTA), final pH 7.4. On the day of use, one tablet of Roche EDTA-free protease inhibitor cocktail table (Roche, Hertfordshire, UK) and one tablet of PhosSTOP Easy pack phosphatase inhibitor (Sigma Aldrich Co Ltd, Irvine, UK) were added for every 10 ml of RIPA lysis buffer used. The samples were homogenized using a bead homogeniser running at 30 Hz for 30 seconds and then centrifuged at 10,000 xg for 10 mins at 4°C. The supernatant containing the protein was transferred to a new tube and kept on ice. 5 µL of supernatant was removed to determine protein concentration, while the rest of the protein was stored at -80°C until needed.

6.4.6.2 Protein Quantification

The protein concentrations were determined using Pierce BCA (bicinchoninic acid) protein assay kit (Thermo fisher Scientific, Loughborough, UK), according to the manufacturer's instructions. The bovine serum albumin (BSA) standards were provided in dilution range 25 ng/µl – 2 µg/µl. The samples were diluted 10x before quantification. Assay was performed in flat bottom 96 well plate and 25 µl of each sample and standards are add to the plate. Working reagent (WR) contains reagents A and B included in the kit, which were mixed at a ratio of 50:1; respectively. WR is then added to the plate by using a multichannel pipette and

then the plate was protected from light and incubated at 37 ºC for 30 minutes. Absorbance at 562 nm was determined for all wells using a Wallac Victor2 plate reader (Wallac, Turku, Finland). Both standards and samples were measured in duplicate and the average calculated. Results were then calculated according to the linear equation based on the standard curve generated.

6.4.6.3 Sample preparation

Protein samples were prepared in a total volume of 20 µl at a concentration of 30 µg/well µl with 4x loading buffer (NuPAGE LDS Sample buffer) as follows:

Reagent	Volume (µl)
Nuclease-free water	(15-X) µl
Protein	X µl
NuPAGE LDS Sample buffer (4X)	5 µl
Total volume	20 µl

Samples were denatured for 10 minutes at 99ºC to ensure proteins were denatured and cooled on ice immediately for at 5 minutes before adding to gels.

6.4.6.4 Sodium dodecyl sulphate-polyacrylamide electrophoresis

Protein were resolved using sodium dodecyl sulphate-polyacrylamide gel electrophoresis (SDS-PAGE). 12% polyacrylamide gel contains 40% (v/v) of N, N'-methylene-bis-acrylamide (polyacrylamide 30%), 25% (v/v) of Tris pH 8.8 (11.25 mM), 0.1% (v/v) SDS, 300 µl ammonium persulphate (APS) and 30 µl of N,N,N',N'Tetramethylethylenediamine (TEMED) were used. A 5% stacking gel containing 13.3% (v/v) polyacrylamide 30%, 25% (v/v) Tris pH 6.8 (3.75 mM), 0.1% (v/v) SDS, 1% (v/v) APS and 0.1% (v/v) TEMED.

Resolving gel

Reagent	Volume
30% acrylamide	12 ml
1.5 M Tris (pH8.8)	7.5 ml
10% SDS	300 µl
H_2O	10.2 ml
TEMED	30 µl
10% APS	300 µl

Stacking gel

Reagent	Volume
30% acrylamide	2 ml
0.5 M Tris (pH6.8)	3.75 ml
10% SDS	159 µl
H_2O	9.1 ml
TEMED	15 µl
10% APS	150 µl

Subsequently, gels were loaded with samples and 15 µl of Precision Plus Protein™ (10–250 kD) ladder (Bio-Rad Laboratories, Watford, UK). Gels were electrophoresed at 150 V in running buffer (50 ml 20x NuPAGE bolt running buffer to 950 ml deionized water) for 1 hour.

6.4.6.5 Protein blotting

Following electrophoresis, the stacking gel was removed and lanes not including protein were cut from the resolving gel. Four pieces of Whatman 3 mm chromatography blotting paper and a piece of Amersham Hybond-P polyvinylidene difluoride membrane (Amersham Bioscience UK Limited, Buckingham, UK). Filter paper and transfer sponges were equilibrated in transfer buffer and membranes were activated with methanol. Transfer buffer consists of 0.025 M Tris pH10.5; 0.2 M Glycine; 20% methanol. Transfer apparatus was prepared as follows (cathode to anode): 1X transfer sponge, 2x Whatman sheets, gel, membrane, 2x Whatman sheets, and 1x transfer sponge. Blots were transferred at 100V for 90 minutes.

Transfer Buffer

Reagent	Volume (2L)
Tris (Base)	6.06 g
Glycine	28.8 g
Methanol	400 ml
Deionized water	1600 ml

6.4.6.6 Antibody probing and washing

Once the membranes had been transferred, membranes were blocked with SEA BLOCK solution (Thermo Scientific, Loughborough, UK) (1:1 dilution with Tris-buffered saline Tween buffer (1xTBS-T)) for 1 hour. Blocking was carried out on a lab shaker (Luckham R100) at 50 oscillations per minute.

SEA BLOCK solution consisted of:

Steelhead salmon serum

Phosphate-buffered saline

0.1% sodium azide

TBS-T (Tris-buffered saline Tween buffer) 0.5% tween (10x Stock)

Reagent	Volume
Tris base	24.2 g
NaCl	87.7 g
Tween 20	5 ml
Distilled water	1000 ml

PH to 7.5 with HCl

Following blocking, the membranes were washed with 1x TBS-T three times for 10 minutes each and then incubated with primary antibody Oatp4 (Oatp1b2)/ $IgG_{1\kappa}$ light chain (Figure 6-2) (Santa Cruz Biotechnology, INC) diluted in blocking buffer at the 1:1000 dilution overnight at 4ºC with shaking. Following overnight incubation, the membrane was washed three times for 10 minutes with 1x TBST-T at room temperature, followed by incubation with 1:15000 dilution of the appropriate secondary antibody, goat anti-mouse IgG (H+L) (Thermo Scientific, Loughborough, UK) for 1 hour at room temperature with shaking. The membrane was then washed with 1x TBS-T three times for 10 minutes followed by washing with phosphate-buffered saline (PBS) (Sigma Aldrich Co Ltd, Irvine, UK) for 1 minute at room temperature with shaking. Proteins were developed using Li-COR (*Li-COR*, Nebraska, USA). The images were visualized and analysed using Image Studio™ Software. Membranes were then incubated with housekeeping protein GAPDH Rabbit / IgG Polyclonal antibody (Thermo Scientific, Loughborough, UK) diluted in blocking buffer at the 1:5000 dilution overnight at 4ºC with shaking.

Following overnight incubation, the membrane was washed three times for 10 minutes with 1x TBST-T at room temperature, followed by incubation with 1:15000 dilution of the appropriate secondary antibody, rabbit anti-mouse IgG (H+L) (Thermo Scientific, Loughborough, UK) for 1 hour at room temperature with shaking. The membrane was then washed with 1x TBS-T three times for 10 minutes followed by washing with phosphate-buffered saline (PBS), for 1 minute at room temperature with shaking. Proteins were developed using Li-COR exactly as described above.

6.4.6.7 Membrane stripping and re-probing

The level of a protein in a sample was measured relative to the level of a housekeeping protein. Membranes were stripped to remove conjugated antibodies and re-probed with antibodies specific to the housekeeper. The membranes were stripped in 10 ml of a mild stripping buffer (0.2 M Glycine, 1% SDS, and 1% Tween20R, pH 2.2) for 10 minutes at room temperature on a shaker at 50 oscillations per minute, then washed with 1x TBS-T 3 times for 10 minutes each. Membranes were then re-incubated overnight at 4 ^{o}C, washed and analysed for the housekeeping protein exactly as described above.

Stripping buffer

Reagent	Volume
Glycine	15 g
SDS	1 g
Tween 20	10 mL
Distilled water	800 mL

Adjust pH to 2.2

Bring volume up to 1 L with distilled water

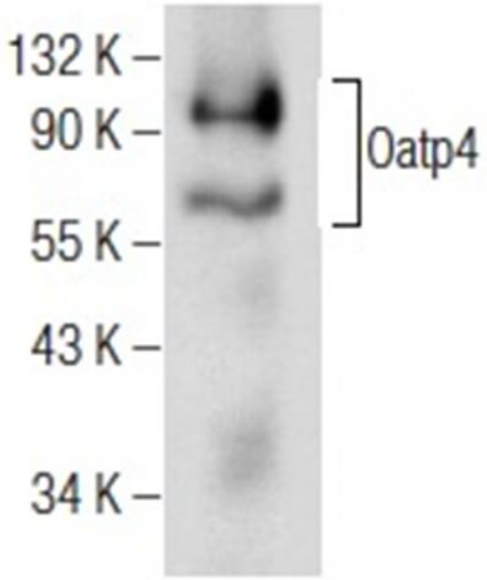

Figure 6-2: Representative image of the Oatp4 (Oatp1b2) expression in liver tissues shows the range and band size provided by the manufacturer (Santa Cruz Biotechnology).

6.4.7 Statistical analysis

All results are displayed as mean ± SEM using Graphpad Prism. Western blot and Taqman gene expression data were analysed using student's T-test. Statistical significance was assumed at P-value less than 0.05.

6.5 Results

6.5.1 Homologue of human SLCO1B1 in rat (Rattus Norvegicus)

The Ensembl genome browser was used to confirm the rat homologue of the human SLCO1B1 gene and the rat Slco1b2 is located on rat chromosome 4 (Figure 6-3).

6.5.2 Comparison of rat Slco1b2 genome sequence between $SHRSP_{Gla}$ and WKY_{Gla}

We have examined 15,000 bp upstream from the transcriptional start site of Slco1b2. We identified two genetic variants within the target Slco1b2 gene when comparing $SHRSP_{Gla}$ and WKY_{Gla} genome sequence using Ensembl genome browser (Rat Rnor_5.0).

(1) An insertion of 9 nucleotides (GTCTATCTA) within an intronic region (intron 3 of 14) on chromosome 4 at position 240,062,637 bp, band 4q44 forward strand in the WKY_{Gla} strain rather than G nucleotide in the $SHRSP_{Gla}$ strain.

(2) Deletion of 4 nucleotides (TATC) within the 3'untranslated region (UTR), on chromosome 4 at position 240,102,755 bp of the WKY_{Gla} genome sequence (Figure 6-4).

6.5.3 miRNA / transcription factors binding sites within Slco1b2 gene and potential impact of the deletion

Here, we used miRTarBase database to identify predicted miRNA binding sites within the target gene Slco1b2 gene. The analysis was carried out in sequences of 3 different species; human, rat and mouse, which showed 3 miRNAs were identified within target human SLCO1B1 (i.e. miR_335_5p, miR_26b_5p and miR_511_5p). One miRNA was also identified within target mouse Slco1b2 (miR_698_3p) using Next-Generation Sequencing (NGS). However, no miRNA has yet been identified in rat Slco1b2 (Figure 6-6).

The analysis was then carried out in sequences of rat and mouse using CLC genomics workbench to rely on the conservation in the target region (i.e. deleted 4 nucleotides TATC) within 3'UTRs between the two species. The Sequence alignment that involved the deleted 4 nucleotides (TATC) (blue highlighted) in rat

showed lack of sequence of conservation when compared to mouse sequence (Figure 6-7).

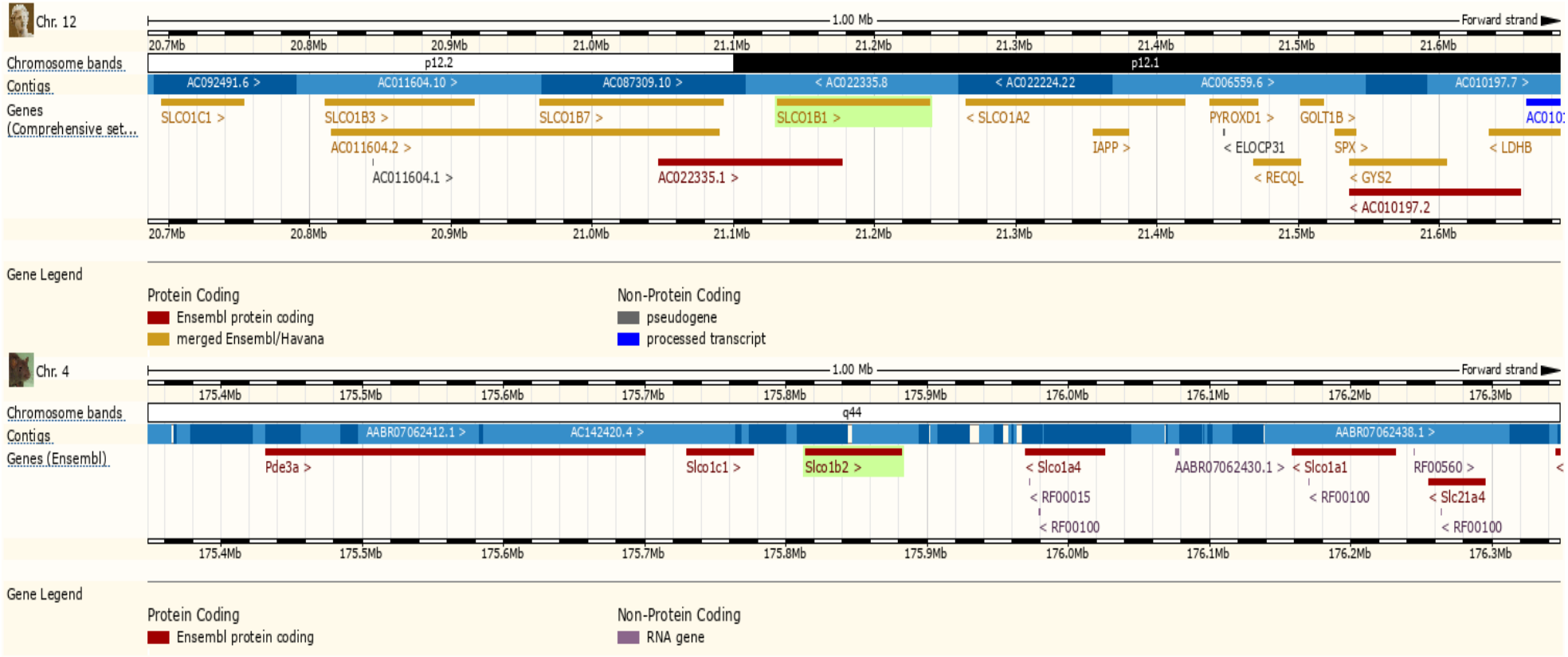

Figure 6-3: Ensembl genome browser (Rat Rnor_5.0) identified human SLCO1B1 and its rat homolog Slcolb2.

Slco1b2, located on rat chromosome 4, is a single rodent homolog of the human SLCO1B1 gene on chromosome 12 (green highlight).

Figure 6-4: Genotype Analysis of Slco1b2 sequence identified an insertion of 9 nucleotides and a deletion of 4 nucleotides in WKY_{Gla} strain compared to $SHRSP_{Gla}$ strain.

Screenshot taken from RGD browser identifying an insertion of 9 nucleotides in WKY_{Gla} at position 240,062,637 bp and a deletion of 4 nucleotides in the WKY_{Gla} strain at position 240,102,755 bp on rat chromosome 4.

Slco1b2 (NM_031650)

```
2161 aatgaaacac ctctttaagg aaagagaaag atacatctgt tgctgtgttt tcaaataccc
2221 ccggggttct ttcactgaaa tttttcatac tttatatgta atagagaatt tataacccta
2281 tgcatttata attaaacaaa ttgcaaatca aaagaaataa gagaaccctt gttagggtat
2341 agctgtgcat ttgtagctaa agatttggag atatataaac aggtattcgc ttaagcattt
2401 ataactcaat aaaatagaga atggggcaag gatggacaaa ggggaaaggg actgtgaaaa
2461 attgttgtct ttaaaaatca aaatttgaat cgtactattc atgccagaag cttctgtgat
2521 aggtgacttc atgatgtggc atattctggt atccccggta agtcaaatat atatatatat
2581 atatatatat atatatatat atatatatat atatatatat ttttttttt ttttttggag
2641 ctggggaccg aacccagagc cttgcgcttg ctaggcaagt gctctaccac tgagttaaat
2701 ccccaaccct aagtcatata tttttaatta ttaattttaa attgtgttta atgacatatc
2761 catcttcttt gtacatactg tacagaatat tgagaataaa acagagacgt ttaggatgtg
2821 agatatctct gtctatctct atctctaccc ctagcttcac ctccttctct gtctccatct
2881 ccctatctat ctatctatct atctatctat ctatctatct atcatctatc tatccatcta
2941 tgtatctgtc tatctattat ctatctatct atctatctat ctatctatct atctatctat
3001 ctatctatct acaatctccc caaatatcta aaattaagat agagtgaatg agacagatat
3061 ctgtagacac tgtattttct tgtgtgatca gatctagtgt ggtggatgat agaagttgaa
3121 cttgctttat tgctatgtgt taaaatattt tgtttgcatt aaaatggcct attgaaatgc
3181 ttttctgttc ctataataaa ataacctgat gaaaaagt
```

Figure 6-5: 3' untranslated downstream sequence of the Slco1b2 (NM_031650) gene in $SHRSP_{Gla}$.

Green highlighted nucleotides represent the stop codon (TAA) and red highlighted nucleotides indicate the position of deletions within 3'UTR of the $WKY_{Gla.}$

A. Human

ID	Species (miRNA)	Species (Target)	miRNA	Target	Validation methods: Strong evidence: Reporter assay	Strong evidence: Western blot	Strong evidence: qPCR	Less strong evidence: Microarray	Less strong evidence: NGS	Less strong evidence: pSILAC	Less strong evidence: Other	Sum	# of papers
MIRT018741	Homo sapiens	Homo sapiens	hsa-miR-335-5p	SLCO1B1				✔				1	1
MIRT030029	Homo sapiens	Homo sapiens	hsa-miR-26b-5p	SLCO1B1				✔				1	1
MIRT732548	Homo sapiens	Homo sapiens	hsa-miR-511-5p	SLCO1B1	✔	✔	✔					3	1

B. Mouse

ID	Species (miRNA)	Species (Target)	miRNA	Target	Validation methods: Strong evidence: Reporter assay	Strong evidence: Western blot	Strong evidence: qPCR	Less strong evidence: Microarray	Less strong evidence: NGS	Less strong evidence: pSILAC	Less strong evidence: Other	Sum	# of papers
MIRT594256	Mus musculus	Mus musculus	mmu-miR-698-3p	Slco1b2					✔			1	1

C. Rat

ID	Species (miRNA)	Species (Target)	miRNA	Target	Validation methods: Strong evidence: Reporter assay	Strong evidence: Western blot	Strong evidence: qPCR	Less strong evidence: Microarray	Less strong evidence: NGS	Less strong evidence: pSILAC	Less strong evidence: Other	Sum	# of papers

Figure 6-6: MiRTarBase analysis showed the identified miRNA within a target (A) human SLCO1B1, (B) mouse Slco1b2 and (C) rat Slco1b2.

MiRTarBase analysis showed (A) three miRNAs within target human SLCO1B1 was identified in several validation methods. In addition, (B) one miRNA was identified within target mouse Slco1b2 using Next-Generation Sequencing (NGS). However, no miRNA was identified in rat Slco1b2 (C).

Figure 6-7: Rat and mouse Slco1b2 3' UTR region sequences.

The rat's sequence alignment that involved the deleted 4 nucleotides (TATC) (blue highlighted, red arrow) showed the absence of conservation when compared to mouse sequence alignment.

6.5.4 Slco1b2 expression in liver tissues of $SHRSP_{Gla}$ and WKY_{Gla}

Slco1b2 mRNA levels were assessed by quantitative real time PCR (qRT-PCR) in liver samples from male WKY_{Gla} and $SHRSP_{Gla}$ aged 16-week old . Slco1b2 mRNA expression was significantly decreased in $SHRSP_{Gla}$ compared to WKY_{Gla} (P=0.008) (Figure 6-8).

6.5.5 Oatp1b2 protein expression in liver tissues of $SHRSP_{Gla}$ and WKY_{Gla}

To further investigate the extent of the changes in Slco1b2 expression, total protein Oatp1b2 levels in the liver tissues from WKY_{Gla} and $SHRSP_{Gla}$ were measured by Western blot. Representative immunoblots are shown in Figure 6-9 A, B.

Smeared bands are detected, which limited the analysis and prevented confident interpretation of the data. However, the analysis was preformed according to the predicted and observed molecular weights of Oatp1b2 provided by Santa Cruz Biotechnology (Figure 6-2). Oatp1b2 protein in $SHRSP_{Gla}$ rat at 5 weeks of age significantly decreased when compared to WKY_{Gla} levels. While protein levels in liver sample from $SHRSP_{Gla}$ rats at 16 weeks and 20 weeks showed no difference to that of WKY_{Gla} rats (Table 6-1), (Table 6-2).

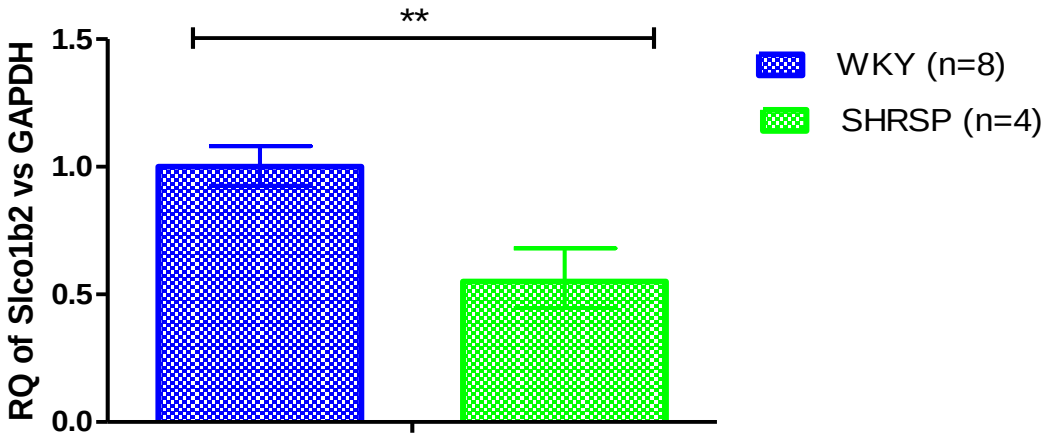

Figure 6-8: The expression level of Slco1b2 in liver tissues of $SHRSP_{Gla}$ and WKY_{Gla} rats.

The expression level of Slco1b2 was significantly decreased in liver tissues of 16-week-old $SHRSP_{Gla}$ (n=4) compared to WKY_{Gla} rats (n=8) (P**<0.01). Values are presented as mean ± SEM.

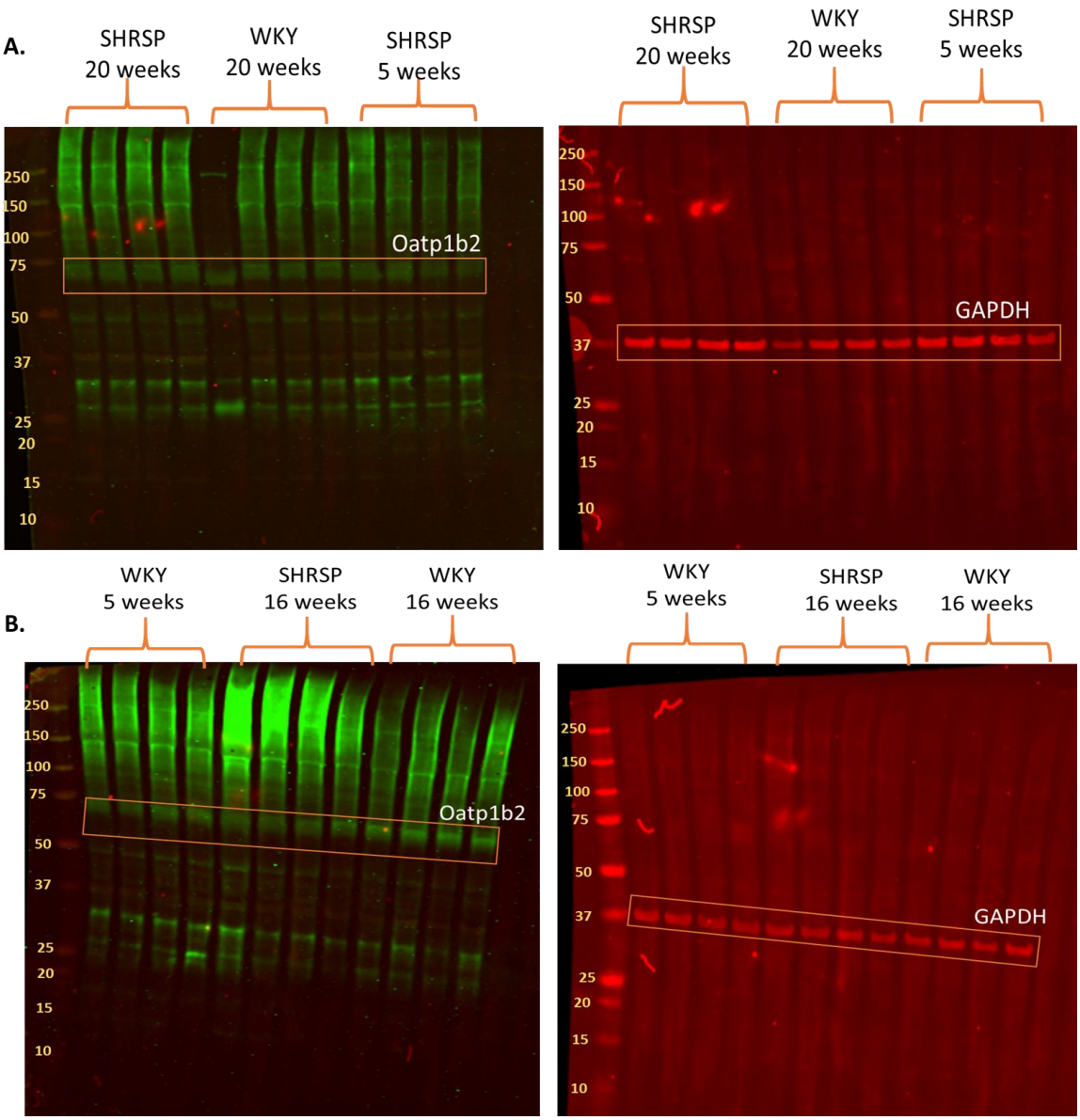

Figure 6-9: Western blot analysis of Oatp1b2 in WKY_{Gla} and $SHRSP_{Gla}$ rats from liver tissue.

Protein lysates from snap frozen liver tissue from $SHRSP_{Gla}$ and WKY_{Gla} rats were prepared, quantified, electrophoresed, blotted, and probed for Oatp1b2. (A) Representative immunoblots of $SHRSP_{Gla}$ at 20 weeks, WKY_{Gla} at 20 weeks and $SHRSP_{Gla}$ at 5 weeks (n=4/group). (B) Representative immunoblots of WKY_{Gla} at 5 weeks, $SHRSP_{Gla}$ at 16 weeks and WKY_{Gla} at 16 weeks (n=4/group). GAPDH bands demonstrates equivalent sample loading, while smearing was observed in Oatp1b2 bands, which limited the analysis.

Table 6-1: Intensity levels of Oatp1b2 in liver tissue of $SHRSP_{Gla}$ compared to WKY_{Gla} (n=4/group).

Age	5 weeks		16 weeks		20 weeks	
Strain	WKY	SHRSP	WKY	SHRSP	WKY	SHRSP
Oatp1b2 intensity	1090	878	1400	1470	1400	1030
	1130	910	1080	1150	1280	1090
	1440	1020	1280	989	1040	1340
	1510	913	1170	1100	1000	1330
TTEST (P value)	0.02		0.67		0.89	

Table 6-2: Protein expression of Oatp1b2 normalized to GAPDH in liver tissue of $SHRSP_{Gla}$ compared to WKY_{Gla} (n=4/group).

Age	5 weeks		16 weeks		20 weeks	
Strain	WKY	SHRSP	WKY	SHRSP	WKY	SHRSP
Oatp1b2/GAPDH	0.06	0.03	0.08	0.11	0.07	0.04
	0.06	0.03	0.07	0.08	0.06	0.04
	0.10	0.03	0.09	0.06	0.04	0.05
	0.12	0.04	0.06	0.07	0.04	0.05
TTEST (P value)	0.01		0.77		0.27	

Due to the presence of smearing, we were unable to detect the exact bands with confidence. Therefore, we relied on the molecular weights of Oatp1b2 provided by the manufacturer for our analysis. Reduction in protein expression levels of Oatp1b2 in liver tissue of 5 weeks old $SHRSP_{Gla}$ compared to WKY_{Gla}.There were no differences in expression levels of Oatp1b2 in liver tissue of $SHRSP_{Gla}$ at 16 weeks and 20 weeks compared to WKY_{Gla}. GAPDH demonstrates equivalent sample loading, and expression levels of Oatp1b2 are displayed as ratio intensity normalised to GAPDH.

6.6 Discussion

The recent studies by Yu *et al.*(2016) and Menni *et al* (2017) have indicated an association between human SLCO1B1 mutations and hexadecanedioate serum levels. These associations would suggest that human SLCO1B1 has a putative role in hexadecanedioate removal from the body and any alteration in this transporter may cause increases in circulating hexadecanedioate levels potentially leading to blood pressure elevation. In this chapter, the rat Slco1b2 homolog was investigated by comparing the genome sequence of the normotensive WKY_{Gla} and hypertensive $SHRSP_{Gla}$ rats and identifying genetic variants (SNPs) between these rat strains. We examined 15,000 bp upstream of the transcriptitonal start site to explore how far SNPs and indels may exist from the affected gene. The analysis demonstrated an insertion of 9 nucleotides (GTCTATCTA) within an intronic region of the WKY_{Gla} strain rather than G nucleotide in the $SHRSP_{Gla}$ strain. Also, there was a deletion of 4 nucleotides (TATC) in the 3'UTR of WKY_{Gla} genome sequence (Figure 6-3).

Intronic variants may affect structure and function of proteins by affecting alternative splicing of mRNA. Alternative splicing is a regulatory process of gene expression, resulting in multiple protein isoforms being encoded by a single gene. *Cis- and trans-acting* regulatory elements regulate the alternative splicing. During this process, *cis-acting* regulatory elements in the precursor mRNA sequence determine which particular exons are included and excluded from the final produced mRNA. Accordingly, proteins are translated from spliced mRNAs. The mechanisms affecting alternative splicing include alteration of either *cis*-acting elements by a direct impact on the expression of one gene or *trans*-acting factors which may affect the expression of many genes (Wang and Cooper, 2007). Time constraints prevented further investigation of the impact of the 9 nucleotides insertion within the intronic region of Slco1b2, however future studies could examine the proximity of the variant to the nearest canonical splice site together with investigation of any potential splice variants.

The 3'UTR plays a role in post-transcriptional regulation of gene expression through mRNA stability and translational efficiency. Mutations affecting the 3'UTR region may interfere with mRNA stability and translation through affecting the termination codon and polyadenylation signal leading to overexpression or

downregulation of proteins (Mignone *et al.*, 2002; Chatterjee and Pal, 2009). MicroRNA (miRNA) binding sites are located within the 3'UTR, and therefore SNPs and indels identified within these regions may affect the binding sequences of miRNAs on their target mRNA and subsequently alter the gene expression levels (Gu *et al.*, 2016). miRNAs are small non-coding RNAs (*trans-acting* elements), which regulate protein-coding gene expression at the post-transcriptional phase either by promoting destabilization/degradation of mRNA or inhibition of translation leading to RNA silencing or regulation of mRNA abundance (Matoulkova *et al.*, 2012). Due to their ubiquitous role in gene regulation, miRNAs are involved in a wide range of physiological processes such as cell proliferation and apoptosis, also their dysregulation has been related to many pathological disorders; such as diabetes and cancer (Vimalraj and Selvamurugan, 2011). The main feature of miRNA function is that a specific miRNA can control multiple mRNA targets that are involved in the same biological pathway which makes them good candidates for novel therapeutics (Wahid *et al.*, 2010; Vimalraj and Selvamurugan, 2011) (Figure 6-11). Bioinformatics approaches using computational methods, are extensively used for identification of predicted miRNA binding sites and their functional annotation (Liu *et al.*, 2014).

The rat genome database incorporated with miRTarBase database have been used in this study to determine whether the identified genetic variants disrupt predicted miRNA binding sites. The analysis carried out by using miRTarBase database showed that no miRNAs within the target gene (Slco1b2) were identified in the rat genome sequence. However, when the analysis was carried on the human SLCO1B1 and mouse Slco1b2, 3 miRNAs were identified in human SLCO1B2 gene by different validation methods (i.e. literature, western blot and qPCR), one miRNA was identified in mouse Slco1b2 gene using next-generation sequencing. The lack of sufficient rat Slco1b2 genome information may have limited further identification of target miRNAs. As mature miRNA and their target sequences can be well conserved across species, the sequence conservation in the 3' UTR was examined between rat and mouse using the CLC genomics workbench. Our analysis showed that a lack of conservation near to the identified deletion region was observed in the sequence of 3'UTR region between rat and mouse making the analysis challenging to predict potential target miRNA.

Several clinical studies have been conducted to investigate genetic variants in the human SLCO1B1 gene and their association with cardiovascular and metabolic diseases. For example, loss of function mutations have been identified in the SLCO1B1 gene among African-American individuals from the Atherosclerosis Risk in Communities (ARIC) study (Yu *et al.*, 2016). This study not only showed an association between SLCO1B1 and hexadecanedioate serum levels, but also demonstrated that one copy of the mutated T allele in SLCO1B1 was associated with increased risk of incident heart failure (Yu *et al.*, 2016).

A single nucleotide polymorphism rs4149056 (known as Val174Ala) that introduced amino acids changes within the transmembrane domains of OATP1B1 (i.e. alteration of the amino acid at position 174 from valine to alanine) has been found to be associated with a decrease OATP1B1 activity and increased plasma levels of statins and subsequent muscle toxicities (Clarke *et al.*, 2014; Pasanen *et al.*, 2007; Hartkoorn *et al.*, 2010; Huang *et al.*, 2012). Furthermore, this SNP rs4149056 was found to be correlated with high levels of tetradecanedioate and hexadecanedioate in plasma samples from individuals on pravastatin/cyclosporine treatment, which indicates the potential utility of tetradecanedioate and hexadecanedioate as quantitative biomarkers of OATP1B1 activity (Yee *et al.*, 2016). Downregulation of OATP activity was found to be associated with impairment in bile acid removal from the blood to hepatocytes leading to increased excretion of sulphated and glucuronic acid conjugated bile acids into the urine (Kullak-Ublick *et al.*, 2000; Gartung and Matern, 1997; Takikawa, 2002).

In the current study, the expression of Slco1b2 was significantly decreased in hypertensive $SHRSP_{Gla}$ rats compared to normotensive WKY_{Gla} rats (Figure 6-8). This could be associated with elevated circulating hexadecanedioate levels as well as increases in bile acid metabolite levels in liver, kidney and adipose tissues of hexadecanedioate-treated rats compared to untreated control WKY rats, as shown in Chapter 4. To confirm this result, protein expression of Oatp1b2 was measured in liver tissue of $SHRSP_{Gla}$ rats compared to WKY_{Gla} rats, which suggested a reduction in Oatp1b2 expression at 5 weeks of age in $SHRSP_{Gla}$ rats compared to WKY_{Gla} rats, whereas no differences were observed in adult rats (Figure 6-10). Previous studies have shown that the expression of Oatp1b2 is low at neonatal stage, significantly rising after weaning age and reaching a peak, which is maintained at high levels during adulthood. However, the expression of Oatp1b2

is shown to decrease in liver tissues of aged rats (Hou *et al.*, 2014; Cheng *et al.*, 2005). RNA and protein represent different molecular stages of the genetic information flow process within a cell, in which these molecules are dynamically produced and degraded. Indeed, proteins may have different half lives as the result of different protein synthesis and degradation that may account for the mRNA and protein discrepancies (Greenbaum *et al.*, 2003). This may explain why expression of the Slco1b2 gene and expression of the Oatp1b2 protein are different in SHRSP rats at 16 weeks of age. Moreover, a potential limitation to this study is the presence of smeared bands of Oatp1b2, which prevent the detection of specific bands of the protein. This may be due to technical reasons e.g. errors or limitations resulting from poor quality Oatp1b2 antibodies for western blotting, which may contribute to the poor quality blots. Further studies would be required to determine whether the differences are due to biological or technical reasons. This could also cause discrepant results between mRNA and protein levels in this study.

In conclusion, this study has identified genetic variants within the Slco1b2 gene that may contribute to altered expression/function of the Oatp1b2 transporter, which may in turn contribute to elevated levels of circulating hexadecanedioate in the SHRSP rat model of hypertension. Further investigation will be required to confirm these findings and determine the underlying mechanisms.

Chapter 7 General Discussion

7.1 Overview Summary

It is well established that hypertension is the major indicator of early cardiovascular risk in populations. The clinical management of hypertension is one of the most common interventions in UK primary care, accounting for approximately £1 billion in drug costs alone (NICE, 2018a). The annual healthcare cost of cardiovascular disease; including hypertension in the UK is estimated at around £16.3 billion (Luengo-Fernández *et al.*, 2006). A substantial reduction in healthcare costs will be achieved if all the hypertensive patients had their blood pressure controlled to target (Elliott, 2003). However, effective blood pressure control to meet the clinical targets in hypertensive patients has been unsuccessful (Kotchen, 2003; Egan *et al.*, 2011), with an increase in an incidence of resistant hypertension (Naseem *et al.*, 2017; Barochiner *et al.*, 2013; Cifkova *et al.*, 2016). Suboptimal therapy is the most common reason for failure to reach the blood pressure target. In addition, the complexity of medical regimens failed to control hypertension due to the challenge of patient adherence (Calhoun *et al.*, 2008; Carey and Whelton, 2018; Krieger *et al.*, 2018). Development of antihypertensive drugs has essentially stalled over the last decade, and there is still much uncertainty and no clear single identifiable cause underlying the pathophysiology of hypertension. There is an urgent need to discover novel pathways that will identify novel drug targets or enable effective targeting of therapy. For those reasons, this study sought to investigate a novel pathway for hypertension, involving hexadecanedioate, since previous work identified a direct association between hexadecanedioate and both blood pressure elevation and mortality (Menni *et al.*, 2015). To allow clinical translation, we require a deeper understanding of the mechanisms by which hexadecanedioate influences blood pressure and it's potential as a therapeutic target. Therefore, this study was designed to examine the functional role of hexadecanedioate on blood pressure and end-organ damage, and identify a putative novel pathway for hypertension. Here we provide evidence to confirm that administration of exogenous hexadecanedioic acid elevated circulating hexadecanedioate levels in parallel with a rise in systolic blood pressure in normotensive WKY rats. Vascular function was also examined, which identified significant increases in vascular reactivity to noradrenaline in mesenteric resistance arteries of WKY rats treated orally with hexadecanedioic acid (Chapter 3).

In support of these findings a metabolomics study was conducted to identify the metabolic effects of hexadecanedioate-induced blood pressure elevation. A previous metabolomic study was carried out in the pulmonary vascular system, which identified increased dicarboxylic fatty acids, including hexadecanedioate in conjunction with disrupted glycolysis in lung tissues from human pulmonary arterial hypertension (Zhao *et al.*, 2014). Similarly, our study exhibited multiple dicarboxylic acids, including hexadecanedioate to be significantly accumulated in cardiovascular tissues obtained from hexadecanedioic acid treated WKY rats. In addition, subtle changes in fatty acid metabolism and energetics-related metabolites were identified, indicating a disruption of ß-oxidation and an increase of ω-oxidation in this condition and pointing to a putative role in elevating blood pressure in both the systemic and pulmonary circulations (Chapter 4). Indeed, impairment of mitochondrial ß-oxidative function is associated with increased dicarboxylate fatty acids, reflecting a shift toward increased use of peroxisomal ω-oxidation. Animals studies have identified that the downregulation of fatty acid ß-oxidation enzymes is also associated with increased use by mitochondria of oxygen-sparing glycolytic pathways for adenosine triphosphate (ATP) production (de las Fuentes *et al.*, 2006). Fatty acid oxidation is a more efficient process for ATP production in comparison with glycolysis (Zhao *et al.*, 2014). Any abnormality in glycolytic and fatty acid metabolism causes metabolic dysfunctions and both are now recognised as a potential biological mechanism leading to pulmonary vascular remodelling, ventricular hypertrophy and systolic heart failure (de las Fuentes *et al.*, 2006; Assad and Hemnes, 2015; Rubattu *et al* , 2016).

Our analysis also identified marked increases in hepatic, renal and adipose levels of bile acid profiles as well as significant increases in hepatic and renal levels of cholesterol in hexadecanedioic acid treated WKY rats (Chapter 4). A previous study were performed by Wu *et al.*(1999) found that serum total bile acids levels were higher in essential hypertensive patients and in spontaneously hypertensive rats. Wu *et al* suggested that bile acids are able to induce hypertension by inhibiting the transcription of both 11ß-hydroxysteroid dehydrogenase (11b-HSD) and CYP11B2 in vasculature, leading to a decrease in aldosterone and an increase in corticosterone production in vessels and increased vasoconstrictor responses to noradrenaline. In fact, aldosterone and bile acids are both produced from cholesterol in a series of reactions. Cholesterol, aldosterone, and bile acids are

involved in development of hypertension. However, the associations between bile acids, cholesterol and hexadecandioate in hypertension remain to be identified and further investigations are required to determine the underlying mechanisms.

For a better understanding of the role of hexadecandioate in blood pressure regulation, molecular levels of ω-oxidation pathway were examined. Our gene expression analysis identified a significant reduction in the final enzyme of the ω-oxidation pathway, aldehydehydrogenase (ALDH1L2 isoform), in liver tissues obtained from hypertensive SHRSP rats compared to normotensive WKY (Chapter 5). Our results corroborate findings by Menni *et al* (2017), which verified significant correlations between high circulating levels of hexadecanedioate and the levels of encoding enzymes involved in the ω-oxidation pathway. For further investigation, pharmacological intervention studies were carried out to examine the enzymes involved in the ω-oxidation pathway by perturbing the endogenous ω-oxidation pathway utilising specific inhibitors and agonists for several enzymes in the pathway. Here we identified a significant reduction in blood pressure of the hypertensive SHRSP rat model after inhibition of aldehyde dehydrogenase enzyme by administration of the specific antagonist (disulfiram). It would be important to measure the level of hexadecandioate in plasma samples and the protein expression of ALDH in these treated rats. Also, it would be beneficial to activate the ALDH enzyme by specific agonist (Alda-1) in normotensive WKY rats to fully confirm the effect of altering endogenous hexadecandioate levels and gain a better understanding of the role of ALDH in hypertension. Unfortunately, time and budget limitations in the present study prevented a more in-depth investigation.

Although a number of GWAS on blood pressure and hypertension have been published, two GWAS studies have determined an association between hypertension and ω-oxidation pathway genes, including ALDH and ADH. Firstly, a GWAS study carried out by Adeyemo *et al* (2009) identified an association between rs991316 SNPs in ADH7 and rs1550576 SNPs in ALDH1A2 and hypertension in African Americans populations. Secondly, ALDH2 gene was found to be associated with blood pressure and hypertension in Asian ancestry (Yang *et al*., 2012). Therefore, further investigation is needed to verify the role of ω-oxidation enzymes, ALDH and ADH in elevation of hexadecanedioate levels.

Interestingly, administration of the CYP4A enzyme in the ω-oxidation pathway by the agonist (fenofibrate), which showed a significant reduction in blood pressure with significant increase in the hepatic and renal expression of CYP4A in fenofibrate-treated WKY rats compared to vehicle-treated WKY rats (Chapter 5). The unexpected reduction in blood pressure may point to the role of peroxisome proliferator-activated receptor-alpha (PPAR-α), which may also be activated by fenofibrate administration leading to reductions in blood pressure and sodium retention (Lee *et al.*, 2011). Activation of PPAR-α increases the expression of renal tubular CYP4A expression, thus increasing the production of 20-hydroxyeicosatetraenoic acid (20-HETE) which leads to reduces sodium retention and blood pressure (Lee *et al.*, 2011). It would be important to conduct future studies in fenofibrate-treated SHRSP rats, since blood pressure reductions have also been identified with fenofibrate treatment in DOCA-salt hypertension rats as well as in salt-sensitive hypertensive patients (Lee *et al.*, 2011; Gilbert *et al.*, 2013). Nevertheless, the mechanisms underlying the reduction of blood pressure are still unknown.

The dicarboxylic fatty acid, hexadecanedioate is mainly metabolised in liver, and transported across the hepatocyte sinusoidal membrane by organic-anion-transporting polypeptide (OATP) encoded by solute carrier organic anion (SLCO) gene. We hypothesized that mutations in this transporter may lead to elevated circulating levels of hexadecanedioate and subsequently may cause elevation of blood pressure. Several studies have been successful in identifying the association between elevated circulating hexadecanedioate levels and SNPs (rs414056) in human SLCO1B1 gene (Yu *et al.*, 2016; Yee *et al.*, 2016; Menni *et al.*, 2017). These SNPs have been previously identified as being association with risk of statin related myopathy (Ramsey *et al.*, 2014; Bakar *et al.*, 2017). In this thesis, we have extended these studies by preliminary investigation of the genome sequences of the rat homolog, the Slco1b2 gene in two rat models, the spontaneously hypertensive stroke-prone (SHRSP) and normotensive Wistar–Kyoto (WKY) rats and identified SNPs within their genome sequences. Our results have identified two genetic variants within WKY sequence; which are a deletion of 4 nucleotides within 3'untranslated region (UTR) and an insertion of 9 nucleotides within the intronic region on chromosome 4 (Chapter 6). These mutations may interfere with the Slco1b2 gene expression resulting in dysregulation of protein function. Hepatic

mRNA expression of Slco1b2 was also examined to verify this result, which showed a significant downregulation of Slco1b2 mRNA levels in hypertensive SHRSP rats compared to normotensive WKY (Chapter 6). This suggests that the genetic polymorphism in this gene may affect SLCO function, leading to reduced hepatic uptake of hexadecanedioate and other metabolites. Xiang *et al*. (2009) found that OATP1B1 mutation also altered the uptake of certain bile acid profiles. This may explain the results of elevated bile acid metabolomic profiles in many of the examined tissues (i.e. adipose, kidney and liver) of hexadecanedioic acid-treated WKY rats (Chapter 4). Therefore, these findings indicate that under condition of decreased hepatic OATP1B1 levels, these changes can reduce hepatic clearance of circulating hexadecanedioate in hypertensive SHRSP rats. This may explain why baseline circulating hexadecanedioate levels were significantly higher in SHRSP rats compared with WKY rats (Menni *et al*., 2015).

7.2 Future perspectives

In this thesis, we have confirmed the role of hexadecanedioate on vascular function assessed by wire myography. However, we still not entirely sure about the molecular mechanisms, which influence vascular tone and contractile response observed during blood pressure elevation. As we know, perturbing vascular smooth muscle cell signalling influences vascular reactivity and tone leading to vascular resistance and hypertension (Touyz *et al*., 2018). Therefore, further investigation is needed to prove the mechanism of hexadecanedioate in vascular tissues. One way to do that is by *in vitro* analysis of vascular cells to understand how elevated circulating levels of hexadecanedioate contribute to increased vascular reactivity and blood pressure elevation. Vascular smooth muscle cells and endothelial cells of aorta and mesenteric resistant arteries are obtained from SHRSP and WKY rats could be isolated and cultured. Vascular cells could be treated with a range of hexadecanedioate concentrations ($1x10^{-8}$ to $3x10^{-5}$ mol/l) or vehicle. The expression of critical ion transporters, channels, and signalling molecules involved in calcium homeostasis could be examined by qRT-PCR and western analysis. This would include, voltage dependent Ca^{2+} channels, transient receptor potential channel (TRPC), plasma membrane calcium ATPase (PMCA), sarco/endoplasmic reticulum calcium pump (SERCA), and Na^{+}/Ca^{2+} exchangers.

The previous unpublished SILAC studies mentioned in Chapter 1, Section 1.14, have demonstrated significantly increased aldehyde dehydrogenase protein levels in vascular smooth muscle cells from SHRSP rats, suggesting potential ω-oxidation pathway dysregulation. It is essential to examine the impact of disulfiram treatment on these cellular mechanisms. Similarly to the proposed in vitro studies with hexadecanedioate, vascular smooth muscle cells and endothelial cells isolated from aorta and mesenteric resistant arteries of SHRSP could be treated with disulfiram (5 μmol/l) or vehicle and the expression of critical Ca^{2+} ion signalling molecules examined by measuring the expressions of relevant proteins and mRNAs. In fact, intracellular calcium $[Ca^{2+}]_i$ of vascular smooth muscle cell not only regulates the contractile response but also impacts on the activity of several calcium dependent transcription factors and proteins (Touyz *et al.*, 2018). Therefore, intracellular calcium concentration $[Ca^{2+}]_i$ should be measured using direct fluorescence methods to determine the short-term hexadecanedioate treatment on Ca^{2+} in vascular smooth muscle cells (VSMCs) of WKY and SHRSP rats.

In our study, the mutation within the Slco1b2 genome sequence encoding the Oatp1b2 protein was confirmand between the two rat strains, SHRSP and WKY. However, the physiologic and pharmacologic roles of OATPs of the 1B subfamily and hepatic reuptake of hexadecanedioate are still not clearly understood. To investigate the roles of Oatp1b2 in hexadecanedioate clearance and its association to blood pressure elevation, knockout mice (Slco1a/1b-/-) could be utilized, which have been previously generated by Van de Steeg *et al.*, (2010). It would be important to measure blood pressure together with hexadecanedioate, bilirubin and bile acids levels in plasma and liver samples in these knockout mice compared to wild type. Confirmation of a functional role for Slco1b2 on hexadecanedioate levels in a different species would provide important corroborative evidence for our findings in the rat.

In this thesis, we proposed that examining in parallel alterations at both the whole animal, metabolomics and molecular levels, would not only help to identify novel therapeutic targets but also help to provide a better understanding of pathophysiology of hypertension. However, the current study has limitations due to the enormous complexity of biological systems, which makes the reliable predictions about the biological role of novel targets difficult. It is suggested that these difficulties impact our ability to determine the main organ(s) affected by

elevation of the hexadecanedioate levels. Limitations also arise from the short duration of the animal studies and pathophysiologic processes compared to a lifetime of development of hypertension in humans. In addition, it was difficult to determine the direct ortholog of ω-oxidation enzymes shared between rat and human. Some of our studies were stastically under powered. Although, it would be benifical to increase the animals number, that was impossible within the time frame of this thesis.

This project was conducted to provide better understanding of the effect of hexadecanedioate in elevation of blood pressure and involved initial studies to determine the underling pathways and mechanisms. From our findings, we can suggest a number of targets, which are associated with altered hexadecanedioate levels and consequently development of hypertension; including aldehydehydrogenase (ALDH) and solute carrier organic anion (SLCO). Identification of these putative targets will be important for the scientific and medical researcher community in the cardiovascular field to advance understanding of hypertension and intermediate phenotypes. It is anticipated that a clearer understanding of hypertension pathogenesis will lead to better targeted treatments and thereby reduce the burden of hypertension-related cardiovascular morbidity and mortality. In this case, we can suggest that hexadecanedioate will be shown as “low-hanging fruit” gathered at beginning of an effort that is eventually expected to not only alter our view of pathophysiology of hypertension, but also a promising focal point for novel treatment targets and clinical management.

In conclusion, multiple *in* vivo, *ex* vivo and molecular techniques have been applied in identification of the role of hexadecanedioate in modulating of blood pressure. The data from this multilayered study supports our hypothesis and provides strong corroborative evidence of a causal role for hexadecandioate in blood pressure regulation and identifies novel targets; including ω- oxidation pathway and solute carrier organic anion mechanism in regulation of blood pressure. Further work needs to be prioritised to elucidate the underpinning mechanisms, to allow these findings to be translated ultimately into novel drugs for treatment of hypertension.

Appendices

Table A 1: Biochemical compounds profiled in adipose tissues.

Biochemical metabolites	Super Pathway	Sub Pathway	Mean ±SEM		Fold of change Welch's Two-ample t-Test HEXA/Control	Statistical Values	
			Control	HEXA		p-value	q-value
tetradecanedioate	Lipid	Fatty Acid, Dicarboxylate	0.92 ± 0.04	1.10 ± 0.07	1.19	0.0451	0.9911
hexadecanedioate	Lipid	Fatty Acid, Dicarboxylate	0.67 ± 0.07	1.36 ± 0.11	2.04	0.0008	0.3253
octadecanedioate	Lipid	Fatty Acid, Dicarboxylate	0.86 ± 0.08	1.51 ± 0.28	1.76	0.0416	0.9911
myristoylcarnitine	Lipid	Fatty Acid Metabolism (Acyl Carnitine)	1.73 ± 0.46	0.78 ± 0.34	0.45	0.0592	0.9911
oleoylcarnitine	Lipid	Fatty Acid Metabolism (Acyl Carnitine)	1.86 ± 0.53	0.81 ± 0.14	0.44	0.0738	0.9911
16-hydroxypalmitate	Lipid	Fatty Acid, Monohydroxy	0.91 ± 0.05	1.26 ± 0.15	1.39	0.082	0.9911
1,2-dipalmitoleoyl-GPC (16:1/16:1)*	Lipid	Phospholipid Metabolism	0.76 ± 0.12	1.20 ± 0.09	1.58	0.0385	0.9911
1-oleoyl-GPI (18:1)*	Lipid	Lysolipid	1.08 ± 0.25	0.59 ± 0.09	0.55	0.0826	0.9911
1-palmitoleoylglycerol (16:1)*	Lipid	Monoacylglycerol	0.85 ± 0.16	1.35 ± 0.17	1.59	0.0574	0.9911
sphingomyelin(d18:1/20:1, d18:2/20:0)*	Lipid	Sphingolipid Metabolism	0.85 ± 0.16	1.42 ± 0.31	1.67	0.096	0.9911
taurocholate	Lipid	Primary Bile Acid Metabolism	0.33 ± 0.10	3.12 ± 1.38	9.55	0.0035	0.5904
taurochenodeoxycholate	Lipid	Primary Bile Acid Metabolism	0.45 ± 0.20	3.07 ± 1.60	6.82	0.0151	0.9911
tauro-alpha-muricholate	Lipid	Primary Bile Acid Metabolism	0.41 ± 0.16	1.92 ± 0.77	4.74	0.0706	0.9911
tauro-beta-muricholate	Lipid	Primary Bile Acid Metabolism	0.25 ± 0.09	2.85 ± 1.09	11.24	0.0013	0.3253
Taurodeoxycholate	Lipid	Secondary Bile Acid metabolism	0.33 ± 0.14	4.55 ± 2.67	13.98	0.0061	0.7659
Sedoheptulose-7-hosphate	Carbohydrate	Pentose Phosphate Pathway	1.10 ± 0.0	0.96 ± 0.0	0.87	0.0416	0.9911

Table A 2: Biochemical compounds profiled in kidney tissues.

Biochemical metabolites	Super Pathway	Sub Pathway	Mean ±SEM		Fold of change Welch's Two-ample t-Test HEXA/Control	Statistical Values	
			Control	HEXA		p-value	q-value
3-phosphoserine	Amino Acid	Glycine, Serine and Threonine Metabolism	1.25 ± 0.11	0.82 ± 0.09	0.66	0.0222	0.3176
N-acetylasparagine	Amino Acid	Alanine and Aspartate Metabolism	1.12 ± 0.06	0.89 ± 0.04	0.79	0.0095	0.3176
N-acetylglutamine	Amino Acid	Glutamate Metabolism	1.03 ± 0.04	0.91 ± 0.06	0.88	0.0989	0.4515
1-methylhistidine	Amino Acid	Histidine Metabolism	1.034 ± 0.02	0.95 ± 0.03	0.92	0.0715	0.4515
N-acetyl-3-methylhistidine*	Amino Acid	Histidine Metabolism	1.19 ± 0.14	0.84 ± 0.12	0.71	0.0998	0.4515
imidazole lactate	Amino Acid	Histidine Metabolism	0.90 ± 0.04	1.09 ± 0.07	1.22	0.0433	0.3819
1-methylimidazoleacetate	Amino Acid	Histidine Metabolism	0.77 ± 0.05	1.51 ± 0.16	1.96	0.0014	0.2872
N2-acetyllysine	Amino Acid	Lysine Metabolism	1.16 ± 0.07	0.93 ± 0.03	0.80	0.0306	0.3176
kynurenine	Amino Acid	Tryptophan Metabolism	0.91 ± 0.43	2.95 ± 1.14	3.25	0.0667	0.4515
alpha-hydroxyisovalerate	Amino Acid	Leucine, Isoleucine and Valine Metabolism	0.89 ± 0.04	1.29 ± 0.10	1.45	0.0062	0.3176
N-acetylvaline	Amino Acid	Leucine, Isoleucine and Valine Metabolism	1.10 ± 0.04	0.90 ± 0.042	0.82	0.0122	0.3176
hypotaurine	Amino Acid	Methionine, Cysteine, SAM and Taurine Metabolism	0.71 ± 0.08	1.37 ± 0.14	1.92	0.0027	0.2995
taurine	Amino Acid	Methionine, Cysteine, SAM and Taurine Metabolism	0.83 ± 0.08	1.52 ± 0.31	1.83	0.0815	0.4515
taurocyamine	Amino Acid	Methionine, Cysteine, SAM and Taurine Metabolism	1.18 ± 0.13	0.86 ± 0.10	0.73	0.0761	0.4515
arginine	Amino Acid	Urea cycle; Arginine and Proline Metabolism	0.91 ± 0.06	1.14 ± 0.10	1.26	0.0886	0.4515

proline	Amino Acid	Urea cycle; Arginine and Proline Metabolism	0.96 ± 0.03	1.06 ± 0.02	1.11	0.0204	0.3176
N-delta-acetylornithine	Amino Acid	Urea cycle; Arginine and Proline Metabolism	0.88 ± 0.06	1.01 ± 0.03	1.15	0.0955	0.4515
N-methylproline	Amino Acid	Urea cycle; Arginine and Proline Metabolism	0.89 ± 0.06	1.04 ± 0.03	1.16	0.0374	0.3602
creatine	Amino Acid	Creatine Metabolism	0.94 ± 0.02	1.07 ± 0.06	1.13	0.0985	0.4515
guanidinoacetate	Amino Acid	Creatine Metabolism	0.89 ± 0.05	1.14 ± 0.04	1.28	0.0103	0.3176
putrescine	Amino Acid	Polyamine Metabolism	0.76 ± 0.13	1.56 ± 0.20	2.05	0.0176	0.3176
N-acetylputrescine	Amino Acid	Polyamine Metabolism	0.62 ± 0.01	1.15 ± 0.23	1.85	0.0738	0.4515
guanidinosuccinate	Amino Acid	Guanidino and Acetamido Metabolism	0.86 ± 0.09	1.16 ± 0.12	1.35	0.0866	0.4515
glucose 6-phosphate	Carbohydrate	Glycolysis, Gluconeogenesis, and Pyruvate Metabolism	1.16 ± 0.08	0.91 ± 0.05	0.79	0.0276	0.3176
arabitol/xylitol	Carbohydrate	Pentose Metabolism	1.19 ± 0.09	0.91 ± 0.03	0.76	0.0182	0.3176
maltotetraose	Carbohydrate	Glycogen Metabolism	0.79 ± 0.09	1.22 ± 0.09	1.53	0.0247	0.3176
maltotriose	Carbohydrate	Glycogen Metabolism	0.86 ± 0.07	1.15 ± 0.06	1.34	0.0266	0.3176
maltose	Carbohydrate	Glycogen Metabolism	0.92 ± 0.04	1.04 ± 0.02	1.13	0.0397	0.3653
galactose 1-phosphate	Carbohydrate	Fructose, Mannose and Galactose Metabolism	1.13 ± 0.08	0.94 ± 0.04	0.83	0.0526	0.4195
glucuronate	Carbohydrate	Aminosugar Metabolism	1.13 ± 0.06	0.82 ±0.07	0.72	0.0173	0.3176
tricarballylate	Energy	TCA Cycle	0.85 ± 0.08	1.28 ± 0.18	1.50	0.0523	0.4195
myristate (14:0)	Lipid	Long Chain Fatty Acid	0.81 ± 0.06	1.88 ± 0.70	2.33	0.0853	0.4515
myristoleate (14:1n5)	Lipid	Long Chain Fatty Acid	0.74 ± 0.09	1.73 ± 0.44	2.33	0.0195	0.3176
palmitoleate (16:1n7)	Lipid	Long Chain Fatty Acid	0.76 ± 0.06	2.59 ± 0.03	3.42	0.08	0.4515
10-heptadecenoate (17:1n7)	Lipid	Long Chain Fatty Acid	0.77 ± 0.09	2.57 ± 1.20	3.32	0.0636	0.4474

10-nonadecenoate (19:1n9)	Lipid	Long Chain Fatty Acid	0.80 ± 0.08	2.72 ± 1.40	3.39	0.0831	0.4515
15-methylpalmitate	Lipid	Fatty Acid, Branched	0.81 ± 0.05	2.35 ± 1.12	2.90	0.0912	0.4515
sebacate (decanedioate)	Lipid	Fatty Acid, Dicarboxylate	1.31 ± 0.15	0.89 ± 0.03	0.68	0.0245	0.3176
hexadecanedioate	Lipid	Fatty Acid, Dicarboxylate	0.89 ± 0.01	1.31 ± 0.08	1.46	0.0029	0.2995
malonylcarnitine	Lipid	Fatty Acid Synthesis	1.10 ± 0.05	0.87 ± 0.08	0.79	0.0405	0.3653
butyrylcarnitine	Lipid	Fatty Acid Metabolism (Acyl Carnitine)	0.67 ± 0.14	1.33 ± 0.16	1.99	0.0345	0.3492
propionylcarnitine	Lipid	Fatty Acid Metabolism (Acyl Carnitine)	0.91 ± 0.11	1.20 ± 1.04	1.32	0.0895	0.4515
3-hydroxybutyrylcarnitine (2)	Lipid	Fatty Acid Metabolism (Acyl Carnitine)	0.88 ± 0.05	1.06 ± 0.03	1.21	0.0304	0.3176
3-hydroxybutyrate (BHBA)	Lipid	Ketone Bodies	0.88 ± 0.05	1.05 ± 0.03	1.20	0.0153	0.3176
myo-inositol	Lipid	Inositol Metabolism	1.05 ± 0.02	0.97 ± 0.01	0.93	0.0105	0.3176
trimethylamine N-oxide	Lipid	Phospholipid Metabolism	0.84 ± 0.09	1.47 ± 0.16	1.74	0.0181	0.3176
1-palmitoyl-2-palmitoleoyl-GPC (16:0/16:1)*	Lipid	Phospholipid Metabolism	0.89 ± 0.05	1.24 ± 0.10	1.38	0.0166	0.3176
1-stearoyl-2-arachidonoyl-GPI (18:0/20:4)	Lipid	Phospholipid Metabolism	1.05 ± 0.03	0.96 ± 0.03	0.91	0.0637	0.4474
1-palmitoyl-2-oleoyl-GPG (16:0/18:1)	Lipid	Phospholipid Metabolism	0.88 ± 0.04	1.11 ± 0.04	1.26	0.0038	0.3161
1-palmitoyl-2-oleoyl-GPE (16:0/18:1)	Lipid	Phospholipid Metabolism	0.89 ± 0.05	1.17 ± 0.08	1.31	0.0228	0.3176
1-oleoyl-2-linoleoyl-GPE (18:1/18:2)*	Lipid	Phospholipid Metabolism	1.07 ± 0.05	0.94 ± 0.16	0.88	0.0954	0.4515
1-palmitoleoyl-GPC (16:1)*	Lipid	Lysolipid	0.79 ± 0.08	1.38 ± 0.05	1.73	0.0008	0.2872
1-(1-enyl-palmitoyl)-2-arachidonoyl-GPC (P-16:0/20:4)*	Lipid	Plasmalogen	1.09 ± 0.03	0.90 ± 0.04	0.83	0.0069	0.3176
glycerol	Lipid	Glycerolipid Metabolism	0.81 ± 0.07	1.13 ± 0.09	1.40	0.0196	0.3176

1-palmitoleoylglycerol (16:1)*	Lipid	Monoacylglycerol	0.69 ± 0.13	3.07 ± 1.30	4.43	0.0226	0.3176
sphingomyelin (d18:1/20:0, d16:1/22:0)*	Lipid	Sphingolipid Metabolism	1.06 ± 0.05	0.92 ± 0.04	0.87	0.0797	0.4515
palmitoyl dihydrosphingomyelin (d18:0/16:0)*	Lipid	Sphingolipid Metabolism	1.06 ± 0.05	0.92 ± 0.05	0.87	0.0959	0.4515
7-hydroxycholesterol (alpha or beta)	Lipid	Sterol	1.49 ± 0.31	0.79 ± 0.11	0.53	0.0634	0.4474
glycocholate	Lipid	Primary Bile Acid Metabolism	1.35 ± 0.18	0.63 ±0.17	0.46	0.0565	0.4255
chenodeoxycholate	Lipid	Primary Bile Acid Metabolism	1.49 ± 0.43	0.77 ± 0.23	0.51	0.0973	0.4515
glycochenodeoxycholate	Lipid	Primary Bile Acid Metabolism	1.51 ± 0.29	0.65 ± 0.29	0.43	0.0548	0.4203
tauro-alpha-muricholate	Lipid	Primary Bile Acid Metabolism	0.68 ± 0.13	1.17 ± 0.05	1.73	0.0285	0.3176
tauro-beta-muricholate	Lipid	Primary Bile Acid Metabolism	0.60 ± 0.19	1.50 ± 0.26	2.50	0.0241	0.3176
glycodeoxycholate	Lipid	Secondary Bile Acid Metabolism	1.75 ± 0.31	0.45 ± 0.16	0.26	0.0073	0.3176
glycolithocholate	Lipid	Secondary Bile Acid Metabolism	1.56 ± 0.7	0.49 ± 0.19	0.31	0.0799	0.4515
tauroursodeoxycholate	Lipid	Secondary Bile Acid Metabolism	0.68 ± 0.14	1.39 ± 0.18	2.06	0.0158	0.3176
glycohyodeoxycholate	Lipid	Secondary Bile Acid Metabolism	1.26 ± 0.12	0.48 ± 0.214	0.38	0.0472	0.3994
orotate	Nucleotide	Pyrimidine Metabolism, Orotate containing	0.92 ± 0.05	1.39 ± 0.14	1.52	0.0176	0.3176
pseudouridine	Nucleotide	Pyrimidine Metabolism, Uracil containing	1.09 ± 0.06	0.96 ± 0.04	0.88	0.0917	0.4515
1-methylnicotinamide	Cofactors and Vitamins	Nicotinate and Nicotinamide Metabolism	1.40 ± 0.19	0.95 ± 0.05	0.68	0.0545	0.4203
riboflavin (Vitamin B2)	Cofactors and Vitamins	Riboflavin Metabolism	1.09 ± 0.06	0.94 ± 0.03	0.86	0.0694	0.4515
flavin adenine dinucleotide (FAD)	Cofactors and Vitamins	Riboflavin Metabolism	1.06 ± 0.03	0.97 ± 0.03	0.91	0.0405	0.3653
flavin mononucleotide (FMN)	Cofactors and Vitamins	Riboflavin Metabolism	1.05 ± 0.03	0.93 ± 0.04	0.89	0.0273	0.3176

alpha-tocopherol	Cofactors and Vitamins	Tocopherol Metabolism	0.78 ± 0.15	1.12 ± 0.08	1.43	0.0843	0.4515
5-methyltetrahydrofolate (5MeTHF)	Cofactors and Vitamins	Folate Metabolism	0.84 ± 0.07	1.19 ± 0.09	1.42	0.0184	0.3176
pterin	Cofactors and Vitamins	Pterin Metabolism	1.30 ± 0.11	0.85 ± 0.10	0.65	0.0354	0.3497
thiamin monophosphat	Cofactors and Vitamins	Thiamine Metabolism	1.07 ± 0.03	0.96 ± 0.03	0.90	0.0459	0.396
thiamin diphosphate	Cofactors and Vitamins	Thiamine Metabolism	1.04 ± 0.03	0.89 ± 0.05	0.85	0.0587	0.4342
retinol (Vitamin A)	Cofactors and Vitamins	Vitamin A Metabolism	0.63 ± 0.18	1.24 ± 0.12	1.96	0.0702	0.4515
pyridoxamine phosphate	Cofactors and Vitamins	Vitamin A Metabolism	1.07 ± 0.03	0.95 ± 0.05	0.89	0.0829	0.4515
hippurate	Xenobiotics	Benzoate Metabolism	0.88 ± 0.08	1.17 ± 0.09	1.32	0.0526	0.4195
catechol sulfate	Xenobiotics	Benzoate Metabolism	0.66 ± 0.15	1.49 ± 0.40	2.25	0.0293	0.3176

Table A 3: Biochemical compounds profiled in brain tissues.

Biochemical metabolites	Super Pathway	Sub Pathway	Mean ±SEM		Fold of Change Welch's Two-Sample t-Test (HEXA/Control)	Statistical Values	
			Control	HEXA		p-value	q-value
N-acetyl-3-methylhistidine*	Amino acid	Histidine Metabolism	1.24 ± 0.13	0.78 ± 0.18	0.63	0.0893	0.9868
beta-hydroxyisovalerate	Amino acid	Leucine, Isoleucine and Valine Metabolism	0.96 ± 0.06	1.21 ± 0.11	1.26	0.0854	0.9868
alpha-hydroxyisovalerate	Amino acid	Leucine, Isoleucine and Valine Metabolism	0.85 ± 0.08	1.11 ± 0.06	1.30	0.054	0.9868
urea	Amino acid	Urea cycle; Arginine and Proline Metabolism	0.94 ± 0.04	1.09 ± 0.05	1.17	0.0611	0.9868
anserine	Peptide	Dipeptide Derivative	1.13 ± 0.07	0.77 ± 0.22	0.68	0.0917	0.9868
myristate (14:0)	Lipid	Long Chain Fatty Acid	0.90 ± 0.05	1.11 ± 0.05	1.23	0.0184	0.9868
palmitate (16:0)	Lipid	Long Chain Fatty Acid	0.89 ± 0.04	1.22 ± 0.09	1.36	0.0143	0.9868
palmitoleate (16:1n7)	Lipid	Long Chain Fatty Acid	0.79 ± 0.09	1.11 ± 0.08	1.39	0.045	0.9868
stearate (18:0)	Lipid	Long Chain Fatty Acid	0.87 ± 0.07	1.16 ± 0.07	1.33	0.0239	0.9868
nonadecanoate (19:0)	Lipid	Long Chain Fatty Acid	0.91 ± 0.05	1.07 ± 0.07	1.18	0.0878	0.9868
arachidate (20:0)	Lipid	Long Chain Fatty Acid	0.94 ± 0.04	1.09 ± 0.07	1.16	0.0742	0.9868
oleate/vaccenate (18:1)	Lipid	Long Chain Fatty Acid	0.90 ± 0.02	1.31 ± 0.09	1.45	0.0061	0.9175
eicosapentaenoate (EPA; 20:5n3)	Lipid	Polyunsaturated Fatty Acid (n3 and n6)	0.87 ± 0.09	1.23 ± 0.14	1.42	0.0593	0.9868
docosahexaenoate (DHA; 22:6n3)	Lipid	Polyunsaturated Fatty Acid (n3 and n6)	0.88 ± 0.02	1.33 ± 0.10	1.52	0.0036	0.9175
linoleate (18:2n6)	Lipid	Polyunsaturated Fatty Acid (n3 and n6)	0.79 ± 0.09	1.06 ± 0.07	1.33	0.0651	0.9868

dihomo-linolenate (20:3n3 or n6)	Lipid	Polyunsaturated Fatty Acid (n3 and n6)	0.87 ± 0.09	1.29 ± 0.07	1.49	0.0103	0.9868
arachidonate (20:4n6)	Lipid	Polyunsaturated Fatty Acid (n3 and n6)	0.88 ± 0.06	1.27 ± 0.12	1.44	0.0178	0.9868
adrenate (22:4n6)	Lipid	Polyunsaturated Fatty Acid (n3 and n6)	0.88 ± 0.05	1.34 ± 0.10	1.52	0.0043	0.9175
docosapentaenoate (n6 DPA; 22:5n6)	Lipid	Polyunsaturated Fatty Acid (n3 and n6)	0.84 ± 0.09	1.32 ± 0.17	1.58	0.0352	0.9868
dihomo-linoleate (20:2n6)	Lipid	Polyunsaturated Fatty Acid (n3 and n6)	0.89 ± 0.06	1.23 ± 0.14	1.37	0.0784	0.9868
1-stearoyl-2-oleoyl-GPE (18:0/18:1)	Lipid	Phospholipid Metabolism	0.92 ± 0.06	1.15 ± 0.09	1.24	0.0781	0.9868
1-stearoyl-GPI (18:0)	Lipid	Lysolipid	0.77 ± 0.11	1.23 ± 0.15	1.60	0.0402	0.9868
sphingosine	Lipid	Sphingolipid Metabolism	0.94 ± 0.03	1.11 ± 0.08	1.19	0.0887	0.9868
4-cholesten-3-one	Lipid	Sterol	0.92 ± 0.21	0.49 ± 0.0	0.54	0.0895	0.9868
corticosterone	Lipid	Steroid	0.78 ± 0.21	1.20 ± 0.13	1.54	0.0773	0.9868
adenosine 3'-monophosphate (3'-AMP)	Nucleotide	Purine Metabolism, Adenine containing	1.19 ± 0.10	0.80 ± 0.12	0.68	0.0599	0.9868
flavin adenine dinucleotide (FAD)	Cofactors and Vitamins	Riboflavin Metabolism	0.99 ± 0.01	1.09 ± 0.05	1.11	0.0877	0.9868
coenzyme A	Cofactors and Vitamins	Pantothenate and CoA Metabolism	1.17 ± 0.10	0.91 ± 0.10	0.77	0.0985	0.9868
dihydrobiopterin	Cofactors and Vitamins	Tetrahydrobiopterin Metabolism	0.83 ± 0.08	1.20 ± 0.12	1.45	0.037	0.9868
pyridoxamine phosphate	Cofactors and Vitamins	Vitamin B6 Metabolism	0.97 ± 0.03	1.06 ± 0.04	1.09	0.0984	0.9868

Table A 4: Biochemical compounds profiled in liver tissues.

Biochemical metabolites	Super Pathway	Sub Pathway	Mean ±SEM		Fold of Change Welch's Two-Sample t-Test (HEXA/Control)	Statistical Values	
			Control	HEXA		p-value	q-value
glycine	Amino Acid	Glycine, Serine and Threonine Metabolism	1.06 ± 0.03	0.97 ± 0.03	0.91	0.074	0.4467
betaine	Amino Acid	Glycine, Serine and Threonine Metabolism	1.05 ± 0.05	0.90 ± 0.05	0.86	0.0543	0.4467
betaine aldehyde	Amino Acid	Glycine, Serine and Threonine Metabolism	1.04 ± 0.05	0.91 ± 0.05	0.88	0.0831	0.4467
N-acetylglutamate	Amino Acid	Glutamate Metabolism	1.08 ± 0.04	0.87 ± 0.06	0.80	0.0261	0.4467
4-hydroxyglutamate	Amino Acid	Glutamate Metabolism	1.19 ± 0.09	0.97 ± 0.03	0.81	0.0724	0.4467
histidine	Amino Acid	Histidine Metabolism	1.03 ± 0.01	0.96 ±0.03	0.93	0.0998	0.4467
imidazole lactate	Amino Acid	Histidine Metabolism	0.87 ± 0.06	1.09 ± 0.07	1.25	0.04	0.4467
1-methylimidazoleacetate	Amino Acid	Histidine Metabolism	0.79 ± 0.08	1.52 ± 0.20	1.91	0.0052	0.4467
4-imidazoleacetate	Amino Acid	Histidine Metabolism	0.79 ± 0.11	1.12 ± 0.09	1.41	0.0598	0.4467
N-acetyltyrosine	Amino Acid	Phenylalanine and Tyrosine Metabolism	1.26 ± 0.01	0.90 ± 0.07	0.72	0.0559	0.4467
o-Tyrosine	Amino Acid	Phenylalanine and Tyrosine Metabolism	1.12 ± 0.04	0.93 ± 0.032	0.82	0.0051	0.4467
N-acetyltryptophan	Amino Acid	Tryptophan Metabolism	1.15 ± 0.12	0.85 ± 0.09	0.74	0.0976	0.4467
N-acetylleucine	Amino Acid	Leucine, Isoleucine and Valine Metabolism	1.22 ± 0.11	0.93 ± 0.07	0.76	0.0574	0.4467
4-methyl-2-oxopentanoate	Amino Acid	Leucine, Isoleucine and Valine Metabolism	1.12 ± 0.09	0.92 ± 0.55	0.82	0.0984	0.4467
N-acetylisoleucine	Amino Acid	Leucine, Isoleucine and Valine Metabolism	1.11 ± 0.08	0.89 ± 0.06	0.80	0.0653	0.4467
valine	Amino Acid	Leucine, Isoleucine and Valine Metabolism	1.05 ± 0.03	0.96 ± 0.04	0.91	0.0967	0.4467

S-adenosylhomocysteine (SAH)	Amino Acid	Methionine, Cysteine, SAM and Taurine Metabolism	1.09 ± 0.05	0.96 ± 0.03	0.88	0.0372	0.4467
S-methylcysteine	Amino Acid	Methionine, Cysteine, SAM and Taurine Metabolism	1.07 ± 0.03	0.91 ± 0.04	0.85	0.0123	0.4467
taurocyamine	Amino Acid	Methionine, Cysteine, SAM and Taurine Metabolism	1.16 ± 0.04	0.92 ± 0.04	0.80	0.0052	0.4467
ornithine	Amino Acid	Urea cycle; Arginine and Proline Metabolism	1.12 ± 0.09	0.92 ± 0.06	0.82	0.0982	0.4467
N-delta-acetylornithine	Amino Acid	Urea cycle; Arginine and Proline Metabolism	0.95 ± 0.06	1.16 ± 0.08	1.22	0.0684	0.4467
cysteine-glutathione disulfide	Amino Acid	Glutathione Metabolism	0.67 ± 0.08	1.09 ± 0.17	1.61	0.0591	0.4467
5-oxoproline	Amino Acid	Glutathione Metabolism	1.09 ±0.05	0.88 ± 0.04	0.81	0.0078	0.4467
gamma-glutamylglycine	Peptide	Gamma-glutamyl Amino Acid	1.15 ± 0.05	0.96 ± 0.02	0.83	0.0106	0.4467
gamma-glutamylmethionine	Peptide	Gamma-glutamyl Amino Acid	1.08 ± 0.04	0.93 ± 0.06	0.86	0.0596	0.4467
gamma-glutamyltyrosine	Peptide	Gamma-glutamyl Amino Acid	1.08 ± 0.06	0.91 ±0.06	0.85	0.0821	0.4467
gamma-glutamylvaline	Peptide	Gamma-glutamyl Amino Acid	1.18 ± 0.08	0.92 ± 0.12	0.78	0.0925	0.4467
arabonate/xylonate	Carbohydrate	Pentose Metabolism	1.23 ± 0.15	0.88 ± 0.13	0.71	0.0815	0.4467
UDP-glucuronate	Carbohydrate	Nucleotide Sugar	0.79 ± 0.05	1.22 ± 0.17	1.55	0.0502	0.4467
UDP-N-acetylgalactosamine	Carbohydrate	Nucleotide Sugar	0.82 ± 0.09	1.17 ± 0.08	1.42	0.0295	0.4467
glucuronate	Carbohydrate	Aminosugar Metabolism	1.09 ± 0.06	0.85 ± 0.08	0.78	0.0505	0.4467
N-acetyl-glucosamine 1-phosphate	Carbohydrate	Aminosugar Metabolism	0.83 ± 0.02	1.35 ± 0.02	1.62	0.0889	0.4467
alpha-ketoglutarate	Energy	TCA Cycle	1.23 ± 0.0	0.93 ± 0.0	0.76	0.0905	0.4467
phosphate	Energy	Oxidative Phosphorylation	1.04 ± 0.0	0.96 ± 0.0	0.92	0.0264	0.4467

margarate (17:0)	Lipid	Long Chain Fatty Acid	0.94 ± 0.06	1.13 ± 0.07	1.20	0.0687	0.4467
10-heptadecenoate (17:1n7)	Lipid	Long Chain Fatty Acid	0.92 ± 0.10	1.18 ± 0.08	1.27	0.0804	0.4467
10-nonadecenoate (19:1n9)	Lipid	Long Chain Fatty Acid	0.87 ± 0.18	1.35 ± 0.18	1.56	0.0765	0.4467
stearidonate (18:4n3)	Lipid	Polyunsaturated Fatty Acid (n3 and n6)	1.08 ± 0.07	0.91 ± 0.04	0.84	0.0814	0.4467
dihomo-linoleate (20:2n6)	Lipid	Polyunsaturated Fatty Acid (n3 and n6)	0.90 ± 0.09	1.19 ± 0.10	1.33	0.0571	0.4467
15-methylpalmitate	Lipid	Fatty Acid, Branched	0.93 ± 0.04	1.60 ± 0.26	1.72	0.0469	0.4467
17-methylstearate	Lipid	Fatty Acid, Branched	0.98 ± 0.08	1.42 ± 0.22	1.44	0.0999	0.4467
hexadecanedioate	Lipid	Fatty Acid, Dicarboxylate	0.90 ± 0.05	1.23 ± 0.13	1.37	0.0421	0.4467
hexanoylglycine	Lipid	Fatty Acid Metabolism (Acyl Glycine)	1.08 ± 0.04	0.80 ± 0.07	0.74	0.016	0.4467
linoleoylcarnitine*	Lipid	Fatty Acid Metabolism (Acyl Carnitine)	0.93 ± 0.05	1.07 ± 0.04	1.15	0.054	0.4467
4-hydroxybutyrate (GHB)	Lipid	Fatty Acid, Monohydroxy	0.96 ± 0.04	1.12 ± 0.05	1.17	0.0442	0.4467
2-hydroxypalmitate	Lipid	Fatty Acid, Monohydroxy	1.07 ± 0.04	0.92 ± 0.04	0.86	0.0224	0.4467
prostaglandin F2alpha	Lipid	Eicosanoid	1.28 ± 0.15	0.81 ± 0.09	0.63	0.0238	0.4467
1-stearoyl-2-linoleoyl-GPC (18:0/18:2)*	Lipid	Phospholipid Metabolism	0.91 ± 0.05	1.05 ± 0.05	1.15	0.0942	0.4467
1-oleoyl-2-linolenoyl-GPC (18:1/18:3)	Lipid	Phospholipid Metabolism	0.65 ± 0.14	1.18 ± 0.19	1.81	0.0991	0.4467
1-stearoyl-2-linoleoyl-GPE (18:0/18:2)*	Lipid	Phospholipid Metabolism	0.96 ± 0.03	1.09 ± 0.05	1.15	0.0579	0.4467
1,2-dioleoyl-GPE (18:1/18:1)	Lipid	Phospholipid Metabolism	0.97 ± 0.01	1.09 ± 0.05	1.12	0.0951	0.4467
1,2-dilinoleoyl-GPC (18:2/18:2)	Lipid	Phospholipid Metabolism	0.85 ± 0.08	1.06 ± 0.06	1.24	0.0707	0.4467
1-oleoyl-2-linoleoyl-GPE (18:1/18:2)*	Lipid	Phospholipid Metabolism	0.98 ± 0.02	1.08 ± 0.03	1.10	0.0449	0.4467

1,2-distearoyl-GPC (18:0/18:0)	Lipid	Phospholipid Metabolism	0.89 ± 0.06	1.06 ± 0.04	1.18	0.0631	0.4467
1-linoleoyl-2-arachidonoyl-GPC (18:2/20:4)*	Lipid	Phospholipid Metabolism	0.95 ± 0.03	1.11 ± 0.08	1.18	0.0888	0.4467
1-lignoceroyl-GPC (24:0)	Lipid	Lysolipid	0.90 ± 0.05	1.07 ± 0.05	1.18	0.0364	0.4467
1-(1-enyl-stearoyl)-2-oleoyl-GPE (P-18:0/18:1)	Lipid	Plasmalogen	0.91 ± 0.04	1.07 ± 0.06	1.17	0.0681	0.4467
1-(1-enyl-stearoyl)-2-linoleoyl-GPE (P-18:0/18:2)*	Lipid	Plasmalogen	0.89 ± 0.06	1.12 ± 0.06	1.26	0.0227	0.4467
1-(1-enyl-stearoyl)-2-arachidonoyl-GPE (P-18:0/20:4)*	Lipid	Plasmalogen	0.97 ± 0.02	1.07 ± 0.04	1.11	0.0539	0.4467
1-myristoylglycerol (14:0)	Lipid	Monoacylglycerol	0.82 ± 0.08	1.66 ± 0.51	2.04	0.0935	0.4467
N-palmitoyl-sphinganine (d18:0/16:0)	Lipid	Sphingolipid Metabolism	0.92 ± 0.04	1.12 ± 0.07	1.22	0.0483	0.4467
behenoyl sphingomyelin (d18:1/22:0)*	Lipid	Sphingolipid Metabolism	0.94 ± 0.04	1.08 ± 0.04	1.14	0.0426	0.4467
sphingomyelin (d18:1/21:0, d17:1/22:0, d16:1/23:0)*	Lipid	Sphingolipid Metabolism	0.94 ± 0.05	1.14 ± 0.08	1.21	0.0749	0.4467
tricosanoyl sphingomyelin (d18:1/23:0)*	Lipid	Sphingolipid Metabolism	0.84 ± 0.05	1.14 ± 0.11	1.35	0.0338	0.4467
cholesterol	Lipid	Sterol	0.92 ± 0.03	1.03 ± 0.01	1.12	0.0106	0.4467
campesterol	Lipid	Sterol	0.89 ± 0.05	1.07 ± 0.04	1.20	0.0241	0.4467
tauro-alpha-muricholate	Lipid	Primary Bile Acid Metabolism	0.66 ± 0.18	1.48 ± 0.33	2.23	0.0542	0.4467
tauro-beta-muricholate	Lipid	Primary Bile Acid Metabolism	0.71 ± 0.14	2.25 ± 0.67	3.16	0.0472	0.4467
glycodeoxycholate	Lipid	Secondary Bile Acid Metabolism	1.67 ± 0.44	0.45 ± 0.16	0.27	0.0179	0.4467

3-methylcytidine	Nucleotide	Purine Metabolism, Adenine containing	1.09 ± 0.05	0.86 ± 0.08	0.78	0.0751	0.4467
5-methylcytidine	Nucleotide	Purine Metabolism, Adenine containing	1.07 ± 0.03	0.95 ± 0.02	0.88	0.0159	0.4467
quinolinate	Cofactors and Vitamins	Purine Metabolism, Adenine containing	0.88 ± 0.11	1.24 ± 0.14	1.41	0.0561	0.4467
N1-Methyl-2-pyridone-5-carboxamide	Cofactors and Vitamins e	Nicotinate and Nicotinamide Metabolism	1.09 ± 0.12	0.78 ± 0.10	0.71	0.0552	0.4467
pyridoxal	Cofactors and Vitamins	Vitamin B6 Metabolism	1.06 ± 0.05	0.94 ± 0.05	0.88	0.0693	0.4467
pyridoxate	Cofactors and Vitamins	Vitamin B6 Metabolism	1.44 ± 0.19	0.86 ± 0.08	0.60	0.0568	0.4467

Table A 5: Biochemical compounds profiled in aorta tissues.

Biochemical metabolites	Super Pathway	Sub Pathway	Mean ±SEM		Fold of Change Welch's Two-Sample t-Test (HEXA/Control)	Statistical Values	
			Control	HEXA		p-value	q-value
glycine	Amino acids	Glycine, Serine and Threonine Metabolism	1.41 ± 0.72	1.13 ± 0.054	0.80	0.0122	0.6182
serine	Amino acids	Glycine, Serine and Threonine Metabolism	1.34 ± 0.05	1.12 ± 0.96	0.84	0.0953	0.6182
asparagine	Amino acids	Alanine and Aspartate Metabolism	0.89 ± 0.02	0.79 ± 0.04	0.89	0.0606	0.6182
pyroglutamine*	Amino acids	Glutamate Metabolism	1.56 ± 0.06	1.23 ± 0.11	0.79	0.0471	0.6182
histidine	Amino acids	Histidine Metabolism	1.47 ± 0.10	1.18 ± 0.09	0.8	0.0652	0.6182
imidazole lactate	Amino acids	Histidine Metabolism	0.73 ± 0.05	1.00 ± 0.11	1.38	0.0769	0.6182
phenyllactate (PLA)	Amino acids	Phenylalanine and Tyrosine Metabolism	0.82 ± 0.07	0.99 ± 0.05	1.21	0.0723	0.6182
3-methoxytyrosine	Amino acids	Phenylalanine and Tyrosine Metabolism	1.08 ± 0.12	0.73 ± 0.15	0.68	0.0953	0.6182
indolelactate	Amino acids	Tryptophan Metabolism	1.13 ± 0.07	1.43 ± 0.11	1.27	0.0497	0.6182
valine	Amino acids	Leucine, Isoleucine and Valine	1.84 ± 0.08	1.56 ± 0.11	0.84	0.0805	0.6182
taurocyamine	Amino acids	Methionine, Cysteine, SAM and Taurine Metabolism	0.63 ± 0.03	0.49 ± 0.03	0.78	0.0141	0.6182
creatinine	Amino acids	Creatine Metabolism	0.55 ± 0.03	0.47 ± 0.02	0.85	0.0561	0.6182
gamma-glutamylglycine	Amino acids	Gamma-glutamyl Amino Acid	1.75 ± 0.47	0.95 ± 0.12	0.54	0.0787	0.6182
gamma-glutamylvaline	Amino acids	Gamma-glutamyl Amino Acid	0.86 ± 0.09	1.17 ± 0.11	1.35	0.0756	0.6182
1,5-anhydroglucitol (1,5-AG)	Carbohydrate	Glycolysis, Gluconeogenesis, and Pyruvate Metabolism	1.06 ± 0.09	0.81 ± 0.05	0.77	0.0457	0.6182
mannitol/sorbitol	Carbohydrate	Fructose, Mannose and Galactose Metabolism	0.56 ± 0.04	0.72 ± 0.06	1.29	0.0371	0.6182
citrate	Energy	TCA Cycle	1.14 ± 0.10	1.62 ± 0.27	1.43	0.0992	0.6182

succinylcarnitine	Energy	TCA Cycle	0.43 ± 0.07	0.77 ± 0.13	1.79	0.0473	0.6182
arachidonate (20:4n6)	Lipid	Polyunsaturated Fatty Acid (n3 and n6)	1.77 ± 0.14	1.29 ± 0.15	0.72	0.0525	0.6182
12-HETE	Lipid	Eicosanoid	2.10 ± 0.19	1.51 ± 0.24	0.74	0.0908	0.6182
1,2-dipalmitoyl-GPC (16:0/16:0)	Lipid	Phospholipid Metabolism	1.12 ± 0.03	0.99 ± 0.03	0.89	0.0186	0.6182
1-oleoyl-2-linoleoyl-GPC (18:1/18:2)*	Lipid	Phospholipid Metabolism	1.17 ± 0.08	0.97 ± 0.03	0.82	0.0528	0.6182
1-palmitoyl-2-stearoyl-GPC (16:0/18:0)	Lipid	Phospholipid Metabolism	1.19 ± 0.02	1.02 ± 0.04	0.86	0.0112	0.6182
1-stearoyl-2-oleoyl-GPG (18:0/18:1)	Lipid	Phospholipid Metabolism	0.69 ± 0.09	0.93 ± 0.04	1.33	0.0718	0.6182
1-linoleoyl-2-arachidonoyl-GPC (18:2/20:4n6)*	Lipid	Phospholipid Metabolism	1.19 ± 0.10	0.86 ± 0.08	0.72	0.0398	0.6182
1-palmitoyl-GPE (16:0)	Lipid	Lysolipid	2.19 ± 0.14	1.62 ± 0.11	0.74	0.008	0.6182
1-stearoyl-GPE (18:0)	Lipid	Lysolipid	2.08 ± 0.16	1.50 ± 0.14	0.72	0.0264	0.6182
1-oleoyl-GPE (18:1)	Lipid	Lysolipid	2.70 ± 0.24	1.9 ± 0.09	0.71	0.0219	0.6182
1-(1-enyl-palmitoyl)-2-arachidonoyl-GPE (P-16:0/20:4)*	Lipid	Plasmalogen	1.00 ± 0.03	0.89 ± 0.03	0.88	0.0197	0.6182
1-(1-enyl-stearoyl)-2-arachidonoyl-GPE (P-18:0/20:4)*	Lipid	Plasmalogen	1.00 ± 0.03	0.88 ± 0.04	0.88	0.0584	0.6182
1-(1-enyl-palmitoyl)-GPE (P-16:0)*	Lipid	Lysoplasmalogen	1.38 ± 0.16	0.94 ± 0.05	0.68	0.0309	0.6182
1-(1-enyl-oleoyl)-GPE (P-18:1)*	Lipid	Lysoplasmalogen	1.43 ± 0.19	0.96 ± 0.06	0.67	0.0478	0.6182
N-palmitoyl-sphingosine (d18:1/16:0)	Lipid	Sphingolipid Metabolism	2.4 ± 0.21	1.85 ± 0.12	0.77	0.0638	0.6182
tauro-beta-muricholate	Lipid	Primary Bile Acid Metabolism	0.32 ± 0.13	2.12 ± 0.88	6.55	0.0029	0.6182
deoxycholate	Lipid	Secondary Bile Acid Metabolism	0.42 ± 0.00	0.79 ± 0.19	1.91	0.0917	0.6182

glycodeoxycholate	Lipid	Secondary Bile Acid Metabolism	1.12 ± 0.23	0.45 ± 0.05	0.40	0.0337	0.6182
N1-methyladenosine	Nucleotide	Purine Metabolism, Adenine containing	0.80 ± 0.06	0.62 ± 0.06	0.72	0.0134	0.6182
N6-succinyladenosine	Nucleotide	Purine Metabolism, Adenine containing	0.20 ± 0.05	0.35 ± 0.05	1.70	0.061	0.6182
2'-deoxyuridine	Nucleotide	Pyrimidine Metabolism, Uracil containing	1.28 ± 0.06	0.72 ± 0.09	0.57	0.0079	0.6182
cytosine	Nucleotide	Pyrimidine Metabolism, Cytidine containing	0.97 ± 0.14	1.40 ± 0.17	1.45	0.0919	0.6182
nicotinate ribonucleoside	Cofactors and Vitamins	Nicotinate and Nicotinamide Metabolism	0.92 ± 0.06	0.75 ± 0.02	0.82	0.0432	0.6182
nicotinamide adenine dinucleotide (NAD+)	Cofactors and Vitamins	Nicotinate and Nicotinamide Metabolism	0.91 ± 0.07	1.42 ± 0.16	1.55	0.0187	0.6182
pyridoxate	Cofactors and Vitamins	Vitamin B6 Metabolism	2.34 ± 0.32	1.53 ± 0.22	0.65	0.0614	0.6182
catechol sulfate	Xenobiotics	Benzoate Metabolism	0.84 ± 0.22	1.37 ± 0.15	1.63	0.0955	0.6182

Table A 6: Biochemical compounds profiled in heart tissues.

Biochemical metabolites	Super Pathway	Sub Pathway	Mean ±SEM		Fold of Change Welch's Two-Sample t-Test (HEXA/Control)	Statistical Values	
			Control	HEXA		p-value	q-value
threonine	Amino acids	Glycine, Serine and Threonine Metabolism	0.61 ± 0.02	0.72 ± 0.02	1.18	0.0053	0.2036
asparagine	Amino acids	Alanine and Aspartate Metabolism	1.17 ± 0.04	1.29 ± 0.03	1.11	0.038	0.2036
N-acetylaspartate (NAA)	Amino acids	Alanine and Aspartate Metabolism	1.67 ± 0.04	1.33 ± 0.05	0.8	0.0018	0.2036
N-acetylglutamine	Amino acids	Glutamate Metabolism	1.32 ± 0.11	1.09 ± 0.04	0.82	0.0903	0.2036
1-methylimidazoleacetate	Amino acids	Histidine Metabolism	0.53 ± 0.06	0.79 ± 0.07	1.47	0.0313	0.2036
N6,N6,N6-trimethyllysine	Amino acids	Lysine Metabolism	0.89 ± 0.05	1.02 ± 0.04	1.15	0.0948	0.2036
phenyllactate (PLA)	Amino acids	Phenylalanine and Tyrosine Metabolism	0.82 ± 0.05	1.33 ± 0.21	1.63	0.0482	0.2036
tyrosine	Amino acids	Phenylalanine and Tyrosine Metabolism	0.57 ± 0.04	0.67 ± 0.03	1.18	0.0584	0.2036
3-(4-hydroxyphenyl)lactate	Amino acids	Phenylalanine and Tyrosine Metabolism	1.49 ± 0.05	1.82 ± 0.08	1.22	0.0529	0.2036
tryptophan	Amino acids	Tryptophan Metabolism	0.63 ± 0.04	0.74 ± 0.01	1.19	0.0427	0.2036
C-glycosyltryptophan	Amino acids	Tryptophan Metabolism	0.99 ± 0.05	1.304 ± 0.06	1.32	0.01	0.2036
leucine	Amino acids	Leucine, Isoleucine and Valine Metabolism	0.57 ± 0.05	0.67 ± 0.02	1.18	0.0837	0.2036
beta-hydroxyisovaleroylcarnitine	Amino acids	Leucine, Isoleucine and Valine Metabolism	1.65 ± 0.12	2.07 ± 0.14	1.26	0.0444	0.2036
alpha-hydroxyisovaleroyl carnitine*	Amino acids	Leucine, Isoleucine and Valine Metabolism	0.86 ± 0.11	1.15 ± 0.07	1.34	0.0907	0.2036
methylsuccinate	Amino acids	Leucine, Isoleucine and Valine Metabolism	1.71 ± 0.17	1.17 ± 0.07	0.68	0.0141	0.2036

isoleucine	Amino acids	Leucine, Isoleucine and Valine Metabolism	0.71 ± 0.03	0.82 ± 0.02	1.16	0.0266	0.2036
tiglylcarnitine	Amino acids	Leucine, Isoleucine and Valine Metabolism	1.47 ± 0.12	2.02 ± 0.10	1.37	0.0108	0.2036
methionine	Amino acids	Methionine, Cysteine, SAM and Taurine Metabolism	0.67 ± 0.04	0.80 ± 0.02	1.20	0.0266	0.2036
S-adenosylmethionine (SAM)	Amino acids	Methionine, Cysteine, SAM and Taurine	1.39 ± 0.07	1.66 ± 0.07	1.19	0.0254	0.2036
S-adenosylhomocysteine (SAH)	Amino acids	Methionine, Cysteine, SAM and Taurine Metabolism	0.81 ± 0.07	0.97 ± 0.05	1.20	0.0782	0.2036
argininosuccinate	Amino acids	Urea cycle; Arginine and Proline Metabolism	1.10 ± 0.06	1.43 ± 0.12	1.29	0.0438	0.2036
dimethylarginine (SDMA + ADMA)	Amino acids	Urea cycle; Arginine and Proline Metabolism	0.89 ± 0.05	1.06 ± 0.06	1.18	0.0541	0.2036
N-delta-acetylornithine	Amino acids	Urea cycle; Arginine and Proline Metabolism	1.15 ± 0.05	1.36 ± 0.08	1.18	0.079	0.2036
glucose	Carbohydrate	Glycolysis, Gluconeogenesis, and Pyruvate Metabolism	0.74 ± 0.06	0.96 ± 0.09	1.30	0.0822	0.2036
glucose 6-phosphate	Carbohydrate	Glycolysis, Gluconeogenesis, and Pyruvate Metabolism	0.77 ± 0.15	1.42 ± 0.28	1.85	0.0692	0.2036
3-phosphoglycerate	Carbohydrate	Glycolysis, Gluconeogenesis, and Pyruvate Metabolism	2.87 ± 0.59	1.67 ± 0.12	0.58	0.0929	0.2036
ribulose/xylulose	Carbohydrate	Pentose Metabolism	2.03 ± 0.23	2.70 ± 0.16	1.33	0.0649	0.2036
maltotetraose	Carbohydrate	Glycogen Metabolism	0.46 ± 0.11	1.40 ± 0.60	3.02	0.0925	0.2036
maltotriose	Carbohydrate	Glycogen Metabolism	0.47 ± 0.08	1.07 ± 0.27	2.27	0.0431	0.2036
maltose	Carbohydrate	Glycogen Metabolism	0.473 ± 0.05	0.86 ± 0.11	1.82	0.0132	0.2036
fructose	Carbohydrate	Fructose, Mannose and Galactose Metabolism	1.31 ± 0.22	2.12 ± 0.19	1.61	0.055	0.2036

glucosamine-6-phosphate	Carbohydrate	Aminosugar Metabolism	0.82 ± 0.16	1.52 ± 0.25	1.85	0.0619	0.2036
N-acetylneuraminate	Carbohydrate	Aminosugar Metabolism	1.59 ± 0.10	1.96 ± 0.10	1.23	0.042	0.2036
fumarate	Energy	TCA Cycle	1.14 ± 0.03	1.28 ± 0.03	1.12	0.0144	0.2036
phosphate	Energy	Oxidative Phosphorylation	1.55 ± 0.05	1.38 ± 0.05	0.89	0.0382	0.2036
linoleate (18:2n6)	Lipid	Polyunsaturated Fatty Acid (n3 and n6)	0.22 ± 0.13	0.52 ± 0.16	2.39	0.0955	0.2036
hexadecanedioate	Lipid	Fatty Acid, Dicarboxylate	0.63 ± 0.06	0.98 ± 0.08	1.57	0.0091	0.2036
malonylcarnitine	Lipid	Fatty Acid Synthesis	1.69 ± 0.05	1.91 ± 0.09	1.13	0.0546	0.2036
butyrylcarnitine	Lipid	Fatty Acid Metabolism (also BCAA Metabolism)	0.59 ± 0.27	1.19 ± 0.10	1.99	0.0801	0.2036
3-hydroxybutyrylcarnitine (1)	Lipid	Fatty Acid Metabolism(Acyl Carnitine)	2.26 ± 0.24	3.03 ± 0.21	1.34	0.0377	0.2036
3-hydroxybutyrylcarnitine (2)	Lipid	Fatty Acid Metabolism(Acyl Carnitine)	2.24 ± 0.31	3.64 ± 0.31	1.62	0.0188	0.2036
palmitoylcarnitine	Lipid	Fatty Acid Metabolism(Acyl Carnitine)	0.76 ± 0.19	1.72 ± 0.36	2.28	0.0409	0.2036
stearoylcarnitine	Lipid	Fatty Acid Metabolism(Acyl Carnitine)	0.45 ± 0.14	1.65 ± 0.48	3.65	0.0241	0.2036
linoleoylcarnitine*	Lipid	Fatty Acid Metabolism (Acyl Carnitine)	0.49 ± 0.08	2.83 ± 0.71	5.72	0.0022	0.2036
oleoylcarnitine	Lipid	Fatty Acid Metabolism (Acyl Carnitine)	0.51 ± 0.02	3.81 ± 1.14	7.48	0.0076	0.2036
myo-inositol	Lipid	Inositol Metabolism	0.29 ± 0.005	0.27 ± 0.002	0.93	0.0078	0.2036
phosphoethanolamine	Lipid	Phospholipid Metabolism	0.78 ± 0.03	0.68 ± 0.023	0.87	0.0324	0.2036
trimethylamine N-oxide	Lipid	Phospholipid Metabolism	0.79 ± 0.14	1.37 ± 0.07	1.74	0.026	0.2036

1-palmitoyl-2-linoleoyl-GPC (16:0/18:2)	Lipid	Phospholipid Metabolism	0.48 ± 0.14	0.92 ± 0.07	1.91	0.071	0.2036
1,2-dioleoyl-GPC (18:1/18:1)*	Lipid	Phospholipid Metabolism	0.33 ± 0.11	0.76 ± 0.13	2.30	0.0432	0.2036
1-stearoyl-2-linoleoyl-GPC (18:0/18:2)*	Lipid	Phospholipid Metabolism	0.61 ± 0.18	1.20 ± 0.12	1.97	0.0711	0.2036
1-palmitoyl-2-palmitoleoyl-GPC (16:0/16:1)*	Lipid	Phospholipid Metabolism	0.21 ± 0.06	0.41 ± 0.05	1.95	0.0678	0.2036
1-oleoyl-2-linoleoyl-GPC (18:1/18:2)*	Lipid	Phospholipid Metabolism	0.53 ± 0.17	1.09 ± 0.15	2.06	0.0712	0.2036
1-palmitoyl-2-linoleoyl-GPI (16:0/18:2)	Lipid	Phospholipid Metabolism	0.66 ± 0.16	1.06 ± 0.02	1.6	0.0914	0.2036
1-palmitoyl-2-oleoyl-GPE (16:0/18:1)	Lipid	Phospholipid Metabolism	0.28 ± 0.07	0.62 ± 0.08	2.22	0.043	0.2036
1-stearoyl-2-oleoyl-GPE (18:0/18:1)	Lipid	Phospholipid Metabolism	0.19 ± 0.05	0.41 ± 0.06	2.11	0.0349	0.2036
1-palmitoyl-2-arachidonoyl-GPE (16:0/20:4)*	Lipid	Phospholipid Metabolism	0.37 ± 0.09	0.68 ± 0.07	1.84	0.0757	0.2036
1-palmitoyl-2-linoleoyl-GPE (16:0/18:2)	Lipid	Phospholipid Metabolism	0.56 ± 0.14	1.18 ± 0.14	2.10	0.0459	0.2036
1-stearoyl-2-linoleoyl-GPE (18:0/18:2)*	Lipid	Phospholipid Metabolism	0.69 ± 0.17	1.49 ± 0.21	2.15	0.0402	0.2036
1,2-dioleoyl-GPE (18:1/18:1)	Lipid	Phospholipid Metabolism	0.22 ± 0.06	0.56 ± 0.10	2.59	0.0275	0.2036
1-palmitoyl-2-linolenoyl-GPC (16:0/18:3)*	Lipid	Phospholipid Metabolism	0.23 ± 0.09	0.49 ± 0.08	2.14	0.0715	0.2036
1-palmitoleoyl-2-linoleoyl-GPC (16:1/18:2)*	Lipid	Phospholipid Metabolism	0.35 ± 0.14	0.86 ± 0.13	2.49	0.0536	0.2036
1,2-dilinoleoyl-GPC (18:2/18:2)	Lipid	Phospholipid Metabolism	0.59 ± 0.23	1.56 ± 0.27	2.60	0.0442	0.2036
1-oleoyl-2-linoleoyl-GPE (18:1/18:2)*	Lipid	Phospholipid Metabolism	0.49 ± 0.60	1.14 ± 0.27	2.30	0.0388	0.2036
1-palmitoleoyl-GPC (16:1)*	Lipid	Lysolipid	0.19 ± 0.082	0.48 ± 0.11	2.47	0.0592	0.2036
1-stearoyl-GPC (18:0)	Lipid	Lysolipid	0.40 ± 0.15	0.77 ± 0.14	1.91	0.093	0.2036

1-palmitoyl-GPE (16:0)	Lipid	Lysolipid	0.16 ± 0.06	0.36 ± 0.08	2.29	0.0637	0.2036
1-stearoyl-GPE (18:0)	Lipid	Lysolipid	0.25 ± 0.09	0.60 ± 0.13	2.41	0.0554	0.2036
1-oleoyl-GPE (18:1)	Lipid	Lysolipid	0.09 ± 0.04	0.25 ± 0.07	2.91	0.0458	0.2036
1-stearoyl-GPI (18:0)	Lipid	Lysolipid	0.18 ± 0.05	0.84 ± 0.49	4.62	0.0946	0.2036
1-oleoyl-GPI (18:1)*	Lipid	Lysolipid	0.19 ± 0.07	0.57 ± 0.19	3.07	0.0682	0.2036
1-linoleoyl-GPI (18:2)*	Lipid	Lysolipid	0.41 ± 0.16	0.88 ± 0.20	2.13	0.0688	0.2036
1-(1-enyl-palmitoyl)-2-oleoyl-GPE (P-16:0/18:1)*	Lipid	Plasmalogen	0.45 ± 0.12	0.96 ± 0.13	2.11	0.0385	0.2036
1-(1-enyl-palmitoyl)-2-linoleoyl-GPE (P-16:0/18:2)*	Lipid	Plasmalogen	1.04 ± 0.26	2.11 ± 0.29	2.04	0.05	0.2036
1-(1-enyl-palmitoyl)-2-palmitoyl-GPC (P-16:0/16:0)*	Lipid	Plasmalogen	0.40 ± 0.16	0.72 ± 0.082	1.80	0.0777	0.2036
1-(1-enyl-palmitoyl)-2-oleoyl-GPC (P-16:0/18:1)*	Lipid	Plasmalogen	0.24 ± 0.08	0.44 ± 0.07	1.84	0.0482	0.2036
1-(1-enyl-stearoyl)-2-oleoyl-GPE (P-18:0/18:1)	Lipid	Plasmalogen	0.29 ± 0.06	0.64 ± 0.11	2.23	0.0143	0.2036
1-(1-enyl-stearoyl)-2-linoleoyl-GPE (P-18:0/18:2)*	Lipid	Plasmalogen	1.09 ± 0.27	2.29 ± 0.32	2.09	0.0503	0.2036
1-(1-enyl-palmitoyl)-2-linoleoyl-GPC (P-16:0/18:2)*	Lipid	Plasmalogen	0.49 ± 0.23	1.16 ± 0.24	2.31	0.0629	0.2036
1-(1-enyl-palmitoyl)-GPC (P-16:0)*	Lipid	Lysoplasmalogen	0.77 ± 0.33	1.78 ± 0.33	2.31	0.0532	0.2036
1-(1-enyl-palmitoyl)-GPE (P-16:0)*	Lipid	Lysoplasmalogen	0.48 ± 0.17	1.19 ± 0.24	2.47	0.0468	0.2036
1-(1-enyl-oleoyl)-GPE (P-18:1)*	Lipid	Lysoplasmalogen	0.56 ± 0.21	1.55 ± 0.35	2.77	0.0438	0.2036

1-(1-enyl-stearoyl)-GPE (P-18:0)*	Lipid	Lysoplasmalogen	0.45 ± 0.15	1.09 ± 0.29	2.41	0.0617	0.2036
1-oleoylglycerol (18:1)	Lipid	Monoacylglycerol	0.22 ± 0.09	0.48 ± 0.09	2.16	0.0406	0.2036
2-oleoylglycerol (18:1)	Lipid	Monoacylglycerol	0.28 ± 0.21	0.75 ± 0.20	2.69	0.0592	0.2036
1-palmitoyl-3-linoleoyl-glycerol (16:0/18:2)*	Lipid	Diacylglycerol	0.29 ± 0.19	0.56 ±0.11	1.90	0.0845	0.2036
N-palmitoyl-sphingosine (d18:1/16:0)	Lipid	Sphingolipid Metabolism	0.21 ± 0.07	0.42 ± 0.07	1.97	0.0647	0.2036
sphingomyelin (d18:1/24:1, d18:2/24:0)*	Lipid	Sphingolipid Metabolism	0.38 ± 0.13	0.64 ± 0.07	1.70	0.0975	0.2036
sphingomyelin (d18:1/20:0, d16:1/22:0)*	Lipid	Sphingolipid Metabolism	1.24 ± 0.46	2.32 ± 0.37	1.88	0.097	0.2036
palmitoyl dihydrosphingomyelin (d18:0/16:0)*	Lipid	Sphingolipid Metabolism	0.31 ± 0.06	0.47 ± 0.05	1.53	0.0543	0.2036
sphingomyelin (d18:2/24:1, d18:1/24:2)*	Lipid	Sphingolipid Metabolism	0.45 ± 0.15	0.79 ± 0.09	1.79	0.0766	0.2036
3-hydroxy-3-methylglutarate	Lipid	Mevalonate Metabolism	0.67 ± 0.01	0.59 ± 0.01	0.89	0.0024	0.2036
cholesterol	Lipid	Sterol	0.49 ± 0.21	0.97 ± 0.14	1.94	0.0907	0.2036
beta-sitosterol	Lipid	Sterol	0.51 ± 0.19	1.18 ± 0.18	2.31	0.0324	0.2036
xanthosine	Nucleotide	Purine Metabolism, (Hypo)Xanthine/Inosine containing	0.62 ± 0.08	0.89 ± 0.07	1.43	0.0401	0.2036
2'-deoxyinosine	Nucleotide	Purine Metabolism, (Hypo)Xanthine/Inosine containing	0.72 ± 0.06	1.10 ± 0.16	1.53	0.0651	0.2036
adenosine 5'-diphosphate (ADP)	Nucleotide	Purine Metabolism, Adenine containing	2.39 ± 0.99	4.31 ± 0.54	1.81	0.0987	0.2036
adenosine 3'-monophosphate (3'-AMP)	Nucleotide	Purine Metabolism, Adenine containing	0.47 ± 0.08	0.82 ± 0.09	1.74	0.0215	0.2036

adenosine 2'-monophosphate (2'-AMP)	Nucleotide	Purine Metabolism, Adenine containing	0.61 ± 0.17	0.94 ± 0.09	1.54	0.0757	0.2036
adenosine	Nucleotide	Purine Metabolism, Adenine containing	0.53 ± 0.14	0.95 ± 0.18	1.78	0.0829	0.2036
N1-methyladenosine	Nucleotide	Purine Metabolism, Adenine containing	1.01 ± 0.05	1.40 ± 0.11	1.39	0.0147	0.2036
N6-succinyladenosine	Nucleotide	Purine Metabolism, Adenine containing	1.99 ± 0.19	2.72 ± 0.19	1.37	0.0335	0.2036
guanine	Nucleotide	Purine Metabolism, Guanine containing	0.58 ± 0.11	1.18 ± 0.17	2.05	0.0181	0.2036
2'-deoxyguanosine	Nucleotide	Purine Metabolism, Guanine containing	0.89 ± 0.07	1.72 ± 0.37	1.94	0.0809	0.2036
pseudouridine	Nucleotide	Pyrimidine Metabolism, Uracil containing	0.99 ± 0.06	1.13 ± 0.04	1.13	0.0907	0.2036
5-methyluridine (ribothymidine)	Nucleotide	Pyrimidine Metabolism, Uracil containing	0.93 ± 0.04	1.19 ± 0.08	1.29	0.0129	0.2036
cytidine	Nucleotide	Pyrimidine Metabolism, Cytidine containing	1.04 ± 0.03	1.20 ± 0.05	1.16	0.0168	0.2036
5-methyl-2'-deoxycytidine	Nucleotide	Pyrimidine Metabolism, Cytidine containing	0.62 ± 0.04	0.75 ± 0.04	1.20	0.0838	0.2036
nicotinate ribonucleoside	Cofactors and Vitamins	Nicotinate and Nicotinamide Metabolism	1.45 ± 0.24	2.35 ± 0.41	1.62	0.0869	0.2036
nicotinamide riboside	Cofactors and Vitamins	Nicotinate and Nicotinamide Metabolism	1.39 ± 0.07	1.70 ± 0.14	1.22	0.0915	0.2036
nicotinamide adenine dinucleotide (NAD+)	Cofactors and Vitamins	Nicotinate and Nicotinamide Metabolism	0.74 ± 0.09	1.09 ± 0.09	1.48	0.0297	0.2036
riboflavin (Vitamin B2)	Cofactors and Vitamins	Riboflavin Metabolism	0.52 ± 0.06	0.81 ± 0.12	1.57	0.0702	0.2036
flavin mononucleotide (FMN)	Cofactors and Vitamins	Riboflavin Metabolism	0.55 ± 0.12	0.94 ± 0.15	1.72	0.0952	0.2036
pantothenate	Cofactors and Vitamins	Pantothenate and CoA Metabolism	0.83 ± 0.05	0.94 ± 0.04	1.13	0.0997	0.2036

coenzyme A	Cofactors and Vitamins	Pantothenate and CoA Metabolism	1.62 ± 0.22	0.86 ± 0.24	0.53	0.0305	0.2036
biliverdin	Cofactors and Vitamins	Hemoglobin and Porphyrin Metabolism	1.06 ± 0.12	1.53 ± 0.12	1.44	0.029	0.2036
thiamin (Vitamin B1)	Cofactors and Vitamins	Thiamine Metabolism	0.47 ± 0.04	0.66 ± 0.06	1.42	0.0201	0.2036
retinol (Vitamin A)	Cofactors and Vitamins	retinol (Vitamin A)	0.27 ± 0.06	0.54 ± 0.10	2.02	0.0652	0.2036

List of References

Aarsland, A., Aarsaether, N., Bremer, J. and Berge, R.K. (1989) Alkylthioacetic acids (3-thia fatty acids) as non-beta-oxidizable fatty acid analogues: a new group of hypolipidemic drugs. III. Dissociation of cholesterol- and triglyceride-lowering effects and the induction of peroxisomal beta-oxidation. *Journal of lipid research*, 30, 1711–1718.

Acker, M.A., Parides, M.K., Perrault, L.P., Moskowitz, A.J., Gelijns, A.C., Voisine, P., Smith, P.K., Hung, J.W., Blackstone, E.H., Puskas, J.D., Argenziano, M., Gammie, J.S., Mack, M., Ascheim, D.D., Bagiella, E., Moquete, E.G., Ferguson, T.B., Horvath, K.A., Geller, N.L., *et al.* (2014) Mitral-Valve Repair versus Replacement for Severe Ischemic Mitral Regurgitation. *New England Journal of Medicine*, 370 (1), 23–32. Available from: doi:10.1056/NEJMoa1312808.

Ackermann, U. (2004) Regulation of arterial blood pressure. *Surgery (Oxford)*, 22 (5), 120a–120f. Available from: doi:10.1383/surg.22.5.120a.33383.

Adams, S.H., Hoppel, C.L., Lok, K.H., Zhao, L., Wong, S.W., Minkler, P.E., Hwang, D.H., Newman, J.W. and Garvey, W.T. (2009) Plasma acylcarnitine profiles suggest incomplete long-chain fatty acid -oxidation and altered tricarboxylic acid cycle activity in type 2 diabetic african-american women. *Journal of Nutrition*, 139 (6), 1073–1081. Available from: doi:10.3945/jn.108.103754.

Adeyemo, A., Gerry, N., Chen, G., Herbert, A., Doumatey, A., Huang, H., Zhou, J., Lashley, K., Chen, Y., Christman, M. and Rotimi, C. (2009) A genome-wide association study of hypertension and blood pressure in african americans. *PLoS Genetics*, 5 (7), 1–11. Available from: doi:10.1371/journal.pgen.1000564.

De Aguiar Vallim, T.Q., Tarling, E.J. and Edwards, P.A. (2013) Pleiotropic roles of bile acids in metabolism. *Cell Metabolism*, 17 (5), 657–669. Available from: doi:10.1016/j.cmet.2013.03.013.

Ajouz, H., Mukherji, D. and Shamseddine, A. (2014) Secondary bile acids: an underrecognized cause of colon cancer. *World Journal of Surgical Oncology*, 12 (164), 1–5. Available from: doi:10.1186/1477-7819-12-164.

Anderson, N.H., Devlin, A.M., Graham, D., Morton, J.J., Hamilton, C.A., Reid, J.L., Schork, N.J. and Dominiczak, A.F. (1999) Telemetry for Cardiovascular Monitoring in a Pharmacological Study : New Approaches to Data Analysis. *Hypertension*, 33 (2), 248–255. Available from: doi:10.1161/01.HYP.33.1.248.

Ashfaq, S., Abramson, J.L., Jones, D.P., Rhodes, S.D., Weintraub, W.S., Hooper, W.C., Vaccarino, V., Alexander, R.W., Harrison, D.G. and Quyyumi, A.A. (2008) Endothelial function and aminothiol biomarkers of oxidative stress in healthy adults. *Hypertension*, 52 (1), 80–85. Available from: doi:10.1161/HYPERTENSIONAHA.107.097386.

Assad, T.R. and Hemnes, A.R. (2015) Metabolic dysfunction in pulmonary arterial hypertension. *Curr Hypertens Rep*, 17 (3), 1–17. Available from: doi:10.1007/s11906-014-0524-y.

Atanur, S.S., Diaz, A.G., Maratou, K., Sarkis, A., Rotival, M., Game, L., Tschannen, M.R., Kaisaki, P.J., Otto, G.W., Ma, M.C.J., Keane, T.M., Hummel, O., Saar, K., Chen, W., Guryev, V., Gopalakrishnan, K., Garrett, M.R., Joe, B., Citterio, L., *et al.* (2013) Genome sequencing reveals loci under artificial selection that underlie disease phenotypes in the laboratory rat. *Cell*, 154 (3), 691–703. Available from: doi:10.1016/j.cell.2013.06.040.

Atkinson, L.L., Kelly, S.E., Russell, J.C., Bar-Tana, J. and Lopaschuk, G.D. (2002) MEDICA 16 inhibits hepatic acetyl-CoA carboxylase and reduces plasma triacylglycerol levels in insulin-resistant JCR:LA-cp rats. *Diabetes*, 51 (5), 1548–1555. Available from: doi:10.2337/diabetes.51.5.1548.

Bähr, A. and Wolf, E. (2012) Domestic animal models for biomedical research. *Reproduction in Domestic Animals*, 47 (4), 59–71. Available from: doi:10.1111/j.1439-0531.2012.02056.x.

Bakar, N.S., Neely, D., Avery, P., Brown, C., Daly, A.K. and Kamali, F. (2017) Genetic and clinical factors are associated with statin-related myotoxicity of moderate severity: a case-control study. *Clinical Pharmacology and Therapeutics*, 00 (00), 1–10. Available from: doi:10.1002/cpt.887.

Bakris, G.L. and Mensah, G.A. (2003) Pathogenesis and Clinical Physiology of Hypertension The Physiology of Normal BP Control. *Curr Probl Cardiol*, 28, 137–155. Available from: doi:10.1016/S0146-2806(03)00019-7.

Bansilal, S., Castellano, J.M. and Fuster, V. (2015) Global burden of CVD: Focus on secondary prevention of cardiovascular disease. *International Journal of Cardiology*, 201, S1–S7. Available from: doi:10.1016/S0167-5273(15)31026-3.

Bar-Tana, J., Rose-Kahn, G., Frenkel, B., Shafer, Z. and Fainaru, M. (1988) Hypolipidemic effect of ß, ß'-methyl-substituted hexadecanedioic acid (MEDICA 16) in normal and nephrotic rats. *Journal of Lipid Research*, 29 (4), 431–441.

Barochiner, J., Alfie, J., Aparicio, L.S., Cuffaro, P.E., Rada, M.A., Morales, M.S., Galarza, C.R. and Waisman, G.D. (2013) Prevalence and clinical profile of resistant hypertension among treated hypertensive subjects. *Clin Exp Hypertens*, 35 (6), 412–417. Available from: doi:10.3109/10641963.2012.739236.

Barré-Sinoussi, F. and Montagutelli, X. (2015) Animal models are essential to biological research: issues and perspectives. *Future Science*, 1 (4). Available from: doi:10.4155/fso.15.63.

Bartlett, K. and Eaton, S. (2004) Mitochondrial ß-oxidation. *European Journal of Biochemistry*, 271 (3), 462–469. Available from: doi:10.1046/j.1432-1033.2003.03947.x.

Barupal, D.K. and Fiehn, O. (2017) Chemical Similarity Enrichment Analysis (ChemRICH) as alternative to biochemical pathway mapping for metabolomic datasets. *nature scientific Reports*, 7 (1), 1–11. Available from: doi:10.1038/s41598-017-15231-w.

Beilin, L.J. (2004) Hypertension research in the 21st century: where is the gold? *Journal of Hypertension*, 22 (12), 2243–2251. Available from: doi:10.1097/00004872-200412000-00002.

Bernal-Mizrachi, C., Weng, S., Feng, C., Finck, B.N., Knutsen, R.H., Leone, T.C., Coleman, T., Mecham, R.P., Kelly, D.P. and Semenkovich, C.F. (2003) Dexamethasone induction of hypertension and diabetes is PPAR-α dependent in LDL receptor-null mice. *Nature Medicine*, 9 (8), 1069–1075. Available from: doi:10.1038/nm898.

Boleda, M.D., Saubi, N., Farres, J. and Pares, X. (1993) Physiological Substrates for Rat Alcohol Dehydrogenase Classes: Aldehydes of Lipid Peroxidation, ω-Hydroxyfatty Acids, and Retinoids. *Biochemistry and Biophysics*.307 (1) pp.85–90. Available from: doi:10.1006/abbi.1993.1564.

Bolk, J., van der Ploeg, T., Cornel, J.H., Arnold, A.E., Sepers, J. and Umans, V.A.W.M. (2001) Impaired glucose metabolism predicts mortality after a myocardial infarction. *International Journal of Cardiology*, 79 (2–3), 207–214. Available from: doi:S0167527301004223.

Booth, S.C., Weljie, A.M. and Turner, R.J. (2013) Computational tools for the

secondary analysis of metabolomics experiments. *Computational and Structural Biotechnology Journal*, 4 (5), 1–13. Available from: doi:10.5936/csbj.201301003.

Borràs, E., Coutelle, C., Rosell, A., Fernández-Muixi, F., Broch, M., Crosas, B., Hjelmqvist, L., Lorenzo, A., Gutiérrez, C., Santos, M., Szczepanek, M., Heilig, M., Quattrocchi, P., Farrés, J., Vidal, F., Richart, C., Mach, T., Bogdal, J., Jörnvall, H., *et al*. (2000) Genetic polymorphism of alcohol dehydrogenase in europeans: The ADH2*2 allele decreases the risk for alcoholism and is associated with ADH3*1. *Hepatology*, 31 (4), 984–989. Available from: doi:10.1053/he.2000.5978.

Bragulat, E., de la Sierra, A., Antonio, M.T. and Coca, A. (2001) Endothelial Dysfunction in Salt-Sensitive Essential Hypertension. *Hypertension*, 37 (2), 444–448. Available from: doi:10.1161/01.HYP.37.2.444.

Brittain, E.L., Talati, M., Fessel, J.P., Zhu, H., Penner, N., Calcutt, M.W., West, J.D., Funke, M., Lewis, G.D., Gerszten, R.E., Hamid, R., Pugh, M.E., Austin, E.D., Newman, J.H. and Hemnes, A.R. (2016) Fatty acid metabolic defects and right ventricular lipotoxicity in human pulmonary arterial hypertension. *Circulation*, 133 (20), 1–54. Available from: doi:10.1161/CIRCULATIONAHA.115.019351.

Brown, M.J. (2018) Comments on the 2018 ESC / ESH Guidelines for the management of arterial hypertension. *European Guidelines*, Available from: doi:10.30824/ 1806-8.

Brozovich, F. V, Nicholson, C.J., Degen, C. V, Gao, Y.Z., Aggarwal, M. and Morgan, K.G. (2016) Mechanisms of Vascular Smooth Muscle Contraction and the Basis for Pharmacologic Treatment of Smooth Muscle Disorders. *Pharmacological reviews*, 68 (2), 476–532. Available from: doi:10.1124/pr.115.010652.

Bygdeman, S., Perman, E. and Sjöstrand, N. (1962) Mechanism of the hypotension during the antabuse-alcohol reaction in rabbits. *Experientia*, 8, 51–52.

Calhoun, D.A., Jones, D., Textor, S., Goff, D.C., Murphy, T.P., Toto, R.D., White, A., Cushman, W.C., White, W., Sica, D., Ferdinand, K., Giles, T.D., Falkner, B. and Carey, R.M. (2008) Resistant hypertension: diagnosis, evaluation, and treatment: a scientific statement from the american heart association professional education committee of the council for high blood pressure research. *Circulation*, 117 (25), e510–e526. Available from: doi:10.1161/CIRCULATIONAHA.108.189141.

Caline Koh-Tan, H.H., Dashti, M., Wang, T., Beattie, W., McClure, J., Young, B., Dominiczak, A.F., McBride, M.W. and Graham, D. (2017) Dissecting the genetic components of a quantitative trait locus for blood pressure and renal pathology on rat chromosome 3. *Journal of Hypertension*, 35 (2), 319–329. Available from: doi:10.1097/HJH.0000000000001155.

Campbell, F.M., Kozak, R., Wagner, A., Altarejos, J.Y., Dyck, J.R.B., Belke, D.D., Severson, D.L., Kelly, D.P. and Lopaschuk, G.D. (2002) A role for peroxisome proliferator-activated receptor α (PPARα) in the control of cardiac malonyl-CoA levels. *Journal of Biological Chemistry*, 277 (6), 4098–4103. Available from: doi:10.1074/jbc.M106054200.

Carey, R.M., Jin, X. and Siragy, H.M. (2001) Role of the Angiotensin AT 2 Receptor in Blood Pressure Regulation and Therapeutic Implications. *the American Journal of Hypertension*, 14, 98S–102S.

Carey, R.M. and Whelton, P.K. (2018) Prevention, detection, evaluation, and management of high blood pressure in adults: synopsis of the 2017 american college of cardiology/american heart association hypertension guideline.

Annals of Internal Medicine, 168, 351–358. Available from: doi:10.7326/M17-3203.

Carretero, O. and Oparil, S. (2000) Essential Hypertension. *Circulation*, 101, 329–335. Available from: doi:10.1161/01.CIR.101.3.329.

Carvajal, K. and Moreno-Sánchez, R. (2003) Heart metabolic disturbances in cardiovascular diseases. *Archives of Medical Research*, 34 (2), 89–99. Available from: doi:10.1016/S0188-4409(03)00004-3.

Chapleau, M.W. (2012) Baroreceptor Reflexes. In: *Primer on the Autonomic Nervous System*. Third Edit. Elsevier Inc. pp. 161–165. Available from: doi:10.1016/B978-0-12-386525-0.00033-0.

Chatterjee, S. and Pal, J.K. (2009) Role of 5′- and 3′-untranslated regions of mRNAs in human diseases. *Biology of the Cell*, 101 (5), 251–262. Available from: doi:10.1042/BC20080104.

Chen, X. tian, Yang, S., Yang, Y. ming, Zhao, H. long, Chen, Y. chun, Zhao, X. hai, Wen, J. bo, Tian, Y. rui, Yan, W. li and Shen, C. (2017) Exploring the relationship of peripheral total bilirubin, red blood cell, and hemoglobin with blood pressure during childhood and adolescence. *Jornal de Pediatria*, Available from: doi:10.1016/j.jped.2017.07.018.

Cheng, X., Maher, J., Chen, C. and Klaassen, C.D. (2005) Tissue distribution and ontogeny of mouse organic anion transporting polypeptides (Oatps). *Drug Metabolism and Disposition*, 33 (7), 1062–1073. Available from: doi:10.1124/dmd.105.003640.

Chiang, J.Y.L. (2013) Bile Acid Metabolism and Signalling. *Compr Physiol*, 3 (3), 1191–1212. Available from: doi:10.1002/cphy.c120023.

Chiang, J.Y.L. (2009) Bile acids: regulation of synthesis. *Journal of Lipid Research*, 50 (10), 1955–1966. Available from: doi:10.1194/jlr.R900010-JLR200.

Chin, H.J., Song, Y.R., Kim, H.S., Park, M., Yoon, H.J., Na, K.Y., Kim, Y., Chae, D.W. and Kim, S. (2009) The bilirubin level is negatively correlated with the incidence of hypertension in normotensive Korean population. *Journal of Korean Medical Science*, 24 (SUPPL.1), 50–56. Available from: doi:10.3346/jkms.2009.24.S1.S50.

Chobanian, A. V, Bakris, G.L., Black, H.R., Cushman, W.C., Green, L.A., Izzo, J.L., Jones, D.W., Materson, B.J., Oparil, S., Wright, J.T. and Roccella, E.J. (2003) The Seventh Report of the Joint National Committee on Prevention , Detection , Evaluation , and Treatment of High Blood Pressure. *Journal American Medical Association*, 289 (19), 2560–2572.

Choi, H.Y., Park, H.C. and Ha, S.K. (2015) Salt sensitivity and hypertension: A paradigm shift from kidney malfunction to vascular endothelial dysfunction. *Electrolyte and Blood Pressure*, 13 (1), 7–16. Available from: doi:10.5049/EBP.2015.13.1.7.

Chu, J., Wang, R.Y. and Hill, N.S. (2002) Update in clinical toxicology. *American Journal of Respiratory and Critical Care Medicine*, 166 (1), 9–15. Available from: doi:10.1164/rccm.2108138.

Cifkova, R., Fodor, G. and Wohlfahrt, P. (2016) Changes in hypertension prevalence, awareness, treatment, and control in high-, middle-, and low-income countries: an update. *Current Hypertension Reports*, 18 (62), 1–6. Available from: doi:10.1007/s11906-016-0669-y.

De Ciuceis, C., Porteri, E., Rizzoni, D., Corbellini, C., La Boria, E., Boari, G.E.M., Pilu, A., Mittempergher, F., Di Betta, E., Casella, C., Nascimbeni, R., Rosei, C.A., Ruggeri, G., Caimi, L. and Rosei, E.A. (2011) Effects of weight loss on structural and functional alterations of subcutaneous small arteries in obese patients. *Hypertension*, 58, 29–36. Available from:

doi:10.1161/HYPERTENSIONAHA.111.171082.
Clarke, J.D., Hardwick, R.N., Lake, A.D., Lickteig, A.J., Goedken, M.J., Klaassen, C.D. and Cherrington, N.J. (2014) Synergistic interaction between genetics and disease on pravastatin disposition. *J Hepatol*, 61 (1), 139–147. Available from: doi:doi:10.1016/j.jhep.2014.02.021.
Cohen, J.D. (2009) Hypertension epidemiology and economic burden: refining risk assessment to lower costs. *Managed care*, 18 (10), 51–58.
Cowan, E., Kumar, P., Burch, K.J., Grieve, D.J., Green, B.D. and Graham, S.F. (2016) Treatment of lean and diet-induced obesity (DIO) mice with a novel stable obestatin analogue alters plasma metabolite levels as detected by untargeted LC–MS metabolomics. *Metabolomics*, 12 (124), 1–14. Available from: doi:10.1007/s11306-016-1063-0.
D'Elia, L. and Strazzullo, P. (2018) Excess Body Weight, Insulin Resistance and Isolated Systolic Hypertension: Potential Pathophysiological Links. *High Blood Pressure and Cardiovascular Prevention*, 25, 17–23. Available from: doi:10.1007/s40292-017-0240-1.
Demir, M., Demir, C. and Keçeoğlu, S. (2014) Relationship between serum bilirubin concentration and nondipper hypertension. *International Journal of Clinical and Experimental Medicine*, 7 (5), 1454–1458.
Desvergne, B. and Wahli, W. (1995) PPAR: a Key Nuclear Factor in Nutrient / Gene Interactions? In: *Inducible Gene Expression*. Birkhäuser. pp. 142–176.
Dhar, M., Sepkovic, D.W., Hirani, V., Magnusson, R.P. and Lasker, J.M. (2008) Omega oxidation of 3-hydroxy fatty acids by the human CYP4F gene subfamily enzyme CYP4F11. *Journal of lipid research*, 49 (3), 612–624. Available from: doi:10.1194/jlr.M700450-JLR200.
Dodd, M.S., Ball, D.R., Schroeder, M.A., Le Page, L.M., Atherton, H.J., Heather, L.C., Seymour, A.-M., Ashrafian, H., Watkins, H., Clarke, K. and Tyler, D.J. (2012) In vivo alterations in cardiac metabolism and function in the spontaneously hypertensive rat heart. *Cardiovascular Research*, 95 (1), 69–76. Available from: doi:10.1093/cvr/cvs164.
Drenjacnevic-Peric, I., Jelaković, B., Lombard, J.H., Kunert, M.P., Kibel, A. and Gros, M. (2011) High-salt diet and hypertension: Focus on the renin-angiotensin system. *Kidney and Blood Pressure Research*, 34, 1–11. Available from: doi:10.1159/000320387.
Dunn, K.M., Renic, M., Flasch, A.K., Harder, D.R., Falck, J. and Roman, R.J. (2008) Elevated production of 20-HETE in the cerebral vasculature contributes to severity of ischemic stroke and oxidative stress in spontaneously hypertensive rats. *American journal of physiology. Heart and circulatory physiology*, 295, H2455–H2465. Available from: doi:10.1152/ajpheart.00512.2008.
Egan, B.M., Zhao, Y., Axon, R.N., Brzezinski, W.A. and Ferdinand, K.C. (2011) Uncontrolled and apparent treatment resistant hypertension in the United States, 1988 to 2008. *Circulation*, 124 (9), 1046–1058. Available from: doi:10.1161/CIRCULATIONAHA.111.030189.
Elliott, W.J. (2003) The economic impact of hypertension. *Journal of clinical hypertension*, 5 (2), 3–13. Available from: doi:10.1111/j.1524-6175.2003.02463.x.
Evans, A., Brown, W., Kenyon, C., Maxted, K. and Smith, D. (1994) Improved system for measuring systolic blood pressure in the conscious rat. *Med Biol Eng Comput*, 32 (1), 101–102.
Fabian, M.R., Sonenberg, N. and Filipowicz, W. (2010) Regulation of mRNA translation and stability by microRNAs. *Annual Review of Biochemistry*, 79 (1), 351–379. Available from: doi:10.1146/annurev-biochem-060308-103103.

Fer, M., Corcos, L., Dréano, Y., Plée-Gautier, E., Salaün, J.-P., Berthou, F. and Amet, Y. (2008) Cytochromes P450 from family 4 are the main omega hydroxylating enzymes in humans: CYP4F3B is the prominent player in PUFA metabolism. *Journal of Lipid Research*, 49 (11), 2379–2389. Available from: doi:10.1194/jlr.M800199-JLR200.

Ferdinandusse, S., Denis, S., van Roermund, C.W.T., Wanders, R.J.A. and Dacremont, G. (2004) Identification of the peroxisomal ß-oxidation enzymes involved in the degradation of long-chain dicarboxylic acids. *Journal of Lipid Research*, 45 (6), 1104–1111. Available from: doi:10.1194/jlr.M300512-JLR200.

Feron, O. (2009) Pyruvate into lactate and back: from the warburg effect to symbiotic energy fuel exchange in cancer cells. *Radiotherapy and Oncology*, 92 (3), 329–333. Available from: doi:10.1016/j.radonc.2009.06.025.

Fessel, J.P., Hamid, R., Wittmann, B.M., Robinson, L.J., Blackwell, T., Tada, Y., Tanabe, N., Tatsumi, K., Hemnes, A.R. and West, J.D. (2012) Metabolomic analysis of bone morphogenetic protein receptor type 2 mutations in human pulmonary endothelium reveals widespread metabolic reprogramming. *Pulmonary Circulation*, 2 (2), 201–213. Available from: doi:10.4103/2045-8932.97606.

Fillmore, N., Mori, J. and Lopaschuk, G.D. (2014) Mitochondrial fatty acid oxidation alterations in heart failure, ischaemic heart disease and diabetic cardiomyopathy. *British Journal of Pharmacology*, 171, 2080–2090. Available from: doi:10.1111/bph.12475.

Fiorucci, S., Mencarelli, A., Palladino, G. and Cipriani, S. (2009) Bile-acid-activated receptors: targeting TGR5 and farnesoid-X-receptor in lipid and glucose disorders. *Trends in Pharmacological Sciences*, 30 (11), 570–580. Available from: doi:10.1016/j.tips.2009.08.001.

Flachs, P., Horakova, O., Brauner, P., Rossmeisl, M., Pecina, P., Franssen-Van Hal, N., Ruzickova, J., Sponarova, J., Drahota, Z., Vlcek, C., Keijer, J., Houstek, J. and Kopecky, J. (2005) Polyunsaturated fatty acids of marine origin upregulate mitochondrial biogenesis and induce ß-oxidation in white fat. *Diabetologia*, 48 (11), 2365–2375. Available from: doi:10.1007/s00125-005-1944-7.

Fowler, E.D., Benoist, D., Drinkhill, M.J., Stones, R., Helmes, M., Wüst, R.C.I., Stienen, G.J.M., Steele, D.S. and White, E. (2015) Decreased creatine kinase is linked to diastolic dysfunction in rats with right heart failure induced by pulmonary artery hypertension. *Journal of Molecular and Cellular Cardiology*, 86, 1–8. Available from: doi:10.1016/j.yjmcc.2015.06.016.

Frenkel, B., Bishara-Shieban, J. and Bar-Tana, J. (1994) The effect of ß,ß'-tetramethylhexadecanedioic acid (MEDICA 16) on plasma very-low-density lipoprotein metabolism in rats: role of apolipoprotein C-III. *Biochemical Journal*, 298, 409–414.

Frenkel, B., Mayorek, N., Hertz, R. and Bar-Tana, J. (1988) The hypochylomicronemic effect of ß,ß'-methyl-substituted hexadecanedioic acid (MEDICA 16) is mediated by a decrease in apolipoprotein C-III. *Journal of Biological Chemistry*, 263 (17), 8491–8497.

Friis, U.G., Madsen, K., Stubbe, J., Hansen, P.B.L., Svenningsen, P., Bie, P., Skøtt, O. and Jensen, B.L. (2013) Regulation of renin secretion by renal juxtaglomerular cells. *Pflugers Archiv European Journal of Physiology*, 465 (1), 25–37. Available from: doi:10.1007/s00424-012-1126-7.

Frisoli, T.M., Schmieder, R.E., Grodzicki, T. and Messerli, F.H. (2012) Salt and hypertension: Is salt dietary reduction worth the effort? *The American Journal of Medicine*, 125, 433–439. Available from:

doi:10.1016/j.amjmed.2011.10.023.
Fruchart, J.C. (2009) Peroxisome proliferator-activated receptor-alpha (PPARα): At the crossroads of obesity, diabetes and cardiovascular disease. *Atherosclerosis*, 205 (1), 1–8. Available from: doi:10.1016/j.atherosclerosis.2009.03.008.
Funder, J.W. (2017) Apparent mineralocorticoid excess. *Journal of Steroid Biochemistry and Molecular Biology*, 165, 151–153. Available from: doi:10.1016/j.jsbmb.2016.03.010.
Gainer, J. V., Lipkowitz, M.S., Yu, C., Waterman, M.R., Dawson, E.P., Capdevila, J.H. and Brown, N.J. (2008) Association of a CYP4A11 Variant and Blood Pressure in Black Men. *Journal of the American Society of Nephrology*, 19 (8), 1606–1612. Available from: doi:10.1681/ASN.2008010063.
Gartung, C. and Matern, S. (1997) Molecular regulation of sinusoidal liver bile acid transporters during cholestasis. *Yale Journal of Biology and Medicine*, 70 (4), 355–363.
Gaval-Cruz, M. and Weinshenker, D. (2009) Mechanisms of Disulfiram-induced Cocaine Abstinence: Antabuse and Cocaine Relapse. *Molecular Interventions*, 9 (4), 175–187. Available from: doi:10.1124/mi.9.4.6.
Geissler, S., Zwarg, M., Knütter, I., Markwardt, F. and Brandsch, M. (2010) The bioactive dipeptide anserine is transported by human proton-coupled peptide transporters. *The FEBS Journal*, 277 (3), 790–795. Available from: doi:10.1111/j.1742-4658.2009.07528.x.
George, J., Mathur, R., Shah, A.D., Pujades-Rodriguez, M., Denaxas, S., Smeeth, L., Timmis, A. and Hemingway, H. (2017) Ethnicity and the first diagnosis of a wide range of cardiovascular diseases: Associations in a linked electronic health record cohort of 1 million patients. *PLoS ONE*, 12 (6), 1–17. Available from: doi:10.1371/journal.pone.0178945.
Gilbert, K., Nian, H., Yu, C., Luther, J.M. and Brown, N.J. (2013) Fenofibrate lowers blood pressure in salt-sensitive but not salt-resistant hypertension. *Journal of Hypertension*, 31 (4), 820–829. Available from: doi:10.1097/HJH.0b013e32835e8227.
Gokce, N. (2004) L -Arginine and hypertension. *The Journal of Nutrition*, 134 (10), 2807S–2811S.
Gong, Y., McDonough, C.W., Padmanabhan, S. and Johnson, J.A. (2014) Hypertension Pharmacogenomics. In: *Handbook of Pharmacogenomics and Stratified Medicine*. Elsevier Inc. pp. 747–778. Available from: doi:10.1016/B978-0-12-386882-4.00032-3.
Gordan, R., Gwathmey, J.K. and Xie, L.-H. (2015) Autonomic and endocrine control of cardiovascular function. *World Journal of Cardiology*, 7 (4), 204–214. Available from: doi:10.4330/wjc.v7.i4.204.
Gowda, G.A.N. and Raftery, D. (2013) Biomarker discovery and translation in metabolomics. *Curr Metabolomics*, 1 (3), 227–240. Available from: doi:10.2174/2213235X113019990005.
Graham, D., Hamilton, C., Beattie, E., Spiers, A. and Dominiczak, A.F. (2004) Comparison of the effects of omapatrilat and irbesartan/ hydrochlorothiazide on endothelial function and cardiac hypertrophy in the stroke-prone spontaneously hypertensive rat: Sex differences. *Journal of Hypertension*, 22 (2), 329–337. Available from: doi:10.1097/00004872-200402000-00017.
Graham, D., Mcbride, M.W., Brain, N.J.R. and Dominiczak, A.F. (2005) Congenic / Consomic Models of Hypertension. In: *Methods in Molecular Medicine*. pp. 3–15.

Greenbaum, D., Williams, K., Greenbaum, D., Colangelo, C., Williams, K. and Gerstein, M. (2003) Comparing protein abundance and mRNA expression levels on a genomic scale comparing protein abundance and mRNA expression levels on a genomic scale. *Genome Biology*, 4 (9), 1–8. Available from: doi:10.1186/gb-2003-4-9-117.

Grego, A. V. and Mingrone, G. (1995) Dicarboxylic acids, an alternate fuel substrate in parenteral nutrition: an update. *Clinical Nutrition*, 14 (3), 143–148. Available from: doi:10.1016/S0261-5614(95)80011-5.

Griffiths, W.J., Koal, T., Wang, Y., Kohl, M., Enot, D.P. and Deigner, H.P. (2010) Targeted metabolomics for biomarker discovery. *Angewandte Chemie - International Edition*, 49 (32), 5426–5445. Available from: doi:10.1002/anie.200905579.

Grossman, E. and Messerli, F.H. (2008) Secondary hypertension: Interfering substances. *Journal of Clinical Hypertension*, 10 (7), 556–566. Available from: doi:10.1111/j.1751-7176.2008.07758.x.

Gu, S., Rong, H., Zhang, G., Kang, L., Yang, M. and Guan, H. (2016) Functional SNP in 3′-UTR microRNA-binding site of ZNF350 confers risk for age-related cataract. *Human Mutation Variation Society*, 37 (11), 1223–1230. Available from: doi:10.1002/humu.23073.

Guerrero-García, C. and Rubio-Guerra, A.F. (2018) Combination therapy in the treatment of hypertension. *Drugs in Context*, 7 (212531), 1–9. Available from: doi:DOI: 10.7573/dic.212531.

Guo, S.X., Yan, Y.Z., Mu, L.T., Niu, Q., He, J., Liu, J.M., Li, S.G., Zhang, J.Y., Guo, H. and Rui, D.S. (2015) Association of serum free fatty acids with hypertension and insulin resistance among rural Uyghur adults in far Western China. *International Journal of Environmental Research and Public Health*, 12 (6), 6582–6590. Available from: doi:10.3390/ijerph120606582.

Guyenet, P.G. (2006) The sympathetic control of blood pressure. *Nature Reviews Neuroscience*, 7 (5), 335–346. Available from: doi:10.1038/nrn1902.

Ha, S.K. (2014) Dietary Salt Intake and Hypertension. *Electrolytes & Blood Pressure*, 12, 7–18. Available from: doi:10.5049/EBP.2014.12.1.7.

Hagenbuch, B. (2007) Cellular entry of thyroid hormones by organic anion transporting polypeptides. *Best Practice and Research*, 21 (2), 209–221. Available from: doi:10.1016/j.beem.2007.03.004.

Haider, A.W., Larson, M.G., Franklin, S.S. and Levy, D. (2003) Systolic blood pressure, diastolic blood pressure, and pulse pressure as predictors of risk for congestive heart failure in the Framingham Heart Study. *Ann Intern.Med*, 138, 10–16.

Hajri, T., Ibrahimi, A., Coburn, C.T., Knapp, F.F., Kurtz, T., Pravenec, M. and Abumrad, N.A. (2001) Defective fatty acid uptake in the spontaneously hypertensive rat is a primary determinant of altered glucose metabolism, hyperinsulinemia, and myocardial hypertrophy. *Journal of Biological Chemistry*, 276 (26), 23661–23666. Available from: doi:10.1074/jbc.M100942200.

Hall, J.E., Granger, J.P. and Hall, M.E. (2013) Physiology and Pathophysiology of Hypertension. In: *Seldin and Geibisch's The Kidney*. 5th edition. pp. 1319–1352. Available from: doi:10.1016/B978-0-12-381462-3.00039-2.

Hardwick, J.P., Osei-Hyiaman, D., Wiland, H., Abdelmegeed, M.A. and Song, B.J. (2009) PPAR/RXR regulation of fatty acid metabolism and fatty acid ω-hydroxylase (CYP4) isozymes: Implications for prevention of lipotoxicity in fatty liver disease. *PPAR Research*, 2009, 1–20. Available from: doi:10.1155/2009/952734.

Harrap, S.B., Hopper, J.L., Hoang, H.N. and Giles, G.G. (2000) Familial patterns

of covariation for cardiovascular risk factors in adults: The Victorian Family Heart Study. *American Journal of Epidemiology*, 152 (8), 704–715. Available from: doi:10.1093/aje/152.8.704.

Harrison-bernard, L.M. (2009) The renal renin-angiotensin system. *Advances in Physiology Education*, 33, 270–274. Available from: doi:10.1152/advan.00049.2009.

Harrison, D., Gongora, M.C., Guzik, T. and Julian, W. (2007) Oxidative stress and hypertension. *Journal of the American Society of Hypertension*, 1 (1), 33–40. Available from: doi:10.1007/978-1-4471-5198-2_15.

Hartkoorn, R.C., Kwan, W.S., Shallcross, V., Chaikan, A., Liptrott, N., Egan, D., Sora, E.S., James, C.E., Gibbons, S., Bray, P.G., Back, D.J., Khoo, S.H. and Owen, A. (2010) HIV protease inhibitors are substrates for OATP1A2, OATP1B1 and OATP1B3 and lopinavir plasma concentrations are influenced by SLCO1B1 polymorphisms. *Pharmacogenet Genomics*, 20 (2), 112–120. Available from: doi:10.1097/FPC.0b013e328335b02d.

Haufe, S., Utz, W., Engeli, S., Kast, P., Böhnke, J., Pofahl, M., Traber, J., Haas, V., Hermsdorf, M., Mähler, A., Busjahn, A., Wiesner, S., Otto, C., Mehling, H., Luft, F.C., Boschmann, M., Schulz-Menger, J. and Jordan, J. (2012) Left ventricular mass and function with reduced-fat or reduced-carbohydrate hypocaloric diets in overweight and obese subjects. *Hypertension*, 59, 70–75. Available from: doi:10.1161/HYPERTENSIONAHA.111.178616.

Hewitson, T.D., Holt, S.G. and Smith, E.R. (2015) Animal models to study links between cardiovascular disease and renal failure and their relevance to human pathology. *Frontiers in Immunology*, 6 (465), 1–9. Available from: doi:10.3389/fimmu.2015.00465.

Hiltunen, T.P., Rimpelä, J.M., Mohney, R.P., Stirdivant, S.M. and Kontula, K.K. (2017) Effects of four different antihypertensive drugs on plasma metabolomic profiles in patients with essential hypertension. *PLoS ONE*, 12 (11), 1–16. Available from: doi:10.1371/journal.pone.0187729.

Ho, M., Yo, C., Liu, C., Chen, C. and Lee, C. (2007) Refractive hypotension in a patient with disulfiram-ethanol reaction. *Am J Med Sci*, 333 (1), 53–55.

Hoagland, K.M., Flasch, A.K. and Roman, R.J. (2003) Inhibitors of 20-HETE formation promote salt-sensitive hypertension in rats. *Hypertension*, 42 (2), 669–673. Available from: doi:10.1161/01.HYP.0000084634.97353.1A.

Holle, R., Happich, M., Löwel, H. and Wichmann, H. (2005) KORA - A Research Platform for Population Based Health Research. *Das Gesundheitswesen*, 67 (S 01), 19–25. Available from: doi:10.1055/s-2005-858235.

Van der Hooft, J.J.J., Padmanabhan, S., Burgess, K.E.V. and Barrett, M.P. (2016) Urinary antihypertensive drug metabolite screening using molecular networking coupled to high-resolution mass spectrometry fragmentation. *Metabolomics*, 12 (125), 1–15. Available from: doi:10.1007/s11306-016-1064-z.

Hoshi, T., Wissuwa, B., Tian, Y., Tajima, N., Xu, R., Bauer, M., Heinemann, S.H. and Hou, S. (2013) Omega-3 fatty acids lower blood pressure by directly activating large-conductance Ca2+-dependent K+ channels. *Proceedings of the National Academy of Sciences*, 110 (12), 4816–4821. Available from: doi:10.1073/pnas.1221997110.

Hou, W.Y., Xu, S.F., Zhu, Q.N., Lu, Y.F., Cheng, X.G. and Liu, J. (2014) Age- and sex-related differences of organic anion-transporting polypeptide gene expression in livers of rats. *Toxicology and Applied Pharmacology*, 280 (2), 370–377. Available from: doi:10.1016/j.taap.2014.08.020.

Houten, S.M. and Wanders, R.J.A. (2010) A general introduction to the biochemistry of mitochondrial fatty acid ß-oxidation. *Journal of Inherited*

Metabolic Disease, 33, 469–477. Available from: doi:10.1007/s10545-010-9061-2.

Hsu, L.C., Tani, K., Fujiyoshi, T., Kurachi, K. and Yoshida, A. (1985) Cloning of cDNAs for human aldehyde dehydrogenases 1 and 2. *The National Academy of Sciences*, 82 (11), 3771–3775. Available from: doi:10.1073/pnas.82.11.3771.

Huang, S., Chen, L. and Giacomini, K.M. (2012) Pharmacogenomic mechanisms of drug toxicity. In: *Principles of Clinical Pharmacology*. Third Edit. Elsevier Inc. pp. 285–306. Available from: doi:10.1016/B978-0-12-385471-1.00017-9.

Hubers, S.A. and Brown, N.J. (2016) Combined Angiotensin Receptor Antagonism and Neprilysin Inhibition. *Circulation*, 133 (11), 1115–1124. Available from: doi:10.1161/CIRCULATIONAHA.115.018622.

Hunt, S.C., Williams, R.R. and Barlow, G.K. (1986) A comparison of positive family history definitions for defining risk of future disease. *Journal of Chronic Diseases*, 39 (10), 809–821. Available from: doi:10.1016/0021-9681(86)90083-4.

Hylemon, P.B., Zhou, H., Pandak, W.M., Ren, S., Gil, G. and Dent, P. (2009) Bile acids as regulatory molecules. *Journal of Lipid Research*, 50 (8), 1509–1520. Available from: doi:10.1194/jlr.R900007-JLR200.

Ingwall, J.S., Kramer, M.F., Fifer, M.A., Lorell, B.H., Shemin, R., Grossman, W. and Allen, P. (1985) The creatine kinase system in normal and diseased human myocardium. *New England Journal of Medicine*, 313 (17), 1050–1054.

Intengan, H.D. and Schiffrin, E.L. (2000) Structure and mechanical properties of resistance arteries in hypertension: role of adhesion molecules and extracellular matrix determinants. *Hypertension*, 36, 312–318. Available from: doi:10.1161/01.HYP.36.3.312.

Intengan, H.D. and Schiffrin, E.L. (2001) Vascular remodeling in hypertension Roles of apoptosis, inflammation, and fibrosis. *Hypertension*, 38 (2), 581–587. Available from: doi:10.1161/hy09t1.096249.

Izzard, A.S. and Heagerty, A.M. (1999) Impaired flow-dependent dilatation in distal mesenteric arteries from the spontaneously hypertensive rat. *Journal of Physiology*, 518 (1), 239–245. Available from: doi:10.1111/j.1469-7793.1999.0239r.x.

Jackson, B., Brocker, C., Thompson, D.C., Black, W., Vasiliou, K., Nebert, D.W. and Vasiliou, V. (2011) Update on the aldehyde dehydrogenase gene (ALDH) superfamily. *Human Genomics*, 5 (4), 283–303. Available from: doi:10.1186/1479-7364-5-4-283.

James, P.A., Oparil, S., Carter, B.L., Cushman, W.C., Dennison-Himmelfarb, C., Handler, J., Lackland, D.T., LeFevre, M.L., MacKenzie, T.D., Ogedegbe, O., Smith, S.C., Svetkey, L.P., Taler, S.J., Townsend, R.R., Wright, J.T., Narva, A.S. and Ortiz, E. (2014) 2014 Evidence-Based Guideline for the Management of High Blood Pressure in Adults Report From the Panel Members Appointed to the Eighth Joint National Committee (JNC 8). *Journal American Medical Association*, 311 (5), 507–520. Available from: doi:10.1001/jama.2013.284427.

Jiang, G. and Zhang, B.B. (2003) Glucagon and regulation of glucose metabolism. *American Journal of Physiology - Endocrinology And Metabolism*, 284 (4), E671–E678. Available from: doi:10.1152/ajpendo.00492.2002.

Johnston, J.B., Ouellet, H., Podust, L.M. and Ortiz de Montellano, P.R. (2011) Structural control of cytochrome P450-catalyzed ω- hydroxylation. *Arch Biochem Biophys*, 507 (1), 86–94. Available from: doi:10.1016/j.abb.2010.08.011.

Kageyama, S., Hanada, E., Ii, H., Tomita, K., Yoshiki, T. and Kawauchi, A.

(2015) Gamma-glutamylcyclotransferase: a novel target molecule for cancer diagnosis and treatment. *BioMed Research International*, 2015, 1–5. Available from: doi:10.1155/2015/345219.

Kalra, G., Sousa, A. De and Shrivastava, A. (2014) Disulfiram in the management of alcohol dependence : A comprehensive clinical review. *Open Journal of Psychiatry*, 4, 43–52. Available from: doi:10.4236/ojpsych.2014.41007.

Kang, K.T. (2014) Endothelium-derived relaxing factors of small resistance arteries in hypertension. *Toxicological Research*, 30 (3), 141–148. Available from: doi:10.5487/TR.2014.30.3.141.

Keech, A., Simes, R.J., Barter, P., Best, J., Scott, R., Taskinen, M.R., Forder, P., Pillai, A., Davis, T., Glasziou, P., Drury, P., Kesäniemi, Y.A., Sullivan, D., Hunt, D., Colman, P., D'Emden, M., Whiting, M., Ehnholm, C. and Laakso, M. (2005) Effects of long-term fenofibrate therapy on cardiovascular events in 9795 people with type 2 diabetes mellitus (the FIELD study): Randomised controlled trial. *Lancet*, 366, 1849–1861. Available from: doi:10.1016/S0140-6736(05)67667-2.

Kitzenberg, D., Colgan, S.P. and Glover, L.E. (2016) Creatine kinase in ischemic and inflammatory disorders. *Clinical and Translational Medicine*, 5 (31), 1–10. Available from: doi:10.1186/s40169-016-0114-5.

Ko, B. and Bakris, G. (2008) The Renin-Angiotensin-Aldosterone System and the Kidney. In: *Textbook of Nephro-Endocrinology*. Second Edi. Elsevier Inc. pp. 167–180. Available from: doi:10.1016/B978-0-12-373870-7.00013-2.

Koh-Tan, H.H.C., McBride, M.W., McClure, J.D., Beattie, E., Young, B., Dominiczak, A.F. and Graham, D. (2013) Interaction between chromosome 2 and 3 regulates pulse pressure in the stroke-prone spontaneously hypertensive rat. *Hypertension*, 62 (1), 33–40. Available from: doi:10.1161/HYPERTENSIONAHA.111.00814.

Köhler, R., Grundig, A., Brakemeier, S., Rothermund, L., Distler, A., Kreutz, R. and Hoyer, J. (2001) Regulation of pressure-activated channel in intact vascular endothelium of stroke-prone spontaneously hypertensive rats. *American Journal of Hypertension*, 14 (7 I), 716–721. Available from: doi:10.1016/S0895-7061(01)01306-1.

Kotchen, T.A. (2003) Trends in prevalence , awareness , in the united states , 1988-2000. *Journal of the American Medical Association*, 290 (2), 199–206.

Krieger, E.M., Drager, L.F., Giorgi, D.M.A., Pereira, A.C., Barreto-Filho, J.A.S., Nogueira, A.R., Mill, J.G., Lotufo, P.A., Amodeo, C., Batista, M.C., Bodanese, L.C., Carvalho, A.C.C., Castro, I., Chaves, H., Costa, E.A.S., Feitosa, G.S., Franco, R.J.S., Fuchs, F.D., Guimarães, A.C., *et al*. (2018) Spironolactone versus clonidine as a fourth-drug therapy for resistant hypertension: the ReHOT randomized study (resistant hypertension optimal treatment). *Hypertension*, 71 (4), 681–690. Available from: doi:10.1161/HYPERTENSIONAHA.117.10662.

Kroetz, D.L., Yook, P., Costet, P., Bianchi, P. and Pineau, T. (1998) Peroxisome proliferator-activated receptor α controls the hepatic CYP4A induction adaptive response to starvation and diabetes. *Journal of Biological Chemistry*, 273 (47), 31581–31589. Available from: doi:10.1074/jbc.273.47.31581.

Kulik, A., Ruel, M., Jneid, H., Ferguson, T.B., Hiratzka, L.F., Ikonomidis, J.S., Lopez-Jimenez, F., McNallan, S.M., Patel, M., Roger, V.L., Sellke, F.W., Sica, D.A. and Zimmerman, L. (2015) Secondary prevention after coronary artery bypass graft surgery: A scientific statement from the American Heart Association. *Circulation*, 131 (10), 927–964. Available from: doi:10.1161/CIR.0000000000000182.

Kulkarni, R., Ramdurg, S. and Bairy, B. (2014) Disulfiram-induced reversible hypertension: A prospective case series and review of the literature. *Indian Journal of Psychological Medicine*, 36 (4), 434–438. Available from: doi:10.4103/0253-7176.140744.

Kulkarni, R.R. and Bairy, B. (2013) Disulfiram induced reversible hypertension: A prospective case study and brief review. *Indian Journal of Psychological Medicine*, 35 (2), 217–219. Available from: doi:10.4103/0253-7176.116263.

Kullak-Ublick, G.A., Stieger, B., Hagenbuch, B. and Meier, P.J. (2000) Hepatic Transport of Bile Salts. *Seminars in Liver Disease*, 20 (3), 273–292. Available from: doi:10.1055/s-2000-9426.

Kunz, R., Friedrich, C., Wolbers, M. and Mann, J.F.. (2008) Meta-analysis: effect of monotherapy and combination therapy with inhibitors of the renin angiotensin system on proteinuria in renal disease. *Ann Intern Med*, 148 (1), 30–48. Available from: doi:10.7326/0003-4819-148-1-200801010-00190.

Ladage, D., Schwinger, R.H.G. and Brixius, K. (2013) Cardio-Selective Beta-Blocker: Pharmacological Evidence and Their Influence on Exercise Capacity. *Cardiovascular Therapeutics*, 31 (2), 76–83. Available from: doi:10.1111/j.1755-5922.2011.00306.x.

Lai, Y. (2013) Organic anion-transporting polypeptides (OATPs/SLCOs). In: *Transporters in Drug Discovery and Development*. pp. 353–454. Available from: doi:10.1533/9781908818287.353.

Larsson, C., Pahlman, I., Ansell, R. and Rigoulet, M. (1998) The importance of the glycerol 3 -phosphate shuttle during aerobic growth of Saccharomyces cerevisiae. *Yeast*, 14, 347–357. Available from: doi:10.1002/(SICI)1097-0061(19980315)14.

Larsson, E., Wahlstrand, B., Hedblad, B., Hedner, T., Kjeldsen, S.E., Melander, O. and Lindahl, P. (2013) Hypertension and Genetic Variation in Endothelial-Specific Genes. *PLoS ONE*, 8 (4), 1–7. Available from: doi:10.1371/journal.pone.0062035.

de las Fuentes, L., Soto, P.F., Cupps, B.P., Pasque, M.K., Herrero, P., Gropler, R.J., Waggoner, A.D. and Dávila-Román, V.G. (2006) Hypertensive left ventricular hypertrophy is associated with abnormal myocardial fatty acid metabolism and myocardial efficiency. *Journal of Nuclear Cardiology*, 13 (3), 369–377. Available from: doi:10.1016/j.nuclcard.2006.01.021.

Laurent, S. (2017) Antihypertensive drugs. *Pharmacological Research*, 124, 116–125. Available from: doi:10.1016/j.phrs.2017.07.026.

Laurent, S., Schlaich, M. and Esler, M. (2012) New drugs, procedures, and devices for hypertension. *The Lancet*, 380, 591–600. Available from: doi:10.1016/S0140-6736(12)60825-3.

Lecerf, J.-M. (2009) Fatty acids and cardiovascular disease. *Nutrition Reviews*, 67 (5), 273–283. Available from: doi:10.1111/j.1753-4887.2009.00194.x.

Lee, D.L., Wilson, J.L., Duan, R., Hudson, T. and El-Marakby, A. (2011) Peroxisome proliferator-activated receptor-α activation decreases mean arterial pressure, plasma interleukin-6, and COX-2 while increasing renal CYP4A expression in an acute model of DOCA-salt hypertension. *PPAR Research*, 2011, 1–7. Available from: doi:10.1155/2011/502631.

Lefebvre, P., Cariou, B., Lien, F., Kuipers, F. and Staels, B. (2009) Role of bile acids and bile acid receptors in metabolic regulation. *Physiol Rev*, 89, 147–191. Available from: doi:10.1152/physrev.00010.2008.

Leong, X.-F., Ng, C.-Y. and Kamsiah, J. (2015) Animal Models in Cardiovascular Research: Hypertension and Atherosclerosis. *BioMed Research International*, 1–11. Available from: doi:10.1155/2015/528757.

Li, C., Li, J., Weng, X., Lan, X. and Chi, X. (2015) Farnesoid X receptor agonist

CDCA reduces blood pressure and regulates vascular tone in spontaneously hypertensive rats. *Journal of the American Society of Hypertension*, 9 (7), 507–516. Available from: doi:10.1016/j.jash.2015.04.006.

Liskova, S., Petrova, M., Karen, P., Behuliak, M. and Zicha, J. (2014) Contribution of Ca2+-dependent Cl- channels to norepinephrine-induced contraction of femoral artery is replaced by increasing EDCF contribution during ageing. *BioMed Research International*, 2014, 1–9. Available from: doi:10.1155/2014/289361.

Liu, B., Li, J. and Cairns, M.J. (2014) Identifying miRNAs, targets and functions. *Briefings in Bioinformatics*, 15 (1), 1–19. Available from: doi:10.1093/bib/bbs075.

Liu, X., Byrd, J.B. and Rodriguez, C.J. (2018) Use of physician-recommended non-pharmacological strategies for hypertension control among hypertensive patients. *Journal of Clinical Hypertension*, 20 (3), 518–527. Available from: doi:10.1111/jch.13203.

Longo, N. (2016) Primary carnitine deficiency and newborn screening for disorders of the carnitine cycle. *Annals of Nutrition and Metabolism*, 68 (3), 5–9. Available from: doi:10.1159/000448321.

Longo, N., Amat di San Filippo, C. and Pasquali, M. (2006) Disorders of carnitine transport and the carnitine cycle. *American Journal of Medical Genetics Part C: Seminars in Medical Genetics*, 142C (2), 77–85. Available from: doi:10.1002/ajmg.c.30087.

Lopaschuk, G.D., Ussher, J.R., Folmes, C.D.L., Jaswal, J.S. and Stanley, W.C. (2010) Myocardial fatty acid metabolism in health and disease. *Physiol Rev.*, 90, 207–258. Available from: doi:10.1152/physrev.00015.2009.

Loperena, R. and Harrison, D.G. (2017) Oxidative Stress and Hypertensive Diseases. *Med Clin North Am*, 101 (1), 169–193. Available from: doi:10.1016/j.mcna.2016.08.004.

Lu, Y., A., J., Guangji, W., Hao, H., Qing, H., Yan, B., Zha, W., Gu, S., Ren, H., Zhang, Y., Fan, X., Zhang, M. and Hao, K. (2008) Gas chromatography/time-of-flight mass spectrometry based metabonomic approach to differentiating hypertension- and age-related metabolic variation in spontaneously hypertensive rats. *Rapid Communications in Mass Spectrometry*, 22, 2882–2888. Available from: doi:10.1002/rcm.3670.

Luengo-Fernández, R., Leal, J., Gray, A., Petersen, S. and Rayner, M. (2006) Cost of cardiovascular diseases in the united kingdom. *Heart*, 92 (10), 1384–1389. Available from: doi:10.1136/hrt.2005.072173.

Luft, F.C. (2003) Mendelian forms of human hypertension and mechanisms of disease. *Clinical medicine & research*, 1 (4), 291–300. Available from: doi:10.3121/cmr.1.4.291.

Lund, L.H. (2016) ACE inhibitors in African Americans with hypertension associated with worse outcomes as compared to other antihypertensives. *Evidence Based Medicine*, 21 (1), 33–34. Available from: doi:10.1136/ebmed-2015-110258.

Lüscher, T.F. and Vanhoutte, P.M. (1986) Endothelium-dependent contractions to acetylcholine in the aorta of the spontaneously hypertensive rat. *Hypertension*, 8 (4), 344–348. Available from: doi:10.1161/01.HYP.8.4.344.

Ma, X., Zheng, S., Shu, Y., Wang, Y. and Chen, X. (2016) Association of the Glu504Lys polymorphism in the aldehyde dehydrogenase 2 gene with endothelium-dependent dilation disorder in Chinese Han patients with essential hypertension. *Internal Medicine Journal*, 46 (5), 608–615. Available from: doi:10.1111/imj.12983.

Madsen, R., Lundstedt, T. and Trygg, J. (2010) Chemometrics in metabolomics-a

review in human disease diagnosis. *Analytica Chimica Acta*, 659, 23–33. Available from: doi:10.1016/j.aca.2009.11.042.

Makani, H., Bangalore, S., Desouza, K.A., Shah, A. and Messerli, F.H. (2013) Efficacy and safety of dual blockade of the renin-angiotensin system: Meta-analysis of randomised trials. *BMJ*, 346 (f360), 1–15. Available from: doi:10.1136/bmj.f360.

Maltesen, R.G., Hanifa, M.A., Kucheryavskiy, S., Pedersen, S., Kristensen, S.R., Rasmussen, B.S. and Wimmer, R. (2016) Predictive biomarkers and metabolic hallmark of postoperative hypoxaemia. *Metabolomics*, 12 (87), 1–15. Available from: doi:10.1007/s11306-016-1018-5.

Marr, C.M. and Reimer, J.M. (2009) The Cardiovascular System. In: *The Equine Manual*. Elsevier. pp. 455–483. Available from: https://doi.org/10.1016/B978-0-7020-2769-7.50013-7.

Marsin, A.S., Bertrand, L., Rider, M.H., Deprez, J., Beauloye, C., Vincent, M.F., Van den Berghe, G., Carling, D. and Hue, L. (2000) Phosphorylation and activation of heart PFK-2 by AMPK has a role in the stimulation of glycolysis during ischaemia. *Current Biology*, 10 (20), 1247–1255. Available from: doi:10.1016/S0960-9822(00)00742-9.

Martinez-Lemus, L.A. (2012) The Dynamic Structure of Arterioles. *Basic Clin Pharmacol Toxicol*, 110 (1), 5–11. Available from: doi:10.1111/j.1742-7843.2011.00813.x.

Matoulkova, E., Michalova, E., Vojtesek, B. and Hrstka, R. (2012) The role of the 3′ untranslated region in post-transcriptional regulation of protein expression in mammalian cells. *RNA Biology*, 9 (5), 563–576. Available from: doi:10.4161/rna.20231.

Matsuzawa, Y., Guddeti, R.R., Kwon, T.-G., Lerman, L.O. and Lerman, A. (2015) Secondary Prevention Strategy of Cardiovascular Disease Using Endothelial Function Testing. *Circulation Journal*, 79 (4), 685–694. Available from: doi:10.1253/circj.CJ-15-0068.

Mayorek, N., Kalderon, B., Itach, E. and Bar-Tana, J. (1997) Sensitization to insulin induced by ß,ß'-methyl-substituted hexadecanedioic acid (MEDICA 16) in obese Zucker rats in vivo. *Diabetes*, 46 (12), 1958–1964. Available from: doi:10.2337/diabetes.46.12.1958.

McMahon, G.T. and Dluhy, R.G. (2004) Glucocorticoid-Remediable Aldosteronism. *Cardiology in Review Volume*, 12 (1), 44–48. Available from: doi:10.1097/01.crd.0000096417.42861.ce.

Mégarbane, B. (2010) Treatment of patients with ethylene glycol or methanol poisoning: Focus on fomepizole. *Dove Press Journal*, 2, 67–75. Available from: doi:10.2147/OAEM.S5346.

Menni, C., Graham, D., Kastenmüller, G., Alharbi, N.H.J., Alsanosi, S.M., Mcbride, M., Mangino, M., Titcombe, P., Shin, S.Y., Psatha, M., Geisendorfer, T., Huber, A., Peters, A., Wang-Sattler, R., Xu, T., Brosnan, M.J., Trimmer, J., Reichel, C., Mohney, R.P., *et al*. (2015) Metabolomic Identification of a Novel Pathway of Blood Pressure Regulation Involving Hexadecanedioate. *Hypertension*, 66 (2), 422–429. Available from: doi:10.1161/HYPERTENSIONAHA.115.05544.

Menni, C., Metrustry, S.J., Ehret, G., Dominiczak, A.F., Chowienczyk, P., Spector, T.D., Padmanabhan, S. and Valdes, A.M. (2017) Molecular pathways associated with blood pressure and hexadecanedioate levels. *PLoS ONE*, 12 (4), 1–12. Available from: doi:10.1371/journal. pone.0175479.

Mignone, F., Gissi, C., Liuni, S. and Pesole, G. (2002) Untranslated regions of mRNAs. *Genome biology*, 3 (3), 1–10. Available from: doi:10.1186/gb-2002-3-3-reviews0004.

Mingrone, G., Castagneto-Gissey, L. and Macé, K. (2013) Use of dicarboxylic acids in type 2 diabetes. *British Journal of Clinical Pharmacology*, 75 (3), 671–676. Available from: doi:10.1111/j.1365-2125.2012.04177.x.

Miura, Y. (2013) The biological significance of ω-oxidation of fatty acids. *The Japan Academy*, 89 (8), 370–382. Available from: doi:10.2183/pjab.89.370.

Miyata, N., Taniguchi, K., Seki, T., Ishimoto, T., Sato-Watanabe, M., Yasuda, Y., Doi, M., Kametani, S., Tomishima, Y., Ueki, T., Sato, M. and Kameo, K. (2001) HET0016, a potent and selective inhibitor of 20-HETE synthesizing enzyme. *British Journal of Pharmacology*, 133 (3), 325–329. Available from: doi:10.1038/sj.bjp.0704101.

Moayyeri, A., Hammond, C.J., Hart, D.J. and Spector, T.D. (2013) The UK adult twin registry (twinsUK resource). *Twin Research and Human Genetics*, 16 (1), 144–149. Available from: doi:10.1017/thg.2012.89.

Mongeau, J.-G., Biron, P. and Sing, C.F. (1986) The Influence of Genetics and Household Environment upon the Variability of Normal Blood Pressure: The Montreal Adoption Survey. *Clin Exp Hypertens A*, 8 (4–5), 653–60. Available from: doi:10.3109/10641968609046581e.

Monteiro, M.S., Carvalho, M., Bastos, M.L. and Guedes de Pinho, P. (2013) Metabolomics Analysis for Biomarker Discovery: Advances and Challenges. *Current Medicinal Chemistry*, 20 (2), 257–271. Available from: doi:10.2174/092986713804806621.

Moreels, S., Neyrinck, A. and Desmet, W. (2012) Intractable hypotension and myocardial ischaemia induced by co-ingestion of ethanol and disulfiram. *Acta Cardiol*, 67 (4), 491–493.

Mori, T.A., Burke, V., Beilin, L.J. and Puddey, I.B. (2015) Randomized controlled intervention of the effects of alcohol on blood pressure in premenopausal women. *Hypertension*, 66 (3), 517–523. Available from: doi:10.1161/HYPERTENSIONAHA.115.05773.

Mozaffarian, D., Benjamin, E.J., Go, A.S., Arnett, D.K., Blaha, M.J., Cushman, M., De Ferranti, S., Després, J.P., Fullerton, H.J., Howard, V.J., Huffman, M.D., Judd, S.E., Kissela, B.M., Lackland, D.T., Lichtman, J.H., Lisabeth, L.D., Liu, S., Mackey, R.H., Matchar, D.B., *et al*. (2015) Heart disease and stroke statistics-2015 update : A report from the American Heart Association. *Circulation*, 131 (4), e29–e39. Available from: doi:10.1161/CIR.0000000000000152.

Muntner, P., Barrett Bowling, C. and Shimbo, D. (2014) Systolic Blood Pressure Goals to Reduce Cardiovascular Disease Among Older Adults. *The American Journal of the Medical Sciences*, 348 (2), 129–134. Available from: doi:10.1097/MAJ.0000000000000314.

Nabika, T., Ohara, H., Kato, N. and Isomura, M. (2012) The stroke-prone spontaneously hypertensive rat: Still a useful model for post-GWAS genetic studies? *Hypertension Research*, 35, 477–484. Available from: doi:10.1038/hr.2012.30.

Nagai, N., Yoshioka, C., Mano, Y., Ito, Y., Okamoto, N. and Shimomura, Y. (2015) Effect of eye drops containing disulfiram and low-substituted methylcellulose in reducing intraocular pressure in rabbit models. *Current Eye Research*, 40 (10), 990–1000. Available from: doi:10.3109/02713683.2014.971187.

Namsolleck, P. and Unger, T. (2014) Aldosterone synthase inhibitors in cardiovascular and renal diseases. *Nephrology Dialysis Transplantation*, 29, i62–i68. Available from: doi:10.1093/ndt/gft402.

Naseem, R., Adam, A.M., Khan, F., Dossal, A., Khan, I., Khan, A., Paul, H., Jawed, H., Aslam, A., Syed, F.M., Niazi, M.A., Nadeem, S., Khan, A., Zia, A.

and Arshad, M.H. (2017) Prevalence and characteristics of resistant hypertensive patients in an asian population. *Indian Heart Journal*, 69 (4), 442–446. Available from: doi:10.1016/j.ihj.2017.01.012.

Newgard, C.B., An, J., Bain, J.R., Muehlbauer, M.J., Stevens, R.D., Lien, L.F., Haqq, A.M., Shah, S.H., Arlotto, M., Slentz, C. a, Gallup, D., Ilkayeva, O., Wenner, B.R., Yancy, W.E., Musante, G., Surwit, R., Millington, D.S., Butler, M.D. and Svetkey, L.P. (2013) A branched-chain amino acid-related metabolic signature that differentiates obese and lean humans and contributes to insulin resistance. *Cell Metab*, 9 (4), 311–326. Available from: doi:10.1016/j.cmet.2009.02.002.

NICE (2018a) Hypertension in adults : diagnosis and management. *Clinical guideline*, 1–25. Available from: nice.org.uk/guidance/cg127%0A.

NICE (2018b) *Treatment steps for hypertension*. 2018. Available from: https://pathways.nice.org.uk/pathways/hypertension.

Nichols, M., Townsend, N., Scarborough, P. and Rayner, M. (2014) cardiovascular disease in Europe 2014: Epidemiological update. *European Heart Journal*, 35, 2950–2959. Available from: doi:10.1093/eurheartj/ehu299.

Nikodijević, B., Trajkov, T., Glavaš, E., Gudeska, S. and Vetadžokoska, D. (1971) Inhibition of noradrenaline biosynthesis and the level of blood pressure in spontaneously hypertensive rats and metacorticoid rats. *Naunyn-Schmiedebergs Archiv für Pharmakologie*, 268 (2), 185–191. Available from: doi:10.1007/BF01020073.

O'Shea, P.M., Griffin, T.P. and Fitzgibbon, M. (2017) Hypertension: The role of biochemistry in the diagnosis and management. *Clinica Chimica Acta*, 465, 131–143. Available from: doi:10.1016/j.cca.2016.12.014.

Ohsawa, I., Kamino, K., Nagasaka, K., Ando, F., Niino, N., Shimokata, H. and Ohta, S. (2003) Genetic deficiency of a mitochondrial aldehyde dehydrogenase increases serum lipid peroxides in community-dwelling females. *Journal of Human Genetics*, 48 (8), 404–409. Available from: doi:10.1007/s10038-003-0046-y.

Okamoto, K., Hazama, F., Yamori, Y., Haebara, H. and Nagaoka, A. (1975) Pathogenesis and prevention of stroke in spontaneously hypertensive rats. *Clinical Science and Molecular Medicine*, 2, 161s–163s.

de Oliveira, F.A., Shahin, M.H., Gong, Y., McDonough, C.W., Beitelshees, A.L., Gums, J.G., Chapman, A.B., Boerwinkle, E., Turner, S.T., Frye, R.F., Fiehn, O., Kaddurah-Daouk, R., Johnson, J.A. and Cooper-DeHoff, R.M. (2016) Novel plasma biomarker of atenolol-induced hyperglycemia identified through a metabolomics-genomics integrative approach. *Metabolomics*, 12 (129), 1–9. Available from: doi:10.1007/s11306-016-1076-8.

Olson, E. and Graham, D. (2014) Animal Models in Pharmacogenomics. In: *Handbook of Pharmacogenomics and Stratified Medicine*. Elsevier Inc. pp. 73–87. Available from: doi:10.1016/B978-0-12-386882-4.00005-0.

Orywal, K. and Szmitkowski, M. (2017) Alcohol dehydrogenase and aldehyde dehydrogenase in malignant neoplasms. *Clinical and Experimental Medicine*, 17 (2), 131–139. Available from: doi:10.1007/s10238-016-0408-3.

Ota, M., Hisada, A., Lu, X., Nakashita, C., Masuda, S. and Katoh, T. (2016) Associations between aldehyde dehydrogenase 2 (ALDH2) genetic polymorphisms, drinking status, and hypertension risk in Japanese adult male workers: a case–control study. *Environmental Health and Preventive Medicine*, 21 (1), 1–8. Available from: doi:10.1007/s12199-015-0490-2.

Pacurari, M., Kafoury, R., Tchounwou, P.B. and Ndebele, K. (2014) The renin-angiotensin-aldosterone system in vascular inflammation and remodeling. *International Journal of Inflammation*, 2014, 1–13. Available from:

doi:10.1155/2014/689360.
Padmanabhan, S., Tan, L.-E. and Dominiczak, A.F. (2018) Genetics of Blood Pressure and Hypertension. In: *Disorders of Blood Pressure Regulation Phenotypes, Mechanisms, Therapeutic Options*. Springer International Publishing AG. pp. 135–154. Available from: doi:https://doi.org/10.1007/978-3-319-59918-2.
Pasanen, M., Fredrikson, H., Neuvonen, P.J. and Niemi, M. (2007) Different effects of SLCO1B1 polymorphism on the pharmacokinetics atorvastatin and rosuvastatin. *Clinical Pharmacology and Therapeutics*, 82 (6), 726–733. Available from: doi:10.1038/sj.clpt.6100220.
Peachey, J., Brien, J., Roach, C. and Loomis, C. (1981) A comparative review of the pharmacological and toxicological properties of disulfiram and calcium carbimide. *Clin Psychopharmacol*, 1, 21–26.
Peng, B., Li, H. and Peng, X.X. (2015) Functional metabolomics: from biomarker discovery to metabolome reprogramming. *Protein and Cell*, 6 (9), 628–637. Available from: doi:10.1007/s13238-015-0185-x.
Pettersen, J.E. (1973) In vitro studies on the metabolism of hexadecanedioic acid and its mono-l-carnitine- ester. *Biochimica et Biophysica Acta (BBA)/Lipids and Lipid Metabolism*, 306 (1), 1–14. Available from: doi:10.1016/0005-2760(73)90201-4.
Pettersen, J.E. and Aas, M. (1974) Subcellular localization of hexadecanedioic acid activation in human liver. *Journal of Lipid Research*, 15, 551–556.
Piepoli, M.F., Corrà, U., Adamopoulos, S., Benzer, W., Bjarnason-Wehrens, B., Cupples, M., Dendale, P., Doherty, P., Gaita, D., Höfer, S., McGee, H., Mendes, M., Niebauer, J., Pogosova, N., Garcia-Porrero, E., Rauch, B., Schmid, J.P. and Giannuzzi, P. (2014) Secondary prevention in the clinical management of patients with cardiovascular diseases. Core components, standards and outcome measures for referral and delivery. *European Journal of Preventive Cardiology*, 21 (6), 664–681. Available from: doi:10.1177/2047487312449597.
Piepoli, M.F., Hoes, A.W., Agewall, S., Albus, C., Brotons, C., Catapano, A.L., Cooney, M.T., Corrà, U., Cosyns, B., Deaton, C., Graham, I., Hall, M.S., Hobbs, F.D.R., Løchen, M.L., Löllgen, H., Marques-Vidal, P., Perk, J., Prescott, E., Redon, J., *et al*. (2016) 2016 European Guidelines on cardiovascular disease prevention in clinical practice: The Sixth Joint Task Force of the European Society of Cardiology and Other Societies on Cardiovascular Disease Prevention in Clinical Practice (constituted by representati. *Atherosclerosis*, 252, 207–274. Available from: doi:10.1016/j.atherosclerosis.2016.05.037.
Pintérová, M., Kuneš, J. and Zicha, J. (2011) Altered neural and vascular mechanisms in hypertension. *Physiological Research*, 60, 381–402.
Poirier, Y., Antonenkov, V.D., Glumoff, T. and Hiltunen, J.K. (2006) Peroxisomal ß-oxidation-a metabolic pathway with multiple functions. *Biochimica et biophysica acta*, 1763 (12), 1413–1426. Available from: doi:10.1016/j.bbamcr.2006.08.034.
Poole, D.C. and Erickson, H.H. (2014) Heart and vessels: Function during exercise and training adaptations. In: *Equine Sports Medicine and Surgery: Second Edition*. Second Edi. Elsevier Ltd. pp. 667–694. Available from: doi:10.1016/B978-0-7020-4771-8.00031-4.
Popolo, A., Adesso, S., Pinto, A., Autore, G. and Marzocco, S. (2014) L-Arginine and its metabolites in kidney and cardiovascular disease. *Amino Acids*, 46 (10), 2271–2286. Available from: doi:10.1007/s00726-014-1825-9.
Prancheva, M., Krasteva, S., Tufkova, S., Karaivanova, T., Nizamova, V. and

Iliev, Y. (2010) Severe hypotension and ischemic stroke after disulfiram-ethanol reaction. *Folia Med (Plovdiv).*, 52 (3), 70–73.

Rahmouni, K. (2014) Obesity-associated hypertension: Recent progress in deciphering the pathogenesis. *Hypertension*, 64, 215–221. Available from: doi:10.1161/HYPERTENSIONAHA.114.00920.

Rakhshandehroo, M., Knoch, B., Müller, M. and Kersten, S. (2010) Peroxisome proliferator-activated receptor alpha target genes. *PPAR Research*, 2010, 1–20. Available from: doi:10.1155/2010/612089.

Ramsey, L.B., Johnson, S.G., Caudle, K.E., Haidar, C.E., Voora, D., Wilke, R.A., Maxwell, W.D., McLeod, H.L., Krauss, R.M., Roden, D.M., Feng, Q., Cooper-Dehoff, R.M., Gong, L., Klein, T.E., Wadelius, M. and Niemi, M. (2014) The clinical pharmacogenetics implementation consortium guideline for SLCO1B1 and simvastatin-induced myopathy: 2014 update. *Clinical Pharmacology and Therapeutics*, 96 (4), 423–428. Available from: doi:10.1038/clpt.2014.125.

Reddy, J.K. and Rao, M.S. (2006) Lipid metabolism and liver inflammation. II. Fatty liver disease and fatty acid oxidation. *American Journal Of Physiology Gastrointestinal Liver Physiology*, 290, G852–G858. Available from: doi:10.1152/ajpgi.00521.2005.

Remy, S., Chenouard, V., Tesson, L., Usal, C., Ménoret, S., Brusselle, L., Heslan, J.M., Nguyen, T.H., Bellien, J., Merot, J., De Cian, A., Giovannangeli, C., Concordet, J.P. and Anegon, I. (2017) Generation of gene-edited rats by delivery of CRISPR/Cas9 protein and donor DNA into intact zygotes using electroporation. *Scientific Reports*, 7 (1), 1–13. Available from: doi:10.1038/s41598-017-16328-y.

Renna, N.F., De Las Heras, N. and Miatello, R.M. (2013) Pathophysiology of vascular remodeling in hypertension. *International Journal of Hypertension*, 2013, 1–7. Available from: doi:10.1155/2013/808353.

Te Riet, L., Van Esch, J.H.M., Roks, A.J.M., Van Den Meiracker, A.H. and Danser, A.H.J. (2015) Hypertension: Renin-Angiotensin-Aldosterone System Alterations. *Circulation Research*, 116 (6), 960–975. Available from: doi:10.1161/CIRCRESAHA.116.303587.

Rizza, S., Copetti, M., Rossi, C., Cianfarani, M.A., Zucchelli, M., Luzi, A., Pecchioli, C., Porzio, O., Di Cola, G., Urbani, A., Pellegrini, F. and Federici, M. (2014) Metabolomics signature improves the prediction of cardiovascular events in elderly subjects. *Atherosclerosis*, 232 (2), 260–264. Available from: doi:10.1016/j.atherosclerosis.2013.10.029.

Roth, M., Obaidat, A. and Hagenbuch, B. (2012) OATPs, OATs and OCTs: The organic anion and cation transporters of the SLCO and SLC22A gene superfamilies. *British Journal of Pharmacology*, 165 (5), 1260–1287. Available from: doi:10.1111/j.1476-5381.2011.01724.x.

Rubattu, S., Stanzione, R. and Volpe, M. (2016) Mitochondrial dysfunction contributes to hypertensive target organ damage: lessons from an animal model of human disease. *Oxidative Medicine and Cellular Longevity*, 2016, 1–10. Available from: doi:10.1155/2016/1067801.

Rubins, H.B., Robins, S.J., Collins, D., Nelson, D.B., Elam, M.B., Schaefer, E.J., Faas, F.H. and Anderson, J.W. (2002) Diabetes, Plasma Insulin, and Cardiovascular Disease. *Arch Intern Med*, 162, 2597–2604.

Rupasinghe, H.P.V., Sekhon-Loodu, S., Mantso, T. and Panayiotidis, M.I. (2016) Phytochemicals in regulating fatty acid ß-oxidation: Potential underlying mechanisms and their involvement in obesity and weight loss. *Pharmacology and Therapeutics*, 165, 153–163. Available from: doi:10.1016/j.pharmthera.2016.06.005.

Ruppert, V. and Maisch, B. (2003) Genetics of Human Hypertension. *Herz*, 28 (8),

655–662. Available from: doi:10.1007/s00059-003-2516-6.
Russell, J.C., Dolphin, P.J., Hameed, M., Stewart, B., Koeslag, D.G., Rose-Kahn, G. and Bar- Tana, J. (1991) Hypolipidemic effect of ß,ß'-tetramethyl hexadecanedioic acid (MEDICA 16) in hyperlipidemic JCR:LA-corpulent rats. *Arteriosclerosis, Thrombosis, and Vascular Biology*, 11 (3), 602–609. Available from: doi:10.1161/01.ATV.11.3.602.
Russo, A., Di Gaetano, C., Cugliari, G. and Matullo, G. (2018) Advances in the genetics of hypertension: The effect of rare variants. *International Journal of Molecular Sciences*, 19 (688), 1–21. Available from: doi:10.3390/ijms19030688.
Saeidi, M., Soroush, A., Komasi, S., Moemeni, K. and Heydarpour, B. (2015) Attitudes Toward Cardiovascular Disease Risk Factors Among Patients Referred to a Cardiac Rehabilitation Center: Importance of Psychological Attitudes. *Shiraz E-Medical Journal*, 16 (7). Available from: doi:10.17795/semj22281.
Samson, R., Qi, A., Jaiswal, A., Le Jemtel, T.H. and Oparil, S. (2017) Obesity-Associated Hypertension: the Upcoming Phenotype in African-American Women. *Current Hypertension Reports*, 19 (41), 1–11. Available from: doi:10.1007/s11906-017-0738-x.
Sanders, R.-J., Ofman, R., Dacremont, G., Wanders, R.J.A. and Kemp, S. (2008a) Characterization of the human -oxidation pathway for -hydroxy-very-long-chain fatty acids. *The FASEB Journal*, 22 (6), 2064–2071. Available from: doi:10.1096/fj.07-099150.
Sanders, R.-J., Ofman, R., Dacremont, G., Wanders, R.J.A. and Kemp, S. (2008b) Characterization of the human ω -oxidation pathway for ω-hydroxy-very-long-chain fatty acids. *The FASEB Journal*, 22 (6), 2064–2071. Available from: doi:10.1096/fj.07-099150.
Sanders, R., Ofman, R., Duran, M., Kemp, S. and Wanders, R.J.A. (2006) ω-oxidation of very long-chain fatty acids in human liver microsomes: implications for x-linked adrenoleukoystrophy. *Journal of Biological Chemistry*, 281 (19), 1–11. Available from: doi:10.1074/jbc.M513481200.
Sandoo, A., Veldhuijzen van Zanten, J.J.C.S., Metsios, G.S., Carroll, D. and Kitas, G.D. (2010) The Endothelium and Its Role in Regulating Vascular Tone. *The Open Cardiovascular Medicine Journal*, 4 (1), 302–312. Available from: doi:10.2174/1874192401004010302.
Santos, C.R. and Schulze, A. (2012) Lipid metabolism in cancer. *The FEBS Journal*, 279, 2610–2623. Available from: doi:10.1111/j.1742-4658.2012.08644.x.
Sarwar, M., Islam, M., Al Baker, S.M. and Hasnat, A. (2013) Resistant Hypertension: Underlying Causes and Treatment. *Drug Research*, 63, 217–223. Available from: doi:10.1055/s-0033-1337930.
Sear, J.W. (2013) Antihypertensive Drugs and Vasodilators. In: *Pharmacology and Physiology for Anesthesia: Foundations and Clinical Application*. Elsevier Inc. pp. 405–425. Available from: doi:10.1016/B978-1-4377-1679-5.00023-5.
Segarra, G., Cortina, B., Mauricio, M.D., Novella, S., Lluch, P., Navarrete-Navarro, J., Noguera, I. and Medina, P. (2016) Effects of asymmetric dimethylarginine on renal arteries in portal hypertension and cirrhosis. *World Journal of Gastroenterology*, 22 (48), 10545–10556. Available from: doi:10.3748/wjg.v22.i48.10545.
Sesso, H.D., Stampfer, M.J., Rosner, B., Hennekens, C.H., Gaziano, J.M., Manson, J.E. and Glynn, R.J. (2000) Systolic and diastolic blood pressure, pulse pressure, and mean arterial pressure as predictors of cardiovascular disease risk in Men. *Hypertension*, 36, 801–807. Available from:

doi:10.1161/01.HYP.36.5.801.
Shaddy, R., Canter, C., Halnon, N., Kochilas, L., Rossano, J., Bonnet, D., Bush, C., Zhao, Z., Kantor, P., Burch, M. and Chen, F. (2017) Design for the sacubitril/valsartan (LCZ696) compared with enalapril study of pediatric patients with heart failure due to systemic left ventricle systolic dysfunction (PANORAMA-HF study). *American Heart Journal*, 193, 23–34. Available from: doi:10.1016/j.ahj.2017.07.006.
Shapiro, H., Kolodziejczyk, A.A., Halstuch, D. and Elinav, E. (2018) Bile acids in glucose metabolism in health and disease. *The Journal of Experimental Medicine*, 215 (9), 1–14. Available from: doi:10.1084/jem.20171965.
Sheppard, J.P., Martin, U. and McManus, R.J. (2017) Diagnosis and management of resistant hypertension. *Heart*, 103, 1–9. Available from: doi:10.1136/heartjnl-2015-308297.
Sim, K.G., Hammond, J. and Wilcken, B. (2002) Strategies for the diagnosis of mitochondrial fatty acid ß-oxidation disorders. *Clinica chimica acta*, 323, 37–58. Available from: doi:S0009898102001821.
Singh, H., Cheng, J., Deng, H., Kemp, R., Ishizuka, T., Nasjletti, A. and Schwartzman, M.L. (2007) Vascular cytochrome P450 4A expression and 20-hydroxyeicosatetraenoic acid synthesis contribute to endothelial dysfunction in androgen-induced hypertension. *Hypertension*, 50 (1), 1–8. Available from: doi:10.1161/HYPERTENSIONAHA.107.089599.
Singh, K.D. and Karnik, S.S. (2016) Angiotensin Receptors: Structure, Function, Signaling and Clinical Applications. *Journal Cell Signal*, 1 (2), 1–8. Available from: doi:10.4172/jcs.1000111.
Singh, M., Mensah, G.A. and Bakris, G. (2010) Pathogenesis and clinical physiology of hypertension. *Cardiology clinics*, 20 (2), 545–559.
Sinnott, S.-J., Smeeth, L., Williamson, E. and Douglas, I.J. (2017) Trends for prevalence and incidence of resistant hypertension: population based cohort study in the UK 1995-2015. *Bmj*, 358 (j3984), 1–8. Available from: doi:10.1136/bmj.j3984.
Soyka, M. and Müller, C.A. (2017) Pharmacotherapy of alcoholism–an update on approved and off-label medications. *Expert Opinion on Pharmacotherapy*, 18 (12), 1187–1199. Available from: doi:10.1080/14656566.2017.1349098.
Sparks, M.A., Crowley, S.D., Gurley, S.B., Mirotsou, M. and Coffman, T.M. (2014) Classical Renin-Angiotensin System in Kidney Physiology. *Comprehensive Physiology*, 4 (3), 1201–1228. Available from: doi:10.1002/cphy.c130040.
Spratlin, J.L., Serkova, N.J. and Eckhardt, S.G. (2009) Clinical applications of metabolomics in oncology: a review. *Clin Cancer Res. Author*, 15 (2), 431–440. Available from: doi:10.1158/1078-0432.CCR-08-1059.
Stambuk, N. and Konjevoda, P. (2002) Relationship of plasma creatine kinase and cardiovascular function in myocardial infarction. *Croatica Chemica Acta*, 75 (4), 891–898.
Stanhewicz, A.E. and Kenney, W.L. (2015) Determinants of water and sodium intake and output. *Nutrition Reviews*, 73 (S2), 73–82. Available from: doi:10.1093/nutrit/nuv033.
Van de Steeg, E., Wagenaar, E., Van der Kruijssen, C.M.M., Burggraaf, J.E.C., de Waart, D.R., Oude Elferink, R.P.J., Kenworthy, K.E. and Schinkel, A.H. (2010) Organic anion transporting polypeptide 1a/1b–knockout mice provide insights into hepatic handling of bilirubin, bile acids, and drugs. *The Journal of Clinical Investigation*, 120 (8), 2942–2952. Available from: doi:10.1172/JCI42168DS1.
Subramanian, S., DeRosa, M.A., Bernal-Mizrachi, C., Laffely, N., Cade, W.T., Yarasheski, K.E., Cryer, P.E. and Semenkovich, C.F. (2006) PPARα activation

elevates blood pressure and does not correct glucocorticoid-induced insulin resistance in humans. *American journal of physiology Endocrinology and metabolism*, 291, E1365–E1371. Available from: doi:10.1152/ajpendo.00230.2006.

Sumbria, R. and Fisher, M. (2017) Endothelium. In: *Primer on Cerebrovascular Diseases*. Second Edi. Elsevier. pp. 47–51. Available from: doi:10.1016/B978-0-12-803058-5.00008-4.

Sussulini, A. (2017) *Metabolomics: From Fundamentals to Clinical Applications*. springer. Available from: doi:10.1007/978-3-319-47656-8.

Syddall, H.E., Simmonds, S.J., Martin, H.J., Watson, C., Dennison, E.M., Cooper, C. and Sayer;, A.A. (2010) Cohort profile: The Hertfordshire Ageing Study (HAS). *International Journal of Epidemiology*, 39 (1), 36–43. Available from: doi:10.1093/ije/dyn275.

Takahashi, S., Fukami, T., Masuo, Y., Brocker, C.N., Xie, C., Krausz, K.W., Wolf, C.R., Henderson, C.J. and Gonzalez, F.J. (2016) Cyp2c70 is responsible for the species difference in bile acid metabolism between mice and humans. *Journal of Lipid Research*, 57 (12), 2130–2137. Available from: doi:10.1194/jlr.M071183.

Takikawa, H. (2002) Hepatobiliary transport of bile acids and organic anions. *Journal of Hepatobiliary Pancreatic Surgery*, 9 (4), 443–447.

Talati, M. and Hemnes, A. (2015) Fatty acid metabolism in pulmonary arterial hypertension: role in right ventricular dysfunction and hypertrophy. *Pulmonary circulation*, 5 (2), 269–278. Available from: doi:10.1086/681227.

Tapiero, H., Mathé, G., Couvreur, P. and Tew, K.D. (2002) I. Arginine. *Biomed Pharmacother*, 56 (9), 439–445. Available from: doi:10.1016/s0753-3322(02)00284-6.

Tarnoki, A.D., Tarnoki, D.L. and Molnar, A.A. (2014) Past, present and future of cardiovascular twin studies. *Cor et Vasa*, 56, e486–e493. Available from: doi:10.1016/j.crvasa.2014.07.005.

Taylor, D.A. and Abdel-Rahman, A.A. (2009) Novel Strategies and Targets for the Management of Hypertension. *Advances in Pharmacology*, 57 (08), 291–345. Available from: doi:10.1016/S1054-3589(08)57008-6.

Tein, I. (2014) Lipid Storage Myopathies Due to Fatty Acid Oxidation Defects. In: *Neuromuscular Disorders of Infancy, Childhood, and Adolescence*. Second. Elsevier Inc. pp. 761–795. Available from: doi:10.1016/B978-0-12-417044-5.00040-8.

Thakkar, N., Lockhart, A.C. and Lee, W. (2015) Role of organic anion-transporting polypeptides (OATPs) in cancer therapy. *The AAPS Journal*, 17 (3), 535–545. Available from: doi:10.1208/s12248-015-9740-x.

Timpson, N.J., Harbord, R., Smith, G.D., Zacho, J., Tybjærg-Hansen, A. and Nordestgaard, B.G. (2009) Does greater adiposity increase blood pressure and hypertension risk?: Mendelian randomization using the FTO/MC4R genotype. *Hypertension*, 54, 84–90. Available from: doi:10.1161/HYPERTENSIONAHA.109.130005.

Tobe, S. and Lewanczuck, R. (2009) Resistant hypertension. *Canadian Journal of Cardiology*, 6 (5), 315–317. Available from: doi:10.1161/HYPERTENSIONAHA.111.00601.

Toka, H.R. (2018) Monogenic Forms of Hypertension. In: *Disorders of Blood Pressure Regulation Phenotypes, Mechanisms, Therapeutic Options*. Springer International Publishing AG. pp. 157–175. Available from: doi:10.1007/978-3-319-59918-2.

Tordjman, K., Bernal-Mizrachi, C., Zemany, L., Weng, S., Feng, C., Zhang, F., Leone, T.C., Coleman, T., Kelly, D.P. and Semenkovich, C.F. (2001) PPARα

deficiency reduces insulin resistance and atherosclerosis in apoE-null mice. *The Journal of clinical investigation*, 107 (8), 1025–1034. Available from: doi:10.1172/JCI11497.

Toth, P., Csiszar, A., Sosnowska, D., Tucsek, Z., Cseplo, P., Springo, Z., Tarantini, S., Sonntag, W.E., Ungvari, Z. and Koller, A. (2013) Treatment with the cytochrome P450 ω-hydroxylase inhibitor HET0016 attenuates cerebrovascular inflammation, oxidative stress and improves vasomotor function in spontaneously hypertensive rats. *British Journal of Pharmacology*, 168 (8), 1878–1888. Available from: doi:10.1111/bph.12079.

Touyz, R.M., Alves-Lopes, R., Rios, F.J., Camargo, L.L., Anagnostopoulou, A., Arner, A. and Montezano, A.C. (2018) Vascular smooth muscle contraction in hypertension. *Cardiovascular Research*, 114, 529–539. Available from: doi:10.1093/cvr/cvy023.

Tsunoda, F., Asztalos, I.B., Horvath, K. V., Steiner, G., Schaefer, E.J. and Asztalos, B.F. (2016) Fenofibrate, HDL, and cardiovascular disease in Type-2 diabetes: The DAIS trial. *Atherosclerosis*, 247, 35–39. Available from: doi:10.1016/j.atherosclerosis.2016.01.028.

Tummers-de Lind van Wijngaarden, R.F.A., Havenith, T., Hurkens, K., de Vries, F. and Hulsewe-Evers, H. (2013) A patient with a life-threatening disulfiram-ethanol reaction. *Ned Tijdschr Geneeskd*, 157 (1), A5240.

Tzur, R., Rose-kahn, G., Adler, J.H. and Bar-tana, J. (1988) Hypolipidemic, antiobesity, and hypoglycemic-hypoinsulinemic effects of ß,ß'-methyl-substituted hexadecanedioic acid in sand Rats. *Diabetes*, 37, 1618–1624.

Uno, T. and Hisa, Y. (2016) Autonomic Nervous System. In: *Neuroanatomy and Neurophysiology of the Larynx*. pp. 30–44.

Vasdev, S., Singal, P. and Gill, V. (2009) The antihypertensive effect of cysteine. *International Journal of Angiology*, 18 (1), 7–21. Available from: doi:10.1055/s-0031-1278316.

Vasiliou, V. and Nebert, D.W. (2005) Analysis and update of the human aldehyde dehydrogenase (ALDH) gene family. *Human Genomics*, 2 (2), 138–143. Available from: doi:10.1186/1479-7364-2-2-138.

Ventura, H.O., Taler, S.J. and Strobeck, J.E. (2005) Hypertension as a hemodynamic disease: The role of impedance cardiography in diagnostic, prognostic, and therapeutic decision making. *American Journal of Hypertension*, 18 (2), 26S–43S. Available from: doi:10.1016/j.amjhyper.2004.11.002.

Vimalraj, S. and Selvamurugan, N. (2011) MicroRNAs : synthesis , gene regulation and osteoblast differentiation. *Mol ecular Biology*, 15, 7–18.

Vishwanath, V.A. (2016) Fatty acid beta-oxidation disorders: A brief review. *Annals of Neurosciences*, 23 (1), 51–55. Available from: doi:10.1159/000443556.

Wahid, F., Shehzad, A., Khan, T. and Kim, Y.Y. (2010) MicroRNAs: synthesis, mechanism, function, and recent clinical trials. *Molecular Cell Research*, 1803 (11), 1231–1243. Available from: doi:10.1016/j.bbamcr.2010.06.013.

Wakil, S.J. and Abu-Elheiga, L.A. (2009) Fatty acid metabolism: target for metabolic syndrome. *Journal of Lipid Research*, 50, S138–S143. Available from: doi:10.1194/jlr.R800079-JLR200.

Wamelink, M.M.C., Struys, E.A. and Jakobs, C. (2008) The biochemistry, metabolism and inherited defects of the pentose phosphate pathway: a review. *Journal of Inherited Metabolic Disease*, 31 (6), 703–717. Available from: doi:10.1007/s10545-008-1015-6.

Wanders, R.J.A., Komen, J. and Kemp, S. (2011) Fatty acid omega-oxidation as a rescue pathway for fatty acid oxidation disorders in humans. *The FEBS*

Journal, 278 (2), 182–194. Available from: doi:10.1111/j.1742-4658.2010.07947.x.

Wang, G.S. and Cooper, T.A. (2007) Splicing in disease: Disruption of the splicing code and the decoding machinery. *Nature Reviews Genetics*, 8 (10), 749–761. Available from: doi:10.1038/nrg2164.

Wang, L. and Bautista, L.E. (2015) Serum bilirubin and the risk of hypertension. *International Journal of Epidemiology*, 44 (1), 142–152. Available from: doi:10.1093/ije/dyu242.

Wang, S., Ma, A., Song, S., Quan, Q., Zhao, X. and Zheng, X. (2008) Fasting serum free fatty acid composition, waist/hip ratio and insulin activity in essential hypertensive patients. *Hypertension Research*, 31 (4), 623–632. Available from: doi:10.1291/hypres.31.623.

Wang, Y., Seto, S.-W. and Golledge, J. (2014) Angiotensin II, sympathetic nerve activity and chronic heart failure. *Heart Failure Reviews*, 19 (2), 187–198. Available from: doi:10.1007/s10741-012-9368-1.

Wang, Z., Tang, W.H.W., Cho, L., Brennan, D. and Hazen, S.L. (2009) Targeted metabolomic evaluation of arginine methylation and cardiovascular risks: potential mechanisms beyond nitric oxide synthase inhibition. *Arterioscler Thromb Vasc Biol*, 29 (9), 1383–1391. Available from: doi:10.1161/ATVBAHA.109.185645.

Weisbrod, R.M., Shiang, T., Sayah, L. Al, Fry, J.L., Bajpai, S., Reinhart-King, C.A., Lob, H.E., Santhanam, L., Mitchell, G., Cohen, R.A. and Seta, F. (2013) Arterial stiffening precedes systolic hypertension in diet-induced obesity. *Hypertension*, 62, 1105–1110. Available from: doi:10.1161/HYPERTENSIONAHA.113.01744.

Whelton, P.K. and Carey, R.M. (2018) 2017 ACC/AHA/AAPA/ABC/ACPM/AGS/APhA/ASH/ASPC/NMA/PCNA Guideline for the Prevention, Detection, Evaluation, and Management of High Blood Pressure in Adults. *Nature Reviews Cardiology*, 71 (19), e127–e248. Available from: doi:10.1016/j.jacc.2017.11.006.

Williams, J.M., Murphy, S., Burke, M. and Roman, R.J. (2011a) 20-HETE: a new target for the treatment of hypertension. *Journal of Cardiovascular Pharmacol*, 56 (4), 336–344. Available from: doi:10.1097/FJC.0b013e3181f04b1c.20-HETE.

Williams, J.S., Hopkins, P.N., Jeunemaitre, X. and Brown, N.J. (2011b) CYP4A11 T8590C polymorphism, salt-sensitive hypertension, and renal blood flow. *Journal of Hypertension*, 29 (10), 1913–1918. Available from: doi:10.1097/HJH.0b013e32834aa786.

de Wit, C., Bolz, S.S., Kaas, J. and Pohl, U. (1998) Myogenic effects enhance norepinephrine constriction: inhibition by nitric oxide and felodipine. *Kidney international*, 54 (67), S122–S126. Available from: doi:10.1046/j.1523-1755.1998.06723.x.

World Health Organization (2018a) *Cardiovascular diseases (CVDs)*. 2018. Available from: http://www.who.int/en/news-room/fact-sheets/detail/cardiovascular-diseases-(cvds).

World Health Organization (2018b) *Global health observatory (GHO) data Raised blood pressure*. 2018. Available from: http://www.who.int/gho/ncd/risk_factors/blood_pressure_prevalence_text/en/.

World Health Organization (2018c) *Salt reduction*. 2018. Available from: http://www.who.int/en/news-room/fact-sheets/detail/salt-reduction.

Wu, P., Zhang, Y., Liu, Y., Wang, X., Guo, Z., Zhang, Y., Liang, X. and Lai, W. (1999) Effects of cholic acid on blood pressure and production of vascular

aldosterone and corticosterone. *Steroids*, 64 (4), 291–295. Available from: doi:10.1016/S0039-128X(99)00005-7.

Xiang, X., Han, Y., Neuvonen, M., Pasanen, M.K., Kalliokoski, A., Backman, J.T., Laitila, J., Neuvonen, P.J. and Niemi, M. (2009) Effect of SLCO1B1 polymorphism on the plasma concentrations of bile acids and bile acid synthesis marker in humans. *Pharmacogenetics and Genomics*, 19 (6), 447–457. Available from: doi:10.1097/FPC.0b013e32832bcf7b.

Yamori, Y., Tomimoto, K., Ooshima, A., Hazama, F. and Okamoto, K. (1974) Proceedings: Developmental course of hypertension in the SHR-substrains susceptible to hypertensive cerebrovascular lesions. *Japanese heart journal*, 15 (2), 209–210. Available from: doi:10.1536/ihj.15.209.

Yang, H.C., Liang, Y.J., Chen, J.W., Chiang, K.M., Chung, C.M., Ho, H.Y., Ting, C.T., Lin, T.H., Sheu, S.H., Tsai, W.C., Chen, J.H., Leu, H.B., Yin, W.H., Chiu, T.Y., Chern, C.I., Lin, S.J., Tomlinson, B., Guo, Y., Sham, P.C., *et al*. (2012) Identification of IGF1, SLC4A4, WWOX, and SFMBT1 as hypertension susceptibility genes in han chinese with a genome-wide gene-based association study. *PLoS ONE*, 7 (3), 1–14. Available from: doi:10.1371/journal.pone.0032907.

Yang, X.-F., Chen, Y.-Z., Su, J.-L., Wang, F.-Y. and Wang, L.-X. (2009) Relationship between Serum Bilirubin and Carotid Atherosclerosis in Hypertensive Patients. *Internal Medicine*, 48 (18), 1595–1599. Available from: doi:10.2169/internalmedicine.48.2286.

Yasunami, M., Chen, C.S. and Yoshida, A. (1991) A human alcohol dehydrogenase gene (ADH6) encoding an additional class of isozyme. *The National Academy of Sciences*, 88 (17), 7610–7614. Available from: doi:10.1073/pnas.88.17.7610.

Ye, Y., Gong, G., Ochiai, K., Liu, J. and Zhang (2001a) High-energy phosphate metabolism and creatine kinase in failing hearts. *Circulation*, 103, 1570–1576. Available from: doi:10.1161/01.CIR.103.11.1570.

Ye, Y., Wang, C., Zhang, J., Cho, Y.K., Gong, G., Murakami, Y. and Bache, R.J. (2001b) Myocardial creatine kinase kinetics and isoform expression in hearts with severe LV hypertrophy. *Am.J.Physiol Heart Circ.Physiol*, 281, H376–H386.

Yee, S.W., Giacomini, M.M., Hsueh, C.H., Weitz, D., Liang, X., Goswami, S., Kinchen, J.M., Coelho, A., Zur, A.A., Mertsch, K., Brian, W., Kroetz, D.L. and Giacomini, K.M. (2016) Metabolomic and genome-wide association studies reveal potential endogenous biomarkers for OATP1B1. *Clinical Pharmacology and Therapeutics*, 100 (5), 524–536. Available from: doi:10.1002/cpt.434.

Yokoyama, A., Mizukami, T., Matsui, T., Yokoyama, T., Kimura, M., Matsushita, S., Higuchi, S. and Maruyama, K. (2013) Genetic polymorphisms of alcohol dehydrogenase-1B and aldehyde dehydrogenase-2 and liver cirrhosis, chronic calcific pancreatitis, diabetes mellitus, and hypertension among Japanese alcoholic men. *Alcoholism: Clinical and Experimental Research*, 37 (8), 1391–1401. Available from: doi:10.1111/acer.12108.

Yoshida, A., Rzhetsky, A., Hsu, L.C. and Chang, C. (1998) Human aldehyde dehydrogenase gene family. *European journal of biochemistry*, 251 (3), 549–557. Available from: doi:10.1046/j.1432-1327.1998.2510549.x.

Yu, B., Li, A.H., Metcalf, G.A., Muzny, D.M., Morrison, A.C., White, S., Mosley, T.H., Gibbs, R.A. and Boerwinkle, E. (2016) Loss-of-function variants influence the human serum metabolome. *Science advances*, 2 (8), 1–5. Available from: doi:10.1126/sciadv.1600800.

Yue, T., Bao, W., Jucker, B.M., Gu, J., Romanic, A.M., Brown, P.J., Cui, J.,

Thudium, D.T., Boyce, R., Burns-Kurtis, C.L., Mirabile, R.C., Aravindhan, K., Ohlstein, E.H. and Background—Peroxisome (2003) Activation of Peroxisome Proliferator-Activated Receptor- α Protects the Heart From Ischemia/Reperfusion Injury. *Circulation*, 108, 2393–2399. Available from: doi:10.1161/01.CIR.0000093187.42015.6C.

Zaher, H., Meyer zu Schwabedissen, H.E., Tirona, R.G., Cox, M.L., Obert, L.A., Agrawal, N., Palandra, J., Stock, J.L., Kim, R.B., Ware, J.A., Meyer, H.E., Tirona, R.G., Cox, M.L., Obert, L.A., Agrawal, N., Palandra, J., Stock, J.L., Kim, R.B. and Ware, J.A. (2008) Targeted disruption of murine organic anion-transporting polypeptide 1b2 (Oatp1b2/Slco1b2) significantly alters disposition of prototypical drug substrates pravastatin and rifampin. *Molecular Pharmacology*, 74 (2), 320–329. Available from: doi:10.1124/mol.108.046458.

Zhang-James, Y., Middleton, F.A. and Faraone, S. V. (2013) Genetic architecture of Wistar-Kyoto rat and spontaneously hypertensive rat substrains from different sources. *Physiological Genomics*, 45 (13), 528–538. Available from: doi:10.1152/physiolgenomics.00002.2013.

Zhang, Y., Wu, J.H.Y., Vickers, J.J., Ong, S.L.H., Temple, S.E.L., Mori, T.A., Croft, K.D. and Whitworth, J.A. (2009) The role of 20-hydroxyeicosatetraenoic acid in adrenocorticotrophic hormone and dexamethasone-induced hypertension. *Journal of Hypertension*, 27 (8), 1609–1616. Available from: doi:10.1097/HJH.0b013e32832cc56c.

Zhao, Y., Peng, J., Lu, C., Hsin, M., Mura, M., Wu, L., Chu, L., Zamel, R., Machuca, T., Waddell, T., Liu, M., Keshavjee, S., Granton, J. and De Perrot, M. (2014) Metabolomic heterogeneity of pulmonary arterial hypertension. *PLoS ONE*, 9 (2), 1–11. Available from: doi:10.1371/journal.pone.0088727.

Zhou, H. and Hylemon, P.B. (2014) Bile acids are nutrient signaling hormones. *Steroids*, 86, 62–68. Available from: doi:10.1016/j.steroids.2014.04.016.

Zhou, M.-S., Schulman, I.H., Pagano, P.J., Jaimes, E.A. and Raij, L. (2006) *Reduced NAD (P) H Oxidase in Low Renin Hypertension Link Among Angiotensin II, Atherogenesis, and Blood Pressure*. 47, 81–86. Available from: doi:10.1161/01.HYP.0000197182.65554.c7.

Zhou, M.S., Adam, A.G., Jaimes, E.A. and Raij, L. (2003) In Salt-Sensitive Hypertension, Increased Superoxide Production Is Linked to Functional Upregulation of Angiotensin II. *Hypertension*, 42, 945–951. Available from: doi:10.1161/01.HYP.0000094220.06020.C8.